

Hanafi Ismail
Sapuan S. M.
Ilyas R. A. *Editors*

Recycled Polymer Blends and Composites

Processing, Properties, and Applications

 Springer

Recycled Polymer Blends and Composites

Hanafi Ismail • Sapuan S. M. • Ilyas R. A.
Editors

Recycled Polymer Blends and Composites

Processing, Properties, and Applications

 Springer

Editors

Hanafi Ismail
School of Materials and Mineral Resources
Engineering, Engineering Campus
Universiti Sains Malaysia
Nibong Tebal, Penang, Malaysia

Sapuan S. M.
Advanced Engineering Materials and
Composites Research Center (AEMC)
Faculty of Engineering
Universiti Putra Malaysia
Seri Kembangan, Selangor, Malaysia

Ilyas R. A.
Centre for Advanced Composite
Materials (CACM)
Universiti Teknologi Malaysia
Johor Bahru, Johor, Malaysia

ISBN 978-3-031-37045-8 ISBN 978-3-031-37046-5 (eBook)
<https://doi.org/10.1007/978-3-031-37046-5>

© The Editor(s) (if applicable) and The Author(s), under exclusive license to Springer Nature Switzerland AG 2023

This work is subject to copyright. All rights are solely and exclusively licensed by the Publisher, whether the whole or part of the material is concerned, specifically the rights of translation, reprinting, reuse of illustrations, recitation, broadcasting, reproduction on microfilms or in any other physical way, and transmission or information storage and retrieval, electronic adaptation, computer software, or by similar or dissimilar methodology now known or hereafter developed.

The use of general descriptive names, registered names, trademarks, service marks, etc. in this publication does not imply, even in the absence of a specific statement, that such names are exempt from the relevant protective laws and regulations and therefore free for general use.

The publisher, the authors, and the editors are safe to assume that the advice and information in this book are believed to be true and accurate at the date of publication. Neither the publisher nor the authors or the editors give a warranty, expressed or implied, with respect to the material contained herein or for any errors or omissions that may have been made. The publisher remains neutral with regard to jurisdictional claims in published maps and institutional affiliations.

This Springer imprint is published by the registered company Springer Nature Switzerland AG
The registered company address is: Gewerbestrasse 11, 6330 Cham, Switzerland

Paper in this product is recyclable.

Contents

Zooming into Recycling of Composites	1
Ilyas R. A., A. H. Nordin, H. S. N. Hawanis, J. Tarique, Sapuan S. M., M. R. M. Asyraf, M. Rafidah, Hanafi Ismail, and M. Y. M. Zuhri	
Recycling of Polymeric Membranes	17
Maicon Sérgio Nascimento dos Santos, João Henrique Cabral Wancura, Carolina Elisa Demaman Oro, Rogério Marcos Dallago, Giovani Leone Zabet, and Marcus Vinícius Tres	
Composites Based on Polymeric Matrices Recycled from Different Wastes and Natural Fibers	35
Galder Kortaberria	
Mechanical Properties of Recycled Polyolefin Composites	49
Ruey Shan Chen, Mohd Nazry Salleh, and Sinyee Gan	
Polymeric Substances Recycled from Excess Sludge in Wastewater Treatment Plant	67
Da-Qi Cao	
Recycling of Ground Tire Rubber According to the Literature	97
Fabiula Danielli Bastos de Sousa	
Polymer Processing Technology to Recycle Polymer Blends	111
Daniel C. Licea Saucedo, Rubén González Nuñez, Milton O. Vázquez Lepe, and Denis Rodrigue	
Sustainable Materials from Recycled Polypropylene Waste and Green Fillers: Processing, Properties, and Applications	133
Noraiham Mohamad, Hairul Effendy Ab Maulod, and Jeefferie Abd Razak	

Comparative Studies of Natural Rubber/Virgin Ethylene Propylene Diene Rubber and Natural Rubber/Recycled Ethylene Propylene Diene Rubber and Natural Rubber/Blends	179
Nabil Hayeemasae and Hanafi Ismail	
Optimization of Accelerators on the Properties of Natural Rubber/Recycled Ethylene Propylene Diene Rubber Blends	209
Nabil Hayeemasae and Hanafi Ismail	
Compatibilization of Natural Rubber/Recycled Ethylene Propylene Diene Rubber Blends	227
Nabil Hayeemasae and Hanafi Ismail	
Effect of Metal Oxide Content on the Mechanical and Thermal Properties of Natural Rubber/Recycled Chloroprene Rubber Blends	255
Nabil Hayeemasae, Siti Zuliana Salleh, and Hanafi Ismail	
Chloroprene Rubber Waste as Blend Component with Natural Rubber, Epoxidized Natural Rubber, and Styrene Butadiene Rubber	271
Nabil Hayeemasae, Siti Zuliana Salleh, and Hanafi Ismail	
Recycled Cellulose and Cellulose-Based Materials by Gamma Rays and Its Use as Reinforcement in Composites	291
Irna Zukeyt Garduño-Jaimes, Gonzalo Martínez-Barrera, Enrique Viguera-Santiago, and Julián Cruz-Olivares	
Tensile, Thermal Properties, and Biodegradability Test of Paddy Straw Powder-Filled Polyhydroxybutyrate-3-Valerate (PHBV) Biocomposites: Acrylation Pretreatment	307
Noorulnajwa Diyana Yaacob, Hanafi Ismail, and Sam Sung Ting	
Comparison Between Natural Rubber, Liquid Natural Rubber, and Recycled Natural Rubber as Secondary Matrix in Epoxy/Natural Rubber/Graphene Nano-platelet System	323
K. W. Kam, P. L. Teh, and C. K. Yeoh	
Recycling of Commonly Used Waste Plastics to Fabricate Membranes for Filtration Applications	347
Abichal Ghosh, Anirban Roy, and A. K. Ghosh	
Recycled Polymer Bio-based Composites: A Review of Compatibility and Performance Issues	363
Khalid Alzebdeh, Nasr Al Hinai, Mahmoud Al Safy, and Mahmoud Nassar	
Production and Recycling of Biocomposites: Present Trends and Future Perspectives	389
Venitalitya A. S. Augustia and Achmad Chafidz	

Recycled Polyethylene Blends and Composites: Current Trend, Technology, and Challenges 405
Yamuna Munusamy, Zunaida Zakaria, Hanafi Ismail,
and Nor Azura Abdul Rahim

Recycled Polyethylene Terephthalate Blends and Composites: Impact of PET Waste, Engineering Design, and Their Applications 417
Zunaida Zakaria, Hakimah Osman, Nor Azura Abdul Rahim,
Yamuna Munusamy, and Hanafi Ismail

Index 437

Zooming into Recycling of Composites



Ilyas R. A., A. H. Nordin, H. S. N. Hawanis, J. Tarique, Sapuan S. M.,
M. R. M. Asyraf, M. Rafidah, Hanafi Ismail, and M. Y. M. Zuhri

1 Introduction

Plastics have supplanted other materials in the modern economy because they are inexpensive, lightweight, and adaptable (MacArthur 2017; Tarique et al. 2021b). The annual production of plastic expanded from 2 to 380 Mt. between the year 1950 and 2018, but this was also accompanied by the production of an estimated 6300 Mt. of plastics garbage, of which around 9% was recycled, 12% was burned, and 79% was dumped in the environment or sent to landfills. It is currently projected that 90% of plastic products are utilized once and then disposed of (2018). However, because of the prohibitive costs of collection and a lack of the necessary infrastructure, almost 50% of the plastic was wasted after only one usage (Kedzierski et al.

Ilyas R. A. (✉)

Faculty of Chemical and Energy Engineering, Universiti Teknologi Malaysia, Johor, Malaysia

Centre for Advanced Composite Materials (CACM), Universiti Teknologi Malaysia,
Johor Bahru, Johor, Malaysia

Institute of Tropical Forest and Forest Products (INTROP), Universiti Putra Malaysia,
Serdang, Selangor, Malaysia

Centre of Excellence for Biomass Utilization, Universiti Malaysia Perlis,
Arau, Perlis, Malaysia

e-mail: ahmadilyas@utm.my

A. H. Nordin · H. S. N. Hawanis

Faculty of Chemical and Energy Engineering, Universiti Teknologi Malaysia, Johor, Malaysia

J. Tarique

Advanced Engineering Materials and Composites Research Centre (AEMC),
Department of Mechanical and Manufacturing Engineering, Faculty of Engineering,
Universiti Putra Malaysia, Serdang, Selangor, Malaysia

Institute of Energy Infrastructure, Universiti Tenaga Nasional, Jalan IKRAM-UNITEN,
Kajang, Selangor, Malaysia

2020). By 2050, landfills and the natural environment are predicted to accumulate 12 billion tons of plastic trash (Yong et al. 2020). In addition, the COVID-19 outbreak has greatly increased the usage of personal protective equipment, disposable dinnerware, and plastic-wrapped food, which could lead to a new environmental crisis (Vanapalli et al. 2021). Polyethylene terephthalate (PET), polyethylene (PE), polypropylene (PP), polyvinyl chloride (PVC), and polystyrene (PS) are only a few of the polymers that make up plastic debris in general (Chen et al. 2021).

However, global assessments of plastic waste management losses (Jambeck et al. 2015), microplastic (plastics < 5 mm in length) losses across the whole plastic value chain (Boucher and Friot 2017), and micro- and macroplastics (plastics \geq 5 mm in length) transportation in rivers have indicated that massive volumes of plastics are ejected into the ocean. According to the United Nation Environment Program, 3.0 Mt. of microplastics and 5.3 Mt. of macroplastics are discarded into the environment each year (Ryberg et al. 2018), a significant portion of which is likely to end up as ocean plastic pollution. As a result, it is essential to keep advancing our awareness of plastic losses along the plastics value chain, as well as to develop suitable procedures to limit the environmental implications of plastic. Plastic recycling is critical not only because of the high costs of garbage disposal but also because of possibility of recovering energy from plastics and the fact that recycled items are less expensive than virgin items. Numerous more stringent legal laws in European nations constrain the ability to store plastic waste, requiring additional logical plastics management and the implementation of various technologies for plastic waste neutralization and recycling (Adelodun 2021; Tarique et al. 2022b).

Sapuan S. M.

Advanced Engineering Materials and Composites Research Center (AEMC),
Faculty of Engineering, Universiti Putra Malaysia, Seri Kembangan, Selangor, Malaysia

Laboratory of Biocomposite Technology, Institute of Tropical Forest, and Forest Products
(INTROP), Universiti Putra Malaysia, Serdang, Selangor, Malaysia

M. R. M. Asyraf

Engineering Design Research Group (EDRG), Faculty of Mechanical Engineering,
Universiti Teknologi Malaysia, Johor Bahru, Johor, Malaysia

Centre for Advanced Composite Materials (CACM), Universiti Teknologi Malaysia,
Johor Bahru, Johor, Malaysia

M. Rafidah

Department of Civil Engineering, Faculty of Engineering, Universiti Putra Malaysia,
Serdang, Selangor, Malaysia

H. Ismail

School of Materials and Mineral Resources Engineering, Engineering Campus,
Universiti Sains Malaysia, Nibong Tebal, Penang, Malaysia

M. Y. M. Zuhri

Advanced Engineering Materials and Composites Research Centre (AEMC),
Department of Mechanical and Manufacturing Engineering, Faculty of Engineering,
Universiti Putra Malaysia, Serdang, Selangor, Malaysia

According to a recent study, in order to stop the trend of rising environmental plastic pollution, a concerted worldwide effort to minimize plastic waste in every stage of the plastic lifecycle is required. For instance, Borrelle et al. (2020) evaluated the effects of lowering plastic waste output, raising waste plastic collection and recycling, and identifying and removing plastic pollution on environmental recovery. Lau et al. (2020) investigated the effects of various future scenarios that involved using alternative materials, collecting and recycling more plastic, and limiting the usage of plastics. Both groups reached the same conclusion: notwithstanding the prospect of greater costs connected with the collecting, sorting, quality control, and use of recovered plastics, rapid global cooperation is essential to decrease plastic pollution. Recycling plastic trash is also anticipated to be an effective countermeasure to the creation of ecological plastic pollution, e.g., marine pollution.

Composite materials offer better quality and a long-life duration to design engineers. Higher strength, lighter weight, and less maintenance have resulted in several engineering applications, particularly in the transportation industry, for dramatically reduced energy usage and environmental effect (CO₂). In general, three different types of composite materials have been developed and are widely employed in a wide range of technical applications: polymer–matrix composites (PMC), metal–matrix composites (MMC), and ceramic–matrix composites (CMC). These composite materials must be well managed by good waste management system. Thus, this chapter focused on the recycling on the composite materials.

2 Recycling of Plastics

Many developments are concentrating on global plastics technologies, biopolymers synthesis, the recycling sector, and waste management, with the goal of converting plastic waste into a trading opportunity for industries and manufacturers. Numerous studies on the recycling of plastic trash are currently growing exponentially, and the leading journals include *Waste Management*, the *Journal of Applied Polymer Science*, and the *Journal of Cleaner Production* (Jiang et al. 2022). The waste plastic would break down into microplastics, which would eventually be released into the leachate or an underground river or the soil (He et al. 2019). A landfill is similar to a confined tank that undergoes intricate biochemical processes and physical alterations. Additionally, landfills permanently squander land resources due to the inability of plastic to disintegrate (Chen et al. 2020). Researchers have attempted to recycle plastic garbage in an effort to avoid the issues with landfill disposal and traditional incineration that have been highlighted above. In this context, the typical methods for recycling plastic trash and their description, benefits, and drawbacks are given in Table 1. Chemical recycling, also known as tertiary recycling (Martínez Narro et al. 2019), could be accomplished using solvolysis, pyrolysis, or gasification, as described in American Society for Testing and Materials' (ASTM) D5033 standard. Chemical recycling is more popular than mechanical and biological recycling because of the mechanism that turns plastic waste into highly valuable

Table 1 Three most common plastic recycling processes

Recycling technique	Chemical Yang et al. (2021) and De-la-Torre et al. (2020)	Mechanical Sharuddin et al. (2016)	Biological Hwang et al. (2019)
Description	Pyrolysis, solvolysis, and gasification turn plastic into chemical feedstocks	Plastic is remelted or reprocessed to become relatively low plastic	Microorganisms make enzymes that break plastic polymer bonds into monomers
Benefits	Transformed into chemical raw material Adhere to principles of sustainability Processability of the end product	Widespread application Efficient disposal procedure Low operational cost Widespread adoption Adaptable source of material	Environmentally friendly
Drawbacks	Expensive dynamic catalyst High temperature Uses a lot of energy Restricts the scope of possible uses in industry	Negative impact on the environment The product has inferior mechanical characteristics It can only be used with monolayer plastics	Chemical and mechanical processes are faster compared to biological recycling

chemical feedstocks, fuel, and monomer (Klemeš et al. 2021). However, mechanical recycling, such as milling, washing, and pelletizing, is currently the most widely used technology for the large-scale recycling of plastic solid waste (Garcia and Robertson 2017). However, this method produces a lot of untreated wastewater, which may contain significant amounts of microplastics and endanger aquatic ecosystems. The sorting, shredding, cleaning, and melting steps during the recycling procedure also require a significant amount of labor and electricity expenditures. The biological recycling of plastic waste is accomplished through the extraction of enzymes or the culture of microorganisms (Koshti et al. 2018). So far, by using this technique, only plastics having hydrolyzable ester or amide linkages in the foremost chain can currently be converted to oligomers or monomers (Wei et al. 2020).

3 Polymer Blends

Polymers based on renewable resources have grown in popularity over the last 20 years as a result of environmental concerns and limited petroleum resources. For example, polymers can be derived from natural monomers such as starch, protein, and cellulose; synthetic polymers can be derived from natural monomers such as polylactic acid (PLA); and polymers can be derived from microbial fermentation such as polyhydroxybutyrate (PHB). Although PLA and starch have received the most attention in the research community, other materials such as poly(3-hydroxybutyrate-co-3-hydroxyhexanoate)/poly(vinyl phenol) (Cai et al. 2012),

thermoplastic phenol formaldehyde resin/poly(ϵ -caprolactone) (PCL) (Yang et al. 2011), poly(3-hydroxybutyrate) (PHB)/PCL (Hinüber et al. 2011), and poly(butylene succinate) should be considered. The characteristics of renewable resources-based polymers may be enhanced by blending and composite production, like many other petroleum-based polymers. Natural polymers have several native uses. For instance, polysaccharides operate in membranes and intracellular communication, whereas proteins are structural materials and catalysts (Yu et al. 2006). Polymers could be produced by nature to be utilized in fibers, adhesives, coatings, gels, foaming agents, films, thermoplastics, and thermoset resins. One of the key disadvantages of biodegradable polymers made from renewable resources is their hydrophilic nature, quick decomposition rate, and, in certain cases, worse mechanical properties, particularly in moist situations. Blending natural and synthetic polymers may, in theory, dramatically enhance the characteristics of natural polymers.

Polymer blending is a popular approach for modifying characteristics since it is low-cost and employs standard technology. The primary aim of developing a perfect blend of two or more polymers is to optimize the greatest possible performance of the blends rather than to drastically change the characteristics of the components. Several starch–polyolefin blends were developed in the 1970s and 1980s. However, since these mixtures were not biodegradable, the advantage of using biodegradable polysaccharides was lost.

4 Recycling of Blends with Limited Compatibilization

In this era, global communities have been shifting toward a greener environment that employed sustainable materials such as natural and recycled-based materials to reduce manufacturing costs and preserve the environment (Tarique et al. 2021c; Asyraf and Rafidah 2022; Asyraf et al. 2022b, c, d). In this case, the increase in demand for polymer-based materials in various usages has led researchers to explore many new fields (Ilyas et al. 2020, 2021b, 2022; Asyraf et al. 2022a). Because the usage of polymers in their pure state could occasionally be restricted, altering the polymers by using filler components can have beneficial effects (Ilyas et al. 2021a; Norizan et al. 2022; Rahman et al. 2022; Tarique et al. 2022a; Norraahim et al. 2022). The polymeric materials may be modified using this method of composite preparation based on the needs of the applications (Tarique et al. 2021a). However, at the end of their lifecycle, the material needs to be recycled as it can no longer function as at the beginning of its initial state. Depending on the kind of ingredient in the composite and the intended use of the recovered products, several alternative recycling processes have been developed and established to date for recycling old polymer composite materials.

In this point of view, the polymeric material can be broken down into recycled polymer blends, which can be fitted with suitable physical properties without compatibilization (Dorigato 2021). Considering that a large part of plastic waste is constituted by polyolefins (PO), particular attention should be given to recycled blends constituted by

polyethylene and polypropylene. In this case, recycling polymer constituents have good miscibility such as polypropylene with a low quantity of linear low-density polyethylene (LLDPE). Besides, the polymer blends should be commingled plastics having similar chemical structures, like recycled resins with virgin ones, LLDPE with low-density polyethylene (LDPE), and metallocene PO with Ziegler-Natta PO. Moreover, recycling blends with co-continuous morphology and having a concentration of the dispersed phase below 10 vol%. In the end, the application should be able to develop materials to be implemented only for aesthetic and nonstructural purposes.

Taufiq et al. (2017) studied the influence of processing temperature on the mechanical properties and morphology of a recycled PP/PE blend derived from rejected/unused disposable diapers. For this purpose, a PP/PE (70/30 wt%) combination was compounded at 180 °C using an internal mixer. In three different temperatures of 180, 190, and 200 °C, the compounds were then crushed and compression-molded. In this study, virgin PP and LLDPE were also taken into consideration for comparison. As the processing temperature increased from 180 to 200 °C, the stress at break of the recycled mix (r-PP/PE) decreased from 9.4 to 8.3 MPa. A similar impact was also observed in the virgin blend during the breakdown of polymer chains. Similarly, when the processing temperature increased, the elastic modulus of r-PP/PE fell from 285 to 226 MPa. Figure 1 shows the strain under maximum load for r-PP/PE and virgin (v-PP/PE) blends. It is noticeable that the strain increased from 3.3% to 17.2% as the temperature was raised from 180 to 200 °C. This benefit was credited to the higher compounding temperatures' ability to provide enhanced microstructural uniformity, as can be seen in the SEM micrographs shown in Fig. 2a, b.

Adam et al. (2017) investigated the mechanical characteristics of blends produced by combining the most significant polymers found in recovered printers. As a result, extrusion and injection molding were used to produce samples of high-impact polystyrene (HIPS) that were 90% PS, 10% ABS, and 100% HIPS. The mechanical characteristics of blends made by combining the most significant polymers found in recovered printers were studied. Hence, extrusion and injection molding were used to create samples of high-impact polystyrene (HIPS) that were 90%

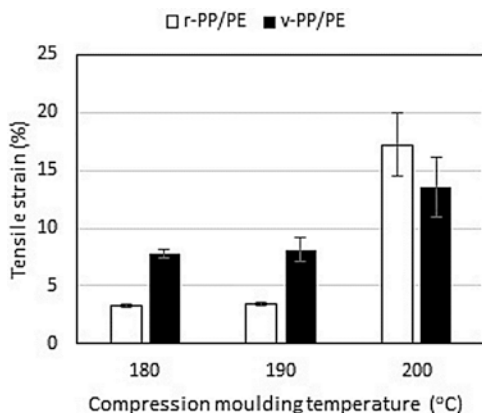


Fig. 1 Tensile strain of r-PP/PE and v-PP/PE blends at varied molding temperatures. (Reprinted from Ref. Taufiq et al. 2017)

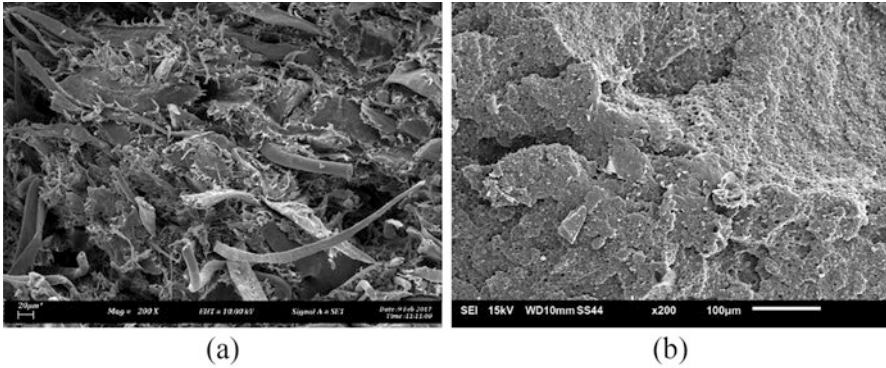


Fig. 2 SEM micrographs of r-PP/PE blend molded at (a) 180 °C and (b) 200 °C. (Reprinted from Ref. Taufiq et al. 2017)

Table 2 Tensile properties polymer blends restored from printers

Polymer blends configurations	Yield strength (MPa)	Strain at break (%)
HIPS-90%/ABS-10%	39	46.2
HIPS-90%/PS-10%	37.5	39.1
HIPS-100%	45.1	14.9

Adapted from Ref. Adam et al. (2017)

PS, 10% ABS, and 100% HIPS. The best blends were HIPS-90%/ABS-10%, which had a yield strength of 39.0 MPa and strain at break of 46.2%, and HIPS-90%/PS-10%, which had a σ_y value of 37.5 MPa and ϵ_b value of 39.1%. As stated in Table 2, the yield strength for the HIPS-100% sample was determined to be 45.1 MPa, and the elongation at break was 14.9%. In contrast to the formulation with HIPS, the strain at break values were much greater in the blends with PS, with a 24.2% improvement in the former over the latter. Due to the inclusion of an elastomeric component in the printers’ HIPS, the blends with HIPS had a σ_y value of 45.1 MPa, which varied by 3.7 MPa.

4.1 Recycling of Blends from Commingled Plastics

At present, due to the lack of globally applicable composite recycling operations, the recycling of waste plastics is now a fascinating field in the waste management industry. The three primary issues that constrain the recycling of polymers and polymer composites are maintaining the quality of recycled plastics, the expense of recycling, and the harm to the environment. The four acknowledged elements that have the greatest impact on the quality of the recirculates are cross-polymer contamination in the disposal site, additives applied to the polymer composites, non-polymer impurities, and deterioration of polymer composites over time. The causes

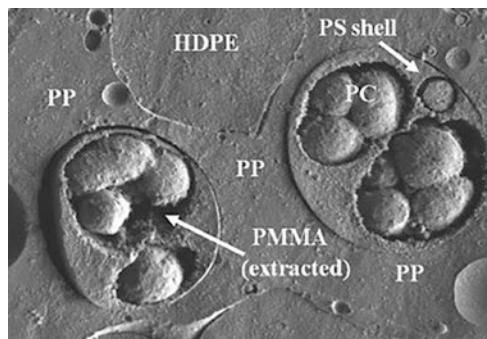


Fig. 3 SEM micrograph of combination HDPE/PP/PS/PMMA/PC after 30 min annealing with 20% EPDM. PMMA was selectively chiseled. (Reprinted from Ref. Le Corroller and Favis (2012), with the permission of John Wiley and Sons)

of the contamination may result from the postproduction stages of plastics directly using additives (binders, colors, and others) or through the phases of trash collection and management (Hopewell et al. 2020). Despite the fact that recycling has been the subject of much research, accurate statistics and data about the caliber of recycled plastics are still inadequate. This information is crucial for ensuring the possibility of recycling and enhancing the yield from recycling (Jose and Joseph 2012; Hopewell et al. 2020). It will help us better understand the pollutants that impact plastic recycling.

In general, the existence of many surfaces in immiscible polymer mixtures is the primary issue with recycling blends made up of commingled polymers. Le Corroller and Favis (2012) studied phase encapsulation and thermodynamically driven polymer segregation, both of which were used to concentrate a minor phase within one of the two major phases. If the HDPE/PP interface was suitably compatible, it was possible to determine encapsulated PS/PMMA/PC droplets within the PP matrix in a co-continuous mix of HDPE and PP, as seen in the SEM micrograph of Fig. 3. Thus, it was feasible to enhance the stiffness, tensile strength, and ductility of the resultant materials by utilizing the most appropriate processing settings.

Furthermore, it was discovered that the addition of two copolymers, specifically vinyl alcohol and anhydride, allowed blends with polar matrices such as PVC, PC, PMMA, thermoplastic polyurethane (TPU), polyamides, polyesters, SAN, or ABS to be made compatible. For instance, blends of TPU with EVAc, modified cellulose, and/or polyalkylene oxide have been found to have good physical, optical, and barrier properties and to process without degrading at the molten stage.

5 Recycling of Bioplastics-Based Blends

Plastics that are biodegradable and/or made from renewable resources are referred to as bioplastics. Examples of the most common bioplastics include poly(lactic acid) (PLA), polyhydroxyalkanoates (PHAs), poly(butylene succinate) (PBS), and

thermoplastic starch (TPS). By 2025, 2.89 Mt. of bioplastic would have reportedly been produced worldwide (Beltrán et al. 2021). Most commercial bioplastics such as PLA degrade slowly under ambient conditions, which may cause severe environmental pollution. Thus, the use of efficient management systems for bioplastic products must be achieved to enhance the sustainability of bioplastics. These bioplastics offer other methods for waste disposal, i.e., recycling that reduces the quantity of plastic waste in the environment. Recycling is one of the effective methods since it allows for the reduction of emissions, the carbon footprint, and the use of raw resources. The common recycling methods of bioplastics are mechanical and chemical recycling, where mechanical recycling was found as a favorable recycling method (Scaffaro et al. 2011).

5.1 Mechanical Recycling of Blends Containing Bioplastics

Mechanical recycling refers to the physical processing of waste. It is recognized as the primary method for recovering bioplastic since it is often less costly, needs relatively basic technology, and has a smaller environmental effect than chemical recycling. In general, mechanical recycling involves multiple phases, including waste collection, screening, and sorting. These phases include several processes such as grinding, washing, drying, compounding, extrusion, and granulation.

Using numerous extrusions and injections of a 50/50 wt% PLA/PS polymer blend, Hamad et al. (2011) mechanically recycled a hybrid PLA blend. The results revealed that stress and strain at blend break fell dramatically after two processing cycles, although Young's modulus was unaffected. It was recorded that after four processing cycles, Young's modulus showed the least reduction by 26%, the strain at break showed a higher reduction of 73%, and the stress at break showed the biggest change, i.e., 79%. The compounded PLA/PS mix had an apparent viscosity of 3100 Pa.s, and it became less viscous after each processing cycle due to the reduction of the molecular weights with the processing cycles.

In order to study the recycling of impact-modified PLA, Scaffaro et al. (2011) introduced two kinds of impact modifiers to PLA in different amounts. The mechanical characteristics were greatly enhanced by adding low concentrations of impact modifiers; however, it was discovered that frequent recycling significantly decreased the impact strength. This effect may have been caused by a change in crystallinity as a result of each processing step's reduced molecular weight, which caused the recycled materials stiffer, less deformable, and exhibit lower water absorption and impact resistance than the original material.

Chaitanya et al. (2019) investigated the impact of mechanical recycling on the thermal and mechanical behavior of PLA/sisal biocomposites, as well as the maximum number of recycles that are permitted within the acceptable behavioral range. Extrusion was used in this work to recycle the biocomposites eight times. Up until the third recycling, the tensile strength of injection-molded biocomposites decreased by 20.9%. The authors also reported a severe reduction in storage and loss of

modulus of PLA after the third recycle. Recycled biocomposites' morphological and thermal evaluation also showed that the fiber and matrix had degraded significantly. Hydrolysis was identified as one of the reasons for PLA degradation upon recycling by infrared spectroscopy. It is not advised to recycle PLA/sisal biocomposites more than three times.

Beltrán et al. (2020) studied the effect of thermal treatments of PLA residues on the structure and properties of recycled PLA. In this work, two different accelerated aging procedures were applied as shown in Fig. 1 to simulate residues with different levels of degradation. It was found that both polycondensation and degradation processes occurred during thermal treatments, and the net outcome was determined by the degradation level of the residue as well as the time and temperature of the treatment. The different aging processes and the reprocessing caused the PLA samples to degrade, which resulted in an increase in carboxyl end groups, a decrease in intrinsic viscosity, and a reduction in thermal stability. It was also discovered that thermal treatments of aged PLA promoted polycondensation reactions that led to the elimination of carboxyl end groups and increased the average molecular weight of the residue and significantly improved the mechanical and thermal characteristics of the recycled plastic. They also concluded that it is crucial to have proper process conditions, as the treatments also resulted in degradation reactions when excessive temperatures or long residence durations were applied. The degree of degradation of the aged plastic also affected the outcomes. Thermal treatments were insufficient to restore the structure and characteristics of the starting material when significantly degraded residues were taken into account. However, when the aged PLA was only slightly degraded, thermal treatment at 110 °C for 8 h resulted in the partial recovery of the initial intrinsic viscosity and the production of recycled materials with structure, thermal stability, hardness, and thermal behavior that are very similar to those of virgin plastic. These findings imply that thermal treatments are a simple, inexpensive, and ecologically beneficial way to increase PLA's recyclable content and, hence, reduce the environmental impact of this material (Fig. 4).

In the next study, Beltrán et al. (2021) studied the effect of the addition of two organic fillers namely chitosan and silk fibroin nanoparticles during the recycling process of PLA for improving the properties of the recycled plastic for packaging application. After being exposed to two distinct aging protocols, the initial granulated PLA was melted and reprocessed with either chitosan with low and high molecular weights or silk fibroin nanoparticles that were made using two separate ways. The varied aging protocols combined with the degradation that occurred during the melt reprocessing caused the recycled polymer to lose intrinsic viscosity, Vickers hardness, thermal stability, and increased permeability. It was noted that the performance of recycled plastics is influenced by the type and volume of filler, as well as the degree of degradation of the aged polymer. When high molecular weight chitosan and fibroin were added to recycled PLA made from degraded PLA, the polymer was somewhat degraded, but when recycled PLA was made from highly hydrolyzed plastic, the inherent viscosity improved with all of the fillers. Despite PLA's degradation, chitosan and, to a lesser extent, silk fibroin nanoparticles demonstrated a reinforcing impact on mechanically recycled PLA.

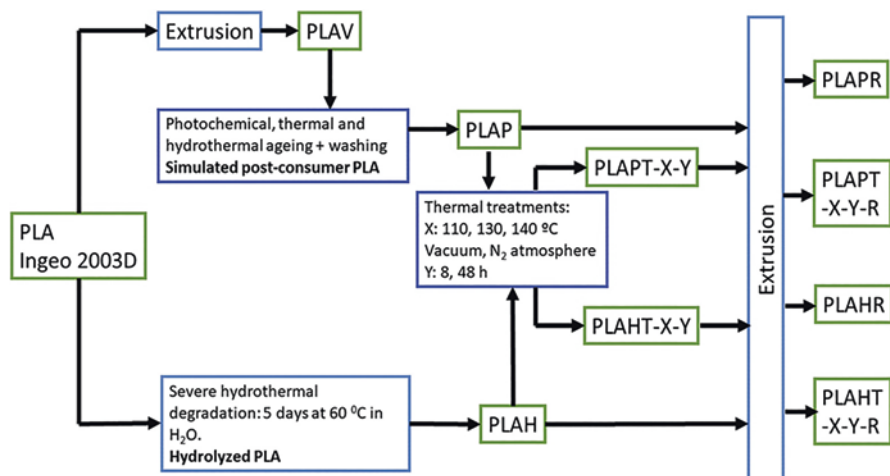


Fig. 4 Mechanical recycling process and thermal treatments of PLA. (Beltrán et al. 2020)

5.2 Chemical Recycling of Blends Containing Bioplastics

Chemical recycling involves turning waste materials into valuable chemicals such as monomers and oligomers, which may then be reintroduced into the polymer value chain and used for polymerization. As mechanical recycling is typically accompanied by degraded plastic properties, chemical recycling was found as an alternative way to recycle bioplastic into alternative feedstocks for monomers and intermediate products (Niaounakis 2019). Chemical recycling techniques include cracking, gasification, and chemolysis or solvolysis (Piemonte et al. 2013; Morici et al. 2022).

Tsuneizumi et al. (2010) explored two methods for the selective chemical recycling of PLLA/PE and PLLA/PBS blends. The first method used the chemical recycling of PLLA after the direct separation of PLLA and PE from the PLLA/PE blend based on their solubility in toluene. The lactic acid oligomer was created by the second approach, which involved the selective breakdown of PLLA in a PLLA/PE blend. In another work, according to a study by La Mantia et al. (2012), low levels of PLA in PET waste can have a big impact on how the material behaves under non-isothermal elongational flow. Thermal stability was not severely impacted; however, the mechanical qualities were only notably impacted under certain conditions. Feng et al. (2018) produced a low molecular weight PLA (L-PLA) with different hydroxyl and carboxyl end-groups via direct polycondensation of L-lactic acid using stannous benzoate ($\text{Sn}(\text{ArCOO})_2$) as a catalyst at high temperature and high vacuum. It was recorded that under the catalysis of Sn, the pyrolysis of PLA resulted in the selective production of lactide, and with different end-groups for PLA, the activation energy of the pyrolysis process differed. Wang et al. (2020) used 1,3-dimethylimidazolium-2-carboxylate as an organocatalyst for the glycolysis of waste PET. It

was recorded that PET was entirely depolymerized in less than an hour at 180 °C, with up to 60% of BHET was recovered by precipitation after chilling the reaction fluid. The 1,3-dimethylimidazolium acetate performed substantially worse as a catalyst under similar circumstances, indicating that catalysis was accomplished through the production of a nucleophilic N-heterocyclic carbene.

A catalytic thermal degradation method was studied by Ariffin et al. (2010) on the highly selective transformation of poly[(*R*)-3-hydroxybutyric acid] (PHB) into trans-crotonic acid during pyrolysis. In this study, the presence of Mg compounds, MgO and Mg(OH)₂, as catalysts were investigated. It was suggested that the Mg catalysts were functioning throughout the initial and primary processes, stimulating the entirety of the elimination reactions, resulting in a decrease in the degradation temperature and a fully selective transformation of PHB. Fukushima et al. (2013) reported the aminolysis process, specifically organocatalysis of the aminolytic depolymerization of waste PET using 1,5,7-triazabicyclo[4.4.0]dec-5-ene (TBD), producing a broad range of crystalline terephthalamides. Due to the terephthalic moiety and amide hydrogen bonding, this varied group of monomers has enormous promise as building blocks for high-performance materials, with acceptable thermal and mechanical characteristics.

6 Conclusions

It is currently projected that 90% of plastic products are utilized once and then disposed of. However, because of the prohibitive costs of collection and a lack of the necessary infrastructure, almost 50% of the plastic was wasted after only one use. By 2050, landfills and the natural environment are predicted to accumulate 12 billion tons of plastic trash. In addition, the COVID-19 outbreak has greatly increased the usage of personal protective equipment, disposable dinnerware, and plastic-wrapped food, which could lead to a new environmental crisis. Polyethylene terephthalate (PET), polyethylene (PE), polypropylene (PP), polyvinyl chloride (PVC), and polystyrene (PS) are only a few of the polymers that make up plastic debris in general. According to a recent study, in order to stop the trend of rising environmental plastic pollution, a concerted worldwide effort to minimize plastic waste in every stage of the plastic lifecycle is required. Thus, rapid global cooperation is essential to decrease plastic pollution. Recycling plastic trash is also anticipated to be an effective countermeasure to the creation of ecological plastic pollution, e.g., marine pollution. There are three most common plastic recycling processes such as chemical, mechanical, and biological recycling. Chemical recycling, also known as tertiary recycling [20], could be accomplished using solvolysis, pyrolysis, or gasification, as described in American Society for Testing and Materials' (ASTM) D5033 standard. Chemical recycling is more popular than mechanical and biological recycling because of the mechanism that turns plastic waste into highly valuable chemical feedstocks, fuel, and monomer. However, mechanical recycling, such as milling, washing, and pelletizing, is currently the most widely used technology for

the large-scale recycling of plastic solid waste. However, this method produces a lot of untreated wastewater, which may contain significant amounts of microplastics and endanger aquatic ecosystems. The sorting, shredding, cleaning, and melting steps during the recycling procedure also require a significant amount of labor and electricity expenditures. The biological recycling of plastic waste is accomplished through the extraction of enzymes or the culture of microorganisms. So far, by using this technique, only plastics having hydrolyzable ester or amide linkages in the foremost chain can currently be converted to oligomers or monomers. The common recycling methods of bioplastics are mechanical and chemical, where mechanical recycling was found as a favorable recycling method.

Acknowledgments The authors would like to express their gratitude for the financial support received from the Universiti Teknologi Malaysia for the project, “The impact of Malaysian bamboos’ chemical and fibre characteristics on their pulp and paper properties,” grant number PY/2022/02318–Q.J130000.3851.21H99. The research has been carried out under the program, Research Excellence Consortium (JPT (BPKI) 1000/016/018/25 (57)), provided by the Ministry of Higher Education (MOHE) Malaysia.

References

- Adam AP, Gonçalves JVRV, Robinson LC et al (2017) Recycling and mechanical characterization of polymer blends present in printers. *Mat Res* 20:202–208
- Adelodun AA (2021) Plastic recovery and utilization: from ocean pollution to green economy. *Front Environ Sci* 9:683403
- Ariffin H, Nishida H, Shirai Y, Hassan MA (2010) Highly selective transformation of poly[(R)-3-hydroxybutyric acid] into trans-crotonic acid by catalytic thermal degradation. *Polym Degrad Stab* 95:1375–1381. <https://doi.org/10.1016/j.polymdegradstab.2010.01.018>
- Asyraf MRM, Rafidah M (2022) Mechanical and thermal performance of sugar palm fibre thermo-set polymer composites: a short review. *J Nat Fibre Polym Compos* 1:2
- Asyraf MRM, Khan T, Syamsir A, Supian ABM (2022a) Synthetic and natural fiber-reinforced polymer matrix composites for advanced applications. *Materials (Basel)* 15:6030
- Asyraf MRM, Syamsir A, Supian ABM et al (2022b) Sugar palm fibre-reinforced polymer composites: influence of chemical treatments on its mechanical properties. *Materials (Basel)* 15. <https://doi.org/10.3390/ma15113852>
- Asyraf MRM, Syamsir A, Zahari NM et al (2022c) Product development of natural fibre-composites for various applications: design for sustainability. *Polymers (Basel)* 14:920. <https://doi.org/10.3390/polym14050920>
- Asyraf MZ, Suriani MJ, Ruzaidi CM et al (2022d) Development of natural fibre-reinforced polymer composites ballistic helmet using concurrent engineering approach: a brief review. *Sustainability* 14:7092
- Beltrán FR, Climent-Pascual E, de la Orden MU, Martínez Urreaga J (2020) Effect of solid-state polymerization on the structure and properties of mechanically recycled poly(lactic acid). *Polym Degrad Stab* 171. <https://doi.org/10.1016/j.polymdegradstab.2019.109045>
- Beltrán FR, Gaspar G, Dadras Chomachayi M et al (2021) Influence of addition of organic fillers on the properties of mechanically recycled PLA. *Environ Sci Pollut Res* 28:24291–24304. <https://doi.org/10.1007/s11356-020-08025-7>
- Borrelle SB, Ringma J, Law KL et al (2020) Predicted growth in plastic waste exceeds efforts to mitigate plastic pollution. *Science* 369:1515–1518

- Boucher J, Friot D (2017) Primary microplastics in the oceans: a global evaluation of sources. Iucn Gland, Gland
- Cai H, Yu J, Qiu Z (2012) Miscibility and crystallization of biodegradable poly (3-hydroxybutyrate-co-3-hydroxyhexanoate)/poly (vinyl phenol) blends. *Polym Eng Sci* 52:233–241
- Chaitanya S, Singh I, Song J II (2019) Recyclability analysis of PLA/Sisal fiber biocomposites. *Compos. Part B Eng* 173:106895. <https://doi.org/10.1016/j.compositesb.2019.05.106>
- Chen S, Liu Z, Jiang S, Hou H (2020) Carbonization: a feasible route for reutilization of plastic wastes. *Sci Total Environ* 710:136250
- Chen Y, Awasthi AK, Wei F et al (2021) Single-use plastics: production, usage, disposal, and adverse impacts. *Sci Total Environ* 752:141772
- De-la-Torre GE, Dioses-Salinas DC, Pizarro-Ortega CI, Saldaña-Serrano M (2020) Global distribution of two polystyrene-derived contaminants in the marine environment: a review. *Mar Pollut Bull* 161:111729
- Dorigato A (2021) Recycling of polymer blends. *Adv Ind Eng Polym Res* 4:53–69
- Feng L, Feng S, Bian X et al (2018) Pyrolysis mechanism of poly(lactic acid) for giving lactide under the catalysis of tin. *Polym Degrad Stab* 157:212–223. <https://doi.org/10.1016/j.polymdegradstab.2018.10.008>
- Fukushima K, Lecuyer JM, Wei DS et al (2013) Advanced chemical recycling of poly(ethylene terephthalate) through organocatalytic aminolysis. *Polym Chem* 4:1610–1616. <https://doi.org/10.1039/c2py20793a>
- Garcia JM, Robertson ML (2017) The future of plastics recycling. *Science* 358:870–872
- Hamad K, Kaseem M, Deri F (2011) Effect of recycling on rheological and mechanical properties of poly(lactic acid)/polystyrene polymer blend. *J Mater Sci* 46:3013–3019. <https://doi.org/10.1007/s10853-010-5179-8>
- He P, Chen L, Shao L et al (2019) Municipal solid waste (MSW) landfill: a source of microplastics?—Evidence of microplastics in landfill leachate. *Water Res* 159:38–45
- Hinüber C, Häußler L, Vogel R et al (2011) Hollow fibers made from a poly (3-hydroxybutyrate)/poly-ε-caprolactone blend. *Express Polym Lett* 5:643–652
- Hopewell J, Dvorak R, Kosior E (2020) Plastics recycling: challenges and opportunities. *Philosophical Transactions of the Royal Society B: Biological Sciences* 364: 2115–2126.
- Hwang J, Choi D, Han S et al (2019) An assessment of the toxicity of polypropylene microplastics in human derived cells. *Sci Total Environ* 684:657–669
- Ilyas RA, Sapuan SM, Asyraf MRM et al (2020) Introduction to biofiller-reinforced degradable polymer composites. In: Jumaidin R, Sapuan SM, Ismail H (eds) *Biofiller-reinforced biodegradable polymer composites*, 1st edn. CRC Press, Boca Raton, pp 1–23
- Ilyas RA, Azmi A, Nurazzi NM et al (2021a) Oxygen permeability properties of nanocellulose reinforced biopolymer nanocomposites. *Mater Today Proc.* <https://doi.org/10.1016/j.matpr.2021.10.420>
- Ilyas RA, Sapuan SM, Asyraf MRM et al (2021b) Polymer composites filled with metal derivatives: a review of flame retardants. *Polymers (Basel)* 13:1701. <https://doi.org/10.3390/polym13111701>
- Ilyas RA, Zuhri MYM, Norraahim MNF et al (2022) Natural fiber-reinforced polycaprolactone green and hybrid biocomposites for various advanced applications. *Polymers (Basel)* 14:182. <https://doi.org/10.3390/polym14010182>
- Jambeck JR, Geyer R, Wilcox C et al (2015) Plastic waste inputs from land into the ocean. *Science* 347:768–771
- Jiang J, Shi K, Zhang X et al (2022) From plastic waste to wealth using chemical recycling: a review. *J Environ Chem Eng* 10:106867. <https://doi.org/10.1016/j.jece.2021.106867>
- Jose JP, Joseph K (2012) Advances in polymer composites: macro-and microcomposites—state of the art, new challenges, and opportunities. *Polym Compos* 1:1–16
- Kedzierski M, Frère D, Le Maguer G, Bruzard S (2020) Why is there plastic packaging in the natural environment? Understanding the roots of our individual plastic waste management behaviours. *Sci Total Environ* 740:139985

- Klemeš JJ, Van FY, Jiang P (2021) Plastics: friends or foes? The circularity and plastic waste footprint. *Energy Sources Part A Recover Util Environ Eff* 43:1549–1565
- Koshti R, Mehta L, Samarth N (2018) Biological recycling of polyethylene terephthalate: a mini-review. *J Polym Environ* 26:3520–3529
- La Mantia FP, Botta L, Morreale M, Scaffaro R (2012) Effect of small amounts of poly(lactic acid) on the recycling of poly(ethylene terephthalate) bottles. *Polym Degrad Stab* 97:21–24. <https://doi.org/10.1016/j.polyimdegradstab.2011.10.017>
- Lau WWY, Shiran Y, Bailey RM et al (2020) Evaluating scenarios toward zero plastic pollution. *Science* 369:1455–1461
- Le Corroller P, Favis BD (2012) Droplet-in-droplet polymer blend microstructures: a potential route toward the recycling of co-mingled plastics. *Macromol Chem Phys* 213:2062–2074
- MacArthur E (2017) Beyond plastic waste. *Science* 358:843
- Martínez Narro G, Pozos Vázquez C, Mercado González MO (2019) Viscosity reduction of heavy crude oil by dilution with hydrocarbons obtained via chemical recycling of plastic wastes. *Pet Sci Technol* 37:1347–1354
- Morici E, Carroccio SC, Bruno E et al (2022) Recycled (bio)plastics and (bio)plastic composites: a trade opportunity in a green future. *Polymers (Basel)* 14:1–24. <https://doi.org/10.3390/polym14102038>
- Niaounakis M (2019) Recycling of biopolymers – the patent perspective. *Eur Polym J* 114:464–475. <https://doi.org/10.1016/j.eurpolymj.2019.02.027>
- Norizan MN, Shazleen SS, Alias AH et al (2022) Nanocellulose-based nanocomposites for sustainable applications: a review. *Nanomaterials* 12. <https://doi.org/10.3390/nano12193483>
- Norrahim MNF, Knight VF, Nurazzi NM et al (2022) The frontiers of functionalized nanocellulose-based composites and their application as chemical sensors. *Polymers (Basel)* 14:4461. <https://doi.org/10.3390/polym14204461>
- Piemonte V, Sabatini S, Gironi F (2013) Chemical recycling of PLA: a great opportunity towards the sustainable development? *J Polym Environ* 21:640–647. <https://doi.org/10.1007/s10924-013-0608-9>
- Rahman I, Singh P, Dev N et al (2022) Improvements in the engineering properties of cementitious composites using nano-sized cement and nano-sized additives. *Materials (Basel)* 15:8066
- Ryberg MW, Laurent A, Hauschild M (2018) Mapping of global plastics value chain and plastics losses to the environment: with a particular focus on marine environment
- Scaffaro R, Morreale M, Mirabella F, La Mantia FP (2011) Preparation and recycling of plasticized PLA. *Macromol Mater Eng* 296:141–150. <https://doi.org/10.1002/mame.201000221>
- Sharuddin SDA, Abnisa F, Daud WMAW, Aroua MK (2016) A review on pyrolysis of plastic wastes. *Energy Convers Manag* 115:308–326
- Tarique J, Sapuan SM, Khalina A et al (2021a) Recent developments in sustainable arrowroot (*Maranta arundinacea* Linn) starch biopolymers, fibres, biopolymer composites and their potential industrial applications: a review. *J Mater Res Technol* 13:1191–1219. <https://doi.org/10.1016/j.jmrt.2021.05.047>
- Tarique J, Sapuan SM, Khalina A (2021b) Effect of glycerol plasticizer loading on the physical, mechanical, thermal, and barrier properties of arrowroot (*Maranta arundinacea*) starch biopolymers. *Sci Rep* 11:1–17
- Tarique J, Sapuan SM, Khalina A (2021c) Extraction and characterization of a novel natural lignocellulosic (Bagasse and Husk) fibers from arrowroot (*Maranta Arundinacea*). *J Nat Fibers*:1–17. <https://doi.org/10.1080/15440478.2021.1993418>
- Tarique J, Sapuan SM, Khalina A et al (2022a) Thermal, flammability, and antimicrobial properties of arrowroot (*Maranta arundinacea*) fiber reinforced arrowroot starch biopolymer composites for food packaging applications. *Int J Biol Macromol*. <https://doi.org/10.1016/J.IJBIOMAC.2022.05.104>
- Tarique J, Zainudin ES, Sapuan SM et al (2022b) Physical, mechanical, and morphological performances of arrowroot (*Maranta arundinacea*) fiber reinforced arrowroot starch biopolymer composites. *Polymers (Basel)* 14:388. <https://doi.org/10.3390/polym14030388>

- Taufiq MJ, Mustafa Z, Mansor MR (2017) Utilisation of recycled thermoplastics sourced from rejected-unused disposable diapers as polymer blends. *J Mech Eng Sci* 11:3137–3143
- Tsuneizumi Y, Kuwahara M, Okamoto K, Matsumura S (2010) Chemical recycling of poly(lactic acid)-based polymer blends using environmentally benign catalysts. *Polym Degrad Stab* 95:1387–1393. <https://doi.org/10.1016/j.polyimdegradstab.2010.01.019>
- Vanapalli KR, Sharma HB, Ranjan VP et al (2021) Challenges and strategies for effective plastic waste management during and post COVID-19 pandemic. *Sci Total Environ* 750:141514
- Wang L, Nelson GA, Toland J, Holbrey JD (2020) Glycolysis of PET using 1,3-dimethylimidazolium-2-carboxylate as an organocatalyst. *ACS Sustain Chem Eng* 8:13362–13368. <https://doi.org/10.1021/acssuschemeng.0c04108>
- Wei R, Tiso T, Bertling J et al (2020) Possibilities and limitations of biotechnological plastic degradation and recycling. *Nat Catal* 3:867–871
- Yang J, Liu MK, Zhang B et al (2011) Intrinsic fluorescence studies of compatibility in thermoplastic phenol formaldehyde resin/poly (ϵ -caprolactone) blends. *Express Polym Lett* 5(8):698–707
- Yang L, Gao J, Liu Y et al (2021) Biodegradation of expanded polystyrene and low-density polyethylene foams in larvae of *Tenebrio molitor* Linnaeus (Coleoptera: Tenebrionidae): broad versus limited extent depolymerization and microbe-dependence versus independence. *Chemosphere* 262:127818
- Yong CQY, Valiyaveetil S, Tang BL (2020) Toxicity of microplastics and nanoplastics in mammalian systems. *Int J Environ Res Public Health* 17:1509
- Yu L, Dean K, Li L (2006) Polymer blends and composites from renewable resources. *Prog Polym Sci* 31:576–602. <https://doi.org/10.1016/j.progpolymsci.2006.03.002>
- (2018). The future of plastic. *Nat Commun* 9:2157. <https://doi.org/10.1038/s41467-018-04565-2>

Recycling of Polymeric Membranes



Maicon Sérgio Nascimento dos Santos, João Henrique Cabral Wancura, Carolina Elisa Demaman Oro, Rogério Marcos Dallago, Giovani Leone Zobot, and Marcus Vinícius Tres

1 Introduction

The membrane separation process (MSP) approach has been extensively applied in a range of industries, expressly in food-related (Argenta and Scheer 2020; Castro-Muñoz et al. 2021), beverages (Conidi et al. 2020; Junior et al. 2021), effluents treatment (Hube et al. 2020), biomedical and pharmaceutical (Sharma et al. 2021; Boateng et al. 2021), biofuel production (Gojun et al. 2021) sectors, among others. Consequently, the intensification in the scale-up of treatment with membranes and the interest in technologies aimed at separation processes observed in recent years have resulted in an effective procedure with great advances in energy and sustainable context (Shao 2020). Nonetheless, this scenario could become a serious obstacle, as the rate at which large amounts of membrane masses have been discarded annually, which results in dramatic problems for human health and the environment (Potrich et al. 2020).

Currently, intense exploitation of polymer-based membranes in the industrial consumer market has been noticed, mainly due to their reduced footprint, practicality, economic viability, and production proportions (Yadav et al. 2021). The implementation of the MSP has been favorably applicable as a remedial strategy for a range of contaminants in a system (Rabajczyk et al. 2021). However, the growth

M. S. N. dos Santos · G. L. Zobot · M. V. Tres (✉)
Laboratory of Agroindustrial Processes Engineering (LAPE),
Federal University of Santa Maria (UFSM), Cachoeira do Sul, RS, Brazil
e-mail: marcus.tres@ufsm.br

J. H. C. Wancura
Laboratory of Biomass and Biofuels (L2B), Federal University of Santa Maria (UFSM),
Santa Maria, RS, Brazil

C. E. D. Oro · R. M. Dallago
Department of Food Engineering, URI Erechim, Erechim, RS, Brazil

of waste production from MSP processes and the directing of membranes and polymers to landfills without proper treatment have been widely discussed topics regarding the maintenance of the environment and human health. Appropriately, the disposal of membranes and waste in landfills is a serious economic dilemma that threatens the circular economy and leads to immediate conflicts with sustainable and recycling purposes (Landaburu-Aguirre et al. 2016; Contreras-Martínez et al. 2021). Estimates report that just considering reverse osmosis (RO) membranes, more than 840,000 modules are discarded annually (Lejarazu-Larrañaga et al. 2020).

Commonly, membranes have a significantly restricted life cycle. Even with advances in expanding the useful life of these materials, the manipulation interval of membranes is normally up to 7 years (De Paula et al. 2017). This particularity is a result of the effects of severe operations of these materials, causing critical fouling and deterioration and limiting their use in subsequent applications (Zhang et al. 2021a, b). The fouling intensity is caused by external conditions during the performance and by alterations in the composition of the membrane under conditions of physicochemical deterioration, drastically affecting the transfer of solute and solvent via membrane (Landaburu-Aguirre et al. 2016). Besides, energy demand and lucrative attributes, permeation performance, product characterization, and remaining treatment are remarkable impediments to provide or limit the membrane recycling potentiality (Warsinger et al. 2018).

Consequently, the inappropriate disposal of these materials in abundance causes serious impacts, highlighting the growing demand for strategies and alternatives that aim to minimize disposal in environments and perpetuate the conservation of these locations (De Paula et al. 2017). Furthermore, studies suggest that important measures must be adopted not only in the procedure for extracting and separating components but also in the recycling of membranes and remaining treatment (Landaburu-Aguirre et al. 2016). Membrane recycling involves three direct steps: (1) rejuvenation (minimization of fouling intensity), (2) minor treatment procedures, and (3) subsequent implementation (Moradi et al. 2019). Exploiting the recycling of these materials makes the process economically viable and a practicable strategy for environmental perspectives (Ahmed and Jamal 2021).

Additionally, the performance of the number of scientific studies aimed at polymeric membrane reuse, in industrial and scientific approaches, is an important tool to verify the expansion of the subject. Polymeric membrane recycling has been extensively investigated in the last years as an innovative alternative with economic and energetic advantages. Accordingly, basic research to verify the volume of scientific publications from 2010 to 2020 was encouraged in the Scopus® scientific platform. To perform the range of data demanded, the following keywords were used: *polymeric/membrane/recycling* (Fig. 1).

According to the application of the polymeric membrane recycling dynamics, the academic performance observed in Fig. 1 shows the improvement of this subject over the years. As reported by the Scopus® database, 17 manuscripts were published in 2017, almost three times the number of studies published in 2010. Even though the period from 2018 to 2020 presented an insignificant reduction compared to 2017, considering the entire temporal range, the scenario of polymeric membrane

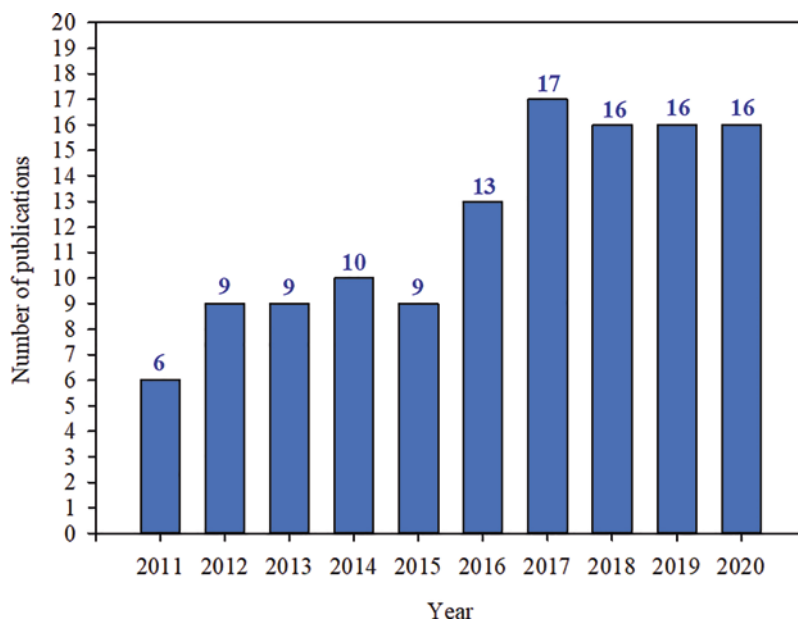


Fig. 1 Global number of scientific studies on the polymeric membranes recycling dynamics subject in a temporal range from 2010 to 2020 according to the Scopus® database platform with *polymeric/membrane/reuse* keywords

recycling is optimistic and several studies have been encouraged for practical applications in the next years.

Therefore, the aim of this review was to clarify the dynamics of recycling polymeric membranes under reuse perspectives in various industrial segments. Particularly, the main polymeric components of the membranes and the recycling processes were investigated, mainly with the impact of portraying environmental-friendly alternatives that identify the advances regarding the application of these materials in the MSP processes. The significant preference for using MSP as a separation tool in different industrial fields revealed the consequences of degradation processes in the life cycle of polymer-based membranes, which has been a target for prospecting reuse strategies and technologies. The effects and impacts verified globally reappear as a key point for the adoption of innovative actions that promote a stable balance between membrane production and the environment.

2 Main Polymers Used in Membrane Manufacturing

The main polymers used in membrane technology are polysulfone (PSU), polyethersulfone (PES), polyacrylonitrile (PAN), polyamide (PA), polyethylene (PE), polypropylene (PP), cellulose acetate (CA), polyvinylimidazole (PVIM),

poly(vinylidenedifluoride) (PVDF), poly(tetrafluoroethylene) (PTFE), polydimethylsiloxane (PDMS), polycarbonate (PC), and poly(ethyleneterephthalate) (PET) (Khaki et al. 2021; Yang et al. 2021; Nunes et al. 2020). In addition to the choice of polymer, the success of the MSP depends on the application and the level of resistance required for the process. Furthermore, different polymers can be used because of the membrane manufacturing method.

Overall, the main used polymers from 2015 to 2020 were cellulose acetate derivatives, polyimides, polyethers, and polynorbornenes (Deng et al. 2021). Furthermore, combinations of polymers, such as blends of polyethersulfone and polyvinylpyrrolidone (PVP) or polyethersulfone and modified polyethersulfone, are known and applied industrially.

Additionally, conjugated polymers have been studied due to their excellent chemical and physical properties. Conjugated polymers have π -bond and include polyaniline (PANI), polypyrrole (PPy), polythiophene (PT), polyacetylene, poly(*p*-phenylene), poly(phenylene vinylene), and their other derivatives (Saini et al. 2021).

The manufacture of polymeric membranes can employ the base polymers or a mixture of other compounds to achieve the desired properties for the process. Accordingly, polymer inclusion membranes (PIMs) are considered environmentally friendly and consist of a polymer, plasticizer, and carrier base, usually in a ratio of 40:40:20 (w/w) (Keskin et al. 2021). The most used base polymers are polyvinyl chloride (PVC), polyvinylidene difluoride (PVDF), and polyvinylidene fluoride-*co*-hexafluoropropylene (PVDF-HFP); cellulose triacetate (CTA), cellulose acetate propionate (CAP), cellulose tribenzoate (CTB), and cellulose acetate butyrate (CAB); polybutylene adipate-*co*-terephthalate (PBAT), polyacrylonitrile (PAN), polytetrafluoroethylene (PTFE), polyethersulfone (PES), and polypropylene (PP) (Zhang et al. 2021a, b; Keskin et al. 2021).

Notably, the choice of the polymer depends on the desirable characteristics of the membrane and the method of manufacture. The chemical and physical characteristics of the membranes are important elements to guide the success of the process and their shelf-life.

3 Application of MSP

The MSP has become an interesting alternative to produce significant quality products. Its application allowed reaching regulatory standards in diverse types of manufacture, due to their higher removal rate of low molecular weights organic pollutants, reducing risks associated with the source and its contaminants as well as its modularity and capacity to engage with other systems. This section presents promising areas where MSP has been applied.

3.1 Water Purification

The majority of applications of processes that use membranes are related to water treatment, whether wastewater containing some specific type of contaminant from an industrial sector or as a step of purification to obtain potable water (Warsinger et al. 2018). Access to potable water is a challenge for many regions of the planet, and developing a feasible process is fundamental (Yusuf et al. 2020). Accordingly, Fan et al. (2020) investigated the operating parameters of a combined dual-membrane (ultra- and nanofiltration) process for brackish water treatment and its application performance in a municipal drinking water treatment plant. Results presented by Fan et al. (2020) showed that ultrafiltration guaranteed the inlet water quality of nanofiltration, and nanofiltration could efficiently reject salts and organics, with a chloride removal of over 95%.

Furthermore, Chakraborty et al. (2021) reported the production of two Janus-type bilayer polymer membranes using polyvinylidene fluoride, Nylon 6,10, and cotton fabric. Janus membranes are a unique class of polymers having divergent hydrophilic and hydrophobic properties on both sides of their interface. The fabrication technique of the membranes (doctor blading method) is simple and scalable. The water contact angle measured by the authors confirmed hydrophobic and hydrophilic natures. Furthermore, porosity (gravimetric) and equilibrium water content measurements confirmed that the Janus membranes have good water permeability and porosity for oil–water separation and application for water purification.

3.2 Beverages

In beverage industries, membranes are typically applied for clarification (wine, beer, and juices industries), sterilization (wine, beer, and milk industries), removing bacteria and spores without chemical and color-changing, dealcoholization (beer and wine), concentration, and compound extraction (Jain and De 2019; Peyravi et al. 2020; Reis et al. 2019). Accordingly, Luo et al. (2016) developed an integrated membrane process consisting of a tubular ultrafiltration and nanofiltration system to refine crude sugarcane juice at a pilot plant scale. With a volume reduction ratio of 20, the authors reported that the membrane system was able to operate at a rate of 70 L/m²/h, with a color removal kept more than 95% and a sucrose recovery of up to 98% in the two-stage system.

3.3 Biofuels

Another interesting application of the MSP is the environmental-friendly purification of biofuels. The technique is an alternative to conventional biodiesel washing, achieving high purified biodiesel, and is feasible from an economic perspective

(Alves et al. 2013; Biniiaz et al. 2021). The membrane technique was investigated to dehydrate bioethanol as an option to the distillation, which demands high taxes of energy (Khalid et al. 2019). Tajziehchi and Sadrameli (2021) used statistical design to evaluate the process parameters (temperature, transmembrane pressure, and water addition) for crude biodiesel purification through ultrafiltration. The authors observed the simultaneous reduction of impurities, such as free glycerol, diglyceride, and triglyceride, to the limits imposed by international standards at 30 °C and pressures lower than 2 bar, with a permeated flux of 20 kg/m²/h.

3.4 Medical

In (bio)medical applications, most of the membranes are cellulose-based or synthetic polymer membranes. Considering the application of membranes for medical purposes, hemodialysis is the most dominant therapeutic application, followed by blood oxygenation procedures and filters for infusion solutions (Jose et al. 2018). Besides, membranes can be applied for blood purification, filtration for removal of molecular fractions of specific components, liver dialysis, artificial pancreas, therapeutic apheresis, and drug delivery systems (Bai et al. 2021; Fissell et al. 2007; Woźniak-Budych 2021).

4 Degradative Processes

The shelf-life of most polymeric membranes for common uses, such as water desalination and juice filtration, is 5–10 years (Bandara et al. 2019). Polymeric membranes have porous structures (micro- and nanopore), which can suffer damage and rupture due to deformations and crack propagation that significantly interferes with shelf-life (Kodaira et al. 2021). This damage can be mechanical or chemical and lead to membrane degradation. Mechanical degradation is easily avoided by adding one more layer of polymer to the membrane or additives. However, chemical degradation is not well understood and can be accelerated by operational parameters such as temperature and pressure (Futter et al. 2019). Moreover, sodium, lithium, calcium, copper, nickel, and iron (III) ions are considered ions that contribute to membrane degradation (Khatib et al. 2019).

Furthermore, thinning of membranes, poisoning of metals, degradation due to thermal effect, bipolar plate, degradation of the flow plate (embrittlement), and flow plate are important causes of chemical degradation in polymer electrolyte membranes (Khatib et al. 2019). The authors also reported that stresses, compression, and nonuniform compression are also correlated with membrane crack and consequent degradation.

Shelf-life studies under different experimental conditions and with different membranes are important and must be conducted whenever there is a new process

or process change. For example, Le Petit et al. (2021) showed that the new biocide was validated for reverse osmosis (RO) polyamide membrane but should be avoided in hydrophobic ultrafiltration polyethersulfone (PES)/polyvinylpyrrolidone (PVP) membrane.

As an example of new processes, fuel cells are one of the applications of polymeric membranes, which are characterized by ion exchange and have a flat-sheet configuration (Nunes et al. 2020). Thus, polymer electrolyte membrane fuel cells (PEMFCs) are a new technology that aims to replace internal combustion engines and thus reduces carbon emissions (Whiteley et al. 2020). Appropriately, the study conducted by Vassiliev et al. (2019) presented one of the first shelf-life studies of PEMFCs based on phosphoric acid doped polybenzimidazole membranes with a direct dimethyl ether anode. The authors reported membrane degradation for more than 200 h at temperatures of 160 and 200 °C, which was explained by the mechanisms of increased polarization resistance and specific area. In the same context of studying the shelf-life of membranes, Bandara et al. (2019) showed that chitosan (CS)–polyethyleneimine (PEI)–graphene oxide (GO) nanocomposite membrane coating is able to remove suspended particles, bacteria, and heavy metals effectively of samples of wastewater and seawater with different pH values, salinity, and total hardness in accelerated shelf-life experiments around 9–12 months.

5 Technologies Applied to the Recycling of Membranes

The basic principle of most membranes is the selection of specific components through pores of different dimensions. The MSP involves the characteristics of the contaminant, and especially the membranes such as material composition, pore size, and driving force (Warsinger et al. 2018). One of the biggest challenges for membrane-based treatments in different industrial segments is membrane fouling. The advancement of fouling is a result of the accumulation of organic, inorganic, biological, and colloidal materials on the membrane surface (Alkhatib et al. 2021). The degradation caused by the agglomeration of these substances in the active layer of the membrane acts directly on the performance of the separation process, inducing drastic modifications in the permeability and selectivity of the product (Khaless et al. 2021). Appropriately, the scarcity of the adoption of processes aimed at eliminating fouling and periodic membrane cleaning treatments generates high costs and higher disposal of waste in the environment (Tin et al. 2017). Significant factors that affect membrane fouling magnitude are related to (1) membrane composition, (2) process parameterization, (3) agent characteristics, (4) contaminant properties, (5) cleaning procedure conditions, and (6) concentration polarization, closely related to the deposition of effluents in the superficial apportion of the membrane (Bokhary et al. 2018; Alsawaftah et al. 2021).

Accordingly, Fig. 2 reports the major components that influence the membrane fouling background. The exposure of membranes to specific agents and the level of performance are determining factors that enable the recycling of end-of-life

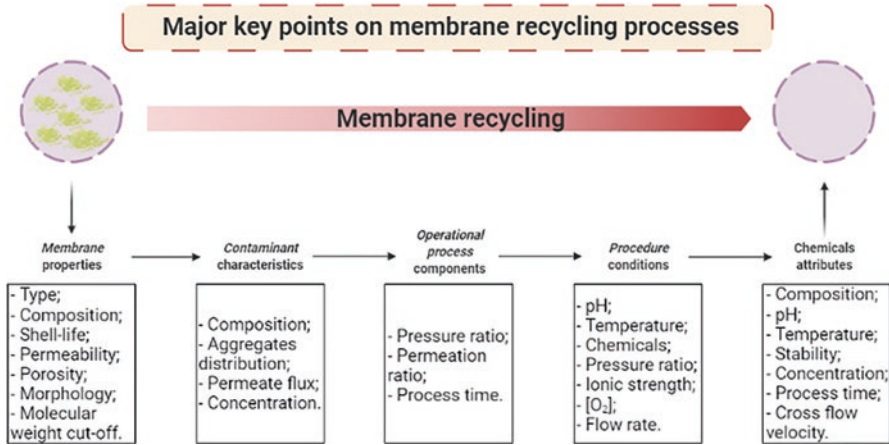


Fig. 2 Overview of the major components that involve the membrane fouling process

membranes (Landaburu-Aguirre et al. 2016). Studies indicated sodium hypochlorite and potassium permanganate as prominent components for a notable reduction in the level of fouling and increased permeability (De Paula et al. 2017). This scenario is the result of the modification of the morphological structure of membranes by the action of oxidizing agents, promoting the opening of the pores and facilitating the passage of the solution (Govardhan et al. 2020). Furthermore, these constituents conducted the minimization of permeate flow, which altered the quality of the final product (Laqbaqbi et al. 2017). Finally, parameters related to process and operating conditions considerably affect the permeability stability of membranes, as well as economic and sustainable attributions. External operating and process conditions affect pore balance, altering flux rates and may reduce membrane life-cycle (Alsawafah et al. 2021).

Therefore, the alternatives involving the cleaning and recycling processes of membranes can be physical, chemical, and physicochemical, and the membrane particularities and fouling level are significant properties to be highlighted (Landaburu-Aguirre et al. 2016). Chemical treatment is widely applied in membrane cleaning processes since chemical agents act in the re-stability of permeability. It is essential that chemical cleaning is conducted periodically, once the chemical action affects the surface structure of the membrane and, consequently, its deterioration (Gul et al. 2021). A range of chemicals has been used as cleaning agents such as acids, alkalis, oxidants, and surfactants (Li et al. 2019). Sodium hypochlorite (NaClO) (Ding et al. 2020), hydrogen peroxide (H₂O₂) (Li et al. 2019), titanium dioxide (TiO₂) (Zhang et al. 2017), sodium hydroxide (NaOH), sodium chloride (NaCl), and hydrochloric acid (HCl) (Zhang et al. 2019) are agents widely discussed in scientific studies and in industries and have been investigated by their decontamination potential. These compounds are widely used due to their ease of acquisition, cost-effectiveness, and contaminant removal performance (Gruskevica and Mezule 2021).

Alternatively, physical treatment technologies are based on the application of mechanical forces that cause displacement and extraction of contaminants from the membrane surface (Landaburu-Aguirre et al. 2016). Physical procedures involve agitation (Gul et al. 2021), ultrasonic bubbles (Reuter et al. 2017), CO₂ bubbles (Alnajjar et al. 2021), osmotic backwashing and flushing (Zhang and Dong 2018), sponge ball purification (Alsawaftah et al. 2021), and so on. Once these techniques are insufficient without the application of a chemical element, the addition of these methods with chemical agents has shown the improvement of the performance of removing contaminants and expanding the life cycle of membranes (Gul et al. 2021). This attribute is resulted by the agility of cleaning of physical technologies and the significant action of chemical agents in contact with contaminants. Accordingly, Table 1 reports the major technologies applied to the membrane fouling background, highlighting the treatments discussed previously.

Finally, some new technological strategies have been employed for cleaning and decontaminating membranes recently. The clean-in-place (CIP) is based on the integrated application of alkaline and acid detergents, disinfectants, and hot water in membrane systems (Vitzilaiou et al. 2019). The reduced use of chemicals and the high efficiency of contaminant removal point this technology as a prominent alternative to be explored in the coming years (Park et al. 2018). Moreover, recent studies highlighted that technologies and integration of techniques for the removal of microbial biofilms present in membranes is an interesting and encouraging approach (Nguyen et al. 2012; Vitzilaiou et al. 2019). Microbial biofouling is the deposition of microorganisms present in brackish solutions, synthesizing a film of high concentration of organic materials and microbial growth, which prevent the continuous flow of permeate and accumulate substances on the membrane surface (Kucera 2019). As biofouling remediation strategies, the silver application, ultraviolet (UV), ozone, and nano photocatalytic disinfection are highlighted (Al-Abri et al. 2019).

6 Challenges that Involve the Recycle of Polymeric Membranes

Although the recycling of polymeric membranes is a preferable way to reduce undesirable wastes and land-filling activities, recovering monomers and other materials with aggregate value, some challenges involving the procedure were highlighted by distinct authors (Chanda 2021; Utekar et al. 2021; Ignatyev et al. 2014; Hopewell et al. 2009; Dorigato 2021; Dogu et al. 2021; Valerio et al. 2020). Some of these items were described as follows:

- Contamination is the first obstacle in the recycling process of polymer membranes. For an appropriate reclaim and recycling, a preliminary decontamination step of the membranes is required. Nonetheless, if the decontamination process is costly, how to proceed?

Table 1 Advantages and limitations of the dominant technologies applied to the membrane fouling approach

	Membrane type	Advantages	Limitations	References
Chemical	UF ^a , NF ^b , UF ^c , and RO ^d	High reaction velocity High microorganism removal High flow rate Significant colloids and organic components elimination Elevated oxidation Process easiness Accessible injection	Costs with chemical solvents Uncertain stability Membrane shelf-life reduction Low efficiency Chemical corrosion predisposition Environmental impasse Carcinogens generation Inhibitors generation at higher temperatures Operation parameters requirement High precipitation propensity Necessity for application periodicity Suitable for certain types of membrane pH adjustment requirement Production of additional by-products	Maddah and Chogle (2017), Nascimbén Santos et al. (2020), Landaburu-Aguirre et al. (2016), Alsawftah et al. (2021), and Bokhary et al. (2018)

(continued)

Table 1 (continued)

	Membrane type	Advantages	Limitations	References
Physical	UF ^a , NF ^b , and UF ^c	No chemicals are required No chemical corrosion Easy installation High foulants removal Reduced installation and operation costs High colloids and suspended components removal High microorganism removal Receptiveness to supplemental techniques	High energy demand High reaction time Mutagenic by-products formation Reduced bacteria removal efficiency Incomplete biofouling disruption Necessity for additional technologies In many cases, membranes are susceptible to tearing and rewetting Costs increase Cooling system requirement No harmful by-products synthesis	Mohan and Nagalakshmi (2020), Landaburu-Aguirre et al. (2016), Alsawftah et al. (2021), Bokhary et al. (2018), Alkhatib et al. (2021), and Maddah and Chogle (2017)
Physicochemical	UF ^a , NF ^b , and UF ^c	Reduced chemicals demand High reaction velocity Higher efficiency than chemical or physical technologies individually	Formation of degradation compounds	Bokhary et al. (2018) and Mohan and Nagalakshmi (2020)

^aUltrafiltration, ^bNanofiltration, ^cUltrafiltration, and ^dReverse Osmosis

- Polymer membranes are formed by composite materials that are prepared by a combination of reinforcement, matrix materials, and fillers compounds. Therefore, the recycling method must consider that the reactivity among all these materials is different and the process could be complicated.
- If the membrane is composed of thermosetting resins, an additional problem must be considered: this type of material cannot be remolded again since it is reticulated.

- Another important topic is the separation and classification of the different polymers that composed the membranes. After the recycling process, there is a significant challenge and a tedious step.
- It is typically reported that the main commercial technique for recycling polymeric membranes (mechanical recycling, which includes reducing the size of the waste to reinforce it in different materials) degraded the mechanical properties of the membrane components.
- Membrane recycling by a conventional technique (such as chemical recycling) results in a waste management concern by the generation of liquefied waste, hazardous compounds, and solid waste since dangerous solvents can be used.
- Although the membranes technology is emergent, but not yet a disseminated technique, the inconsistent supply of recyclable materials limits a long-term business.

7 General Overview and Conclusions

Membrane separation processes (MSP) are a rapidly growing technology that has conquered industrial processes. The use of membranes eliminates some steps and considerably reduces the use of chemical reagents, especially in the treatment of effluents. It was possible due to the numerous researches conducted in recent years that allowed the improvement of the membrane manufacturing process. Nevertheless, membranes present a considerably restricted life cycle. This panorama led to large amounts of membranes and environmentally oriented waste, extolling strategies for recycling these materials as cost-friendly and eco-friendly alternatives in MSP processes.

Accordingly, this chapter detailed the dynamics of recycling polymeric membranes for reuse in a variety of applications. The intensification of MSP processes in a range of employments indicated the importance of degradation processes in the life cycle of membranes, manifesting significant reuse strategies and technologies. The performance of membrane reuse in the current scenario is a central topic for future actions that aspire a balance between membrane production and manipulation and the environment.

References

- Ahmed J, Jamal Y (2021) A pilot application of recycled discarded RO membranes for low strength gray water reclamation. *Environ Sci Pollut Res* 28(26):34042–34050. <https://doi.org/10.1007/s11356-020-11117-z>
- Al-Abri M, Al-Ghafri B, Bora T, Dobretsov S, Dutta J, Castelletto S, Rosa L, Boretti A (2019) Chlorination disadvantages and alternative routes for biofouling control in reverse osmosis desalination. *Npj Clean Water* 2(1). <https://doi.org/10.1038/s41545-018-0024-8>
- Alkhatib A, Ayari MA, Hawari AH (2021) Fouling mitigation strategies for different foulants in membrane distillation. *Chem Eng Process Process Intensif* 167(March):108517. <https://doi.org/10.1016/j.cep.2021.108517>

- Alnajjar H, Tabatabai A, Alpatova A, Leiknes T, Ghaffour N (2021) Organic fouling control in reverse osmosis (RO) by effective membrane cleaning using saturated CO₂ solution. *Sep Purif Technol* 264(August 2020):118410. <https://doi.org/10.1016/j.seppur.2021.118410>
- Alsawafah N, Abuwatfa W, Darwish N, Hussein G (2021) A comprehensive review on membrane fouling: mathematical modelling, prediction, diagnosis, and mitigation. *Water* 13(9). <https://doi.org/10.3390/w13091327>
- Alves MJ, Nascimento SM, Pereira IG, Martins MI, Cardoso VL, Reis M (2013) Biodiesel purification using micro and ultrafiltration membranes. *Renew Energy* 58(October):15–20. <https://doi.org/10.1016/j.renene.2013.02.035>
- Argenta AB, Scheer ADP (2020) Membrane separation processes applied to whey: a review. *Food Rev Int* 36(5):499–528. <https://doi.org/10.1080/87559129.2019.1649694>
- Bai W, Feng J, Luo C, Zhang P, Wang H, Yang Y, Zhao Y, Fan H (2021) A comprehensive review on oxygen transport membranes: development history, current status, and future directions. *Int J Hydrog Energy* 46:36257. <https://doi.org/10.1016/j.ijhydene.2021.08.177>
- Bandara PC, Nadres ET, Peña-Bahamonde J, Rodrigues DF (2019) Impact of water chemistry, shelf-life, and regeneration in the removal of different chemical and biological contaminants in water by a model polymeric graphene oxide nanocomposite membrane coating. *J Water Process Eng* 32(July):100967. <https://doi.org/10.1016/j.jwpe.2019.100967>
- Biniiaz P, Roostaie T, Rahimpour MR (2021) Biofuel purification and upgrading using novel integrated membrane technology. In: *Advances in bioenergy and microfluidic applications*. Elsevier, Amsterdam, pp 69–86. <https://doi.org/10.1016/B978-0-12-821601-9.00003-0>
- Boateng ID, Soetanto DA, Li F, Yang XM, Li YY (2021) Separation and purification of polyphenols from *Ginkgo Biloba* L. leaves by bulk ionic liquid membrane and optimizing parameters. *Ind Crop Prod* 170(July):113828. <https://doi.org/10.1016/j.indcrop.2021.113828>
- Bokhary A, Tikka A, Leitch M, Liao B (2018) Membrane fouling prevention and control strategies in pulp and paper industry applications: a review. *J Membr Sci Res* 4(4):181–197. <https://doi.org/10.22079/JMSR.2018.83337.1185>
- Castro-Muñoz R, Díaz-Montes E, Cassano A, Gontarek E (2021) Membrane separation processes for the extraction and purification of steviol glycosides: an overview. *Crit Rev Food Sci Nutr* 61(13):2152–2174. <https://doi.org/10.1080/10408398.2020.1772717>
- Chakraborty T, Chandra KP, Trivedi MU, Tripathi B, Pandey MK (2021) Fabrication of Janus type bi-layer polymeric membranes for advance water purification. *Mater Today: Proc* (in press). <https://doi.org/10.1016/j.matpr.2020.11.753>
- Chanda M (2021) Chemical aspects of polymer recycling. *Adv Ind Eng Polym Res* 4(3):133–150. <https://doi.org/10.1016/j.aiepr.2021.06.002>
- Conidi C, Castro-Muñoz R, Cassano A (2020) Membrane-based operations in the fruit juice processing industry: a review. *Beverages* 6(1):1–39. <https://doi.org/10.3390/beverages6010018>
- Contreras-Martínez J, García-Payo C, Khayet M (2021) Electrospun nanostructured membrane engineering using reverse osmosis recycled modules: membrane distillation application. *Nanomaterials* 11(6). <https://doi.org/10.3390/nano11061601>
- De Paula EC, Gomes JCL, Amaral MCS (2017) Recycling of end-of-life reverse osmosis membranes by oxidative treatment: a technical evaluation. *Water Sci Technol* 76(3):605–622. <https://doi.org/10.2166/wst.2017.238>
- Deng J, Huang Z, Sundell BJ, Harrigan DJ, Sharber SA, Zhang K, Guo R, Galizia M (2021) State of the art and prospects of chemically and thermally aggressive membrane gas separations: insights from polymer science. *Polymer* 229(July):123988. <https://doi.org/10.1016/j.polymer.2021.123988>
- Ding J, Wang S, Xie P, Zou Y, Wan Y, Chen Y, Wiesner MR (2020) Chemical cleaning of algae-fouled ultrafiltration (UF) membrane by sodium hypochlorite (NaClO): characterization of membrane and formation of halogenated by-products. *J Membr Sci* 598:117662. <https://doi.org/10.1016/j.memsci.2019.117662>
- Dogu O, Pelucchi M, Van de Vijver R, Van Steenberge PHM, D'hooge DR, Cuoci A, Mehl M, Frassoldati A, Faravelli T, Van Geem KM (2021) The chemistry of chemical recycling of solid

- plastic waste via pyrolysis and gasification: state-of-the-art, challenges, and future directions. *Prog Energy Combust Sci* 84(May):100901. <https://doi.org/10.1016/j.peccs.2020.100901>
- Dorigato A (2021) Recycling of polymer blends. *Adv Ind Eng Polym Res* 4(2):53–69. <https://doi.org/10.1016/j.aiepr.2021.02.005>
- Fan G, Li Z, Yan Z, Wei Z, Xiao Y, Chen S, Shanguan H, Lin H, Chang H (2020) Operating parameters optimization of combined UF/NF dual-membrane process for brackish water treatment and its application performance in municipal drinking water treatment plant. *J Water Process Eng* 38(December):101547. <https://doi.org/10.1016/j.jwpe.2020.101547>
- Fissell WH, Fleischman AJ, David Humes H, Roy S (2007) Development of continuous implantable renal replacement: past and future. *Transl Res* 150(6):327–336. <https://doi.org/10.1016/j.trsl.2007.06.001>
- Futter GA, Latz A, Jahnke T (2019) Physical modeling of chemical membrane degradation in polymer electrolyte membrane fuel cells: influence of pressure, relative humidity and cell voltage. *J Power Sources* 410–411(September 2018):78–90. <https://doi.org/10.1016/j.jpowsour.2018.10.085>
- Gojun M, Šalić A, Zelić B (2021) Integrated microsystems for lipase-catalyzed biodiesel production and glycerol removal by extraction or ultrafiltration. *Renew Energy* 180:213–221. <https://doi.org/10.1016/j.renene.2021.08.064>
- Govardhan B, Fatima S, Madhumala M, Sridhar S (2020) Modification of used commercial reverse osmosis membranes to nanofiltration modules for the production of mineral-rich packaged drinking water. *Appl Water Sci* 10(11):1–17. <https://doi.org/10.1007/s13201-020-01312-1>
- Gruskevica K, Mezule L (2021) Cleaning methods for ceramic ultrafiltration membranes affected by organic fouling. *Membranes* 11(2):1–15. <https://doi.org/10.3390/membranes11020131>
- Gul A, Hruza J, Yalcinkaya F (2021) Fouling and chemical cleaning of microfiltration membranes: a mini-review. *Polymers* 13(6). <https://doi.org/10.3390/polym13060846>
- Hopewell J, Dvorak R, Kosior E (2009) Plastics recycling: challenges and opportunities. *Philos Trans R Soc B Biol Sci* 364(1526):2115–2126. <https://doi.org/10.1098/rstb.2008.0311>
- Hube S, Eskafi M, Hrafnkelsdóttir KF, Bjarnadóttir B, Bjarnadóttir MÁ, Axelsdóttir S, Bing W (2020) Direct membrane filtration for wastewater treatment and resource recovery: a review. *Sci Total Environ* 710:136375. <https://doi.org/10.1016/j.scitotenv.2019.136375>
- Ignatyev IA, Thielemans W, Beke BV (2014) Recycling of polymers: a review. *ChemSusChem* 7(6):1579–1593. <https://doi.org/10.1002/cssc.201300898>
- Jain A, De S (2019) Processing of beverages by membranes. In: *Processing and sustainability of beverages*. Elsevier, Duxford, pp 517–560. <https://doi.org/10.1016/B978-0-12-815259-1.00015-X>
- Jose AJ, Kappen J, Alagar M (2018) Polymeric membranes: classification, preparation, structure physiochemical, and transport mechanisms. In: *Fundamental biomaterials: polymers*. Elsevier, Duxford, pp 21–35. <https://doi.org/10.1016/B978-0-08-102194-1.00002-5>
- Junior DAA, Oro CED, Dos Santos MSN, Dallago RM, Tres MV (2021) Integration of improved methods for the treatment of wastewater from a soft drink industry. *Biointerface Res Appl Chem* 11(5):12946–12957. <https://doi.org/10.33263/BRIAC115.1294612957>
- Keskin B, Zeytuncu-Gökoğlu B, Koyuncu I (2021) Polymer inclusion membrane applications for transport of metal ions: a critical review. *Chemosphere* 279:130604. <https://doi.org/10.1016/j.chemosphere.2021.130604>
- Khaki E, Abyar H, Nowrouzi M, Younesi H, Abdollahi M, Enderati MG (2021) Comparative life cycle assessment of polymeric membranes: polyacrylonitrile, polyvinylimidazole and poly (Acrylonitrile-Co-Vinylimidazole) applied for CO₂ sequestration. *Environ Technol Innov* 22:101507. <https://doi.org/10.1016/j.eti.2021.101507>
- Khaless K, Achiou B, Boulif R, Benhida R (2021) Recycling of spent reverse osmosis membranes for second use in the clarification of wet-process phosphoric acid. *Minerals* 11(6):1–10. <https://doi.org/10.3390/min11060637>
- Khalid A, Aslam M, Qyyum MA, Faisal A, Khan AL, Ahmed F, Lee M et al (2019) Membrane separation processes for dehydration of bioethanol from fermentation broths: recent developments, challenges, and prospects. *Renew Sust Energ Rev* 105(May):427–443. <https://doi.org/10.1016/j.rser.2019.02.002>

- Khatib FN, Wilberforce T, Ijaodola O, Ogungbemi E, Zaki El-Hassan A, Durrant JT, Olabi AG (2019) Material degradation of components in Polymer Electrolyte Membrane (PEM) electrolytic cell and mitigation mechanisms: a review. *Renew Sust Energy Rev* 111(May):1–14. <https://doi.org/10.1016/j.rser.2019.05.007>
- Kodaira Y, Miura T, Ito S, Emori K, Yonezu A, Nagatsuka H (2021) Evaluation of crack propagation behavior of porous polymer membranes. *Polym Test* 96:107124. <https://doi.org/10.1016/j.polymertesting.2021.107124>
- Kucera J (2019) Biofouling of polyamide membranes: fouling mechanisms, current mitigation and cleaning strategies, and future prospects. *Membranes* 9(9). <https://doi.org/10.3390/membranes9090111>
- Landaburu-Aguirre J, García-Pacheco R, Molina S, Rodríguez-Sáez L, Rabadán J, García-Calvo E (2016) Fouling prevention, preparing for re-use and membrane recycling. Towards circular economy in RO desalination. *Desalination* 393:16–30. <https://doi.org/10.1016/j.desal.2016.04.002>
- Laqbaqbi M, Sanmartino JA, Khayet M, García-Payo C, Chaouch M (2017) Fouling in membrane distillation, osmotic distillation and osmotic membrane distillation. *Appl Sci (Switzerland)* 7(4). <https://doi.org/10.3390/app7040334>
- Le Petit L, Rabiller-Baudry M, Touin R, Chataignier R, Thomas P, Connan O, Périon R (2021) Efficient and rapid multiscale approach of polymer membrane degradation and stability: application to formulation of harmless non-oxidative biocide for polyamide and PES/PVP membranes. *Sep Purif Technol* 259:118054. <https://doi.org/10.1016/j.seppur.2020.118054>
- Lejarazu-Larrañaga A, Ortiz JM, Molina S, Zhao Y, García-Calvo E (2020) Nitrate-selective anion exchange membranes prepared using discarded reverse osmosis membranes as support. *Membranes* 10(12):1–18. <https://doi.org/10.3390/membranes10120377>
- Li K, Li S, Huang T, Dong C, Li J, Zhao B, Zhang S (2019) Chemical cleaning of ultrafiltration membrane fouled by humic substances: comparison between hydrogen peroxide and sodium hypochlorite. *Int J Environ Res Public Health* 16(14). <https://doi.org/10.3390/ijerph16142568>
- Luo J, Hang X, Zhai W, Qi B, Song W, Chen X, Wan Y (2016) Refining sugarcane juice by an integrated membrane process: filtration behavior of polymeric membrane at high temperature. *J Membr Sci* 509(July):105–115. <https://doi.org/10.1016/j.memsci.2016.02.053>
- Maddah H, Chogle A (2017) Biofouling in reverse osmosis: phenomena, monitoring, controlling and remediation. *Appl Water Sci* 7(6):2637–2651. <https://doi.org/10.1007/s13201-016-0493-1>
- Mohan SM, Nagalakshmi S (2020) A review on aerobic self-forming dynamic membrane bioreactor: formation, performance, fouling and cleaning. *J Water Process Eng* 37(May):101541. <https://doi.org/10.1016/j.jwpe.2020.101541>
- Moradi MR, Pihlajamäki A, Hesampour M, Ahlgren J, Mänttari M (2019) End-of-life RO membranes recycling: reuse as NF membranes by polyelectrolyte layer-by-layer deposition. *J Membr Sci* 584(October 2018):300–308. <https://doi.org/10.1016/j.memsci.2019.04.060>
- Nguyen T, Roddick FA, Fan L (2012) Biofouling of water treatment membranes: a review of the underlying causes, monitoring techniques and control measures. *Membranes* 2(4):804–840. <https://doi.org/10.3390/membranes2040804>
- Nunes SP, Zeynep Culfaz-Emecen P, Ramon GZ, Visser T, Koops GH, Jin W, Ulbricht M (2020) Thinking the future of membranes: perspectives for advanced and new membrane materials and manufacturing processes. *J Membr Sci* 598:117761. <https://doi.org/10.1016/j.memsci.2019.117761>
- Park S, Kang JS, Lee JJ, Vo TKQ, Kim HS (2018) Application of physical and chemical enhanced backwashing to reduce membrane fouling in the water treatment process using ceramic membranes. *Membranes* 8(4). <https://doi.org/10.3390/membranes8040110>
- Peyravi M, Jahanshahi M, Banafati S (2020) Application of membrane technology in beverage production and safety. In: Safety issues in beverage production. Elsevier, Duxford, pp 271–308. <https://doi.org/10.1016/B978-0-12-816679-6.00008-5>
- Potrich E, Miyoshi SC, Machado PFS, Furlan FF, Ribeiro MPA, Tardioli PW, Giordano RLC, Cruz AJG, Giordano RC (2020) Replacing hexane by ethanol for soybean oil extraction: modeling,

- simulation, and techno-economic-environmental analysis. *J Clean Prod* 244:118660. <https://doi.org/10.1016/j.jclepro.2019.118660>
- Rabajczyk A, Zielecka M, Cygańczuk K, Pastuszka Ł, Jurecki L (2021) The use of polymer membranes to counteract the risk of environmental of soil and water contamination. *Membranes* 11(6). <https://doi.org/10.3390/membranes11060426>
- Reis MHM, Madrona GS, Ferreira FB, de Santana Magalhães F, Bindaes MMM, Cardoso VL (2019) Membrane filtration processes for the treatment of nonalcoholic beverages. In: *Engineering tools in the beverage industry*. Elsevier, Oxford, pp 175–207. <https://doi.org/10.1016/B978-0-12-815258-4.00006-8>
- Reuter F, Lauterborn S, Mettin R, Lauterborn W (2017) Membrane cleaning with ultrasonically driven bubbles. *Ultrason Sonochem* 37(December):542–560. <https://doi.org/10.1016/j.ultsonch.2016.12.012>
- Saini N, Pandey K, Awasthi K (2021) Conjugate polymer-based membranes for gas separation applications: current status and future prospects. *Mater Today Chem* 22:100558. <https://doi.org/10.1016/j.mtchem.2021.100558>
- Santos N, Érika ZL, Hodúr C, Arthanareeswaran G, Veréb G (2020) Photocatalytic membrane filtration and its advantages over conventional approaches in the treatment of oily wastewater: a review. *Asia Pac J Chem Eng* 15(5):1–29. <https://doi.org/10.1002/apj.2533>
- Shao L (2020) Grand challenges in emerging separation technologies. *Front Environ Chem* 1(May):1–5. <https://doi.org/10.3389/fenvc.2020.00003>
- Sharma R, Geranpayehvaghei M, Ejeian F, Razmjou A, Asadnia M (2021) Recent advances in polymeric nanostructured ion selective membranes for biomedical applications. *Talanta* 235(August):122815. <https://doi.org/10.1016/j.talanta.2021.122815>
- Tajziehchi K, Sadrameli SM (2021) Optimization for free glycerol, diglyceride, and triglyceride reduction in biodiesel using ultrafiltration polymeric membrane: effect of process parameters. *Process Saf Environ Prot* 148(April):34–46. <https://doi.org/10.1016/j.psep.2020.09.047>
- Tin MM, Ma GA, Nakagoe O, Tanabe S, Kodamatani H, Nghiem LD, Fujioka T (2017) Membrane fouling, chemical cleaning and separation performance assessment of a chlorine-resistant nanofiltration membrane for water recycling applications. *Sep Purif Technol* 189:170–175. <https://doi.org/10.1016/j.seppur.2017.07.080>
- Utekar S, Suriya VK, More N, Rao A (2021) Comprehensive study of recycling of thermosetting polymer composites – driving force, challenges and methods. *Compos Part B* 207(September 2020):108596. <https://doi.org/10.1016/j.compositesb.2020.108596>
- Valerio O, Muthuraj R, Codou A (2020) Strategies for polymer to polymer recycling from waste: current trends and opportunities for improving the circular economy of polymers in South America. *Curr Opin Green Sustain Chem* 25(October):100381. <https://doi.org/10.1016/j.cogsc.2020.100381>
- Vassiliev A, Reumert AK, Jensen JO, Aili D (2019) Durability and degradation of vapor-fed direct dimethyl ether high temperature polymer electrolyte membrane fuel cells. *J Power Sources* 432(May):30–37. <https://doi.org/10.1016/j.jpowsour.2019.05.062>
- Vitzilaiou E, Stoica IM, Knøchel S (2019) Microbial biofilm communities on reverse osmosis membranes in whey water processing before and after cleaning. *J Membr Sci* 587(June):117174. <https://doi.org/10.1016/j.memsci.2019.117174>
- Warsinger DM, Chakraborty S, Tow EW, Plumlee MH, Bellona C, Loutatidou S, Karimi L et al (2018) A review of polymeric membranes and processes for potable water reuse. *Prog Polym Sci* 81(June):209–237. <https://doi.org/10.1016/j.progpolymsci.2018.01.004>
- Whiteley M, Dunnett S, Jackson L (2020) Simulation of polymer electrolyte membrane fuel cell degradation using an integrated Petri net and 0D model. *Reliab Eng Syst Saf* 196(November 2019):106741. <https://doi.org/10.1016/j.res.2019.106741>
- Woźniak-Budych MJ (2021) Polymeric membranes for biomedical applications. *Phys Sci Rev O*. <https://doi.org/10.1515/psr-2021-0052>
- Yadav P, Ismail N, Essalhi M, Tysklind M, Athanassiadis D, Tavajohi N (2021) Assessment of the environmental impact of polymeric membrane production. *J Membr Sci* 622(January):118987. <https://doi.org/10.1016/j.memsci.2020.118987>

- Yang S, Wang J, Wang Y, Ding Y, Zhang W, Liu F (2021) Interfacial polymerized polyamide nanofiltration membrane by demulsification of hexane-in-water droplets through hydrophobic PTFE membrane: membrane performance and formation mechanism. *Sep Purif Technol* 275(July):119227. <https://doi.org/10.1016/j.seppur.2021.119227>
- Yusuf A, Sodiq A, Giwa A, Eke J, Pikuda O, De Luca G, Di Salvo JL, Chakraborty S (2020) A review of emerging trends in membrane science and technology for sustainable water treatment. *J Clean Prod* 266(September):121867. <https://doi.org/10.1016/j.jclepro.2020.121867>
- Zhang W, Dong B (2018) Effects of physical and chemical aspects on membrane fouling and cleaning using interfacial free energy analysis in forward osmosis. *Environ Sci Pollut Res* 25(22):21555–21567. <https://doi.org/10.1007/s11356-018-2239-0>
- Zhang RX, Braeken L, Liu TY, Luis P, Wang XL, Van der Bruggen B (2017) Remarkable anti-fouling performance of TiO₂-modified TFC membranes with mussel-inspired polydopamine binding. *Appl Sci (Switzerland)* 7(1). <https://doi.org/10.3390/app7010081>
- Zhang B, Shuili Y, Youbing Zhu Y, Gao SX, Shi W, Tay JH (2019) Efficiencies and mechanisms of the chemical cleaning of fouled polytetrafluoroethylene (PTFE) membranes during the microfiltration of alkali/surfactant/polymer flooding oilfield wastewater. *RSC Adv* 9(63):36940–36950. <https://doi.org/10.1039/c9ra06745k>
- Zhang Q, Wang Q, Huang S, Jiang Y, Chen Z (2021a) Preparation and electrochemical study of PVDF-HFP/LATP/g-C₃N₄ composite polymer electrolyte membrane. *Inorg Chem Commun* 131(July):108793. <https://doi.org/10.1016/j.inoche.2021.108793>
- Zhang J, Xiao K, Liu Z, Gao T, Liang S, Huang X (2021b) Large-scale membrane bioreactors for industrial wastewater treatment in China: technical and economic features, driving forces, and perspectives. *Engineering* 7(6):868–880. <https://doi.org/10.1016/j.eng.2020.09.012>

Composites Based on Polymeric Matrices Recycled from Different Wastes and Natural Fibers



Galder Kortaberria

1 Introduction

The increase in material production and consumption is leading to a fast exhaustion of the virgin resources. Plastics or polymers are among the most widely produced and used materials. In 2018, the production of plastics was around 359 million metric tons worldwide, and it appears that this will continue to grow year after year (Garside 2020). In fact, 62 million metric tons were produced in Europe this year 2018. China, the largest plastic producer in the world, accounts for more than one quarter of the global production. In 2019, 39.9% of European plastic demand came from packaging industry, while 19.9% was from building one. The most demanded plastics were poly(ethylene) (PE) for films, tubes, toys, and containers, poly(propylene) (PP) for food packaging, pipes, or car accessories, and poly(ethylene terephthalate) (PET) mainly for bottles (PlasticsEurope 2019). Figure 1 shows the evolution of plastic production since 1950.

If plastic production continues to grow as predicted, around 2000 tons of polymeric materials will be produced by 2050 (UNEP 2016), resulting in waste accumulation if waste management and reuse/recycling are not properly considered and developed. The use of recycled polymers in different applications or as matrices in composites is an urgent requirement to reduce polymeric waste and find value-added applications for them. Consequently, plastic recycling has attracted a great interest in different sectors (Ilyas et al. 2021). Thermoplastic polymers are the most commonly used and, consequently, the most recycled ones. Among their main advantages is their relatively easy processability by several methods, resulting in different products obtained by changing operating conditions, which can be easily

G. Kortaberria (✉)

Group 'Materials + Technologies' (GMT), University of the Basque Country UPV/EHU, Donostia-San Sebastián, Spain

e-mail: galder.cortaberria@ehu.eus

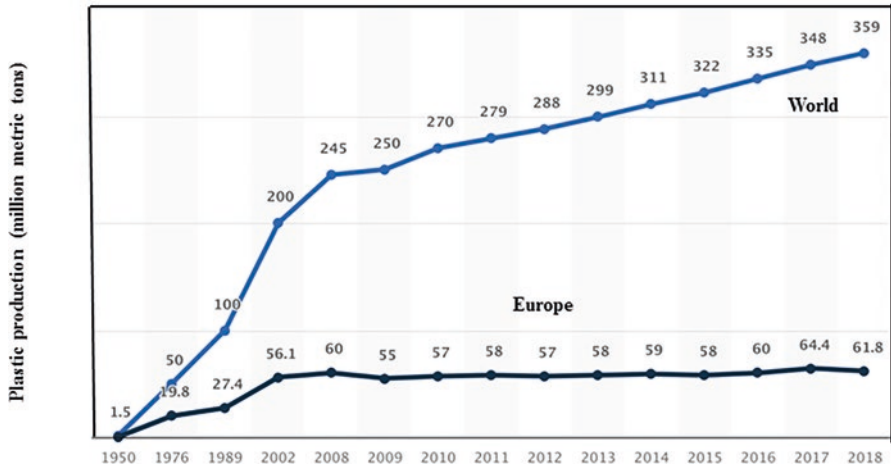


Fig. 1 Evolution of plastic production, in millions of metric tons, since 1950 in Europe and the world

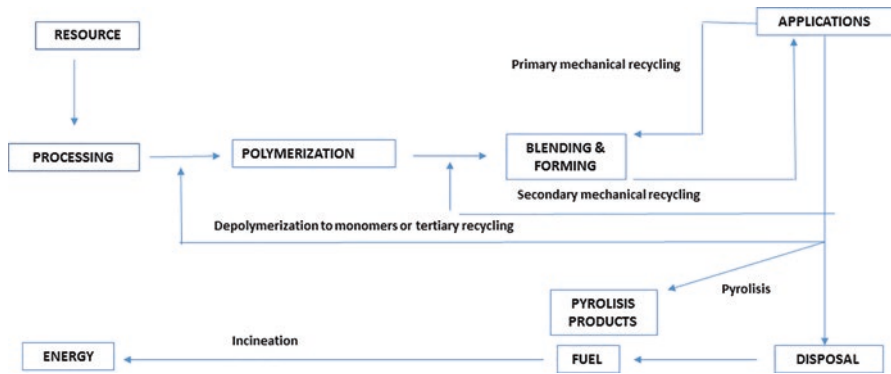


Fig. 2 The most common polymer recycling methods

mixed with additives, fillers, or reinforcements (Favis and Le Corroller 2017; Saleh and Danmaliki 2017). The recycling and incineration are the most often used recovery methods of thermoplastic polymers. While the incineration presents some problems such as the production of toxic gases and the residual ash that could contain heavy metals such as lead and cadmium, recycling helps to reduce environmental problems besides saving material and energy (Francis 2016). The recycling processes can be classified into four main types as shown in Fig. 2: primary recycling, secondary or mechanical recycling, chemical or tertiary recycling, and feedstock or quaternary recycling.

The primary recycling is the most used one, due to their simplicity and low cost, consisting of the reuse of products in their original structure. The main disadvantage is that each material presents a limit on the number of cycles (Francis 2016; Singh

et al. 2017). The secondary or mechanical recycling can only be applied to thermoplastic polymers, because they can be remelted and reprocessed into end products. In this process, plastic wastes are cut, shredded, and washed into granulates, flakes, or pellets, and then melted to make the new product by extrusion. Sometimes this reprocessed material is also blended with virgin material to obtain better properties (Grigore 2017). By chemical recycling, polymers are completely or partially depolymerized to obtain monomers or oligomers, respectively, which can be used for further polymerization processes (Mendiburu-Valor et al. 2021; Olah et al. 2008). Glycolysis, hydrolysis, and methanolysis can be underlined as the main depolymerization reactions even though there are some others. Finally, the aim of quaternary recycling is the energy recovery, the main process being represented by the incineration, which generates considerable energy. However, it is not ecologically acceptable because toxic substances such as dioxins are generated (in the case of heavy metals, chlorine-containing polymers, toxic carbon, and oxygen-based free radicals).

Taking a look to Table 1, in which together with the worldwide plastic production, data about the wastes management are also shown, one can realize the dramatic situation. The latest available data revealed that 75% of generated plastic was landfilled which means a loss of resources. Therefore, the enhancement of the waste management is imperative.

On the other hand, natural fiber-based composites consist of a sustainable alternative to the synthetic material-based composites. Natural fibers have several advantages over their synthetic counterparts: abundant availability, lower cost, lower environmental impact, and easier processing. Natural fibers can be classified into many different categories, as shown in Fig. 3 (Al-Maadeed and Labidi 2014).

Natural fibers are an abundant and renewable resource, being their cost relatively low compared with other conventional fibers, presenting low density and relatively high mechanical properties (Xie et al. 2010). They are eco-friendly and biodegradable, and they reduce the problem of solid waste production when used to replace nondegradable fillers. Due to their nonabrasive behavior, they can be used in larger amounts as polymer filler than nonorganic ones, which could damage the machinery because of their abrasive character.

Thermoplastics obtained from waste can be properly combined with natural fibers such as kenaf, jute, flax, and hemp to create so-called biocomposites, which

Table 1 Data on plastics production and waste management (in thousands of US tons) from 1960 to 2018, as obtained from the American Chemistry Council, the National Association for PET Container Resources, and the Association of Plastic Recyclers

Management pathway	1960	1970	1980	1990	2000	2005	2010	2017	2018
Generation	390	2900	6830	17,130	25,550	29,380	31,400	35,410	35,680
Recycled	–	–	20	1480	1480	1780	2500	3000	3090
Composted	–	–	–	–	–	–	–	–	–
Energy recovery	–	–	140	2980	4120	4330	4530	5590	5620
Landfilled	390	2900	6670	13,780	19,950	23,270	24,370	26,820	26,970

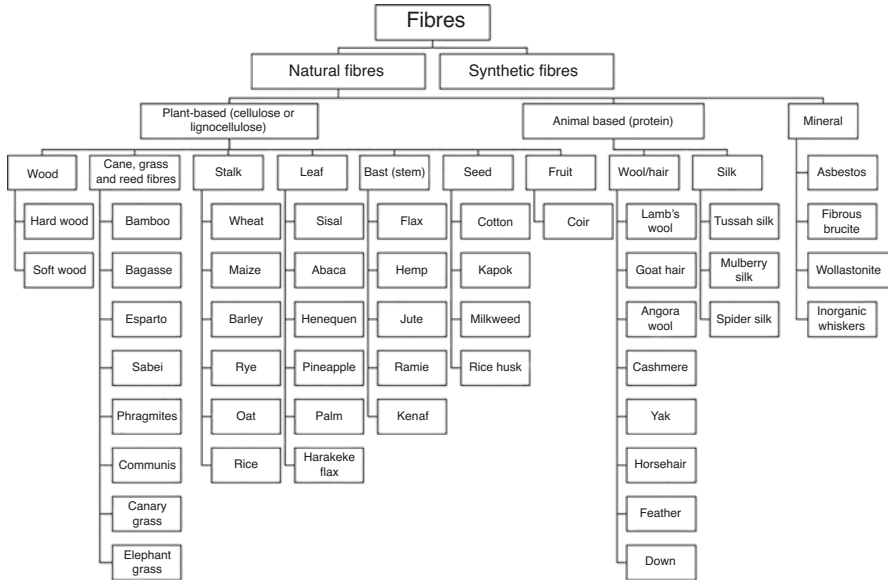


Fig. 3 Classification of natural fibers. (Reproduced with permission of Al-Maadeed and Labidi (2014), copyright Woodhead Publishing, Elsevier, 2014)

have several advantages over synthetic fiber-based composites such as acceptable mechanical properties, lightweight, low cost, and biodegradability (Adhikary et al. 2008; Cho et al. 2007). In fact, many authors have prepared composites based on natural fibers, not only with thermoplastic polymers but also with thermosetting ones (Bourmaud et al. 2011; Cho et al. 2009; Lee et al. 2008). Natural fiber-based composites, however, also have some disadvantages such as relatively high moisture sorption or the poor compatibility between fiber and matrix, which necessitates the use of compatibilizers or the functionalization of the surface with acids or alkalis, modifying their surface properties, improving their thermal stability and compatibility, as well as the removal of potential impurities (Fahim and Elhaggar 2012).

The aim of this review chapter is to show the main advances developed during the last years on the preparation and characterization of composites based on recycled thermoplastics (mainly polyethylene terephthalate (PET) and polypropylene (PP)) and natural fibers from different origins (woven flax, cotton fibers, sugar cane fibers, kenaf or rice straw fibers, among others).

2 Biocomposites Based on Recycled PET

PET is a semicrystalline aromatic–aliphatic thermoplastic polyester used in the production of food packaging, mainly for bottles (51%), other food packaging (9.1%), sheets and films (13.8%), as well as for nonfood products (6.1%) (Wei et al. 2017).

PET consumption has increased in recent years, with a demand of around four million tons in Europe in 2018 (Plastics Europe 2019), mainly due to its suitable properties such as flexibility, low density and low cost, high mechanical, physical, and chemical properties, and low gas transmission permeability (Chapa-Martínez et al. 2016; Mendiburu-Valor et al. 2021). Wastes coming from manufacture and post-urban residues constitute the main PET waste sources, which should be managed and recycled. The development of composites with natural fibers has been one of the ways for reusing recycled PET. The behavior of natural fiber-based composites greatly depends on fiber type, content, geometry, and interface properties (Khan et al. 2018; Ku et al. 2011; Mohammed et al. 2015). Many studies can be found in the literature, with the aim of improving the mechanical properties of recycled PET/natural fiber composites. In this way, Zou et al. (2011) successfully prepared composites from polyester and cotton blend fabrics. PET/cotton blend composites were prepared by using plasticizers such as 2-phenyl phenol and glycerol for decreasing the melting temperature of PET, reducing the preparation time. Moreover, even though some studies also probed the possibility of obtaining regenerated cellulosic fibers from waste PET and cotton blend textiles (Yabuki et al. 2003), some authors claimed that the physical and chemical techniques of recycling pure PET are not conclusive for recovering PET from waste PET/cotton blended fabrics because it is intricately mixed with cotton fibers, making mechanical separation difficult. Moreover, as PET is only soluble in a few expensive solvents, dissolving it from mixtures is difficult. In this way, Palakurthi (2016) developed composites based on separated and recycled PET and cotton textiles for their potential use in home furnishings and other textile products. The author used plain woven fabrics of 100% cotton and 100% PET obtained from wastes of textile industry. She analyzed the effect of plasticizers and alkali treatments by decreasing the processing temperatures, in order to protect the cotton during the process, showing that plasticizer reduced the melting point, allowing the composites to be prepared at lower temperatures, presenting improved mechanical properties due to the lower damage caused to cotton fabrics.

With similar constituents, Carrete (2019) produced natural fiber-reinforced polymer composites from post-consumer textile cotton waste and PET from water bottles by surface modifications of cotton fibers. This novel composite material, obtained as a monofilament feedstock for 3D printing, toughened the recycled PET matrix. They hydrolyzed fibers from white denim cloth (as a representation of bleached fibers) as well as fibers from post-consumer denim jeans, in order to increase the compatibility with polymeric matrix, increasing the interfacial adhesion. Functionalization with a silane was also used for this purpose. They concluded that cotton fibers were successfully modified and toughened the matrix, increasing impact resistance. They showed that the fiber–matrix adhesion was sufficient to resist brittle fracture modes using scanning electron microscopy (SEM) images of impact fracture surfaces. They concluded by pointing out that their study showed that mechanical properties of PET were improved, particularly the dampening characteristics and impact strength.

Some further studies on composites with various natural fibers can be found in the literature. In this way, Ardekani et al. (2014) studied the mechanical and thermal properties of composites made from recycled newspaper fibers and recycled PET, with styrene-ethylene-butylene-styrene grafted maleic anhydride (SEBS-g-MA) as compatibilizer. They found that tensile and flexural strength of the composite increased with addition of up to 5 wt% of fiber; however, for higher fiber contents, both parameters decreased due to insufficient wettability between the fibers and the matrix. Corradini et al. (2008) prepared composites based on bagasse fiber and recycled PET, with ethylene/*n*-butyl acrylate/glycidyl methacrylate (EBGMA) and ethylene-methyl acrylate (EMA) as compatibilizers. SEM and dynamic mechanical analysis (DMA) revealed that adhesion of fiber with PET was more effective with EBGMA than that of EMA. However, they found that the incorporation of fiber decreased tensile properties of PET.

Dehghani et al. (2013) also prepared composites based on recycled PET and date palm leaf fiber, by using maleated block copolymer of SEBS-g-MA as compatibilizer, through injection molding. They reported that tensile strength increased with fiber addition, due to the better stress transfer between the phases, improved by the surface modification of the fiber. Flexure strength increased up to 5 wt% of fiber loading and it remained unaffected for higher contents. The compatibilizer increased the impact strength of recycled PET. Santos et al. (2014) prepared composites based on recycled PET and sisal fibers by thermal processing. They used three different plasticizers in order to decrease the melting point of PET: glycerol, castor oil, and tributyl citrate. They found that PET stiffness decreased with fiber and plasticizer addition due to restricted intermolecular interaction.

Some authors also used polymer blends based on recycled PET, reinforced with natural fibers, for preparing composites. In this way, Chaiwutthinan et al. (2019) prepared composites based on blends of recycled PET and poly(butyleneadipate-*co*-terephthalate) (PBAT) reinforced with wood flour. They found that PBAT decreased the tensile and flexural properties of PET, while impact strength and elongation at break were increased. Even though flexural strength and Young's modulus increased, due to the high stiffness of wood that reduced polymer chain mobility, the thermal stability decreased. Mosavi-Mirkolaei et al. (2019) prepared composites based on blends of recycled high-density polyethylene (HDPE), low-density polyethylene (LDPE), and PET with beech wood flour by using ethylene-glycidyl methacrylate copolymer (E-GMA) as compatibilizer. Developed composites presented improved mechanical properties and water resistance due to the increase in crystallinity, and interfacial bonding among the polymer and the filler. Martinez Lopez et al. (2020) used sawdust as reinforcement for waste thermoplastic PET, HDPE, and PP blend with the aim of preparing a composite board. They also added calcium carbonate (CaCO₃) and found that the higher the sawdust content, the lower the mechanical properties, increasing the rigidity of the matrix. Finally, Dairi et al. (2017) prepared composites based on recycled PP/PET blends and wood flour, with maleic anhydride grafted polypropylene (MAPP) as compatibilizer. They found that flexural strength and modulus, as well as tensile modulus, increased with wood flour

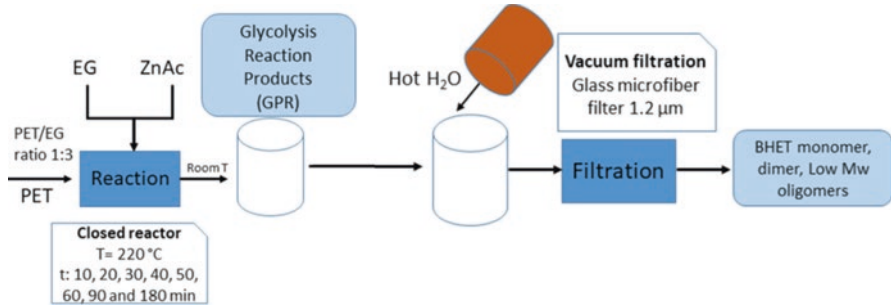


Fig. 4 PET glycolysis reaction and obtained products

content, probably due to the effect of MAPP, which favored a good interface interaction between constituents.

As was stated above, the tertiary or chemical recycling is another way for recovering primary materials from polymeric wastes for further use in the synthesis of new materials. In this way, unsaturated polyester resin obtained by chemical recycling of PET (from BHET monomer) is a potential matrix material for composites reinforced with natural fibers. Figure 4 shows the chemical recycling procedure for BHET obtained from PET wastes.

Several authors have developed related studies, such as Ahmad et al. (2008), who prepared composites with sawdust and analyzed the effects of alkali treatment, filler content, and size on mechanical properties. They found that tensile and flexure modulus increased with filler content, but tensile and flexural strength decreased. They concluded by pointing out that the smaller the size of sawdust, the higher the strength and modulus because of the higher surface area for filler–matrix interaction. Farahani et al. (2012) prepared composites based on kenaf fiber and unsaturated polyester (UPR) from PET recycling, using different size fibers. They found a decrease in tensile strength with fiber addition. However, the impact strength of the composites was improved for all sizes used. Tan et al. (2011) prepared composites based on UPR from PET waste and empty fruit bunch after modifying fiber surface with NaOH, silane, and maleic anhydride (MA). They observed that fiber treatment enhanced the tensile properties and impact strength.

3 Biocomposites Based on Recycled PP

PP is one of the most used thermoplastics in many industrial applications, which can be processed through extrusion and injection molding, both with synthetic glass or carbon fibers and natural ones. In recent years, several authors have prepared composites reinforced with natural fibers, from different origins, and recycled PP as polymeric matrix. In this way, Quynh Truong Hoang et al. (2010) prepared composites reinforced with short spruce fiber. They analyzed the effect of recycling PP five

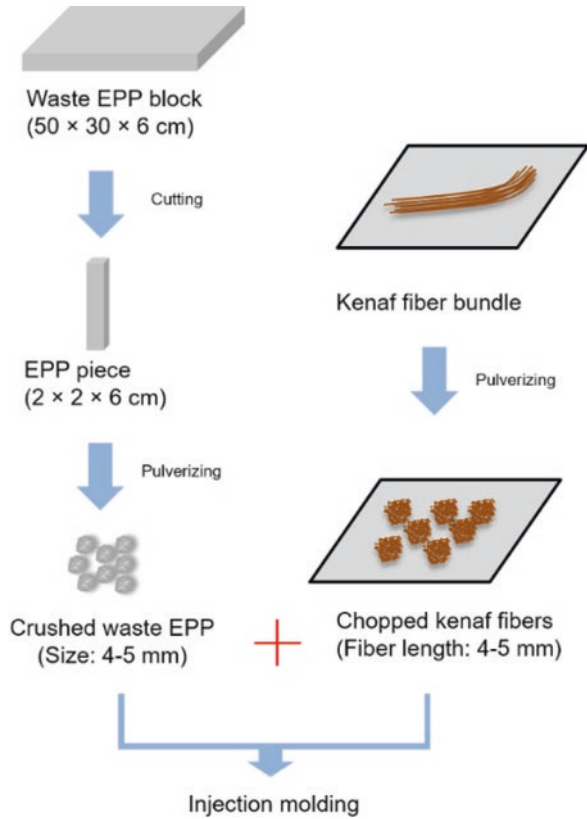
and ten times, together with that of the fiber amount. They showed the effect of fibers increasing degree of crystallinity of PP, with the development of a new crystalline β phase using differential scanning calorimetry (DSC) and wide-angle X-ray spectroscopy (WAXS). Using tensile tests, they showed that the fiber embrittled the materials. Using fracture tests coupled with digital image correlation, they found the better accommodation of overstrains at the crack tip in the composite material. They pointed out the promising material developed. Srebrenkoska et al. (2009) studied the possibility of using recycled PP for preparing composites with kenaf fibers and rice hulls as reinforcements, with maleic anhydride grafted PP (MAPP) as compatibilizer. They found that flexural strength and thermal stability of composites with recycled PP were similar to those of composites with neat PP, while those reinforced with kenaf fibers presented better properties than those based on rice hulls. As mechanical and thermal properties of recycled PP were very similar than those of virgin PP, and taking into account the reinforcing effect of natural fibers, the authors claimed the possibility of using recycled PP for the production of composites with potential applications as construction building materials in housing systems.

In his thesis, Rios (2015) prepared and characterized composites based on recycled PP and both as-received and NaOH-treated coconut fibers. Scanning electron microscopy (SEM) and X-ray tomography (XRT) were performed for morphological analysis, while unidirectional tensile test followed by digital image correlation (DIC) and infrared thermography were used for mechanical analysis. He concluded that NaOH treatment reduced impurities. He found that Young's modulus and tensile strength decreased with increasing fiber diameters. Moreover, the critical damage was determined, showing that composites fabricated with recycled PP had more time for rupture propagation. Damage evolution using strain fields from DIC demonstrated that the longitudinal strains are predominant in relation to the transverse ones on the damage process. He presented a detailed experimental and theoretical study of mechanical properties and damage process.

Hidalgo-Salazar et al. (2018) studied the morphological, mechanical, and thermal studies on composites based on recycled PP, coffee husk, and coir coconut biocomposites prepared by extrusion and injection molding, with MAPP as compatibilizing agent. They showed that both fibers improved the flexural modulus and thermal properties of composites, which, on the other hand, showed poor impact properties. Both fibers acted as nucleating agents, generating an increase of the thermal stability of PP phase. The compatibilizer significantly improved the mechanical strength and impact behavior of biocomposites.

Abdullah and Che Aslan (2019) used Mengkuang leaf fiber from Malaysia to reinforce recycled PP and evaluated tensile, flexural, and impact properties of composites. The effect of both NaOH treatment and MAPP compatibilizer was analyzed. Tensile and flexural properties showed improvements, especially those with MAPP and alkaline treatment, compared to neat PP. However, they also observed a decrease in the impact strength of composites. Kim and Cho (2020) reinforced a matrix of recycled waste expanded PP (EPP) with kenaf fibers, by

Fig. 5 Crushed waste expanded polypropylene and chopped kenaf fibers obtained by pulverizing waste EPP blocks and kenaf fiber bundles, respectively, prior to injection molding. (Reproduced with permission of Kim and Cho (2020), MDPI)



using chopped kenaf fibers and crushed EPP waste. Figure 5 shows an scheme of composites preparation.

They found that flexural properties, impact strength, and heat deflection temperature (HDT) of composites were enhanced by using waste EPP, compared to that of those prepared with virgin PP. The flexural modulus and strength of the composites with waste EPP were 98% and 55% higher than with virgin PP at the same kenaf contents, respectively. They claimed that waste EPP would be suitable for replacing conventional PP matrix in natural fiber composites.

Bogataj et al. (2019) used cellulose (CF) and newsprint (NP) fibers to prepare composites with recycled PP, with the addition of impact modifier and compatibilizing agent, by extrusion melting and injection molding. Tensile strength of the composites filled with CF and NP fibers was 36 and 29 MPa, respectively, which is higher than the value of 23 MPa obtained for neat recycled PP. The fiber increased the Young's modulus of composites. They claimed that waste paper in the form of recovered cellulose or reclaimed newsprint fiber constitute a promising alternative to inorganic fillers.

Pineapple fibers are also used for preparing composites with recycled PP, as did Reichert et al. (2020) with fibers from pineapple crown waste (both mercerized and

neat) and PP recycled from cups. Mercerization increased crystallization degree and partially removed hemicellulose and lignin. All composites have higher values of the elastic modulus than neat recycled PP; however, they found no differences in the elastic modulus between the different types and amounts of fibers.

Finally, there have been some attempts to prepare composites with natural fibers and recycled PP for 3D printing applications. In this way, Stoof and Pickering (2017) reinforced recycled PP with harakeke natural fibers and gypsum powder for applications in fused deposition modeling (FDM). The authors developed a novel method of measuring the shrinkage effects in 3D printed components. They found improvements of 77% and 275% in tensile strength and Young's modulus, respectively. The composite with the least shrinkage contained 30 wt% harakeke with a shrinkage value of 0.34%, resulting in a net reduction of 84% relative to plain PP. Morales et al. (2021) developed sustainable 3D printing filaments based on rice husk (RH), an agricultural residue, and recycled PP, analyzing the influence of fiber weight ratio on the physical, thermal, mechanical, and morphological properties of 3D printing parts. They found that the degradation process of composites started earlier than for the neat PP because of the lignocellulosic fiber components. Mechanical tests showed that tensile strength increased when using a raster angle of 0° than specimens printed at 90° because of the weaker inter-layer bonding compared to in-layer one. During the printing process, composites presented lower warping than printed neat PP. Thus, they conclude by pointing out that 3D printable eco-friendly natural fiber composite filaments with low density and low cost could be developed and used for 3D printing applications.

4 Conclusions

- With the aim of reducing the impact of increasing plastic wastes, the development of composite materials with recycled plastics (mainly PET and PP) and natural fibers has increased in recent years.
- Even though some attempts have been made to directly recover PET from composites, as in most cases, PET recycling techniques are not suitable for that purpose, composites based on previously recycled PET and natural fibers constitute the majority found in the literature.
- Several authors have successfully prepared composites of recycled PET and different fibers such as cotton, bagasse, or sisal ones, among others, using compatibilizers for better adhesion or plasticizers to decrease processing temperature.
- Composites based on recycled polymer blends based on PET (with PBAT, HDPE, LDPE, or PP, among others) and natural fibers such as wood flour or saw dust have also been successfully prepared, with the use of compatibilizer to improve characteristics.
- Composites based on polymers, such as UPR derived from the chemical recycling of PET and natural fibers, have also been prepared in a promising way.

- Composites with recycled PP as matrix and natural fibers have also been developed, particularly by treating fiber surface with NaOH or using compatibilizers such as MAPP.
- Even though most of fibers led to the improvement of flexural or tensile properties, as found by several authors for different fibers such as spruce ones, coconut or coffee husk, pineapple or cellulose, impact properties were not improved, presenting poor impact behavior in most of the cases.
- A promising way for 3D printing applications is being developed based on composites with recycled PP and natural fibers.

References

- Abdullah MZ, Che Aslan NH (2019) Performance evaluation of composite from recycled polypropylene reinforced with Mengkuang leaf Fiber. *Resources* 8:97–106. <https://doi.org/10.3390/resources8020097>
- Adhikary KB, Pang S, Staiger MP (2008) Dimensional stability and mechanical behaviour of wood-plastic composites based on recycled and virgin high-density polyethylene. *Compos Part B Eng* 39:807–815. <https://doi.org/10.1016/j.compositesb.2007.10.005>
- Ahmad I, Mosadeghzad Z, Daik R, Ramli A (2008) The effect of alkali treatment and filler size on the properties of sawdust/UPR composites based on recycled PET wastes. *J Appl Polym Sci* 109:3651–3658. <https://doi.org/10.1002/app28488>
- Al-Maadeed MA, Labidi S (2014) Recycled polymers in natural fiber-reinforced polymer composites. In: Hodzic A, Shanks R (eds) *Natural fiber composites*. Woodhead Publishing/Elsevier
- Ardekani SM, Dehghani A, Al-Maadeed MA, Wahit MU, Hassan A (2014) Mechanical and thermal properties of recycled poly(ethylene terephthalate) reinforced newspaper fiber composites. *Fibers Polym* 15:1531–1538. <https://doi.org/10.1007/s12221-014-1531-y>
- Bogatay VZ, Fajs P, Peñalva C, Omahen M, Cop M, Henttonen A (2019) Utilization of recycled polypropylene, cellulose and newsprint fibres for production of green composites 7:36–46. <https://doi.org/10.31025/2611-4135/2019.13857>
- Bourmaud A, Le Duigou A, Baley C (2011) What is the technical and environmental interest in reusing a recycled polypropylene-hemp fibre composite? *Polym Degrad Stab* 96:1732–1739. <https://doi.org/10.1016/j.polymdegradstab.2011.08.003>
- Carrete I (2019) Development and characterization of polyethylene terephthalate (PET)-cotton natural fiber-reinforced composites from waste materials. Dissertation, University of Texas at El Paso
- Chaiwutthinan P, Pimpong A, Larpkasemsuk A, Chuayjuljit S, Boonmahitthisud A (2019) Wood plastic composites based on recycled poly(ethyleneterephthalate) and poly(butylene adipate-co-terephthalate). *J Metal Mater Min* 29:87–97. <https://doi.org/10.14456/jmmm.2019.23>
- Chapa-Martínez CA, Hinojosa-Reyes L, Hernández-Ramírez A, Ruiz-Ruiz E, Maya-Treviño L, Guzmán-Mar JL (2016) An evaluation of the migration of antimony from polyethylene terephthalate (PET) plastic used for bottled drinking water. *Sci Total Environ* 565:511–518. <https://doi.org/10.1016/j.scitotenv.2016.04.184>
- Cho D, Seo JM, Park WH, Han SO, Hwang TW, Choi CH, Jung SJ (2007) Fiber surface treatments for improvement of the interfacial adhesion and flexural and thermal properties of jute/poly(lactic acid) biocomposites. *J Biobased Mater Bioenergy* 1:331–340. <https://doi.org/10.1166/jbmb.2007.007>
- Cho D, Lee HS, Han SO (2009) Effect of fiber surface modification on the interfacial and mechanical properties of Kenaf Fiber-reinforced thermoplastic and thermosetting polymer composites. *Compos Interfaces* 16:711–729. <https://doi.org/10.1163/092764409X12477427307537>

- Corradini E, Ito EN, Marconcini JM, Rios CT, Agnelli JAM, Mattoso LHC (2008) Interfacial behavior of composites of recycled poly(ethylene terephthalate) and sugarcane bagasse fiber. *Polym Test* 28:183–187. <https://doi.org/10.1016/j.polymertesting.2008.11.014>
- Dairi B, Djidjelli H, Boukerrou A, Migneault S, Koubaa A (2017) Morphological, mechanical, and physical properties of composites made with wood flour reinforced polypropylene/recycled poly(ethylene terephthalate) blends. *Polym Compos* 38:101–113. <https://doi.org/10.1002/pc.23745>
- Rios AS (2015) Mechanical behavior of recycled polypropylene reinforced by coconut fibers using X-ray tomography and digital image correlation. *Mechanical engineering [physics.class-ph]*. Université Paris-Saclay; Universidade federal do Ceará. NNT:2015SACLN023
- Dehghani A, Madadi Ardekani S, Al-Maadeed MA, Hassan A, Wahit MU (2013) Mechanical and thermal properties of date palm leaf fiber reinforced recycled PET composites. *Mater Des* 52:841–848. <https://doi.org/10.1016/j.matdes.2013.06.022>
- Fahim IS, Elhaggar S (2012) Reinforcement of plastic waste with treated natural fibers. *Nat Resour* 3:6–10. <https://doi.org/10.4236/nr.2012.31002>
- Farahani GN, Ahmad I, Mosadeghzad Z (2012) Effect of fiber content, fiber length and alkali treatment on properties of kenaf fiber/UPR composites based on recycled PET wastes. *Polym Plast Technol Eng* 51:634–639. <https://doi.org/10.1080/03602559.2012.659314>
- Favis BD, Le Corroller P (2017) Polymeric material and process for recycling plastic blends. U.S. Patent 9, 670, 344, 6 July 2017
- Francis R (2016) *Recycling of polymers: methods, characterization and applications*. Wiley, Hoboken
- Garside M (2020) Global plastic production 1950–2018. Available from: <https://www.statista.com/statistics/282732/global-production-of-plastics-since-1950>
- Grigore ME (2017) Methods of recycling, properties and applications of recycled thermoplastic polymers. *Recycling* 2:24–35. <https://doi.org/10.3390/recycling2040024>
- Hidalgo-Salazar MA, Correa-Aguirre JP, Montalvo-Navarrete JM, Lopez-Rodríguez DF, Rojas-González AF (2018) Recycled polypropylene-coffee husk and coir coconut biocomposites: morphological, mechanical, thermal and environmental studies. In: Evingür GA, Achilias DS (eds) *Thermosoftening plastics*. In Tech Open, Rijeka
- Ilyas RA, Sapuan SM, Sabaruddin FA, Atikah MSN, Ibrahim R, Asyraf MRM, Huzaifah MRM, SaifulAzry SOA, Ainun ZMA (2021) Reuse and recycle of biobased packaging products. In: Sapuan SM, Ilyas RA (eds) *Bio-based packaging: material, environmental and economic aspects*. Wiley, Hoboken
- Khan MZR, Srivastava SK, Gupta MK (2018) Tensile and flexural properties of natural fiber reinforced polymer composites: a review. *J Reinf Plast Compos* 37:1435–1455. <https://doi.org/10.1177/0731684418799528>
- Kim J, Cho D (2020) Effects of waste expanded polypropylene as recycled matrix on the flexural, impact, and heat deflection temperature properties of Kenaf Fiber/PP composites. *Polymers* 12:2578–2587. <https://doi.org/10.3390/polym12112578>
- Ku H, Wang H, Pattarachaiyakoo N, Trada M (2011) A review on the tensile properties of natural fiber reinforced polymer composites. *Compos Part B Eng* 42:856–873. <https://doi.org/10.1016/j.compositesb.2011.01.010>
- Lee HS, Cho D, Han SO (2008) Effect of natural Fiber surface treatments on the interfacial and mechanical properties of henequen/polypropylene biocomposites. *Macromol Res* 16:411–417. <https://doi.org/10.1007/BF03218538>
- Martinez Lopez Y, Paes JB, Gustavo D, Gonçalves FG, M'endez FC, Theodoro Nantet AC (2020) Production of wood-plastic composites using *Cedrela odorata* sawdust waste and recycled thermoplastics mixture from post-consumer products – a sustainable approach for cleaner production in Cuba. *J Clean Prod* 244:118723. <https://doi.org/10.1016/j.jclepro.2019.118723>
- Mendiburu-Valor E, Mondragon G, Gonzalez N, Kortaberria G, Eceiza A, Peña-Rodríguez C (2021) Improving the efficiency for the production of bis-(2-hydroxy- 2-ethyl) terephthalate (BHET) from the glycolysis reaction of poly(ethylene terephthalate) (PET) in a pressure reactor. *Polymers* 13:1461–1475. <https://doi.org/10.3390/polym13091461>

- Mohammed L, Ansari MNM, Pua G, Jawaid M, Islam MS (2015) A review on natural fiber reinforced polymer composite and its applications. *Int J Polym Sci* 2015:Article ID 243947. <https://doi.org/10.1155/2015/243947>
- Morales MA, Atencio Martinez CL, Maranon A, Hernandez C, Michaud V, Porras A (2021) Development and characterization of Rice husk and recycled polypropylene composite filaments for 3D printing. *Polymers* 13:1067–1074. <https://doi.org/10.3390/polym13071067>
- Mosavi-Mirkolaei ST, Najafi SK, Tajvidi M (2019) Physical and mechanical properties of wood-plastic composites made with microfibrillar blends of LDPE, HDPE and PET. *Fibers Polym* 20:2156–2165. <https://doi.org/10.1007/s12221-019-1089-9>
- Olah GA, Goeppert A, Prakash GS (2008) Chemical recycling of carbon dioxide to methanol and dimethyl ether: from greenhouse gas to renewable, environmentally carbon neutral fuels and synthetic hydrocarbons. *J Org Chem* 74:487–498. <https://doi.org/10.1021/jo801260f>
- Palakurthi M (2016) Development of composites from waste PET-cotton textiles. Dissertation, University of Nebraska-Lincoln
- PlasticsEurope (2019) *Plastics – the facts 2018*. PlasticsEurope, Brussels
- Quynh Truong Hoang T, Lagattu F, Brillaud J (2010) Natural Fiber-reinforced recycled polypropylene: microstructural and mechanical properties. *J Reinf Plast Compos* 29:209–217. <https://doi.org/10.1177/0731684408096931>
- Reichert AA, Ribas de Sá M, Hochmuller E, da Silva G, Gonçalves Beatrice CA, Fajardo AR, Dantas de Oliveira A (2020) Utilization of pineapple crown Fiber and recycled polypropylene for production of sustainable composites. *J Renewable Mater* 8:1327–1341. <https://doi.org/10.32604/jrm.2020.010291>
- Saleh TA, Danmaliki GI (2017) Polymer consumption, environmental concerns, possible disposal options, and recycling for water treatment. In: Saleh TA (ed) *Advanced nanomaterials for water engineering, treatment, and hydraulics*. IGI Global, Hershey
- Santos RPDO, Castro DO, Ruvolo-Filho AC, Frollini E (2014) Processing and thermal properties of composites based on recycled PET, sisal fibers, and renewable plasticizers. *J Appl Polym Sci* 131:1–13. <https://doi.org/10.1002/app.40386>
- Singh N, Hui D, Singh R, Ahuja I, Feo L, Fraternali F (2017) Recycling of plastic solid waste: a state of art review and future applications. *Compos Part B Eng* 115:409–422. <https://doi.org/10.1016/j.compositesb.2016.09.013>
- Srebrenkoska V, Bogoeva-Gaceva G, Avella M, Ericco ME, Gentile G (2009) Utilization of recycled polypropylene for production of eco-composites. *Polym Plast Technol Eng* 48:1113–1120. <https://doi.org/10.1080/03602550903147247>
- Stoof D, Pickering KL (2017) 3D printing of natural fibre reinforced recycled polypropylene. In: Bickerton S, Lin RJ, Somashekar AA, Singh I, Srivatsan TS (eds) *Processing and fabrication of advanced materials – XXV*. University of Auckland, Auckland, pp 668–691
- Tan C, Ahmad I, Heng M (2011) Characterization of polyester composites from recycled polyethylene terephthalate reinforced with empty fruit bunch fibers. *Mater Des* 32:4493–4501. <https://doi.org/10.1016/j.matdes.2011.03.037>
- UNEP, United Nations Environment Programme (2016) *Marine plastic debris and microplastics – global lessons and research to inspire action and guide policy change*. United Nations Environment Programme, Nairobi
- Wei HS, Liu KT, Chang YC, Chan CH, Lee CC, Kuo CC (2017) Superior mechanical properties of hybrid organic-inorganic superhydrophilic thin film on plastic substrate. *Surf Coat Technol* 320:377–382
- Xie Y, Hill CAS, Xiao Z, Militz H, Mai C (2010) Silane coupling agents used for natural fibre/polymer composites: a review. *Compos Part A Appl Sci Manuf* 41:806–819. <https://doi.org/10.1016/j.compositesa.2010.03.005>
- Yabuki K, Tanaka Y, Kobayashi H (2003) U.S. Patent No. 6,527,987. U.S. Patent and Trademark Office, Washington, DC
- Zou Y, Reddy N, Yang Y (2011) Reusing polyester/cotton blend fabrics for composites. *Compos Part B Eng* 42:763–770. <https://doi.org/10.1016/j.compositesb.2011.01.022>

Mechanical Properties of Recycled Polyolefin Composites



Ruey Shan Chen, Mohd Nazry Salleh, and Sinyee Gan

1 Introduction

Humans have been evolving and employing materials as devices to solve problems since the Stone Age for many thousands of years. Materials are essential components for increasing human productivity and living conditions. It represents human power to understand the world and alter nature through social productive force, science, and technology (Wang et al. 2011). At the fast pace of current science technology and innovation, demand for the stringent specific materials with multifunctional and yet environmental-friendly elements has emerged in the material engineering fields. High-performance plastics and composites, which first arose in the twentieth century, have invaded the national economy and people's lives in a variety of areas at an unprecedented rate of growth in history (Wang et al. 2011). They have become the substitutes for traditional materials such as steel, iron, wood, and so on, with improved performance but lower weight and density.

R. S. Chen (✉)

Department of Applied Physics, Faculty of Science and Technology,
Universiti Kebangsaan Malaysia, Bangi, Selangor, Malaysia

Advanced Polymer Group, Center of Excellence Geopolymer and Green Technology
(CEGeoGTech), Universiti Malaysia Perlis, Arau, Perlis, Malaysia
e-mail: chen@ukm.edu.my

M. N. Salleh

Advanced Polymer Group, Center of Excellence Geopolymer and Green Technology
(CEGeoGTech), Universiti Malaysia Perlis, Arau, Perlis, Malaysia

Faculty of Chemical Engineering Technology, Universiti Malaysia Perlis,
Arau, Perlis, Malaysia

S. Gan

Malaysian Palm Oil Board, Kajang, Selangor, Malaysia

© The Author(s), under exclusive license to Springer Nature
Switzerland AG 2023

H. Ismail et al. (eds.), *Recycled Polymer Blends and Composites*,
https://doi.org/10.1007/978-3-031-37046-5_4

Composite is a multiphase system material produced from a matrix and reinforcement constituents together (usually fiber) to achieve superior mechanical properties without dissolving or blending together. Composite materials have appeared in our daily lives, especially in infrastructure and therapeutic application, petroleum and natural gas transportation, sports, aerospace, as well as many other fields and sectors (Ngo 2020). They have numerous features such as high corrosion resistance, design flexibility, durability, low weight, and higher mechanical strength. Many composite materials were created from laboratory experiments to practical fabrication during War World II (Johnson 2018). The composite inventors attempted to bring composites into other areas such as aircraft, building, and logistics. In the early 1980s, composites were first used in construction fields in Asia and Europe, when an all-composites-based materials pedestrian bridge was built in Aberfeldy, Scotland (Ngo 2020). The composite sector has still been growing nowadays, with most of the development concentrated on renewable energy.

Composites can be generally classified into three categories based on their primary matrix phase in the composites, which are metal matrix composites (MMC), ceramic matrix composites (CMC), and polymer matrix composites (PMC), as illustrated in Fig. 1. The composite components created by using certain processes from metallic, nonmetallic, and polymeric constituents may keep the benefits of the original components while also resolving some flaws and showing some new characteristics (Wang et al. 2011). PMC is an engineering material designed with significantly different physical and chemical properties by using two or more constituent materials to reinforce a neat polymer. It comprises a variety of short or continuous long fibers that are embedded in an organic polymer matrix (Advani and Hsiao 2012).

PMC can be classified based on whether the matrix is a thermoset or thermoplastic (Zia et al. 2017). The levels of mechanical properties such as strength and stiffness are commonly used to distinguish types of PMC. Reinforced plastics are generally composed of thermoplastic resins with high modulus, high strength, high elastic elongation, good chemical and solvent resistance, and low density with

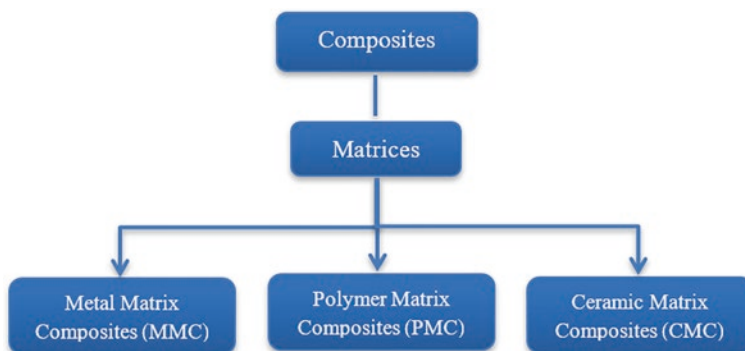


Fig. 1 Classification of composites

reinforcing phase. An advanced composite offers greater strength and stiffness, which are usually used in high-performance applications such as automobile, marine, and aerospace structures over 15 years (Advani and Hsiao 2012). Composite materials usually achieve good mechanical properties, which is contributed from the strong bond of interfacial adhesive bonding between the polymer matrix with the stiff reinforcement. The following are four characteristics of a polymer matrix composite: (1) non-homogeneous materials with a different microscopically interface; (2) there are substantial large differences in the performance of each material component; (3) composites should have improvement in properties; and (4) volume fraction of material components are larger than 10% (Wang et al. 2011).


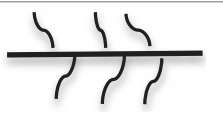

Fibers or filaments, whiskers, particulates, and so on are typical examples of reinforcement used in polymer matrix composites. The fiber is the load bear component in the composites and stronger than the matrix due to high strength and modulus properties. The matrix phase is required to have good adhesion properties to bond with the reinforcing phase in order to effectively transfer applied stress to the reinforcement. Simultaneously, the polymer matrix can be used to distribute the tensile stress uniformly throughout the composites and absorb energy in the polymer chains during elongation (Wang et al. 2011). Fiber–matrix debonding usually happens in thermomechanical loading due to the poor wetting properties between the matrix and the reinforcement with different size of porosity (Talreja and Varna 2015).

1.1 Recycled Polyolefins Phase

Polyolefin is a group of macromolecules with the chemical formula (CH_2CHR), which is synthesized by the polymerization of olefin monomer units. It is also known as polyalkene and the most common polyolefins are polypropylene (PP) and polyethylene (PE) (Hong et al. 2002). PE is the largest volume of polyolefin with a variety of grades based on their molecular weight, density, side branching, and so on, as shown in Table 1. These thermoplastic polymers can be molded into a wide range of products or various applications when it is heated and solidified upon cooling. They have a unique characteristic with the processing frequency as the chemical reaction is reversible and softened when heating. Because of its lightweight, inexpensive, and durable properties, the development of thermoplastic has dramatically risen, resulting in a global crisis with disposal of plastic wastes. The plastic wastes have been accumulated and treated as debris in landfill and other natural environment (Grigore 2017). This is because plastic materials have been mass produced around 60 years since the industrial age and most of them are not biodegradable (Andrady 1994). For instance, plastic bags need up to 300–1000 years for photodegradation in the soil, in which the plastics will break down to small toxicity particles that are immensely harmful to environment (Ilyas et al. 2021).

Low-density polyethylene (LDPE), linear low-density polyethylene (LLDPE), high-density polyethylene (HDPE), polypropylene (PP), polyethylene terephthalate

Table 1 Classification of PE based on density, molecular weight (MW), percentage of crystallinity, and polymer conformation (Pruitt 2017)

Polymer	Conformation	Density (g/cm ³)	Molecular weight (g/mol)	% Crystallinity	Application
LDPE		0.910–0.925	30,000–50,000	30–40	Packaging, film, catheters
LLDPE		0.919–0.925	192,000	30–45	Plastic bags, sheets, plastic wraps, toys, etc.
MDPE	Shorter side branching than LDPE	0.926–0.940	60,000–100,000	50–60	Facial implants
HDPE		0.941–0.970	200,000–500,000	70–90	Tendons, catheters
Ultra-high molecular weight PE (UHMWPE)	Longer and linear chains than HDPE, which effectively transfer load	0.925–0.935	4–6 million	45–60	Orthopedic bearings

(PET), and polystyrene (PS) are the common families of polyolefin. They are widely used in industrial and commercial packaging, household products, containers, and so on. This generates a significant number of polyolefins, particularly packaging, which might possibly be recovered for recycling. Even though the recycling process of these materials may be challenging, the mechanical properties such as tensile strength of the recovered plastics are still rather good for some applications. However, poor stiffness and creep resistance of recycling polyolefin components are restricted in their usage (Selke and Wichman 2004). This can be overcome by incorporating a secondary reinforcing phase to improve the rigidity and stiffness of the recycled plastic. For composites, the interface is not considered to be changed during recycling, but the resulting mechanical performance of in-plant recycled fiber glass-reinforced nylon demonstrated that instead the fiber length had a strong influence on the strength (Eriksson et al. 1996).

In 2019, over 380 million tons of postconsumer plastic wastes were produced, and the report showed that the global packaging industries generated 42% and 17% by the construction sector (Rafey and Siddiqui 2021). It is estimated that the global plastic consumption by 2050 will increase to 500 million tons of which the major consumer is the single-use plastics-based products (Ncube et al. 2021). Therefore, plastic trash has earned public attention and criticism due to its high visibility, voluminous nature, slow degradability, and short service life. Due to the sustainability of the environment, recycling of polymeric materials is one way to reduce the environmental impact and resource depletion. Basically, recycling is the act of collecting

and converting the plastic wastes that would be discarded as garbage and developing them into a reusable product to extend the service periods. These plastic wastes include water bottles, plastic bags, food wrappers, plastic containers, plastic insulator covers, and so on. In fact, recycling minimizes the amount of plastic waste disposed in landfills and incinerators and helps protect the environment by decreasing the demand for raw materials extraction such as mining, logging, and quarrying. This might significantly contribute to energy saving as well as the conservation of natural resources such as lumber, water, and minerals. Apart from that, recycling also helps to prevent severe pollution such as greenhouse effect, air pollution caused by plastic wastes incineration, water pollution (landfill), ecosystem imbalance, extinction of wildlife, and so on (Karlsson 2004).

Recycling can be accomplished by either mechanically, chemically, and energetically. Mechanical recycling is accomplished by physical techniques such as grinding, remelting, and reprocessing. While chemical recycling is done by decomposition of polymers to monomers or other low molecular weight compounds that can be utilized to create new goods. The recycling through energetically is worked through heat or electricity generated from incineration of plastic wastes. Nevertheless, recycling of polyolefins is more challenging than plastic produced from crude oil refining. Polymers can easily undergo chemical and physical changes during manufacturing and industrial production. They are subjected to oxygen reactions at every step of their life cycle. The formation of new functional groups during the oxidation process increases the recycle more vulnerable to heat and photodegradation. Besides, recovery plastics usually interact with the non-polymeric impurities and contaminants, which may affect the long-term service life and mechanical stability of application (Karlsson 2004). In recent decades, numerous research studies have been conducted on the blends (Aumnate et al. 2019; Barbosa et al. 2017; Matei et al. 2017; Pimentel et al. 2018; Thodsaratpreeyakul et al. 2018) and composites based on postconsumer or recycled polymers from different polymer types such as PE (Yu et al. 2018; Murat et al. 2020; Ilori et al. 2018; Chen et al. 2020; Beigloo et al. 2017; Akter et al. 2021), PP (Narayanan et al. 2018; Meftah et al. 2018; Karina et al. 2017; Bogataj et al. 2019; Abdullah and Che Aslan 2019), polyethylene terephthalate (PET) (Baek et al. 2018; Monti et al. 2021), and so on.

1.2 Reinforcing Phase

The dispersed phase is sometimes called the reinforcing phase that is added to increase mechanical strength of the polymer matrix. Fibers, sheets, or particles that are usually embedded in the polymer matrix phase can act as the reinforcing phase. Fibers are potential to reduce the weight of products and the cost of materials, while improving the renewability without compromising the composite's characteristics (Safri et al. 2018; Awais et al. 2020). The dispersion phase improves the strength of polymer matrix composites by distributing reinforcing filler in the primary matrix phase. With its stiffness and hardness properties, the reinforcing filler works as a

barrier to prevent the composites from deforming, moving dislocations, and sliding over each other when stress is applied (Akaluzia et al. 2021).

Particle-reinforced composites have a large volume fraction of particles dispersed in the matrix and the load is shared by the particles and the matrix. The diameter of the dispersed phase is often equiaxed roughly the same in all directions. Particle-reinforced composites make up the majority of commercial polymer composites. Most of these polymers serve as micron-sized particles, which often provide greater heat stability and modulus. In contrast, nano-sized particles such as nanoclay can increase physical and mechanical characteristics. Smaller particles will provide more surface area of interaction with the matrix, while longer fibers offer better reinforcing properties and better durability. However, the overall performance of the composite is determined by the effective interface adhesion between matrix and dispersed phase (Advani and Hsiao 2012).

Meanwhile, continuous fiber reinforcements often exhibit the greater mechanical characteristics such as rigidity and tensile strength. These fibers can be used in many different applications over a wide range, including continuous random mat, woven fabric, stitched fabric, and unidirectional or bidirectional fabric (Advani and Hsiao 2012). In fiber-reinforced composites, the reinforcement is the major load-bearing element and can be categorized into natural, synthetic, and semisynthetic. Fiber-reinforced composites usually include fiber glass and carbon fiber composites. If the composite is properly designed and manufactured, it can combine the strength of the reinforcement with the toughness of the matrix to create a combination of desired properties, which is not found in any single traditional material. Many composites have benefits in manipulating the desired properties of the final product. This means that the characteristics such as strength and stiffness can be readily altered by changing the volume or orientation of the reinforcing material (Oseli et al. 2020; Elkazaz et al. 2020).

2 Mechanical Properties of Recycled Polyolefin-Based Composites

2.1 Effect of Recycled Polyolefin Types and Blend Composition

Table 2 describes some recent previous studies of various recycled polyolefin blends and their mechanical performances. In the study of rPP/rLDPE by Aumnate et al. (2019), the tensile strength and Young's modulus of rPP decreased with the rLDPE content, but the improvement of elongation was observed by adding the more ductile LDPE. Interestingly, the Young's modulus of rPP/rLDPE was slightly higher, but there was no real change in tensile stress and strain as compared to virgin one. Based on the finding, the researchers proposed that this blend could be used in injection-molded or blow-molded applications such as bottles, containers, outdoor

Table 2 Mechanical properties of the various recycled polyolefin blends

Recycled polyolefin	Formulation	Mechanical performance findings	References
rPP/rLDPE	25, 50, 75, 100 wt%	Elongation of PP was improved with the addition of LDPE Comparable tensile properties compared to those of virgin PP/LDPE	Aumnate et al. (2019)
rPET/PC	25, 50, 75, 100 wt%	Flexural strength increased with the PC content up to 75 wt% Flexural modulus reduced with the PC addition	Thodsaratpreeyakul et al. (2018)
rPP/elastomer	10 wt%	Tensile and impact properties increased Tensile strength: 2.06 MPa (rPP), 8.90–11.70 MPa (rPP/elastomer) Elongation at break: 2.83% (rPP), 10.96–12.89% (rPP/elastomer) Izod impact: 4.35 kJ/m ² (rPP), 8.55–21.78 kJ/m ² (rPP/elastomer)	Matei et al. (2017)
vPP/rPP	20, 40, 60, 80 wt%	Yield strength (35.86–37.24 MPa) and elastic modulus (1395.10–1481.62 MPa) of vPP reduced with increasing the rPP content	Pimentel et al. (2018)
vPP/rPP	10, 20, 30, 100 wt%	Yield strength (20.83–21.65 MPa), elastic modulus (1702.69–1761.11 MPa), impact strength (6.67–49.53 kJ/m ²) of vPP reduced with increasing the rPP content	Barbosa et al. (2017)

Note: *PP* polypropylene, *LDPE* low-density polyethylene, *PET* polyethylene terephthalate, *PC* polycarbonate, “*r*” recycled, “*v*” virgin

decking, fencing, picnic tables, pipe, films, and sack bags. Matei et al. (2017) reported a marked increase in mechanical properties of rPET by blending with three types of elastomers. The improved elongation and impact strength in rPET/10 wt% elastomer blend is attributed to the elastomeric phase that favors the flow of rPP and stress transfer from the rPP matrix. Moreover, the flexible interface between rPP and elastomer can prevent crack propagation.

Aside from blending with different types of polyolefin, literature also established the blending of virgin polyolefin material with recycled source of same polymer type. Pimentel et al. (2018) prepared vPP/rPP blends with similar yield strength and elastic modulus as the pure vPP, as the decrease of tensile properties with the increasing rPP content was only less than 7%. The decline in elastic modulus indicates the reduced stiffness, which is contributed by the rPP of having lower molecular weight and shorter chains due to the degradation during reprocessing. The similar observation of mechanical properties of vPP/rPP blend with different formulation was reported by Barbosa et al. (2017).

2.2 Effect of Natural Reinforcements

Based on the literature review, there are numerous recycled PE- and PP-based biocomposites reinforced with various types of natural fibers such as plant leaves (Abdullah and Che Aslan 2019; Narayanan et al. 2018), rice husk (Rajendran Royan et al. 2018; Chen et al. 2015a, b, 2020), sawdust (Fletes and Rodrigue 2021; Murat et al. 2020; Silva et al. 2017), coconut (Akter et al. 2021), and so on. Overall, the addition of natural fiber at an appropriate loading has promoted a small increment in mechanical strength and a consequent decrement when the fiber loading exceeds the optimum level (Table 3). In this regard, different composite formulation shows different optimum loading level.

The maximum value of the tensile strength, for example, was found to be 20.22 MPa for 15 wt% coconut fiber-reinforced rHDPE composite (Akter et al. 2021), 22.2 MPa for 70 wt% rice husk-reinforced rHDPE/rPET composite (Chen et al. 2020), and 16.5 MPa for 30 wt% dried banana leaf-reinforced rPP composite (Narayanan et al. 2018). A higher strength means a harder but less formable material (Bogataj et al. 2019). The increase in tensile strength of the biocomposites is attributed to the homogeneous distribution of fibers in the composite material and the reasonable interfacial bonding between the matrix and fiber (Akter et al. 2021). It is interesting to note that rPP/rice straw lignin composite exhibited a slightly higher strength than those of PP-based composite as stated in Karina et al. (2017), which might be due to the probable cross-linking generated during production of rPP. On the other hand, the reduction of tensile strength, especially at high fiber content, could be ascribed to the inadequate amount of matrix resin with fiber agglomeration and poor interfacial adhesion or low compatibility between the fiber and matrix (Karina et al. 2017; Narayanan et al. 2018). In this regard, surface treatment or coupling agent could be applied to improve the compatibility and miscibility as well as interfacial bonding between the fiber and matrix phases, thereby increasing the tensile strength as shown in maleic anhydride polyethylene (MAPP)-coupled rPP/treated mengkuang leaf fiber composites (Abdullah and Che Aslan 2019).

Young's modulus is established as a measurement of a material's stiffness (Akter et al. 2021). As expected, the incorporation of natural fiber is commonly resulted in an increase in modulus, which is consistent with the stiff characteristic of natural fiber (Murat et al. 2020). Commonly, the neat PE or PP without reinforcing filler is more ductile and a longer time is required to achieve breaking compared the polymer/natural fiber-blended composites. This can be demonstrated by the decline in elongation at break with fiber addition, as stated in the reports of rPE/sawdust composite (Murat et al. 2020) and rPP/lignin composites (Karina et al. 2017). In many cases, the elongation result was similar to the impact strength trend, where higher fiber loading reduced the impact strength, and this indicates that more brittle material was obtained (Murat et al. 2020; Akter et al. 2021).

Table 3 Influence of natural fiber and its loading on the mechanical properties of the recycled polyolefin composites

Matrix	Natural fiber and loading	Mechanical performance findings	References
rHDPE	Coconut (5, 10, 15, 20 wt%)	Tensile strength: 14.76 MPa (rHDPE), 12.89–20.22 MPa (rHDPE/coconut) Flexural strength: 14.84 MPa (rHDPE), 17.25–27.41 MPa (rHDPE/coconut) Izod impact: 0.032 J/mm (rHDPE), 0.038–0.075 J/mm (rHDPE/coconut) Elastic and flexural modulus: inconsistent trend	Akter et al. (2021)
rHDPE/ rLDPE	Sawdust (20, 30 wt%)	Tensile strength, impact strength, and elongation decreased, whereas elastic modulus increased with sawdust addition	Murat et al. (2020)
rHDPE/ rPET	Rice husk (40, 50, 60, 70, 80 wt%)	Tensile properties of neat blend (strength of 19.1 MPa, modulus of 821.41 MPa) increased with rice husk addition from 40 to 70 wt% (strength of 22.2 MPa, modulus of ~1800 MPa) and decreased at 80 wt%	Chen et al. (2020)
rPP	Mengkuang leaf, ML (40 wt%)	Tensile strength: 18.1 MPa (rPP), 15.6 MPa (rPP/ML), 23.1 MPa (rPP/treated ML/MAPP) Tensile modulus: 1.6 GPa (rPP), 3.2 GPa (rPP/ML), 5.1 MPa (rPP/treated ML/MAPP) Flexural strength: 25.3 MPa (rPP), 27.7 MPa (rPP/ML), 34.9 MPa (rPP/treated ML/MAPP) Flexural modulus: 0.93 GPa (rPP), 2.03 GPa (rPP/ML), 2.23 MPa (rPP/treated ML/MAPP) Izod impact: 46.9 J/m (rPP), 23.7 J/m (rPP/ML), 30.6 J/m (rPP/treated ML/MAPP)	Abdullah and Che Aslan (2019)
rPP	Cellulose or newsprint (40 wt%)	Tensile strength and modulus increased but elongation reduced for rPP/cellulose (36 MPa, 447 MPa, 11%) and rPP/newsprint (29 MPa, 564 MPa, 9%) compared to rPP (23 MPa, 384 MPa, 49%), respectively	Bogataj et al. (2019)
rPP	Dried banana leaves (10, 20, 30, 40 wt%)	Tensile (16.5 MPa) and flexural (22.6 MPa) strengths of rPP increased up to 30 wt% (26.1 MPa) and 10 wt% (28.4 MPa), respectively, and both properties reduced afterward	Narayanan et al. (2018)
rPP PP	Rice straw lignin (10–70%)	Tensile strength (7.1–37.8 MPa for rPP-based, 6.8–34.0 MPa for PP-based) and elongation (0.7–44.0% for rPP-based, 0.7–700% for PP-based) reduced, while tensile modulus (1.22–1.44 GPa for rPP-based, 1.06–1.38 GPa for PP-based) increased with lignin content	Karina et al. (2017)

Note: *HDPE* high-density polyethylene, *LDPE* low-density polyethylene, *PET* polyethylene terephthalate, *MAPP* maleic anhydride polypropylene, *PP* polypropylene, “*r*” recycled, “*v*” – virgin

From the perspective of matrix types, the finding of Murat et al. (2020) showed that LDPE exhibited greater elongation rate but lower strength as compared to HDPE matrix. In the study of Karina et al. (2017), the tensile properties demonstrated no real changes in term of strength, modulus, and elongation, and thus it suggests the feasible substitution of rPP for virgin PP material.

2.3 Effect of Artificial Reinforcements

Based on the literature work in this study, glass fiber and carbon fiber are common synthetic-reinforcing fillers used in rPP and rPET composites. In Table 4, the recent works of recycled polyolefin/synthetic fiber composites showed a variety of investigation focuses. In the study of Monti et al. (2021), the addition of copolymers in rPET/glass had slightly reduced the stiffness (as represented by elastic modulus) where the highest reduction was presented by the reactive copolymer of E-MA/24-GMA. This is associated to the chemical interaction between the PET chain and the GMA group. On the other hand, the rPET/glass fiber with added copolymers exhibited higher ductility as represented by increased strain at break, which is due to the better interaction of PET chains with polar moiety of the copolymer. In consequence, this chemical bonding is able to hinder the initiation and propagation of the cracks, which reflects the enhanced impact strength. The rPET flakes from the used drinking bottles were integrated into PP-carbon fiber composites by Kaymakçı and co-researchers (2020). In the presence of MAPP coupling agent, the improved

Table 4 Mechanical properties of the recycled polyolefin/synthetic fiber composites

Matrix	Synthetic fiber and loading	Investigation scope	Mechanical performance findings	References
rPET	Glass (20 wt%)	Types of ethylene copolymers (E-MA/24, E-MA/24-GMA, E-MAA)	With copolymers, the stress and elastic modulus were reduced in the range of 10%, whereas the strain at break and impact strength were increased by 10–30% and 7–60%, respectively	Monti et al. (2021)
PP/rPET	Carbon (10 wt%)	Inclusion and loading of rPET (2.5, 5.0, 7.5, 10.0, 12.5, 15.0 wt%)	Addition of rPET flakes increased the tensile stress, modulus, and strain. A marked improvement in tensile stress and modulus was achieved at 5.0 wt%	Kaymakçı et al. (2020)
rPP or PP	Recycled carbon (20 wt%)	Presence of carbon fiber and strain rate tension (0.01, 0.1, 10, 100 s ⁻¹)	Better mechanical performance of rPP/carbon than the PP/carbon Mechanical properties were affected by increasing strain rate	Meftah et al. (2018)
rPET	Recycled carbon fiber mat	Thermoforming condition: processing temperatures (250, 260, 270, 280 °C), hold time (1, 3, 5, 10 min)	The optimum condition was found at 270 °C and 5 min, with tensile strength of 54.3 MPa, modulus of 2.4 GPa, and elongation of 2.6%	Baek et al. (2018)

Note: PET polyethylene terephthalate, PP polypropylene, E-MA/24 copolymer of ethylene and methyl acrylate (24 wt%), E-MA/24-GMA random terpolymer of ethylene, methyl acrylate (24 wt%), and glycidyl methacrylate (8%), E-MAA copolymer of ethylene and methacrylic acid, partially neutralized with Na⁺, “r” recycled, “v” virgin

tensile stress and strain suggests the good compatibility between the PP matrix and rPET microfibrils. In another rPP/recycled carbon composites (Meftah et al. 2018), the effect of strain rate was studied. Results showed that at a low strain rate of 0.1 s^{-1} , a good fiber–matrix adherence could lead to high local plasticity of the matrix, whereas local deformation is more concentrated around the fibers during the intermediate strain rate of 10 s^{-1} , and finally no matrix ductility is visible at 100 s^{-1} .

2.4 Effects of Nano-Size Filler

Table 5 shows the mechanical properties of the recycled polyolefin/nanofiller composites. In general, the state-of-the-art literature has shown the improvement of mechanical properties of composite with the aid of nanofiller. As described by Velásquez et al. (2021), nanofiller is a potential alternative to enhance the performances of the recycled or degraded plastic, which has a different molar mass distribution compared to vPP, dependent upon its source and grade. In order to obtain a comparable ductility with the vPP/rPP blend, organoclay of 1 wt% has increased the ductility of nanocomposites as depicted from the increased Young's modulus values

Table 5 Mechanical properties of the recycled polyolefin/nanofiller composites

Matrix	Nanofiller and loading	Mechanical performance findings	References
vPP/rPP (50/50)	NP-clay or P-clay (1, 3, 5 wt%)	Tensile strength and elongation of vPP/rPP (23.5 MPa, 199%) reduced significantly with organoclay loading (17.1–24.0 MPa and 21–36% for NP-clay; 12.9–22.8 MPa and 41–59% for P-clay) Young's modulus of vPP/rPP (473 MPa) was improved at 1 wt%, by 12% for NP-clay and 14% for P-clay	Velásquez et al. (2021)
rHDPE/rPET (75/25)	Cloisite 10A clay (1, 3, 5, 7, 9 wt%)	(i) With 5 phr E-GMA, the optimum flexural strength (24.5 MPa) and modulus (1178 MPa) were obtained (ii) Two-step compounding method gave better flexural strength (32.2 MPa) and modulus (1269 MPa) than one-step method (iii) Among the rotor speeds (30–150 rpm), 90 rpm was the optimum (flexural strength: 34.4 MPa, flexural modulus: 1318 MPa) (iv) With increasing clay loading, the flexural properties increased	Chen et al. (2017)
rPP/4 wt% PANI	Graphene (0.5–3 phr)	Presence of graphene reduced the tensile properties, yet 1.5–2.0 phr was the optimum loading	Husin et al. (2015)

Note: *PP* polypropylene, *HDPE* high-density polyethylene, *PET* polyethylene terephthalate, *PANI* polyaniline, *NP-clay* non-polar modified organoclay, *P-clay* polar modified organoclay, “*r*” recycled, “*v*” virgin

in Table 5. This is greatly due to the rigidity of the silicate structures and the intercalation of the clay layers by the polymer chains. Nevertheless, the tensile strength and elongation of vPP/rPP blend were reduced significantly with the introduction of nanoclay, especially at high clay concentration, which is possibly attributed to the severe tactoid structure formation and weakened interfacial adhesion. In short words, the mechanical properties of nanocomposite depend on the structures of PP/clay nanocomposites rather than their crystallinity as proven by Velásquez et al. (2021). On the other hand, Chen et al. 2017 proposed that the speed of rotation of the twin screw extruder and extrusion temperature would affect the mechanical properties of nanofiller-reinforced composites. According to their findings, the clay nanofiller improved the stiffness of the nanocomposite while decreased the tensile and impact strengths, and higher extrusion temperature led to greater mechanical properties. The small amount of clay content also resulted in higher elongation at breaks of the nanoclay-reinforced polymer composite. While the increasing of nanoclay reinforcement has enhanced the flexural properties and modulus of the nanocomposite (Chen et al. (2017)). Graphene is one of the most popular nanofillers being investigated in the twenty-first century. Husin et al. (2015) have reported that the higher graphene nanofiller amount could promote increment in tensile strength and tensile modulus of the rPP/PANI nanocomposites. The greater mechanical properties were attributed to the uniform dispersion of the nanofiller, stiffness of the platelets, and effective stress transfer between the matrix and nanofiller.

2.5 *Effects of Hybrid Filler*

The agricultural biomass waste is an effective alternative for a sustainable development, thus it is widely used in the composite field. Even though single fiber is frequently reinforced in composites materials, the hybridization of biofillers has shown significant improvement in properties of composite, especially mechanical and thermal properties. Table 6 shows mechanical properties of recycled polyolefin composites reinforced with hybrid fillers. Yu et al. (2018) investigated the influence of hybrid fillers (particleboard dust and basalt fibers) reinforcement in HDPE composite. The hybrid fillers of low-cost particleboard dust not only improve the recyclability of the composite but also reduce its production cost. The 40 wt% of particleboard dust hybrid filler promoted high tensile and flexural properties of hybrid filler composite with lower degree of crystallization. In another study, Ilori et al. (2018) investigated the effect of talc/glass hybrid fillers on mechanical properties of the composite under weathering or non-weathering situation. The increase of filler amount (from 0 to 40 wt%) led to greater impact strength and hardness of the rLDPE composites regardless of the weathering condition. The reinforcement of hybrid glass and talc fillers in polymer composites was proven to improve its resistivity in degradation. The combination of nanofiller and biomass fiber is tremendously exploited as the single fiber filler reinforcement lacks of outstanding improvement in composite field.

Table 6 Mechanical properties of hybrid fillers-reinforced recycled polyolefin composites

Matrix	Hybrid fillers and loading	Mechanical performance findings	References
vHDPE/ rHDPE (50/50)	Particleboard dust/basalt (50 wt%) Ratio: 2:1, 1:1, 1:2	Tensile and flexural properties were increased (by 24–46% for tensile strength, 228–320% for tensile modulus, 114–150% for flexural strength, 175–245% for flexural modulus) but impact strength was reduced by 30–38% with combined fillers, irrespective of filler ratio	Yu et al. (2018)
rLDPE	Talc/glass (10, 20, 30, 40 wt%, ratio 1:1)	Tensile strength, impact strength, and hardness were slightly improved with the presence of filler	Ilori et al. (2018)
rHDPE/ rPET (75/25)	Cloisite 10A clay (3 phr)/rice husk (70 wt%)	Inclusion of clay with coupling agent (MAPE or E-GMA) slightly increased tensile properties, and the addition of rice husk showed a further notable improvement	Chen and Ahmad (2017)
rHDPE	Wood flour (30 wt%)/ graphene (0.5, 1.5, 2.5 wt%)	Addition of 0.5 wt% graphene led to optimum flexural strength (24.77 MPa), flexural modulus (1778.5 MPa), and impact strength (32.61 J/m ²) of rHDPE/wood composite (20.5 MPa, 1604.6 MPa, 19.35 J/m ² , respectively)	Beigloo et al. (2017)

Note: *HDPE* high-density polyethylene, *LDPE* low-density polyethylene, *PET* polyethylene terephthalate, “r” recycled, “v” virgin

Our research team has carried out the reinforcement of nanoclay and rice husk hybrid fillers into recycled HDPE/PET polymer composites. The synergy effect and great interfacial interaction of nanofiller and biomass fiber rice husk (up to 70 wt%) have enhanced the mechanical properties of polymer composite (Chen and Ahmad 2017). Based on the investigation of Beigloo et al. (2017), the addition of graphene filler in composite has shown a promising improvement in durability, flexural and tensile properties. Thus, graphene was added into the wood flour-reinforced plastic composites to further improve the mechanical properties. From their findings, the incorporation of 0.5 wt% nanographene has significantly promoted the flexural modulus, flexural strength, and notched impact strength of the wood–plastic composites. This can be explained that nanofillers could enhance the connectivity of the polymer composite and fibers, thereby resulting in its excellent surface adhesion between the graphene and epoxy as well as a better slenderness ratio.

3 Conclusions

Recycled or postconsumer thermoplastics have gained extensive attention among the researchers in developing green composites. This book chapter discussed the recent research works based on recycled thermoplastic including blends, and bio-, nano-, and hybrid composites. Based on the literatures, several conclusions can be reached as follows:

- Recycled thermoplastics can provide comparable mechanical properties compared to virgin ones while offering lower price and serving as a solution to plastic waste.
- Through incorporating natural fibers including agricultural wastes onto postconsumer thermoplastics, certain mechanical properties of the resultant composites can be increased.
- By reinforcing thermoplastic with a small amount of nanoparticles, an effective improvement of mechanical performance can be obtained, promoting additional functional properties.
- Hybridization is shown to be a potential way to offer synergistic effect of overall performance in composites.

Future works can focus on the development of new green and value-added composites based on recycled polyolefins with different formulation and modification to achieve desired comparable properties for targeted application.

Acknowledgments The authors would like to acknowledge Universiti Kebangsaan Malaysia (UKM) and Ministry of Higher Education Malaysia (Fundamental Research Grant Scheme with code FRGS/1/2022/TK09/UKM/02/8).

References

- Abdullah MZ, Che Aslan NH (2019) Performance evaluation of composite from recycled polypropylene reinforced with Mengkuang leaf fiber. *Resources* 8:97. <https://doi.org/10.3390/resources8020097>
- Advani SG, Hsiao K-T (2012) Introduction to composites and manufacturing processes. In: *Manufacturing techniques for polymer matrix composites (PMCs)*. Elsevier, Sawston, United Kingdom, pp 1–12
- Akaluzia RO, Edoziuno FO, Adediran AA, Odoni BU, Edibo S, Olayanju TMA (2021) Evaluation of the effect of reinforcement particle sizes on the impact and hardness properties of hardwood charcoal particulate-polyester resin composites. *Mater Today Proc* 38:570–577. <https://doi.org/10.1016/j.matpr.2020.02.980>
- Akter R, Budrun Neher MA, Gafur RH, Ahmed F (2021) Study of the physical and mechanical properties of coconut spathe fiber reinforced obsolete polymer composites. *Mater Sci Appl* 12:223–238. <https://doi.org/10.4236/msa.2021.125015>
- Andrady AL (1994) Assessment of environmental biodegradation of synthetic polymers. *J Macromol Sci Polym Rev* 34:25–76. <https://doi.org/10.1080/15321799408009632>
- Aumnan C, Rudolph N, Sarmadi M (2019) Recycling of polypropylene/polyethylene blends: effect of chain structure on the crystallization behaviors. *Polymers* 11:1456. <https://doi.org/10.3390/polym11091456>
- Awais H, Nawab Y, Adnan Amjad A, Anjang HMA, Abidin MSZ (2020) Environmental benign natural fibre reinforced thermoplastic composites: a review. *Compos Part C Open Access* 100082. <https://doi.org/10.1016/j.jcomc.2020.100082>
- Baek Y-M, Shin P-S, Kim J-H, Park H-S, Dong-Jun Kwon K, DeVries L, Park J-M (2018) Investigation of interfacial and mechanical properties of various thermally-recycled carbon fibers/recycled PET composites. *Fibers Polym* 19:1767–1775. <https://doi.org/10.1007/s12221-018-8305-x>

- Barbosa LG, Piaia M, Henrique Ceni G (2017) Analysis of impact and tensile properties of recycled polypropylene. *Int J Mater Eng* 7:117–120. <https://doi.org/10.5923/j.jime.20170706.03>
- Beigloo JG, Eslam HK, Hemmasi AH, Bazayr B, Ghasemi I (2017) Effect of nanographene on physical, mechanical, and thermal properties and morphology of nanocomposite made of recycled high density polyethylene and wood flour. *Bioresources* 12:1382–1394. <https://doi.org/10.15376/biores.12.1.1382-1394>
- Bogataj VZ, Fajš P, Omahen M, Peñalva C, Henttonen A, Cop M (2019) Utilization of recycled polypropylene, cellulose and newsprint fibres for production of green composites. *Detritus* Volume 07-September 2019, 1
- Chen RS, Ahmad S (2017) Mechanical performance and flame retardancy of rice husk/organoclay--reinforced blend of recycled plastics. *Mater Chem Phys* 198:57–65
- Chen RS, Ab Ghani MH, Salleh MN, Ahmad S, Tarawneh M'a A (2015a) Mechanical, water absorption, and morphology of recycled polymer blend rice husk flour biocomposites. *J Appl Polym Sci* 132:2461–2472. <https://doi.org/10.1002/app.41494>
- Chen RS, Ghani MHA, Ahmad S, Salleh MN, Tarawneh M'a A (2015b) Rice husk flour biocomposites based on recycled high-density polyethylene/polyethylene terephthalate blend: effect of high filler loading on physical, mechanical and thermal properties. *J Compos Mater* 49:1241–1253. <https://doi.org/10.1177/0021998314533361>
- Chen RS, Ahmad S, Gan S (2017) Characterization of recycled thermoplastics-based nanocomposites: polymer-clay compatibility, blending procedure, processing condition, and clay content effects. *Compos B Eng* 131:91–99. <https://doi.org/10.1016/j.compositesb.2017.07.057>
- Chen RS, Ahmad S, Gan S, Tarawneh M'a A (2020) High loading rice husk green composites: dimensional stability, tensile behavior and prediction, and combustion properties. *J Thermoplast Compos Mater* 33:882–897. <https://doi.org/10.1177/0892705718815536>
- Elkazaz E, Crosby WA, Ollick AM, Elhadary M (2020) Effect of fiber volume fraction on the mechanical properties of randomly oriented glass fiber reinforced polyurethane elastomer with crosshead speeds. *Alex Eng J* 59:209–216. <https://doi.org/10.1016/j.aej.2019.12.024>
- Eriksson P-A, Albertsson A-C, Boydell P, Prautzsch G, Månson J-AE (1996) Prediction of mechanical properties of recycled fiberglass reinforced polyamide 66. *Polym Compos* 17:830–839. <https://doi.org/10.1002/PC.10676>
- Fletes RCV, Rodrigue D (2021) Effect of wood fiber surface treatment on the properties of recycled HDPE/maple fiber composites. *J Compos Sci* 5:177. <https://doi.org/10.3390/jcs5070177>
- Grigore ME (2017) Methods of recycling, properties and applications of recycled thermoplastic polymers. *Recycling* 2:24. <https://doi.org/10.3390/recycling2040024>
- Hong SC, Jia S, Teodorescu M, Kowalewski T, Matyjaszewski K, Gottfried AC, Brookhart M (2002) Polyolefin graft copolymers via living polymerization techniques: preparation of poly(n-butyl acrylate)-graft-polyethylene through the combination of Pd-mediated living olefin polymerization and atom transfer radical polymerization. *J Polym Sci A Polym Chem* 40:2736–2749. <https://doi.org/10.1002/pola.10348>
- Husin MR, Arsad A, Al-Othman O (2015) Effect of graphene loading on mechanical and morphological properties of recycled polypropylene/polyaniline nanocomposites. In: *MATEC web of conferences*
- Ilori OO, Idowu IA, Adeleke KM (2018) Comparing the effect of fillers on the mechanical properties of recycled low density polyethylene composites under non-weathered and weathered conditions. *Eur J Eng Technol Res* 3:17–20. <https://doi.org/10.24018/ejers.2018.3.5.707>
- Ilyas RA, Sapuan SM, Sabaruddin FA, Atikah MSN, Rushdan Ibrahim MRM, Asyraf MRMH, SaifulAzry SOA, Ainun ZMA (2021) Reuse and recycle of biobased packaging products. In: *Bio-based packaging: material, environmental and economic aspects*. Wiley, Hoboken, pp 413–426
- Johnson T (2018) History of composites. The evolution of lightweight composite materials. ThoughtCo. <https://www.thoughtco.com/history-of-composites-820404>

- Karina M, Syampurwadi A, Satoto R, Irmawati Y, Puspitasari T (2017) Physical and mechanical properties of recycled polypropylene composites reinforced with rice straw lignin. *Bioresources* 12:5801–5811. <https://doi.org/10.15376/biores.12.3.5801-5811>
- Karlsson S (2004) Recycled polyolefins. Material properties and means for quality determination. *Long Term Properties Polyolefins*:201–230. <https://doi.org/10.1007/b94173>
- Kaymakçı O, Ergin EB, Uyanık N (2020) Development of cost effective in-situ microfibrillar recycled PET/carbon fiber/polypropylene matrix composites with high mechanical properties. In: AIP conference proceedings
- Matei E, Răpă M, Andras AA, Predescu AM, Pantilimon C, Pica A, Predescu C (2017) Recycled polypropylene improved with thermoplastic elastomers. *Int J Polym Sci* 2017:1–10. <https://doi.org/10.1155/2017/7525923>
- Meftah H, Tamboura S, Fitoussi J, Bendaly H, Tcharkhtchi A (2018) Characterization of a new fully recycled carbon fiber reinforced composite subjected to high strain rate tension. *Appl Compos Mater* 25:507–526. <https://doi.org/10.1007/s10443-017-9632-6>
- Monti M, Scrivani MT, Kociolek I, Larsen ÅG, Olafsen K, Lambertini V (2021) Enhanced impact strength of recycled PET/glass fiber composites. *Polymers* 13:1471. <https://doi.org/10.3390/polym13091471>
- Murat BIS, Kamaluzaman MS, Azman MHN, Misroh MF (2020) Assessment of mechanical properties of recycled HDPE and LDPE plastic wastes. In: IOP conference series: materials science and engineering
- Narayanan T, Razak JA, Ahmad A, Tamri J (2018) Characterization on mechanical properties of recycled polypropylene reinforced dried banana leaves degradable composites. *SkillsMalaysia J* 4:47–53. <https://doi.org/10.5281/zenodo.5069141>
- Ncube LK, Ude AU, Ogunmuyiwa EN, Zulkifli R, Beas IN (2021) An overview of plastic waste generation and management in food packaging industries. *Recycling* 6:12. <https://doi.org/10.3390/recycling6010012>
- Ngo T-D (2020) Introduction to composite materials. In: Ngo T-D (ed) *Composite and nanocomposite materials – from knowledge to industrial applications*. IntechOpen, pp 1–27. London, UK
- Oseli A, Prodan T, Susič E, Perše LS (2020) The effect of short fiber orientation on long term shear behavior of 40% glass fiber reinforced polyphenylene sulfide. *Polym Test* 81:106262. <https://doi.org/10.1016/j.polymertesting.2019.106262>
- Pimentel IT, Acevedo NIA, Rocha MCG (2018) Rheological and mechanical properties of recycled polypropylene/virgin polypropylene blends. In: XXI Encontro Nacional de Modelagem Computacional e IX Encontro de Ciências e Tecnologia de Materiais, pp 1–8
- Pruitt LA (2017) 1.23 load-bearing medical polymers (non-degradable). *Comprehensive Biomaterials II*, 507–515. <https://doi.org/10.1016/b978-0-12-803581-8.10214-0>
- Rafey A, Siddiqui FZ (2021) A review of plastic waste management in India—challenges and opportunities. *Int J Environ Anal Chem*:1–17. <https://doi.org/10.1080/03067319.2021.1917560>
- Royan R, Royan N, Sulong AB, Yuhana NY, Chen RS, Ghani MHA, Ahmad S (2018) UV/O3 treatment as a surface modification of rice husk towards preparation of novel biocomposites. *PLoS One* 13:e0197345. <https://doi.org/10.1371/journal.pone.0197345>
- Safri SN, Azrie MT, Sultan H, Jawaid M, Jayakrishna K (2018) Impact behaviour of hybrid composites for structural applications: a review. *Compos B Eng* 133:112–121. <https://doi.org/10.1016/j.compositesb.2017.09.008>
- Selke SE, Wichman I (2004) Wood fiber/polyolefin composites. *Compos A: Appl Sci Manuf* 35:321–326. <https://doi.org/10.1016/j.compositesa.2003.09.010>
- Silva CB d, Martins AB, Catto AL, Santana RMC (2017) Effect of natural ageing on the properties of recycled polypropylene/ethylene vinyl acetate/wood flour composites. *Matéria (Rio de Janeiro)* 22:1–12. <https://doi.org/10.1590/S1517-707620170002.0168>
- Talreja R, Varna J (2015) *Modeling damage, fatigue and failure of composite materials*. Elsevier, Amsterdam, Netherlands

- Thodsaratpreeyakul W, Uawongsuwan P, Negoro T (2018) Properties of recycled-polyethylene terephthalate/polycarbonate blend fabricated by vented barrel injection molding. *Mater Sci Appl* 9:174. <https://doi.org/10.4236/msa.2018.91012>
- Velásquez E, Espinoza S, Valenzuela X, Garrido L, Galotto MJ, Guarda A, López de Dicastillo C (2021) Effect of organic modifier types on the physical–mechanical properties and overall migration of post-consumer polypropylene/clay nanocomposites for food packaging. *Polymers* 13:1502. <https://doi.org/10.3390/polym13091502>
- Wang R-M, Zheng S-R, Zheng YG (2011) *Polymer matrix composites and technology*. Elsevier, Amsterdam, Netherlands
- Yu M, Mao H, Huang R, Ge Z, Tian P, Sun L, Qinglin W, Sun K (2018) Mechanical and thermal properties of R-high density polyethylene composites reinforced with wheat straw particle-board dust and basalt fiber. *Int J Polym Sci* 2018:1–11. <https://doi.org/10.1155/2018/5101937>
- Zia KM, Zuber M, Ali M (2017) *Algae based polymers, blends, and composites: chemistry, biotechnology and materials science*. Elsevier, Amsterdam

Polymeric Substances Recycled from Excess Sludge in Wastewater Treatment Plant



Da-Qi Cao

1 Introduction

Excess sludge production by wastewater treatment plants (WWTPs) is a serious environmental problem that necessitates the development of effective sludge treatment/disposal methods (Cao 2021; Cao et al. 2018a, b, 2020c, 2021b). In addition to various wastewater treatment methods, resource recovery has become one of the future approaches that satisfy the concept of sustainable development (van Loosdrecht and Brdjanovic 2014; Winkler and van Loosdrecht 2022). The recovery of resources in wastewater, such as phosphates (Remmen et al. 2019), bioplastics (Guest et al. 2009; Ilyas et al. 2021), cellulose (Ruiken et al. 2013), alginates (Cao et al. 2017, 2020a, b, 2021a), and extracellular polymeric substances (EPSs) (Cao et al. 2018a, 2018b, 2020c, 2021b), is a forefront approach pertinent to many applications, except for recycling of reclaimed water.

Excess sludge mainly consists of cell bodies and EPSs, with EPSs accounting for 10–40% of the sludge dry weight. EPSs, mainly derived from the secretion of microbial cells and cell autolysis, are mixtures of various macromolecular substances, such as polysaccharides, proteins, humus, nucleic acid, and DNA. Among these substances, polysaccharides and proteins are the major components, accounting for 75–89% of the EPS composition. The recovered EPSs can be used as

Da-Qi Cao, Doctor of Engineering (Nagoya University), Associate Professor, Research interest: Recovery of resources from wastewater, Removal of trace organic contaminants and heavy metal ions in wastewater, Membrane separation, Preparation of novel membrane.

D.-Q. Cao (✉)

Sino-Dutch R&D Centre for Future Wastewater Treatment Technologies/Key Laboratory of Urban Stormwater System and Water Environment, Beijing University of Civil Engineering and Architecture, Beijing, China

Yau Mathematical Sciences Center, Tsinghua University, Beijing, China

adsorbents for heavy metal ions (Cao et al. 2018b, 2020c, 2021b), flame retardants (Kim et al. 2020), bio-flocculants (More et al. 2012), soil conditioners (Cao et al. 2017), animal feed additives (Matassa et al. 2015), and novel materials used for clothes and jewelry (van Loosdrecht and Brdjanovic. 2014). EPS recovery from excess sludge can not only enhance the dewatering performance of sludge but also promote sludge reduction, through which the load in the subsequent treatment and disposal of excess sludge can be decreased.

In particular, a recent innovation that targets all of these key issues is the aerobic granular sludge (AGS) technology, which allows for the simultaneous removal (or recovery) of nitrogen, carbon, and phosphate while reducing the footprint by up to 75% (Winkler and van Loosdrecht 2022). The AGS process produces alginate, a typical EPS, which account for up to 20 dry wt% of AGS (Cao et al. 2017) and are widely used in the food industry, textile printing, and paper and pharmaceuticals production (Cao et al. 2017, 2020a, b, 2021a). Alginate is a linear block copolymer of β -D-mannuronic acid and its isomer, α -L-guluronic acid, connected by α (1 \rightarrow 4) glycosidic bonds. Alginate has attracted extensive interest in various fields because of the properties of water retention, thickening, biocompatibility, and gel formation. Hence, the recovery of alginate from wastewater can expand the access to alginate and provide high economic added value to sewage treatment.

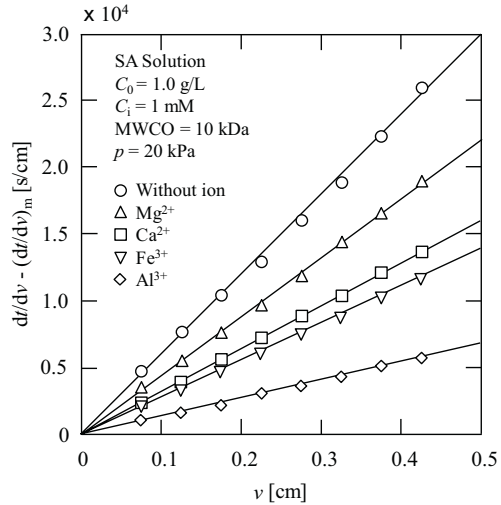
The moisture content of the EPS/alginate solution recycled in wastewater is up to 99.8%. Thus, dewatering and concentration comprises the dominant bottleneck for EPS/alginate recovery. At the same time, the application and extraction method of the recycled substances are also the research focuses currently. Therefore, the aims of this chapter are to discuss first membrane recoveries of alginate and EPSs, then to introduce heavy metal ion adsorption properties of EPSs and surfactant-enhanced ultrasonic extraction of polymeric substances, and finally to outlook five bottlenecks for polymeric substance recovery from excess sludge.

2 Membrane Recovery of Alginate

2.1 Ultrafiltration (UF) Concentration of Sodium Alginate (SA) Solution

Constant-pressure dead-end filtration with metal ions individually and in combination was carried out to evaluate membrane filtration properties for the concentration of the SA solution. The UF behaviors of SA solutions without metal ions and with the addition of 1 mM metal ion (Mg^{2+} , Ca^{2+} , Fe^{3+} , and Al^{3+}) are shown in Fig. 1. Theoretically, the relationship between the reciprocal of the filtration rate (dt/dv) and the cumulative filtrate volume collected per unit effective membrane area, v , is linear in accordance with the Ruth filtration rate equation:

Fig. 1 UF behaviors of SA solutions without metal ions and with various metal ions of 1 mM. (The figure is reprinted with the copyright permission (Cao et al. 2020a))



$$\frac{dt}{dv} = \frac{2}{K_v} v + \left(\frac{dt}{dv} \right)_m, \quad (1)$$

where t is the filtration time and v is the cumulative filtrate volume collected per unit effective membrane area. $(dt/dv)_m$ is equivalent to the flow resistance of the membrane and is an intercept on the (dt/dv) axis according to the Ruth plots of (dt/dv) as a function of v , which is the value of the reciprocal of the filtration rate at the start of filtration when no cake is formed. K_v is the Ruth filtration coefficient, indicating the filterability of the feed as defined by:

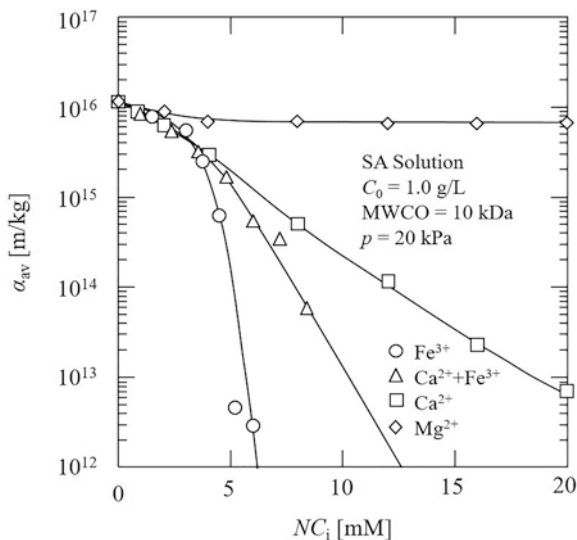
$$K_v = \frac{2p(1-ms)}{\mu\rho s\alpha_{av}}, \quad (2)$$

where p is the applied filtration pressure, m is the ratio of the mass of wet cake to the mass of particles, colloids, or polymers in the cake, s is the mass fraction of particles, colloids, or polymers in suspension, μ is the viscosity of the filtrate, ρ is the density of the filtrate, and α_{av} is the cake average specific resistance. As the term $(1 - ms)$ may be approximated by unity in filtrations conducted with dilute particles, colloids, or polymers, Eq. (2) reduces to:

$$K_v = \frac{2p}{\mu\rho s\alpha_{av}}. \quad (3)$$

Hence, the flux decline can be analyzed using the Ruth cake filtration model, although gel-like cake layers that contained both small and large metal ions-alginate particles as well as SA were found on membrane surfaces.

Fig. 2 Relationships between cake average filtration resistance, α_{av} , and the total charge concentration of metal ions, NC_i , in UF of SA solutions with Ca^{2+} , Mg^{2+} , Fe^{3+} , and $Ca^{2+} + Fe^{3+}$. (The figure is reprinted with the copyright permission (Cao et al. 2020a))



The Ruth plots in the figure, expressed as $\{(dt/dv) - (dt/dv)_m\}$ vs. v , indicate a linear relationship irrespective of the types of metal ions, in accordance with the Ruth filtration rate equation and regardless of the different forms of membrane fouling. Additionally, the declines in the filtration rate gradually slowed in the presence of the metal ion, and the ability of trivalent ions to reduce membrane fouling was noted to be more effective than that of bivalent ions, arranged in the order of $Mg^{2+} < Ca^{2+} < Fe^{3+} < Al^{3+}$ (filtration resistance mitigation).

The cake average filtration resistance, α_{av} , was calculated by Eq. (3), as shown in Fig. 2. Here, the abscissa is the total charge concentration, NC_i , which is the product of the metal ion concentration (C_i) and the ion charge number (N); $Ca^{2+} + Fe^{3+}$ is a mixture with the molar mass rate of Ca^{2+} and Fe^{3+} of 3:2, corresponding to the NC_i rate of Ca^{2+} and Fe^{3+} of 1:1. Figure 2 shows that when the total charge concentration is low ($NC_i < 5 \text{ mM}$), the α_{av} values of the four solutions are almost the same, indicating that they have the same mitigation role of membrane fouling. For the total charge concentration of $NC_i > 5 \text{ mM}$, the mitigation roles of membrane fouling increased significantly in the presence of Ca^{2+} or Fe^{3+} . However, the mitigation role remained constant for Mg^{2+} with the increase of NC_i . These results are arranged in the order of $Fe^{3+} > Fe^{3+} + Ca^{2+} > Ca^{2+} > Mg^{2+}$ (filtration resistance mitigation).

2.2 Filtration Coefficient and Recovery Rate of Alginate

The components such as particles, colloids, and polymers are included in the suspensions formed by SA solutions on the addition of metal ions. Hence, the components contributing to membrane fouling or the formation of a filter cake on the

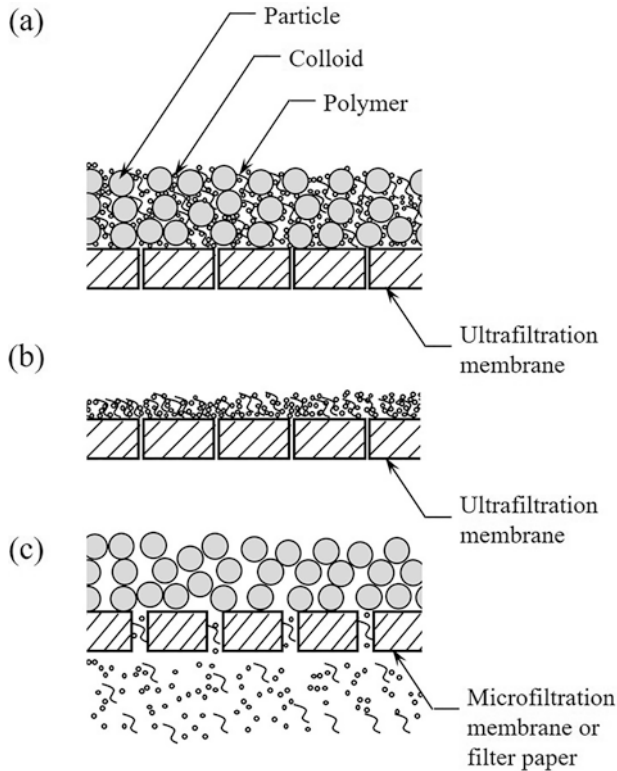


Fig. 3 Schematic of membrane fouling for sodium alginate solutions after the addition of metal ions: (a) ultrafiltration of suspension, (b) ultrafiltration of supernatant, and (c) microfiltration or filtration of suspension using a filter paper. (The figure is reprinted with the copyright permission (Cao et al. 2017))

membrane for suspensions are particles, colloids, and polymers (Fig. 3a), while for the supernatant the main materials are colloids and polymers (Fig. 3b), due to the higher settling velocity of particles during filtration. Colloids or polymers contributed to membrane resistance during the filtration of the suspension formed in the alginate solution by the addition of metal ions. The increase of K_v during the filtration of an SA solution in the presence of metal ions was mainly caused by the decrease in the concentration and α_{av} of components such as colloids and polymers. Hence, the colloids and polymers present in the suspension, which are considered to be the dominant factors for membrane fouling, may be filtered out with the filtrate (Fig. 3c); for instance, during microfiltration or filtration using a filter paper, filtration resistance may markedly decrease while alginate recovery is still effective, because colloids and polymers constituted a small portion of the alginate in the suspension formed by the SA solution with the added metal ions.

Table 1 shows the measured K_v and the alginate recovery rates, R_r , in the filtration of SA solution in the presence of Ca^{2+} . The recovery rate of alginate was calculated by

Table 1 Ruth filtration coefficients K_v and alginate recovery rates for a 10 kDa membrane, as well as 1 μm membrane and a filter paper of 7 μm at an applied pressure of 20 kPa

C_{i0} (mM)	Membrane of 10 kDa		Membrane of 1 μm		Filter paper of 7 μm	
	K_v (cm^2/s)	R_r (%)	K_v (cm^2/s)	R_r (%)	K_v (cm^2/s)	R_r (%)
1	6.20×10^{-5}	100.00	7.69×10^{-5}	59.26	1.18	67.95
2	1.34×10^{-4}	100.00	1.15×10^{-4}	97.92	1.08×10^{-4}	94.56
4	8.00×10^{-4}	100.00	7.73×10^{-4}	96.83	1.11×10^{-3}	92.45
6	3.92×10^{-3}	100.00	1.18×10^{-3}	97.38	3.38×10^{-2}	96.51
8	1.77×10^{-2}	100.00	7.47×10^{-3}	97.55	2.09	97.80
10	4.17×10^{-2}	100.00	0.47	98.53	5.44	97.90

$$R_r = 1 - \frac{C_f}{C_0}. \quad (4)$$

Here, R_r is the alginate recovery rate after filtration, C_f is the mass concentration of alginate in the filtrate at a cumulative filtrate volume collected per unit effective membrane area, $v = 1$ cm, because R_r is constant for a filtration experiment after filtration with $v = 1$ cm. At the molar concentration of calcium ion in the initial suspension, $C_{i0} < 2$ mM, R_r was less than 70% for the 1- μm membrane and 7- μm filter paper because of the formation of fewer large particles. However, at $C_{i0} \geq 2$ mM, the K_v value, which is indicative of the feed filterability, was one to two orders of magnitude greater than that observed using the 10 kDa membrane, and R_r was greater than 92% for a 1- μm membrane and 7- μm filter paper. For 7- μm filter paper, at $C_{i0} = 1$ mM, K_v was very large (1.18 cm^2/s), possibly because most of the colloids and polymers present in the suspension were filtered out with the filtrate. In addition, K_v for the 1- μm membrane and 7- μm filter paper exponentially increased with increasing concentration of Ca^{2+} added, as was observed for the 10 kDa membrane. Notably, the intrinsic resistance of a clean 10 kDa membrane ($5.94 \times 10^{12} \text{ m}^{-1}$) was considerably greater than those of the 1- μm membrane and 7- μm filter paper.

2.3 Forward Osmosis Recovery with Useful Reverse Solute Diffusion

The concentrated substances were formed and deposited on the membrane on the feed side when CaCl_2 was used as the draw solute in the forward osmosis (FO) of SA, and the typical images are shown in Fig. 4. This is because SA in feed side on the FO membrane is attracted to and combines with permeable Ca^{2+} in the draw side. The Ca^{2+} that penetrated through the FO membrane from the drive side reacted with the concentrated SA on the FO membrane and calcium alginate (Ca-Alg) was

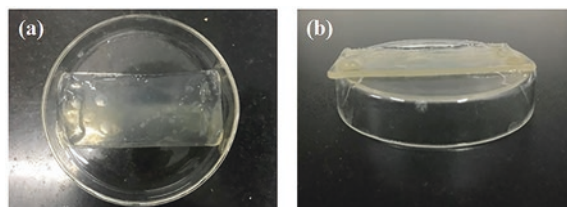


Fig. 4 Typical images of concentrated substances formed on the feed side of a forward-osmosis membrane: (a) Top view and (b) side view. (The figure is reprinted with the copyright permission (Cao et al. 2021a))

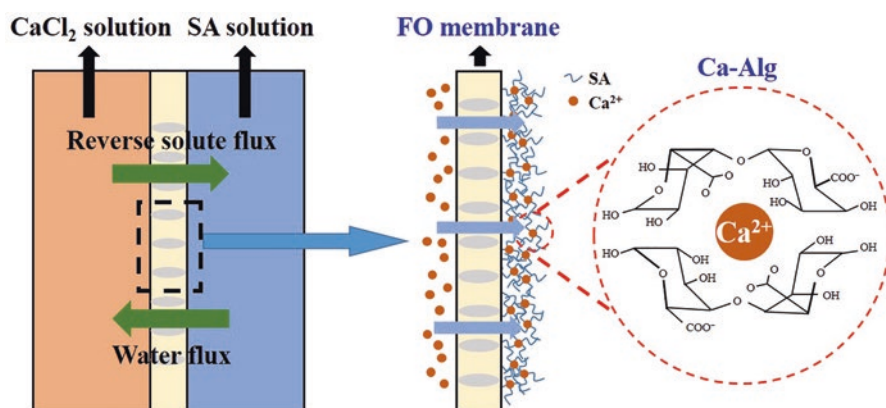


Fig. 5 Formation mechanism of calcium alginate (Ca-Alg) on feed side for sodium alginate (SA) concentration in forward osmosis (FO) with calcium salt as a draw solute. (The figure is reprinted with the copyright permission (Cao et al. 2021a))

formed. Figure 5 shows the formation mechanism of the concentrated substances on the feed side of the FO membrane. The reverse solute flux (RSF) of Ca^{2+} in the FO was limited; therefore, the intermolecular binding is preferred over intramolecular binding (bridging) (Zhang et al. 2018). The continuous RSF of Ca^{2+} gives rise to polymer bundle formation, and eventually transforms into an egg-box structure (Braccini and Perez 2001).

A moderate RSF of Ca^{2+} was required to form Ca-Alg on the FO membrane on the feed side, which is the limitation of the FO alginate concentration. The low reverse osmosis of Ca^{2+} is not enough to combine with SA to form Ca-Alg, while the high reverse osmosis of Ca^{2+} leads to a rapid decline in water flux. The concentration of CaCl_2 in the draw solution influences not only the water flux but also the RSF of Ca^{2+} , which changes the material properties of Ca-Alg formed on the FO membrane on the feed side. Furthermore, the properties of the FO membrane affect the RSF of Ca^{2+} , which depends on the novel design of the FO membrane and its properties. Therefore, the concentration of calcium salt as draw solute and FO-membrane type are the key points of future research for alginate recovery via FO.

2.4 Properties of Recycled Materials

2.4.1 Moisture Content of Filter Cake

The filter cake's moisture contents were 99.35%, 96.18%, 93.64%, and 92.32% in the UF of SA solution with the control (no metal ions), 1 mM Ca^{2+} , 1 mM Fe^{3+} , and 0.5 mM Ca^{2+} + 0.5 mM Fe^{3+} , respectively. Therefore, the moisture content of the filter cake decreased markedly in the presence of metal ions. Hence, the addition of multivalent metal ions is not only effective in mitigating membrane fouling but also decreases the moisture content of the filter cake during UF recovery.

2.4.2 Photomicrographs

Figure 6a–e shows the typical photomicrographs of the filter cake. Figure 6a shows the microstructure of SA as the control, and a three-dimensional rotating chain is observed. As shown in Fig. 6, the microstructure of the materials formed by the interaction of SA and metal ions is obviously different. In general, the addition of metal ions changed the chain structure of alginate to form larger flocs. Figure 6b is the image of Mg^{2+} binding with alginate, with long chains disappearing and inclusions appearing. Figure 6c shows that Ca^{2+} binds to alginate to form a more stable colloidal structure known as an egg-box structure. Figure 6d shows the SA microstructure with the addition of Fe^{3+} . Compared with the calcium alginate in Fig. 6c, additional clumps and some flower-like structures were formed. In Fig. 6e,

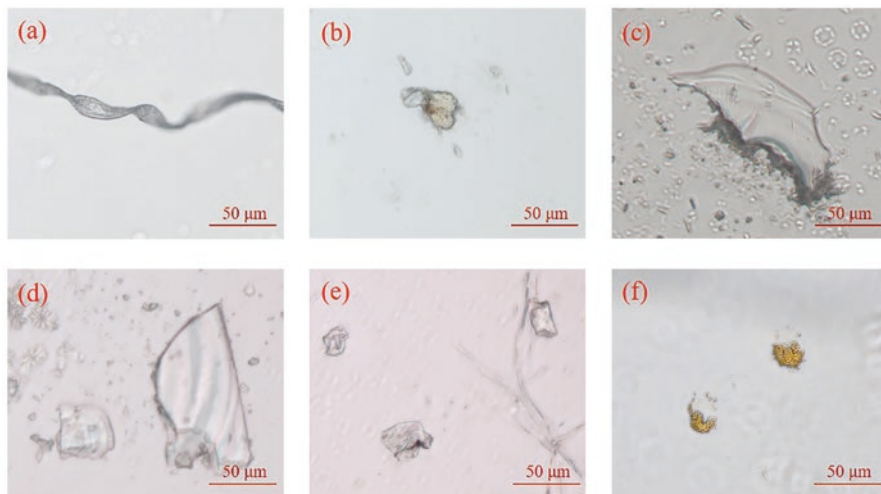
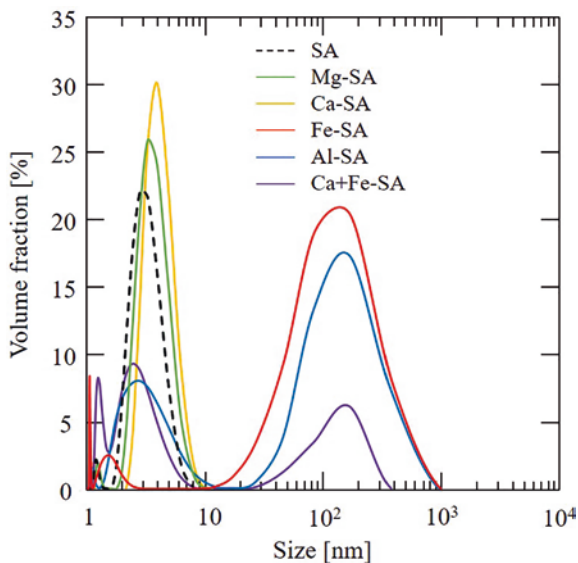


Fig. 6 Typical photomicrographs of recycled materials (filter cake): (a) SA, (b) Mg-SA, (c) Ca-SA, (d) Fe-SA, (e) Al-SA, and (f) Ca + Fe-SA. (The figure is reprinted with the copyright permission (Cao et al. 2020a))

Fig. 7 Typical size distributions of colloids and polymers present in the suspension formed in SA solution with the addition of various metal ions. (The figure is reprinted with the copyright permission (Cao et al. 2020a))



the case of Al^{3+} is similar to that of Fe^{3+} as shown in Fig. 6d. Specifically, as shown in Fig. 6f, after adding 0.5 mM Ca^{2+} and 0.5 mM Fe^{3+} , a yellow flocculent was formed instead of the block structure. Therefore, observing the microstructures of different types of alginates may provide an optical basis for further broadening the application direction of alginates such as new nanomaterials.

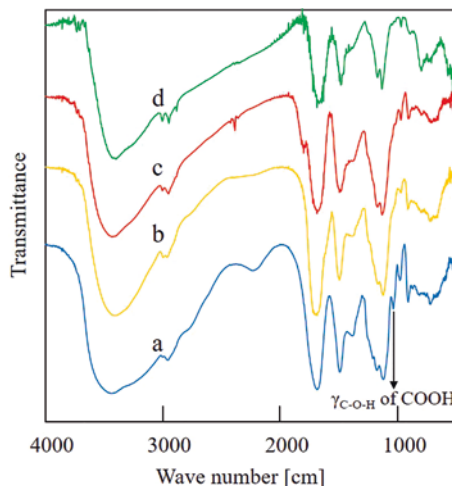
2.4.3 Size Distributions

Figure 7 shows the typical size distributions of colloids and polymers present in the suspension formed in 1.0 g/L SA solution with the addition of various metal ions. The figure shows that after adding metal ions, the particle size peak shifts to the right, meaning that larger particles are formed. Compared with the micrograph structure in Fig. 6, these results further confirmed that the reason for adding metal ions to reduce filtration resistance was that metal ions combined with SA and larger flocs were formed.

2.4.4 Fourier Transform Infrared (FTIR) Spectra

Figure 8 shows the FTIR spectra of SA and its products in reaction with metal ions: 1.0 g/L SA and 1 mM metal ions were used. Compared with SA (Fig. 8a), both Fe^{3+} and Ca^{2+} reacted with the hydroxyl groups on the carboxyl group ($-\text{COOH}$) in SA. Both show similar results in that the characteristic peak of carboxylic acid disappeared in the product as shown in Fig. 8b, c. Figure 8d shows the FTIR spectra of

Fig. 8 FTIR spectra of SA and its products in reaction with metal ions: (a) SA, (b) SA-Ca, (c) SA-Fe, and (d) SA-Fe (pH = 7). (The figure is reprinted with the copyright permission (Cao et al. 2020a))



the suspension formed by SA with Fe^{3+} at pH 7. Fe^{3+} exists in the form of hydroxide iron ($\text{Fe}(\text{OH})_3$) in this example. As shown in Fig. 8d, the characteristic peak of the carboxylic acid decreases, confirming that the hydroxide iron interacts with SA at pH 7.

2.4.5 X-ray Photoelectron Spectroscopy (XPS) Spectra

The XPS spectra in the energy range 0–1200 eV for SA and its products with metal ions are presented in Fig. 9. The figure shows that the characteristic peaks of C 1s, O 1s, Na 1s, Ca 2p, and Fe 2p can be observed for various materials formed by SA and metal ions. Compared with SA (Fig. 9a), the characteristic peaks of Ca 2p (Fig. 9b), Fe 2p (Fig. 9c), and Ca 2p and Fe 2p (Fig. 9d) were observed with the additions of Ca^{2+} , Fe^{3+} , and $\text{Ca}^{2+} + \text{Fe}^{3+}$, respectively. The Ca 2p peak can be further interpreted as a component peak with binding energies of 350.68 and 347.68 eV in Fig. 9b, d, respectively. Two peaks of Fe 2p at binding energies of around 713.08 and 724.08 eV are observed in Fig. 9c, d, respectively. However, the content of Na^+ decreases in the presence of metal ions as shown in Fig. 9b–d because Ca-alginate or Fe-alginate is formed. Therefore, the cation exchange is the interaction mechanism between SA and multivalent metal ions.

Specifically, as shown in Fig. 9d, the characteristic peaks of calcium and iron appear while the strength of Na^+ is undetectable, suggesting that the addition of mixed metal ions can bind to SA more completely. When comparing the spectra of Ca 2p and Fe 2p, as shown in Fig. 9b, c, respectively, the contents of metal ions bound to SA changed. The relative strength of iron ions increased while the calcium ions decreased. Considering the filtration behavior, the reduction of filtration resistance is mainly related to the addition of iron ions. Iron ions can occupy more

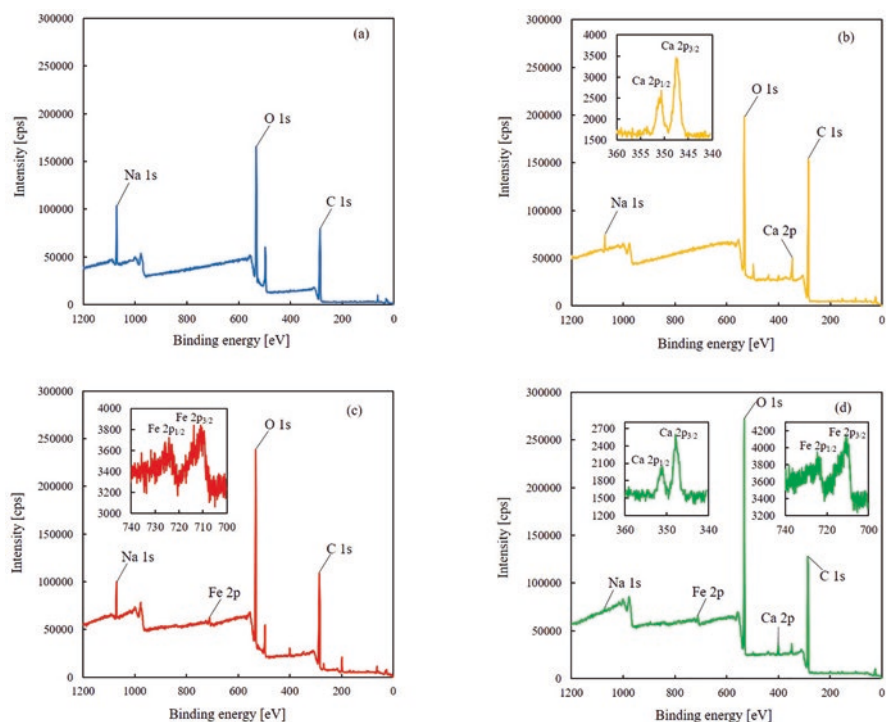


Fig. 9 XPS spectra of SA and its products in reaction with metal ions: (a) SA, (b) Ca-SA, (c) Fe-SA, and (d) Ca + Fe-SA. (The figure is reprinted with the copyright permission (Cao et al. 2020a))

binding sites for SA than calcium ions, thereby decreasing the membrane fouling. Alginate is a complex mixture and does not show uniformity, which may cause deviations in XPS analyses. Based on the unique structure of alginates and its special interaction with metal ions, the introduction of combined metal ions into alginates has become a promising method for the development of new materials.

2.4.6 Scanning Electron Microscope (SEM)

Through the analysis of SEM images, the cross sections of filter cakes formed by 1.0 g/L SA solution with and without various metal ions are shown in Fig. 10. Compared with the filter cake of the SA solution without metal ions (Fig. 10a), the filter cake of the SA solution with metal ions was porous and showed stripping near the surface of the membrane (Fig. 10b–d). The cake with Fe³⁺ (Fig. 10c) was obviously loose as compared to that with Ca²⁺ (Fig. 10b), and the porosity of the filter cake may be arranged in the order of Fe-SA > Ca + Fe-SA > Ca-SA > SA.

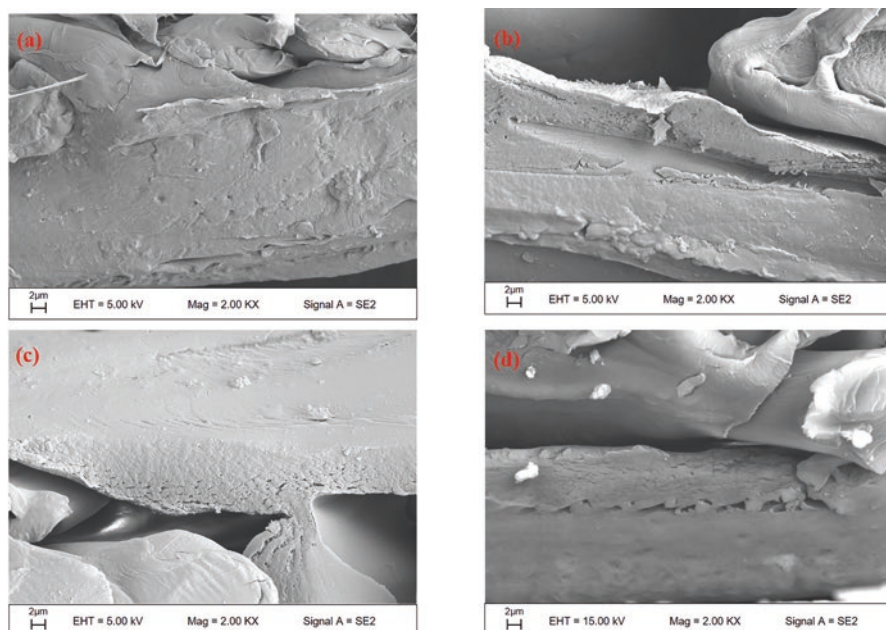


Fig. 10 SEM images of the cross sections of filter cakes formed by SA solution without and with various metal ions at 20 kPa: (a) SA, (b) Ca-SA, (c) Fe-SA, and (d) Ca + Fe-SA. (The figure is reprinted with the copyright permission (Cao et al. 2020a))

3 Membrane Recovery of EPSs and Their Heavy Metal Ion Adsorption Properties

3.1 Membrane Concentration of EPS Solutions in the Presence of Ca^{2+}

Ca^{2+} addition reduces the extent of membrane fouling during EPS isolation since the interactions between Ca^{2+} and EPS carboxylate groups increase the size and reduce the concentration of colloids/polymers in EPS suspensions (Cao et al. 2018b). The separation efficiencies of both membranes are evaluated by measuring EPS concentrations in the corresponding filtrates. Figure 11 shows the relationship between the EPS recovery efficiencies, R , and the added Ca^{2+} concentration for both membranes. As shown in the figure, unlike in the case of simulated EPS (sodium alginate) solution, for which high ultra-/microfiltration recovery efficiencies (>90%) were obtained (Cao et al. 2017), the efficiency of EPS recovery by microfiltration (0.5 μm) increased with increasing concentration of added Ca^{2+} (triangles and the fitted curve in Fig. 5), reaching values of up to 67.0% (dotted line in Fig. 11). This behavior is ascribed to the filtering out of substances that do not interact with Ca^{2+} (Cao et al. 2018a). On the other hand, the EPS recovery efficiency achieved by ultrafiltration

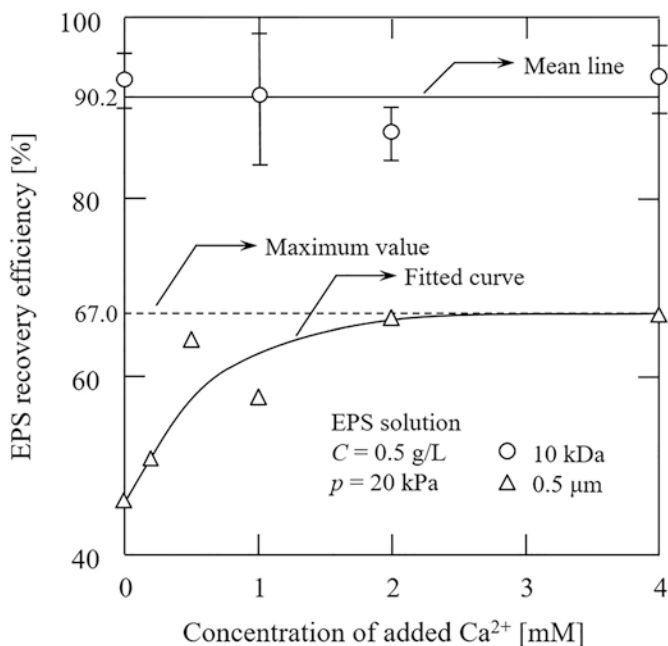


Fig. 11 Relationships between EPS recovery efficiency and concentration of added Ca²⁺ observed in ultrafiltration (10 kDa) and microfiltration (0.5 μm). (The figure is reprinted with the copyright permission (Cao et al. 2018b))

(10 kDa) was almost independent of Ca²⁺ concentration (circles in Fig. 11), probably because Ca²⁺ did not interact with EPSs with $M_w < 10$ kDa and the average efficiency of EPS recovery (90.2%, the mean line in Fig. 11) exceeded 90%. Therefore, ultrafiltration was confirmed to be well suited for highly efficient EPS recovery, and all subsequent filtration experiments were conducted using the 10-kDa ultrafiltration membrane.

3.2 MF Separation of Polysaccharides and Proteins in EPS

The separation and recovery of polysaccharides and proteins contained in EPSs is currently attracting increased research attention. Sodium alginate (SA) and bovine serum albumin (BSA) are used as a model polysaccharide and protein, respectively, to investigate the separation performance of membrane filtration in the presence of Ca²⁺. Figure 12 shows the concentrations of SA and BSA in the filtrate and the filtration behaviors for unstirred dead-end microfiltration in the presence of 1–10 mM added Ca²⁺. For a Ca²⁺ concentration (C_{0i}) of 1 mM, the filtration behavior was similar to that observed for $C_{0i} = 8$ and 10 mM, i.e., a slow increase of flux decline was detected (Fig. 12b), whereas the concentrations of SA and BSA in the filtrate were

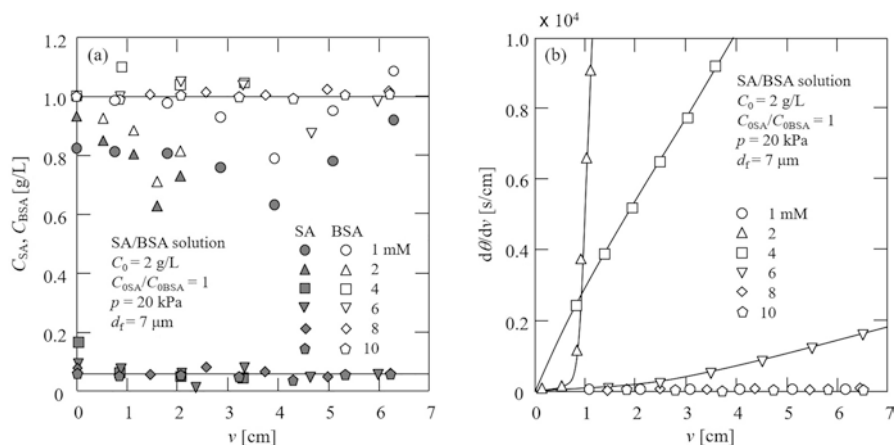


Fig. 12 (a) Filtration progress-dependent concentrations of SA and BSA in the filtrate for various concentrations of Ca^{2+} ; (b) filtration behaviors of mixed SA/BSA solutions containing various concentrations of Ca^{2+} . (The figure is reprinted with the copyright permission (Cao et al. 2018a))

identical to those in the unfiltered solution (Fig. 12a). This behavior was ascribed to the fact that the generated calcium alginate colloids were small enough to pass through the 7- μm -sized pores, and hence, SA and BSA could not be separated from each other. On the other hand, at $C_{0i} = 2$ –10 mM, the larger aggregates of calcium alginate were retained by the filter paper (Cao et al. 2017) (Fig. 12a), as reflected by the decrease of filtration resistance with increasing Ca^{2+} concentration (Fig. 12b). For $C_{0i} = 2$ mM, the filtrate still contained large amounts of SA (Fig. 12a), probably due to the shortage of Ca^{2+} . Conversely, at $C_{0i} \geq 4$ mM, the concentration of BSA in the filtrate was close to 1.0 g/L, whereas that of SA was extremely low, with both concentrations remain unchanged with progressing filtration (Fig. 12a). Therefore, $C_{0i} = 4$ mM can be considered as the minimal concentration required for an effective separation of SA and BSA. On the other hand, the recovery rate of polysaccharose approached 80% for an EPS solution containing 8 mM Ca^{2+} , using filter paper with $d_f = 7 \mu\text{m}$ (Cao et al. 2018a). Therefore, polysaccharides in EPS can be effectively separated by microfiltration with the addition of Ca^{2+} .

SA is a complex polymer composed of monomers M and G joined into homo-(MM and GG) and heteropolymeric (MG) blocks capable of binding Ca^{2+} and other ions. The above binding ability imparts the gel with a certain level of mechanical strength, which is its most prominent feature. Since BSA is a globular protein containing a variety of amino acids that cannot bind Ca^{2+} , the addition of Ca^{2+} results in the formation of calcium alginate aggregates with sizes exceeding that of BSA, which enables efficient BSA/SA separation at sufficient concentrations of Ca^{2+} .

Figure 13 schematically represents the processes occurring during unstirred and stirred dead-end filtration in the mixed solution of SA and BSA containing Ca^{2+} . As shown in Fig. 13a, the aggregates of calcium alginate are retained on the filter paper, while BSA is filtered out, which results in efficient separation. On the other hand,

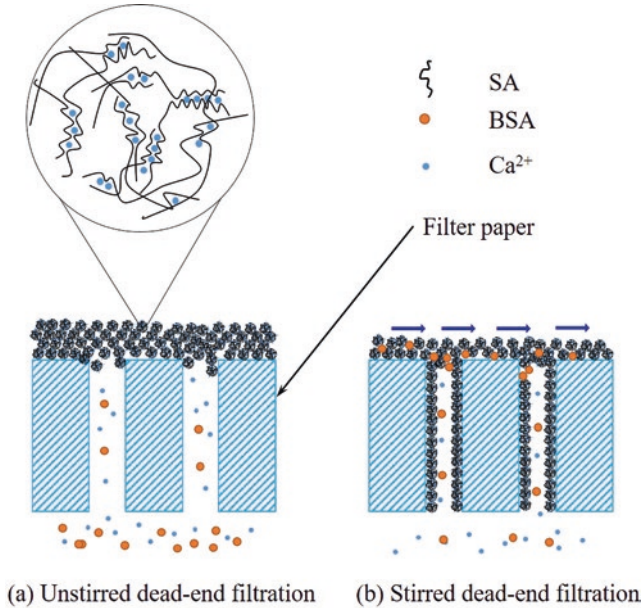


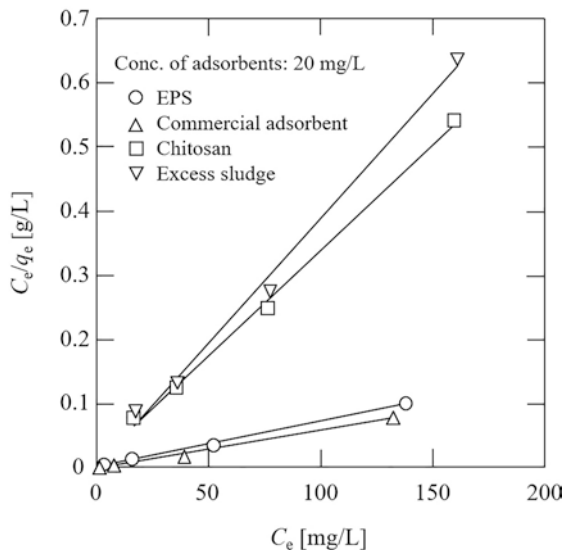
Fig. 13 Schematic representation of processes occurring during unstimulated and stimulated dead-end filtration experiments performed using mixed SA/BSA solutions containing Ca^{2+} . (The figure is reprinted with the copyright permission (Cao et al. 2018a))

Fig. 13b explains the results obtained for the influence of filtration surface shear, illustrating why filtration surface shear does not influence the separation efficiency and filtration resistance in unstimulated dead-end filtration. Notably, pore blockage becomes more severe with decreasing d_f , which results in decreased SA/BSA separation efficiency. The filtration resistance is known to depend on cake and pore blocking. Generally, cake fouling can be reduced by the application of hydraulic shear forces such as agitation, which makes the cake thinner. Hence, the higher filtration resistance observed for stimulated dead-end filtration can be ascribed to the disturbing flow forcing the particles or colloids into the pores of filtering paper to result in their serious blockage (Cao et al. 2018a).

3.3 Adsorption Behaviors of Heavy Metal Ions on EPS

Figure 14 shows the adsorption behaviors of Pb^{2+} on EPS, dry excess sludge, a commercial adsorbent, and chitosan, and the adsorption isotherms were characterized by fitting the experimental data to the Langmuir model, which can effectively describe the adsorption behaviors of heavy metal ions (HMIs) on EPS (Cao et al. 2018b, 2020c):

Fig. 14 Langmuir sorption isotherms of Pb^{2+} on EPS, commercial adsorbent, chitosan, and dry excess sludge. Here, the concentration of all adsorbents was 20 mg/L, the initial concentration of Pb^{2+} was 0.1–0.8 mM, and the experimental temperature was 25 °C. (The figure is reprinted with the copyright permission (Cao et al. 2020c))



$$\frac{C_e}{q_e} = \frac{1}{Q_{\max} K} + \frac{C_e}{Q_{\max}}, \quad (5)$$

where C_e is the concentration of HMIs in solution at equilibrium, q_e is the amount of HMIs adsorbed on the composite adsorbent at equilibrium, Q_{\max} is the amount of HMIs adsorbed to afford monolayer coverage, and K is the Langmuir adsorption equilibrium constant. The EPS extracted from excess sludge was clearly far more effective at adsorbing Pb^{2+} than dry excess sludge and chitosan. Furthermore, the experimental data were compared with results of commercially available products with a similar adsorption capacity, as shown in Fig. 14. This comparison revealed that EPSs recovered from excess sludge can be used as alternative Pb^{2+} adsorbents.

Having established that the filtration resistance of the EPS solutions decreased in the presence of Ca^{2+} , the next step was to investigate the heavy metal adsorption performance of the recovered products (cake or EPS-Ca) formed during the membrane separation of metal ion-containing EPS solutions (Cao et al. 2018b). Figure 15 shows the capacities of EPS (extracted from Dongba excess sludge by the cation exchange resin (CER) method) and EPS-Ca for the removal of Cu^{2+} , Cd^{2+} , and Pb^{2+} . The obtained results demonstrate that both adsorbents exhibit essentially identical removal capacities regardless of the metal ion type and revealed that all removal efficiencies exceeded 80% and were larger for Cu^{2+} and Cd^{2+} than for Pb^{2+} ; i.e., EPS- Ca^{2+} interactions did not affect the performance of EPS for heavy metal ion adsorption. The above behavior can be explained by the fact that heavy metal ions have higher affinities for EPS than Ca^{2+} and are primarily bound by virtue of interactions with carboxyl ($-\text{COOH}$) and hydroxyl ($-\text{OH}$) groups present in EPS. Consequently, heavy metal ions can react with EPS-Ca by ionic exchange to form EPS-heavy metal complexes and free Ca^{2+} . Figure 16 shows the relationships

Fig. 15 Removal capacities of EPS and product of EPS–Ca²⁺ interaction (EPS–Ca) for different heavy metal ions. (The figure is reprinted with the copyright permission (Cao et al. 2018b))

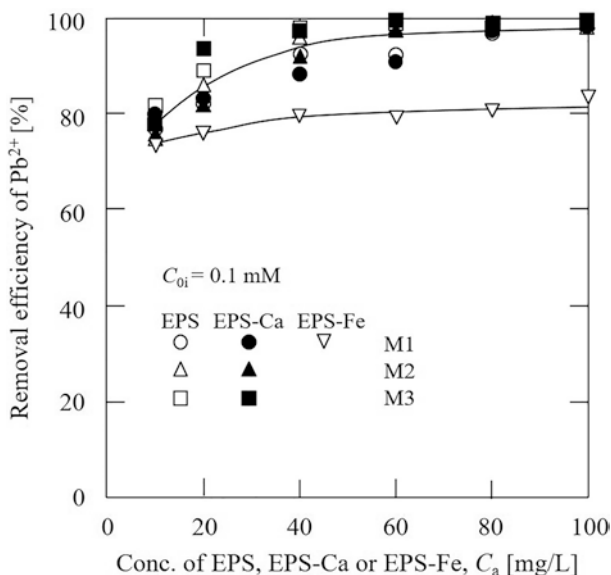
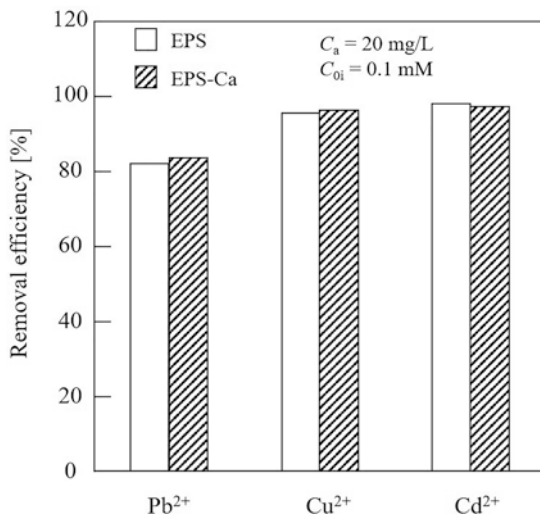


Fig. 16 Pb²⁺ removal efficiencies obtained using 0.1 mM Pb²⁺ and various concentrations of EPSs, EPS-Ca, and product of EPS–Fe³⁺ interaction (EPS-Fe). The EPS solutions were extracted using three typical methods (M1, M2, and M3). M1, CER extraction method; M2, formaldehyde–NaOH extraction method; M3, high-temperature sodium carbonate extraction method. (The figure is reprinted with the copyright permission (Cao et al. 2018b))

Table 2 Pb²⁺ adsorption properties of EPS, EPS-Ca, and a selected commercial adsorbent

Adsorbent ^a	Adsorbent loading (mg/L)	Pb ²⁺ concentration (mg/L)	Removal efficiency (%)	Q_{\max} (mg/g)
EPS (M1) ^b	20	8.2–65.6	16–82	555.56
EPS-Ca (M1)	20	8.2–65.6	13–83	454.55
EPS (M2)	20	8.2–65.6	17–86	588.24
EPS-Ca (M2)	20	8.2–65.6	23–82	833.33
EPS (M3)	20	8.2–65.6	18–89	625.00
EPS-Ca (M3)	20	8.2–65.6	16–93	555.56
Commercial adsorbent	20	8.2–65.6	20–95	666.67

^aEPS was extracted from Dongba excess sludge

^bSymbols in bracket denote the method of EPS extraction

between the efficiency of Pb²⁺ removal and the concentrations of EPS, EPS-Ca, and EPS-Fe for EPSs extracted by M1, M2, and M3. Notably, the Pb²⁺ removal efficiency improved markedly with increasing EPS concentration (reaching values of ~100% for 0.1 g/L EPS), whereas the extraction method had virtually no effect. Similar to the results shown in Fig. 15, EPS and EPS-Ca showed identical adsorption properties regardless of the employed extraction method, which demonstrated that Ca²⁺ addition does not affect the ability of EPS to absorb heavy metal ions. However, the heavy metal adsorption capacity of EPS-Fe was much lower than that of EPS, although Fe³⁺ could also mitigate EPS membrane fouling. The addition of Fe³⁺ was therefore concluded to be an ineffective means of reducing filtration resistance for EPS membrane recovery.

Furthermore, the adsorption of Pb²⁺ on EPS and EPS-Ca was characterized by fitting the experimental data (C_e/q_e vs. C_e) to the Langmuir model. The obtained results are summarized in Table 2. Comparison of the experimental data with results of commercially available products and other adsorbents reported in the literature over the past 5 years (Cao et al. 2018b) revealed that EPSs recovered from waste sludge can be used as alternative Pb²⁺ adsorbents.

3.4 Removal of Heavy Metal Ions by UF with Recovery of EPSs

To achieve the dual goal of EPS concentration/recovery and removal of heavy metal ions (HMIs), two-stage constant pressure dead-end UF was developed, as shown in Fig. 17. The first step involved the EPS concentration process: the UF membrane was used to filter the EPS solution to form a dense EPS cake layer on the surface of the membrane to obtain a filter membrane with an EPS cake layer at the filtration pressure p_1 , as shown in Fig. 17a. The second step involved the removal of HMIs; after the EPS cake was completely formed, heavy-metal-containing wastewater was filtered through the cake at the filtration pressure p_2 . Here, the HMIs were adsorbed

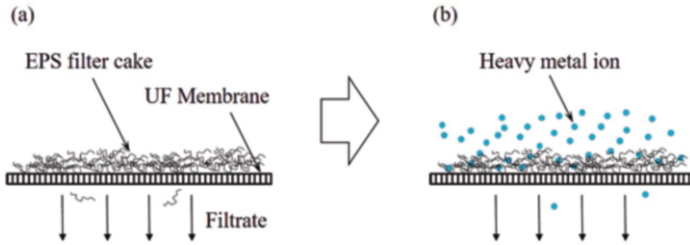


Fig. 17 Schematic diagram of extracellular polymer substance (EPS)-enhanced ultrafiltration (UF), i.e., EPS-UF, combining the recovery of EPSs from excess sludge and the removal of HMIs: (a) First stage: formation of EPS filter cake in UF; (b) Second stage: adsorption removal of HMIs by the EPS filter cake. (The figure is reprinted with the copyright permission (Cao et al. 2020c))

Table 3 Effect of filtration pressure p on initial filtration rate J_0 , filtration resistance R_t , and removal efficiency of Pb^{2+} η_i in EPS-UF

Stage 1 (UF)				Stage 2 (EPS-UF)				η_i (%)
p_1 (kPa)	J_{01} (10^{-5} m/s)	R_{t1} ($v = 0$ cm) (10^{12} m $^{-1}$)	R_{t1} ($v = 5$ cm) (10^{12} m $^{-1}$)	p_2 (kPa)	J_{02} (10^{-5} m/s)	R_{t2} ($v = 0$ cm) (10^{12} m $^{-1}$)	R_{t2} ($v = 5$ cm) (10^{12} m $^{-1}$)	
100	1.66	6.29	10.05	20	0.30	7.97	8.01	97.7 ± 1.2
100	1.65	6.49	10.21	100	1.32	7.92	6.46	94.8 ± 2.1
100	1.62	6.96	8.58	200	1.64	14.57	14.29	78.9 ± 10.5
20	0.43	4.44	5.90	100	1.50	6.82	5.79	95.0 ± 2.1
200	3.47	6.97	8.95	100	1.79	6.54	5.96	93.1 ± 2.1

by EPS contained in the cake layer to remove the HMIs, as shown in Fig. 17b. Notably, in order to obtain a fixed cake, all dead-end filtration tests were conducted under constant pressure conditions using a novel filter, in which the filtration area was suddenly reduced at a distance of 1.0 mm from the membrane surface (Cao et al. 2013).

The filtration rate, J , is given by Darcy’s law as follows:

$$J = \frac{P}{\mu R_t}, \tag{6}$$

where R_t is the total filtration resistance. The above equation clearly shows that the filtration rate, J , is an indication of the total filtration resistance R_t . Table 3 shows the typical experimental data. For the first stage (UF, EPS concentration process), the filtration resistance R_{t1} was lower with low applied filtration pressure p_1 than with high p_1 although the initial filtration rate was slower for low p_1 , and R_{t1} increased with filtration progress because of the high compressibility of the EPS filter cake. For the second stage (EPS-UF, removal process of HMIs), the filtration rate could not be increased by applying a higher filtration pressure ($p_2 = 200$ kPa) because of the high compressibility of the EPS filter cake, and the removal efficiency of Pb^{2+}

Table 4 Effect of HMIs patterns on removal efficiency of HMIs in EPS-UF at $p_1 = p_2 = 100$ kPa

Initial conc. of HMIs in aqueous solution (μM)			Removal efficiency of HMIs (%)		
Pb^{2+}	Cu^{2+}	Cd^{2+}	Pb^{2+}	Cu^{2+}	Cd^{2+}
10	0	0	94.8 ± 2.1	–	–
0	10	0	–	88.9 ± 5.0	–
0	0	10	–	–	89.2 ± 6.7
5	5	0	94.9 ± 2.5	96.0 ± 2.2	–

decreased markedly (only 78.9%). This is probably because the interaction between EPS and Pb^{2+} changed the structure and ingredient of the EPS cake. It is noteworthy that the filtration resistance R_{f2} decreased with filtration progress precisely because of the changed EPS cake.

In the table, a 10 kDa membrane, 100 mL of a 0.1 g/L EPS solution, and 180 mL of a 10 μM Pb^{2+} solution are used.

Various HMIs are usually encountered in actual wastewater; therefore, the removal efficiencies for single solutions of metal ions such as Cu^{2+} and Cd^{2+} and a binary solution of Pb^{2+} and Cu^{2+} were also investigated in EPS-UF after the formation of the EPS. As shown in Table 4, the results indicate that EPS-UF is effective for removing various HMIs in wastewater, with high removal efficiency. Nevertheless, the mechanisms of interaction between EPS-cake and HMIs are extremely complicated because of the complex EPSs containing various substances such as polysaccharides, proteins, humus, nucleic acid, and DNA.

In the table, a 10 kDa membrane, 100 mL of 0.1 g/L EPS solution and 180 mL aqueous solution of HMIs are used.

Significantly, unlike SA, the detailed EPSs formula or compounds cannot be obtained since the biomaterials extracted from the microorganisms in excess sludge are the mixtures of various macromolecular substances. The properties of recycled EPSs depend on sludge source, extraction method, operating condition, and so on. The characteristics of the typical EPSs such as photomicrograph, size distribution, FTIR, XPS, and SEM can be found in the previous studies (Cao et al. 2018b, 2020c, 2021b).

4 Surfactant-Enhanced Ultrasonic Extraction of Polymeric Substances

4.1 Effect of Surfactant on Extraction Efficiency

Figure 18a shows the relationship between the extraction efficiency of polymeric substances (PSs) and surfactant concentration for various pulse ultrasonic times (effective ultrasonic time, t_p). As shown in the figure, the extraction efficiency of PSs increased first and then decreased with an increasing concentration of

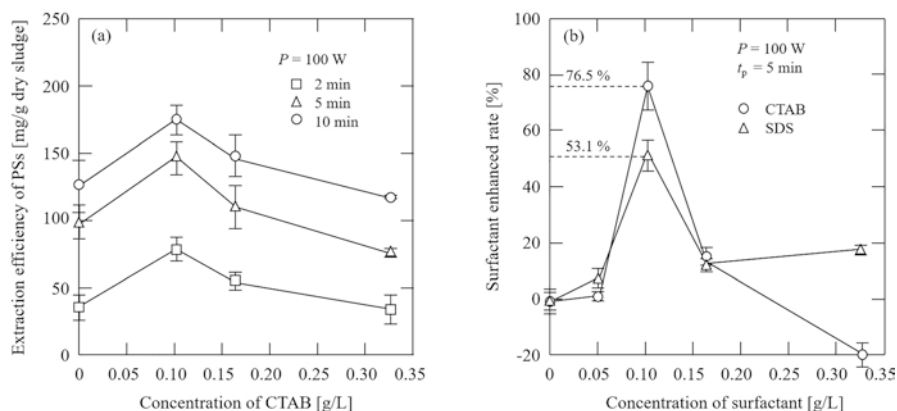


Fig. 18 (a) Relationship between the extraction efficiency of polymeric substances (PSs) and the concentration of cetyltrimethylammonium bromide (CTAB) for various pulse ultrasonic times, t_p . (b) Relationship between the surfactant enhanced rate and concentration of surfactant for the extraction of PSs via ultrasonication with CTAB and sodium dodecyl sulfate (SDS). (The figure is reprinted with the copyright permission (Cao et al. 2021b))

cetyltrimethylammonium bromide (CTAB), regardless of the effective ultrasonic time, and the maximum value was reached when the concentration of CTAB was 0.1 g/L. Furthermore, the highest extraction efficiency of PSs (up to 176.02 mg/g dry sludge for the CTAB of 0.1 g/L) is for 10 min, while the increase rate of the extraction amount of PSs decreased with further increase in the effective ultrasonic time. Figure 18b shows the relationship between the surfactant-enhanced extraction rate and the concentration of surfactant for CTAB and sodium dodecyl sulfate (SDS). Both surfactants had a similar effect on the extraction of PSs from excess sludge; the extraction rate first increased and then decreased, although the effect of CTAB (76.5%, 147.9 mg/g dry sludge for 5 min) was larger than that of SDS (53.1%, 126.9 mg/g dry sludge for 5 min) for the surfactant of 0.1 g/L. Furthermore, considering the disposal of the residue generated after the extraction of PSs from excess sludge, the use of CTAB is recommended because of its high efficiency, nontoxicity, and biodegradability (Zhou et al. 2019).

The ultrasonication with and without surfactant was compared with the CER method, which was used in our previous studies because of little damage to the cell (Cao et al. 2018b, 2020c), as shown in Fig. 19a. The extraction efficiency of PSs containing intracellular polymeric substances (IPSS) and EPSs was much higher than that of the CER method probably because the ultrasonication damaged a larger number of cells. Above all, the ultrasonication with surfactant was proposed as a suitable extraction method for the recovery of PSs from excess sludge.

The percentages of polysaccharide, protein, and DNA were evaluated in the PSs extracted via ultrasonication with various concentrations of CTAB, as shown in Fig. 19b. The percentage of proteins in PSs were higher than those of polysaccharides because of the sludge type, and the percentages of polysaccharides, proteins, and DNA together accounted for approximately 50% of the total PSs. The concentration

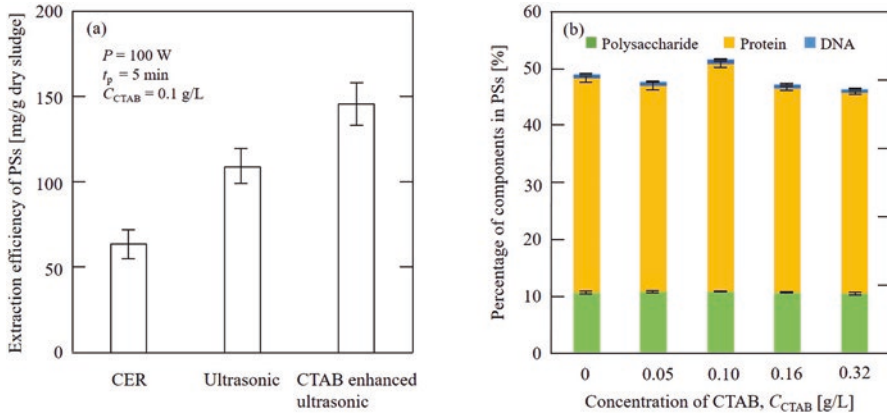


Fig. 19 (a) Extraction efficiency of polymeric substances (PSs) in excess sludge for three extraction methods (centrifugation speed = 10,000 rpm, centrifugation time = 20 min). (b) Percentages of polysaccharides, proteins, and DNA in the PSs extracted via ultrasonication with various concentration of cetyltrimethylammonium bromide (CTAB). (The figure is reprinted with the copyright permission (Cao et al. 2021b))

changes of the surfactant had a negligible effect on their percentages, most likely because the composition of components in the EPSs and IPSs is uniform. Specifically, the percentage of DNA remained constant, indicating that the increase in CTAB concentrations did not enhance the breakdown of cells in the excess sludge under the experimental conditions.

4.2 Mechanisms of Surfactant-Enhanced Ultrasonication Extraction

The increase in the amount of PSs recovered from excess sludge by ultrasonication with the surfactants was caused by the release of the organic matter into the medium because of floc disintegration and cell lysis. Figure 20 shows four mechanisms of surfactant-enhanced ultrasonication to extract PSs from excess sludge (Cao et al. 2021b). The release of PSs may have been caused by one or more of these mechanisms. Case 1: The aqueous medium, with a low surface tension owing to the presence of hydrophobic and hydrophilic groups in surfactants, increases cavitation, and therefore, the energy consumption of the ultrasonic process was reduced (Fig. 20a). Case 2: The surfactants broke the non-covalent bonds between EPSs and microbial cells, which resulted in a separation of EPSs from the surface of the cell membranes (Fig. 20b). Case 3: Through the principle of mutual solubility, linear hydrocarbon chains in the surfactants formed micelles, which accelerated the release of EPSs from sludge flocs or the surfactant solubilized PSs, such as polysaccharide and protein present in the sludge flocs (Fig. 20c). Case 4: The surfactants, containing polar

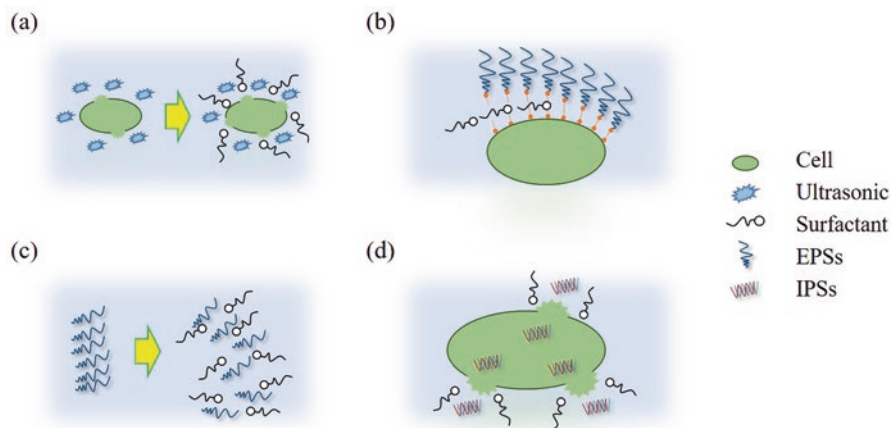


Fig. 20 Four mechanisms of surfactant-enhanced ultrasonication extraction: (a) the aqueous medium, with a low surface tension owing to the presence of hydrophobic and hydrophilic groups in surfactants, increases cavitation; (b) the surfactants break non-covalent bonds between extracellular polymeric substances (EPSs) and microbial cells, resulting in the separation of EPSs from the surface of cell membranes; (c) the surfactants solubilize polymeric substances (PSs), such as polysaccharides and proteins present in the sludge flocs, through the principle of mutual solubility; (d) the surfactants, containing polar functional groups, destroy lipid bilayers, causing cell lysis and the release of intracellular polymeric substances (IPs). (The figure is reprinted with the copyright permission (Cao et al. 2021b))

functional groups, destroyed lipid bilayers, which caused cell lysis and the release of IPs (Fig. 20d).

With an increase in the surfactant concentration, the surfactant-enhanced ultrasonic extraction efficiency reached its maximum near the critical micelle concentration (CMC), which was approximately 0.1 g/L in this study. When the concentration of surfactant is greater than CMC, the surfactant gets adsorbed to the cell and neutralizes negatively charged functional groups in the cell wall and EPSs, and long alkyl chains connect the cell and PSs to enhance aggregation. This has a negative impact on the extraction of PSs from excess sludge, resulting in a decrease in the extraction efficiency.

4.3 Characteristics of Polymeric Substances

4.3.1 Size Distribution

Figure 21a shows the size distributions of PSs. PSs extracted from the excess sludge via ultrasonication without a surfactant (denoted as PS_u) showed three peaks with average particle diameters of 80.75, 520.1, and 5092 nm, respectively, and the corresponding volume fractions were 27.3%, 28.0%, and 44.7%, respectively. PSs

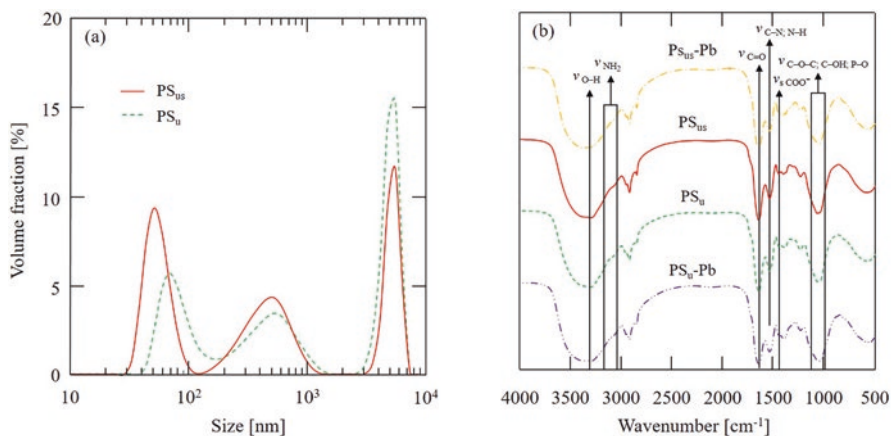


Fig. 21 (a) Typical size distributions of PS_{us} and PS_u ; (b) Fourier transform infrared spectra of different PSs. (The figure is reprinted with the copyright permission (Cao et al. 2021b))

extracted from the excess sludge via ultrasonication with a CTAB content of 0.1 g/L (denoted as PS_{us}) also showed three peaks, with average particle diameters of 54.92, 483.6, and 5256 nm, respectively, corresponding to respective volume fractions of 38.2%, 32.3%, and 29.5%, respectively. Therefore, the size of PSs extracted via ultrasonication with a surfactant was smaller than that extracted without a surfactant, indicating that smaller extracellular materials in excess sludge could be extracted ultrasonically using surfactants. The reasons may be the smaller size of IPSs released and solubility increase of smaller PSs due to the miscibility of surfactant.

4.3.2 FTIR Analysis

The FTIR spectra of PS_{us} and PS_u are shown in Fig. 21b. Both treatments showed the same characteristic peaks at 3350, 3110, 1658, 1544, 1420, and 1060 cm^{-1} , indicating the presence of various functional groups, such as O–H, $-NH_2$, C=O, C–N, N–H, COO^- , C–O–C, C–OH, and P–O, in PSs, regardless of the presence or absence of the surfactant. In other words, proteins, polysaccharides, lipids, DNA, and aromatic compounds were contained in both PSs. Therefore, the surfactant had no effect on the properties of PSs extracted from excess sludge via ultrasonication.

4.3.3 XPS Analysis

XPS was used to elucidate the composition of PS_{us} and PS_u in detail. The peaks, such as O 1s (531 eV), N 1s (399 eV), C 1s (284.8 eV), P 2p (132 eV), Ca 2p (348 eV), and Si 2p (103 eV), appeared in both full spectra, as shown in Fig. 22a, b, which indicated that the extracted PSs were mainly composed of organic substances

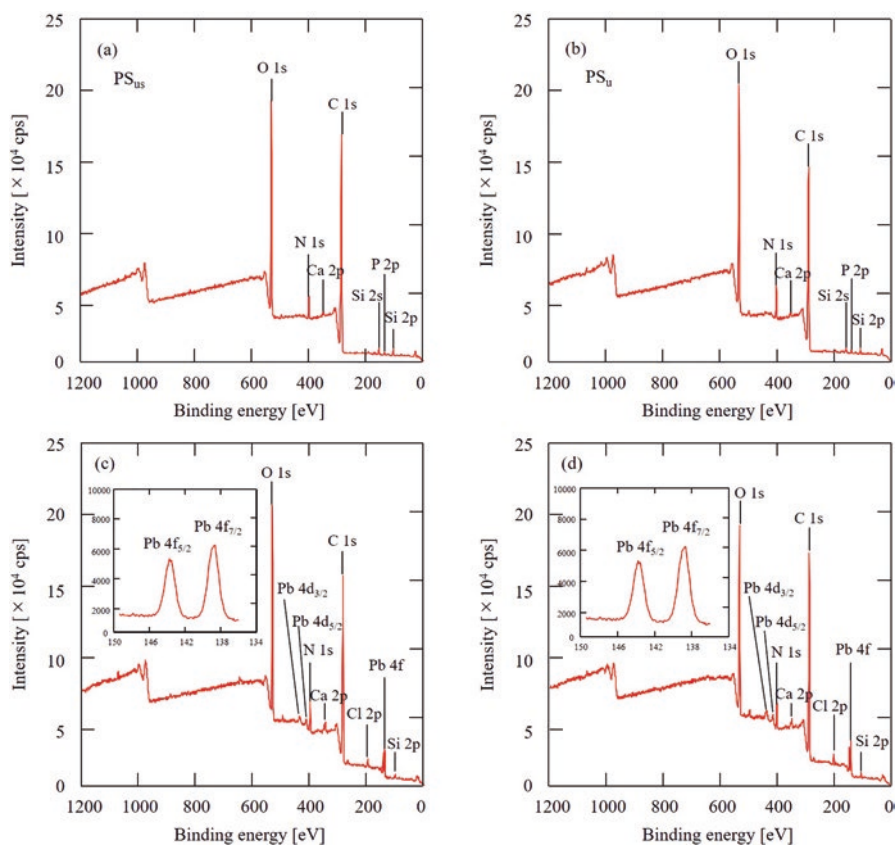


Fig. 22 X-ray photoelectron spectroscopy spectra of (a) PS_{us} , (b) PS_u , (c) PS_u -Pb, and (d) PS_{us} -Pb. (The figure is reprinted with the copyright permission (Cao et al. 2021b))

and certain inorganic substances. Table 5 shows the elemental composition of both PSs, and the contents of C, H, O, N, and P had only minor differences. Specifically, the metal contents in the PS_{us} decreased significantly (Al: 0.18% \rightarrow 0%; Na: 0.15% \rightarrow 0%; Ca: 0.24% \rightarrow 0.11%), which may have caused by the interaction between CTAB and the metal ions in the excess sludge. CTAB, a surface chemical modification reagent for cells in excess sludge, was bound to the cations (Al^{3+} , Ca^{2+} , Na^+) to the hydrophobic anionic groups on the surface of the cell. Notably, the inorganic fraction, which is frequently neglected in EPS studies, can influence the physicochemical properties of PSs, and therefore, PS_{us} may have more superior characteristics than PS_u .

The high-resolution scans (C 1 s, O 1 s, and N 1 s) of XPS are shown in Fig. 23. As shown in the figure, similar functional groups are contained in PS_{us} and PS_u , and the peaks of C 1 s, O 1 s, and N 1 s are resolved into four-, two-, and two-component peaks, respectively. Table 6 lists the chemical functional groups of PSs. Here, C-(C, H) predominantly originates from hydrocarbon-like compounds, including

Table 5 Elemental composition obtained via X-ray photoelectron spectroscopy of PS_{us} and PS_u

Element	PS _u (%)	PS _{us} (%)
C	67.52 ± 0.34	71.41 ± 0.33
N	5.37 ± 0.29	3.72 ± 0.27
O	24.32 ± 0.24	22.30 ± 0.22
P	0.57 ± 0.09	0.57 ± 0.10
S	0.43 ± 0.10	0.39 ± 0.11
Si	1.22 ± 0.12	1.50 ± 0.15
Ca	0.24 ± 0.07	0.11 ± 0.06
Al	0.18 ± 0.08	0 ^a
Na	0.15 ± 0.08	0

^aThe content is below the detection limit of method, and therefore, 0% is mentioned

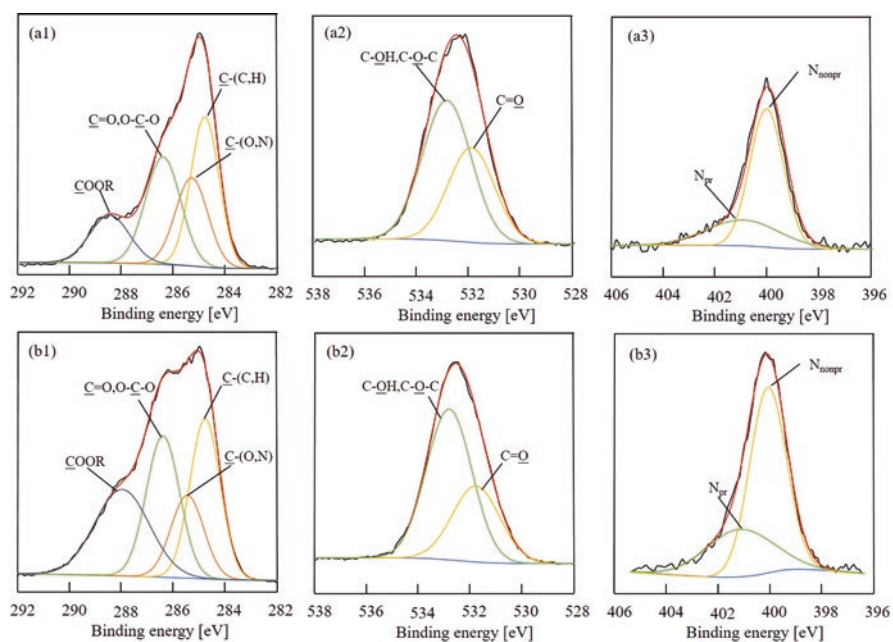


Fig. 23 High-resolution X-ray photoelectron spectroscopy scans (C 1 s (left), O 1 s (middle), and N 1 s (right)) of PS_{us} (top row, a1–a3) and PS_u (bottom row, b1–b3). (The figure is reprinted with the copyright permission (Cao et al. 2021b))

polysaccharides or side chains of amino acids and lipids; C–(O, N) originates from amide, alcohol, or amine groups in proteins and polysaccharides; C=O and O–C–O are typically present in carboxylate, carbonyl, amide, acetal, or hemiacetal groups; O=C–OH and O=C–OR originate from the carboxyl or ester groups in carboxylate and uronic acids; O=C originates from carbonyl, carboxylate, amide, or ester groups; C–O–C and C–O–H are present in alcohol, hemiacetal, or acetal groups;

Table 6 Contents of functional groups (molar ratio with respect to C) in various polymeric substances (PSs)

Region	Position (eV)	Functional groups	PS _u (%)	PS _{us} (%)	PS _u -Pb (%)	PS _{us} -Pb (%)
C 1 s	284.8	C-(C, H)	28.53	14.79	49.01	52.95
	286.3	C-(C, N)	15.95	29.60	13.7	14.76
	288.0	C=O, O-C-O	27.79	22.45	21.12	19.16
	289.0	O=C-OH, O=C-OR	27.73	33.16	16.17	12.14
N 1 s	400.1	N _{nonpr}	70.49	68.38	42.36	28.97
	401.6	N _{pr}	29.51	31.62	57.64	70.03
O 1 s	531.4	O=C	34.26	60.88	42.35	42.00
	532.7	C-O-C, C-O-H	65.74	39.12	57.65	58.00

non-protonated nitrogen (N_{nonpr}) is present in amides and amines; protonated amines (N_{pr}) are commonly found in amino acids or amino sugars.

The differences in the contents of functional groups in the C 1 s spectrum are mainly attributed to the varying contents of proteins, nucleic acids, and other organic substances in PS_u and PS_{us}. For the O 1 s spectrum, the C-O-C and C-O-H content in the PS_u was higher because of the different contents of polysaccharides. The phenol-sulfuric acid method was used to measure the contents of polysaccharide in this study, and its contents in both PSs showed minimal differences; however, the contents of functional groups differed considerably. This was probably because the surfactants can precipitate acidic polysaccharides, resulting in different functional groups in the polysaccharide. The appearance of N_{pr} indicated that the ultrasonic treatment had caused some proteins to be hydrolyzed to a certain extent. The number of N_{pr} in the PS_{us} is larger than that in the PS_u, which may originate from IPSs.

4.4 Adsorption Properties of Pb²⁺ on Polymeric Substances

The adsorption of PSs recovered from excess sludge on HMIs is one of their most typical properties, and therefore, the adsorption experiments for Pb²⁺ on the extracted PS_u, PS_{us}, and a commercial adsorbent were performed (Cao et al. 2021b). Both PSs exhibited a similar efficiency in adsorbing Pb²⁺ compared to the results of the commercially available products with a similar adsorption capacity. The amounts of Pb²⁺ adsorbed to afford monolayer coverage (Q_{\max}) for PS_{us}, PS_u, and the commercial adsorbent were 526.32, 500.00, and 500.00 mg/g, respectively. In addition, the Q_{\max} values of PSs obtained were similar to those of EPSs (555.56 mg/g) reported in the previous study (Cao et al. 2018b), indicating that the adsorption capacity of PSs extracted from excess sludge on Pb²⁺ is negligibly affected by the extraction methods. This comparison revealed that the PSs recovered from excess sludge using ultrasonication with a surfactant can be used as alternative Pb²⁺ adsorbents.

FTIR spectra of PSs with adsorbed Pb^{2+} (PSs-Pb) is shown in Fig. 21b. The band at 3350 cm^{-1} was detected for PS_{us} and PS_{u} , suggesting the presence of $-\text{OH}$ in sugars, phenols, and alcohols. After the adsorption of Pb^{2+} , a conspicuous displacement is observed for PS_{us} with adsorbed Pb^{2+} ($\text{PS}_{\text{us}}\text{-Pb}$) and PS_{u} with adsorbed Pb^{2+} ($\text{PS}_{\text{u}}\text{-Pb}$), indicating that $-\text{OH}$ has an adsorption effect on Pb^{2+} . The intensity at 1658 cm^{-1} is weakened, indicating that amide I is involved in adsorption. There is a significant change from 1300 to 1500 cm^{-1} , where the characteristic peaks in the band are derived from carboxyl-containing and hydrocarbon-like compounds, and the band at 1420 cm^{-1} corresponds to the vibration of $-\text{C}=\text{O}$, usually from the carboxylate structure. Considering the peak height and peak area, the adsorption of Pb^{2+} reduces the content of $-\text{COOH}$ and increases the content of $-\text{COO}^-$, indicating that $-\text{COOH}$ is also involved in the Pb^{2+} adsorption process. The characteristic peaks are shifted at $900\text{--}1200\text{ cm}^{-1}$, and different characteristic peaks appear, indicating that the phosphate group is also involved in adsorption.

XPS spectra of $\text{PS}_{\text{u}}\text{-Pb}$ and $\text{PS}_{\text{us}}\text{-Pb}$ are shown in Fig. 22c, d. The Pb 4f peak showed a strong representative double peak, indicating that the polymer substance was adsorbed to Pb^{2+} . The appearance of Pb $4f_{7/2}$ and Pb $4f_{5/2}$ peaks indicates that Pb^{2+} reacted with the PSs in the form of divalent ions to generate Pb-O , indicating that Pb^{2+} mainly adsorbed with the oxygen-containing functional groups in the PSs. Therefore, the Pb^{2+} adsorption with PSs can be divided into two parts with one as the electrostatic adsorption and the other as the reaction with the functional groups in PSs to form complexes such as R-COOPb^+ , $(\text{R-COO})_2\text{Pb}$, R-OPb^+ , and $(\text{R-O})_2\text{Pb}$. The Cl 1 s (1300 eV) peak appears because PbCl_2 was used as the Pb^{2+} sample in the experiments.

To explore the types of functional groups that adsorb Pb^{2+} in PSs, high-resolution scans (C 1 s, O 1 s, and N 1 s) of XPS were analyzed for both PSs adsorbed Pb^{2+} , and the detailed information on the main functional group content in PSs-Pb was obtained as shown in Table 6. The peaks of C 1 s, O 1 s, and N 1 s for both PSs-Pb were resolved into the component peaks of 4, 2, and 2, respectively. The content of $\text{O}=\text{C}$ increased in $\text{PS}_{\text{u}}\text{-Pb}$ as shown in the high-resolution XPS scans of O 1 s, probably because $-\text{COOH}$ can interact with HMIs through ion exchange or complexation. For both PSs-Pb, the content of the N_{pr} with higher binding energy increased. This can be explained by two reasons: (i) the pH value changed during the adsorption process, resulting in an increase in NH_4^+ content; (ii) the interaction of HMIs with N in the amine group. The increase in N_{pr} content was mainly related to the adsorption of Pb^{2+} because the pH value did not change. When the electron cloud density of the nitrogen atom decreases, its binding energy becomes higher. Therefore, the peak at 401.6 eV with higher binding energy appeared, and it can be attributed to N_{nonpr} , such as $-\text{C-NH}$ and $-\text{C-NH}_2$, which forms a complex with HMIs.

5 Challenges and Future Perspective

Recovery of polymeric substances from excess sludge is one of the most important research objectives in wastewater treatment. The challenges and future perspective contain the following five aspects (Cao 2021): (1) optimization of various extraction methods such as ultrasonication, heating, high-temperature Na_2CO_3 , HCHO – NaOH , EDTA, CER, and H_2SO_4 methods; (2) directed recovery of typical materials such as alginate, polyhydroxyalkanoate, and poly- β -hydroxybutyrate; (3) novel concentration technologies such as microfiltration, ultrafiltration, and forward osmosis; (4) efficient separation and purification technologies for removal of heavy metal ions and organic pollutants from recycled materials; (5) potential applications such as adsorbent, bio-flocculant, animal feed additive, fire retardant, soil conditioner, and novel nano-materials for clothes and jewelry.

Acknowledgments This study was partially supported by the Beijing Nova Program (Z211100002121154), the Beijing Natural Science Foundation (8222043), the Project of Cultivation for young top-notch Talents of Beijing Municipal Institutions (BPHR202203083), and Beijing Energy Conservation & Sustainable Urban and Rural Development Provincial and Ministry Co-construction Collaboration Innovation Center. The funding agencies did not influence the study design, data collection, analysis and interpretation, report writing, or the decision to submit this article for publication.

References

- Braccini I, Perez S (2001) Molecular basis of Ca^{2+} -induced gelation in alginates and pectins: the egg-box model revisited. *Biomacromolecules* 2:1089–1096. <https://doi.org/10.1021/bm010008g>
- Cao DQ (ed) (2021) Recycling of polymeric substances from sewage. Chinese Chemical Industry Press. <http://www.cip.com.cn/Book/Index/48659>
- Cao DQ, Iritani E, Katagiri N (2013) Properties of filter cake formed during dead-end microfiltration of O/W emulsion. *J Chem Eng Jpn* 46:593–600. <https://doi.org/10.1252/jcej.13we066>
- Cao DQ, Hao XD, Wang Z et al (2017) Membrane recovery of alginate in an aqueous solution by the addition of calcium ions: analyses of resistance reduction and fouling mechanism. *J Membr Sci* 535:312–321. <https://doi.org/10.1016/j.memsci.2017.04.050>
- Cao DQ, Song X, Hao XD et al (2018a) Ca^{2+} -aided separation of polysaccharides and proteins by microfiltration: implications for sludge processing. *Sep Purif Technol* 202:318–325. <https://doi.org/10.1016/j.seppur.2018.03.070>
- Cao DQ, Song X, Fang XM et al (2018b) Membrane filtration-based recovery of extracellular polymer substances from excess sludge and analysis of their heavy metal ion adsorption properties. *Chem Eng J* 354:866–874. <https://doi.org/10.1016/j.cej.2018.08.121>
- Cao DQ, Jin JY, Wang QH et al (2020a) Ultrafiltration recovery of alginate: membrane fouling mitigation by multivalent metal ions and properties of recycled materials. *Chin J Chem Eng* 28:2881–2889. <https://doi.org/10.1016/j.cjche.2020.05.014>
- Cao DQ, Sun XZ, Jin JY et al (2020b) Recovery of extracellular polymeric substance: impact factors in forward osmosis separation of sodium alginate. *Environ Eng* 38:1–6. <https://doi.org/10.13205/j.hjgc.202008012>

- Cao DQ, Wang X, Wang QH et al (2020c) Removal of heavy metal ions by ultrafiltration with recovery of extracellular polymer substances from excess sludge. *J Membr Sci* 606:118103. <https://doi.org/10.1016/j.memsci.2020.118103>
- Cao DQ, Sun XZ, Yang XX et al (2021a) News on alginate recovery by forward osmosis: reverse solute diffusion is useful. *Chemosphere* 285:131483. <https://doi.org/10.1016/j.chemosphere.2021.131483>
- Cao DQ, Tian F, Wang X et al (2021b) Recovery of polymeric substances from excess sludge: surfactant-enhanced ultrasonic extraction and properties analysis. *Chemosphere* 283:131181. <https://doi.org/10.1016/j.chemosphere.2021.131181>
- Guest JS, Skerlos SJ, Barnard JL (2009) A new planning and design paradigm to achieve sustainable resource recovery from wastewater. *Environ Sci Technol* 43:6126–6130. <https://doi-org.xjplg.80599.net/10.1021/es9010515>
- Ilyas RA, Sapuan SM, Sabaruddin FA et al (2021) Reuse and recycle of biobased packaging products. In: Sapuan SM, Ilyas RA (eds) *Bio-based packaging: material, environmental and economic aspects*. Wiley, West Sussex
- Kim NK, Mao N, Lin R et al (2020) Flame retardant property of flax fabrics coated by extracellular polymeric substances recovered from both activated sludge and aerobic granular sludge. *Water Res* 170:115344. <https://doi.org/10.1016/j.watres.2019.115344>
- Matassa S, Batstone DJ, Huelsen T et al (2015) Can direct conversion of used nitrogen to new feed and protein help feed the world? *Environ Sci Technol* 49:5247–5254. <https://doi-org.xjplg.80599.net/10.1021/es505432w>
- More TT, Yan S, Hoang NV et al (2012) Bacterial polymer production using pre-treated sludge as raw material and its flocculation and dewatering potential. *Bioresour Technol* 121:425–431. <https://doi.org/10.1016/j.biortech.2012.06.075>
- Remmen K, Müller B, Köser J et al (2019) Phosphorus recovery in an acidic environment using layer-by-layer modified membranes. *J Membr Sci* 582:254–263. <https://doi.org/10.1016/j.memsci.2019.03.023>
- Ruiken CJ, Breuer G, Klaversma E (2013) Sieving wastewater-cellulose recovery, economic and energy evaluation. *Water Res* 47:43–48. <https://doi.org/10.1016/j.watres.2012.08.023>
- van Loosdrecht MCM, Brdjanovic D (2014) Anticipating the next century of wastewater treatment. *Science* 344:1452–1453. <https://www.science.org/doi/10.1126/science.1255183>
- Winkler MKH, van Loosdrecht MCM (2022) Intensifying existing urban wastewater. *Science* 375:377–378. <https://www.science.org/doi/10.1126/science.abm3900>
- Zhang MJ, Hong HC, Lin HJ et al (2018) Mechanistic insights into alginate fouling caused by calcium ions based on terahertz time-domain spectra analyses and DFT calculations. *Water Res* 129:337–346. <https://doi.org/10.1016/j.watres.2017.11.034>
- Zhou Y, Lai YS, Eustance E et al (2019) Promoting *Synechocystis* sp. PCC 6803 harvesting by cationic surfactants: alkyl-chain length and dose control for the release of extracellular polymeric substances and biomass aggregation. *ACS Sustain Chem Eng* 7:2127–2133. <https://doi.org/10.1021/acssuschemeng.8b04776>

Recycling of Ground Tire Rubber According to the Literature



Fabiula Danielli Bastos de Sousa

1 Introduction

The recycling of ground tire rubber (GTR) is far from being an easy task. Due to the tridimensional network formed during the vulcanization of rubber and the additives present in its formulation, vulcanized rubbers cannot flow like thermoplastic polymers, which hinders their recycling.

When disposed in landfills or incorrectly disposed of in the environment, end-of-life tires may cause/aggravate socio-environmental problems. Due to their large size, they may be a perfect place to store rainwater and to proliferate vectors, such as the *aedes aegypti* mosquito, the transmitter of dengue, chikungunya, zika, and yellow fever (de Sousa 2016). So, the recycling of end-of-life tires has extreme importance to minimize or eliminate the problem.

There are several applications of the GTR available in the literature, such as in the production of polymeric blends (Scaffaro et al. 2005; Mujal-Rosas et al. 2011b; de Sousa et al. 2015a, b, 2016, 2019a; Sienkiewicz et al. 2017; de Sousa and Scuracchio 2020), composites (Ghosh et al. 2020; Marín-Genescà et al. 2020a, b; Phiri et al. 2020), the use of GTR in asphalt pavements and concretes (Bignozzi and Sandrolini 2006; Huang et al. 2007; Bravo and de Brito 2012; Lo Presti 2013; Saberian et al. 2020), asphalt binder (Hassanpour-Kasanagh et al. 2020), pyrolysis (De Marco Rodriguez et al. 2001; Williams and Brindle 2003; Acosta et al. 2016), devulcanization of GTR – a method used to restore the flow capability of vulcanized rubbers (De et al. 2006; Garcia et al. 2015; Colom et al. 2016; Edwards et al. 2016; de Sousa et al. 2017, 2019b; Li et al. 2019; de Sousa and Ornaghi Júnior 2020; Saputra et al. 2020), among many others.

Currently, bibliometric studies are widely used to help researchers have an overview of a given research area, through the analysis of the scientific production in a

F. D. B. de Sousa (✉)

Technology Development Center, Universidade Federal de Pelotas, Pelotas, RS, Brazil

period of time. All the data from a group of publications can be analyzed, such as the authors, sources, affiliations, countries, and keywords. To verify the current scenario and evolution of a given research area, and to know the difficulties encountered by this area, the in-depth analysis of the keywords is especially essential, being a crucial tool to outline future researches in that specific area (de Sousa 2022).

In the present work, bibliometric analysis (a quantitative analysis from the data) was performed about the recycling of GTR. Having in mind the importance of the analysis of the authors' keywords, emphasis was given to it to have an overview of the subject. In general, the results have shown that mechanical properties, pyrolysis, and devulcanization are hotspots, whereas waste management, end-of-life tires, natural rubber, tyre recycling, and modification are trends in the recycling of the GTR research area.

2 Review Methodology

A Scopus search was conducted to obtain the bibliographic data inputs on September 12, 2021, by using the keywords (recycling OR reclamation) AND (ground tire rubber* OR ground tyre rubber*) OR (waste tire* OR waste tyre*) OR (scrap tire* OR scrap tyre*) OR (ground rubber tire* OR ground rubber tyre*). Reviews and articles in English were considered from 2001 to 2020.

From Scopus, a scopus.bib file containing the data was taken, and a bibliometric analysis using the Bibliometrix (an R-package) was performed.

3 Results and Discussion

From the Scopus search by using the keywords (recycling OR reclamation) AND (ground tire rubber* OR ground tyre rubber*) OR (waste tire* OR waste tyre*) OR (scrap tire* OR scrap tyre*) OR (ground rubber tire* OR ground rubber tyre*), a total of 469 publications in English were obtained, including 431 articles and 38 reviews from 2001 to 2020. The number of publications per year and per area is shown in Fig. 1.

Based on the results, an increase in the number of publications along the period can be observed, with an annual growth rate of 6.54% (Fig. 1a). Figure 1b depicts the interdisciplinary nature of the area, with a higher number of publications in the following science areas: materials science, engineering, chemistry, and environmental science.

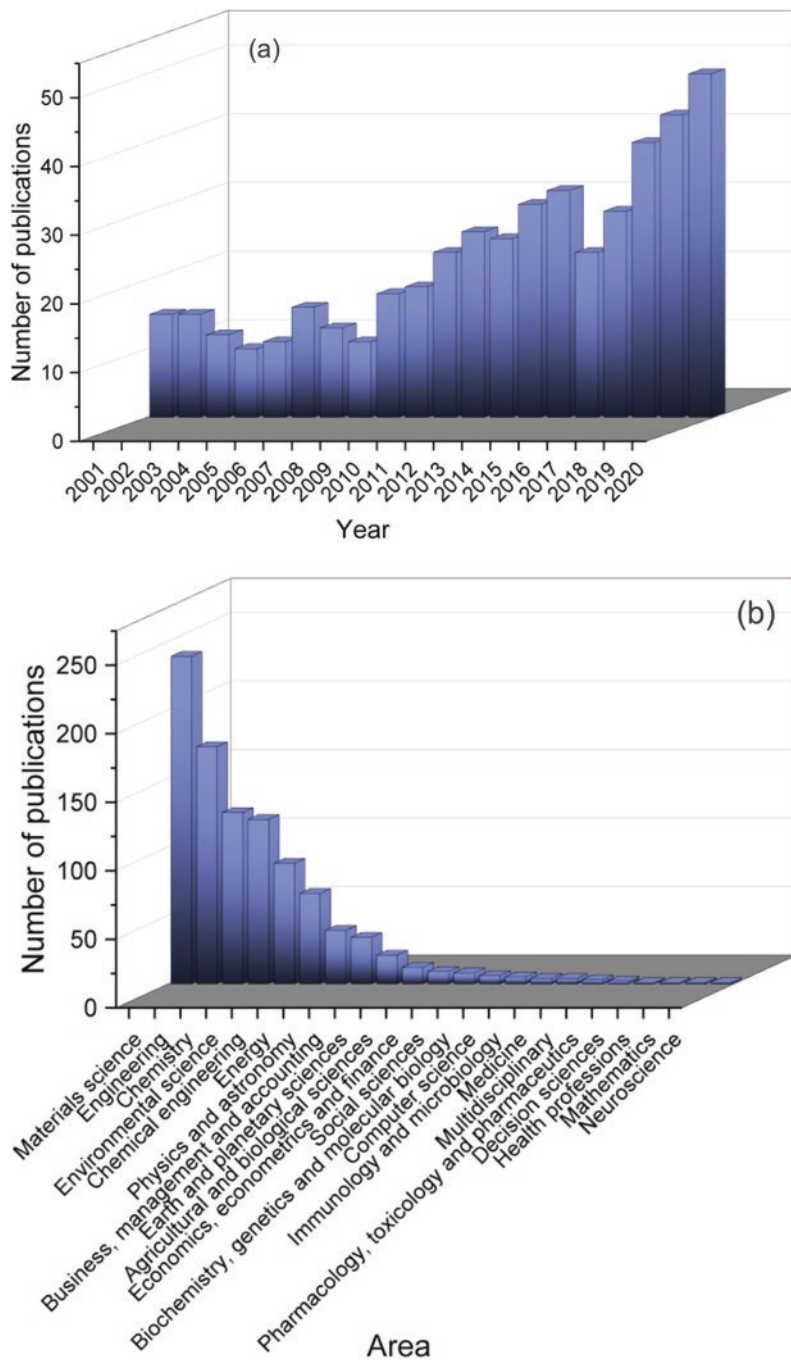


Fig. 1 (a) Number of publications per year. (b) Number of publications per area

3.1 Sources

The most important sources in the field, according to the number of publications, are (the number of publications in parenthesis): *Journal of Applied Polymer Science* (30), *Construction and Building Materials* (27), *Journal of Cleaner Production* (21), *Waste Management* (21), *Progress in Rubber, Plastics and Recycling Technology* (15), *Rubber Chemistry and Technology* (12), and *Polymer Degradation and Stability* (10). These journals are peer-reviewed, and the results demonstrate their high quality, as well as the authors' confidence in publishing their works in these journals (de Sousa 2021).

3.2 Affiliations and Countries

Based on the first author's affiliation, the affiliations with the highest number of publications are (number of publications in parenthesis) Gdansk University of Technology (44) of Poland, Université Laval (13) of Canada, Beijing University of Chemical Technology (12) of China, Gyeongsang National University (12) of South Korea, and University of Aveiro (12) of Portugal.

The most productive countries are (number of publications in parenthesis) China (105), Spain (102), India (96), Poland (65), Italy (55), the United States (45), Australia (43), the United Kingdom (43), Brazil (38), and Canada (27).

These results demonstrate the importance of the contribution of all the authors since some of the most productive affiliations and countries are not related to the authors with the highest number of publications in the area (to be seen in the sequence). Thus, all authors play an important role within the literature on the GTR recycling.

3.3 Authors

The top-authors' production over time is presented in Fig. 2. The number in parentheses on the right side of the names of each author represents the total number of publications of each one. The size of the circles represents the number of publications per year, and the shade of blue represents the total number of citations (TC) of each author per year.

According to the results, the most prominent author is Formela K with 31 publications, followed by Colom X (14), Mujal-Rosas R (14), Saeb MR (12), and Cañavate J (10), with the number of publications in parenthesis.

Regarding the most cited publications of the top-authors, the one by Formela, Colom, and Cañavate is Colom et al. (Colom et al. 2016), with 61 citations. The publication deals with the Fourier transform infrared spectroscopy (FTIR) and

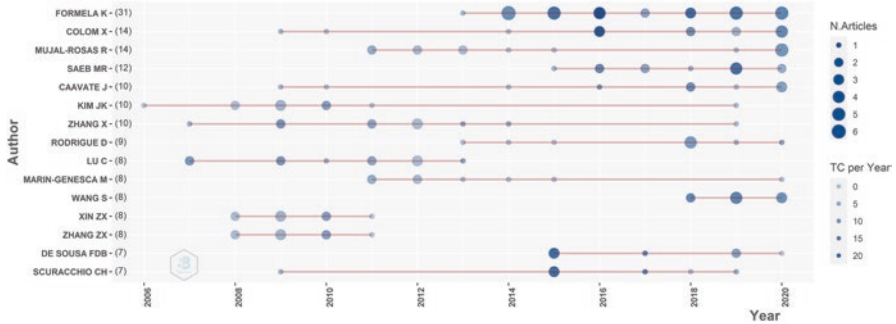


Fig. 2 Top-authors' production over the time

thermogravimetric characterization of GTR devulcanized by microwave treatment. The most cited publication by Mujal-Rosas is Mujal-Rosas et al. (Mujal-Rosas et al. 2011b), with 27 citations. The authors studied the dielectric, thermal, and mechanical properties of the ethylene vinyl acetate reinforced with GTR. The one by Saeb is Formela et al. (Formela et al. 2016), which received 50 citations and investigated the combined impact of plasticizer and shear force on the efficiency of low temperature reclaiming of GTR.

3.4 Publications

Table 1 presents the 10 most relevant publications (top 10), according to the local citation score (LCS) and the global citation score (GCS). LCS refers to the number of citations of publications in the local data set, i.e., it refers to the documents obtained from the Scopus search, whereas GCS refers to the total number of citations of publications in the entire Scopus database (de Sousa 2021). The higher the LCS, the more significant the publication concerning the GTR recycling, and the higher the GCS, the more important the publication is in the literature in general (it may be important to other areas besides the GTR recycling).

Regarding the top 10 GCS publications, some of them discuss the use of GTR in asphalt pavements and concretes (Bignozzi and Sandrolini 2006; Huang et al. 2007; Bravo and de Brito 2012; Lo Presti 2013), some authors (De Marco Rodriguez et al. 2001; Williams and Brindle 2003; Acosta et al. 2016) deal with pyrolysis, Sienkiewicz et al. (Sienkiewicz et al. 2012) investigated the progress in the used tires management in the European Union, and some authors (Ramarad et al. 2015) reviewed the use of waste tires in polymeric blends. Most of them are reviews.

About the top 10 LCS publications, some of them are part of the top 10 GCS publications group. From those not mentioned above, some authors investigated the devulcanization of GTR (De et al. 2006; Garcia et al. 2015; de Sousa et al. 2017), and others discussed the use of GTR in polymeric blends (Scaffaro et al. 2005; Sienkiewicz et al. 2017).

Table 1 Citation scores of the most relevant publications

Group	Publication	GCS	LCS
Top 10 GCS	Lo Presti (Lo Presti 2013)	429	21
	Huang et al. (Huang et al. 2007)	389	6
	De Marco Rodriguez et al. (De Marco Rodriguez et al. 2001)	317	14
	Sienkiewicz et al. (Sienkiewicz et al. 2012)	272	29
	Ramarad et al. (Ramarad et al. 2015)	219	26
	Karger-Kocsis et al. (Karger-Kocsis et al. 2013)	214	31
	Bignozzi and Sandrolini (Bignozzi and Sandrolini 2006)	210	9
	Bravo and de Brito (Bravo and de Brito 2012)	198	10
	Acosta et al. (Acosta et al. 2016)	159	0
	Williams and Brindle (Williams and Brindle 2003)	149	9
Top 10 LCS	Karger-Kocsis et al. (Karger-Kocsis et al. 2013)	214	31
	Sienkiewicz et al. (Sienkiewicz et al. 2012)	272	29
	Ramarad et al. (Ramarad et al. 2015)	219	26
	Lo Presti (Lo Presti 2013)	429	21
	Garcia et al. (Garcia et al. 2015)	93	20
	Scaffaro et al. (Scaffaro et al. 2005)	88	16
	De et al. (De et al. 2006)	99	15
	Sienkiewicz et al. (Sienkiewicz et al. 2017)	117	14
	De Marco Rodriguez et al. (De Marco Rodriguez et al. 2001)	317	14
	de Sousa et al. (de Sousa et al. 2017)	72	12

LCS local citation score, *GCS* global citation score

3.5 Authors' Keywords

From the 469 publications found through the Scopus search, a total of 1192 authors' keywords were found. The 50 most frequent authors' keywords were analyzed and are presented in the word cloud (Fig. 3), apart from the keyword recycling, which is the most frequent one (139 occurrences). This result was expected because it was one of the keywords used in the search for publications in the Scopus database. In the word cloud, the size of the letters represents the frequency of the keyword.

The word cloud provides a panorama of the literature concerning the recycling of GTR. Apart from the keywords used in the Scopus search, the most frequent authors' keywords are (number of occurrences in parenthesis): mechanical properties (43), pyrolysis (20), devulcanization (15), thermal properties (12), waste (12), composites (11), natural rubber (10), waste management (9), dielectric properties (8), and extrusion (8).

According to the word cloud, a concern of the literature regarding the recycling of GTRs is the characterization, demonstrated through the presence of the keywords mechanical properties (Soleimani et al. 2020; Phiri et al. 2020; Marín-Genescà et al. 2020a), thermal properties (Phiri et al. 2020), dielectric properties (Marín-Genescà et al. 2020c), and adsorption (Miguel et al. 2002; Imyim et al. 2016). It also depicts some concerns from the research area through the presence of the keywords waste



Fig. 3 Word cloud containing the 50 main authors’ keywords, apart from the keyword recycling

management (Hejna et al. 2020; Zedler et al. 2020a, b), degradation (Garcia et al. 2015; Edwards et al. 2016; de Sousa et al. 2017), and circular economy (Rhodes 2019; Dobrotá et al. 2020). Some ways of GTR recycling present in the word cloud are pyrolysis (Miguel et al. 2002; Januszewicz et al. 2020), devulcanization (Edwards et al. 2016; Li et al. 2019; Saputra et al. 2020) (by microwaves (de Sousa et al. 2019b; de Sousa and Ornaghi Júnior 2020)), modification (Hejna et al. 2020; Zedler et al. 2020a, b), and some applications such as in blends type of thermoplastic elastomer (Hejna et al. 2019) (with the thermoplastic phase composed of polyethylene (Datta and Włoch 2015) and polypropylene), composites (Ghosh et al. 2020; Marín-Genescà et al. 2020a, b; Phiri et al. 2020), concrete (Saberian et al. 2020), asphalt binder (Hassanpour-Kasanagh et al. 2020), and bitumen. Other no less important keywords are morphology (Datta and Włoch 2015) and compatibilization (Hejna et al. 2019; Zedler et al. 2020b), which are very important in the application of GTR in polymeric blends.

Figure 4 presents the trend topic over the last 20 years based on the authors’ keywords.

According to Fig. 4, some cutting-edge keywords in the area are thermoplastic elastomer and pyrolysis. These authors’ keywords, dealing with some important applications of GTR, were in evidence for a long period, giving way to other topics that are trending in the recent literature. Current trends are evidenced by keywords such as waste management, end-of-life tires, natural rubber, tyre recycling, and modification.

The conceptual structure map of the keywords according to the multiple correspondence analysis (MCA) method is presented in Fig. 5a, and the documents with the highest contribution are shown in Fig. 5b.

Measurable strategies for disentangling the complex keyword association into a few relative groups by MCA are based on the recurrence of the concurrent rate of two keywords (Ding 2011). A two- or three-dimensional structure is formed by the compression of large data with multiple variables, and the similarity between the

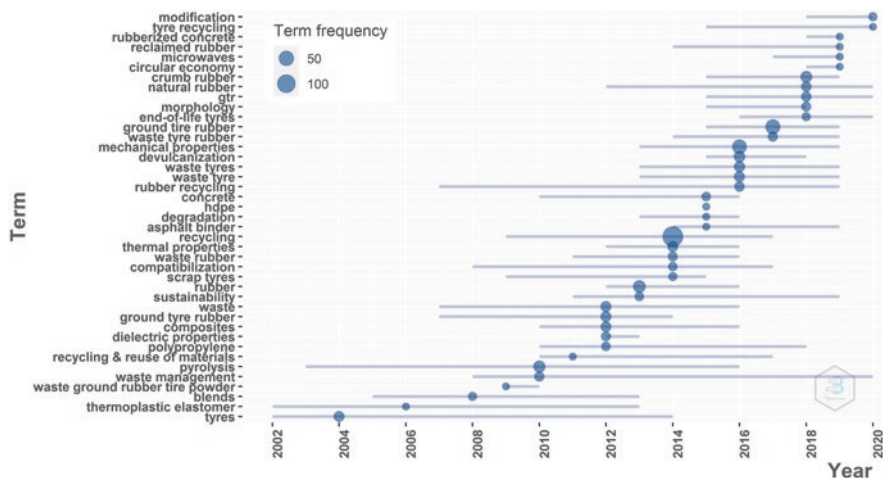


Fig. 4 Trend topic

keywords is demonstrated by the plane distance. The importance of the keyword is shown through its proximity to the central point of the cluster, and narrow themes are near the edge (de Sousa 2021).

Two clusters can be seen in Fig. 5a. The blue one shows the keywords devulcanization, revulcanization, and microwaves. Theoretically, devulcanization can restore the flow capability of the vulcanized rubber and, consequently, its ability to be remolded and reshaped into a new product (de Sousa et al. 2019c). Devulcanization by microwaves is considered an ally to green chemistry due to the increase of energy efficiency, as one of the green chemistry principles highlights the reduction of energy needed to minimize impacts on the environment and the economy (Jessop et al. 2008). The study of the revulcanization of devulcanized rubbers is essential to identify possible applications of the material (de Sousa et al. 2019b, c). So, the blue cluster evidences an important area of the GTR recycling.

Concerning the red cluster, it shows several applications of GTR such as in polymer blends, composites, reclaiming, modification; some possibilities largely used by literature about characterization such as microstructure analysis, dielectric, thermal, and mechanical properties; and some concerns demonstrated by the keywords degradation, circular economy, and waste management. So, this analysis is in accordance with the word cloud (Fig. 3).

In the blue cluster, all the keywords are on the edge, showing that they are connected but narrow themes. In the red cluster, the narrow themes are microstructure analysis, modification, reclaiming, plastics, and circular economy. The keywords on evidence, i.e., the words closest to the center point (shown in detail in Fig. 5a), are ground tyre rubber, rubber, and recycling. It is interesting to notice the proximity between the keywords modification (red cluster) and devulcanization (blue cluster), given that devulcanization can modify the chemical structure of the devulcanized GTR as a whole (de Sousa et al. 2017).

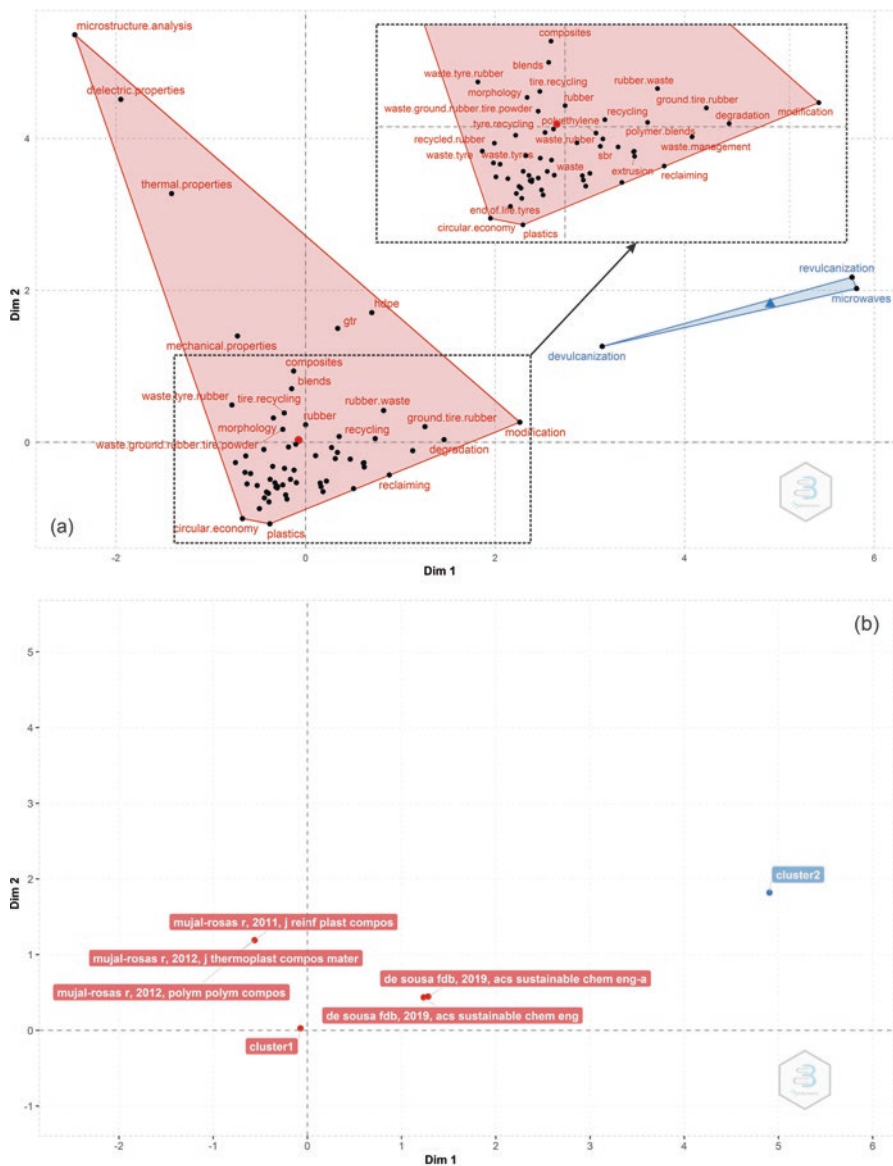


Fig. 5 (a) Conceptual structure map of the keywords according to the MCA method. (b) Factorial map of the publications with the highest contribution

Regarding the documents with the highest contribution in the red cluster (Fig. 5b), the research group of Mujal-Rosas analyzed the properties (dielectric, mechanical, thermal) and microstructure of polypropylene (Mujal-Rosas et al. 2012), high-density polyethylene (Mujal-Rosas et al. 2011a), and ethylene vinyl acetate

(Mujal-Rosas et al. 2011b) composites reinforced by GTR. De Sousa et al. (de Sousa et al. 2019b, c) studied the devulcanization of GTR devulcanized by microwaves.

Concerning the blue cluster, Bibliometrix did not provide results. However, when limiting the results obtained by Scopus with the keywords presented in the blue cluster (Fig. 5b), the most relevant publications, according to the Scopus database, are also the ones by de Sousa et al. (de Sousa et al. 2019b, c).

4 Challenges and Future Perspectives

It is known that recycling has utmost importance to society. It complies with the three criteria of the sustainability tripod because it saves the use of fossil raw material, saves energy and releases less gases to the environment, generates economic development, and increases social equity, because many workers have recycling as the main source of income for the livelihood of their families.

Concerning vulcanized rubbers such as GTR, the difficulties imposed in their recycling are precisely their melt down and remold, which is hindered by their three-dimensional structure (Kim and Lee 2000; Dierkes 2005; Garcia et al. 2015; de Sousa et al. 2017; Marín-Genescà et al. 2020b). The three-dimensional structure is formed by crosslinks, resulted from the initial vulcanization of rubbers. The crosslinks are formed by different sulfidic bonds such as monosulfidic, disulfidic, and polysulfidic bonds, which are mainly the result of the formulation used. Each bond has specific energy necessary to be broken, and it is at this point that the greatest difficulty in recycling rubber is found: to find an efficient, sustainable, and economically viable way to break, preferably the sulfidic bonds, and not the carbon-carbon bonds that form the polymer structure, which promotes degradation of the material.

Furthermore, the irregular disposal of end-of-life tires can cause harmful impacts on the environment and the entire population, since these environments become places conducive to the creation of vectors of diseases and other types of animals that pose risks to human health. The safe disposal of end-of-life tires is a global concern, evidencing a serious environmental issue (Marín-Genescà et al. 2020b), with waste management and circular economy being two great concerns of the literature depicted through the analysis of the authors' keywords. Based on this, countries around the globe have created laws aiming at environmentally correct disposal of these residues. However, academia is constantly searching for other methods to add value to recycled rubber, as described above.

Thus, the literature considers recycling of end-of-life tires and residues of vulcanized rubbers in general to be the biggest challenge in the area. In other words, the biggest challenge in the research area of rubber recycling is how to destroy, even partially, the three-dimensional structure of vulcanized rubbers. Besides, it is necessary that the final recycled materials have properties capable of noble and technological applications (de Sousa et al. 2019c). According to some authors (Rahman

et al. 2020), “sustainability can be ensured in recycling waste if the final product performs to the same degree or better than the existing product at a low cost and, at the same time, entails some environmental benefit.”

The analysis of the authors’ keywords may also show some future perspectives on the research area. As previously stated, some topic trends are waste management, end-of-life tires, natural rubber, tyre recycling, and modification. Additionally, the analysis of the mechanical properties has extreme relevance in the current literature, as it requires a deep knowledge of the recycled rubber properties as a whole for its application; and pyrolysis and devulcanization are two important recycling methods. The literature will constantly continue looking for ways to overcome the challenges of the GTR recycling research area.

5 Conclusions

From a Scopus search concerning the recycling of GTR, the literature of the past 20 years was analyzed by Bibliometrix. From the 469 publications obtained, 1192 authors’ keywords were found and thoroughly analyzed due to their importance in understanding the current and future scenario of the research area. In other words, trends and hotspots in the research area could be identified. Mechanical properties, pyrolysis, and devulcanization are considered hotspots, whereas waste management, end-of-life tires, natural rubber, tyre recycling, and modification are trends in the recycling of the GTR research area.

References

- Acosta R, Fierro V, Martinez de Yuso A et al (2016) Tetracycline adsorption onto activated carbons produced by KOH activation of tyre pyrolysis char. *Chemosphere* 149:168–176. <https://doi.org/10.1016/J.CHEMOSPHERE.2016.01.093>
- Bignozzi MC, Sandrolini F (2006) Tyre rubber waste recycling in self-compacting concrete. *Cem Concr Res* 36:735–739. <https://doi.org/10.1016/j.cemconres.2005.12.011>
- Bravo M, de Brito J (2012) Concrete made with used tyre aggregate: durability-related performance. *J Clean Prod* 25:42–50. <https://doi.org/10.1016/j.jclepro.2011.11.066>
- Colom X, Faliq A, Formela K, Cañavate J (2016) FTIR spectroscopic and thermogravimetric characterization of ground tyre rubber devulcanized by microwave treatment. *Polym Test* 52:200–208. <https://doi.org/10.1016/j.polymertesting.2016.04.020>
- Datta J, Włoch M (2015) Morphology and properties of recycled polyethylene/ground tyre rubber/thermoplastic poly(ester-urethane) blends. *Macromol Res* 2312(23):1117–1125. <https://doi.org/10.1007/S13233-015-3155-5>
- De Marco Rodriguez I, Laresgoiti MF, Cabrero MA et al (2001) Pyrolysis of scrap tyres. *Fuel Process Technol* 72:9–22. [https://doi.org/10.1016/S0378-3820\(01\)00174-6](https://doi.org/10.1016/S0378-3820(01)00174-6)
- de Sousa FDB (2016) Vulcanization of natural rubber: past, present and future perspectives. In: Hamilton JL (ed) *Natural rubber: properties, behavior and applications*. Nova Science Publishers, New York, pp 47–88

- de Sousa FDB (2021) The role of plastic concerning the sustainable development goals: the literature point of view. *Clean Responsible Consum* 3:100020. <https://doi.org/10.1016/j.clrc.2021.100020>
- de Sousa FDB (2022) A simplified bibliometric mapping and analysis about sustainable polymers. *Mater Today Proc* 49:2025–2033. <https://doi.org/10.1016/J.MATPR.2021.08.210>
- de Sousa FDB, Ornaghi Júnior HL (2020) From devulcanization of ground tire rubber by microwaves to revulcanization: a revulcanization kinetic approach using a simple prediction model. *ACS Sustain Chem Eng* 8:16304–16319. <https://doi.org/10.1021/acssuschemeng.0c05996>
- de Sousa FDB, Scuracchio CH (2020) Influence of dynamic revulcanization of ground tire rubber in blends composed of high-density polyethylene/ground tire rubber devulcanized by microwaves. *AIP Conf Proc* 2289:020051-1–020051-5. <https://doi.org/10.1063/5.0028257>
- de Sousa FDB, Gouveia JR, de Camargo Filho PMF et al (2015a) Blends of ground tire rubber devulcanized by microwaves/HDPE – Part A: influence of devulcanization process. *Polímeros* 25:256–264. <https://doi.org/10.1590/0104-1428.1747>
- de Sousa FDB, Gouveia JR, de Camargo Filho PMF et al (2015b) Blends of ground tire rubber devulcanized by microwaves/HDPE-Part B: influence of clay addition. *Polim E Tecnol* 25:382–391. <https://doi.org/10.1590/0104-1428.1955>
- de Sousa FDB, Scuracchio CH, Hu GH, Hoppe S (2016) Effects of processing parameters on the properties of microwave-devulcanized ground tire rubber/polyethylene dynamically revulcanized blends. *J Appl Polym Sci* 133. <https://doi.org/10.1002/app.43503>
- de Sousa FDB, Scuracchio CH, Hu GH, Hoppe S (2017) Devulcanization of waste tire rubber by microwaves. *Polym Degrad Stab* 138:169–181. <https://doi.org/10.1016/j.polymdegradstab.2017.03.008>
- de Sousa FDB, Hu G-H, Hoppe S, Scuracchio CH (2019a) Influence of devulcanization and revulcanization of ground tire rubber in dynamic mechanical properties of blends ground tire rubber/high density polyethylene. *AIP Conf Proc* 2139:090002-1–090002-4. <https://doi.org/10.1063/1.5121674>
- de Sousa FDB, Zanchet A, Ornaghi Júnior HL, Ornaghi FG (2019b) Revulcanization kinetics of waste tire rubber devulcanized by microwaves: challenges in getting recycled tire rubber for technical application. *ACS Sustain Chem Eng* 7:15413–15426. <https://doi.org/10.1021/acssuschemeng.9b02904>
- de Sousa FDB, Zanchet A, Scuracchio CH (2019c) From devulcanization to revulcanization: challenges in getting recycled tire rubber for technical applications. *ACS Sustain Chem Eng* 7:8755–8765. <https://doi.org/10.1021/acssuschemeng.9b00655>
- De D, Das A, De D et al (2006) Reclaiming of ground rubber tire (GRT) by a novel reclaiming agent. *Eur Polym J* 42:917–927. <https://doi.org/10.1016/j.eurpolymj.2005.10.003>
- Dierkes W (2005) Untreated and treated rubber powder. In: De SK, Isayev AI, Khait K (eds) *Rubber recycling*. CRC Press/Taylor & Francis, Boca Raton, pp 136–160
- Ding Y (2011) Scientific collaboration and endorsement: network analysis of coauthorship and citation networks. *J Inflamm* 5:187–203. <https://doi.org/10.1016/j.joi.2010.10.008>
- Dobrotă D, Dobrotă G, Dobrescu T (2020) Improvement of waste tyre recycling technology based on a new tyre markings. *J Clean Prod* 260:121141. <https://doi.org/10.1016/J.JCLEPRO.2020.121141>
- Edwards DW, Danon B, van der Gryp P, Görgens JF (2016) Quantifying and comparing the selectivity for crosslink scission in mechanical and mechanochemical devulcanization processes. *J Appl Polym Sci* 133. <https://doi.org/10.1002/APP.43932>
- Formela K, Klein M, Colom X, Saeb MR (2016) Investigating the combined impact of plasticizer and shear force on the efficiency of low temperature reclaiming of ground tire rubber (GTR). *Polym Degrad Stab* 125:1–11. <https://doi.org/10.1016/j.polymdegradstab.2015.12.022>
- Garcia PS, de Sousa FDB, de Lima JA et al (2015) Devulcanization of ground tire rubber: physical and chemical changes after different microwave exposure times. *Express Polym Lett* 9:1015–1026. <https://doi.org/10.3144/expresspolymlett.2015.91>
- Ghosh J, Hait S, Ghorai S et al (2020) Cradle-to-cradle approach to waste tyres and development of silica based green tyre composites. *Resour Conserv Recycl* 154:104629. <https://doi.org/10.1016/J.RESCONREC.2019.104629>

- Hassanpour-Kasanagh S, Ahmedzade P, Fainleib AM, Behnood A (2020) Rheological properties of asphalt binders modified with recycled materials: a comparison with styrene-butadiene-styrene (SBS). *Constr Build Mater* 230:117047. <https://doi.org/10.1016/J.CONBUILDMAT.2019.117047>
- Hejna A, Klein M, Saeb MR, Formela K (2019) Towards understanding the role of peroxide initiators on compatibilization efficiency of thermoplastic elastomers highly filled with reclaimed GTR. *Polym Test* 73:143–151. <https://doi.org/10.1016/J.POLYMERTESTING.2018.11.005>
- Hejna A, Zedler L, Przybysz-Romatowska M et al (2020) Reclaimed rubber/poly(ϵ -caprolactone) blends: structure, mechanical, and thermal properties. *Polymers (Basel)* 12:1204. <https://doi.org/10.3390/POLYM12051204>
- Huang Y, Bird RN, Heidrich O (2007) A review of the use of recycled solid waste materials in asphalt pavements. *Resour Conserv Recycl* 52:58–73. <https://doi.org/10.1016/J.RESCONREC.2007.02.002>
- Imyim A, Sirithaweessit T, Ruangpornvisuti V (2016) Arsenite and arsenate removal from wastewater using cationic polymer-modified waste tyre rubber. *J Environ Manag* 166:574–578. <https://doi.org/10.1016/J.JENVMAN.2015.11.005>
- Januszewicz K, Kazimierski P, Kosakowski W, Lewandowski WM (2020) Waste tyres pyrolysis for obtaining limonene. *Materials (Basel)* 13:1359. <https://doi.org/10.3390/ma13061359>
- Jessop PG, Trakhtenberg S, Warner J (2008) The twelve principles of green chemistry. In: Flank WH, Abraham MA, Matthews MA (eds) *Innovations in industrial and engineering chemistry: a century of achievements and prospects for the new millennium*. American Chemical Society, Washington, DC, pp 401–436
- Karger-Kocsis J, Meszaros L, Barany T (2013) Ground tyre rubber (GTR) in thermoplastics, thermosets, and rubbers. *J Mater Sci* 48:1–38. <https://doi.org/10.1007/s10853-012-6564-2>
- Kim JK, Lee SH (2000) New technology of crumb rubber compounding for recycling of waste tires. *J Appl Polym Sci* 78:1573–1577. [https://doi.org/10.1002/1097-4628\(20001121\)78:8<1573::aid-app150>3.0.co;2-p](https://doi.org/10.1002/1097-4628(20001121)78:8<1573::aid-app150>3.0.co;2-p)
- Li Y, Shen A, Lyu Z et al (2019) Ground tire rubber thermo-mechanically devulcanized in the presence of waste engine oil as asphalt modifier. *Constr Build Mater* 222:588–600. <https://doi.org/10.1016/J.CONBUILDMAT.2019.06.162>
- Lo Presti D (2013) Recycled tyre rubber modified bitumens for road asphalt mixtures: a literature review. *Constr Build Mater* 49:863–881. <https://doi.org/10.1016/J.CONBUILDMAT.2013.09.007>
- Marín-Genescà M, García-Amorós J, Mujal-Rosas R et al (2020a) Microparticle size and quantities effect on the mechanical features of end of life tires in thermoplastic composites. *Materials (Basel)* 13:5561. <https://doi.org/10.3390/MA13235561>
- Marín-Genescà M, García-Amorós J, Mujal-Rosas R et al (2020b) Study and characterization of the dielectric behavior of low linear density polyethylene composites mixed with ground tire rubber particles. *Polymers (Basel)* 12:1075. <https://doi.org/10.3390/POLYM12051075>
- Marín-Genescà M, García-Amorós J, Mujal-Rosas R et al (2020c) Application properties analysis as a dielectric capacitor of end-of-life tire-reinforced HDPE. *Polymers (Basel)* 12:2675. <https://doi.org/10.3390/POLYM12112675>
- Miguel GS, Fowler GD, Sollars CJ (2002) Adsorption of organic compounds from solution by activated carbons produced from waste tyre rubber. *Sep Sci Technol* 37:663–676. <https://doi.org/10.1081/SS-120001453>
- Mujal-Rosas R, Marin-Genesca M, Orrit-Prat J et al (2011a) Dielectric, mechanical, and thermal characterization of high-density polyethylene composites with ground tire rubber. *J Thermoplast Compos Mater* 25:537–559. <https://doi.org/10.1177/0892705711411344>
- Mujal-Rosas R, Orrit-Prat J, Ramis-Juan X et al (2011b) Study on dielectric, thermal, and mechanical properties of the ethylene vinyl acetate reinforced with ground tire rubber. *J Reinf Plast Compos* 30:581–592. <https://doi.org/10.1177/0731684411399135>
- Mujal-Rosas R, Orrit-Prat J, Ramis-Juan X et al (2012) Study on dielectric, mechanical and thermal properties of polypropylene (PP) composites with ground tyre rubber (GTR). *Polym Polym Compos* 20:797–808. <https://doi.org/10.1177/096739111202000905>

- Phiri MJ, Phiri MM, Mpitso K, Hlangothi SP (2020) Curing, thermal and mechanical properties of waste tyre derived reclaimed rubber–wood flour composites. *Mater Today Commun* 25:101204. <https://doi.org/10.1016/J.MTCOMM.2020.101204>
- Rahman MT, Mohajerani A, Giustozzi F (2020) Recycling of waste materials for asphalt concrete and bitumen: a review. *Materials (Basel)* 13. <https://doi.org/10.3390/MA13071495>
- Ramarad S, Khalid M, Ratnam CT et al (2015) Waste tire rubber in polymer blends: a review on the evolution, properties and future. *Prog Mater Sci* 72:100–140. <https://doi.org/10.1016/J.PMATSCI.2015.02.004>
- Rhodes CJ (2019) Solving the plastic problem: from cradle to grave, to reincarnation. *Sci Prog* 102:218–248. <https://doi.org/10.1177/0036850419867204>
- Saberian M, Li J, Perera STAM et al (2020) An experimental study on the shear behaviour of recycled concrete aggregate incorporating recycled tyre waste. *Constr Build Mater* 264:120266. <https://doi.org/10.1016/J.CONBUILDMAT.2020.120266>
- Saputra R, Walvekar R, Khalid M et al (2020) Devulcanisation of ground rubber tyre by novel ternary deep eutectic solvents. *J Mol Liq* 306:112913. <https://doi.org/10.1016/J.MOLLIQ.2020.112913>
- Scaffaro R, Dintcheva NT, Nocilla MA, La Mantia FP (2005) Formulation, characterization and optimization of the processing condition of blends of recycled polyethylene and ground tyre rubber: mechanical and rheological analysis. *Polym Degrad Stab* 90:281–287. <https://doi.org/10.1016/j.polymdegradstab.2005.03.022>
- Sienkiewicz M, Kucinska-Lipka J, Janik H, Balas A (2012) Progress in used tyres management in the European Union: a review. *Waste Manag* 32:1742–1751. <https://doi.org/10.1016/j.wasman.2012.05.010>
- Sienkiewicz M, Janik H, Borzędowska-Labuda K, Kucińska-Lipka J (2017) Environmentally friendly polymer-rubber composites obtained from waste tyres: a review. *J Clean Prod* 147:560–571. <https://doi.org/10.1016/J.JCLEPRO.2017.01.121>
- Soleimani M, Cree D, Olson L et al (2020) Fabrication of nonextruded recycled rubber–polyethylene composites. *J Appl Polym Sci* 137:49067. <https://doi.org/10.1002/APP.49067>
- Williams PT, Brindle AJ (2003) Aromatic chemicals from the catalytic pyrolysis of scrap tyres. *J Anal Appl Pyrolysis* 67:143–164. [https://doi.org/10.1016/S0165-2370\(02\)00059-1](https://doi.org/10.1016/S0165-2370(02)00059-1)
- Zedler Ł, Burger P, Wang S, Formela K (2020a) Ground tire rubber modified by ethylene-vinyl acetate copolymer: processing, physico-mechanical properties, volatile organic compounds emission and recycling possibility. *Materials (Basel)* 13:4669. <https://doi.org/10.3390/MA13204669>
- Zedler Ł, Kowalkowska-Zedler D, Colom X et al (2020b) Reactive sintering of ground tire rubber (GTR) modified by a trans-polyoctenamer rubber and curing additives. *Polymers (Basel)* 12:3018. <https://doi.org/10.3390/POLYM12123018>

Polymer Processing Technology to Recycle Polymer Blends



Daniel C. Licea Saucedo, Rubén González Nuñez,
Milton O. Vázquez Lepe, and Denis Rodrigue

1 Introduction

Before the era of single-use plastics, the practice of reusing products was performed. Returnable containers were used for the distribution of milk, wine, beer, soda, beverages, and even for some bulk foods. With the turn of the century, more efficient and economic processes allowed the plastic industry to manufacture products with a shorter life cycle. It was easier and cheaper to throw away rather than to reuse. Thus, linear economy became the central dogma in our society: produce, use, and discard. Several items, such as plates, cups, cutlery, food containers, bottles, and packaging materials, became available in large amounts and at affordable prices. Before long, plastic solid waste started accumulating in landfills at an unsustainable rate.

The worldwide plastic production totaled 367 million metric tons in 2020, which fell by 0.3% compared to the 2019 production due to the COVID-19 pandemic (Tiseo 2021). Conventional plastics, such as polyethylene (PE) or polypropylene (PP), take years to decompose; in fact, they only break down into smaller particles called microplastics (MP) (Giacovelli 2018). Microplastics are especially of high concern since they cannot be efficiently recovered from the environment, ultimately ending up in the oceans, where 80% of the total plastic debris originates from land-based sources (Li et al. 2016). Persistent organic pollutants, chemical additives, and residual monomers present in MP may represent a toxic hazard for marine life as

D. C. Licea Saucedo · R. G. Nuñez · M. O. Vázquez Lepe
Departamento de Ingeniería Química, CUCEI, Universidad de Guadalajara,
Guadalajara, Jalisco, México

D. Rodrigue (✉)
Department of Chemical Engineering and CERMA, Université Laval, Quebec, QC, Canada
e-mail: Denis.Rodrigue@gch.ulaval.ca

these small particles can be ingested by marine invertebrates, transported to higher trophic levels, and found in commercial seafood species (Andrady 2017).

It is precisely the negative impact on the environment that triggered a much-needed change in the public's way of thinking and acting. Society has turned toward greener, more sustainable materials. Consumers are now looking for recycled or biodegradable products, even if the price is sometimes slightly higher. Over the last decade, several applications were redesigned and one good example is the development of eco-bricks based on plastics bottles (typically made from polyethylene terephthalate, PET) and filled with commodity plastics such as plastics bags (made from polyethylene, PE), packaging material (made from polypropylene, PP), and polystyrene (PS) containers. The aim of this new way of thinking (designed for recycling) is to sequester plastics that would otherwise end up accumulating in the environment or incinerated.

Recycling still remains the most environmental-friendly way to dispose of solid plastic waste. Not only does it prevent large-scale environmental pollution, but it also lowers the demand for virgin raw materials from nonrenewable sources such as petroleum. Recycling may be the key for meeting the rising demand of plastic production and for the transition toward a greener industry via a circular economy: product design, material sourcing, production, use, postconsumer collection, and recycling.

1.1 Basic Concepts

Plastic recycling consists of physical or chemical processes to recover raw materials as polymers or monomers, respectively, to be used in the manufacture of new products (Moon and Morris 2019). Recently, recycling became a matter of the utmost importance, given the increasing trends in polymer demand and production. For example, more plastic has been manufactured over the last 20 years than in the previous 50 years (Geyer et al. 2017). All plastics can be considered as storage for potential energy since they account for 4% of the global oil production (Singh et al. 2017).

Petroleum-based products, such as plastics, must be used and reused as many times as possible to decrease the demand of virgin raw material, lower costs, and decrease environmental impact. Figure 1 shows the fate of plastic materials in the current waste management scheme.

There are mainly three types of mixtures in plastic solid waste (PSW): municipal solid waste (MSW), waste electric and electronic equipment (WEEE), and automobile shredder residue (ASR) (Dorigato 2021). These mixtures tend to be very complex as they are composed of several resins. In general, they consist of high-density polyethylene (HDPE), low-density polyethylene (LDPE), polyvinylchloride (PVC), polypropylene (PP), polystyrene (PS), polyethylene terephthalate (PET), polymethylmethacrylate (PMMA), acrylonitrile butadiene styrene (ABS) copolymer, and polycarbonate (PC) (Dorigato 2021).

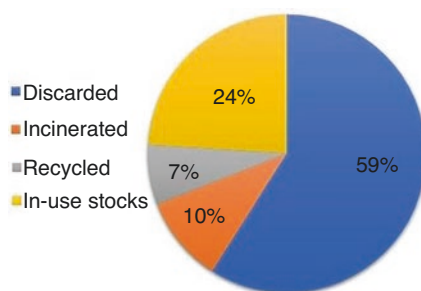


Fig. 1 Global plastic waste management. Recycling accounts for only 7% of the total plastic production. (Geyer et al. 2017)

Plastics recycling can be divided into four main categories: primary, secondary, tertiary, and quaternary recycling (Singh et al. 2017). *Primary recycling*, also known as closed-loop processing or re-extrusion, deals with pollutant-free homopolymer blends. The materials (typically postindustrial) are melted and pelletized to be reprocessed for the same application since they can maintain the properties similar to that of the virgin material (Horodytska et al. 2018). *Secondary recycling* (or open-loop process) is used for the processing of postconsumer polymers for less demanding applications, such as garbage bags, pipes, or agricultural products, due to the presence of contamination (Horodytska et al. 2018). It includes various steps such as size reduction, washing, drying, and pelletizing. Both primary and secondary recycling fall into mechanical recycling. *Tertiary recycling* is a process in which monomers are recovered from plastics solid waste via thermal and catalytic depolymerization/pyrolysis (Al-Salem et al. 2017; Kunwar et al. 2016; Vollmer et al. 2020) from which new products (resins) can be manufactured. When a material cannot be recycled in any of the previous ways, *quaternary recycling* comes into play. Energy recovery is the final alternative for recycling, the most common method used in Europe (Ignatyev et al. 2014). PSW is incinerated to generate heat and electricity with efficiencies of up to 90% (Horodytska et al. 2018). Nevertheless, emissions must be treated with activated charcoal, neutralized, and filtered to prevent environmental pollution (Singh et al. 2017).

Given the complexity of plastic mixtures found in waste streams, problems such as chemical incompatibility or physical inhomogeneity may arise. Thus, separating the components is a crucial step in plastic recycling. Various procedures have been developed to separate different plastic materials: manual sorting, density separation, dissolution sorting, biodegradation, spectroscopic separation, electrostatic sorting, supercritical separation, and selective flotation (Dorigato 2021). Waste collection systems may not be efficient in sorting similar materials such as PE and PP, or PET and PLA (poly(lactic acid), a biopolymer) because of chemical similarity, general appearance, and density, making it difficult to generate “pure” streams (Aumnate et al. 2019; Gere and Czigany 2020). Separation may present great economic and environmental disadvantages as compared to the more attractive option of direct recycling of plastic waste mixtures.

When considering the recycling of plastic mixtures, one must take into account polymer miscibility. A miscible polymer blend is made from a mixture of two or more matrices presenting phase homogeneity and satisfying thermodynamic conditions. An immiscible blend does not satisfy thermodynamic phase stability conditions (Utracki and Favis 1989). Immiscible blends prepared through simple mixing present evident phase separation, affecting the overall mechanical performances (Dorigato 2021). PP with both HDPE and LDPE are immiscible at any ratio and show phase separation during cooling and crystallization (Aumnate et al. 2019). Compatibilization becomes a convenient way to produce new polymeric materials with high performance and for the recycling of plastic waste (Li et al. 2017).

For the mixing of two polymers, compatibility is achieved by using “block or graft copolymers” having “chemical affinity” or reactivity with each component of the blend (Li et al. 2017). This method is not as “effective for ternary or multiphase immiscible polymer blends” since each component adds complexity to the copolymer. For nonreactive (ex situ) compatibilization, premade copolymers (each one miscible with one constituent of the blend) are mixed with the immiscible blend in the melt state (Dorigato 2021; Gere and Czigany 2020). Some polymers may have reactive functional groups in their structure (carboxylic acid, hydroxyl, amine, etc.), so molecules also having reactive functional groups (epoxy, anhydride, carboxylic acid, isocyanate, etc.) may be used as reactive compatibilizers. The reaction is carried out during melt blending, forming in situ copolymers that act as effective compatibilizers (Dorigato 2021; Gere and Czigany 2020).

One of the problems arising during recycling is degradation, which is related to the number of thermo-mechanical cycles the polymers have undergone. Other important factors are differences in melt temperatures, mechanical stress, and oxidation resulting in chain breakup (La Mantia et al. 2017). These changes in the molecular structure/weight distribution can affect the viscosity/elasticity of the material, leading to possible processing difficulties and affecting the properties of the final product. In this case, chain extenders (via their reactive functional groups) can increase molecular weight, thus reinstating melt strength (Gere and Czigany 2020).

In general, mechanical recycling is the preferred choice for thermoplastic polymer blends, given their good processability and versatile properties (Dorigato 2021). Nevertheless, for the reasons mentioned above, some upgrades must be done on plastic waste streams to satisfy technical requirements.

2 Mechanical Recycling

Before new materials can be manufactured from plastic waste, raw materials need to be recovered. This process starts after the collection step, where plastic waste is no longer considered waste, but rather a secondary raw material, referred to as *End-of-life*. These steps may include separation, sorting, baling, washing, grinding, compounding, and pelletizing (Ragaert et al. 2017).

Plastics are then sorted and separated through a combination of manual and automated processes. Near infrared (NIR) technologies are used to identify polymer types, while optical color recognition separates clear from colored fractions (Ragaert et al. 2017; Schyns and Shaver 2021). The use of dyes as molecular tags to simplify plastics sorting via UV-vis spectroscopy has been proposed, though questions arise as to whether these molecules can withstand the extrusion and degradation processes (Schyns and Shaver 2021). A relatively new technique has been proposed based on pulsed laser sources to analyze the carbon and hydrogen content in samples (laser-induced breakdown spectroscopy, LIBS). This method showed the ability of identifying six plastic materials (LDPE, HDPE, PP, PS, PET, and PVC) (Singh et al. 2017). Other sorting technologies include X-rays, froth flotation, magnetic density, electrostatics, melting point, hydrocyclones, and selective dissolution (Ragaert et al. 2017; Schyns and Shaver 2021; Serranti and Bonifazi 2019; Singh et al. 2017). Manual sorting by an operator might be expensive, but highly efficient. Operators are frequently used as quality control, supervising for any false positives or negatives, while correcting any inconsistencies.

Baling of polymers may be needed for transportation when sorting and processing take place in different locations. Frequently, complete separation of PSW is costly, hence bulk PSW is used (Maris et al. 2018). Upon arrival at the facility, subsequent cycles of grinding and washing occur to separate any residual impurities (Ragaert et al. 2017). After drying, regranulation is carried out via extrusion. An extruder typically consists of a hopper, a cylindrical barrel, single or twin screws, a die head, and a motor (Singh et al. 2017). Extrusion is an affordable, large-scale, and solvent-free method used in mechanical recycling to produce regrind material from PSW (Schyns and Shaver 2021). This process induces thermal softening of the material through heat and rotating screws, after which it is fed through a temperature-controlled die, giving the extrudate a fixed shape (usually in the form of a filament for pelletization).

Extruders can be tailor-made to include sections to degas, soften, dry, and filter the extrudate, thus improving the final polymer melt quality. Volatile compounds are removed via open vents or vacuum sections in the barrel, minimizing hydrolysis/acidolysis and improving polymer melt odor. Melt filtration can be used to remove non-melting and nonvolatile compounds such as wood, paper, dust, rubber particles, or higher melting point polymers. Extruders equipped with filters improve blend homogeneity and overall polymer quality (better mechanical and optical properties) (Ragaert et al. 2017; Schyns and Shaver 2021).

An important challenge arising during recycling is degradation. The extrusion process may lead to thermo-oxidative and stress-induced chain scission, chain branching, and cross-linking, which in turn affect the mechanical properties and processability (Ragaert et al. 2017). To prevent free-radical reactions, polymers are extruded with stabilizers. Primary antioxidants protect the chains during the polymer's lifetime, while secondary antioxidants do so during melt processing (Schyns and Shaver 2021).

3 Polymer Blends Recycling

The use of polymer blending technology in plastics recycling is a viable alternative for reducing polymeric waste. While the use of (single-use) plastics has increased due to the COVID-19 outbreak, recycling has decreased by 5.1% (ReportLinker 2020), so only 9% of all the plastic around the world is adequately recycled. However, some countries have recycling rates exceeding 60%. The most collected plastics in the United Kingdom (Schyns and Shaver 2021) are PET (40%), followed by HDPE and LDPE (22%), PP (10%), PS (<2%), and PVC (<2%), while in the United States the values are much lower for PET (15%), PE (9%), PS (2%), PP (1.5%), and PVC (0.2%) (Di et al. 2021). Most countries have regulated and imposed taxes on single-use plastics. However, amid the COVID-19 pandemic, demand for flexible materials (most of which are single-use plastics) increased by “40% in packaging and 17% in other applications, including medical uses” (Silva et al. 2021).

Several plastics are reprocessed in the form of blends following several strategies: (1) recycling with the same virgin polymer, (2) recycling in blend with polymer different from the recycled one, (3) recycling of commingled plastics with a compatibilizer, (4) recycling of commingled plastics with the formation of composites, and more recently, due to an increase in biopolymers production, (5) recycling of bioplastics-based blends. Reviews on this topic have been published (Utracki 2002; La Mantia and Scaffaro 2014; Dorigato 2021). In the next section, these five strategies are discussed in more detail.

3.1 Recycled Homopolymer Blends

One of the most used techniques in the industry is to incorporate into the process postindustrial and/or postconsumer polymers. The main industrial plastics (commodities) are identified by three arrows in a triangular formation with a number inside (1–7), each number representing a different type of polymer. Table 1 shows the relevant work done on the recycling of homopolymer blends.

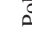







Over the last 20 years, PET has proven to be an important engineering polymer, showing its uniqueness to be recycled over and over. PET is seen as an excellent material for several packaging applications and is widely used for making bottles, fibers, and sheets (Elmari et al. 2017). Extrusion has been shown to be an adequate technique for PET blending. For example, a 70/30 vPET/rPET blend was shown to have similar properties to virgin PET fibers (Lee et al. 2012). Tapia-Picazo et al. (2014) recommended operating conditions and material characteristics for successful recycling: 0.5–0.8 inherent viscosity values, 30–45 rpm screw speed, 270–300 °C and 0.01–0.02% humidity. A blend of 25/75 vPET/rPET was successfully recycled up to 11 times without significant property loss (Pinter et al. 2021).



Table 1 Research on homopolymer and heteropolymer recycled blends and their respective processing strategy

Polymers							
<p>Extrusion (Pinter et al. 2021; Lee et al. 2012; Tapia-Picazo et al. 2014) Injection molding (Snowdon et al. 2020)</p>	<p>Injection molding (Lei et al. 2009; Pawlak et al. 2002)</p>	<p>Compression molding (Akovali and Karababa 1998) Internal mixer (Mamoor et al. 2013; Paci and La Mantia 1999)</p>	<p>Extrusion (Wang et al. 2019; Zhang et al. 2009) Injection molding (Dekva et al. 2019)</p>	<p>Injection molding (Catelli de Souza and Barbosa Caldeira 2015; Inoya et al. 2012) Extrusion (Gallego et al. 2006; Tao and Mai 2007)</p>	<p>Injection molding (Imamura et al. 2014) Melt spinning (Zander et al. 2017)</p>		
<p>Injection molding (Lei et al. 2009; Pawlak et al. 2002)</p>	<p>Injection molding (Sanchez-Soto et al. 2008; Alzereca et al. 2015; Kartalis et al. 2000a, b; Meran et al. 2008) Blow extrusion (Mnif and Elleuch 2015; Ramirez-Vargas et al. 2006) Extrusion (Miller et al. 2001) Rotomolding (Cestari et al. 2021)</p>	<p>Injection molding (Elmaghor et al. 2003)</p>	<p>Blow extrusion (Ramirez-Vargas et al. 2006) Injection molding (Habibi et al. 2017)</p>	<p>Extrusion (Camacho and Karlsson 2002)</p>	<p>Injection molding (Sahnoune et al. 2003; Elmaghor et al. 2003)</p>		

(continued)

Table 1 (continued)

 Polymers	 Internal mixer (Mamoor et al. 2013)	 Extrusion (Lee et al. 2019) Injection molding (Elmaghor et al. 2003)	 Compression molding (Sombatsompop and Thongsang 2001; Wenguang and La Mantia 1996) Rheometry (Popovska-Pavlovska et al. 2000; Maund et al. 1996) Two-roll mill blending (Garcia et al. 2007)	 Compression molding (Ajji 1995) Extrusion (Yoo et al. 2004)	 Two-roll mill blending (Andricic et al. 2008)	 Solution blending (Lin and Lin 1999) Internal mixer (Si et al. 2006)
	Injection molding (Dekva et al. 2019) Internal mixer (Mamoor et al. 2013)	Injection molding (Habibi et al. 2017)	Compression molding (Ajji 1995; Kabdi and Belhaneche-Bensemra 2008) Extrusion (Yoo et al. 2004)	Extrusion (Passos Severino et al. 2021; Jin et al. 2012) Injection molding (Meran et al. 2008) Rotomolding (Diaz et al. 2018)	Injection molding (Saikrishnan et al. 2020; Aummate et al. 2019) Compression molding (Bertin and Robin 2002; Nedkov et al. 2008)	Internal mixer (Fortelny et al. 2004) Dry blending (Olofinnade et al. 2021) Two-roll mill blending (Chouiref and Belhaneche-Bensemra 2012)

	Extrusion (Gallego et al. 2006) Melt spinning (Zander et al. 2017)	Extrusion (Camacho and Karlsson 2002) Compression molding (Bonelli et al. 2001)	Two-roll mill blending (Fadipe 2020; Andrić et al. 2008)	Injection molding (Saikrishnan et al. 2020) Compression molding (Mansor et al. 2019; Bertin and Robin 2002; Nedkov et al. 2008)	Injection molding (Wattanachai et al. 2017; Tai and Yeh 2018; Raj et al. 2013) Extrusion (La Mantia et al. 2021; Meran et al. 2008) Melt spinning (Gregor-Steveć et al. 2009)	Injection molding (Kong et al. 2018; Barreto et al. 2019) Two-roll mill blending (Fadipe 2020) Melt spinning (Zander et al. 2017)
	Melt spinning (Zander et al. 2017)	Injection molding (Sahnoune et al. 2003; Elmaghor et al. 2003)	Solution blending (Lin and Lin 1999)	Dry blending (Olofinmade et al. 2021)	Injection molding (Kong et al. 2018) Melt spinning (Zander et al. 2017)	Injection molding (Hirayama and Saron 2018) Solution blending (García-Ivares et al. 2017)

Bold references indicate the use of additives or compatibilizers

HDPE homopolymers have been recycled through various techniques, such as injection molding (Alzerreca et al. 2015; Kartalis et al. 2000a, b; Meran et al. 2008), blow extrusion (Mnif and Elleuch 2015), and rotomolding (Cestari et al. 2021). Mnif and Elleuch (2015) showed that after only two reprocessing cycles, vHDPE/rHDPE blends presented a significant decrease in viscosity and tensile properties. In order to be reused in the same application, the material needs to be restabilized (Kartalis et al. 2000a, b). However, Alzerreca et al. (2015) concluded that rHDPE can be used for less-demanding applications such as gravity sewer systems, either by reducing pollutant concentration, improving their compatibility, or by increasing tie macromolecule content.

PVC is only second after polyethylene in worldwide consumption, widely used in pipes and construction applications. Sombatsompop and Thongsang (2001) showed that recycling PVC pipes is possible by blending with virgin PVC with concentrations varying from 20% to 80%; while Popovska-Pavlovska et al. (2000) reported up to 50% recyclate of postconsumer oil bottles with adequate processability at a lower temperature, without negative effects on the mechanical and rheological properties.

LDPE (along with HDPE) constitutes half of all the plastics packaging materials. Studies have focused on strategies to recycle LDPE from different sources, such as postconsumer packaging films (Kartalis et al. 2000a, b), mixed MSW (Soto et al. 2018, 2020), and agricultural plastic waste (Briassoulis et al. 2021). Meran et al. (2008) found that the mechanical properties of vLDPE/rLDPE blends linearly decreased as the recycled material content increased. In an attempt to elucidate the number of reprocessing cycles that LDPE can withstand, Jin et al. (2012) recycled the material 100 times, reporting that significant loss of processability and long-time mechanical properties was observed after 40 cycles.

PP accounts for 16% of the global plastic production and is mainly used in packaging, construction, automotive, and sports industries (Bora et al. 2020). Similar to other polyolefins, the mechanical, thermal, and rheological properties of vPP/rPP blends linearly decrease with an increase in recycled material content (Meran et al. 2008; Tai and Yeh 2018). Through simple melt spinning, Gregor-Svetc et al. (2009) obtained monofilaments that were porous, brittle, rigid, and easily broken. Single-screw extrusion proved to be a better processing technique since 70/30 vPP/rPP blends were compatible and maintained adequate mechanical and rheological properties (La Mantia et al. 2021). Raj et al. (2013) showed that for vPP/rPP blends processed by injection molding, a 60/40 ratio provided good flexural strength, although the best results were obtained at 90/10. It was also shown that blends of up to 50% rPP from an automotive source are suitable for a motorcycle saddle application, thus reducing the raw materials' costs by 5–13% (Wattanachai et al. 2017).

PS is highly used in several applications such as packaging, automotive, construction, and electrical and electronic equipment (Thakur et al. 2018). Mechanical recycling of PS foams is especially difficult considering its low density, making transport economically unviable, unless one considers the use of solvents leading to a volume reduction of more than 100 times (Garcia et al. 2009). Despite this

difficulty, high impact polystyrene (HIPS) membranes from recycled plastic waste have been successfully prepared for use in water microfiltration and ultrafiltration (Garcia-Ivars et al. 2017).

3.2 Recycled Binary Blends

Recycled heteropolymer blends are of high interest as a way to easily recycle waste materials. PE and PET, or PE and PP are usually found mixed in plastic waste streams. Extensive research has been done in the area of heteropolymer blends as reported in Table 1. Nevertheless, problems with compatibility are of high concern. The general trend is a decrease in rheological, thermal, and mechanical properties, with very few exceptions. Wang et al. (2019) reported that recycled PET can induce a nucleating effect on LDPE melt crystallization without affecting its crystal form. A rejected–unused diapers project using a 70/30 PP/PE ratio was recycled. The recycled blend showed a weaker performance compared to the virgin blend, but the mechanical properties were still high enough to be competitive along with reduced costs. Saikrishnan et al. (2020) found that, although the rheological and thermal properties were affected, 10% rLDPE/rPP blends showed similar tensile properties with potential to be subjected to multiple reprocessing cycles.

3.3 Recycled Blends with Compatibilizer

Successful compatibilization has been achieved for a homopolymer recycled blend of PET via optimization through a full factorial design. Optimal values for Young's modulus, elongation at break, tensile strength at yield, and Izod impact strength were obtained with the following composition in a corotating twin screw extruder and subsequent injection molding: 25% rPET, 10% biocarbon, Joncryl chain extender, and Elvalov PTW toughening agent (Snowdon et al. 2020). Blends of rHDPE/vHDPE have been processed in a blow molding extruder with up to 70% of recycled materials using two different commercial compatibilizers (Recycloblend and Elvax), showing similar behavior to the virgin material (Ramirez-Vargas et al. 2006). PVC from credit cards was used to make recycled blends for pipes and fittings. Blending was carried out with a two-roll mill, using acrylonitrile butadiene styrene (ABS) and styrene acrylonitrile (SAN) as compatibilizers. Although a reduction in ductile properties was observed with SAN (due to its fragile nature), the use of ABS improved the mechanical properties, which is promising for applications in the building industry (Garcia et al. 2007). LDPE from prepregs was blended with virgin material, bentonite clay, and LDPE-g-MA as compatibilizer (Passos Severino et al. 2021). Specimens from recycled content ranging from 60% to 100% showed similar values to the virgin material for impact strength, Young's

modulus, and deformation at break, which is interesting for a less demanding application such as animal food packaging.

Polymer separation from mixed plastic waste is sometimes costly, so it is preferred to process mixtures instead. In several cases, the recycling of heteropolymer blends is difficult because of polymer degradation, immiscibility, or instability. Great effort has been devoted into the compatibilization of plastic waste (Feldman 2005; Ha et al. 2000; Maris et al. 2018; Martikka and Karki 2019; Vazquez and Barbosa 2016). The main work on recycled blends with compatibilizer addition for several blends is reported in Table 1.

PET, PVC, HDPE, and LDPE are usually found in mixed waste streams. It has been reported that 75/25 rHDPE/rPET blends with ethylene-glycidyl methacrylate (E-GMA) as compatibilizer improved toughness, impact strength, and tensile fracture elongation (Lei et al. 2009). Habibi et al. (2017) proposed a method to blend rHDPE/rLDPE with maleic anhydride polyethylene (MAPE) and ethylene propylene diene monomer (EPDM) rubber as coupling and compatibilizing agents, respectively. It was found that melt blending improved the flexural, tensile, and unnotched impact strengths. Postindustrial PET/LDPE food trays were further compatibilized with ethylene propylene rubber (EPR), which proved successful in retaining tensile strength and stiffness (Dekva et al. 2019). Recycled PVC blended with HDPE and compatibilized with ethylene vinyl acetate (EVA) showed that it is possible to improve impact strength and interfacial adhesion (Lee et al. 2019).

A poly(ethylene-*co*-methyl acrylate-*co*-glycidyl methacrylate) compatibilizer was used to process 90/10 rPET/PP blends (Catelli de Souza and Barbosa Caldeira 2015). The results showed that the compatibilizer acted as a softening agent decreasing the Young's and flexural moduli, flexural yield and strength, as well as increasing the impact strength and elongation at break. Kong et al. (2018) used a styrene-ethylene-propylene-styrene grafted glycidyl methacrylate (SEPS-g-GMA) copolymer for 70/30 rPP/rPS blends. The results showed an increase in impact strength and elongation at break. In addition, an increase in viscosity, storage modulus, and loss modulus pointed toward improved chemical compatibility. A study was performed to add a copolymer made from maleic anhydride functionalized with elastomeric ethylene to blends of recycled LDPE with virgin PS (80/20) (Chouiref and Belhaneche-Bensemra 2012). The results showed a sixfold increase in the elongation at break using 20% of compatibilizer compared to the rLDPE/PS blend without it. Compatibilization of virgin PS with recycled PP and styrene-ethylene-butylene-styrene (SEBS) copolymer showed improvements in "impact strength, elongation at break, thermal stability and heat deflection temperature" (Barreto Luna et al. 2019).

3.4 Recycled Blends with Composites

Commingled plastic recycling is "one of the most effective and alternative methodologies" to produce "sustainable, as well as uniformly distributed, natural fiber reinforced composites" (Nayana and Kandasubramanian 2020). Due to the wide variety

Table 2 Recycling of commingled plastics by the formation of composites

Polymers	Compatibilization	Processing	References
rPET/rHDPE and rice husk	Ethylene glycol dimethylacrylate (EGMA)	Twin-screw extruder (TSE)	Chen et al. (2021)
rPP/rLDPE/rHDPE and date palm fibers	Maleic anhydride grafted polyethylene (MAPE)	TSE at 200 °C	Zadeh et al. (2017)
rHDPE/rPET/rice husk/organoclay-reinforced 75/25/3	MAPE, EGMA	TSE	Chen and Ahmad (2017)
PE/PP wood flour 40/54/3/3	MAPE	TSE	Turku et al. (2017)
LDPE/PP/Nylon 6/EPDM reinforced with MWCNT and kenaf fibers	PP grafted with GMA (glycidyl methacrylate)	Batch mixer	Khan et al. (2015)
rPA6, rPP, and kenaf fibers	MAPP	Single-screw extruder (SSE)	Sukri et al. (2012)
LDPE/LLDPE and coir fibers	Styrene maleic anhydride (SMA)	SSE	Choudury et al. (2007)

of plastics found in MSW, blending of different polymers is necessary because their separation into single components can be difficult, expensive, or even impossible (Khanam and AlMaadeed 2014). Furthermore, as mentioned above, most of them are immiscible and require the use of a compatibilizer (Martikka and Karki 2019). Additionally, the use of synthetic or natural fibers for reinforcement (mechanical properties recovery) is recommended. Reinforced plastic composites are an important class of structural materials that are extensively used in the aerospace, automotive, and construction industries. The main advantage of using thermoplastic materials is their recyclability compared to thermosetting matrices (Pegoretti 2021). Although recycling composites does not fully solve the MSW problems, it provides some solution and reduces the use of virgin plastics (Fakirov 2021).

Table 2 shows some examples of these systems. Most of these studies seek to improve/extend the use of recycled plastics using fibers and compatibilizers to produce materials with good dimensional and thermal stability, as well as good mechanical performance. Other types of properties were also studied, such as fire-retardant performance by recycling mixed plastic waste with multiwalled carbon nanotube (MWCNT) and kenaf fibers (Khan et al. 2015), or by using date palm fibers (Zadeh et al. 2017). In general, natural fibers are preferred to prepare these materials on account of their availability, low cost, bio-based origin, and biodegradability.

3.5 Recycled Bioplastic-Based Blends

Although the production of biopolymers (worldwide) is not yet widespread (1%) (Cinar et al. 2020; Niaounakis 2019), it is necessary to be prepared for the handling and disposal of these materials, mainly because some of them are not biodegradable or compostable. Ilyas et al. (2021) proposed a comprehensive guide for designing,

Table 3 Recycling of bioplastic-based blends

Polymers	Composition	Strategies	Processing	References
PLA/PA	50/50	–	SSE and injection molding	Hamad et al. (2011)
PET/PLA	99.5/0.5, 99/1, 98/2, 95/5 wt/wt	–	Batch mixer	La Mantia et al. (2012)
PET/PLA	PET 0–100% PLA 0–100%	Use of a compatibilizer: ethylene-butyl acrylate-glycidyl methacrylate	Dry blending and melt blending by TSE	Gere and Czigany (2020)
PP/PBAT/TPS	85/7/8	7 cycles of reprocessing	SSE and compression molding	Oliveira et al. (2017) and Oliveira and Barbosa (2020)
LDPE/TPS	70/30, 60/40, 50/50	Virgin and postconsumer LDPE	TSE	Pedroso and Rosa (2005)
PLA/PBAT		5 cycles of reprocessing	SSE	La Mantia et al. (2020)
PLA/PHB	45/55	Multiple extrusion	SSE	Plavec et al. (2020)

handling, and discarding of bio-based packaging products. Mechanical recycling offers the best alternative for bio-based plastics in a complementary way with chemical recycling. Both biopolymers and polymers of fossil origin require high efficiency as well as minimizing the negative environmental impact. According to Briassoulis et al. (2021), the recirculation potential of postconsumer bio-based plastics through mechanical recycling represents a new challenge. Although the amount of biopolymers waste generated is low, some studies on their recyclability are available. This is especially the case for PLA, which is by far the most used biopolymer (Lamberti et al. 2020; Niaounakis 2019). For the recycling of bioplastic-based blends, Table 3 presents a summary of recent studies. Due to the low mechanical performance and high costs of most biodegradable polymers, it is difficult to immediately replace synthetic polymers. Blending conventional and biodegradable materials is a good alternative to develop recyclable products with good mechanical properties. However, this approach calls for special attention, since the biodegradation of these materials “may not be complete and can generate microplastics” (Oliveira and Barbosa 2020). The strategy to recycle biopolymers blends that are biodegradable under industrial compost environment is to evaluate their performance by submitting them to multiple extrusion cycles (Plavec et al. 2020; La Mantia et al. 2020; Oliveira et al. 2017; Oliveira and Barbosa 2020).

4 Conclusion

Based on the current situation, there is still an increasing trend of plastic production and consumption, leading to more waste generated after each part’s end of life. In most cases, complex polymer formulations led to the presence of several types of resins blended together. For this reason, it is difficult, if not impossible, to

completely separate each component producing multiphase systems (polymer blends). In this chapter, several methods to recycle polymer blends were presented and discussed in terms of the materials and equipment used, as well as the possibility to add additives (compatibilizing agents, anti-oxidants, etc.). The main options are:

1. blending with the same virgin polymer (recycled vs. virgin),
2. blending with a different polymer (binary polymer blends),
3. direct use of commingled plastics (no separation) with a compatibilizer (multi-component systems),
4. commingled/blend of plastics with the addition of fillers (composites), and,
5. blending with bioplastics (sustainable bio-based materials).

Although several works have been published on the recycling of polymer blends, there is still some information missing, especially on the structure–properties–performances of the final blends under optimized processing conditions and formulations. This becomes even more complex as new resins are being developed and introduced in the markets to “contaminate” even more the waste streams. More work is also needed to determine the effect of other pollutants (paper, glass, metals, etc.) and the number of cycles on the blends’ degradation and overall performance. Nevertheless, the concepts of sustainable development and circular economy must be applied, as rules and regulations are emerging in this direction.

References

- Ajji A (1995) Morphology and mechanical properties of virgin and recycled polyethylene/polyvinyl chloride blends. *Polym Eng Sci* 35:64–71. <https://doi.org/10.1002/pen.760350109>
- Akovali G, Karababa E (1998) Compatibility study of waste poly(ethylene terephthalate) with poly(vinyl chloride). II *J Appl Polym Sci* 68:765–774. [https://doi.org/10.1002/\(SICI\)1097-4628\(19980502\)68:5<765::AID-APP8>3.0.CO;2-M](https://doi.org/10.1002/(SICI)1097-4628(19980502)68:5<765::AID-APP8>3.0.CO;2-M)
- Al-Salem SM, Antelava A, Constantinou A et al (2017) A review on thermal and catalytic pyrolysis of plastic solid waste (PSW). *J Environ Manag* 197:177–198. <https://doi.org/10.1016/j.jenvman.2017.03.084>
- Alzerreca M, Paris M, Boyron OO et al (2015) Mechanical properties and molecular structure of virgin and recycled HDPE polymers used in gravity sewer systems. *Polym Test* 46:1–8. <https://doi.org/10.1016/j.polymertesting.2015.06.012>
- Andrady AL (2017) The plastic in microplastics. A review. *Mar Pollut Bull* 119:12–22. <https://doi.org/10.1016/j.marpolbul.2017.01.082>
- Andric B, Kovacic T, Klaric I (2008) Properties of recycled material containing poly(vinyl chloride), polypropylene, and calcium carbonate nanofiller. *Polym Eng Sci* 48:572–577. <https://doi.org/10.1002/pen.20986>
- Aumnate C, Rudolph N, Sarmadi M (2019) Recycling of polypropylene/polyethylene blends: effect of chain structure on the crystallization behaviors. *Polymer* 11:1456. <https://doi.org/10.3390/polym11091456>
- Barreto Luna CB, Diniz Siqueira D, Araujo EM et al (2019) Tailoring PS/PP recycled blends compatibilized with SEBS. Evaluation of rheological, mechanical, thermomechanical and morphological characters. *Mater Res Express* 6:075316. <https://doi.org/10.1088/2053-1591/ab131c>

- Bertin S, Robin JJ (2002) Study and characterization of virgin and recycled LDPE/PE blends. *Eur Polym J* 38:2255–2264. [https://doi.org/10.1016/S0014-3057\(02\)00111-8](https://doi.org/10.1016/S0014-3057(02)00111-8)
- Bonelli CM, Martins AF, Mano EB et al (2001) Effect of recycled polypropylene on polypropylene/high density polyethylene blends. *J Appl Polym Sci* 80:1305–1311. <https://doi.org/10.1002/app.1217>
- Bora Raaj R, Wang R, Fengqi Y (2020) Waste polypropylene plastic recycling toward climate change mitigation and circular economy: energy, environmental, and technoeconomic perspectives. *ACS Sustain Chem Eng* 8:16350–16363. <https://doi.org/10.1021/acssuschemeng.0c06311>
- Brissoulis, D., Pikasi, A., & Hiskakis, M. (2021). Recirculation potential of post-consumer/industrial bio-based plastics through mechanical recycling-Techno-economic sustainability criteria and indicators. *Polymer Degradation and Stability*, 183, 109217. <https://doi.org/10.1016/j.polyimdegradstab.2020.109217>
- Camacho W, Karlsson S (2002) Assessment of thermal and thermo-oxidative stability of multi-extruded recycled PP, HDPE and a blend thereof. *Polym Degrad Stab* 78:385–391. [https://doi.org/10.1016/S0141-3910\(02\)00192-1](https://doi.org/10.1016/S0141-3910(02)00192-1)
- Catelli de Souza AM, Barbosa Caldeira C (2015) An investigation on recycled PET/PP and recycled PET/PP-EP compatibilized blends: rheological, morphological, and mechanical properties. *J Appl Polym Sci* 132:41892. <https://doi.org/10.1002/app.41892>
- Cestari SP, Martin PJ, Hanna PR et al (2021) Use of virgin/recycled polyethylene blends in rotational moulding. *J Polym Eng* 41:509–516. <https://doi.org/10.1515/polyeng-2021-0065>
- Chen RS, Ahmad S (2017) Mechanical performance and flame retardancy of rice husk/organoclay-reinforced blend of recycled plastics. *Mater Chem Phys* 198:57–65. <https://doi.org/10.1016/j.matchemphys.2017.05.054>
- Chen RS, Ab Ghani MH, Ahmad S et al (2021) Tensile, thermal degradation and water diffusion behaviour of gamma-radiation induced recycled polymer blend/rice husk composites: experimental and statistical analysis. *Compos Sci Technol* 207:108748. <https://doi.org/10.1016/j.compscitech.2021.108748>
- Choudhury A, Kumar S, Adhikari B (2007) Recycled milk pouch and virgin low-density polyethylene/linear low-density polyethylene based coir fiber composites. *J Appl Polym Sci* 106:775–785. <https://doi.org/10.1002/app.26522>
- Chouiref CC, Belhaneche-Bensemra N (2012) Regenerated LDPE/PS blends: characterization and compatibilization. *Int J Environ Stud* 69:881–887. <https://doi.org/10.1080/00207233.2012.727234>
- Cinar SO, Chong ZK, Kucuker MA et al (2020) Bioplastic production from microalgae: a review. *Int J Environ Res Public Health* 17:3842. <https://doi.org/10.3390/ijerph17113842>
- Dekva L, Deceur C, Van Damme N et al (2019) Compatibilization of PET-PE blends for the recycling of multilayer packaging foils. *AIP Conf Proc* 2055:030005. <https://doi.org/10.1063/1.5084815>
- Di J, Reck BK, Miatto A, Graedel TE et al (2021) United States plastics: large flows, short lifetimes, and negligible recycling. *Resour Conserv Recycl* 167:105440. <https://doi.org/10.1016/j.resconrec.2021.105440>
- Diaz S, Ortega Z, McCourt M, Kearns MP, Benitez AN (2018) Recycling of polymeric fraction of cable waste by rotational moulding. *Waste Manag* 76:199–206. <https://doi.org/10.1016/j.wasman.2018.03.020>
- Dorigato A (2021) Recycling of polymer blends. *Adv Recycl Eng Pol Res* 4:53–69. <https://doi.org/10.1016/j.aiepr.2021.02.005>
- Elamri A, Zdiri K, Harzallah O et al (2017) Progress in polyethylene terephthalate recycling. In: Barber NA (ed) *Polyethylene terephthalate: uses, properties and degradation*. Nova Science Publishers, New York. <https://hal.archives-ouvertes.fr/hal-02953197>
- Elmaghor F, Zhang L, Li H (2003) Recycling of high density polyethylene/poly(vinyl chloride)/polystyrene ternary mixture with the aid of high energy radiation and compatibilizers. *J Appl Polym Sci* 88:2756–2762. <https://doi.org/10.1002/app.11985>
- Fadipe EO (2020) Effects of natural weathering on the tensile strength and embrittlement time of blends of recycled polypropylene with polystyrene, polyvinyl chloride and virgin poly-

- propylene. *FUW Trends Sci Technol J* 5:93–97. <http://www.ftstjournal.com/Digital%20Library/51%20Article%2018.php>
- Fakirov S (2021) A new approach to plastic recycling via the concept of microfibrillar composites. *Adv Ind Eng Polym Res* 4:187–198. <https://doi.org/10.1016/j.aiepr.2021.02.001>
- Feldman D (2005) Polyblend compatibilization. *J Macromol Sci Part A: Pure Appl Chem* 42:587–605. <https://doi.org/10.1081/MA-200056331>
- Fortelny I, Michalkova D, Krulis Z (2004) An efficient method of material recycling of municipal plastic waste. *Polym Degrad Stab* 85:975–979. <https://doi.org/10.1016/j.polymdegradstab.2004.01.024>
- Gallego K, Lopez BL, Gartner C (2006) Study of blends from recycled polymer for properties improvement. *Rev Fac Ing* 37:59–70. <https://revistas.udea.edu.co/index.php/ingenieria/articulo/view/343417>
- Garcia D, Balart R, Parres F et al (2007) Characterization of blends of poly(vinyl chloride) waste for building applications. *J Mater Sci* 42:10143–10151. <https://doi.org/10.1007/s10853-007-2067-y>
- Garcia MT, Gracia I, Duque G, de Lucas A, Rodriguez JF (2009) Study of the solubility and stability of polystyrene wastes in a dissolution recycling process. *Waste Manag* 29:1814–1818. <https://doi.org/10.1016/j.wasman.2009.01.001>
- Garcia-Ivars J, Wang-Xu X, Iborra-Clar MI (2017) Application of post-consumer recycled high-impact polystyrene in the preparation of phase-inversion membranes for low-pressure membrane processes. *Sep Purif Technol* 175:340–351. <https://doi.org/10.1016/j.seppur.2016.11.061>
- Gere D, Czizgany T (2020) Future trends of plastic bottle recycling: compatibilization of PET and PLA. *Polym Test* 81:106160. <https://doi.org/10.1016/j.polymertesting.2019.106160>
- Geyer R, Jambeck JR, Law KL (2017) Production, use, and fate of all plastics ever made. *Sci Adv* 3:e1700782. <https://doi.org/10.1126/sciadv.1700782>
- Giacovelli C (2018) Single use plastic. A roadmap for sustainability. United Nations Environment Programme. <https://wedocs.unep.org/handle/20.500.11822/25496>. Accessed 03 Oct 2021
- Global Plastic Recycling Industry (2020) ReportLinker. https://www.reportlinker.com/p05896556/Global-Plastic-Recycling-Industry.html?utm_source=GNW. Accessed 28 Sep 2021
- Gregor-Svetec D, Tisler-Korljan B, Leskovsek M et al (2009) Monofilaments produced by blending virgin with recycled polypropylene. *Tekstil ve Konfeksiyon* 19:181–188. <https://dergipark.org.tr/tr/pub/tekonfeksiyon/issue/23635/251731>
- Ha CS, Park HD, Cho WJ (2000) Compatibilizers for recycling of the plastic mixture wastes. II The effect of a compatibilizer for binary blends on the properties of ternary blends. *J Appl Polym Sci* 76:1048–1053. [https://doi.org/10.1002/\(SICI\)1097-4628\(20000516\)76:7<1048::AID-APP8>3.0.CO;2-R](https://doi.org/10.1002/(SICI)1097-4628(20000516)76:7<1048::AID-APP8>3.0.CO;2-R)
- Habibi M, Najafi SK, Ghasemi I (2017) Rheological and mechanical properties of composites made from wood flour and recycled LDPE/HDPE blend. *Iran Polym J* 26:949–956. <https://doi.org/10.1007/s13726-017-0579-0>
- Hamad K, Kaseem M, Deri F (2011) Rheological and mechanical characterization of poly(lactic acid)/polypropylene polymer blends. *J Polym Res* 18:1799–1806. <https://doi.org/10.1007/s10965-011-9586-6>
- Hirayama D, Saron C (2018) Morphologic and mechanical properties of blends from recycled acrylonitrile-butadiene-styrene and high-impact polystyrene. *Polymer* 135:271–278. <https://doi.org/10.1016/j.polymer.2017.12.038>
- Horodytska O, Valdés FJ, Fullana A (2018) Plastic flexible films waste management: a state of the art review. *Waste Manag* 77:413–425. <https://doi.org/10.1016/j.wasman.2018.04.023>
- Ignatyev IA, Thielemans W, Vander Beke B (2014) Recycling of polymers: a review. *Chem Sustain Chem* 7:1579–1593. <https://doi.org/10.1002/cssc.201300898>
- Ilyas RA, Sapuan SM, Sabaruddin FA et al (2021) Reuse and recycle of biobased packaging products. In: Sapuan SM, Ilyas RA (eds) *Bio-based packaging: material, environmental and economic aspects*, 1st edn. Wiley, West Sussex. <https://doi.org/10.1002/9781119381228>

- Imamura N, Sakamoto H, Higuchi Y et al (2014) Effectiveness of compatibilizer on mechanical properties of recycled PET blends with PE, PP, and PS. *Mater Sci Appl* 5:548–555. <https://doi.org/10.4236/msa.2014.58057>
- Inoya H, Leong YW, Klinklai W et al (2012) Compatibilization of recycled poly(ethylene terephthalate) and polypropylene blends: effect of polypropylene molecular weight on homogeneity and compatibility. *J Appl Polym Sci* 124:3947–3955. <https://doi.org/10.1002/app.34405>
- Jin H, Gonzalez-Gutierrez J, Oblak P, Zupancic B, Emri I (2012) The effect of extensive mechanical recycling on the properties of low density polyethylene. *Polym Degrad Stab* 97:2262–2272. <https://doi.org/10.1016/j.polymdegradstab.2012.07.039>
- Kabdi SA, Belhaneche-Bensema N (2008) Compatibilization of regenerated low density polyethylene/poly(vinyl chloride) blends. *J Appl Polym Sci* 110:1750–1755. <https://doi.org/10.1002/app.28175>
- Kartalis CN, Papaspyrides CD, Pfaendner R et al (2000a) Mechanical recycling of post-used HDPE crates using the restabilization technique. II: Influence of artificial weathering. *J Appl Polym Sci* 77:1118–1127. [https://doi.org/10.1002/1097-4628\(20000801\)77:5<1118::AID-APP20>3.0.CO;2-J](https://doi.org/10.1002/1097-4628(20000801)77:5<1118::AID-APP20>3.0.CO;2-J)
- Kartalis CN, Papaspyrides CD, Pfaendner R et al (2000b) Recycling of post-used PE packaging film using the restabilization technique. *Polym Degrad Stab* 70:189–197. [https://doi.org/10.1016/S0141-3910\(00\)00106-3](https://doi.org/10.1016/S0141-3910(00)00106-3)
- Khan MA, Kumar SS, Raghu TS et al (2015) Commingled nanocomposites of LDPE/PP/Nylon 6/EPDM reinforced with MWCNT and Kenaf Fiber with enhanced mechanical, thermal and flammability characteristics. *Mater Today Commun* 4:50–62. <https://doi.org/10.1016/j.mtcomm.2015.04.008>
- Khanam NP, AlMaadeed MA (2014) Improvement of ternary recycled polymer blend reinforced with date palm fibre. *Mater Des* 60:532–539. <https://doi.org/10.1016/j.matdes.2014.04.033>
- Kong Y, Li Y, Hu G et al (2018) Preparation of polystyrene-*b*-poly(ethylene/propylene)-*b*-polystyrene grafted glycidyl methacrylate and its compatibility with recycled polypropylene/recycled high impact polystyrene blends. *Polymer* 145:232–241. <https://doi.org/10.1016/j.polymer.2018.05.017>
- Kunwar B, Cheng HN, Chandrashekar SR et al (2016) Plastics to fuel: a review. *Renew Sust Energ Rev* 54:421–428. <https://doi.org/10.1016/j.rser.2015.10.015>
- La Mantia FP, Scaffaro R (2014) Recycling polymer blends. In: Utracki LA, Wilkie CA (eds) *Polymer blends handbook*, 2nd edn. Springer, New York. https://doi.org/10.1007/978-94-007-6064-6_23
- La Mantia FP, Botta L, Morreale M et al (2012) Effect of small amounts of poly(lactic acid) on the recycling of poly(ethylene terephthalate) bottles. *Polym Degrad Stab* 97:21–24. <https://doi.org/10.1016/j.polymdegradstab.2011.10.017>
- La Mantia FP, Morreale M, Botta L et al (2017) Degradation of polymer blends: a brief review. *Polym Degrad Stab* 145:79–92. <https://doi.org/10.1016/j.polymdegradstab.2017.07.011>
- La Mantia FP, Botta L, Mistretta M (2020) Recycling of a biodegradable polymer blend. *Polymer* 20:2297. <https://doi.org/10.3390/polym12102297>
- La Mantia FP, Mistretta MC, Titone V (2021) An additive model to predict the rheological and mechanical properties of polypropylene blends made by virgin and reprocessed components. *Recycling* 6:2. <https://doi.org/10.3390/recycling6010002>
- Lamberti FM, Romain R, Luis A et al (2020) Recycling of bioplastics: routes and benefits. *J Polym Environ* 28:2551–2571. <https://doi.org/10.1007/s10924-020-01795-8>
- Lee JH, Lim KS, Hahm WG et al (2012) Properties of recycled and virgin poly(ethylene terephthalate) blend fibers. *J Appl Polym Sci* 128:1250–1256. <https://doi.org/10.1002/app.38502>
- Lee R, Park SH, Baek JS et al (2019) Mechanical properties and thermal stability of waste PVC/HDPE blend prepared by twin-screw extruder. *Elastom Compos* 54:7–13. <https://doi.org/10.7473/EC.2019.54.1.7>
- Lei Y, Wu Q, Zhang Q (2009) Morphology and properties of microfibrillar composites based on recycled poly(ethylene terephthalate) and high density polyethylene. *Compos Part A* 40:904–912. <https://doi.org/10.1016/j.compositesa.2009.04.017>

- Li WC, Tse HF, Fok L (2016) Plastic waste in the marine environment: a review of sources, occurrence and effects. *Sci Total Environ* 566–567:333–349. <https://doi.org/10.1016/j.scitotenv.2016.05.084>
- Li H, Sui X, Xie XM (2017) High-strength and super-tough PA6/PS/PP/SEBS quaternary blends compatibilized by using a highly-effective multi-phase compatibilizer: toward efficient recycling of waste plastics. *Polymer* 123:240–246. <https://doi.org/10.1016/j.polymer.2017.07.024>
- Lin HR, Lin CT (1999) Mechanical properties and morphology of recycled plastic wastes by solution blending. *Polym-Plast Technol Eng* 38:1031–1050. <https://doi.org/10.1080/03602559909351629>
- Mamoor GM, Shahid W, Mushtaq A et al (2013) Recycling of mixed plastics waste containing polyethylene, polyvinylchloride and polyethylene terephthalate. *Chem Eng Res Bull* 16:25–32. <https://doi.org/10.3329/ceerb.v16i1.17471>
- Mansor MR, Taufiq MJ, Mustafa Z et al (2019) Thermal and mechanical behavior of recycled polypropylene/polyethylene blends of rejected-unused disposable diapers. *J Adv Manuf Technol* 13:13–23. <https://jamt.utem.edu.my/jamt/article/view/5734>
- Maris J, Bourdon S, Brossard JM et al (2018) Mechanical recycling: compatibilization of mixed thermoplastic wastes. *Polym Degrad Stab* 147:245–266. <https://doi.org/10.1016/j.polymdegradstab.2017.11.001>
- Martikka O, Karki T (2019) Promoting recycling of mixed waste polymers in wood-polymer composites using compatibilizers. *Recycling* 4:6. <https://doi.org/10.3390/recycling4010006>
- Maud B, Arnold JC, Isaac DH (1996) Mechanical properties and stability of recycled post-consumer poly(vinyl chloride) bottle compounds. *Key Eng Mater* 118–119:19–26. <https://doi.org/10.4028/www.scientific.net/KEM.118-119.19>
- Meran C, Ozturk O, Yuksel M (2008) Examination of the possibility of recycling and utilizing recycled polyethylene and polypropylene. *Mater Des* 29:701–705. <https://doi.org/10.1016/j.matdes.2007.02.007>
- Miller P, Sbarski I, Iovenitti P et al (2001) Rheological properties of blends of recycled HDPE and virgin polyolefins. *Polym Recycl* 6:181–186
- Mnif R, Elleuch R (2015) Effects of reprocessing cycles and ageing on the rheological and mechanical properties of virgin-recycled HDPE blends. *Mater Tech* 103:704. <https://doi.org/10.1051/mattech/2015056>
- Moon D, Morris J (2019) Chapter six: plastic waste management. In: Kistler A, Muffett C (eds) *Plastic and climate. The hidden costs of a plastic planet*. Center for International Environmental Law. <https://www.ciel.org/plasticandclimate/>. Accessed 03 Oct 2021
- Nayana V, Kandasubramanian B (2020) Advanced polymeric composites via commingling for critical engineering applications. *Polym Test* 91:106774. <https://doi.org/10.1016/j.polymertesting.2020.106774>
- Nedkov T, Lednický F, Mihailova M (2008) Compatibilization of PP/PE blends and scraps with Royalene: mechanical properties, SAXS, and WAXS. *J Appl Polym Sci* 109:226–233. <https://doi.org/10.1002/app.27993>
- Niaounakis M (2019) Recycling of biopolymers – the patent perspective. *Eur Polym J* 114:464–475. <https://doi.org/10.1016/j.eurpolymj.2019.02.027>
- Oliveira T, Barbosa R (2020) Fungal degradation of reprocessed PP/PBAT/thermoplastic starch blends. *J Mater Res Technol* 9:2338–2349. <https://doi.org/10.1016/j.jmrt.2019.12.065>
- Oliveira T, Oliveira R, Barbosa R et al (2017) Effect of reprocessing cycles on the degradation of PP/PBAT-thermoplastic starch blends. *Carbohydr Polym* 168:52–60. <https://doi.org/10.1016/j.carbpol.2017.03.054>
- Olofinnade O, Chandra S, Chakraborty P (2021) Recycling of high impact polystyrene and low-density polyethylene plastic wastes in lightweight based concrete for sustainable construction. *Mater Today Proc* 38:2151–2156. <https://doi.org/10.1016/j.matpr.2020.05.176>
- Paci M, La Mantia FP (1999) Influence of small amounts of polyvinylchloride on the recycling of polyethylene terephthalate. *Polym Degrad Stab* 63:11–14. [https://doi.org/10.1016/S0141-3910\(98\)00053-6](https://doi.org/10.1016/S0141-3910(98)00053-6)

- Passos Severino PR, Braga NF, Morgado GF et al (2021) The use of recycled low-density polyethylene films from protective prepreg for the development of nanocomposites with bentonite clay. *J Appl Polym Sci* 138:50559. <https://doi.org/10.1002/app.50559>
- Pawlak A, Morawiec J, Pazzagli F et al (2002) Recycling of postconsumer poly(ethylene terephthalate) and high-density polyethylene by compatibilized blending. *J Appl Polym Sci* 86:1473–1485. <https://doi.org/10.1002/app.11307>
- Pedroso AG, Rosa DS (2005) Mechanical, thermal and morphological characterization of recycled LDPE/corn starch blends. *Carbohydr Polym* 59:1–9. <https://doi.org/10.1016/j.carbpol.2004.08.018>
- Pegoretti A (2021) Towards sustainable structural composites: a review on the recycling of continuous-fiber-reinforced thermoplastics. *Adv Ind Eng Polym Res* 4:105–115
- Pinter E, Welle F, Mayrhofer E et al (2021) Circularity study on PET bottle-to-bottle recycling. *Sustainability* 13:7370. <https://doi.org/10.3390/su13137370>
- Plavec R, Hlavaia I, Sijavka O et al (2020) Recycling possibilities of bioplastics based on PLA/PHB blends. *Polym Test* 92:106880. <https://doi.org/10.1016/j.polymertesting.2020.106880>
- Popovska-Pavlovska F, Trajkovska A, Trajkovska A et al (2000) Rheological behaviour of VPVC/RPVC blends. *Macromol Symp* 149:191–195. [https://doi.org/10.1002/1521-3900\(200001\)149:1<191::AID-MASY191>3.0.CO;2-0](https://doi.org/10.1002/1521-3900(200001)149:1<191::AID-MASY191>3.0.CO;2-0)
- Ragaert K, Delva L, Van Geem K (2017) Mechanical and chemical recycling of solid plastic waste. *Waste Manag* 69:24–58. <https://doi.org/10.1016/j.wasman.2017.07.044>
- Raj MM, Patel HV, Raj LM et al (2013) Studies on mechanical properties of recycled polypropylene blended with virgin polypropylene. *Int J Sci Invent Today* 2:194–203. http://www.ijst.com/search_ijst.php
- Ramirez-Vargas E, Sandoval-Arellano Z, Hernandez-Valdez JS et al (2006) Compatibility of HDPE/postconsumer HDPE blends using compatibilizing agents. *J Appl Polym Sci* 100:3696–3706. <https://doi.org/10.1002/app.23214>
- Sahnoune F, Lopez Cuesta JM, Crespy A (2003) Improvement of the mechanical properties of an HDPE/PS blend by compatibilization and incorporation of CaCO₃. *Polym Eng Sci* 43:647–660. <https://doi.org/10.1002/pen.10053>
- Saikrishnan S, Jubinville D, Tzoganakis C et al (2020) Thermo-mechanical degradation of polypropylene (PP) and low-density polyethylene (LDPE) blends exposed to simulated recycling. *Polym Degrad Stab* 182:109390. <https://doi.org/10.1016/j.polymdegradstab.2020.109390>
- Sanchez-Soto M, Rossa A, Sanchez AJ et al (2008) Blends of HDPE wastes: study of the properties. *Waste Manag* 28:2565–2573. <https://doi.org/10.1016/j.wasman.2007.10.010>
- Schyns ZO, Shaver MP (2021) Mechanical recycling of packaging plastics: a review. *Macromol Rapid Commun* 42:1–27. <https://doi.org/10.1002/marc.202000415>
- Serranti S, Bonifazi G (2019) 2 – techniques for separation of plastic wastes. In: Pacheco-Torgal F, Khatib K, Colangelo F, Tuladhar R (eds) *Use of recycled plastics in eco-efficient concrete*, 1st edn. Woodhead Publishing, Cambridge
- Si M, Araki T, Ade H et al (2006) Compatibilizing bulk polymer blends by using organoclays. *Macromolecules* 39:4793–4801. <https://doi.org/10.1021/ma060125+>
- Silva ALP, Prata JC, Walker TR et al (2021) Increased plastic pollution due to COVID-19 pandemic: challenges and recommendations. *Chem Eng J* 401:126683–126689. <https://doi.org/10.1016/j.cej.2020.126683>
- Singh N, Hui D, Singh R et al (2017) Recycling of plastic solid waste: a state of the art review and future applications. *Compos Part B* 115:409–422. <https://doi.org/10.1016/j.compositesb.2016.09.013>
- Snowdon MR, Abdelwahab M, Mohanty AK et al (2020) Mechanical optimization of virgin and recycled poly(ethylene terephthalate) biocomposites with sustainable biocarbon through a factorial design. *Result Mater* 5:10060. <https://doi.org/10.1016/j.rinma.2020.100060>

- Sombatsompop N, Thongsang S (2001) Rheology, morphology, and mechanical and thermal properties of recycled PVC pipes. *J Appl Polym Sci* 82:2478–2486. <https://doi.org/10.1002/app.2098>
- Soto JM, Blazquez G, Calero M, Quesada L, Godoy V, Martin-Lara MA (2018) A real case study of mechanical recycling as an alternative for managing of polyethylene plastic film presented in mixed municipal solid waste. *J Clean Prod* 203:777–787. <https://doi.org/10.1016/j.jclepro.2018.08.302>
- Soto JM, Martin-Lara MA, Blazquez G, Godoy V, Quesada L, Calero M (2020) Novel pre-treatment of dirty post-consumer polyethylene film for its mechanical recycling. *Process Saf Environ Prot* 139:315–324. <https://doi.org/10.1016/j.psep.2020.04.044>
- Sukri SM, Suradi NL, Arsad A et al (2012) Green composites based on recycled polyamide-6/ recycled polypropylene kenaf composites: mechanical, thermal and morphological properties. *J Polym Eng* 32:291–299. <https://doi.org/10.1515/polyeng-2012-0016>
- Tai HS, Yeh JL (2018) Evaluation and verification of the virgin-recycled mixing ratio of polypropylene plastic. *J Chin Inst Eng* 41:1. <https://doi.org/10.1080/02533839.2017.1419074>
- Takhrur S, Verma A, Sharma B et al (2018) Recent developments in recycling of polystyrene based plastics. *Curr Opin Green Sustain Chem* 13:32–38. <https://doi.org/10.1016/j.cogsc.2018.03.011>
- Tao Y, Mai K (2007) Non-isothermal crystallization and melting behavior of compatibilized polypropylene/recycled poly(ethylene terephthalate) blends. *Eur Polym J* 43:3538–3549. <https://doi.org/10.1016/j.eurpolymj.2007.05.007>
- Tapia-Picazo JC, Luna-Bárceñas JG, Garcia-Chavez A et al (2014) Polyester fiber production using virgin and recycled PET. *Fibers Polym* 15:547–552. <https://doi.org/10.1007/s12221-014-0547-7>
- Tiseo I (2021) Annual production of plastics worldwide from 1950 to 2020. Statista <https://www-statistacom/statistics/282732/global-production-of-plastics-since-1950/>. Accessed 03 Oct 2021
- Turku I, Keskisaari A, Kärki T et al (2017) Characterization of wood plastic composites manufactured from recycled plastic blends. *Compos Struct* 161:469–476. <https://doi.org/10.1016/j.compstruct.2016.11.073>
- Utracki LA (2002) Role of polymers blends' technology in polymer recycling. In: Utracki LA (ed) *Polymer blends handbook*, 1st edn. Springer, New York
- Utracki LA, Favis BD (1989) *Polymer alloys and blends*. In: Cheremisinoff NP (ed) *Handbook of polymer science and technology*. Marcel Dekker, Inc, New York
- Vazquez YV, Barbosa SE (2016) Recycling of mixed plastic waste from electrical and electronic equipment. Added value by compatibilization. *Waste Manag* 53:196–203. <https://doi.org/10.1016/j.wasman.2016.04.022>
- Vollmer I, Jenks MJ, Roelands MC et al (2020) Beyond mechanical recycling: giving new life to plastic waste. *Angew Chem Int Ed* 59:15402–15423. <https://doi.org/10.1002/anie.201915651>
- Wang D, Yang B, Chen QT et al (2019) A facile evaluation on melt crystallization kinetics and thermal properties of low-density polyethylene (LDPE)/recycled polyethylene terephthalate (RPET) blends. *Adv Ind Eng Polym Res* 2:126–135. <https://doi.org/10.1016/j.aiepr.2019.05.002>
- Wattanachai P, Buasathain B, Antonio C et al (2017) Open loop recycling of recycled polypropylene for motorcycle saddle application. *ASEAN J Chem Eng* 17:60–76. <https://doi.org/10.22146/ajche.49556>
- Wenguang M, La Mantia FP (1996) Processing and mechanical properties of recycled PVC and of homopolymer blends with virgin PVC. *J Appl Polym Sci* 59:759–767. [https://doi.org/10.1002/\(SICI\)1097-4628\(19960131\)59:5<759::AID-APP1>3.0.CO;2-V](https://doi.org/10.1002/(SICI)1097-4628(19960131)59:5<759::AID-APP1>3.0.CO;2-V)
- Yoo Y, Park JC, Won JC et al (2004) Morphology and mechanical properties of recycled PVC blends (III) – morphologies and mechanical properties of recycled PVC/PE blends with different kinds of compatibilizers and mixing conditions. *Polymer* 28:468–477. <http://journal.polymer-korea.or.kr/journal/archive/view/2397>

- Zadeh KM, Ponnamma D, Al-Maadeed MAA (2017) Date palm fibre filled recycled ternary polymer blend composites with enhanced flame. *Polym Test* 61:341–348. <https://doi.org/10.1016/j.polymertesting.2017.05.006>
- Zander NE, Gillan M, Sweetser D (2017) Composite fibers from recycled plastics using melt centrifugal spinning. *Materials* 10:1044–1057. <https://doi.org/10.3390/ma10091044>
- Zhang Y, Zhang H, Yu Y et al (2009) Recycled poly(ethylene terephthalate)/linear low-density polyethylene blends through physical processing. *J Appl Polym Sci* 114:1187–1194. <https://doi.org/10.1002/app.30030>

Sustainable Materials from Recycled Polypropylene Waste and Green Fillers: Processing, Properties, and Applications



Noraiham Mohamad, Hairul Effendy Ab Maulod, and Jeefferie Abd Razak

1 Introduction

Globally, the demand of plastics has continued to grow (Schyns et al. 2021). The circulating plastic-waste volumes has increased from 260 million tons in 2016 to 460 million tons per year by 2030 (Hundertmark et al. 2021). However, approximately half of all plastic manufactured is used primarily for single-use disposable applications such as packaging (PlasticsEurope 2019), agricultural films, and disposable consumer items, all of which end up as a plastic waste (Mohamad et al. 2014; Hopewell 2009). The fast growth in municipal trash creation is globally necessitating an urgent need for a better-managed disposal option. The expansion of garbage landfills has contributed to noise, dust, and stink, as well as bioaerosols generated shortly after opening and possibly for several decades afterward (Othman 2007). Furthermore, landfills add to the greenhouse impact through gas emissions, which is a global issue.

Recycling or reusing plastics in circulation is critical for avoiding the increased inadvertent or intentional release of polymeric materials into the environment and reducing environmental pollution (Schyns et al. 2021). In 2016, only a total of 16% of polymers in flow were collected for recycling, whereas about 40% were disposed of in landfills, and approximately 25% were burnt (Hundertmark et al. 2021). Recently, European governments have boosted their efforts to raise recycling rates.

N. Mohamad (✉) · J. Abd Razak
Fakulti Kejuruteraan Pembuatan, Universiti Teknikal Malaysia Melaka,
Durian Tunggal, Melaka, Malaysia
e-mail: noraiham@utem.edu.my

H. E. Ab Maulod
Fakulti Teknologi Kejuruteraan Mekanikal & Pembuatan, Universiti Teknikal Malaysia
Melaka, Durian Tunggal, Melaka, Malaysia

In 2018, Europe collected a total of 29.1 million tons of post-consumer plastic garbage, while less than a third of this was recycled, which marked a doubling of the amount recycled and about 39% reduction in plastic waste exports to countries outside the European Union (EU) compared to 2006 levels (Schyns et al. 2021).

Recycling, in which used materials are reprocessed into new goods, reduces the generation of everyday garbage. As compared to virgin products, it prevents the waste of potentially usable materials, reduces the consumption of raw materials and energy usage, and hence reduces greenhouse gas emissions (Ilyas et al. 2021a). Recycling conserves landfill space and minimizes the amounts of virgin materials that should be mined or manufactured in creating new items, thus conserving energy and minimizing global climate change (Atiqah et al. 2021). Nowadays, the polymer matrix-based products' manufacturer has moved toward a new perspective. The interest in biodegradable, green, and more sustainable polymer composites is rapidly growing in industrial applications and fundamental research because of their exciting criteria. The plastic waste materials could be considered low-cost and renewable feedstock for the preparation of greener composites. This would be a high-value waste plastic output (Salwa et al. 2021). Compostable plastic and biodegradable items, such as food packaging bags, can help improve waste management and organic recycling (Ilyas et al. 2021b).

“Sustainable” and “sustainability” can be defined in many ways. Nonetheless, the term is frequently used to refer to the practice of ensuring that the material utilized in a product or component does not deplete natural resources excessively while sustaining a prosperous economy for future generations. Mansor et al. (2020) grouped the so-called natural resources-based green composites materials into three categories. The grouping is usually made from a basic composite's formulation, consisting of (1) reinforcement, (2) matrix, and (3) filler materials. The composites can be formulated into a fully or partially green composite. However, this chapter focuses on a similar matrix type, polypropylene-based waste material with the utilization of various more sustainable filler or reinforcement materials (classified as green fillers in this chapter). Fillers function as a discontinuous phase in the composite and are often spread as well as disseminated throughout the matrix, improving or reinforcing the matrix (Abdul Khalil et al. 2019). When fillers are introduced into the matrix phase, a complex interphase structure is produced, in which the configuration and interaction of the fillers and matrix dictate the composite's properties. The filler and matrix phases can complement or be compatible with one another, resulting in an enhanced composite. Green fillers are materials that can fill or reinforce various matrices to form useful or value-added composite materials. The term “eco” in eco-friendly fillers usually describes fillers that are “ecologically” friendly to the environment for biodegradability. However, this chapter reflects some other fillers that are “economically viable” from the reused fillers and by lower consumption of resources due to improved properties. Hence, the fillers are categorized as green fillers in this chapter.

1.1 Polypropylene

Polypropylene (PP) is a typical thermoplastic that is excellent for various industrial applications, from domestic to engineering products such as bottles to automotive parts, due to its outstanding range of qualities. PP is nondegradable because of its chemically stabilized state for long service life. Thus, the disposal of PP plastic waste poses an environmental issue. Mansor et al. (2020) reported that PE and PP were the most extensively used plastics, accounting for 61% of the US plastics industry. As a result of economic and environmental factors, PP recycling had expanded dramatically.

Polypropylene (PP) is a versatile thermoplastic material having properties between low-density polyethylene (LDPE) and high-density polyethylene (HDPE). Their density of 0.899–0.920 g/cm³ (Grigore 2017) and a combination of hardness, rigidity, and ease of processing make them very useful polyolefin materials (Hindle 2021). Their general characteristics – physically, mechanically, functionally, processability, and serviceability – are depicted in Fig. 1.

Polypropylene was the first stereoregular polymer developed and was made from propylene monomers using two types of polymerizations: Ziegler-Natta and metallocene catalysis (Galli et al. 1995). It is a linear polymer with a structure express as C_nH_{2n} that is similar to polyethylene, except that every other carbon atom in the backbone chain has a methyl group attached to it. There are three types of tacticity or PP chain structures: isotactic, atactic, and syndiotactic. Figure 2 shows the linear hydrocarbon of isotactic PP forms from three monomers.

Isotactic PP molecules form helices due to their “one-handed” structure. This regular structure enables the molecules to crystallize into a hard, somewhat rigid substance that melts at 440 K in its pure state. Atactic chains have an entirely

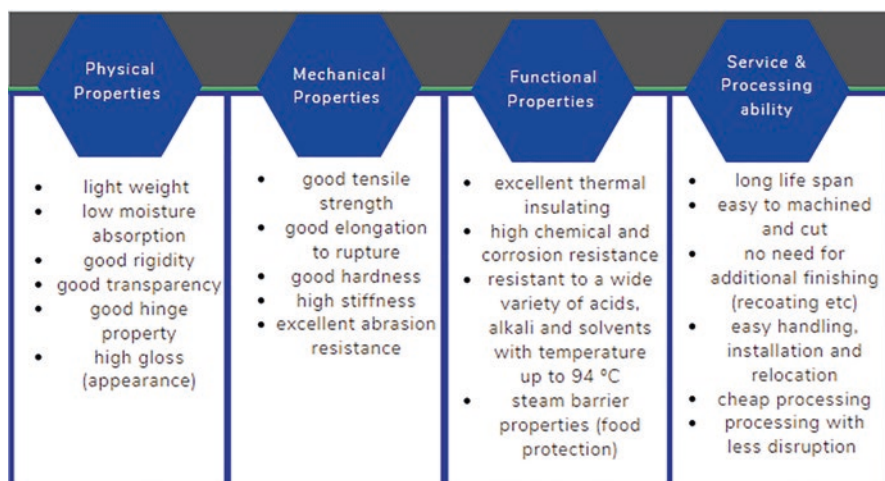
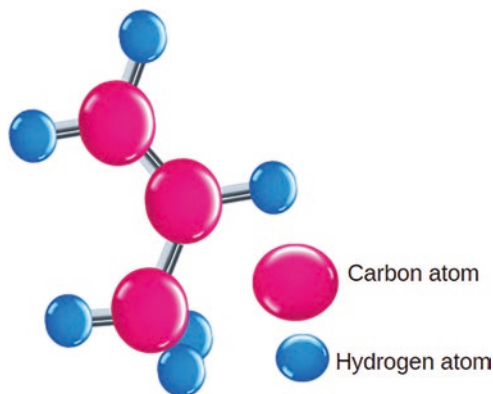


Fig. 1 General characteristics of polypropylene materials

Fig. 2 Ball-and-stick model of polypropylene monomer (propylene)



random structure and so do not crystallize. Atactic PP with a high molecular mass is a rubber-like substance. In the isotactic PP, the methyl groups are on the same side of the chain, while the methyl groups are placed randomly on both sides of the chain in the atactic PP. By utilizing a particular metallocene catalyst, combinations of isotactic and atactic structures are possible (Lower 2017). Syndiotactic PPs are similarly crystalline due to the regularity in their structure. Commercial PP is a primarily isotactic polymer with an atactic content of 1–5% by mass. Besides, there are varieties of PP materials that are homopolymer, random copolymer, and block copolymer. Homopolymer is made up of 100% polypropylene, which has excellent rigidity and heat resistance. PP shows inferior low-temperature impact resistance, and it can be improved through copolymerization with a monomer such as ethylene to form the copolymers.

1.2 Recycled Polypropylene

Waste polypropylene from various products is recycled using a number of methods such as mechanical and chemical recycling to form recycled polypropylene (recycled PP) (Achilias et al. 2007). The recycled PP has been employed in low-cost end products by blending with other virgin thermoplastic materials via mechanical recycling. This technique is nearly identical to recycled PP (Grigore 2017). The recycled PP could be defined as after-serviced or waste PP materials that have undergone several processes (mechanical, chemical, thermal recycling, etc.) in order to regain their processability and properties to be used in the same or other products. The primary challenges in recycling PP stem from the polymer's ease of degradation. Heat, mechanical stress, and UV light could significantly alter PP's structure, composition, and morphology, and thus its properties. According to La Mantia (1999), PP's photooxidative and thermomechanical degradation effects are more significant than other linear polyolefins due to tertiary carbon in its chain. The PP products are exposed to these elements both during their lifetime or service

(primarily via photooxidation) and during processing and recycling (reprocessing cycles) activities. The multi-recycling of recycled PP would further degrade its properties (Othman et al. 2017; Wang et al. 2014).

This chapter will later discuss numerous efforts that developed and characterized waste PP or recycled PP products to identify their potential for future use. The waste PP is gathered from various products and applications such as bottles, waste printed circuit board, manufacturing scraps, damaged tables and chairs, food containers, and so on. Some studies utilize the waste PP directly after the sorting, cleaning, and refining processes into a new blending mixture. However, some researchers utilize it in the form of recycled PP that various suppliers supply. The virgin PP is used as the control samples by most of them. Table 1 compares the general properties of virgin and recycled PP, gathered from multiple studies involving recycled PP. There

Table 1 General properties of virgin and recycled polypropylene

Criteria	Virgin PP	Recycled PP
Compositions	Could be homopolymer (100% PP monomer) or copolymers	Could be a homopolymer (100% PP monomer) or copolymers incorporated with other processing ingredients
Density, ρ (g/cm ³)	0.899–0.920 (Grigore 2017)	0.96–0.99 g/cm ³ (Grigorescu et al. 2020) 910 kg/m ³ (Hung et al. 2016)
Glass transition temperature (°C)	–23 to –10 (Grigore 2017)	Hardly reported by researchers due to the formulation diversity
Melt flow index (g(10 min) ^{–1})	4.14 ± 0.04 to 16.80 ± 0.12 (Ferg and Bolo 2013) 0.2–0.7 (Shubhra et al. 2011)	12.17 ± 0.08 to 14.07 ± 0.15 (Ferg and Bolo 2013) 6.0 (Grigorescu et al. 2020) 3.7 (Hung et al. 2016)
Melting point	163.42 °C (Ferg and Bolo 2013)	165.75–166.05 °C (Ferg and Bolo 2013) 159.60–160.00 °C (Brachet et al. 2008) 107.00 (Zdiri et al. 2018)
Variable melt flow index (g(10 min) ^{–1}) Mass load, 3 kg	22.5–25 (Ferg and Bolo 2013)	7–28.5 (Ferg and Bolo 2013)
Tensile strength, σ_{\max} (MPa)	26–41.40 (Grigore 2017) 29–34 (Shubhra et al. 2011)	20.6 MPa (Grigorescu et al. 2020) 34.4 ± 0.4 (Hung et al. 2016)
Elongation at break (%)	115–350 (Shubhra et al. 2011)	2.83 (Grigorescu et al. 2020) 7.1 ± 0.9 (Hung et al. 2016)
Tensile modulus, E (MPa)	950–1776 (Grigore 2017)	819.3 ± 18.84 MPa (Melo et al. 2020) 1900 (Hung et al. 2016)
Izod impact strength (at 23 °C) (kJ/m ²)	1.7 (Tai et al. 2000) 10–34 ft lb (Shubhra et al. 2011)	10.0 (Grigorescu et al. 2020)
Thermal conductivity (w/m.K)	0.25 (Hadi et al. 2016)	0.33 (Hadi et al. 2016)

are distinct differences between properties exhibited by recycled PP and virgin PP. In general, mechanical properties (tensile strength, tensile modulus, and elongation at break) of recycled PP are lower compared to virgin PP. The ground recycled PP from industrial transport shuttles has shown a significant difference in their percentage elongation at break of only about 2.83% compared to virgin PP. The reported values of homopolymer and copolymer by Shubhra et al. (2011) are in the range of 115–350% instead. Grigorescu et al. (2020) claimed that the recycled PP is originally brittle; hence, the elongation at break is very low.

Meanwhile, there are inconsistent values of properties depicted by the recycled PP themselves. The differentiator is the unique formulation, and different types of PP used for specific products also vary from one manufacturer to another. Manufacturers add various additives to meet the specification required for their products at the most reasonable prices. Therefore, several uncontrollable factors and variables might be the obstacles to the quality or properties uniformity of the recycled PP-based products:

- the difference between types of PP that were initially used by the manufacturer (different structure, configuration, chain's composition, and molecular weight),
- the difference between the formulation of recycled PP products depending on the type of products among different manufacturers,
- the difference in the recycling cycles (for multi-recycling PP), and
- the difference in processing methods and parameters.

However, these factors could be minimized by selecting recycled PP from similar products and sources.

For quality control purposes, the characterization analyses should be conducted frequently to the new batch or recycled PP in order to be utilized in the production line. For example, by using suitable characterization equipment, one could retrace or predict the compositional information of the waste material. In the case of recycled PP from Pb-acid battery casing, XRF elemental analyses were performed by Ferg and Bolo (2013) and Ferg and Rust (2007). They revealed that the waste PP consisted of Pb = 1566–1645 ppm, Br = 538–544 ppm, and Ca = 679–865 ppm. The Pb was most likely present from PbSO₄ or PbO₂ compounds derived from the used battery material, whereas Ca was most likely from CaO₂. It was initially used as a filler in manufacturing the battery case and lid. Meanwhile, the Br was found in a variety of flame-retardant chemicals. They also reported that recycled PP had a slightly higher melting temperature than virgin PP with a melting temperature (T_m) of 163.42 °C. It was assumed to be the contributions of the inorganic fillers and impurities present in the recycled PP. The recycled PP was also presumed to contain small amounts of high-density polyethylene with melting temperature between 120 °C and 130 °C from the tiny DSC endothermic peaks that formed at around 125.31–125.49 °C. The obtained data from variable melt flow index (VMFI) versus the total piston mass load was fitted to the suitable ($y = ax^n$) power function. The power coefficient (n) for the recycled PP samples of $y = 3.225x^{1.732}$ to $y = 3.759x^{1.693}$ was significantly higher than most virgin PP samples of $y = 1.356x^{1.491}$ to $y = 6.040x^{1.312}$. It demonstrated that additives such as fillers, contaminants,

stabilizers, colorants, and flame retardants can affect the flow characteristics of recycled material. Therefore, a close screening for the selection of PP waste or recycled PP is crucial to control the processing parameters and properties of produced recycled PP composite materials.

1.3 Green Fillers for Sustainable Materials

In most cases, the so-called sustainable polymeric materials refer to natural fiber composites, biodegradable composites, and green composites (Mansor et al. 2020; Santhosh Kumar and Somashekhar 2020; Cong et al. 2021). Some popular examples of sustainable polymer composites are biodegradable PLA (polylactic acid) or PVA (polyvinyl alcohol)-based polymer composites, natural fiber-reinforced polymer composites such as sisal fiber-reinforced thermoplastic composites, and more. The terms are used when biodegradable polymers or natural materials are used in formulations. They are inferred regardless of whether the matrix and the filler ingredients are natural, biocompatible, or eco-friendly materials. In most cases, the portion of how extensive these components are in the composites has not been clearly defined, except the filler should always be lesser than the matrix. Their specific ratio would be based on their functionality in the formulation or properties specifications. It is known that recycled thermoplastic materials experience dramatic changes in their physical and mechanical properties. The reusing and recycling of these polymers degrade their chemical structural properties, which calls for other materials or manipulation to their formulation. Therefore, introducing various types of filler materials into recycled polymers, whether organic or inorganic fillers, will result in properties and functional diversity. They could serve as a reinforcing agent, plasticizer, extender, impact modifier, and others: dictating the final seeking properties or product performance.

Green fillers refer to the fillers used either as a filler or reinforcement materials in any polymer matrix, either thermoplastic or thermosets, natural or synthetic. However, in this chapter, the green fillers are categorized based on the type of fillers used in the formulation of recycled PP composites. Figure 3 shows the general classification of green fillers commonly reported to be used as fillers or reinforcement materials in recycled polypropylene (recycled PP)-based composites. They are classified into four main categories, namely (1) natural organic fillers, (2) natural inorganic fillers, (3) advanced fillers, and (4) recycled fillers. Figures 4 and 5 show the images of plastic waste and several types of green fillers used by several studies (Yao et al. 2013; Oladele et al. 2020). Physical dimensional (sizes and shapes) and compositional characteristics of the fillers are essential in determining the properties of produced composites (Yao et al. 2013).

Natural Organic Fillers These fillers are natural or biodegradable materials from organic resources that are safe for the environment. The most commonly used are organic fillers that originated from either plant or animal fibers. They have become

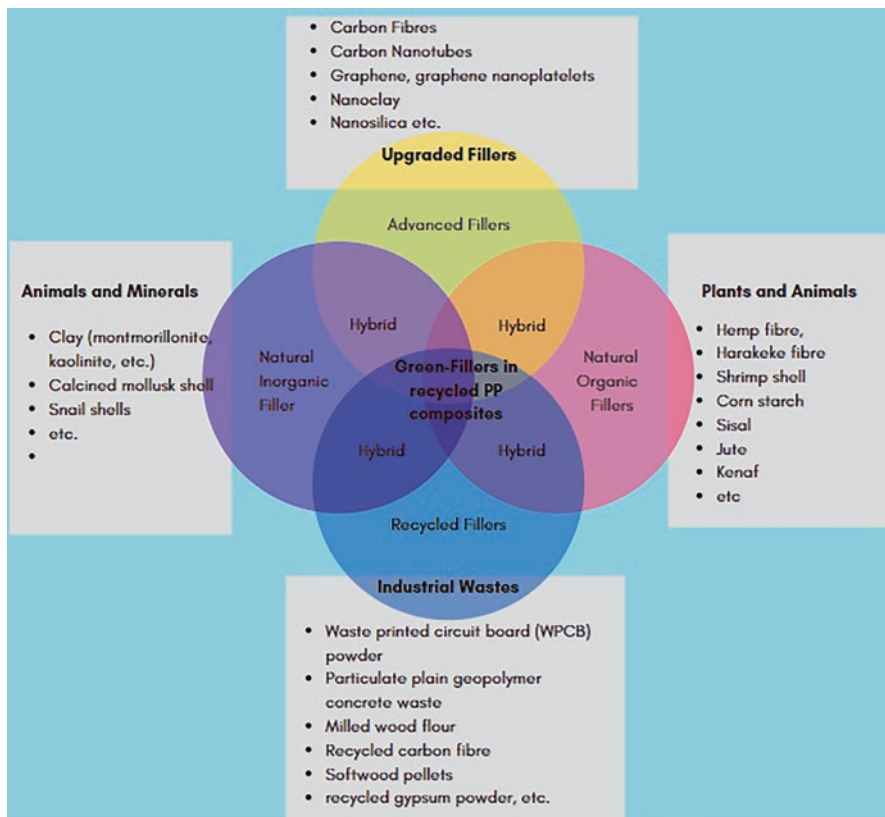


Fig. 3 Classification of green fillers used in recycled polypropylene composites



Fig. 4 (a) Waste plastics, (b) snail shell, and (c) shell powders

the topic of interest in industry and academic research due to its low cost and availability (Cong et al. 2021). Santhosh Kumar and Somashekhar (2020) further classified the plant fibers to (1) wood fibers, either hardwood or softwood, and (2) non-wood fibers, either seed fibers, leaf fibers, bast fibers, fruit fibers, stalk fibers, or grass fibers (Diyana et al. 2021). According to Mansor et al. (2020), plant-derived natural fibers are the most widely used and researched due to their short growth

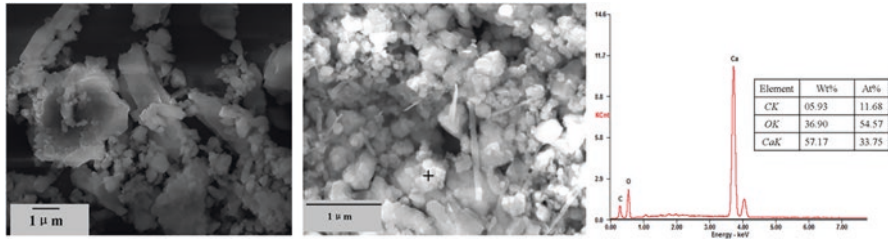


Fig. 5 SEM images of the shell waste. (Yao et al. 2013)

period, renewability, and wide availability. According to Chandrasekar et al. (2021), natural fiber-reinforced thermoplastic-based composites have been used in packaging and structural applications in the automobile, construction, and other industries. The animal origin polysaccharides are chitin and chondroitin. In general, natural fillers enhance the properties of composites due to their low cost, reasonably good mechanical properties, high specific strength, nonabrasive, green, and biodegradable characteristics.

Natural Inorganic Fillers These fillers are natural materials from inorganic resources derived from either minerals or animals. Clay minerals are phyllosilicates formed by the chemical weathering of other silicate minerals. Clay can be manufactured in a lab under controlled pH, temperature, composition, and starting material conditions. It is an alumina-silicate with neutral or negatively charged layers and positive counterions between the layers. Meanwhile, clay is characterized as kaolinite, montmorillonite, illite, chlorite, and fibrous silicate (e.g., sepiolite and palygorskite). Abdul Khalil et al. (2019) stated that the montmorillonite/smectite clay group is the most commonly used clay. It is due to its water stabilizing and rheological qualities. Calcium carbonate (CaCO_3) is another inorganic filler that is frequently used in industry and laboratories. It is typically derived from carbonatite lava, stalactites, stalagmites, skeletons, and some animal shells. However, the required purity, whiteness, thickness, and uniformity are not taken into account. According to Abdul Khalil et al. (2019), it can be obtained by digging carbonate-bearing rock. However, it will result in noise, air, and water pollution.

Advanced Fillers These filler materials can be organic- or inorganic-based materials refined and upgraded further through physical and mechanical processes, heat treatments, chemical modification, or synthetically produced in the laboratory. Some are classified as advanced materials (e.g., carbon fibers and aramid fibers) or nanomaterials (e.g., nanoclay and organoclay). The advancement of processing and nanotechnology has led to nanoclay, which is much preferred in the industries (Abdul Khalil et al. 2019). Polypropylene-based composites reinforced with (1) exfoliated graphite nanoplatelets (xGnPTM), (2) vapor-grown carbon fibers, (3)

polyacrylonitrile (PAN)-based carbon fibers, (4) highly structured carbon black, and (5) montmorillonite clay fabricated by extrusion and injection molding (Kalaitzidou et al. 2007). According to Zdiri et al. (2018), clay, montmorillonite (MMT), calcium carbonate (CaCO_3), carbon nanotubes (CNTs), zinc oxide (ZnO), silica (SiO_2), boehmite alumina (BAL), and graphene (GN) are among the nanomaterials used as fillers in recycled PP matrix.

Recycled Waste Fillers These fillers are natural-based or nonbiodegradable waste materials, either organic or inorganic, reused or recycled by manufacturing or recycling centers. They are placed back into the production/manufacturing lines as recycled feeding materials or fillers in various matrices to reduce their harmful impact on the environment. These fillers' utilization in manufacturing could be considered to adhere to the green policy for multiple industries and considered a greener approach for sustainable resources. Among the recycled fillers are waste printed circuit board (WPCB) powder (Grigorescu et al. 2020), geopolymer concrete waste (GCW) (Ramos et al. 2020), milled wood flour (WF) (Rocha and Rosa 2019), and others. In the report produced by Abdul Rasoul et al. (2020), the addition of PP fibers can strengthen the structural concretes by reducing the formation of micro-cracks and hence increasing their resilience to thermal shock. As a result, concrete waste could be beneficial as a filler in PP matrix composites, but recycled PP in the fiber forms might also be useful in the industry (Tuladhar and Yin 2019).

The generic comparisons of these green fillers with synthetic fibers are tabulated in Table 2. The list is adapted based on the report by Diyana et al. (2021).

Table 2 Comparison of general characteristics of green fillers used in recycled PP composites

	Natural organic fillers	Natural inorganic fillers	Recycled waste fillers	Advanced fillers	Synthetic fibers
Density	Light	Light	Varies (light to high)	Too light	Twice natural fibers
Cost	Low cost	Low cost	Varies (low to moderate)	Expensive	Higher than natural fibers
Renewability	Yes	Yes	No	Yes	No
Recyclability	Yes	Yes	No	No	No
Energy consumption	Low	Moderate	Moderate	High	High
Distribution	Wide	Wide	Varies (low to high)	Very high	High
CO ₂ neutral	Yes	Yes	Varies	Varies	No
Health risk when inhaled	No	Yes	Varies	Varies	Yes
Disposal	Biodegradable	Biodegradable	Varies	No	No

2 Properties of Green Fillers Reinforced Recycled PP Composites

2.1 Mechanical Properties of Recycled PP Matrix Composites

Various filler materials are used to reinforce recycled polypropylene to improve its properties. The requirement for reinforcement is crucial due to the properties' reduction of recycled PP materials compared to their virgin counterparts. A study by Grigorescu et al. (2020) has shown a total of ~10–50% reduction in impact strength. Their ability for plastic deformation dictates this property; hence, it is the most critical mechanical quality to be improved. The deterioration of the materials degrades the quality of recycled PP during their utilization. Research on the effect of reprocessing cycles also showed dramatic changes in their properties (Othman et al. 2017).

To date, various fillers from natural resources, recycled and waste materials, are added into recycled polypropylene or virgin polypropylene to achieve the reliable properties required for different products. Mechanical properties of polymer-filled composites are determined by the efficiency of mechanical stress transfer from matrix material to the fillers. The mechanical strength of a composite depends on:

- the cumulative effect between (1) weakening efforts due to the high stress and (2) reinforcing effect by the fillers, which produces a barrier against crack propagation at load pressure: more micro-cracks are created instead of deeper cracks; and
- the adhesion or interaction between matrix–filler/fibers interfaces (Móczó and Pukánszky 2008; Zdiri et al. 2018).

Table 3 lists several properties that have become the target for most researchers. It also summarizes the contributing factors that claimed to play critical roles in the properties of recycled PP composites based on the type of green fillers used.

In most recycled PP nanocomposites, the nanofillers overloading beyond the optimal level generally reduce the tensile characteristics. According to Zdiri et al. (2018), increasing the nanoclay (NC) loading from 3% to 5% resulted in a decrease in the tensile strength and Young's modulus of recycled PP/clay nanocomposites. The surface attraction between the filler and the polymer matrix was increased at low NC concentrations (<5 wt%). The agglomeration effect on the NC was responsible for this decline. The presence of NC agglomerates from agglomerated clay tactoids induced local stress concentration in nanocomposites. It decreased the clay aspect ratio, reduced the contact surface area between the organoclay and polymer matrix. Even in macrocomposites, stiff particle agglomerates also reduce the thermoplastic matrix deformability, resulting in nonhomogeneity in the stress distribution after external load application (Oladele et al. 2020; Grigorescu et al. 2020; Melo et al. 2020; Khanjanzadeh et al. 2011).

The increase in tensile properties observed with the incorporation of nanofillers does not coincide with their effect on the impact properties. The reasons for this are as follows: (1) stiffening of polymeric chains, (2) agglomerated nanofillers absorb

Table 3 Summary of the effects of various fillers on several properties of recycled PP composites

References	Type of properties	Properties	Contribution factors
Advanced fillers			
Husin et al. (2015)	Mechanical properties	Recycled PP/PANI/GN nanocomposites: ~20% improvement in tensile strength (TS) and elastic modulus (M) at 1.5 and 2 of GN loading	Stiffness of the platelets Effective stress transfer between recycled PP matrix and GN Uniform dispersion of GN in the matrix at these filler concentrations
Hadi et al. (2016)	Thermal properties	Calcium carbonate nanoparticles-filled virgin and recycled PP composites: Thermal conductivity (TC) increased with increasing nanoparticle concentration and crystallinity level Virgin PP + nano-CaCO ₃ (from 3 to 10 wt%): 0.26–0.48 w/m.K Recycled PP + nano-CaCO ₃ (from 3 to 10 wt%): 0.32–0.50 w/m.K	Crystallinity increases with CaCO ₃ CaCO ₃ nanoparticles fill the hole and orient the chain, so the crystallinity increases The intrinsic thermal conductivity of nanoparticles and their vast surface area allow them to transport heat effectively. The effect gets more robust with more significant volume fractions
Pang et al. (2021)	Electrical conductivity	Recycled PP/PANI/GNPs nanocomposites: Electrical conductivity, σ , increased with increasing GNPs loading up to 3 phr from $1.3 \times 10^{-16} \text{ S cm}^{-1}$ (recycled PP) to $4.1 \times 10^{-1} \text{ S cm}^{-1}$	High σ of GNPs; hence, higher concentrations of GNPs provide better networking for electrical conduction Improved physical contact between the dispersed GNPs-PANI chains created conductive networks in the nanocomposites
Natural organic filler			
Mohamad et al. (2014)	Mechanical properties	Recycled PP filled with shrimp shell (SS) composites: Percentage of fine SS particles (100–300 μm) at 8 wt% reached similar TS as recycled PP (~22 MPa) Impact strength increased (7–10 J/m) for fine SS particles loading from 3 to 8 wt%	Finer SS has a higher total surface area that provides a more efficient stress transfer mechanism Smaller SS particle size improves the interfacial bonding between the matrix and filler
	Water absorption	Percentage water absorption increased (1.5–3.3%/7 days) with increasing SS content for SS particles loading from 3 to 8 wt% Higher absorption in coarse SS than fine SS	The –OH group within the SS (presence of chitin) forms hydrogen bonds with water molecules and accelerate the water intake by the sample Higher interaction between fine SS filler with matrix reduces the water absorption at filler–matrix interfaces

(continued)

Table 3 (continued)

References	Type of properties	Properties	Contribution factors
Zaaba et al. (2016)	Mechanical properties	Recycled PP filled with peanut shell composites: TS and elongation at break (EB) decreased, but M increased with increasing recycled PP loadings in composites Recycled PP composites with polyvinyl alcohol (PVOH) showed improved tensile properties	The weak interfacial bonding between the filler and the polymer matrix A more porous structure and filler agglomeration found at higher filler loading PVOH-treated PSP had better interfacial adhesion between the filler and the polymer matrix
	Water absorption	Water absorption increased with the increase of recycled PP loadings and the presence of PVOH in the composites	Recycled PP loadings induced more pores within composites Highly hydrophilic nature of PVOH-treated lignocellulosic filler increased water uptake PVOH is a hydrophilic polymer that absorbs water
Younesi-Kordkheili and Pizzi (2020)	Mechanical properties	Ionic liquid (IL)-treated bagasse fiber-recycled polypropylene composites: Composite made from modified lignin exhibited higher flexural and tensile strengths than those made with unmodified lignin	MAPP increases interfacial adhesion by forming covalent bonding (ester linkages) between the bagasse fiber and polymer. The number of reactive sites was higher in the modified lignin, which improved lignin bonding to natural fibers, and recycled PP increased the panel's dimensional stability
	Water absorption	Water absorption decreased with the increase of lignin contents The addition of ILs to lignin reduced the composite's water absorption slightly more than untreated lignin	Nonpolar hydrocarbon chains and aromatic rings of lignin have hydrophobic characteristic functions as a repellent to water
Natural inorganic filler			
Melo et al. (2020)	Mechanical properties	Calcined mollusk shells reinforced recycled PP composites: Tensile strength decreased from 24.38 ± 0.299 MPa (recycled PP) to 19.08 ± 0.213 MPa (recycled PP/CS) Tensile modulus increased from 819.3 ± 18.84 MPa to 997.3 ± 12.38 MPa	The presence of voids around the hard particles of the shell facilitated the debonding of particles to the matrix

(continued)

Table 3 (continued)

References	Type of properties	Properties	Contribution factors
Oladele et al. (2020)	Mechanical properties	Snail shell particle (SSP)-filled recycled PP composites: TS increased gradually up to 41 MPa with the increase of SSP from 3 to 9 wt% before decreasing at higher loadings	The hard and rigid CaCO ₃ of the SSP enhanced the composite's resistance to deformation by impeding dislocation motion The adequate interfacial adhesion between the filler–matrix phases from chain interdiffusion and entanglement The formation of SSP agglomerates at high SSP loadings aid in TS reduction
	Water absorption	Water absorption rate decreased with the increase of SSP in the composites	The rigid SSP plugged pores and gaps within the matrix The animal-based particles are more hydrophobic
Recycled fillers			
Grigorescu et al. (2020)	Mechanical properties	WPCB reinforced recycled PP composites: Impact strengths decreased with the increased of WPCB loadings: recycled PP+WPCB (from 5 to 30% WPCB): 9–3.77 kJ/m ² recycled PP+SBS blend: 36 kJ/m ² recycled PP+SBS+WPCB (from 5 to 30% WPCB): 25–6 kJ/m ² three times higher impact strength in compatibilized composites recycled PP+SBS+SEBS-MA blend: 37 kJ/m ² recycled PP+SBS+SEBS-MA+WPCB (from 5 to 30 % WPCB): 34–12 kJ/m ²	The presence of stiff glass fibers in the WPCB agglomerates created stress concentration regions Poor interfacial adhesion reduced dispersion of WPCB in recycled PP The addition of elastomer improves resistance to crack propagation Maleic groups physically connect to the WPCB, increasing the interfacial adhesion between the WPCB powder and recycled PP matrix
Hybrid fillers			
Khanjanzadeh et al. (2011)	Mechanical properties	Virgin and recycled PP/wood flour filled with montmorillonite organoclay (NC) composites: 20.3 and 15.6% improvements of TS and M of recycled PP composites. It increased with the addition of NC from 0 to 3 wt%	The high aspect ratio of stiff silicate layers The higher extent of interaction with the polymer chains and good interfacial adhesion between the NC particles and the recycled PP matrix Mobility of polymer chains is restricted under loading

(continued)

Table 3 (continued)

References	Type of properties	Properties	Contribution factors
Ardanuy et al. (2012)	Thermal properties	<p>Composite foams based on recycled polypropylene reinforced with cellulosic fibers:</p> <p>Fibers increased the glass transition temperature of PP (5.4–5.8 °C) in both solid composites and foams up to 11.2 and 12 °C</p> <p>The specific storage modulus (E'_{spec}) was higher in all solid composites than in unfilled PP and increased slightly with cellulose fiber concentration</p>	<p>The cellulose fibers acted as a constraint on polymer mobility, and it decreased molecular mobility of PP, T_g increased</p> <p>E'_{spec} increased due to the stiffer cellulose fibers</p>
Naushad et al. (2016)	Mechanical properties	<p>Cloisite 15A-filled recycled PP nanocomposites and treated and untreated (UT) sisal bio-nanocomposites:</p> <p>Bio-nanocomposites with 40% UT fiber and 5% MA-g-PP had 27% higher TS and 370% higher M than recycled PP</p> <p>Flexural strength and modulus were enhanced by 128 and 269%, respectively than recycled PP</p>	<p>Increase in the degree of dispersion of nanoparticle</p> <p>Improve interaction between filler–matrix due to the presence of compatibilizer, MA-g-PP</p>
Zadeh et al. (2017)	Flammability properties	<p>Date palm fiber-filled recycled PP/HDPE/LDPE ternary blends incorporated $Mg(OH)_2$ flame retardants:</p> <p>Ternary blend burns much faster than natural date palm leaf fibers (DPLF) and flame-retardant composites</p>	<p>The endothermic action of $Mg(OH)_2$ fillers absorb 1.42 MJ kg^{-1} of heat and degrade by losing water</p> <p>The hydrolyzed DPLF has the potential to increase combustion heat</p> <p>Synergistic effects between $Mg(OH)_2$ and hydrolyzed DPLF produced char layer, separating the composite matrix from the heat and oxygen, flammability increased</p>

(continued)

Table 3 (continued)

References	Type of properties	Properties	Contribution factors
	Thermal conductivity	The ternary blend has low heat conductivity, indicating it is insulating A reduction in the TC of ternary blends with DPLF (0.345 W/m.K) compared to the TC of the ternary blend (0.361 W/m.K) The addition of metal hydroxide Mg(OH) ₂ additive enhanced the thermal conductivity of the ternary blend composite containing the flame retardant	The date palm fiber has low thermal conductivity (0.087 W/m.K) The contact between the particles grows as the flame-retardant fraction increases, forming a three-dimensional heat conduction network

Note: Parts per hundred rubber (phr), graphene (GN), polyaniline (PANI), waste printed circuit board (WPCB) powder, ionic liquid-modified lignin (IL), styrene-butadiene block copolymer (SBS), hydrogenated and maleinized styrene-butadiene block copolymer (SEBS-MA)

less impact energy, and (3) the presence of structural voids. Besides, in the case of NC, the unexfoliated aggregates/agglomerates also reduce the impact strength. It reduces nanocomposites' structural stability, diminishes impact energy absorption, and accelerates interface crack propagation. Some investigations have demonstrated that adding an impact modifier such as elastomer to nanocomposites increases their impact resistance (Grigorescu et al. 2020). The elastomer balances the impact resistance and rigidity of the nanocomposites.

2.1.1 Theoretical Interfacial Strength Evaluation Through Micromechanics Models

Several micromechanics models have been presented to analyze fiber–matrix adhesion in recycled PP composites. Naushad et al. (2016) conducted a study “Cloisite 15A” incorporated in recycled polypropylene to form PP nanocomposites and bio-nanocomposites. In their study, the interfacial adhesion in bio-nanocomposites is assessed using yield strength models. Naushad et al. (2016) utilized the Turcsanyi model to determine the bio-nanocomposites' and nanocomposites' tensile strength:

$$\sigma_{\text{comp}} = \sigma \left[\frac{1 - \Phi_f}{1 + 2.5\Phi_f} \right] e^{(B\Phi_f)} \quad (1)$$

where σ_{comp} is the tensile strength of bio-nanocomposites, while σ is the tensile strength for recycled PP and nanocomposites. The Φ_f is the filler volume fraction, and B is the specific constant depending on the type of polymer composites. Some

of the values for B are listed by Turcsányi et al. (1988) in their study. Meanwhile, the theoretical modulus of bio-nanocomposites reported by Naushad et al. (2016) is calculated using the Sato and Furukawa (1963) model:

$$E = E_m \left[\left(1 + \frac{\phi_f^{2/3}}{2 - 2\phi_f^{1/3}} \right) (1 - \psi\xi) - \left(\frac{\phi_f^{2/3} \psi\xi}{(1 - \phi_f^{1/3}) \phi_f} \right) \right] \quad (2)$$

$$\psi = \left(\frac{\phi_f}{3} \right) \left[\frac{(1 + \phi_f^{1/3} - \phi^{2/3})}{(1 - 2\phi_f^{1/3} + \phi^{2/3})} \right] \quad (3)$$

where E_m is the Young's modulus of the matrix (i.e., recycled PP nanocomposites), Φ_f is the fiber volume percentage, and ξ is an adhesion parameter. Meanwhile, ψ is the integral mean value of the filler area fraction in the cross sections (Turcsányi et al. 1988).

Kalaitzidou et al. (2007) compared the actual modulus data to theoretical predictions derived using the Halpin-Tsai and Tandon-Weng models. The PP-based composites in their study were fabricated by melt compounding processes (extrusion and injection molding). The composites were reinforced by zero-dimensional (0-D), one-dimensional (1-D), and two-dimensional (2-D) nanomaterials. The 0-D nanofiller used was a highly structured carbon black; 1-D nanofillers were vapor-grown carbon fibers and PAN-based carbon fibers. Meanwhile, the 2-D nanofillers were exfoliated graphite nanoplatelets (xGnP) and montmorillonite clay. According to Kalaitzidou et al. (2007), apart from the dispersion states within the polymer matrix (aggregated, oriented, and aligned state), the aspect ratio of the nanofiller and the contact at the filler-matrix interface also significantly affect the mechanical properties of the composites, namely the tensile modulus. They compared their experimental data with the values predicted with the Halpin-Tsai model for the tensile and longitudinal modulus of unidirectional fiber-reinforced composites, which is given in Eqs. 4 and 5:

$$E = E_M \left(\frac{1 + \eta\xi V_f}{1 - \eta V_f} \right) \quad (4)$$

$$\eta = \frac{\left(\frac{E_f}{E_M} - 1 \right)}{\left(\frac{E_f}{E_M} + \xi \right)} \quad (5)$$

where E is the composite's modulus, V_f is the fiber volume fraction, E_M denotes the Young's modulus of the matrix, while E_f denotes the longitudinal (E_{11}) modulus of the fiber. Meanwhile, ξ is a function of the filler's aspect ratio, a , which depends on

the geometries and loading conditions of the nanofillers (Halpin 1969). The a is a measure of filler and depends on boundary conditions. Therefore, they selected different ξ for 2-D and 1-D nanofiller-reinforced PP composites. The a values used were $\xi = 2/3a$ for platelets (2-D nanofillers) and $\xi = 2a$ for fibers (1-D nanofillers).

The Tandon-Weng model was used to predict the M values for the effect of nanofillers' orientation in the PP matrix (Kalaitzidou et al. 2007). There were two different nanofillers' orientations: (1) the randomly oriented xGNP nanofillers in xGnP/PP nanocomposites, and (2) the unidirectionally aligned PAN fibers in the PP matrix of PAN/PP composites. Overall, both models were reported to agree with experimental data (tensile modulus) at low nanofiller loadings. However, they showed overprediction at higher nanofiller loadings. The discrepancy between observed and predicted values was speculated due to the model's assumptions. The Tandon-Weng model assumed the nanofillers' isotropy and perfect alignment.

2.2 Water Absorption of Recycled PP Matrix Composites

In general, polymer reinforced with organic natural fillers composites is prone to weaken when exposed to a watery environment. Many studies (Samat et al. 2013; Odusanya et al. 2014; Daramola et al. 2019; Oladele et al. 2020) claimed that the composite's hydrophilicity plays a significant role in water absorption ability. The filler's hydrophilic groups result in poor wettability between the fillers and the polymer matrix, and hence weaker interfacial adhesion between the two components. The chains degradation experienced by recycled PP could make it more vulnerable for its composites. Yet, it depends on whether the natural fillers are highly hydrophilic or hydrophobic. Environmental degradation of composite characteristics can be ascribed to a decrease of adhesion and binding strength at the fiber–matrix interface. It has been demonstrated that water passes across the interface significantly faster than it permeates the matrix (Halpin 1969). Table 3 shows some recycled PP composites systems that exhibit an increase in water absorption when incorporated with shrimp shell (SS) particles (Mohamad et al. 2014) and PVOH-treated lignocellulosic filler (Zaaba et al. 2016).

In comparison, the recycled PP composites filled with bagasse fibers experience a reduction in water affinity. It is due to the nonpolar hydrocarbon chains and aromatic rings of the lignin repel water. According to Oladele et al. (2020), some animal-based particles (natural inorganic fillers) are hydrophobic, unlike plant fibers categorized as natural organic fillers. Hence, when used as polymer matrix reinforcement, they tend to reduce water/moisture intake, unlike plant-based fillers, which increases it. In their study, the resistance to water absorption is attributed to the rigidity of the snail shell particle (SSP) and the plugging of pores and gaps within the recycled PP matrix as the SSP concentration increases. Since SSP fills most pores/voids, it limits the number of available pores that water can fill up. The sample with the best water resistance was increased by 91% compared to the control sample. SSP's hard and rigid CaCO_3 phase in the recycled PP matrix improved the

water repellent properties and their tribological properties. According to Oladele et al. (2020), the water absorption property of polymer matrix composites (PMCs) reinforced with particulate fillers and their derivatives is dependent on:

- the amount of the particle,
- dispersion efficiency,
- immersion temperature,
- the area exposed to water,
- permeability of particulates,
- void content in the PMC, and
- the hydrophilicity of the individual component.

2.3 Electrical Conductivity of Recycled PP Matrix Composites

Apart from their outstanding mechanical capabilities, green fillers may be utilized for various applications due to their multifunctional properties, including electrical conductivity, σ , and electromagnetic interference (EMI) shielding (Ahmad et al. 2018). It served as the foundation for a variety of multifunctional applications of filled polymeric composites. Alshammari et al. (2021) stated that the electrical conductivity and EMI shielding properties are advantageous for energy storage, electronic industry, multifunctional components in vehicles, electrical cables, and EMI shielding for lightning strikes in aerospace and automotive. Table 4 shows the change of electrical conductivity of recycled PP insulator to semiconductor when blended with polyaniline (PANI), which further increases with the incorporation of graphene nanoplatelets (GNPs), even at very low loadings. Their nanocomposites transformed from a low-conductivity semiconductor ($2.25 \times 10^{-8} \text{ S cm}^{-1}$) to a high-conductivity semiconductor ($4.1 \times 10^{-1} \text{ S cm}^{-1}$), as GNPs increased up to 3 phr.

According to Pang et al. (2021), the increase in σ of recycled PP/PANI nanocomposites with increasing GNPs loading may be attributable to several factors:

Table 4 Comparison of electrical conductivity of recycled PP, GNPs, PANI, and its composites

Type of materials	Electrical conductivity, σ (S cm^{-1})	Category	Descriptions
Recycled polypropylene	1.3×10^{-16}	Insulator	Power scale of σ is 10^{-11}
GNPs	1.8×10^5	Conductor	Power scale of σ is larger than $10^{-1} \text{ S cm}^{-1}$
PANI	1.63×10^{-1}	Semiconductor	Power scale of σ ranging from 10^{-9} to $10^{-1} \text{ S cm}^{-1}$
Recycled PP/PANI blend	2.25×10^{-8}	Semiconductor	
Recycled PP/PANI filled with 0.5 phr GNPs nanocomposite	5.6×10^{-6}	Semiconductor	
Recycled PP/PANI filled with 1.5 phr GNPs nanocomposite	7.6×10^{-4}	Semiconductor	
Recycled PP/PANI filled with 3.0 phr GNPs nanocomposite	4.1×10^{-1}	Semiconductor	

- *The intrinsic σ of GNPs.* Thus, higher concentrations of GNPs provide better networking for electrical conduction due to the high σ of GNPs.
- *The filler–matrix interaction.* The increased physical contact between dispersed GNPs-PANI chains forms a conductive network in recycled PP/PANI nanocomposites. As a result, more electrons can flow or jump directly between the conductive filler materials, increasing the σ of the composites.
- *The extent of the amorphous region in the composites.* The increase in σ of the recycled PP/PANI/GNPs nanocomposites can be attributed to the increase in the amorphous area. It facilitates the chain mobility of recycled PP, which contributes to the ease of electron transport, improving the conductivity of composites.

2.4 Thermal Conductivity of Recycled PP Matrix Composites

Thermal stability is a critical factor for the oil and gas pipelines, infrastructure, and buildings in hostile environments, and the automotive industry includes engines, oil tanks, among others (Alshammari et al. 2021). Some other applications in electrical and electronic engineering include electrical insulators, electronic packaging and encapsulation, satellite devices, and others. It requires a good balance between high heat dissipation, low thermal expansion, and low density. One of the parameters indicating the thermal stability of a component is its thermal conductivity. According to Hadi et al. (2016), thermal conductivity qualities are crucial for the products' processing and service life.

Polymer-based materials are usually having significantly less thermal conductivity than metals or ceramic materials. Besides, it is widely reported that recycled polymers showed lower thermal resistance than their counterparts (Hadi et al. 2016; Othman et al. 2017; Zdiri et al. 2018). Therefore, the characterization of thermal properties is essential for the potential of these recycled PP composite materials to be used in temperature-sensitive applications but requires an increase in thermal conductivity. To achieve that, the formulation of these recycled PP is manipulated by incorporating thermally conductive filler materials, either organic or inorganic. Pang et al. (2021) added graphene nanoplatelets (GNPs) to the recycled PP-PANI blend to improve thermal conductivity. They explained the thermal performance of the nanocomposite based on the DSC data analysis. The reported parameters were the melting temperature (T_m), crystallization temperature (T_c), melting enthalpy (ΔH_m^*), and crystallinity percentage (X_c). The nanocomposites experienced T_c increments than their recycled PP counterpart, from 119.2 °C to 123.6 °C. Additionally, the ΔH_m^* decreased from 86.1 J/g (recycled PP) to 40.0 J/g (nanocomposites). From the results, they concluded that the obtained DSC data for nanocomposites reflect enhanced thermal performance. However, no thermal conductivity data support the increase in thermal conductivity exhibited by the materials.

According to Vakili et al. (2011), the DSC data for neat PP nanocomposites revealed different patterns. The ΔH_m^* (J/g) in their work depicted increased values

from 78 J/g (neat PP) to 104.6 J/g (nanocomposites) when 15 phr CaCO₃ nanoparticles were added in the neat PP matrix. Their observation was supported by the increment observed in thermal conductivity, TC (w/m.K), from 0.22±0.04 w/m.K to 0.36 ±0.03 w/m.K when the same amount of nanofillers were added into the neat PP. According to Vakili et al. (2011), it was crucial to compare the experimental data with the existing theoretical models for two-phase mixtures. They stated that numerous theoretical and empirical models for predicting the effective thermal conductivity of two-phase mixtures had been developed. The most straightforward approach for a two-component composite would be to organize the materials in parallel or series concerning heat flow, thereby defining the upper and lower boundaries of effective TC.

For the parallel conduction model (Eq. 6), the value for composite, matrix, and filler are denoted as c , m , and f , respectively. While ϕ is the volume fraction and K represents TC.

$$K_c = \phi_m K_m + \phi_f K_f \quad (6)$$

For the series conduction model (Eq. 7):

$$\left(\frac{1}{K_c} \right) = \left(\frac{\phi_m}{K_m} \right) + \left(\frac{\phi_f}{K_f} \right) \quad (7)$$

In the case of the geometric mean model, the effective TC of the composite is given by Eq. 8:

$$K_c = K_m^{\phi_m} + K_f^{\phi_f} \quad (8)$$

Lewis and Nielsen modified the Halpin–Tsai Eq. 7 for a two-phase system, as stated in Vakili et al. (2011), to account for the effect of particle shape and orientation or type of packing, resulting in Eq. 9:

$$K_c = K_m \left[\frac{(1 + AB\phi_f)}{(1 - B\psi\phi_f)} \right] \quad (9)$$

where B in the equation is calculated based on Eq. 10. There are specific values for A and ϕ_{\max} based on geometric shapes and orientations.

$$\begin{aligned}
 B &= \left[\frac{\left(\frac{K_f}{K_m} - 1 \right)}{\left(\frac{K_f}{K_m} + A \right)} \right] \psi \\
 &= 1 + \phi_f \left[\frac{(1 - \phi_{\max})}{(\phi_{\max}^2)} \right]
 \end{aligned} \tag{10}$$

According to Vakili et al. (2011), Maxwell derived a precise solution for the conductivity of randomly dispersed and noninteracting homogeneous spheres in a homogeneous medium through the use of potential theory, which is represented in Eq. 11, as follows:

$$K_c = \left[\frac{(K_f + 2K_m + 2\phi_f(K_f - K_m))}{(K_f + 2K_m - \phi_f(K_f - K_m))} \right] K_m \tag{11}$$

Vakili et al. (2011) also used other theoretical two-phased composites models referred to as Bruggeman, Botcher, De Loo, and Ce Wen Nan, Eqs. 12, 13, 14 and 15, respectively. They attempted to explain the TC of the produced PP composites. Typically, the TC prediction varies for different nanoparticles depending on many factors, including the type of nanofiller and the filler fraction loading. In their study, the Ce Wen Nan model predicted TC values reasonably well up to 15 phr. However, in most models, the value tends to be underestimated at higher filler loadings, more than 10 phr, and overestimated at low filler loading of about 5 phr.

$$K_c = \left(\frac{K_m}{(1 - \phi_f)^3} \right) \tag{12}$$

$$K_c = \left(\frac{K_m}{(1 - \phi_f)} \right) \tag{13}$$

$$K_c = \left(\frac{K_m(1 + \phi_f)}{(1 - 2\phi_f)} \right) \tag{14}$$

$$K_c = \left(\frac{K_m \left[3 + \phi_f \left(\frac{K_f}{K_m} \right) \right]}{(3 - 2\phi_f)} \right) \tag{15}$$

3 Processing of Recycled PP Composites Based on Type of Green Fillers

For thermoplastic waste materials that are commonly exposed to mechanical recycling (Ilyas et al. 2021c), once collected, they are cleaned, dried, and cut or crushed to a finer size (Tuladhar and Yin 2019). After weighing, there are two major processes typically involve in transforming recycled PP materials into valuable products. The first process is the (1) mixing/compounding process, followed by the (2) fabrication process. Table 5 tabulates the processing methods that various researchers have utilized to make recycled PP composites based on their ingredients and targeted applications or functions.

As a thermoplastic material, polypropylene products can be repeatedly reprocessed by reheating and recooling. It can be melted once reheated above its melting point, fabricated into any shape, and allowed to cool down to room temperature. PP materials are simple to manufacture since their glass transition temperatures (T_g) are substantially lower than ambient temperature and their melting temperatures (T_m) are moderate. At the same time, their semi-crystallinity structure affords them remarkable qualities for a wide range of applications. However, owing to the same criteria, PP has the most significant shrinkage after molding compared to other commodity polymers. In the utilization of recycled PP as a matrix to form composites for various applications, their processability will be much affected by the following:

- Thermal or heating history of the PP from the service life and the number of reprocessing cycles faced by the PP material: A high-throughput continuous compounding process might worsen deterioration problems (Hornsby 2017).
- The types and characteristics of the filler materials used in the formulation:
 - Some fillers are thermally sensitive and can degrade or break down during compounding due to exposure time and temperature. Concerns arise with organic additives such as wood flour, starch, and animal shells. High filler loadings will produce an increase in polymer melt viscosity (Hornsby 2017).
 - Some fillers are hydrophilic, containing hydroxyl groups on their surfaces. Moisture sensitivity is a problem in any polymer melt process. With high surface area or hygroscopic fillers, pre-drying (heat treatment) steps may be required before or during the compounding process. This step eliminates moisture (and other volatiles) present in the material that could degrade the compound's quality. In dealing with natural organic fillers, most research has focused on improving the filler–matrix interface by pre-surface treatment on the fibers via alkaline treatment, chemical treatment, or combined physical–chemical treatment (Cong et al. 2021).

According to Holbery and Houston (2006), the processing temperature limits the production of thermoplastic filled with natural fillers composites. When using natural organic fillers, the production is bound by two fundamental physical restrictions as follows:

Table 5 Processing method for waste PP or recycled PP-based materials and its targeted application

References	Main ingredients	Processing method	Targeted application or function
<i>Recycled fillers</i>			
Grigorescu et al. (2020)	Matrix: Ground recycled PP from industrial transport shuttles (~0.05 × 0.6 mm) Fillers: Waste printed circuit board (WPCB) powder Secondary matrix: Styrene-butadiene block copolymer (SBS)	Melt compounding using Brabender plastometer: Temperature: 185 °C Mixing speed: 60 rpm Duration: 7 min	High-impact strengths composites from the recycled matrix and waste filler from transportation and electronic wastes
Butylina et al. (2012)	Matrix: Recycled PP homopolymer granules with melt mass-flow rate of 3 g/10 min (190 °C, 2.16 kg ⁻¹) Fillers: Softwood pellets (6–8 mm in diameter, with 10–30 mm average length) Others: Coupling agent maleated polypropylene, OREVAC® CA 100	Melt compounding of recycled PP pellets and additives using a Weber CE 7.2 conical twin-screw extruder	Exterior non-structural or semi-structural building wood-polymer composite (WPC) products
Ramos et al. (2020)	Matrix: Recycled PP from blow-molded products Fillers: Particulate plain geopolymer concrete waste (GCW) (smaller than 270 mesh) as filler Others: Oleic acid (99% purity) as a surface modifier to GCW	Melt compounding in a screw extruder: Temperature: 180–200 °C Screw rotating rate: 6 rpm Fabrication through Battenfeld injection machine: Temperature: 200 °C	Producing eco-friendly recycled PP composites for building constructions
Zander et al. (2019)	Blends: Opaque recycled PP from yogurt containers, Clear polyethylene terephthalate (rPET) plastic salad containers, and Clear polystyrene (rPS) from Petri dishes	Melt blending using Thermo Scientific Process 11 Parallel twin-screw extruder	3D printing filaments

(continued)

Table 5 (continued)

References	Main ingredients	Processing method	Targeted application or function
Rocha and Rosa (2019)	<p>Matrix: Recycled polymer from supplier Virgin PP from supplier</p> <p>Fillers: Milled wood flour (WF) from industrial packages transportation's wood pallets</p> <p>Coupling agent: Starch gum from corn starch and distilled water</p> <p>Compatibilizer: Maleic anhydride grafted PP (MAPP)</p>	<p>Double melt compounding using single-screw extruder with L/D 24</p> <p>Heating zones temperature: 175–185 °C</p> <p>Fabrication via compression molding using a hot press:</p> <p>Temperature: 180 °C Pressure: 7 ton Duration: 5 min</p>	Producing eco-friendly alternative coupling agent for producing recycled polymers composites
Szpieg (2011)	<p>Matrix: Recycled PP films from processing waste</p> <p>Fillers: Pyrolysis short-recycled carbon fiber (rCF) preforms, formed through papermaking principles</p>	<p>Press-forming process:</p> <p>Pressing time: 7 min Cooling time: 5 min Applied force: 300 kN Temperature: 210 °C</p>	Producing thermoplastic green composites using waste materials for mechanical performance
<i>Natural organic and inorganic fillers</i>			
Samper et al. (2018)	<p>Matrix: Recycled PP from suppliers</p> <p>Biodegradable polymers (2.5–15 %): Polylactic acid (PLA) Polyhydroxybutyrate (PHB)</p> <p>Fillers: Thermoplastic starch (TPS)</p>	<p>Melt compounding using a twin-screw extruder:</p> <p>Temperature: 200–220 °C Mixing speed: 50 rpm</p> <p>Followed by an injection molding process using a Babyplast standar 6.6 machine</p>	Biodegradable food packaging, agricultural films for farming and crop protection
Melo et al. (2020)	<p>Matrix: Granulated recycled PP from supplier</p> <p>Fillers: Calcined mollusk shell (particulate = 44 µm)</p> <p>Surface modifiers: Cashew nutshell liquid Polyethylene glycol (PEG)</p>	<p>Melt compounding using Haake Polylab OS equipped with roller blades:</p> <p>Duration: 10 min Temperature: 190 °C Mixing speed: 60 rpm</p> <p>Fabrication using injection-molded Battenfeld HM45/210 injector:</p> <p>Injection pressure 400 bar and holding pressure 500 bar Holding time 15 s and cooling time 30 s Temperature profile 170 °C/180 °C Mold temperature 30 °C</p>	Producing thermoplastic green composites using waste materials for mechanical performance and thermal stability

(continued)

Table 5 (continued)

References	Main ingredients	Processing method	Targeted application or function
Oladele et al. (2020)	Matrix: Recycled PP from damaged plastic chairs and tables (granules) Fillers: Pulverized snail shells (particulate = 53–63 μm) Stabilizer: Dioctyl phthalate Plasticizer: Zinc stearate	Two-step hot compression molding process for compounding and fabrication: Temperature: 190 $^{\circ}\text{C}$ Duration: 7 min Pressure: 4 MPa	Lightweight material for automobile application and other commercial purposes
Mohamad et al. (2014)	Matrix: Recycled PP from food container waste (pellets) Fillers: Shrimp shell <i>P. indicus</i> from domestic waste (particulate) Coarse particles: 3–5 mm Fine particles: 100–300 μm	Melt compounding using Haake internal mixer with roller rotor: Temperature: 190 $^{\circ}\text{C}$ Mixing speed: 50 rpm Duration: 15 min Fabrication via compression molding using a hot press: Temperature: 185 $^{\circ}\text{C}$ Duration: 5 min	Potential of producing a sustainable polymer composite for mechanical performance and water resistance
Al-Mulla et al. (2013)	Matrix: Recycled PP granules from supplier Fillers: Corn starch (industrial grade) containing 70 wt% amylopectin and 30 wt% amylose Others: Maleated polypropylene (MAPP) Maleic anhydride Benzoyl peroxide	Double melt blending using an extruder: Screw speed: 100 rpm Barrel temperature: 166–172 $^{\circ}\text{C}$ Film fabrication by mold attached to the single-screw extruder	Potential of producing a biodegradable polymer composite by processability criteria
<i>Hybrid fillers</i>			
Stoof and Pickering, (2018)	Matrix: Granules of pre-consumer recycled PP Fillers: Hemp fiber, Harakeke fiber, and Recycled gypsum powder	Melt compounding using ThermoPrism TSE-16-TC co-rotating twin-screw extruder	3D printing filaments
Cong et al. (2021)	Matrix: Recycled PP from the plastic frame fillers Fillers: Recycled carbon fiber (RCF) 7 μm diameter, 1.75 g/cm^3 density, and 3 mm length Kenaf fiber (KF) 10 mm length Compatibilizer: Maleic anhydride grafted polypropylene (MAPP)	Melt compounding using an internal mixer: Temperature: 190 $^{\circ}\text{C}$ Mixing speed: 40 rpm Duration: 30 min Fabrication under a hot press: Temperature: 200 $^{\circ}\text{C}$ Duration: 1 min Pressure: 5 MPa	Producing lightweight green composites for sustainable parts

- the highest temperature at which the fillers/fiber may be treated, and
- the large difference in surface energy between the natural filler/fiber and the recycled PP matrix.

For long processing times, the highest limit before fiber destruction is typically thought to be around 150 °C, while plant fibers can resist short-term exposures to 220 °C. Discoloration, volatile release, poor interfacial adhesion, and embrittlement of the cellulose components may occur due to prolonged high-temperature exposure. As a result, it is critical to achieve the fastest feasible reaction rate during surface treatment and polymer processing to restrict exposure to cell wall components and prevent degradation.

Developing low-process-temperature surface treatments with good service capabilities is crucial for utilizing plant fibers to produce green composite from polymeric materials.

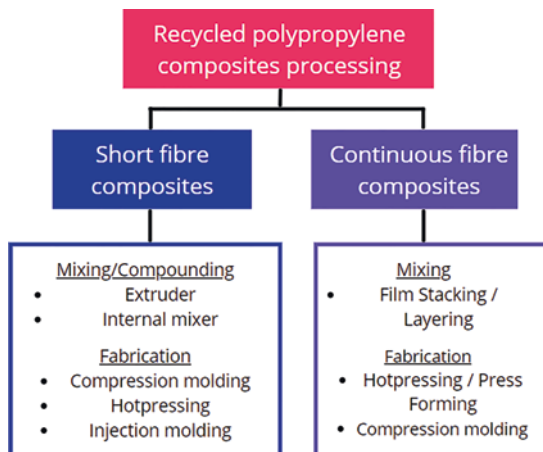
Mixing or compounding a polymer composite is the process of blending various elements with the main ingredients: matrix and filler materials and sometimes accompanied by chemical reactions. The matrix could be from dissimilar polymeric materials, and the fillers could be organic or inorganic materials of various forms with solid and/or liquid additives. Mixing is one of the crucial steps in processing the polymeric materials to attain the required physical, mechanical, and chemical properties of the desired appearance of the product in the processing machine (Zehev and Gogos 2006). Meanwhile, fabrication is the process of transforming the material into final shapes or semi-final shapes in product manufacturing. The obtained forms could require further finishing or not. The properties or performance of particulate-filled thermoplastic composites are highly dependent on the following (Hornsby 2017):

- the mixing processes used to combine the filler and polymer,
- the end processing used to turn the compound into finished products, and
- the final structure generated in the composite.

This usually produces polymer materials with new and improved properties.

There are various methods used to produce recycled PP thermoplastic-based composites (Cong et al. 2021). Since recycled polypropylene (recycled PP) is classified as a thermoplastic material, most reused waste PP or recycled PP-based materials fall within this category. Figure 6 summarizes the major processing strategies for mixing/compounding, melting, and fabricating in producing recycled polypropylene-based composites. The process can be categorized based on types of reinforcing or filler materials, whether short-fiber or continuous-fiber reinforcement. All of the methods utilize the melt compounding approach, as summarized in Table 5.

Fig. 6 Major processing strategies for producing recycled PP matrix composite



3.1 Melt Compounding/Melt Blending for Mixing of Discontinuous Matrix or Filler

Dispersing fillers in polymer matrices can be accomplished in various ways, including in situ polymerization, melting, or solution mixing. It is a crucial and essential procedure for some fields such as biotechnology, polymer handling, natural building, and others. However, for recycled PP composites processing, melt mixing is widely used by taking advantage of thermoplastic properties (Wang et al. 2014). Melt mixing, also referred to as melt compounding or melt blending, disperses nanoparticles in a molten polymer matrix via mechanical shearing action (Brandenburg et al. 2017). It is a straightforward and more adaptable technique for dispersing fillers in recycled PP matrix, mostly the ones involve with the short fibers or particulate fillers. This approach is more convenient to prepare because it is based on existing thermoplastic processing procedures.

Advantages and Disadvantages of Melt Blending Melt compounding or blending is environmentally benign due to the absence of organic solvents. It is become popular due to its compatibility with current industrial processes such as extrusion and injection molding. The primary advantage of this approach is its toxin-free nature, but the downside is the filler's poor dispersion in the polymer matrix, particularly at higher filler loadings. This occurs as a result of the composites' enhanced viscosity. Another downside of this approach is that it may result in fibers buckling or shortening due to the high shear stresses, which are detrimental to the composites' properties.

Figure 7 shows the general operation of producing recycled PP-based polymer pellets. There are five elementary steps of processing: handling of particulate or fibrous solids, melting, pressurizing and pumping, mixing, and devolatilization and stripping. Before the mixing, waste PP and fillers are usually subjected to several preprocessing steps, which are as follows:

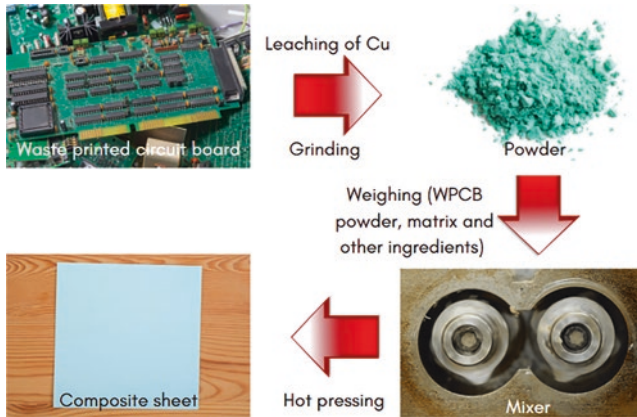


Fig. 7 Schematic representation of the melt compounding process of recycled PP blended with WPCB powders

- The collected waste PP materials would undergo the sorting process to separate them from other types of materials, cleaning to remove dirt and oils, and mechanically cut or crushed into finer sizes (whether granules or pellets). In some cases, it might be subjected to heating and cooling before crushing to obtain the recycled PP.
- The filler materials will undergo the same procedures as waste PP if it is originated from waste materials. In most cases, the fillers will also be subjected to surface modification to improve the interaction between fillers and matrix particles during compounding.

The recycled PP is often melted and blended with the required fillers at a specific amount, usually prepared using an extruder, internal mixer, or injection molding methods. Mixing may include both materials or components in solids or fluids form. It usually incorporates two or more polymers (virgin or reactively modified pellets) and a compatibilizer at low concentrations. It is compulsory to create fine and stable polymer blend morphologies because polymers are commonly incompatible with each other. The processing equipment must melt each polymer quickly, either concurrently or sequentially. It rapidly and efficiently affects the distribution and dispersion of blending of the melt components and the compatibilizer. It is a crucial stride to diminish creation non-consistency in polymer preparation since mechanical, physical, and concoction properties and “appearance” may firmly rely on arrangement consistency.

Using an extruder or internal mixer, recycling PP is usually compounded with other polymers, virgin PP, and other materials or additives. The material is evenly mixed through the mechanically mixing action and heat (Grigorescu et al. 2020). From Table 5, extrusion is the widely utilized method for compounding the recycled PP composites, followed by an internal mixer. Meanwhile, for the fabrication, it is conducted in an injection molding or hot press machine. For continuous fiber

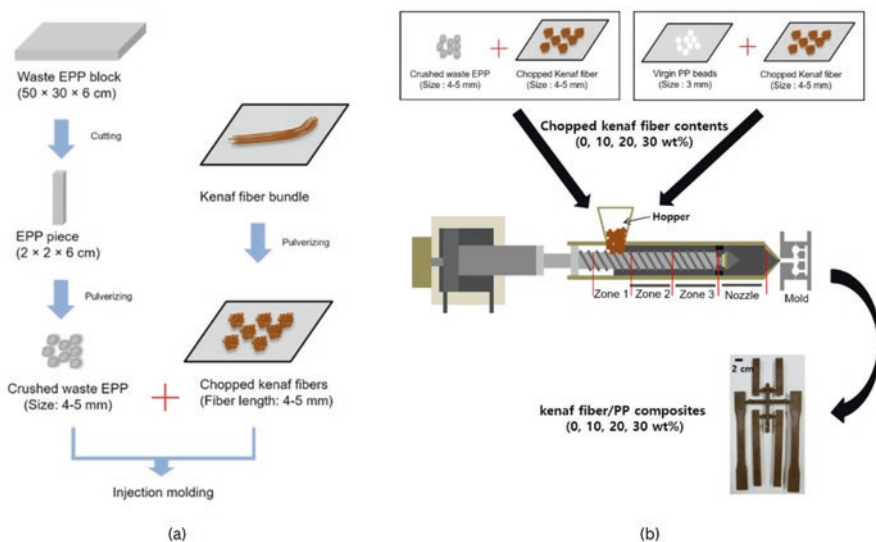


Fig. 8 Illustration of (a) pulverization of waste expanded polypropylene (EPP) blocks and kenaf fiber bundles prior to injection molding for composite preparation, and (b) injection molding of kenaf fiber/PP composites using waste EPP and virgin PP beads. (Kim and Cho 2020)

composites, the recycled PP films with recycled carbon fiber prepreg are melted and fabricated into composites straightaway using a press-forming process (Szpieg 2011). Figure 8 shows the schematic representation of the several processing components generally involved in the production of recycled PP composites. The scheme includes two-step processing of (1) production of crushed waste expanded polypropylene (EPP) and chopped kenaf fiber and (2) melt compounding of chopped kenaf fiber with EPP or virgin PP via injection molding, which is then molded into the specimen. Table 6 compares some of these processes based on their general advantages and disadvantages in making thermoplastic waste composites (Patel et al. 1995; Othman et al. 2017; Veejayplastic 2020).

However, there are recycled PP composites that are prepared via a two-stage processing scheme. The recycled PP and all ingredients are firstly mixed using higher shear mixer/internal mixer or extruder. Then, the molten mixture is discharged from the mixer and fed into an extruder (single- or twin-screw extruder) or refed to the extruder after the mixture was cooled down (Al-Mulla et al. 2013). This approach is to create a continuous compounding operation that targets product consistency. The purpose of these processing steps is not simply to combine the polymers and additives into a molten mass. However, it also functions as a waste pretreatment phase, grinding and drying materials unsuitable for single-screw extrusion. The batch mixing method can be utilized to feed melt to the second stage's single extruder with the appropriate mixer capacity and cycle duration. The extruder, which functions primarily as a melt pump, produces pressure to force the material through a die while further blending, heating, and cooling occur. Cost increases and

Table 6 Comparisons of melt blending/compounding method for recycled PP composites

Twin-screw extruder	High-shear mixer/internal mixer	Injection molding
<i>Advantages</i>		
<p>Great and versatile for compounding hard-to-mix materials (glass-fiber, high loading fillers, and heterogeneous plastics) due to the “gear-pump effect”</p> <p>Provide tailoring to the screw arrangement to meet processing requirements</p> <p>Allow close control to the operating parameters (residence time, degree of shearing, and processing temperature)</p> <p>Allow multiple downstream feed zones that eliminate the pre-blending requirement</p> <p>Allow improved dispersive mixing for broader particles size ranges</p> <p>Possible for an open-ended run or with an attached die</p>	<p>Great and versatile for compounding various types of fillers</p> <p>The ability for mixing mixture containing up to 50 wt% moisture</p> <p>Capable of delivering a high level of mixing unattainable in the continuous screw designs</p> <p>Simplified operations</p> <p>Low energy and maintenance costs</p> <p>Capable for high filler loadings</p> <p>Capable for mixing a wide range and various combinations of ingredients (from flexible to stiff materials) without changing machine parts</p> <p>Capable of reducing or eliminating the requirement or material pretreatment</p>	<p>The most utilized process because of its efficiency</p> <p>Products made through injection molding are stronger than those made through extrusion, which is comparably weaker</p> <p>High production rates</p> <p>High tolerances are repeatable</p> <p>A wide range of materials can be used</p> <p>Low labor costs</p> <p>Minimal scrap losses</p> <p>Little need to finish parts after molding</p>
<i>Disadvantages</i>		
<p>It has limited ability to remove residual moisture of more than 5 wt% from the feed material. Thus, resulting in voids and bubbles in the final solidified product</p> <p>It incurs higher capital costs and higher operating costs due to costly maintenance and more complicated operations</p> <p>Still requires pretreatment for most plastic waste</p>	<p>Controllable variables are limited to blade/rotor speed, degree of heating/cooling, and residence time</p> <p>Batch charging and discharging could affect the productivity and batch-to-batch product consistency</p> <p>More difficult to precisely control melting and mixing</p>	<p>Most expensive due to costly die requirements</p>

more complicated operations and maintenance needs are expected to be offset by predicted cost reductions and simplicity of operation associated with decreased or eliminated pretreatment processes.

3.1.1 Melt Compounding by Screw Extrusion

Screw extrusion operates by converting the flow of material into a well-mixed continuous melt stream. Plastics materials are fed into the feeder. They are mixed, melted, and conveyed by rotating screws in three zones (feed zone, transition/plasticizing zone, and metering/pumping zone). In extrusion, co- and counter-rotating

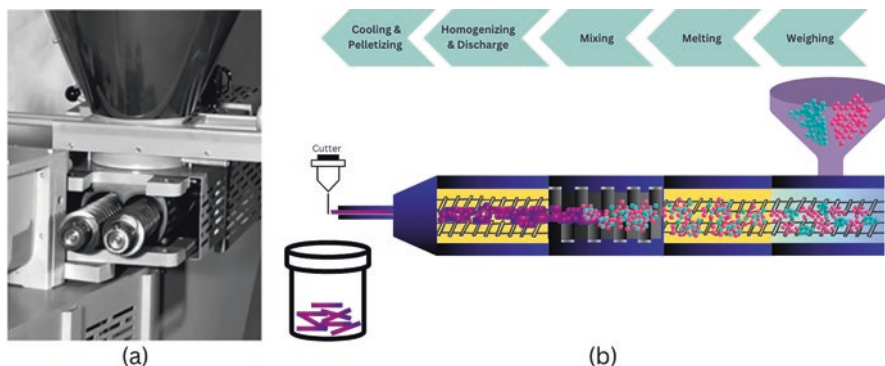


Fig. 9 (a) Conical twin-screw extruder (Butylina et al. 2012) and (b) melt-extrusion mechanism of a thermoplastic melt compounding

polymer mixture can satisfy these mixing and compounding steps significant to blending operations. This process is only suitable for continuous linear and two-dimensional seamless product manufacturing and achieves atypical cross sections. The material is melted by frictional heat from screw rotations and additional external heat applied through the barrel wall during the transition zone. It is categorized as a single-screw or double-screw extruder (co-rotating or counter-rotating with intermeshing and non-intermeshing design). According to Hornsby (2017), standard single-screw extruders have a limited capacity for mixing, producing only very modest amounts of shear strain and stress. Therefore, its drag flow conveying mechanism is incompatible with processing thermoplastics at a high filler content. However, most of the drawbacks of a single-screw extruder could be improved by the twin-screw extruder.

Figure 9 shows the feed zone of a conical twin-screw extruder and the extrusion's general mechanism. In Wang et al. (2014), the molten filaments of PP-based composites were quenched in a cold water bath before being pelletized in a rapid granulator. The pellets were dried in an air-circulating oven for 60 min to reduce moisture before proceeding to the next phase.

3.1.2 Melt Compounding by Internal Mixer

The internal mixer operates as a batch process without external heaters. It is commonly used for its ease of processing, availability, and good dispersion or distribution of the mixing materials. Material and additives are fed through the top of the machine and onto the mixing chamber. Blades of various designs and rotation arrangements rotate at high speed for mixing, fluxing, mastication, or shearing. The internal mixer utilizes high shear and is versatile in the production of recycled PP composites. Since it operates at atmospheric pressures, the moisture content (volatile) in natural fillers or waste materials could be vented out through the production

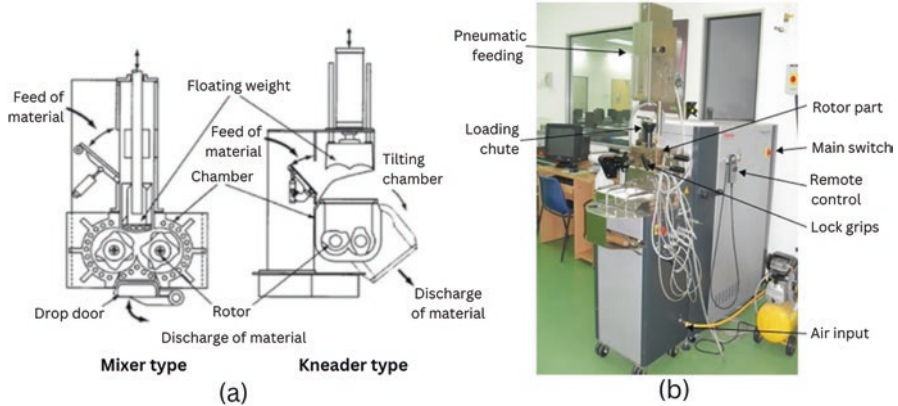


Fig. 10 (a) Types of high shear mixer (Moribe 2012) and (b) Internal mixer

cycle. Therefore, most studies involving natural fillers have selected this method because of the compatibility of mixing the polymer materials and natural fibers (refer to Table 5). However, the discharged mixture from the process still requires further fabrication process for shaping. The parameters of the internal mixer, such as rotor speed and temperature, can be adjusted. As illustrated in Fig. 10, internal mixers are categorized as mixers or kneaders based on their structural and functional characteristics (Moribe 2012).

In general, the mixer type demands a high level of durability to withstand high-load mixing and benefits from increased production capacity due to high volumes and high-speed mixing. Although the drop door method discharges the mixed compound quickly and thus reduces the cycle time between batches, building a frame is required, resulting in an increased installation cost. The kneader type requires a longer discharge time because it uses a chamber tilting system to discharge the rubber compound, but it is easy to install and has a low-cost structure. This type is easy to maintain, but it is not appropriate for high-load mixing since the floating weight's pressing force is low due to its vast breadth fitting in the chamber. Mixers are used for small variety and high amount production; kneaders are used for a huge variety and small quantity production.

3.1.3 Melt Compounding by Injection Molding

Injection molding is a processing technique of forcing melted plastic into a mold cavity. It is versatile to be used with a variety of host materials, including metals and ceramics. It is widely used in manufacturing various products, from the tiniest and simplest to the most robust and intricate components. This process is commonly used to fabricate plastic parts (Othman et al. 2017) and is widely referred to as plastic injection molding. A wide variety of plastic products is manufactured with greatly varying size, complexity, and application. This process can produce

three-dimensional thermoplastic mixture shapes that do not remain constant in a parallel line based on the molten die-casting method. It is highly suitable for three-dimensional product manufacturing, but it requires the use of intricate dies.

From Table 5, it is observed that the injection molding process is widely utilized for the fabrication of recycled PP composites into samples or final products. Cong et al. (2021) stated that recycled carbon fiber-reinforced thermoplastic composites are prepared by this method. The recycled PP materials require further manipulation to develop improved structural and compositional characteristics through the initial mixing and compounding/blending process. Plastic materials are fed into the feed section, compressed, and melted by frictional heat. The readily compounded plastic pellets/granules are melted in injection molding, and the molten mixture is poured into a mold by an injector. The melted composites fill up the die cavities and then cool before the item is ejected as a solid shape. Once the recycled PP composites are cooled, the part can be discharged. The process cycle for injection molding is relatively very short, typically between 2 s and 2 min (Rosato and Rosato 2000).

3.2 Compression Molding Using Hot Pressing/Press-Forming for Fabrication

Initially, compression molding was developed for the powder metallurgy sector. Then, the technology had been successfully used for ceramic components for several decades. A hot press or press-forming machine first consolidated fine green pressed powders into partially or fully sintered components by simultaneously applying increased temperature and compressive force. Pressure increased as a driving factor for densification, lowering the sintering temperature required. According to the manufacturer, this process reduced total grain size, more accurate control over the microstructure, and the ability to grade the ceramic layers functionally. Now, this process is also widely used by plastic molding manufacturers.

In the production of recycled PP composite products, this process is commonly used to fabricate final or intermittent products. It is performed after the mixing stage is completed via melt compounding (refer to Table 5). The process usually fabricates simple or medium shape complexity. During the process, the charge is heated above the melting temperature of the polymer matrix. Then, it is followed by a press-forming step before rapidly cooled to room temperature. The main advantage of this process is its ease of operating and its short processing time. Compression molding is a highly successful process for thermoplastic composite manufacturing. The male and female mold parts can be filled with a specific amount of polymer ingredients or composite mixtures (polymers with fillers) before the compression. Then, both top and bottom molds are heated, sealed, and forced together during the process. Polymer compound fabrication under compression is generally divided into two steps:

1. preheating step to bring polymer to their softening point, and
2. compressing step to deform it.

The polymer melts and conforms to the shape of the mold, releasing a hardened final product. The compression molding parameters, such as temperature, pressure, pressing cycles, and time duration, must be chosen following the thermal characteristics of the underlying polymer material. This procedure is highly time-consuming, expensive, and unsuited for mass production on a big scale (Saravanan and Emami 2021). In contrast to extrusion or injection molding, compression molding can process polymers with a higher molecular weight and melt viscosity.

3.3 Making Recycled Polypropylene Composites Using Press-Forming for Continuous Matrix and Fillers

In Table 5, in most studies, at least two subsequent processes are involved in producing and transforming the recycled PP composites into their final shapes before testing and characterization. The compression molding process is not only utilized to fabricate readily compounded recycled PP composite compounds but it could also be used to produce the composites through a single operation. Szpieg (2011) used this single operation approach to produce recycled PP-reinforced maleic anhydride grafted polypropylene (MAPP)-modified polypropylene (rCF/recycled PP) composite material. They referred to this compression molding method as “press-forming” (Szpieg 2011; Szpieg et al. 2012). The preregs of recovered short carbon fibers were prepared via the papermaking principle. In their study, the tape of scrap PP with tradename PURE[®] was manufactured by Lankhorst Indutech BV, the Netherlands. The polymer films were sandwiched between reinforcing mats, as shown in Fig. 11. The stack was heated and compressed to force the melt-impregnate into the fiber reinforcing. The matrix viscosity must be suitably reduced to avoid heat deterioration and ensure thorough wetting. Besides, insufficient heat could also result in unwetted fibers and a high void content, while overheating could cause material damage.

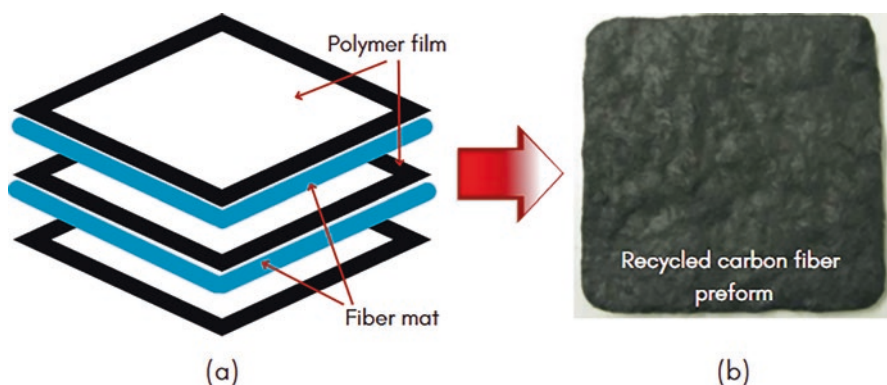


Fig. 11 (a) Film stacking and (b) recycled carbon fibers preform made by papermaking technique

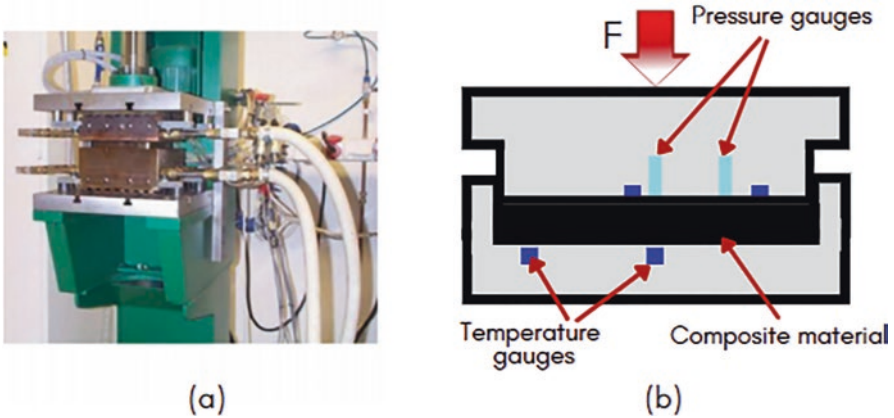


Fig. 12 (a) Press-forming machine and (b) matched die tool used to produce the recycled PP films and the composite material by Szpieg (2011)

The hot press machine employed in their study (Szpieg 2011) was a HASCO Z121/196 196/5 (refer to Fig. 12). The required constituents (recycled PP film and carbon fiber preforms) were calculated and weighed to obtain a nominal fiber volume fraction of 25 and 30%, respectively. The layers of PP film were sandwiched between the carbon fiber preforms in a stack and then placed in the press. The utilized processing parameters were the pressing time of 7 min, the cooling time of 5 min, the applied force (F) of 300 kN, and the temperature of 210 °C.

Process Modeling Theory of Press-Forming of Continuous Matrix and Fillers Composites

During the production of composites, a specific temperature, pressure, and time are required for the reinforcement to be infiltrated. In press-forming, Szpieg (2011) used Darcy's law to calculate the flow front velocity of the molten polymer that infiltrates the fiber preform during the process.

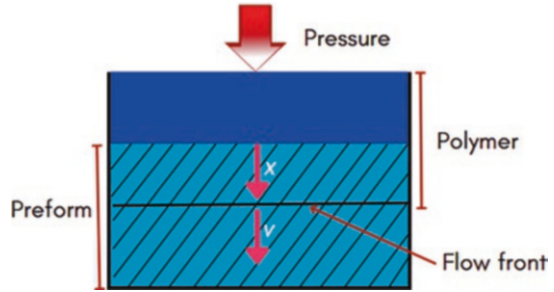
$$v = \frac{d_x}{d_t} = \left(\frac{K}{(1-\phi)\mu} \right) \frac{d_p}{d_x} \quad (16)$$

In Eq. 16, x is the distance at the flow front, as illustrated in Fig. 13. The t is the time, K is the permeability, and ϕ is the fiber volume fraction. Meanwhile, μ (= 1000 Pa s) is the viscosity of the polymer matrix and p is the fluid pressure.

Szpieg (2011) stated that to solve Eq. 16, it should be rearranged. They assumed that the pressure gradient is a constant and therefore needs to be integrated. It results in the following equations:

$$\frac{d_p}{d_x} = \frac{p}{x} \quad (17)$$

Fig. 13 Infiltration process



$$t = \left(x^2 / 2 \right) \left(\mu / K_p \right) \quad (18)$$

Szpieg (2011) approximates the permeability of a fiber network using the Karman-Kozeny equation as follows:

$$K = d^2 (1 - \phi)^3 / C \phi^2 \quad (19)$$

where d is the diameter of the fiber, ϕ denotes the volume of the fiber, and C is a constant. When processing composite materials, it is better to treat the C as a material parameter than a processing parameter. According to Szpieg (2011), the coefficient C for fiber beds with low fiber loadings is close to 180. She arrived at the value based on Jacob Bear's book published in 1989 on the dynamics of fluids in porous media. By combining Eqs. (18) and (19), the time required to enter the preform can be approximated as:

$$t = \left(x^2 / 2K \right) \left(\mu / p \right) = \left(C x^2 \mu \phi^2 / 2d^2 (1 - \phi)^3 k E \phi^\alpha \right) \quad (20)$$

3.4 Strategy for the Improvement of Interaction

In most cases, incorporating micro-sized fillers in the recycled PP resulted in the decrement of their ability to absorb energy during impact. Incorporating WPCB from 5 to 15% in recycled PP, Grigorescu et al. (2020) observed that WPCB was dispersed poorly in the recycled PP matrix. It tended to form agglomerates due to the presence of glass fibers from the WPCB. The poor interfacial adhesion created regions of stress concentrators that reduce the mechanical strength of the recycled PP composites (Guo et al. 2010; Muniyandi et al. 2013). One way to minimize this effect is by adding impact modifiers or elastomers to improve the resistance to crack propagation (Grigorescu et al. 2020). Besides, coupling or compatibility agents can

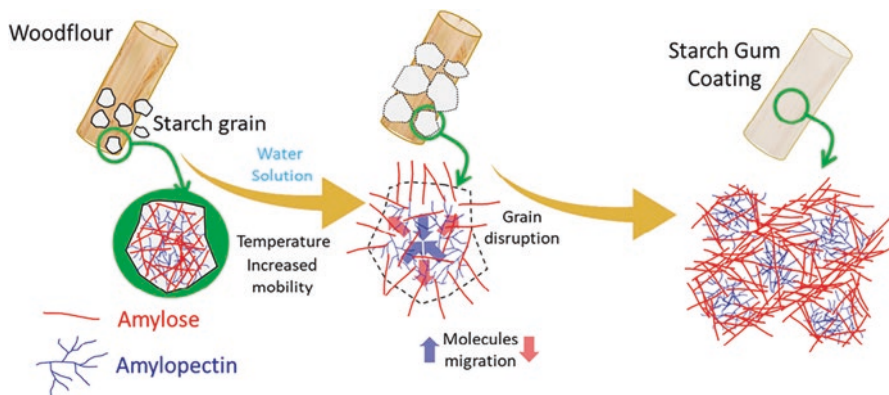


Fig. 14 Schematic of starch gum coating formation over wood flour surfaces. (Rocha and Rosa 2019)

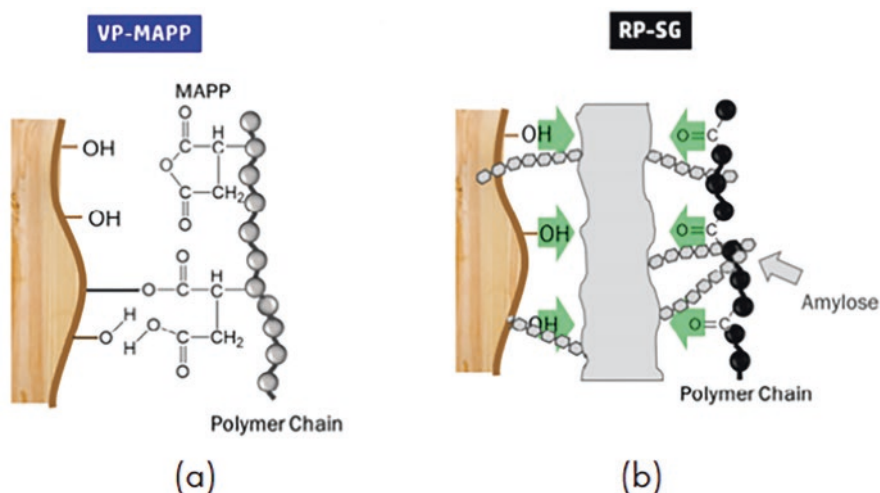
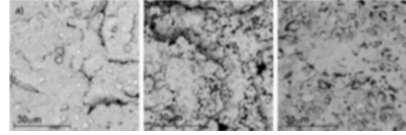


Fig. 15 Schematic of coupling effect from (a) virgin matrix and WF produced by the MAPP and (b) recycled matrix and WF produced by the starch gum coating. (Rocha and Rosa 2019)

be added to modify the surface of the matrix and fillers to increase their interaction. Some researchers carry out chemical modifications before or during the compounding process to improve the interaction between recycled PP and fillers (Rocha and Rosa 2019). Figures 14 and 15 show the schematic of starch gum coating and the coupling effect produced by the starch gum coatings between virgin and recycled PP with wood flour surfaces (Rocha and Rosa 2019).

Meanwhile, miscibility becomes critical when polymeric biomaterials such as polylactic acid (PLA), thermoplastic starch (TPS), or polyhydroxybutyrate (PHB) are added to recycled PP (Samper et al. 2018). The miscibility of various polymers

Fig. 16 SEM images of (a) PP-15PHB, (b) PP-15PLA, and (c) PP-15TPS samples at 3500× magnifications



is determined by their chemical structure, crystalline character, and morphological characteristics. While miscibility is conditional, numerous polymers create immiscible combinations. Figure 16 depicts SEM images of three PP blends with different biodegradable polymers (PLA, PHB, and TPS) at a constant amount. It is observed that all blend samples have spherical droplets in the PP matrix, which reflects the level of miscibility. The phase separation of the components in different blends shows that the blends tested are somewhat immiscible. In polymer recycling, this issue might worsen in the recycled PP composites due to its diverse structural characteristics from the formulation of their original products. A polymeric blend or composites may experience loss in mechanical properties and even superficial lamination due to incompatibility of polymeric matrices. This degradation of attributes is also proportional to the proportions of each component in the blend sample.

Samper et al. (2018) concluded that the biodegradable polymers appear to behave as contaminants in some studies, most likely due to their differing polarity. According to them, it is well established that the solubility parameter, δ , can be used to determine the relative affinity of two polymers. For a compatible mixture, their solubility parameters should be comparable. In this respect, it should be computed by concerning the contribution of each group to the overall molecules' structure using Eq. 21.

$$\delta = \frac{(\rho \sum_j F_j)}{(M_n)} \quad (21)$$

where δ denotes the solubility parameter for each component in $(\text{cal}\cdot\text{cm}^{-3})^{1/2}$, ρ denotes the polymer density in $\text{g}\cdot\text{cm}^{-3}$, and M_n is the molar mass of the repeating unit in $\text{g}\cdot\text{mol}^{-1}$. The \sum_j and F_j represent the sum of all groups' contributions (F , $(\text{cal}\cdot\text{cm}^{-3})^{1/2} \text{mol}^{-1}$).

4 Challenges and Future Perspective

PP is a widely used thermoplastic substance that serves as the foundation for many crucial industries. PP-based products can be found everywhere, and global manufacturing is increasing every year to meet the rising demand. This situation creates pollution and disposal challenges due to its inability to biodegrade. There are still obstacles that prohibit good waste management from delivering long-term environmental solutions for waste PP products. The profitability of their recycling is influenced by two primary economic drivers: (1) the prices of recycled polymer in

comparison to virgin polymer, and (2) the costs of recycling in comparison to alternate kinds of acceptable disposal (Hopewell et al. 2009). Additional challenges arise due to variations in supply quantity and quality compared to virgin polymers. Lack of knowledge regarding recycled plastics' availability, quality, and suitability for specific applications can also hinder the use of recycled materials.

The effort to convert the plastic trash into feedstocks or higher value-added goods by generating recycled PP-based composite materials is prudent and potentially profitable. It seems promising since waste PP has tremendous potential for humankind. It is cheap with high bending strength due to its semi-crystalline form, low coefficient of friction, and chemically resistant to a variety of bases and acids.

Future research on this area should concentrate on designing formulations that reduce the pollution caused by PP materials and their counterparts and enhancing recycling technology. After green and ecologically friendly fillers are added to the production mix, greener and more sustainable composites are generated. The benefits of PP matrix and filler materials and their interactions are integrated into the composite. It has the potential to reduce plastic pollution while also making composites environmentally and economically feasible for businesses. Yet, the manufacturing process and waste management system should be supportive, more ecologically friendly, and sustainable to realize the effort.

5 Conclusions

The motivation for the research and development of recycled PP reinforced by green fillers arises from the need to address the issue of PP waste disposal to landfills, its non-biodegradability, and limited raw materials resources. Therefore, this chapter serves as an essential reference in realizing the potential of recycled PP reinforced by green fillers as sustainable choices in the manufacturing sector. Several highlights from the chapter are as follows:

- There are four types of green fillers that researchers have used to fill the recycled PP, namely (1) natural inorganic fillers, (2) natural organic fillers, (3) advanced fillers, and (4) recycled fillers.
- The filler types, filler–matrix interfacial adhesion, and dispersibility levels play a significant role in controlling the composites' mechanical, thermal, and electrical properties and water absorption.
- Various mathematical models often predict the behavior of thermoplastic composites. Some of the reported mathematical models used for PP composites are briefly introduced in the chapter to raise understanding and spark further material development ideas.
- The melt-based processing methods appear to be the most utilized technique for compounding and fabricating the recycled PP composites regardless of the fillers' types. The used parameters and the targeted properties or application of

the materials are listed to provide the baseline for other future studies on recycled PP composites.

- In most cases, chemical modifications improve composites' properties and performance by enhancing the filler–matrix interaction. It is conducted either as pretreatment on filler materials (before) or during the compounding process of the composites.

Acknowledgment The authors would like to acknowledge Universiti Teknikal Malaysia Melaka for facilities, resources, and for granting the Short Term Grant Scheme PJP/2020/FKP/PP/S01780, which partially contributed to the success of this study.

References

- Abdul Khalil HPS, Chong WN, Owolabi FAT et al (2019) Enhancement of basic properties of polysaccharide-based composites with organic and inorganic fillers: a review. *J Appl Polym Sci* 136(12):47251. <https://doi.org/10.1002/app.47251>
- Abdul Rasoul ZMR, Radhi MS, Alsaad AJ et al (2020) Elevated temperature performance of reinforced concrete beams containing waste polypropylene fibers. *Case Stud Therm Eng* 21:100705(1–9). <https://doi.org/10.1016/j.csite.2020.100705>
- Achiliadis DS, Roupakias C, Megalokononimos P et al (2007) Chemical recycling of plastic wastes made from polyethylene (LDPE and HDPE) and polypropylene (PP). *J Hazard Mater* 149:536–542. <https://doi.org/10.1016/j.jhazmat.2007.06.076>
- Ahmad AF, Abbas Z, Ab Aziz S et al (2018) Synthesis and characterisation of nickel oxide reinforced with polycaprolactone composite for dielectric applications by controlling nickel oxide as a filler. *Results Phys* 11:427–435. <https://doi.org/10.1016/j.rinp.2018.08.041>
- Al-Mulla A, Alfadhel K, Qambar G et al (2013) Rheological study of recycled polypropylene–starch blends. *Polym Bull* 70:2599–2618. <https://doi.org/10.1007/s00289-013-0977-1>
- Alshammari BA, Alsuhybani MS, Almushaikh AM (2021) Comprehensive review of the properties and modifications of carbon fiber-reinforced thermoplastic composites. *Polymers* 13:2474(1–32). <https://doi.org/10.3390/polym13152474>
- Ardanuy M, Antunes M, Velasco JI (2012) Vegetable Fibres from agricultural residues as Thermo-mechanical reinforcement in recycled polypropylene-based green foams. *Waste Manag* 32:256–263. <https://doi.org/10.1016/j.wasman.2011.09.022>
- Atiqah A, Ismail N, Lim KK et al (2021) Properties of recycled metal matrix composites. In: Ilyas RA, Sapuan SM, Bayraktar E (eds) *Recycling of plastics, metals, and their composites*, 1st edn. CRC Press, Boca Raton
- Brachet P, Høydal LT, Hinrichsen EL et al (2008) Modification of mechanical properties of recycled polypropylene from post-consumer containers. *Waste Manag* 28(12):2456–2464. <https://doi.org/10.1016/j.wasman.2007.10.021>
- Brandenburg RF, Lepiński CM, Becker D et al (2017) Influence of mixing methods on the properties of high density polyethylene nanocomposites with different carbon nanoparticles. *Matéria (Rio de Janeiro)* 22(4):1–12. <https://doi.org/10.1590/S1517-707620170004.0222>
- Butylina S, Hyvärinen M, Kärki T (2012) A study of surface changes of wood-polypropylene composites as the result of exterior weathering. *Polym Degrad Stab* 97(3):337–345. <https://doi.org/10.1016/j.polyimdegradstab.2011.12.014>
- Chandrasekar M, Kumar TSM, Senthilkumar K et al (2021) Performance of natural fiber reinforced recycled thermoplastic polymer composites under aging conditions. In: Ilyas RA, Sapuan SM, Bayraktar E (eds) *Recycling of plastics, metals, and their composites*, 1st edn. CRC Press, Boca Raton

- Cong XY, Pierce R, Liu XL (2021) Development of recycled polypropylene-based sustainable composites with recycled carbon fibre/Kenaf fibre hybrid reinforcements. *J Phys Conf Ser* 1765:012013(1–8). <https://doi.org/10.1088/1742-6596/1765/1/012013>
- Daramola OO, Akinwekomi AD, Adediran AA et al (2019) Mechanical performance and water uptake behaviour of treated bamboo fibre reinforced high-density polyethylene composites. *Heliyon* 5(7):e02028(1–6). <https://doi.org/10.1016/j.heliyon.2019.e02028>
- Diyana ZN, Jumaidin R, Selamat MZ et al (2021) Physical properties of thermoplastic starch derived from natural resources and its blends: a review. *Polymers* 13:1396(1–20). <https://doi.org/10.3390/polym13091396>
- Ferg EE, Bolo LL (2013) A correlation between the variable melt flow index and the molecular mass distribution of virgin and recycled polypropylene used in the manufacturing of battery cases. *Polym Test* 32:1452–1459. <https://doi.org/10.1016/j.polymertesting.2013.09.009>
- Ferg EE, Rust N (2007) The effect of Pb and other elements found in recycled polypropylene on the manufacturing of Lead-acid battery cases. *Polym Test* 26:1001–1014. <https://doi.org/10.1016/j.polymertesting.2007.07.001>
- Galli P, Haylock JC, Simonazzi T (1995) Manufacturing and properties of polypropylene copolymers. In: Karger-Kocsis J (ed) *Polypropylene structure, blends and composites. Copolymers and blends, vol 2*. Springer, Dordrecht. https://doi.org/10.1007/978-94-011-0521-7_1
- Grigore ME (2017) Methods of recycling, properties and applications of recycled thermoplastic polymers. *Recycling* 2:24(1–11). <https://doi.org/10.3390/recycling2040024>
- Grigorescu RM, Ghioca P, Iancu L et al (2020) Development of thermoplastic composites based on recycled polypropylene and waste printed circuit boards. *Waste Manag* 118:391–401. <https://doi.org/10.1016/j.wasman.2020.08.050>
- Guo J, Tang Y, Xu Z (2010) Wood plastic composite produced by nonmetals from pulverized waste printed circuit boards. *Environ Sci Technol* 44:463–468. <https://doi.org/10.1021/es902889b>
- Hadi J, Saad NA, Mohamed DH (2016) Thermal behavior of calcium carbonate and zinc oxide nanoparticles filled polypropylene by melt compounding. *Res J Appl Sci. Eng Technol* 13(4):265–272. <https://doi.org/10.19026/rjaset.13.2941>
- Halpin JC (1969) Effects of environmental factors on composite materials, Technical report AFML-TR-67-423, Air Force Materials Laboratory, Air Force Systems Command, vol 45433. Wright-Patterson Air Force Base, Dayton, pp 1–53
- Hindle C (2021) Polypropylene (PP). British Plastic Federal. Available at: <http://www.bpf.co.uk/plastipedia/polymers/pp.aspx>. Accessed 14 Sept 2021
- Holbery J, Houston D (2006) Natural-fiber-reinforced polymer composites in automotive applications. *JOM* 58:80–86. <https://doi.org/10.1007/s11837-006-0234-2>
- Hopewell J, Dvorak R, Kosior E (2009) Plastics recycling: challenges and opportunities. *Phil Trans B* 364:2115–2126. <https://doi.org/10.1098/rstb.2008.0311>
- Hornsby P (2017) Compounding of particulate-filled thermoplastics. In: Rothon R (ed) *Fillers for polymer applications, polymers and polymeric composites: a reference series*. Springer International Publishing. https://doi.org/10.1007/978-3-319-28117-9_3
- Hundertmark T, Mayer M, McNally C et al (2021) How plastics waste recycling could transform the chemical industry. Available at: <https://www.mckinsey.com/industries/chemicals/our-insights/how-plastics-waste-recycling-could-transform-the-chemical-industry>. Accessed 9 Oct 2021
- Hung K-C, Wu T-L, Chen Y-L et al (2016) Assessing the effect of wood acetylation on mechanical properties and extended creep behavior of wood/recycled-polypropylene composites. *Constr Build Mater* 108:139–145. <https://doi.org/10.1016/j.conbuildmat.2016.01.039>
- Husin MR, Arsad A, Al-Othman O (2015) Effect of graphene loading on mechanical and morphological properties of recycled polypropylene/polyaniline nanocomposites. *MATEC Web Conf* 26:01008. <https://doi.org/10.1051/mateconf/20152601008>
- Ilyas RA, Sapuan SM, Bayraktar E (2021a) *Recycling of plastics, metals, and their composites*. CRC Press, Boca Raton. <https://doi.org/10.1201/9781003148760>

- Ilyas RA, Sapuan SM, Sabaruddin FA et al (2021b) Reuse and recycle of biobased packaging products. In: Sapuan S, Ilyas R (eds) Bio-based packaging: material, environmental and economic aspects. Wiley, pp 413–426. <https://doi.org/10.1002/9781119381228.ch23>
- Ilyas RA, Sapuan SM, Jailani AK et al (2021c) Introduction to recycling of polymers and metal composites in: Ilyas RA, Sapuan SM, Bayraktar E (eds) recycling of plastics, metals, and their composites, 1st edn. CRC Press, Boca Raton
- Kalaitzidou K, Fukushima H, Miyagawa H et al (2007) Flexural and tensile moduli of polypropylene nanocomposites and comparison of experimental data to Halpin-Tsai and Tandon-Weng models. *Polym Eng Sci* 47(11):1796–1803. <https://doi.org/10.1002/pen.20879>
- Khanjanzadeh H, Tabarsa T, Shakeri A et al (2011) Effect of Organoclay platelets on the mechanical properties of wood plastic composites formulated with virgin and recycled polypropylene. *Wood Mater Sci Eng* 6:207–212. <https://doi.org/10.1080/17480272.2011.606915>
- Kim J, Cho D (2020) Effects of waste expanded polypropylene as recycled matrix on the flexural, impact, and heat deflection temperature properties of Kenaf fiber/polypropylene composites. *Polymers* 12:2578. <https://doi.org/10.3390/polym12112578>
- La Mantia FP (1999) Recycling of polypropylene. In: Karger-Kocsis J (ed) Polypropylene, Polymer science and technology series, vol 2. Springer, Dordrecht. https://doi.org/10.1007/978-94-011-4421-6_95
- Lower S (2017) Polymers and plastics: an introduction to their structures and properties. <http://www.chem1.com/acad/webtext/states/polymers.html>. Accessed 14 Sept 2021
- Mansor MR, Taufiq MJ, Ab Ghani AF (2020) Natural resources based green composite materials. In: Siddiquee S, Gan Jet Hong M, Mizanur RM (eds) Composite materials: applications in engineering, biomedicine and food science. Springer, Cham. https://doi.org/10.1007/978-3-030-45489-0_7
- Melo PMA, Macêdo OB, Barbosa GP et al (2020) Reuse of natural waste to improve the thermal stability, stiffness, and toughness of postconsumer polypropylene composites. *J Polym Environ* 29:538–551. <https://doi.org/10.1007/s10924-020-01907-4>
- Móczó J, Pukánszky B (2008) Polymer micro and nanocomposites: structure, interactions, properties. *J Ind Eng Chem* 14:535–563. <https://doi.org/10.1016/j.jiec.2008.06.011>
- Mohamad N, Latiff AA, Ab Maulod HE et al (2014) A sustainable polymer composite from recycled polypropylene filled with shrimp Shell waste. *Polym-Plast Technol Eng* 53:167–172. <https://doi.org/10.1080/03602559.2013.843704>
- Moribe T (2012) Advanced intermeshing mixers for energy saving and reduction of environmental impact. *Mitsubishi Heavy Ind Tech Rev* 49(4):38–43. <https://www.mhi.co.jp/technology/review/pdf/e494/e494038.pdf>
- Muniyandi SK, Sohaili J, Hassan A et al (2013) Converting non-metallic printed circuit boards waste into a value added product. *J Environ Health Sci Eng* 11(2):1–9. <https://www.ncbi.nlm.nih.gov/pmc/articles/PMC3915225/pdf/2052-336X-11-2.pdf>
- Naushad MD, Nayak SK, Mohanty S et al (2016) Damage tolerance behaviour of Cloisite 15A incorporated recycled polypropylene nanocomposites and bionanocomposites. *J Exp Nanosci* 11(14):1110–1126. <https://doi.org/10.1080/17458080.2016.1189096>
- Oduşanya AA, Bolasodun B, Madueke CI (2014) Property evaluation of hybrid seashell/snail Shell filler reinforced unsaturated polyester composite in comparison with sea Shell and snail Shell filler reinforced unsaturated polyester composite. *Int J Eng Sci* 3(12):80–90. <https://www.thejjes.com/papers/v3-i12/K031201080090.pdf>
- Oladele O, Adediran AA, Akinwekomi AD et al (2020) Development of ecofriendly snail Shell particulate-reinforced recycled waste plastic composites for automobile application. *Sci World J* 2020:7462758(1–8). <https://doi.org/10.1155/2020/7462758>
- Othman J (2007) Economic valuation of household preference for solid waste Management in Malaysia: a choice modeling approach. *Int Manag Stud* 14(1):189–212. <http://e-journal.uum.edu.my/index.php/ijms/article/view/9235>

- Othman MH, Aisha MM, Khamis SZ (2017) Injection moulding reprocessing cycles effect towards mechanical properties of polypropylene-nanoclay. *Int J Adv Mech Automob Eng* 4(1):88–93. <https://doi.org/10.15242/IJAMAE.E0817004>
- Pang AL, Husin MR, Arsad A et al (2021) Effect of graphene Nanoplatelets on structural, morphological, thermal, and electrical properties of recycled polypropylene/polyaniline nanocomposites. *J Mater Sci Mater Electron* 32:9574–9583. <https://doi.org/10.1007/s10854-021-05620-3>
- Patel BR, Lageraen PR, Kalb PD (1995) Review of potential processing techniques for the encapsulation of wastes in thermoplastic polymers. U.S. Department of Energy, Upton, New York, pp 1–16. https://inis.iaea.org/collection/NCLCollectionStore/_Public/27/029/27029634.pdf
- PlasticsEurope (2019) Plastics – the facts 2019. https://www.plasticseurope.org/application/files/9715/7129/9584/FINAL_web_version_Plastics_the_facts2019_14102019.pdf. Accessed 9 Oct 2021
- Ramos FJHTV, Reis RHM, Grafova I et al (2020) Eco-friendly recycled polypropylene matrix composites incorporated with Geopolymer concrete waste particles. *J Mater Res Technol* 9(3):3084–3090. <https://doi.org/10.1016/j.jmrt.2020.01.054>
- Rocha DB, Rosa DS (2019) Coupling effect of starch coated fibers for recycled polymer/wood composites. *Compos Part B Eng* 172:1–8. <https://doi.org/10.1016/j.compositesb.2019.05.052>
- Rosato DV, Rosato MG (2000) Injection molding handbook. Kluwer Academic Publisher
- Salwa HN, Sapuan SM, Mastura MT et al (2021) Life cycle assessment (LCA) of recycled polymer composites. In: Ilyas R, Sapuan S, Bayraktar E (eds) *Recycling of plastics, metals, and their composites*, 1st edn. CRC Press, Boca Raton
- Samat N, Marini CD, Maritho MA et al (2013) Tensile and impact properties of polypropylene/microcrystalline cellulose treated with different coupling agents. *Compos Interfaces* 20(7):497–506. <https://doi.org/10.1080/15685543.2013.812767>
- Samper MD, Bertomeu D, Arrieta MP et al (2018) Interference of biodegradable plastics in the polypropylene recycling process. *Materials* 11(10):1886(1–18). <https://doi.org/10.3390/ma11101886>
- Santhosh Kumar S, Somashekhar SH (2020) Natural fiber reinforced composites in the context of biodegradability: a review. In: *Encyclopedia of renewable and sustainable materials*, vol 5, pp 160–178. <https://doi.org/10.1016/B978-0-12-803581-8.11418-3>
- Saravanan P, Emami N (2021) Chapter 13: Sustainable tribology: processing and characterization of multiscale thermoplastic composites within hydropower applications. In: Rangappa SM, Siengchin S, Parameswaranpillai J (eds) *Tribology of polymer composites: characterization, properties, and applications*, Series on tribology and surface engineering 2021. Elsevier, Elsevier, Amsterdam. <https://doi.org/10.1016/B978-0-12-819767-7.00013-X>
- Sato Y, Furukawa J (1963) A molecular theory of filler reinforcement based upon the conception of internal deformation (a rough approximation of the internal deformation). *Rubber Chem Technol* 36(4):1081–1106. <https://doi.org/10.5254/1.3539632>
- Schyns ZOG, Shaver MP (2021) Mechanical recycling of packaging plastics: a review. *Macromol Rapid Commun* 42(3):2000415(1–27). <https://doi.org/10.1002/marc.202000415>
- Shubhra QTH, Alam AKMM, Quaiyyum MA (2011) Mechanical properties of polypropylene composites: a review. *J Thermoplast Compos Mater* 26(3):362–391. <https://doi.org/10.1177/0892705711428659>
- Stoof D, Pickering K (2018) Sustainable composite fused deposition modelling filament using recycled pre-consumer polypropylene. *Compos Part B* 135:110–118. <https://doi.org/10.1016/j.compositesb.2017.10.005>
- Szpieg M (2011) Development and characteristics of a fully recycled CF/PP composite. Doctoral thesis, Division of materials science, Department of Engineering Sciences and Mathematics, Luleå University of Technology, SE-971 87 Luleå, Sweden
- Szpieg M, Wysocki M, Asp LE (2012) Mechanical performance and modelling of a fully recycled modified CF/PP composite. *J Compos Mater* 46(12):1503–1517. <https://doi.org/10.1177/0021998311423860>
- Tai CM, Li RKY, Ng CN (2000) Impact behaviour of polypropylene/polyethylene blends. *Polym Test* 19(2):143–154. [https://doi.org/10.1016/S0142-9418\(98\)00080-4](https://doi.org/10.1016/S0142-9418(98)00080-4)

- Thermo Fisher Scientific (2022) Hot melt extrusion. <https://www.thermofisher.com/my/en/home/industrial/pharma-biopharma/drug-formulation-manufacturing/hot-melt-extrusion.html>. Accessed 24 Jan 2022
- Thermo Fisher Scientific Inc (2022) Thermo Scientific™ HAAKE™ Rheomix OS Lab Mixers for the HAAKE™ PolyLab™ OS system. <https://www.fishersci.pt/shop/products/haake-rheomix-os-lab-mixers-the-haake-polylab-os-system/p-4529042>. Accessed 24 Jan 2022
- Tuladhar R, Yin S (2019) Production of recycled polypropylene (PP) fibers from industrial plastic waste through melt spinning process. In: Pacheco-Torgal F, Khatib J, Colangelo F et al (eds) Use of recycled plastics in eco-efficient concrete. Woodhead Publishing. <https://doi.org/10.1016/B978-0-08-102676-2.00004-9>
- Turcsányi B, Pukánszky B, Tüdös F (1988) Composition dependence of tensile yield stress in filled polymers. *J Mater Sci Lett* 7(2):160–162. <https://doi.org/10.1007/BF01730605>
- Vakili MH, Ebadi-Dehaghani H, Haghshenas-Fard M (2011) Crystallization and thermal conductivity of CaCO₃ nanoparticle filled polypropylene. *J Macromol Sci Part B Phys* 50(8):1637–1645. <https://doi.org/10.1080/00222348.2010.543033>
- Veejayplastic (2020) What is the difference between injection molding & extrusion? <http://www.veejayplastic.com/blog/top-5-key-difference-between-extrusion-injection-molding/>. Accessed 9 Sept 2021
- Wang K, Addiego F, Bahlouli N et al (2014) Impact response of recycled polypropylene-based composites under a wide range of temperature: effect of filler content and recycling. *Compos Sci Technol* 95:89–99. <https://doi.org/10.1016/j.compscitech.2014.02.014>
- Yao ZT, Chen T, Li HY et al (2013) Mechanical and thermal properties of polypropylene (PP) composites filled with modified Shell waste. *J Hazard Mater* 262:212–217. <https://doi.org/10.1016/j.jhazmat.2013.08.062>
- Younesi-Kordkheili H, Pizzi A (2020) Ionic liquid- modified lignin as a bio-coupling agent for natural fiber-recycled polypropylene composites. *Compos Part B Eng* 181:107587(1–6). <https://doi.org/10.1016/j.compositesb.2019.107587>
- Zaaba NF, Ismail H, Mariatti M (2016) Utilization of polyvinyl alcohol on properties of recycled polypropylene/Peanut Shell powder composites. *Proc Chem* 19:763–769. <https://doi.org/10.1016/j.proche.2016.03.082>
- Zadeh KM, Ponnamma D, Al-Maadeed MAA (2017) Date palm fibre filled recycled ternary polymer blend composites with enhanced flame retardancy. *Polym Test* 61:341–348. <https://doi.org/10.1016/j.polymertesting.2017.05.006>
- Zander NE, Gillan M, Burckhard Z et al (2019) Recycled polypropylene blends as novel 3D printing materials. *Addit Manuf* 25:122–130. <https://doi.org/10.1016/j.addma.2018.11.009>
- Zdiri K, Elamri A, Hamdaoui M et al (2018) Reinforcement of recycled PP polymers by nanoparticles incorporation. *Green Chem Lett Rev* 11(3):296–311. <https://doi.org/10.1080/17518253.2018.1491645>
- Zehev T, Gogos CG (2006) Principle of polymer process. Wiley, Hoboken

Comparative Studies of Natural Rubber/ Virgin Ethylene Propylene Diene Rubber and Natural Rubber/Recycled Ethylene Propylene Diene Rubber and Natural Rubber/Blends



Nabil Hayemasae and Hanafi Ismail

1 Introduction

Manufacturing of rubber products mostly requires the use of two rubber matrices. This is because these products have the potential of combining the attractive properties from each other. Blending is an economic and technical approach when compared with synthesizing new polymeric materials (Arayaprane and Rempel 2007). The blending of two or more types of rubber is a valuable method for fabricating materials with properties absent in the rubber's component (El-Sabbagh 2003; Chang et al. 1999; Sae-oui et al. 2007). Blending of natural rubber (NR) with other rubbers has been extensively studied especially in manufacturing of tire. However, NR is prone to be deteriorated by thermal oxidation due to the presence of double bond in polymeric backbone. NR generally achieves better resistance to oxidation by blending it with low unsaturated rubbers such as ethylene propylene diene rubber (EPDM). EPDM is polymerized by combining ethylene, propylene, and a small amount of a nonconjugated diene. EPDM generally offers good thermal aging, weathering resistance, and acid–base resistance (Kumar et al. 2002; Delor-Jestin et al. 2000).

To date, an issue to reduce and recycle the rubber waste has put much pressure to rubber manufacturers. Landfill disposal is not the suitable choice for sustainable development of new products (Nabil et al. 2012). Recycling is one of the best choices when considering the environmental and economic advantages. There are

N. Hayemasae (✉)

Department of Rubber Technology and Polymer Science, Faculty of Science and Technology,
Prince of Songkla University, Pattani, Thailand
e-mail: nabil.h@psu.ac.th

H. Ismail

School of Materials and Mineral Resources Engineering, Engineering Campus,
Universiti Sains Malaysia, Nibong Tebal, Penang, Malaysia

many possible applications of rubber waste have been explored. Rubber waste can be an economically useful material such as crumb rubber, reclaimed rubber, and devulcanized rubber (Noriman et al. 2010; Ismail et al. 2006). The use of ground rubber is considered social and economic benefits, as it cheapens the cost of final product by blending finely ground rubber with virgin rubber. Reutilizing of ground EPDM waste is an interesting source of rubber waste due to its increasing growth of EPDM market. Many works have been focused on the post-consumption of EPDM waste. Jacob et al. (2001) studied the effect of ground EPDM vulcanizate on the performance of EPDM rubber. It was found that R-EPDM could replace over 45% of EPDM without significant effect to the performance of the final product. Using waste EPDM in making new material provides a potent in turning the rubber waste into an economic and environmental factor in mind.

As has been clearly stated, the main reason of blending of NR and EPDM is to improve the oxidation resistance of NR. Therefore, detailed investigation on the thermal stability of this blend has been considered. Oxidation of rubber can lose mechanical performance such as tensile properties, tear strength, and abrasion resistance. Hence, the service life is analyzed by thermo-oxidative aging (Abdel-Aziz and Basfar 2000; Lv et al. 2013). The information of how rubber breaks down when exposing to the heat is important (Kleps et al. 2000; Madathingal and Wunder 2011; Zhao et al. 2007). Thermal stability determines from thermogravimetric analysis (TGA) and thermal aging (Aouachria et al. 2011; Bystritskaya et al. 2013), where it was thoroughly focused on the kinetics of thermal degradation obtained from TGA and thermo-oxidative aging. Correlation of activation energy of degradation and crosslinking of rubber was exemplified by Kader and Bhowmick (2003). It was ascribed that crosslink can delay the oxidation rate of rubber at the degradation temperature (Meiorin et al. 2013). It was evidently confirmed after the activation energy, which exhibited high activation energy in the blends that contain high crosslinking. In this study, carbon black (CB) filled NR/EPDM and NR/R-EPDM blends were prepared and compared in terms of compounding properties, mechanical properties, and thermal properties.

2 Materials, Formulation, and Mixing Procedures

Table 1 lists the ingredients focused in this chapter. Natural rubber (SMR 5 L grade) was supplied by the Mardec Berhad, Selangor, Malaysia. Zarm Scientific (M) Sdn. Bhd. was supplied R-EPDM. R-EPDM was ground into powder form to obtain particles ranging from 10 to 200 μm in size (Fig. 1). Figure 2 illustrates the SEM micrograph of recycled EPDM particles at 100 \times magnification. It can be seen that the R-EPDM particles were irregular, rough, and aggregates. The specific gravity of the powdered R-EPDM was 1.06 g/cm^3 . The carbon black content analyzed by TGA was 29.33% (see Fig. 3). Cabot Corporation supplied the N330 grade carbon black (CB). Other compounding ingredients such as zinc oxide, stearic acid, *N*-tert-butyl-2-benzothiazyl sulfonamide (TBBS), and sulfur were obtained from Bayer (M) Ltd. All ingredients were used as received, and a conventional sulfur

Table 1 The blending formulation used for the first series

Materials (phr)	NR/EPDM	NR/R-EPDM
SMR L	90, 80, 70, 60, 50	90, 80, 70, 60, 50
EPDM	10, 20, 30, 40, 50	–
R-EPDM	–	10, 20, 30, 40, 50
ZnO	5.0	5.0
Stearic acid	2.0	2.0
TBBS	1.2	1.2
Sulfur	1.8	1.8
N330	30	30

SMR L Standard Malaysian Rubber L, EPDM ethylene propylene diene rubber, R-EPDM recycled ethylene propylene diene rubber, TBBS *N*-tert-butyl-2-benzothiazyl sulfonamide

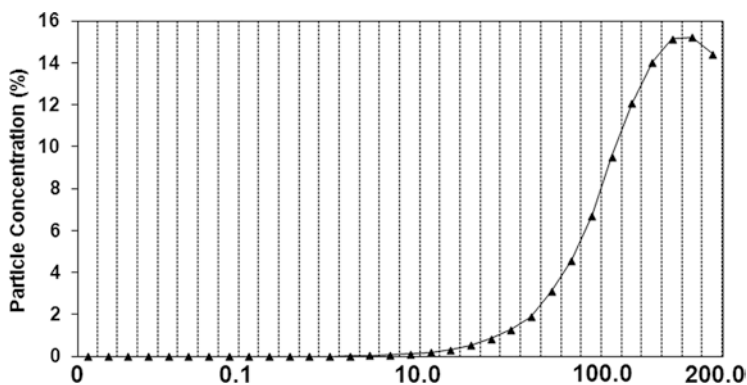


Fig. 1 Particle size distribution of recycled EPDM obtained from particle size analysis (Mastersizer)

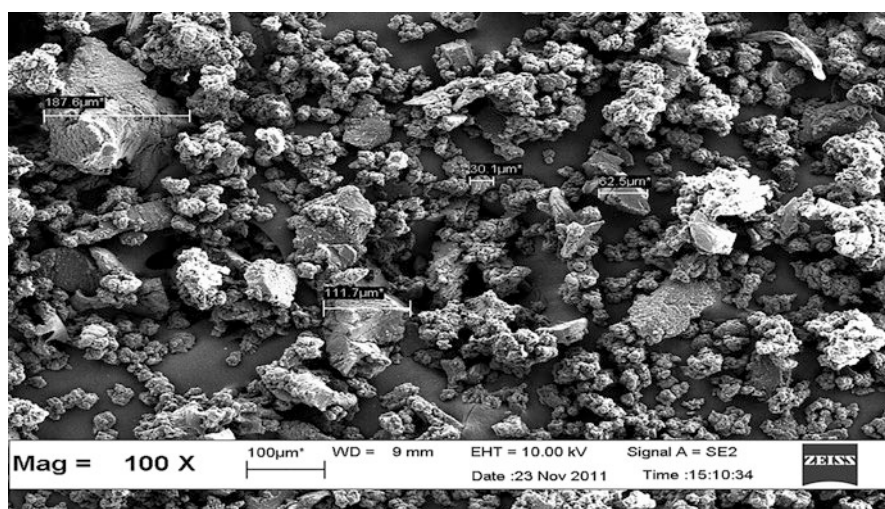


Fig. 2 SEM micrograph of recycled EPDM at 100× magnification

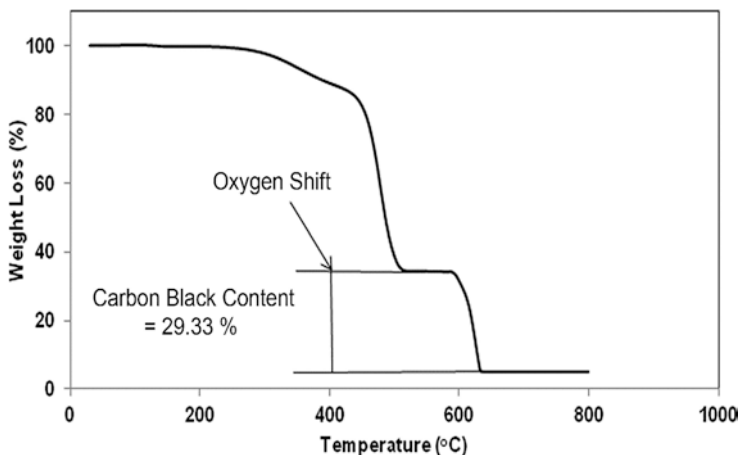


Fig. 3 Weight loss of R-EPDM as a function of temperature (TGA curve)

vulcanization system (CV) was designed. The blend ratio of 90/10, 80/20, 70/30, 60/40, and 50/50 was compounded on a laboratory-sized two-roll mixing mill (Model XK-160). Subsequently, the compounds were compression-molded using a steel mold at 150 °C with a force of 10 MPa based on curing times.

3 Properties of the Rubber Blends

3.1 Cure Characteristics and Dynamic Properties

A Monsanto Moving Die Rheometer (MDR 2000) was used to determine curing properties of the blends. These include scorch time (t_{s2}), curing time (t_{c90}), cure rate index (CRI), and dynamic properties. Samples of the respective compounds were tested at 150 °C. The cure rate index of the blends was calculated as follows.

The curing and dynamic properties are summarized in Table 2. As shown in Table 2, $S'M_L$ increases for increasing blend ratios of virgin EPDM or R-EPDM. $S'M_L$ is commonly indicated to represent the elastic modulus of the uncured compound (Ismail and Anuar 2000), which provides useful data about the processability of the rubber compound. At the same time, $S'M_H$ corresponds to the stiffness, hardness, and modulus of the fully cured compound.

Virgin EPDM or R-EPDM has modified the processability of the blends, particularly at high ratios of virgin EPDM or R-EPDM, and NR/R-EPDM blends showed higher value of $S'M_L$ than those of NR/EPDM blends. This is because R-EPDM consisted of CB (29.33% of CB). It might affect the processability of the blends containing R-EPDM. Virgin EPDM and R-EPDM have also increased the $S'M_H$ values of the blends where the $S'M_H$ of NR/R-EPDM was higher than that of the

NR/EPDM blends. Such finding may be contributed to the higher crosslinks of the NR/R-EPDM blends obtained either from NR itself or the crosslink in R-EPDM. Moreover, the presence of CB in R-EPDM greatly affected the stiffness of NR/R-EPDM blends.

Table 2 also shows the values of torque differences $S'(M_H-M_L)$ of the blends. The torque difference for NR/EPDM increased up to 30 phr of EPDM content and then decreased. The value of $S'(M_H-M_L)$ indirectly correlated to the crosslinking degree (Gardiner 1968). This result indicates that the cure mismatch of NR and EPDM was found when the blend ratio of EPDM exceeded 30 phr. It is known that blending NR and EPDM could lead to a cure incompatibility, leading to a heterogeneous distribution of crosslink density and hence lowering mechanical properties. It was also observed that the viscous torque $S''M_H$ and $\tan \delta (M_H)$ of the blends consecutively increased with increasing blend ratio of virgin EPDM or R-EPDM. The viscous torque is related to the damping characteristics of a rubber compound. The $\tan \delta (M_H)$ obtained from the rheometer was lower for NR/R-EPDM blends than for the NR/EPDM blends. The damping factor ($\tan \delta$) is directly related to its crosslinking (Sae-oui et al. 2007), where lower damping factors indicate greater crosslinking.

The scorch time (ts_2) and curing time (tc_{90}) measures when vulcanization begins and reaches completion. The ts_2 and tc_{90} of the NR/EPDM blends increased gradually with increasing concentrations of virgin EPDM. The augmentation in ts_2 and tc_{90} of NR/EPDM could be attributed to the low vulcanization efficiency of EPDM for the sulfur system, because EPDM has a relatively high saturated content. The differences in diene contents had led to cure incompatibility, particularly in sulfur vulcanization systems, and an increase in ts_2 and tc_{90} (Gardiner 1968). Moreover, ts_2 of NR/R-EPDM blends marginally decreased with R-EPDM, whereas tc_{90} increased. Therefore, the decrement in ts_2 at which vulcanization had begun might be due to

Table 2 Curing characteristics of NR/EPDM and NR/R-EPDM blends

Sample	$S'M_L$	$S'M_H$	$S'(M_H-M_L)$	$S''M_H$	$\tan \delta (M_H)$	ts_2	tc_{90}	CRI
NR/EPDM								
90/10	0.29	10.73	10.44	0.72	0.067	2.65	8.30	17.70
80/20	0.47	11.21	10.74	0.96	0.086	2.69	8.61	16.89
70/30	0.66	12.09	11.43	1.28	0.106	2.70	9.85	13.99
60/40	0.79	12.11	11.32	1.29	0.107	2.73	9.92	13.91
50/50	1.20	12.41	11.21	1.42	0.115	2.88	11.73	11.30
NR/R-EPDM								
90/10	0.24	12.24	12.00	0.68	0.055	2.34	7.53	19.27
80/20	0.47	14.88	14.41	0.89	0.060	2.24	7.91	17.64
70/30	0.76	16.14	15.38	1.05	0.065	2.24	8.31	16.47
60/40	1.27	19.08	17.81	1.26	0.066	2.06	8.61	15.27
50/50	2.54	23.77	21.23	1.71	0.072	1.91	11.38	10.56

$S'M_L$ elastic minimum torque (dN.m), $S'M_H$ elastic maximum torque (dN.m), $S'(M_H-M_L)$ torque difference (dN.m), $S''M_H$ viscous maximum torque (dN.m), $\tan \delta (M_H)$ $\tan \delta$ of maximum torque, ts_2 scorch time (min), tc_{90} curing time (min), CRI cure rate index

the migration of accelerators from R-EPDM to the NR matrix. Gibala et al. (1999) also observed a decrement in ts_2 for SBR compounds incorporating a ground rubber vulcanizate. It was elucidated that to the migration of accelerator from the ground vulcanizate to the virgin matrix. Here, it may be concluded that there is an increment in the number of reactive sites on the NR molecules at the initial vulcanization stage. However, its migration only affected the early stage of vulcanization. Later, the vulcanization time was further increased with the addition of R-EPDM. The cure rate index (CRI) measures the curing rate based on the differences between ts_2 and tc_{90} . The cure rate index indicated that the vulcanization rate decreased slightly with increasing virgin EPDM or R-EPDM levels. This finding confirmed that the higher amount of curative location in the NR phase resulted in a decrease in the number of reactive sites on the rubber molecules and caused a slower rate of the curing process.

3.2 Tensile Properties

Dumbbell-shaped samples were cut from the molded sheets. Tensile tests were performed at a cross-head speed of 500 mm/min and were carried out with a universal tensile machine Instron 3366 according to ISO 37. The tensile properties in terms of tensile strength, stress at 100% elongation (M100), 300% elongation (M300), and elongation at break were investigated. The hardness measurements of the samples were done according to ISO 7691-1 using a manual durometer type Shore A. Resilience was studied using a Wallace Dunlop Tripsometer according to BS 903 Part A8. The rebound resilience was calculated according to the following equation:

$$\text{Resilience (\%)} = \frac{(1 - \cos\theta_2)}{(1 - \cos\theta_1)} \times 100, \quad (1)$$

where θ_1 is the initial angle (45°) and θ_2 is the maximum rebound angle.

Figures 4, 5 and 6 show the tensile properties of NR/EPDM and NR/R-EPDM blends. The results indicated that the tensile strength of these two blends (see Fig. 4) decreased with an increasing blend ratio of virgin EPDM or R-EPDM. The reduction in tensile strength of NR/EPDM and NR/R-EPDM blends was due to incompatibility between the natural rubber and the virgin EPDM or R-EPDM rubber. When more EPDM or R-EPDM was added to the NR, the compatibility between the blends decreased. Virgin EPDM and R-EPDM are low unsaturated rubbers due to their low diene content. Therefore, the blending of EPDM or R-EPDM with highly unsaturated natural rubber resulted in a cure mismatch and reduced the tensile strength eventually (Sahakaro et al. 2009).

The difference in the diene concentrations in each rubber resulted in differences in the polarity, the number of allylic sites for sulfur vulcanization, and reactivity of the crosslink sites (Mangaraj 2002). Curatives, mostly polar molecules, generally

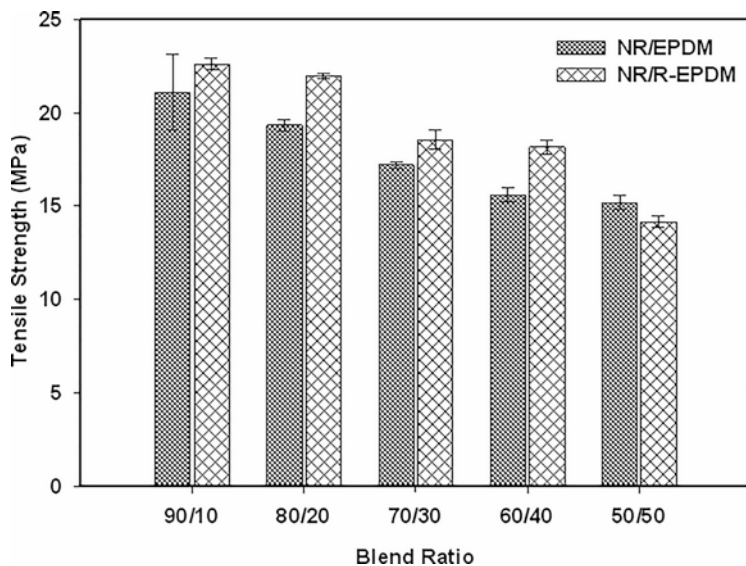


Fig. 4 Tensile strength of NR/EPDM and NR/R-EPDM blends

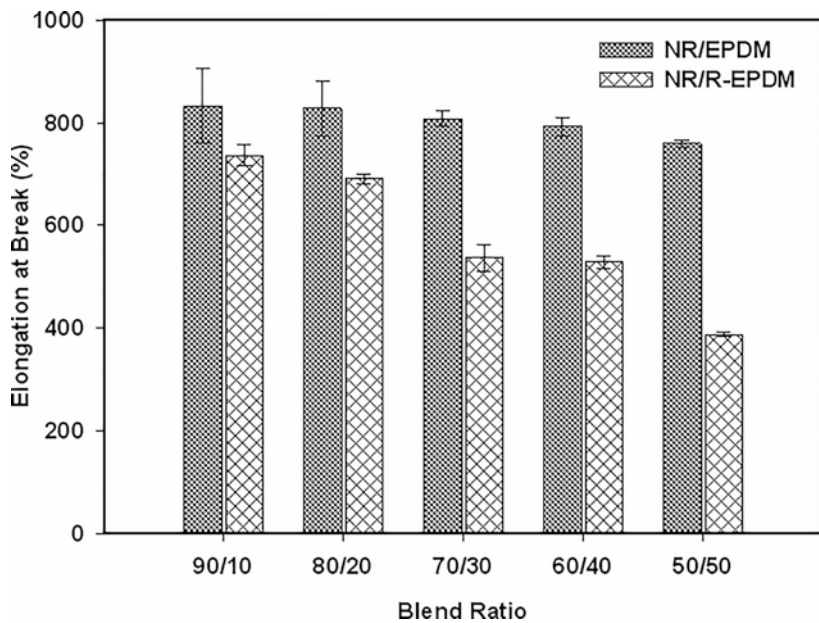


Fig. 5 Elongation at break of NR/EPDM and NR/R-EPDM blends

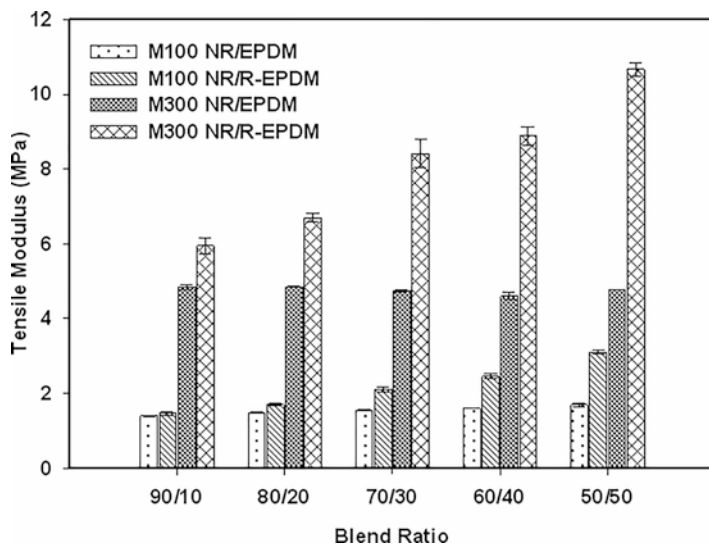


Fig. 6 Tensile modulus at 100% and 300% elongation of NR/EPDM and NR/R-EPDM blends

express higher diffusion into NR, leading to differences in the reactant concentrations and thus an uneven crosslink distribution and inferior tensile strength. In addition, the reduced tensile strength of the NR/R-EPDM blends could be further explained by two factors. First, the number of effective network chains decreased; the curing agent dose was unchanged as the R-EPDM content increased. The curatives were overdosed due to the presence of a three-dimensional network or crosslinked structure that could not be re-vulcanized. As a result, the crosslink density of the blends was too high. In this regard, the average molar mass of the network chain between two successive crosslink points decreased, and the mobility of the chain segment was restricted, limiting the network chain's movement. This restriction would reduce the number of effective network chains, resulting in a decrease in tensile strength (Kader and Bhowmick 2003). Second, the reduction of tensile strength might be due to the aggregation of CB inside the matrix: either the CB from R-EPDM itself (approximately 29.33%, based on TGA result) or CB that was formulated in the compound. Therefore, the CB aggregates tended to be aggregated when a high R-EPDM content was incorporated. The NR/EPDM also exhibited a lower tensile strength than NR/R-EPDM blends. The higher crosslink density obtained from the crosslinked R-EPDM and the CB content of R-EPDM itself is the central potentials in increasing the tensile strength of NR/R-EPDM.

Figure 5 shows the influence of the blend ratio on the elongation at break of NR/EPDM and NR/R-EPDM blends. The elongation at break decreased significantly with an increase in the blend ratio of virgin EPDM or R-EPDM; this behavior was most likely due to the cleavage of the trapped molecules and entanglements, which decreased the flexibility of the rubber (Rooj et al. 2013). The tensile strength and elongation at break are dependent on the NR content. This phenomenon could be

attributed to the high strength in strain-induced crystallized rubber at a high blend ratio of NR (Nabil et al. 2011). The ability of NR to create strain-induced crystallization decreases with an increasing blend ratio of virgin EPDM or R-EPDM. The imbalance location of CB toward the blends leads to lower flexibility. It might cause the lower elongation at break observed at high blend ratios of virgin EPDM or R-EPDM (Sahakaro et al. 2007).

The tensile modulus at 100% elongation (M100) and 300% elongation (M300) and the hardness of NR/EPDM and NR/R-EPDM are illustrated in Figs. 6 and 7. The modulus and hardness of the blends increased slightly with further increases in the concentration of virgin EPDM or R-EPDM. Tensile modulus represents the hardness or stiffness of materials. Therefore, the incorporation of R-EPDM into the rubber matrix increased the stiffness of the vulcanizates. In addition, the flexibility and elasticity of the rubber chain were lower when more R-EPDM was incorporated into the natural rubber, which also resulted in increased rigidity and hardness for the rubber vulcanizates.

3.3 Thermo-Oxidative Ageing

Thermal aging of the blends was done by placing the dumbbell-shaped specimens in an oven equipped with an air circulating system at the test temperature of 100 °C for 48 h, according to ISO 188 Method A. The aged specimens were then measured for tensile properties. The tensile strength and hardness changes after thermal aging

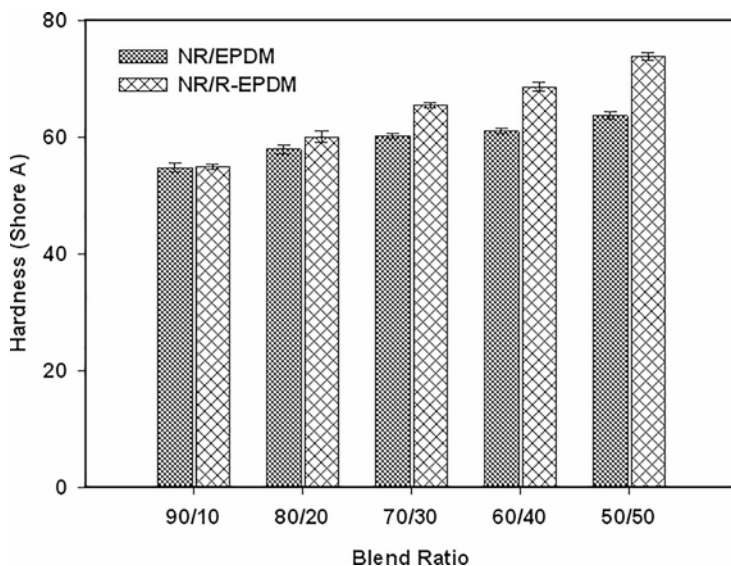


Fig. 7 Hardness (Shore A) of NR/EPDM and NR/R-EPDM blends

determined thermal aging resistance. The retention in each property was evaluated according to Eq. (2):

$$\text{Retention}(\%) = \frac{\text{Value after ageing}}{\text{Value before ageing}} \times 100 \quad (2)$$

Thermal aging plays a significant role in simulating the actual exposure of rubber vulcanizates. Therefore, it can be applied to predict the service life of such rubber vulcanizates. Thermo-oxidative aging of NR/EPDM and NR/R-EPDM blends was carried out, where the changes of tensile properties, hardness, and the functional group were discussed. The changes of tensile strength and elongation at break after thermal aging are shown in Figs. 8 and 9. The tensile strength and elongation at break of all aged samples were reduced upon thermal aging. Reduction in tensile strength could be attributed to the oxidation of polymer, which resulted in chain scissions under thermal exposure (Rattanasom et al. 2005). An increment of the number of shorter chains of the respective polymer obtained from the scission of the larger molecular chains can lead to a decrease in tensile strength and elongation at break. The percentage retention after thermal aging was used to evaluate the thermal stability of polymers. The higher retention indicates the more excellent thermal stability of the rubber blends.

The tensile strength retention of both blends demonstrated lower value at the early stage with the concentration below 30 phr of EPDM. Subsequently, the tensile strength retention of the combinations exhibited a higher value beyond 30 phr of virgin or R-EPDM in the blends. Expectedly, the tensile strength retention of NR/

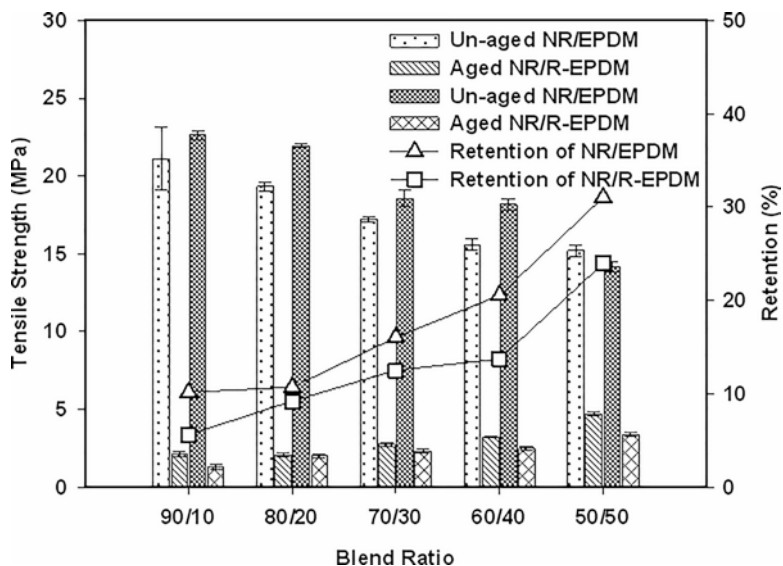


Fig. 8 Tensile strength of NR/EPDM and NR/R-EPDM blends before and after thermal aging

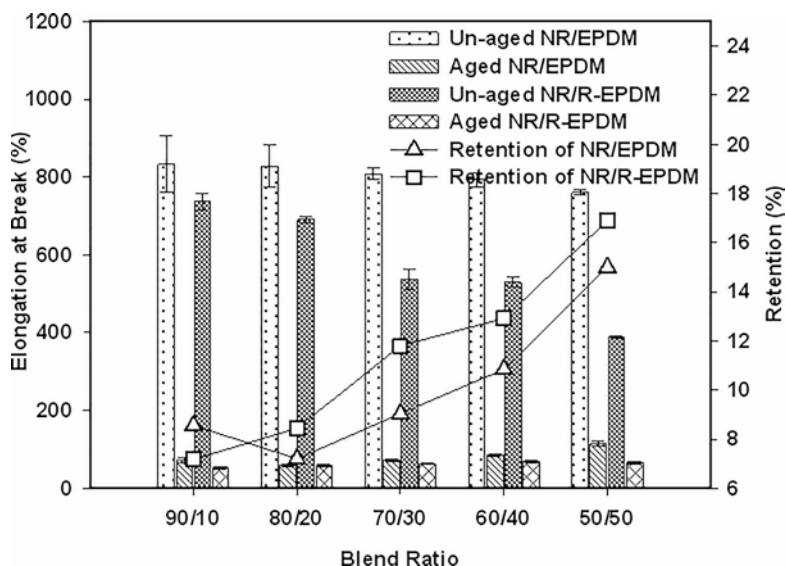


Fig. 9 Elongation at break of NR/EPDM and NR/R-EPDM blends before and after thermal aging

EPDM blends was higher than those of NR/R-EPDM blends. This is associated with R-EPDM used in this study itself being exposed to the environment for a specific time before blending with natural rubber. Therefore, it led to the partial decomposition of R-EPDM via the oxidation process and remained changes in the tensile strength retention.

Tensile modulus at 50% elongation (M_{50}) and hardness of the blends before and after thermo-oxidative aging are illustrated in Figs. 10 and 11. Since the tensile failure of aged samples was mainly below 100% elongation, tensile modulus at 50% elongation was selected to measure the thermal resistance of the blends. It was observed that the modulus and hardness of aged blends increased obviously with increasing virgin EPDM or R-EPDM. This was simply attributed to the formation of additional crosslinks in the blends. Generally, the rubber's radical termination after thermal aging involves the abstraction of hydrogen atoms due to the presence of oxygen. As a result, the oxidative reaction chain with free radicals is produced. Increment of crosslink density after thermal aging was strongly related to the high rate of radical termination in the bulk of polymer; hence, the material was more crosslinked, resulting in higher modulus and hardness (Rabello and White 1997).

Figures 12, 13, and 14 show the FTIR spectra of NR/EPDM and NR/R-EPDM blends before and after aging at 100 °C for 48 h. The assignments at various positions are also listed in Table 3. Five characteristic peaks could be seen in the spectra observed for un-aged NR/EPDM or NR/R-EPDM blends. The asymmetric stretching vibration of methylene in the saturated hydrocarbon backbone was found at 2915.11 cm^{-1} , whereas the peak at 2853 cm^{-1} is assigned to the symmetric stretching vibration of methylene. The peaks at 1450.56–1456.76 cm^{-1} and

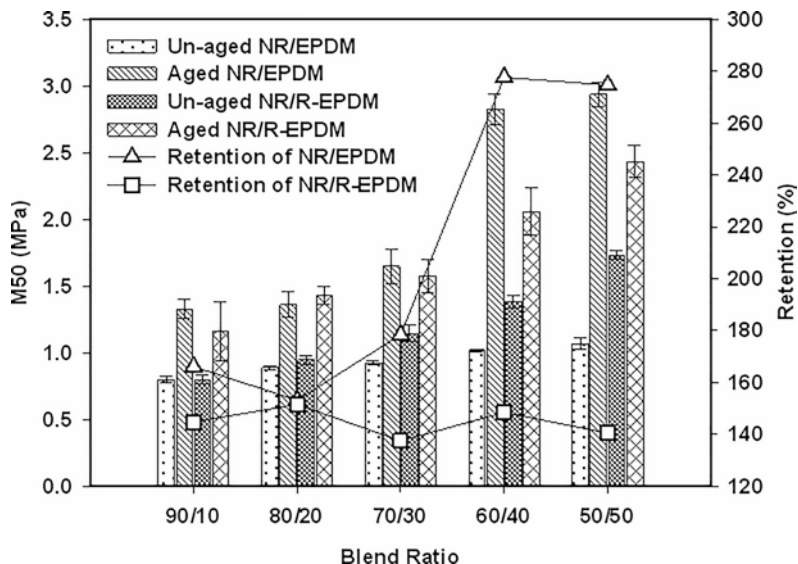


Fig. 10 Tensile modulus at 50% elongation of NR/EPDM and NR/R-EPDM blends before and after thermal aging

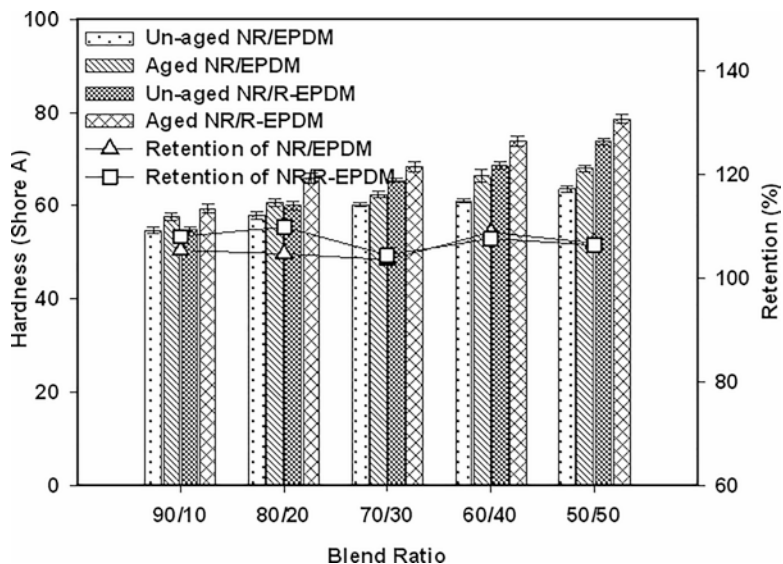


Fig. 11 Hardness (Shore A) of NR/EPDM and NR/R-EPDM blends before and after thermal aging

1372.07–1376.21 cm^{-1} were indicated to CH_2 scissoring vibration and symmetric CH stretching vibration of methyl, respectively. The peak at 719.37–721.43 cm^{-1} was assigned to methylene rocking vibration of $(\text{CH}_2)_n$, where $n > 4$ (Abdel-Aziz

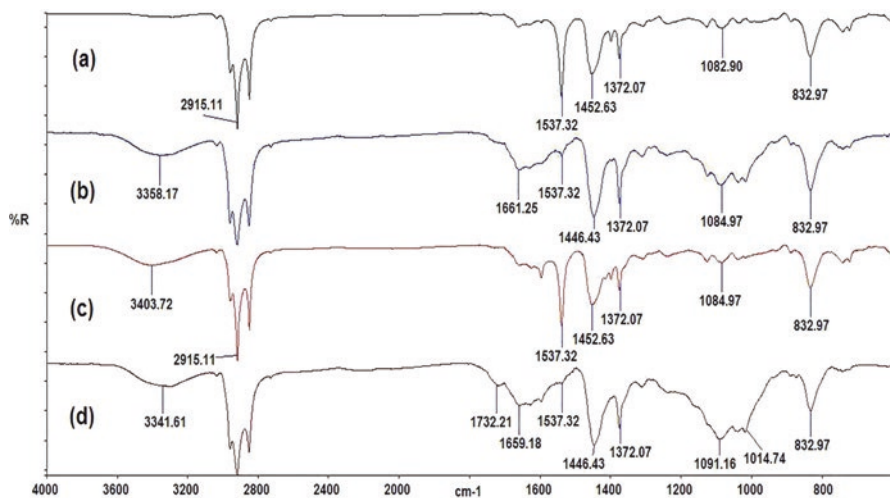


Fig. 12 The FTIR spectra of un-aged and aged blends: (a) un-aged NR/EPDM (90/10), (b) aged NR/EPDM (90/10), (c) un-aged NR/R-EPDM (90/10), and (d) aged NR/R-EPDM (90/10)

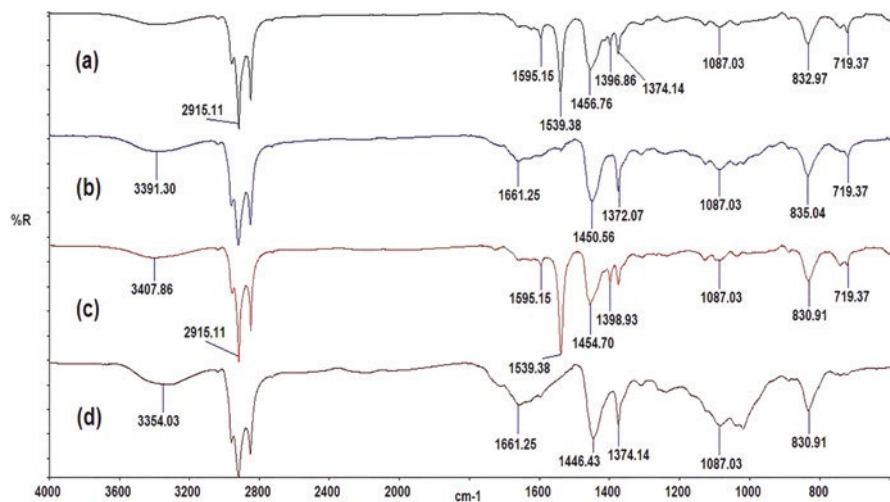


Fig. 13 The FTIR spectra of un-aged and aged blends: (a) un-aged NR/EPDM (70/30), (b) aged NR/EPDM (70/30), (c) un-aged NR/R-EPDM (70/30), and (d) aged NR/R-EPDM (70/30)

and Basfar 2000). After thermal aging at 100 °C for 48 h, there was a slight reduction in the intensity of the bands at 2915.11 cm⁻¹ and 2853 cm⁻¹ in the asymmetric and symmetric stretching vibrations of methyl and methylene, respectively, present in the EPDM backbone.

Additional peaks of the carbonyl region (1850–1550 cm⁻¹) could be observed, and it showed several overlapping bands corresponding to carboxylic acid, ketone,

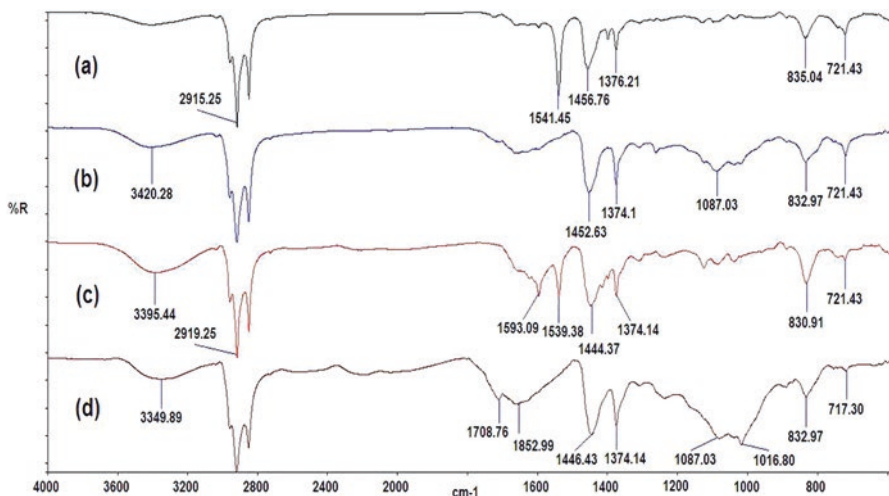


Fig. 14 The FTIR spectra of un-aged and aged blends: (a) un-aged NR/EPDM (50/50), (b) aged NR/EPDM (50/50), (c) un-aged NR/R-EPDM (50/50), and (d) aged NR/R-EPDM (50/50)

Table 3 Fourier transform infrared positions and assignments of NR/EPDM and NR/R-EPDM blends before and after thermal aging

Assignments	Wave number (cm ⁻¹)
C–H stretching	2853 and 2915.11
C=O stretching	1734
Zinc carboxylate absorbance	1580
C=O stretching and carbonyl region	1550–1850
C–H bending and scissoring	1450.56–1456.76
C–H bending and rocking	1372.07–1376.21
C–O stretching	1087 and 1159
C–H bending and rocking	719.37–721.43

ester, and lactones. Gijssman (2002) elucidated that the absorption peak at 1734 cm⁻¹ corresponds to the vibration of the C=O, gaining from the oxidation process of the rubber, while the asymmetric and symmetric vibrations C–O–C are assigned to the peaks at 1159 cm⁻¹ and 1087 cm⁻¹, respectively. In addition to the oxidation process, the absorbance of carbonyl group was found at 1734 cm⁻¹, relative to the absorption band of CH₂ at 1464 cm⁻¹. Delor-Jestin et al. (2000) reported that the presence of zinc oxide in the rubber formulations was also caused the appearance of zinc carboxylates absorbing at 1580 cm⁻¹, which was the main oxidation product. Tomer et al. (2007) noticed that the oxidation of EPDM was initiated after thermal aging. Therefore, the carbonyl group generation started to increase with exposure time. Zhao et al. (2007) made a similar observation when they investigated the FTIR analysis of EPDM upon aging time and introduced the relationship between the relative content of the carbonyl group as a function of aging time.

3.4 Swelling Behavior

Swelling tests were done in toluene following ISO 1817. First, weigh the cured test pieces of dimension 30 mm × 5 mm × 2 mm using an electrical balance and swollen in toluene until equilibrium, which took 72 h at room temperature. Then, took the samples out from the liquid, removed the toluene from the samples' surface, and weighed them again. Calculation of the changes in mass is as follows:

$$\text{Swelling}(\%) = \frac{(W_2 - W_1)}{W_1} \times 100, \quad (3)$$

where W_1 is the initial mass of specimen (g) and W_2 is the mass of sample (g) after immersion in toluene. The swelling results were also used to calculate the molecular weight between crosslinks (M_c) by applying the Flory-Rehner Equation (Flory and Rehner Jr 1943):

$$M_c = \frac{-\rho_p V_s V_r^{1/3}}{\ln(1 - V_r) + V_r + \chi V_r^2}, \quad (4)$$

$$V_r = \frac{1}{1 + Q_m}, \quad (5)$$

where ρ is the density of the rubber (ρ of NR = 0.92 g/cm³, ρ of EPDM = 0.83 g/cm³, and ρ of R-EPDM = 1.06 g/cm³), V_s is the molar volume of the toluene ($V_s = 106.4$ cm³/mol), V_r is the volume fraction of the polymer in the swollen specimen, Q_m is the weight increase of the blends in toluene, and χ is the interaction parameter of the rubber network-solvent (χ of NR = 0.393 and χ of EPDM and R-EPDM = 0.49). The degree of crosslink density is given by:

$$V_c = \frac{1}{2M_c} \quad (6)$$

The swelling resistance and crosslink density of the NR/EPDM and NR/R-EPDM blends are shown in Fig. 15. The swelling percentage was investigated by toluene uptake until equilibrium swelling was reached at room temperature. It is well-recognized that the swelling is directly related to the crosslink density of a network chain (Nabil et al. 2011), with less solvent uptake or penetration into the blends indicating higher crosslink density. Thus, the swelling percentage of NR/EPDM increased with further increases in the concentration of virgin EPDM in NR. This behavior was most likely due to the cure mismatch arising from the different levels of unsaturation between these rubbers. Surprisingly, the swelling percentage of NR/R-EPDM blends decreased with the increasing blend ratio of R-EPDM. This decrease might be due to the crosslink obtained from R-EPDM and

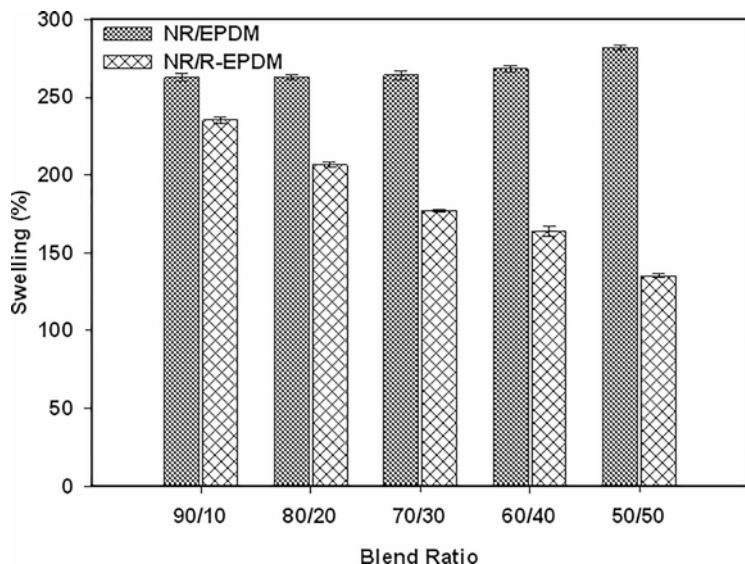


Fig. 15 Swelling resistance of NR/EPDM and NR/R-EPDM blends

CB content from either formulated design or R-EPDM itself, reducing the free volume between rubber matrix molecules and decreasing the toluene swelling.

The crosslink density can be conveniently determined by Flory-Rehner Equation (Flory and Rehner Jr 1943). This parameter includes the actual chemical crosslinks and physical entanglements or loops (Sekkar et al. 2007). The crosslink density of these blends is shown in Fig. 16. The crosslink density of NR/EPDM blends decreased with further increases in EPDM concentration. It is well known that the blending of highly unsaturated NR and low unsaturated EPDM generally result in inferior mechanical properties due to the uneven crosslink density distribution. Saeoui et al. (2007) revealed that the differences in the degree of unsaturation resulted in cure incompatibility, especially in sulfur vulcanization systems. Moreover, highly polar accelerators preferentially locate in highly unsaturated NR phases and promote heterogeneity in terms of accelerator location.

Consequently, the NR phase contains more crosslinks than the EPDM in the NR/EPDM blends. However, the opposite finding is observed for the NR/R-EPDM blend. NR/R-EPDM blends contain CB from either the formulated compound or R-EPDM. Thus, the CB enhanced the extent of crosslinking to the blends. Baccaro et al. (2003) stated that higher crosslink density in the case of higher CB content might be because of two different factors: one is due to the physical linkages or filler-rubber interactions. Another is due to electron acceptor sites on the cluster surfaces of CB, where the rubber macroradicals are chemically bound by mechanochemical degradation during the rubber compounding (Manivannan et al. 1999; Cataldo 2001).

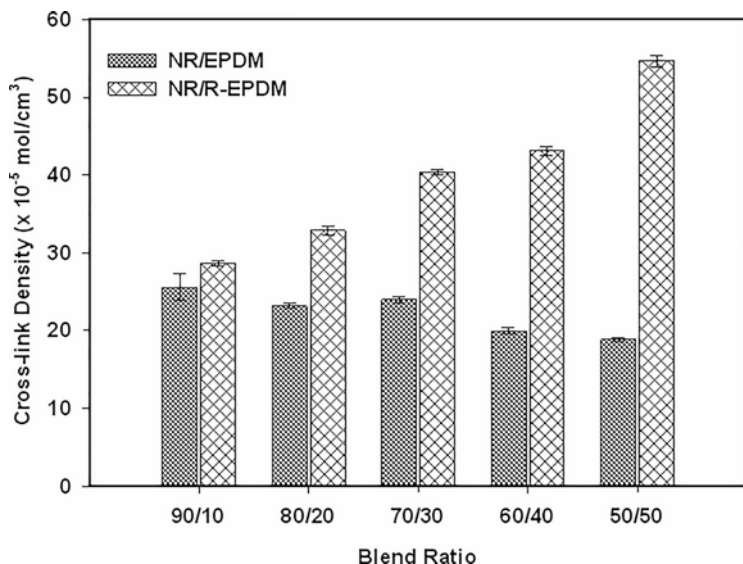


Fig. 16 Crosslink density of NR/EPDM and NR/R-EPDM blends

3.5 Scanning Electron Microscopy (SEM)

The analysis of powdered R-EPDM and tensile fractured surfaces was carried out using a scanning electron microscope (SEM) model Zeiss Supra-35VP to obtain information regarding filler dispersion and to detect the possible presence of micro-defects. In addition, the fractured pieces were coated with a layer of gold-palladium to eliminate electrostatic charge buildup during an examination. Figure 17 shows the SEM micrographs of the tensile fracture surface of NR/EPDM and NR/R-EPDM blends at 100 \times magnifications. Figure 17a–c shows the fractured surfaces of the NR/EPDM blends. At a high loading of NR in the blends, the surface is rougher, with many matrices tearing lines, indicating that more energy was needed to break the sample relative to that observed in Fig. 17b, c, which showed a broader tearing line. Therefore, it could be concluded that the reduction in tensile strength with further increases in the virgin EPDM was in good agreement with the fractured surfaces observed.

In addition, a similar observation was noted for the tensile fractured surfaces of NR/R-EPDM blends (Fig. 17d–f). Figure 17d shows the rougher surface and significantly greater homogeneity relative to the broken surface for the R-EPDM loading at 30 phr (Fig. 17e) compared to the blend containing 50 phr of R-EPDM (Fig. 17f). Figure 17f shows the formation of R-EPDM particulates and a few voids, leading to lower tensile strength. Moreover, the blend homogeneity and matrix tearing lines are more visible for NR/R-EPDM than NR/EPDM blends. This suggested that the coherence of the two rubbers and healthy dispersion of R-EPDM in the NR matrix altered the cracking area, which led to increased resistance to crack propagation and

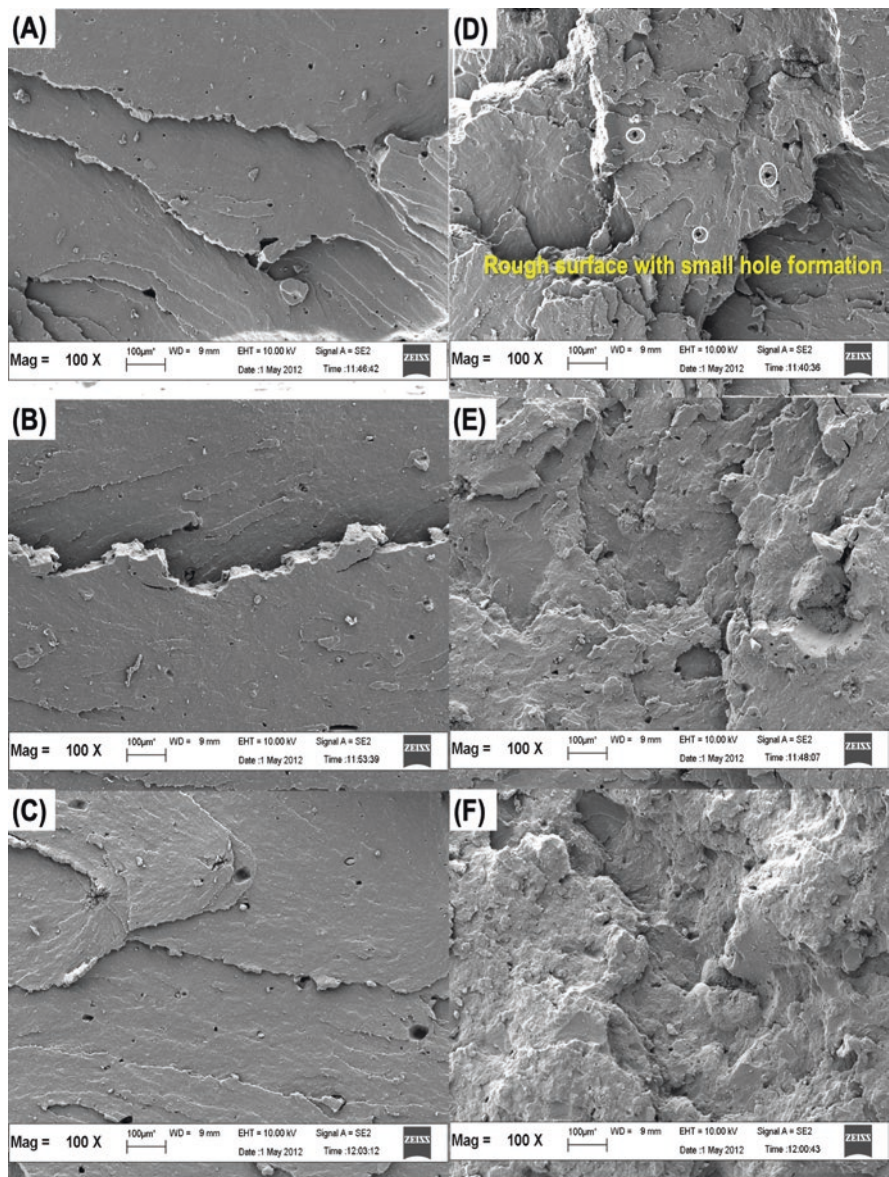


Fig. 17 SEM micrographs of fractured surfaces of carbon-black-filled NR/EPDM and NR/R-EPDM blends: (a) NR/EPDM (90/10), (b) NR/EPDM (70/30), (c) NR/EPDM (50/50), (d) NR/R-EPDM (90/10), (e) NR/R-EPDM (70/30), and (f) NR/R-EPDM (50/50) (magnification 100×)

thus improved the tensile strength. The SEM results for the tensile fractured surfaces followed the results obtained by Ismail and Mathialagan (2012). They reported that the broken surface's roughness and matrix tearing line corresponded to increased tensile strength.

3.6 Thermogravimetric Analysis (TGA)

Thermogravimetric analysis at a different blend ratio of CB filled NR/Virgin EPDM and NR/Recycled EPDM blends was carried out with a Perkin-Elmer Pyris 6 TGA analyzer. The sample was scanned from 30 °C to 600 °C at 30 mL/min nitrogen airflow with a 20 °C/min heating rate. The thermogravimetric analysis measures the amount and speed (velocity) of change in the mass of a sample as a function of temperature or time in a controlled atmosphere. The measurement primarily determines materials' thermal and oxidative stabilities and their compositional properties. The blends' thermal decomposition behavior and derivative weight thermograms are shown in Figs. 18 and 19, respectively. The decomposition temperature at different weight loss and various stages are also summarized in Tables 4 and 5. Two regions of degradation of blends were observed. Here, the initial minor weight loss at around 180–200 °C was due to volatile matter such as stearic acid and the adsorbed water at about 300 °C (Rabello and White 1997).

The first step of degradation of both blends started at about 330 °C and was completed at around 450 °C. The second stage of degradation occurred in the region of 450–520 °C. The former set of the decomposition was due to the degradation of

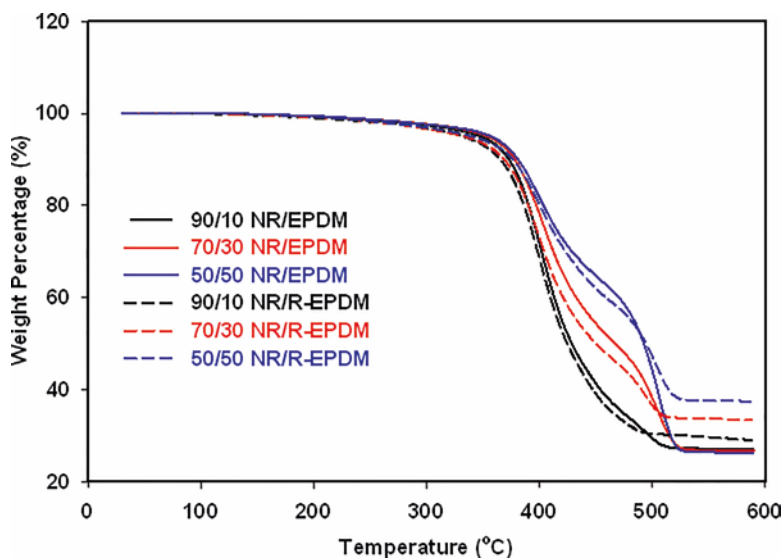


Fig. 18 TG curves of NR/EPDM and NR/R-EPDM blends

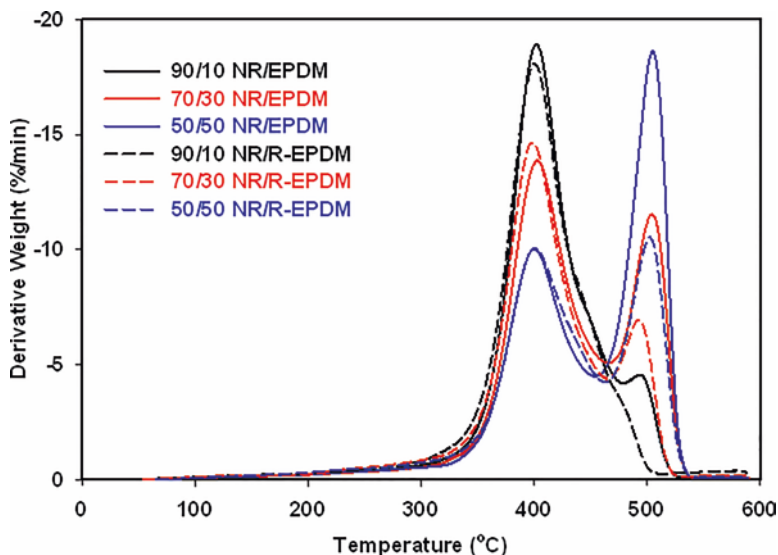


Fig. 19 DTG curves of NR/EPDM and NR/R-EPDM blends

Table 4 The Decomposition temperature at various weight losses of NR/EPDM and NR/R-EPDM blends

Sample codes	Degradation temperature (°C)			
	$T_{-10\%}$	$T_{-30\%}$	$T_{-50\%}$	$T_{-70\%}$
NR/EPDM (90/10)	372.96	401.75	428.52	497.05
NR/EPDM (70/30)	378.02	412.23	466.78	514.72
NR/EPDM (50/50)	380.95	428.85	492.34	516.10
NR/R-EPDM (90/10)	365.27	398.28	424.44	526.82
NR/R-EPDM (70/30)	368.79	403.96	449.88	N/A
NR/R-EPDM (50/50)	376.33	422.97	494.29	N/A

Table 5 The Decomposition temperature at various maximum peak and char residue of NR/EPDM and NR/R-EPDM blends

Sample codes	$T_{\max I}$ (°C)	$T_{\max II}$ (°C)	Char residue (%)
NR/EPDM (90/10)	402	493	26.93
NR/EPDM (70/30)	403	504	26.67
NR/EPDM (50/50)	403	505	26.19
NR/R-EPDM (90/10)	400	483	28.99
NR/R-EPDM (70/30)	400	493	33.31
NR/R-EPDM (50/50)	401	502	37.39

natural rubber (polyisoprene) segments, which corresponded to the significant peak observed from the Derivative Thermogravimetric (DTG) curve. The degradation of the natural rubber segment is sensitive to an oxidized structure and the depletion of

sulfidic crosslinks in natural rubber. Therefore, the later degradation, which could be observed from the DTG curve's small peak area, was attributed to the scission of crosslinked virgin or R-EPDM and conjugated polyene left after the first stage of degradation (Tomer et al. 2007).

Notably, the decomposition temperature at 10, 30, 50, and 70% weight loss of the blends was higher when the blend ratio of virgin EPDM or R-EPDM was increased. This was associated with virgin or R-EPDM, which has higher thermal stability. The decomposition temperature at various maximum peaks (T_{\max}) and char residue of the blends are presented in Table 5. The T_{\max} of the two stages is higher for both blends and increases with the increase in a blend ratio of virgin EPDM or R-EPDM, suggesting that virgin EPDM or R-EPDM are more thermally stable than natural rubber. The char residue obtained for both blends at the final temperature increased as a function of the concentration of the R-EPDM phase. As noticed, R-EPDM contains 29.33% of CB. Increasing the blend ratio of R-EPDM thereby increased the CB content in the blends, leading to a high amount of char residue eventually.

In contrast, the char residue in NR/EPDM blends showed no difference, which was ascribed to the unchanged CB content upon the increment of virgin EPDM. In summary, the decomposition temperature at various weight losses and the maximum peak of NR/EPDM blends were higher than those NR/R-EPDM blends. This was associated with R-EPDM itself, which was exposed to the environment as stated before and lowered the thermal stability of NR/R-EPDM blends.

3.7 Activation Energy of Degradation Process

Both the initial decomposition temperature and the degradation rate correspond to polymers' thermal stability. Observation of kinetic parameters associated with the degradation processes is an exciting topic of study. Thermal analysis studies the durability assessment and lifetime prediction of the rubber products. Such finding is essential for enhancing the service performance of certain products (Saha Deuri et al. 1988). The activation energies of degradation of NR/EPDM and NR/R-EPDM blends at different blend ratios were determined by applying the Coats-Redfern's method (Coats and Redfern 1964):

$$\log \left[\frac{-\log(1-\alpha)}{T^2} \right] = \log \left[\left(\frac{AR}{\beta E} \right) \times \left(\frac{1-2RT}{E} \right) \right] - \frac{E}{2.303RT}, \quad (7)$$

where α is the fractional mass loss at time t , T is the absolute temperature, A is the pre-exponential factor, R is the universal gas constant, β is the heating rate, and E is the activation energy. A plot of $\log[-\log(1-\alpha)/T^2]$ as a function of $1/T$ gives a straight line with the slope equal to $E/2.303R$ and the y-intercept is $\log[(AR)/(\beta E)(1-2RT/E)]$.

According to Coats-Redfern's equation for NR/EPDM and NR/R-EPDM blends, the plots are presented in Figs. 20 and 21. In addition, the kinetic parameters obtained by this approach are summarized in Table 6. The DTG curves show that the NR/EPDM and NR/R-EPDM blends decomposed in two stages, which can be

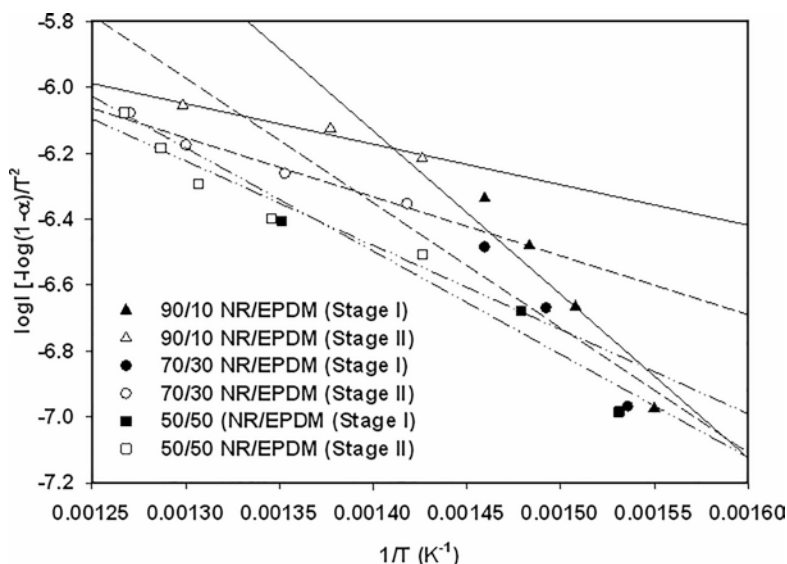


Fig. 20 Coats-Redfern's plots at the different blend ratio of NR/EPDM blends

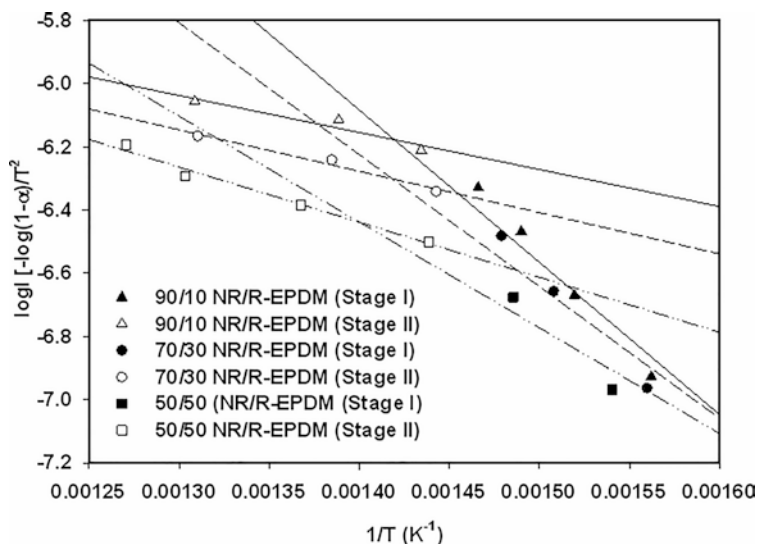


Fig. 21 Coats-Redfern's plots at the different blend ratio of NR/R-EPDM blends

Table 6 Activation energy of NR/EPDM and NR/R-EPDM blends calculated from Coats-Redfern's equation

Sample codes	Stage I		Stage II	
	<i>E</i> (kJ/mol)	Correlation coefficient	<i>E</i> (kJ/mol)	Correlation coefficient
NR/EPDM (90/10)	79.29	0.9038	19.08	0.9752
NR/EPDM (70/30)	62.39	0.8889	29.46	0.9522
NR/EPDM (50/50)	53.78	0.9009	41.13	0.9010
NR/R-EPDM (90/10)	85.58	0.9458	15.76	0.8670
NR/R-EPDM (70/30)	68.83	0.9110	20.22	0.9885
NR/R-EPDM (50/50)	57.93	0.9231	31.83	0.9628

classified from the degradation of natural rubber phase (Stage 1) and virgin EPDM or R-EPDM (Stage 2). For NR/EPDM blends, the first stage (330–450 °C) involved the activation energy of around 79.29, 62.39, and 53.78 kJ/mol in NR/EPDM (90/10), NR/EPDM (70/30), and NR/EPDM (50/50), respectively. On the other hand, NR/R-EPDM blends provided somewhat higher activation energies, at 85.58, 68.83, and 57.93 kJ/mol in a blend ratio of (90/10), (70/30), and (50/50), respectively.

This stage basically could be related to the depletion of sulfidic crosslinks in natural rubber (Abdel-Aziz and Basfar 2000). It was also explored that with further increase in virgin EPDM or R-EPDM content in the blends, the activation energy of this stage started to decrease due to the low natural rubber component. Hence, it required less activated energy to cleave the crosslink. The higher activation energy for NR/R-EPDM blends rather than NR/EPDM blends in this stage could be due to the curative locating more in the natural rubber phase. R-EPDM was mostly cross-linked, resulting in less possible contact with the curatives. The curatives in the natural rubber phase led to higher crosslink density in the natural rubber component.

In the second-stage decomposition, the calculated energies are 19.08, 29.46, and 41.13 kJ/mol of NR/EPDM blends at a ratio of 90/10, 70/30, and 50/50, respectively. Meanwhile, the activation energies of NR/R-EPDM blends are 15.76, 20.22, and 31.83 kJ/mol, respectively. It is found that the activation energy of the blends started to increase following the blend ratio of virgin or R-EPDM. This stage indicated the cleavage of crosslink in the virgin or R-EPDM phase. In addition, the activation energy of NR/EPDM blends, particularly at high virgin EPDM in this stage, exhibited slightly higher than those NR/R-EPDM blends. This is because R-EPDM was mostly crosslinked and exposed to the environment. Therefore, the crosslinkings were partial scissioning, and curatives tend to locate more on the natural rubber phase.

On the other hand, virgin EPDM consists of an entirely reactive diene backbone, leading to higher sulfur crosslinked EPDM. The briefing observed the activation energy between 15.76 and 85.58 kJ/mol. These values correspond to the heat of dissociation for radical homolytic cleavage reaction. Therefore, it is reasonable to infer that the endothermic chain scission could be the most prevalent reaction in the main stage of decomposition (McNeill and Leiper 1985).

3.8 Dynamic Mechanical Analysis

Dynamic mechanical analysis (DMA) properties were measured using a dynamic mechanical analyzer (Perkin Elmer DMA7). The samples were subjected to a cyclic tensile strain with a force amplitude of 0.1 N at a frequency of 10 Hz. Storage modulus and mechanical loss factor ($\tan \delta$) were determined in the temperature range from $-100\text{ }^{\circ}\text{C}$ to $60\text{ }^{\circ}\text{C}$ at a heating rate of $2\text{ }^{\circ}\text{C}/\text{min}$. Figure 22 illustrates the storage modulus (E') as a function of temperature on the properties of NR/EPDM and NR/R-EPDM blends. The raw data is also summarized in Table 7. All the curves show three different regions: a glassy or high modulus region where the segmental movement is restricted, a transition zone where a drastic decrease in the E' values when increasing the temperature, and a rubbery region or the flow region where a considerable reduction in the modulus with temperature. The results revealed that the storage modulus (E') increased with increasing blend ratio of virgin EPDM or R-EPDM. It is well-discussed that the storage modulus is directly related to the stiffness and thus crosslink density (McNeill and Leiper 1985; Rahman et al. 2011). Therefore, a simple explanation for the respective finding is given by the higher degree of crosslinking governed by virgin or R-EPDM, as mentioned earlier on the rigidity phase obtained from ethylene-propylene content and overdosed curative when increasing blend ratio of virgin EPDM or R-EPDM. Two different factors can also elucidate this: one is due to an increment in overall crosslinks density, another being the presence of CB in the R-EPDM. The increase in crosslink density of the blends upon the incorporation of R-EPDM is due to active crosslinking sites in the R-EPDM, which continued to form crosslinking while re-vulcanized: the more

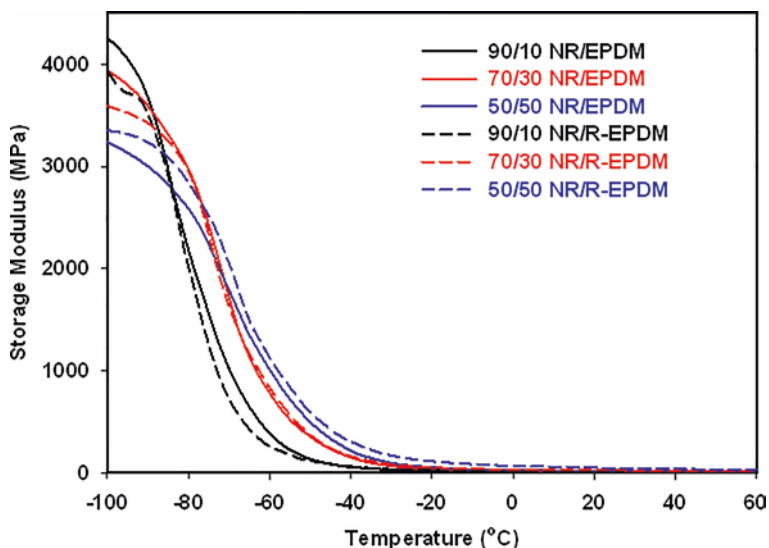
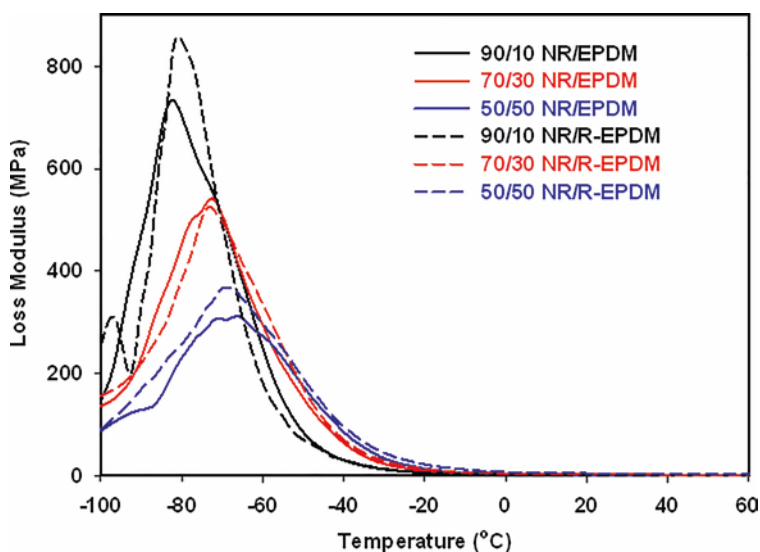


Fig. 22 Storage modulus as a function of temperature of NR/EPDM and NR/R-EPDM blends

Table 7 The effect of blend ratio on the storage modulus at 25 °C, maximum tan delta ($\tan \delta_{\max}$) of NR/EPDM and NR/R-EPDM blends and the glass transition temperature (T_g) of the blends

Sample codes	Storage modulus (MPa)	$\tan \delta_{\max}$	T_g (°C) with respect to $\tan \delta_{\max}$
NR/EPDM (90/10)	8.558	0.6771	-55.72
NR/EPDM (70/30)	14.910	0.4353	-44.16
NR/EPDM (50/50)	15.277	0.3984	-39.35
NR/R-EPDM (90/10)	10.798	0.7305	-63.55
NR/R-EPDM (70/30)	21.815	0.4659	-49.62
NR/R-EPDM (50/50)	44.159	0.3273	-46.38

**Fig. 23** Loss modulus as a function of temperature of NR/EPDM and NR/R-EPDM blends

significant the R-EPDM, the more active crosslinking sites for the formation of crosslink (Coran 1995).

Variation of loss modulus (E'') as functions of temperature is shown in Fig. 23. The loss modulus (E'') peak also corresponded to the maximum heat dissipation per unit deformation (Chuayjuljit and Luecha 2011), which indicated the increment of virgin EPDM or R-EPDM required of highly heat dissipation toward the deformation of the molecule. This observation agreed well with previous TGA profiles that high thermal stability was obtained when increasing the loadings of virgin EPDM or R-EPDM. Similar trend of loss modulus peak (E'') damping characteristic ($\tan \delta$) was found for both blends as the shown in Fig. 24, i.e., highest $\tan \delta$ was observed for the blends at 90/10 (phr/phr). As the damping characteristic is inversely related to the degree of crosslinking, the results again verified that the presence of virgin EPDM and R-EPDM provided the blends with higher degree of crosslinking than a low content of virgin EPDM or R-EPDM. The considerable reduction of $\tan \delta_{\max}$

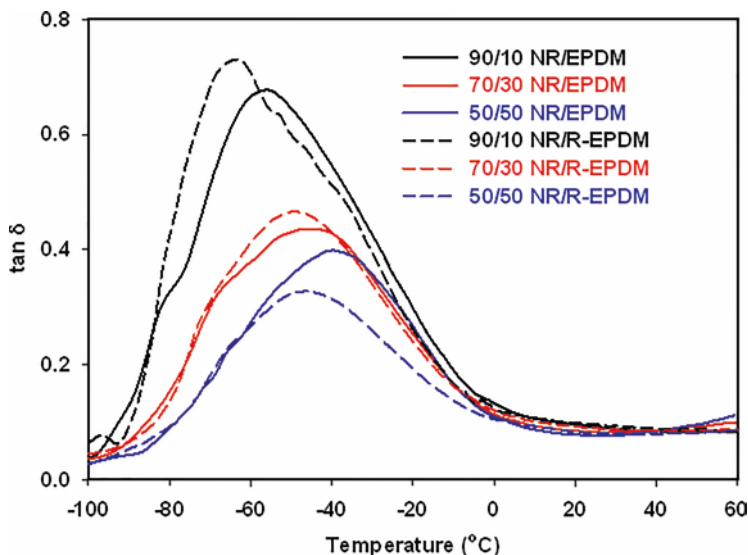


Fig. 24 Damping factor ($\tan \delta$) as a function of temperature of NR/EPDM and NR/R-EPDM blends

may be attributed to filler network of CB either from formulated CB or CB in R-EPDM itself (Nair et al. 2009). The presence of CB remained in the blends or R-EPDM itself also caused an increase in elastic behavior (reduced $\tan \delta_{\max}$). A report by Kumnuantip and Sombatsompop (2003) indicates the reduction of the damping factor of the composite in the presence of CB. It was stated that the CB itself has a shallow loss angle, suggesting that the values of $\tan \delta_{\max}$ in blends were expected to be less than those in the high NR content.

The $\tan \delta_{\max}$ indicates the glass transition temperature (T_g) of the blends. As can be seen from Table 7, T_g of these two blends had increased significantly with the presence of virgin or R-EPDM. The T_g at 10 phr of virgin or R-EPDM in the blends had risen from -55.72 °C and -63.55 °C to -39.35 °C and -46.38 °C of the NR/EPDM (90/10) and NR/R-EPDM (90/10), respectively. EPDM has higher T_g than NR, making the overall T_g of the blends shifted to higher temperature when there is a higher content of virgin EPDM and R-EPDM. Another probable reason might be associated with the molecular restriction in the blends. Theoretically, the T_g of rubber vulcanizates can be increased due to the limitation of molecular movements such as crosslink density (Medalia 1986; Trexler and Lee 1986; Kumnuantip and Sombatsompop 2003).

As stated previously, R-EPDM was crosslinked prior to use as blending component. More crosslinks have made an individual chain harder to move when rubbers are subjected to mechanical stress. Therefore, higher molecular restriction shifts the transition to higher temperature regardless of molecular interactions. In addition, it was also investigated that the presence of virgin or R-EPDM broadened the overall width of the $\tan \delta_{\max}$ peaks, particularly in the rubbery region, indicating the more significant dynamic mechanical losses in this region (Smit 1966). Sombatsompop

(1998) reported that incorporation of recycled polyurethane, which had higher glass transition temperature (T_g) into NR vulcanizates, caused the broader peak of damping factor ($\tan \delta$).

4 Conclusions

The tensile strength and elongation at break decreased when the blend ratio of virgin EPDM or R-EPDM increased. In contrast, the maximum torque, minimum torque, torque difference, scorch time (ts_2), and cure time (tc_{90}) modulus, hardness, and thermal stability showed an increasing trend. Because R-EPDM consists of a crosslinking before blending with natural rubber, greater crosslink density was observed with higher R-EPDM content. This could be confirmed from the augmentation of storage modulus (E') when the blend ratio of recycled EPDM was increased. In addition, SEM micrographs proved that higher surface roughness and matrix tearing lines were observed in the blends containing high content of virgin EPDM or R-EPDM, which is in good agreement with the tensile strength observed.

References

- Abdel-Aziz M, Basfar A (2000) Aging of ethylene-propylene diene rubber (EPDM) vulcanized by γ -radiation. *Polym Test* 19:591–602. [https://doi.org/10.1016/S0142-9418\(99\)00030-6](https://doi.org/10.1016/S0142-9418(99)00030-6)
- Aouachria K, Belhaneche-Bensemra N, Massardier-Nageotte V (2011) Viscoelastic properties, morphology, and thermal stability of rigid and plasticized poly (vinyl chloride)/poly (methyl methacrylate) blends. *J Vinyl Addit Technol* 17:156–163. <https://doi.org/10.1002/vnl.20267>
- Arayaprane W, Rempel G (2007) Properties of NR/EPDM blends with or without methyl methacrylate-butadiene-styrene (MBS) as a compatibilizer. *Int J Mater Struc Reliability* 5:1–12
- Baccaro S, Cataldo F, Cecilia A et al (2003) Interaction between reinforce carbon black and polymeric matrix for industrial applications. *Nucl Instrum Methods Phys Res Sect B* 208:191–194. [https://doi.org/10.1016/S0168-583X\(03\)00638-4](https://doi.org/10.1016/S0168-583X(03)00638-4)
- Bystritskaya EV, Monakhova TV, Ivanov VB (2013) TGA application for optimising the accelerated aging conditions and predictions of thermal aging of rubber. *Polym Test* 32:197–201. <https://doi.org/10.1016/j.polymertesting.2012.10.013>
- Cataldo F (2001) Evidences about carbyne formation together with other carbonaceous material by thermal decomposition of diiodoacetylene. *Fuller Sci Technol* 9:525–542. <https://doi.org/10.1081/FST-100107154>
- Chang YW, Shin YS, Chun H et al (1999) Effects of trans-polyoctylene rubber (TOR) on the properties of NR/EPDM blends. *J Appl Polym Sci* 73:749–756. [https://doi.org/10.1002/\(SICI\)1097-4628\(19990801\)73:5<749::AID-APP15>3.0.CO;2-S](https://doi.org/10.1002/(SICI)1097-4628(19990801)73:5<749::AID-APP15>3.0.CO;2-S)
- Chuayjuljit S, Luecha W (2011) XSBR/NR rubber blends filled with polystyrene-encapsulated nanosilica prepared by in situ differential microemulsion polymerization. *J Elastomers Plast* 43:407–427. <https://doi.org/10.1177/0095244311405001>
- Coats A, Redfern J (1964) Kinetic parameters from thermogravimetric data. *Nature* 201:68–69. <https://doi.org/10.1038/201068a0>
- Coran AY (1995) Vulcanization: conventional and dynamic. *Rubber Chem Technol* 68:351–375. <https://doi.org/10.5254/1.3538748>

- Delor-Jestin FJ, Lacoste N, Barrois-Oudin C et al (2000) Photo-, thermal and natural ageing of ethylene-propylene-diene monomer (EPDM) rubber used in automotive applications. Influence of carbon black, crosslinking and stabilizing agents. *Polym Degrad Stab* 67:469–477. [https://doi.org/10.1016/S0141-3910\(99\)00147-0](https://doi.org/10.1016/S0141-3910(99)00147-0)
- El-Sabbagh SH (2003) Compatibility study of natural rubber and ethylene-propylene diene rubber blends. *Polym Test* 22:93–100. [https://doi.org/10.1016/S0142-9418\(02\)00056-9](https://doi.org/10.1016/S0142-9418(02)00056-9)
- Flory PJ, Rehner J Jr (1943) Statistical mechanics of cross-linked polymer networks II. Swelling. *J Chem Phys* 11:512–520. <https://doi.org/10.1063/1.1723791>
- Gardiner JB (1968) Curative diffusion between dissimilar elastomers and its influence on adhesion. *Rubber Chem Technol* 41:1312–1328. <https://doi.org/10.5254/1.3539198>
- Gibala D, Thomas D, Hamed G (1999) Cure and mechanical behavior of rubber compounds containing ground vulcanizates: part III. Tensile and tear strength. *Rubber Chem Technol* 72:357–360. <https://doi.org/10.5254/1.3538807>
- Gijsman P (2002) New synergists for hindered amine light stabilizers. *Polymer* 43:1573–1579. [https://doi.org/10.1016/S0032-3861\(01\)00708-X](https://doi.org/10.1016/S0032-3861(01)00708-X)
- Ismail H, Anuar H (2000) Palm oil fatty acid as an activator in carbon black filled natural rubber compounds: dynamic properties, curing characteristics, reversion and fatigue studies. *Polym Test* 19:349–359. [https://doi.org/10.1016/s0142-9418\(98\)00102-0](https://doi.org/10.1016/s0142-9418(98)00102-0)
- Ismail H, Mathialagan M (2012) Comparative study on the effect of partial replacement of silica or calcium carbonate by bentonite on the properties of EPDM composites. *Polym Test* 31:199–208. <https://doi.org/10.1016/j.polymertesting.2011.09.002>
- Ismail H, Awang M, Hazizan MA (2006) Effect of waste tire dust (WTD) size on the mechanical and morphological properties of polypropylene/waste tire dust (PP/WTD) blends. *Polym Plast Technol Eng* 45:463–468. <https://doi.org/10.1080/03602550600553739>
- Jacob C, De P, Bhowmick AK et al (2001) Recycling of EPDM waste. I. Effect of ground EPDM vulcanizate on properties of EPDM rubber. *J Appl Polym Sci* 82:3293–3303. <https://doi.org/10.1002/app.2188>
- Kader MA, Bhowmick AK (2003) Thermal ageing, degradation and swelling of acrylate rubber, fluororubber and their blends containing polyfunctional acrylates. *Polym Degrad Stab* 79:283–295. [https://doi.org/10.1016/S0141-3910\(02\)00292-6](https://doi.org/10.1016/S0141-3910(02)00292-6)
- Kleps T, Piaskiewicz M, Parasiewicz W (2000) The use of thermogravimetry in the study of rubber devulcanization. *J Therm Anal Calorim* 60:271–277. <https://doi.org/10.1023/a:1010134315762>
- Kumar A, Dipak G, Basu K (2002) Natural rubber-ethylene propylene diene rubber covulcanization: effect of reinforcing fillers. *J Appl Polym Sci* 84:1001–1010. <https://doi.org/10.1002/app.10361>
- Kumnuantip C, Sombatsompop N (2003) Dynamic mechanical properties and swelling behaviour of NR/reclaimed rubber blends. *Mater Lett* 57:3167–3174. [https://doi.org/10.1016/S0167-577X\(03\)00019-3](https://doi.org/10.1016/S0167-577X(03)00019-3)
- Lv Y, Huang Y, Kong M et al (2013) Improved thermal oxidation stability of polypropylene films in the presence of β -nucleating agent. *Polym Test* 32:179–186. <https://doi.org/10.1016/j.polymertesting.2012.10.008>
- Madathingal RR, Wunder SL (2011) Thermal degradation of poly(methyl methacrylate) on SiO₂ nanoparticles as a function of SiO₂ size and silanol density. *Thermochim Acta* 526:83–89. <https://doi.org/10.1016/j.tca.2011.08.026>
- Mangaraj D (2002) Elastomer blends. *Rubber Chem Technol* 75:365–427. <https://doi.org/10.5254/1.3547677>
- Manivannan A, Chirila M, Giles N et al (1999) Microstructure, dangling bonds and impurities in activated carbons. *Carbon* 37:1741–1747. [https://doi.org/10.1016/S0008-6223\(99\)00052-4](https://doi.org/10.1016/S0008-6223(99)00052-4)
- McNeill I, Leiper H (1985) Degradation studies of some polyesters and polycarbonates-2. Poly lactide: degradation under isothermal conditions, thermal degradation mechanism and photolysis of the polymer. *Polym Degrad Stab* 11:309–326. [https://doi.org/10.1016/0141-3910\(85\)90035-7](https://doi.org/10.1016/0141-3910(85)90035-7)
- Medalia AI (1986) Electrical conduction in carbon black composites. *Rubber Chem Technol* 59:432–454. <https://doi.org/10.5254/1.3538209>

- Meiorin C, Mosiewicki MA, Aranguren MI (2013) Ageing of thermosets based on tung oil/styrene/divinylbenzene. *Polym Test* 32:249–255. <https://doi.org/10.1016/j.polymertesting.2012.10.009>
- Nabil H, Ismail H, Azura A (2011) Recycled polyethylene terephthalate filled natural rubber compounds: effects of filler loading and types of matrix. *J Elastomers Plast* 43:429–449. <https://doi.org/10.1177/0095244311405503>
- Nabil H, Ismail H, Rashid AA (2012) Effects of partial replacement of commercial fillers by recycled poly(ethylene terephthalate) powder on the properties of natural rubber composites. *J Vinyl Addit Technol* 18:139–146. <https://doi.org/10.1002/vnl.20291>
- Nair TM, Kumaran M, Unnikrishnan G et al (2009) Dynamic mechanical analysis of ethylene-propylene-diene monomer rubber and styrene-butadiene rubber blends. *J Appl Polym Sci* 112:72–81. <https://doi.org/10.1002/app.29367>
- Noriman N, Ismail H, Rashid A (2010) Characterization of styrene butadiene rubber/recycled acrylonitrile-butadiene rubber (SBR/NBRr) blends: the effects of epoxidized natural rubber (ENR-50) as a compatibilizer. *Polym Test* 29:200–208. <https://doi.org/10.1002/app.29367>
- Rabello M, White J (1997) Photodegradation of polypropylene containing a nucleating agent. *J Appl Polym Sci* 64:2505–2517. [https://doi.org/10.1002/\(SICI\)1097-4628\(19970627\)64:13<2505::AID-APP4>3.0.CO;2-H](https://doi.org/10.1002/(SICI)1097-4628(19970627)64:13<2505::AID-APP4>3.0.CO;2-H)
- Rahman M, Hamdan S, Ahmed AS et al (2011) Thermogravimetric analysis and dynamic Young's modulus measurement of N, N-dimethylacetamide-impregnated wood polymer composites. *J Vinyl Addit Technol* 17:177–183. <https://doi.org/10.1002/vnl.20275>
- Rattanasom N, Poonsuk A, Makmoon T (2005) Effect of curing system on the mechanical properties and heat aging resistance of natural rubber/tire tread reclaimed rubber blends. *Polym Test* 24:728–732. <https://doi.org/10.1016/j.polymertesting.2005.04.008>
- Roop S, Das A, Morozov IA, Stöckelhuber KW et al (2013) Influence of “expanded clay” on the microstructure and fatigue crack growth behavior of carbon black filled NR composites. *Compos Sci Technol* 76:61–68. <https://doi.org/10.1016/j.compscitech.2012.12.020>
- Sae-oui P, Sirisinha C, Thepsuwan U (2007) Influence of accelerator type on properties of NR/EPDM blends. *Polym Test* 26:1062–1067. <https://doi.org/10.1016/j.polymertesting.2007.07.004>
- Saha Deuri A, Bhowmick AK, Ghosh R et al (1988) Thermal and ablative properties of rocket insulator compound based on EPDM. *Polym Degrad Stab* 21:21–28. [https://doi.org/10.1016/0141-3910\(88\)90062-6](https://doi.org/10.1016/0141-3910(88)90062-6)
- Sahakaro K, Naskar N, Datta RN et al (2007) Blending of NR/BR/EPDM by reactive processing for tire sidewall applications. I. Preparation, cure characteristics and mechanical properties. *J Appl Polym Sci* 103:2538–2546. <https://doi.org/10.1002/app.25088>
- Sahakaro K, Pongpaiboon C, Nakason C (2009) Improved mechanical properties of NR/EPDM blends by controlling the migration of curative and filler via reactive processing technique. *J Appl Polym Sci* 111:2035–2043. <https://doi.org/10.1002/app.29193>
- Sekkar V, Narayanaswamy K, Scariah K et al (2007) Evaluation by various experimental approaches of the crosslink density of urethane networks based on hydroxyl-terminated polybutadiene. *J Appl Polym Sci* 103:3129–3133. <https://doi.org/10.1002/app.24751>
- Smit P (1966) The glass transition in carbon black reinforced rubber. *Rheol Acta* 5:277–283. <https://doi.org/10.1007/bf02009735>
- Sombatsompop N (1998) Dynamic mechanical properties of ground flexible polyurethane foam particles and carbon-black-filled rubber vulcanisates. *Polym Plast Technol Eng* 37:1–18. <https://doi.org/10.1080/03602559808006909>
- Tomer N, Delor-Jestin F, Singh R et al (2007) Cross-linking assessment after accelerated ageing of ethylene propylene diene monomer rubber. *Polym Degrad Stab* 92:457–463. <https://doi.org/10.1016/j.polymdegradstab.2006.11.013>
- Trexler HE, Lee MC (1986) Effect of types of carbon black and cure conditions on dynamic mechanical properties of elastomers. *J Appl Polym Sci* 32:3899–3912. <https://doi.org/10.1002/app.1986.070320309>
- Zhao Q, Li X, Gao J (2007) Aging of ethylene-propylene-diene monomer (EPDM) in artificial weathering environment. *Polym Degrad Stab* 92:1841–1846. <https://doi.org/10.1016/j.polymdegradstab.2007.07.001>

Optimization of Accelerators on the Properties of Natural Rubber/ Recycled Ethylene Propylene Diene Rubber Blends



Nabil Hayemasae and Hanafi Ismail

1 Introduction

The development of effective recycling technology will be an exciting activity because previous solutions to recycle rubber wastes have been landfill and pyrolysis, which resulted in changing ecosystems and pollutants (Mathew et al. 1996; Ismail et al. 2002; Ismail and Suryadiansyah 2002). Therefore, having cost-effective ways to change rubber waste into a processable rubber matrix is a great challenge in the rubber industry (Ismail et al. 2006; Yazdani et al. 2011; Zhang et al. 2011). Grinding the rubber waste and further use it as blending component is an easy and cost-effective technique to manufacture new rubber material.

Blending improves the overall properties and reduces the final product's cost (Sahakaro et al. 2009). Ethylene propylene diene rubber (EPDM) waste is another rubber waste that is available concerning the continuous growth of the EPDM market. It can be used as blending component in many types of rubber. Natural rubber (NR) is one of the good examples. EPDM waste (w-EPDM) was blended with NR. They claimed that w-EPDM improved the oxidative resistance to NR, but the durability of the blend is still challenge as NR is incompatible with w-EPDM. The unsaturation variance makes this blend incompatible cure, especially in sulfur vulcanization systems. Another problem concerning this blend is the migration of sulfur or accelerators from one to another phases. This has brought to a reduction in mechanical performance of the blend. Ground rubber waste generally contains a

N. Hayemasae (✉)

Department of Rubber Technology and Polymer Science, Faculty of Science and Technology,
Prince of Songkla University, Pattani, Thailand
e-mail: nabil.h@psu.ac.th

H. Ismail

School of Materials and Mineral Resources Engineering, Engineering Campus,
Universiti Sains Malaysia, Nibong Tebal, Penang, Malaysia

certain content of free sulfur and/or accelerators. The migration of sulfur in this blend also depends on the content of free sulfur. Morita (1980) found that accelerator migrates from rubber waste to virgin rubber. It made the blend scorchy and shortened the curing time. Layer (1992) tried to reheat the accelerated rubber, and it was reported that the accelerator fragments are not bonded to the network, suggesting that such fragments may be functioned at the later stage during vulcanization. Gibala and Hamed (1994) emphasized that migration of free curatives is a big concern for preparing the rubber blend containing ground rubber waste.

Many studies have tried to overcome the drawbacks of blending NR and EPDM. These include the introduction of compatibilizers (Chang et al. 1999; Sirqueira and Soares 2002; Ghosh et al. 2001), modifying the EPDM rubber (Botros 2002; Sahakaro et al. 2007), applying double-stage vulcanization, and optimizing the accelerator types (Marković et al. 2009; Sae-oui et al. 2007; Palaty and Joseph 2007). The last example is interesting in terms of practical aspect. Therefore, in this chapter, effects of accelerator types on performance of NR/w-EPDM blends were focused. The accelerators introduced in this study were *N*-tert-butyl-2-benzothiazole-sulfonamide (TBBS), *N*-cyclohexyl-benzothiazole-sulfenamide (CBS), tetramethyl thiuram disulfide (TMTD), and 2-mercapto benzothiazole (MBT). The properties were evaluated from the overall findings such as mechanical properties, thermal stability, and other related characteristics.

2 Materials and Preparation

Table 1 lists the ingredients used in this study. Natural rubber (SMR 5 L grade) was manufactured by Mardec Berhad, Selangor, Malaysia. w-EPDM was collected by Zarm Scientific (M) Sdn. Bhd., Penang, Malaysia. w-EPDM was ground before blending with NR. SEM image of w-EPDM can be seen from Fig. 1. The specific gravity of the w-EPDM was 1.06 g/cm³ and carbon black (CB) content in w-EPDM

Table 1 The blending formulation used for blending

Materials (phr)	Sample codes			
	TBBS	CBS	TMTD	MBT
SMR L	70.0	70.0	70.0	70.0
R-EPDM	30.0	30.0	30.0	30.0
ZnO	5.0	5.0	5.0	5.0
Steric acid	2.0	2.0	2.0	2.0
TBBS	1.2	–	–	–
CBS	–	1.2	–	–
TMTD	–	–	1.2	–
MBT	–	–	–	1.2
Sulfur	1.8	1.8	1.8	1.8
N330	30.0	30.0	30.0	30.0

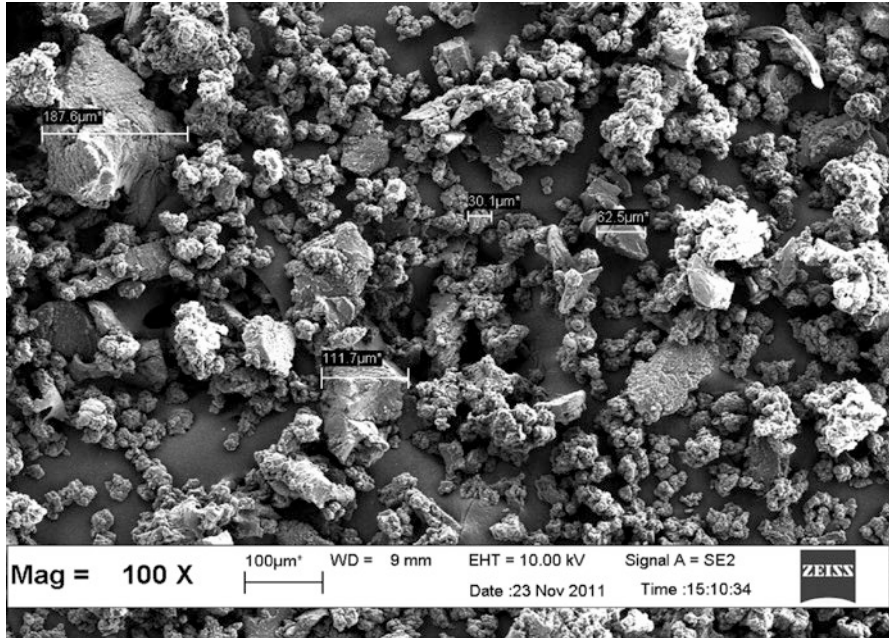


Fig. 1 SEM micrograph of recycled EPDM at 100× magnification

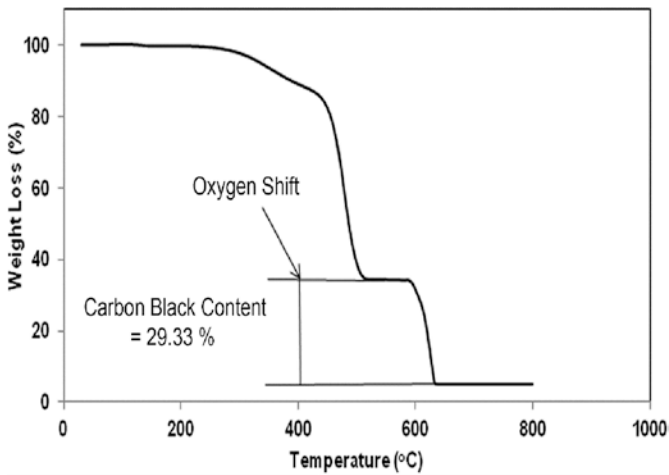


Fig. 2 Weight loss of R-EPDM as a function of temperature (TGA curve)

is 29.33%, which was analyzed by thermogravimetric analysis (TGA) (see Fig. 2). N330 grade CB was manufactured by Cabot Corporation. Other ingredients such as stearic acid, zinc oxide, TBBS, CBS, TMTD, MBT, and sulfur were purchased from Bayer (M) Ltd.

The compounding of the blends with various accelerators were added on a laboratory-sized (160 mm × 320 mm) two-roll mixing mill (Model XK-160). A semi-efficient sulfur vulcanization system (Semi-EV) was used. The blend ratio of 70/30 (phr/phr) of NR/w-EPDM was prepared. Samples of the respective blends were compression-molded by using stainless steel mold at 150 °C based on the respective curing times.

3 Properties of Rubber Blends

3.1 Cure Characteristics

A Monsanto Moving Die Rheometer (MDR 2000) was a tool to measure the curing properties of the blends. This is followed by ASTM D 2240–93. The accelerator type strongly influences cure characteristics. The effects of accelerators on $S'M_L$ and $S'M_H$ are summarized in Table 2. The $S'M_L$ of TBBS, CBS, TMTD, and MBT accelerated NR/w-EPDM blends were almost similar. Accelerator's type did not influence the $S'M_L$ value. $S'M_L$ was recorded at the early stage of curing. Therefore, no crosslinking reaction was taken place at this step.

On the other hand, TMTD exhibited higher $S'M_H$ value than those of CBS, TBBS, and MBT, respectively. TMTD is classified as a sulfur donor accelerator; it can be used for vulcanization with less addition of sulfur as the sulfur content in this study is controlled. This indicated that higher crosslink was gained for TMTD-based NR/w-EPDM and affected the stiffness of the blends. In addition, a less molecular movement leads to higher stiffness to the blends (Sae-Oui et al. 2010; Nabil et al. 2011). This correlated well with the hardness value, which was discussed later in the following section.

The $S'(M_H-M_L)$ is also summarized in Table 2. The results revealed that the MBT-accelerated blend expressed the lowest cure and crosslinking density. TMTD, TBBS, and CBS showed more pronounced choices to accomplish sufficient crosslinking density. CBS and TBBS are classified as sulfenamide accelerators that act as a delayed action accelerator, providing longer ts_2 and, thus, safer processability than TMTD-accelerated blends. These two accelerators also gave lower crosslink

Table 2 Cure characteristics of blends

Sample codes	TBBS	CBS	TMTD	MBT
$S'M_L$	0.76	0.76	0.77	0.70
$S'M_H$	16.14	16.61	20.82	12.17
$S'(M_H-M_L)$	15.38	15.85	20.05	11.47
Tan δ @ M_H	0.065	0.142	0.057	0.136
ts_2	2.24	1.85	1.27	1.66
tc_{90}	8.31	8.27	2.89	11.29
CRI	16.47	15.58	61.73	10.38

density, as measured by torque difference results. However, it was still higher than MBT-accelerated blends. It was found that the highest crosslink density was observed for TMTD-accelerated blend due to its action as sulfur donor. However, since the content of curatives used in this study was controlled, the TMTD then expressed the highest rate of crosslinking, which later fastened the curing process to the blend (Sahakaro et al. 2007, 2009). Another relevant reason might be the nature of TMTD. Zinc dimethyl dithiocarbamate is usually formed after the generation of an active accelerator complex by sulfur insertion. It is a well-known fact that zinc dimethyl dithiocarbamate is grouped as an ultra-fast accelerator for tuber compounds. Therefore, it clearly shows the remarkable effect of the curing process on the blend. Table 2 also shows the $\tan \delta @ M_H$ of the blends. The $\tan \delta$ indicates dissipated mechanical energy or the so-called hysteresis loss of the compound (Ismail and Anuar 2000). MBT may provide lowest hysteresis loss.

3.2 Tensile Properties

Tensile properties of the blends were measured according to ASTM D412. Figure 3 shows the elongation at break and tensile strength of blends. High tensile strength was observed for the blends accelerated by sulfenamide accelerators (particularly CBS), followed by TMTD- and MBT-accelerated blends, respectively. As stated earlier, CBS and TBBS are grouped as safe accelerator in terms of scorch time. Then, CBS and TBBS had sufficient time to foam certain interaction with ZnO and

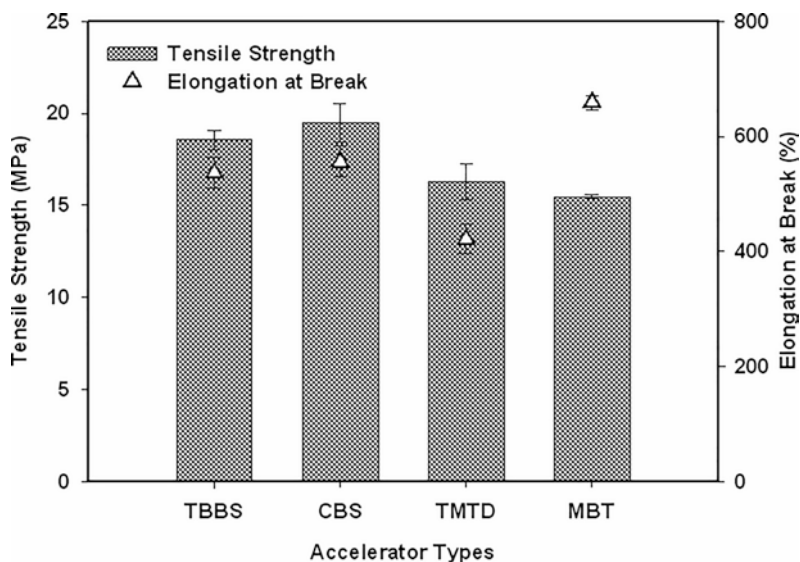


Fig. 3 Effects of accelerators on the tensile strength and elongation at break of NR/R-EPDM blends

thus reacted with rubber chain. The melting point of accelerators also affected the blending properties. The melting point of CBS is found to be 97 °C, which is the lowest when compared to TBBS (105 °C), TMTD (142–148 °C), and MBT (173 °C), respectively. Lower melting point accelerators have a higher possibility to soluble with the matrix and complete the interaction earlier, resulting in enhanced the compatibility and durability of the blends. Moreover, rubber-bound intermediates were produced before forming polysulfides crosslinks. These polysulfides crosslinks also provided monosulfide and disulfide crosslinks. Therefore, the blends accelerated with CBS systems may have dominant polysulfides, disulfides, and monosulfide networks, respectively. Longer crosslinking chains make individual chain move easier and entangled (Ismail et al. 2003). The polysulfides crosslinks may give such elasticity and hence enhance the tensile strength.

The tensile modulus at 100% (M100) and 300% (M300) strains and hardness results are illustrated in Fig. 4. The lowest values of M100 and M300 were observed for MBT-accelerated system followed by CBS-, TBBS-, and TMTD-accelerated blends. Using MBT may cause to give inadequate stiffness and hardness compared to other accelerators. The hardness values of the blends agreed well with the tensile moduli. The highest stiffness in TMTD-accelerated blend is corresponding to the nature of TMTD. The combination use of sulfur and TMTD can enhance the crosslinking density, which is then reflected in the stiffness of the blend eventually. In addition, the stiffness observed in this study corresponded well with the elongation at break of the blends. High tensile moduli reduced the flexibility of rubber chains.

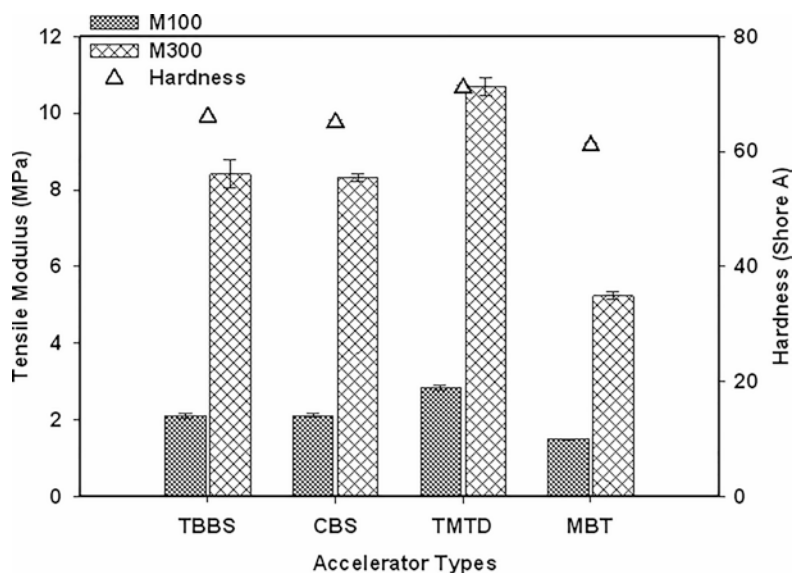


Fig. 4 Effects of accelerators on the M100, M300, and hardness of NR/R-EPDM blends

3.3 Thermo-Oxidative Ageing

Thermal aging was studied by placing rubber samples in an oven at 100 °C for 48 h, according to ASTM D573. The hardness and tensile properties of aged samples were tested where the thermal resistance was evaluated from the retention. Retention was calculated according to Eq. (1):

$$\text{Retention}(\%) = \frac{\text{Value after ageing}}{\text{Value before ageing}} \times 100 \tag{1}$$

Figures 5 and 6 showed the elongation at break and tensile strength of un-aged and aged blends accelerated by various accelerators. In addition, the hardness and tensile modulus at 100% strain of the same samples are listed in Table 3. The reduction of elongation at break and tensile strength was found for aged samples due to the degradation of rubber. Similar trend of these findings was found regardless of accelerators used. All aged samples were reduced after thermal aging. It can be seen that the retention of elongation at break and tensile strength exhibited similar findings. TMTD-accelerated blends expressed superior retention than CBS-, MBT-, and TBBS-accelerated blends. This is responsible to a high requirement of activation energy to break the bonds under the thermal aging. The higher energy needed for breaking the TMTD-accelerated blend is caused by its crosslink density observed. Higher crosslink density reflects higher thermal resistance of the blends. As

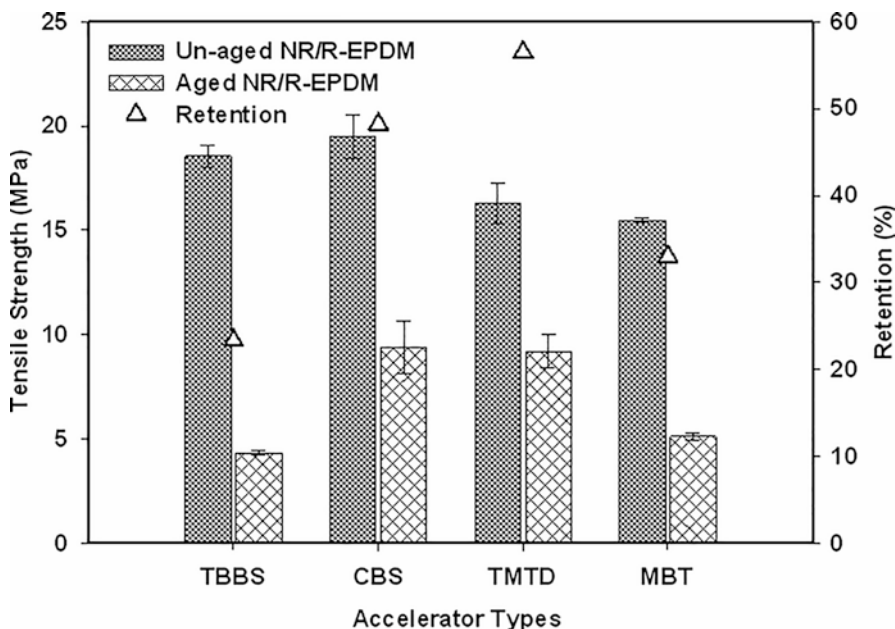


Fig. 5 Effects of accelerators on the tensile strength of un-aged and aged NR/R-EPDM

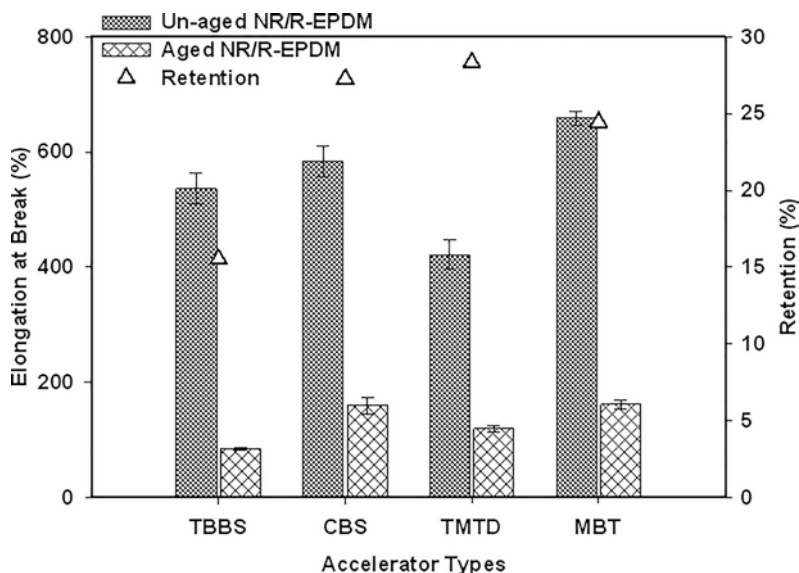


Fig. 6 Effects of accelerators on the elongation at break of un-aged and aged NR/R-EPDM after thermal aging

Table 3 Effects of accelerators on the M100 and hardness result of un-aged and aged NR/R-EPDM blends

Sample code	M100 (MPa)			Hardness (Shore A)		
	Un-aged	Aged	Retention (%)	Un-aged	Aged	Retention (%)
TBBS	2.11	N/A	N/A	66 ± 0.4	68 ± 0.4	103.03
CBS	2.12	5.83	276.27	65 ± 0.5	68 ± 0.7	104.62
TMTD	2.83	7.63	269.01	71 ± 0.7	73 ± 0.5	102.82
MBT	1.49	2.92	195.73	61 ± 0.5	66 ± 0.5	108.20

presented earlier, the TMTD is classified as a sulfur donor accelerator, combined with the elemental sulfur; it can enhance the degree of crosslinking. Thus, the rubber blend showed essentially less reversion, resulting in improved aging characteristics to the blend eventually. Higher retention was observed for modulus and hardness. Scission of rubber chains has made high rate of radical termination. This has increased the crosslink density and stiffness of the material (Rabello and White 1997).

3.4 Swelling Behavior

Swelling tests were measured by immersing test piece in toluene and left to swell for 72 h. The samples were weighed after swelling. Calculation of the changes in mass was as follows:

$$\text{Swelling}(\%) = \frac{(W_2 - W_1)}{W_1} \times 100, \quad (2)$$

where W_1 and W_2 represent the weight of specimen (g) before and after swelling. The results from swelling were later applied for calculating the crosslink density (Flory and Rehner Jr 1943):

$$M_c = \frac{-\rho_p V_s V_r^{1/3}}{\ln(1 - V_r) + V_r + \chi V_r^2}, \quad (3)$$

$$V_r = \frac{1}{1 + Q_m}, \quad (4)$$

where ρ is the density of the rubber (ρ of NR = 0.92 g/cm³, ρ of EPDM = 0.83 g/cm³, and ρ of R-EPDM = 1.06 g/cm³), V_s is the molar volume of the toluene ($V_s = 106.4$ cm³/mol), V_r is the volume fraction of the polymer in the swollen specimen, Q_m is the weight increase of the blends in toluene, and χ is the interaction parameter of the rubber network-solvent (χ of NR = 0.393 and χ of EPDM and R-EPDM = 0.49). The degree of crosslink density is given by:

$$V_c = \frac{1}{2M_c} \quad (6)$$

Figure 7 shows the swelling and crosslink density of NR/w-EPDM blends prepared by various accelerators. The lower swelling to the blends indicates a higher crosslinking density. TMTD-accelerated blend showed superior crosslink density than CBS, TBBS, and MBT consecutively. This result is attributed to the number of network chains and the restriction of the chain segment responsible for the penetration of toluene (Zhao et al. 2007). The highest restriction of the rubber molecule would lead to a decrease in swelling and an increase in crosslink density. The results obtained from the swelling study agree with the torque difference observed previously, suggesting that TMTD-accelerated blend consists of the highest degree of crosslinking.

3.5 Scanning Electron Microscopy (SEM)

SEM images of specimen after blending with NR are shown in Figure 8a–d. Figure 8b shows the image of CBS-accelerated blends where it showed rough surface with many tearing lines, indicating higher force is needed for breaking the sample. This was in good relation to tensile strength value. It is not like other SEM images from other accelerators (see Figure 8b, d), where smoother surfaces were

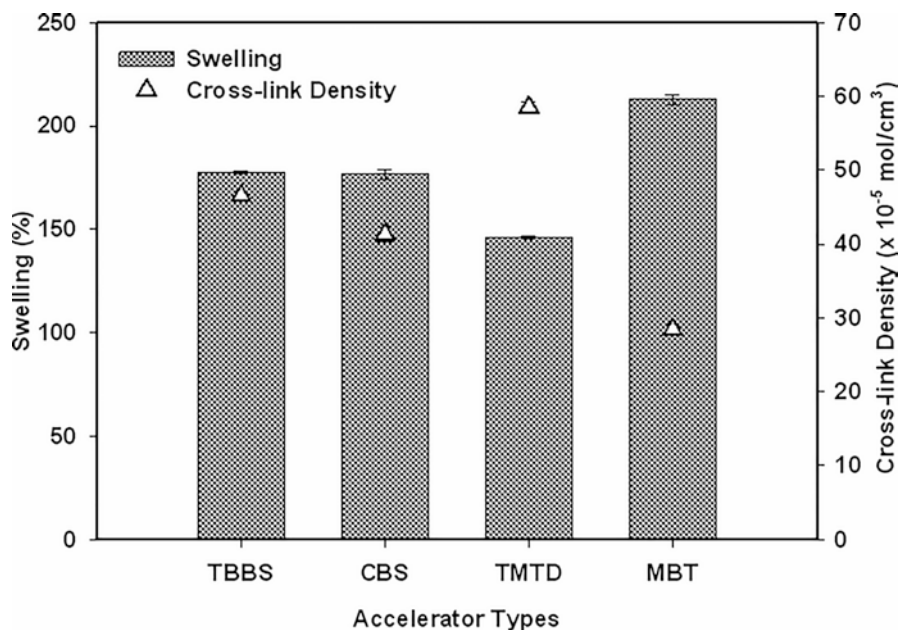


Fig. 7 Effects of accelerators on the swelling resistance and crosslink density of NR/R-EPDM blends

seen throughout the matrix. Particularly, Figure 8d exhibited a very smooth surface, and few voids formation, which agrees with the lower tensile strength received from MBT-accelerated blend. Similar explanation was also mentioned by Noriman et al. (2010), who reported that the higher surface roughness corresponded toward the higher tensile strength observed.

3.6 Thermogravimetric Analysis

Thermogravimetric analysis was also analyzed to monitor the thermal stability of the blends. The thermal decomposition behavior and derivative weight thermograms of the blends are shown in Figs. 9 and 10. The TG outputs are also summarized in Table 4. The initial minor weight loss of low volatile materials started at around 180–200 °C and absorbed water at around 300 °C (Tomer et al. 2007). The degradation of the NR phase started at around 330 °C, while w-EPDM degraded in the region of 450–520 °C. The degradation of the blends is sensitive to the presence of the oxidized structure of sulfidic crosslink in NR and w-EPDM, and other components left after initial degradation (Saha Deuri et al. 1988).

The accelerators affected the decomposition temperature at various weight loss of the blends. The temperatures were also different since the early stage of

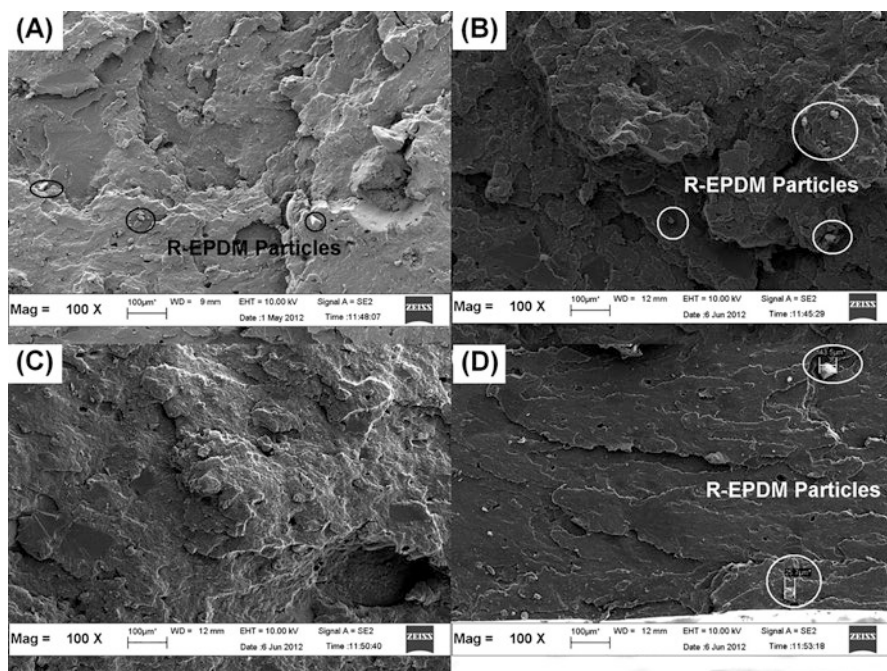


Fig. 8 SEM micrographs of NR/R-EPDM blends: TBBS (a), CBS (b), TMTD (c), and MBT (d) at 100× magnification

decomposition. Superior thermal stability was found for TMTD- and MBT-accelerated blends than those for TBBS- and CBS-accelerated blends. The decomposition temperature of TMTD- and MBT-accelerated blends demonstrated further significance at the decomposition temperature over 50% of weight loss. This finding may be because of high crosslink density of TMTD-accelerated blends. Thus, higher force is required to break the bonds.

Surprisingly, MBT-accelerated blend showed slightly higher thermal stability than that of CBS-accelerated blend at a temperature higher than aging conditions. It was described by Bristow et al. (1963) that MBT-accelerated rubber required more thermal energy, which is greater than 140 °C, to conquer an apparent activation energy of decomposition. This explanation is related to the report by Dick and Annicelli (2001). In addition, it was highlighted that the MBT-type accelerator shows the marching cure in the general rheometer's curve. This indicates a different crosslinking reaction when a particular time is applied after the curing process, suggesting that the MBT-accelerated blend produced more pronounced thermal stability than other accelerators used in the blends.

Table 4 also lists the maximum peaks of thermal decomposition and residue after analyzing. At the first maximum peak ($T_{\max 1}$), it represents the thermal decomposition of NR, while w-EPDM showed the decomposition temperature at the second

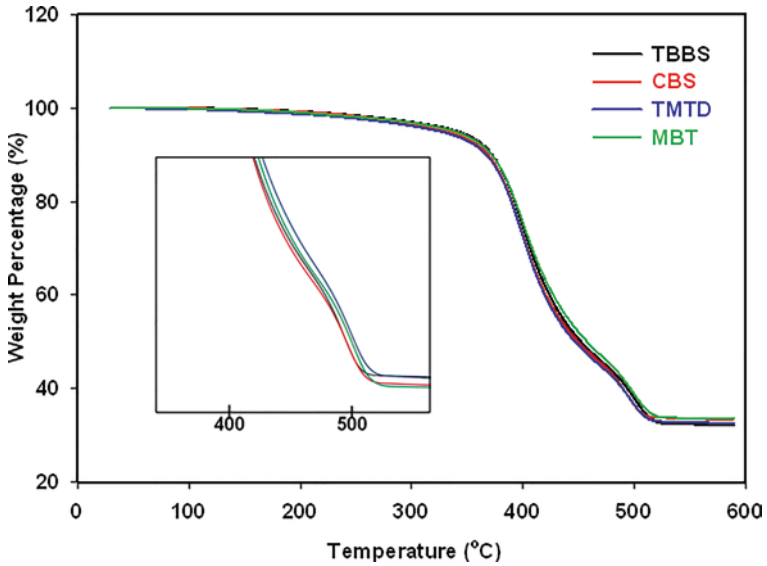


Fig. 9 TG curves of NR/R-EPDM blends at various accelerator types

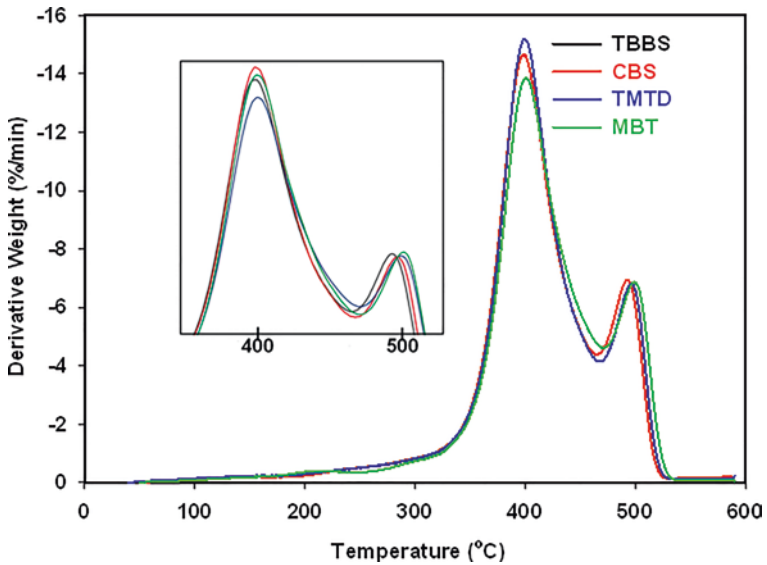
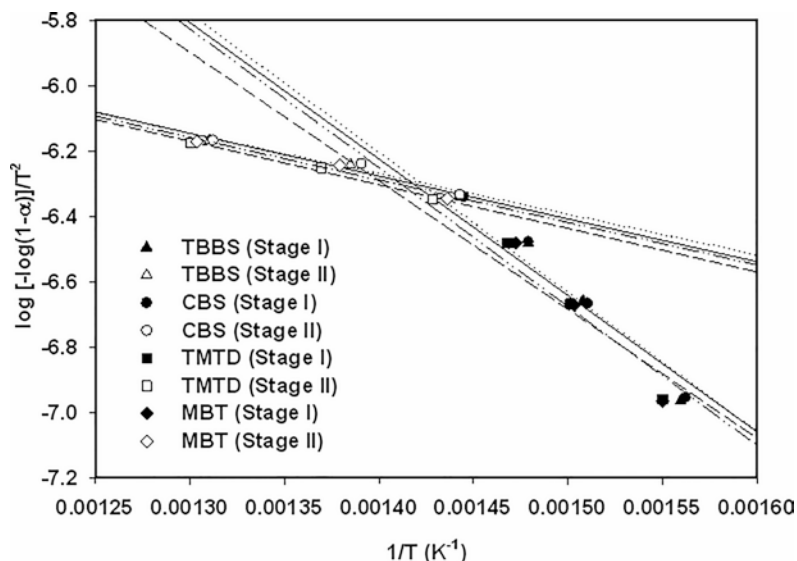


Fig. 10 DTG curves of NR/R-EPDM blends at various accelerator types

maximum peak ($T_{max II}$). Accelerator types had no effect on $T_{max I}$. However, an effect was found at $T_{max II}$ for TMTD-accelerated blends. This is because of its higher crosslink density mentioned earlier. Higher crosslink density required higher energy to conquer an apparent activation energy. Furthermore, accelerator types also did

Table 4 Effects of accelerators on the decomposition temperatures at various weight losses of NR/R-EPDM blends

Sample codes	Degradation temperature (°C)						Char residue (%)
	$T_{-10\%}$	$T_{-30\%}$	$T_{-50\%}$	$T_{-60\%}$	$T_{\max I}$ (°C)	$T_{\max II}$ (°C)	
TBBS	368.79	403.96	449.88	490.14	398	493	33.31
CBS	367.18	403.58	446.97	489.75	399	497	32.55
TMTD	372.05	408.42	457.93	496.77	400	501	33.58
MBT	372.49	406.67	452.27	494.14	400	499	32.33


Fig. 11 Coats-Redfern's plots of NR/R-EPDM blends at various accelerator types

not alter the char residue of the blends as there was not much change in amount of filler (Chakraborty et al. 2011).

3.7 Activation Energy of Degradation Process

Coats-Redfern's method was applied to observe the activation energies of degradation (Coats and Redfern 1964). Coats-Redfern plots for TBBS-, CBS-, TMTD-, and MBT-accelerated NR/w-EPDM blends are presented in Fig. 11, while the obtained activation energies are listed in Table 5. As mentioned earlier, there were two stages of degradation: the degradation of the NR (Stage 1) and w-EPDM (Stage 2). Stage 1 (330–450 °C) involved the activation energy of 68.8, 69.2, 70.9, and 69.2 kJ/mol in TBBS-, CBS-, TMTD-, and MBT-accelerated blends, respectively. Stage 2 (450–520 °C) involved the activation energy of 20.2, 21.4, 23.3, and 21.86 kJ/mol

Table 5 Activation energy calculated from Coats-Redfern's equation of NR/R-EPDM blends at various accelerator types

Sample codes	Stage I		Stage II	
	E (kJ/mol)	Correlation coefficient	E (kJ/mol)	Correlation coefficient
TBBS	68.83	0.9110	20.20	0.9885
CBS	69.24	0.9172	20.23	0.9873
TMTD	70.94	0.9233	23.34	0.9920
MBT	69.15	0.9139	21.86	0.9867

in TBBS-, CBS-, TMTD-, and MBT-accelerated blends, respectively. Higher values indicate that higher energy is required to decompose the molecular network (Kader and Bhowmick 2003). Here, the activation energy observed is responsible for the crosslink density obtained by swelling results. They suggested that TMTD-accelerated blends exhibited the most increased thermal stability among all cases. However, TMTD-accelerated blends gave lower elongation at break and tensile strength compared to CBS- and TBBS-accelerated blends. Apart from that, it is interesting to highlight that CBS-accelerated blends showed good tensile strength together with better thermal stability. This is associated with its low melting point, which leads to higher equilibrium solubility and provides the blend with better properties.

3.8 Dynamic Mechanical Analysis

Dynamic mechanical analysis (DMA) properties were measured using a dynamic mechanical analyzer (Perkin Elmer DMA7). Storage modulus (E'), loss modulus (E''), and damping factor ($\tan \delta$) were determined in the temperature range from -100 °C to 60 °C at a heating rate of 2 °C/min. E' over the change in temperature is illustrated in Fig. 12, while the raw output is also summarized in Table 6.

The results showed that TMTD-accelerated blend possess higher E' followed by TBBS, CBS and MBT, respectively. E' is directly proportionate to the stiffness and thus crosslinking density (Sae-oui et al. 2007; Nair et al. 2009); therefore, it can be observed that the greater crosslinking is given by TMTD- and TBBS-accelerated blends. Variation of E'' over the change in temperature is shown in Fig. 13. E'' peak correlates to maximum heat dissipation per unit deformation (Nair et al. 2009), which indicates that MBT- and CBS-accelerated blends consist of higher heat dissipation toward the deformation of the molecule. A similar trend was observed for the $\tan \delta$, as shown in Fig. 14. The $\tan \delta$ indicates the damping property. The results again confirm that TMTD- and TBBS-accelerated blends possess a high crosslinking density compared to CBS- and MBT-accelerated blends.

A change from the glassy state into the rubbery state is called the glass transition. As noted from the glass transition temperature (T_g) result, MBT caused to broaden the peak, which is attributed to the partially compatible blends and cure mismatch in the blend (Komalan et al. 2007). Moreover, it can be observed that T_g of

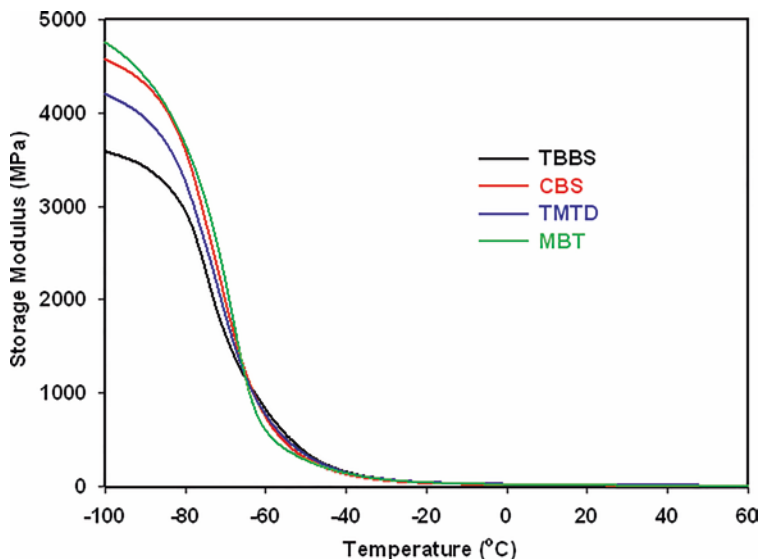


Fig. 12 Storage modulus as a function of temperature of NR/R-EPDM blends at various accelerator types

Table 6 The effect of various accelerators on the dynamic mechanical properties of NR/R-EPDM blends

Sample codes	Parameters at 25 °C		T_g (°C)
	Storage modulus (MPa)	$\tan \delta_{max}$	$\tan \delta_{max}$
TBBS	21.81	0.0888	-49.62
CBS	21.65	0.0882	-50.67
TMTD	22.55	0.0763	-49.90
MBT	18.40	0.1152	-48.89

CBS-accelerated blend possesses lower T_g than those of TMTD-, TBBS-, and MBT-accelerated blends. Less molecular movement makes the transition occur at the earlier stage. As CBS-accelerated blend contains higher polysulfides, disulfides, and monosulfide networks. Longer crosslinks make the chain move easier upon mechanical stress. The results from E' and $\tan \delta$ agreed well with the crosslink density measured by swelling uptake.

4 Conclusions

The effects of accelerators and vulcanizing systems were studied. The results indicated that the CBS-accelerated sulfur vulcanization through the semi-EV system is highly recommended in such a blend. This is because it provides the lowest melting point, which further enhances the blending compatibility. TBBS- and

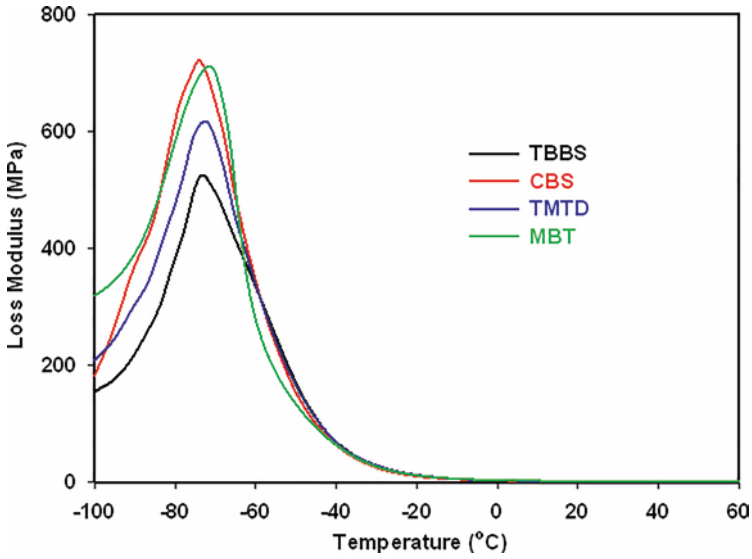


Fig. 13 Loss modulus as a function of temperature of NR/R-EPDM blends at various accelerator types

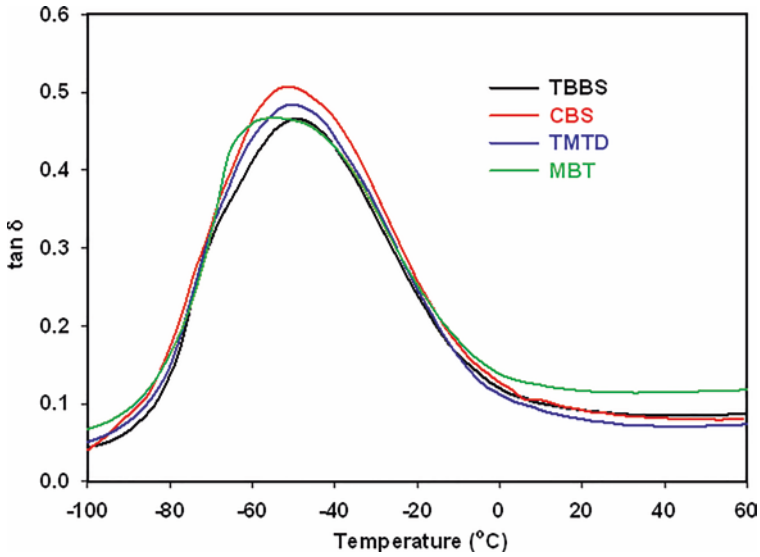


Fig. 14 Damping factor ($\tan \delta$) as a function of temperature of NR/R-EPDM blends at various accelerator types

TMTD-accelerated blends showed higher crosslink density than CBS-accelerated blend. However, CBS-accelerated blend showed highest strength, better thermal stability and elongation at break, satisfactory modulus, hardness, and dynamic mechanical properties.

References

- Botros S (2002) Preparation and characteristics of NR/EPDM rubber blends. *Polym Plast Technol Eng* 41:341–359. <https://doi.org/10.1081/PPT-120002572>
- Bristow G, Watson W, Bateman L (1963) In: Bateman L (ed) *The chemistry and physics of rubber-like substances*. Applied Science Publishers, London, p 417
- Chakraborty S, Roy P, Pathak A et al (2011) Composition analysis of carbon black-filled polychloroprene rubber compound by thermo-oxidative degradation of the compound. *J Elastomers Plast* 43:499–508. <https://doi.org/10.1177/0095244311413442>
- Chang YW, Shin YS, Chun H et al (1999) Effects of trans-polyoctylene rubber (TOR) on the properties of NR/EPDM blends. *J Appl Polym Sci* 73:749–756. [https://doi.org/10.1002/\(SICI\)1097-4628\(19990801\)73:5<749::AID-APP15>3.0.CO;2-S](https://doi.org/10.1002/(SICI)1097-4628(19990801)73:5<749::AID-APP15>3.0.CO;2-S)
- Coats A, Redfern J (1964) Kinetic parameters from thermogravimetric data. *Nature* 201:68–69. <https://doi.org/10.1038/201068a0>
- Dick J, Annicelli R (2001) *Rubber technology: compounding and testing for performance*. Hanser Gardner Publications, Cincinnati
- Flory PJ, Rehner J Jr (1943) Statistical mechanics of cross-linked polymer networks II. Swelling. *J Chem Phys* 11:512–520. <https://doi.org/10.1063/1.1723791>
- Ghosh AK, Debnath SC, Naskar N et al (2001) NR-EPDM covulcanization: A novel approach. *J Appl Polym Sci* 81:800–808. <https://doi.org/10.1002/app.1498>
- Gibala D, Hamed GR (1994) Cure and mechanical behavior of rubber compounds containing ground vulcanizates. Part I-cure behavior. *Rubber Chem Technol* 67:636–648. <https://doi.org/10.5254/1.3538699>
- Ismail H, Anuar H (2000) Palm oil fatty acid as an activator in carbon black filled natural rubber compounds: dynamic properties, curing characteristics, reversion and fatigue studies. *Polym Test* 19:349–359. [https://doi.org/10.1016/s0142-9418\(98\)00102-0](https://doi.org/10.1016/s0142-9418(98)00102-0)
- Ismail H, Suryadiansyah S (2002) Properties of polypropylene/natural rubber/recycle rubber powder blends. *Polym Plast Technol Eng* 41:833–845. <https://doi.org/10.1081/PPT-120014391>
- Ismail H, Nordin R, Noor A (2002) Cure characteristics, tensile properties and swelling behaviour of recycled rubber powder-filled natural rubber compounds. *Polym Test* 21:565–569. [https://doi.org/10.1016/S0142-9418\(01\)00125-8](https://doi.org/10.1016/S0142-9418(01)00125-8)
- Ismail H, Jaffri R, Rozman H (2003) The effects of filler loading and vulcanisation system on properties of oil palm wood flour-natural rubber composites. *J Elastomers Plast* 35:181–192. <https://doi.org/10.1177/0095244303035002006>
- Ismail H, Awang M, Hazizan MA (2006) Effect of waste tire dust (WTD) size on the mechanical and morphological properties of polypropylene/waste tire dust (PP/WTD) blends. *Polym Plast Technol Eng* 45:463–468. <https://doi.org/10.1080/03602550600553739>
- Kader MA, Bhowmick AK (2003) Thermal ageing, degradation and swelling of acrylate rubber, fluororubber and their blends containing polyfunctional acrylates. *Polym Degrad Stab* 79:283–295. [https://doi.org/10.1016/S0141-3910\(02\)00292-6](https://doi.org/10.1016/S0141-3910(02)00292-6)
- Komalán C, George K, Kumar P et al (2007) Dynamic mechanical analysis of binary and ternary polymer blends based on nylon copolymer/EPDM rubber and EPM grafted maleic anhydride compatibilizer. *Express Polym Lett* 1:641–653. <https://doi.org/10.3144/expresspolymlett.2007.88>

- Layer RW (1992) Recuring vulcanizates. I. A novel way to study the mechanism of vulcanization. *Rubber Chem Technol* 65:211–222. <https://doi.org/10.5254/1.3538601>
- Marković G, Radovanović B, Marinović-Cincović M et al (2009) The effect of accelerators on curing characteristics and properties of natural rubber/chlorosulphonated polyethylene rubber blend. *Mater Manuf Process* 24:1224–1228. <https://doi.org/10.1080/10426910902967087>
- Mathew G, Singh R, Lakshminarayanan R et al (1996) Use of natural rubber prophylactics waste as a potential filler in styrene-butadiene rubber compounds. *J Appl Polym Sci* 61:2035–2050. [https://doi.org/10.1002/\(SICI\)1097-4628\(19960912\)61:11<2035::AID-APP19>3.0.CO;2-7](https://doi.org/10.1002/(SICI)1097-4628(19960912)61:11<2035::AID-APP19>3.0.CO;2-7)
- Morita E (1980) SN compounds as delayed action chemicals in vulcanization. *Rubber Chem Technol* 53:393–436. <https://doi.org/10.5254/1.3535050>
- Nabil H, Ismail H, Azura A (2011) Recycled polyethylene terephthalate filled natural rubber compounds: effects of filler loading and types of matrix. *J Elastomers Plast* 43:429–449. <https://doi.org/10.1177/0095244311405503>
- Nair TM, Kumaran M, Unnikrishnan G et al (2009) Dynamic mechanical analysis of ethylene-propylene-diene monomer rubber and styrene-butadiene rubber blends. *J Appl Polym Sci* 112:72–81. <https://doi.org/10.1002/app.29367>
- Noriman N, Ismail H, Rashid A (2010) Characterization of styrene butadiene rubber/recycled acrylonitrile-butadiene rubber (SBR/NBRr) blends: the effects of epoxidized natural rubber (ENR-50) as a compatibilizer. *Polym Test* 29:200–208. <https://doi.org/10.1016/j.polymertesting.2009.11.002>
- Palaty S, Joseph R (2007) Studies on xanthate/dithiocarbamate accelerator combination in NR/BR blends. *J Appl Polym Sci* 103:3516–3520. <https://doi.org/10.1002/app.25225>
- Rabello M, White J (1997) Photodegradation of polypropylene containing a nucleating agent. *J Appl Polym Sci* 64:2505–2517. [https://doi.org/10.1002/\(SICI\)1097-4628\(19970627\)64:13<2505::AID-APP4>3.0.CO;2-H](https://doi.org/10.1002/(SICI)1097-4628(19970627)64:13<2505::AID-APP4>3.0.CO;2-H)
- Sae-oui P, Sirisinha C, Thepsuwan U et al (2007) Influence of accelerator type on properties of NR/EPDM blends. *Polym Test* 26:1062–1067. <https://doi.org/10.1016/j.polymertesting.2007.07.004>
- Sae-Oui P, Sirisinha C, Hatthapanit K (2010) Properties of natural rubber filled with ultra fine acrylate rubber powder. *J Elastomers Plast* 42:139–150. <https://doi.org/10.1177/0095244310362733>
- Saha Deuri A, Bhowmick AK, Ghosh R et al (1988) Thermal and ablative properties of rocket insulator compound based on EPDM. *Polym Degrad Stab* 21:21–28. [https://doi.org/10.1016/0141-3910\(88\)90062-6](https://doi.org/10.1016/0141-3910(88)90062-6)
- Sahakaro K, Talma AG, Datta RN et al (2007) Blending of NR/BR/EPDM by reactive processing for tire sidewall applications. II. Characterization. *J Appl Polym Sci* 103:2547–2554. <https://doi.org/10.1002/app.25113>
- Sahakaro K, Pongpaiboon C, Nakason C (2009) Improved mechanical properties of NR/EPDM blends by controlling the migration of curative and filler via reactive processing technique. *J Appl Polym Sci* 111:2035–2043. <https://doi.org/10.1002/app.29193>
- Sirqueira AS, Soares BG (2002) Mercapto-modified copolymers in elastomer blends. IV. The compatibilization of natural rubber/EPDM blends. *J Appl Polym Sci* 83:2892–2900. <https://doi.org/10.1002/app.10283>
- Tomer N, Delor-Jestin F, Singh R et al (2007) Cross-linking assessment after accelerated ageing of ethylene propylene diene monomer rubber. *Polym Degrad Stab* 92:457–463. <https://doi.org/10.1016/j.polymdegradstab.2006.11.013>
- Yazdani H, Karrabi M, Ghasmi I et al (2011) Devulcanization of waste tires using a twin-screw extruder: the effects of processing conditions. *J Vinyl Addit Technol* 17:64–69. <https://doi.org/10.1002/vnl.20257>
- Zhang ZX, Fan J, Pal K et al (2011) Influence of compatibilizers and processing temperature on microcellular injection-molded polypropylene/(waste tire powder) composites. *J Vinyl Addit Technol* 17:254–259. <https://doi.org/10.1002/vnl.20271>
- Zhao Q, Li X, Gao J (2007) Aging of ethylene-propylene-diene monomer (EPDM) in artificial weathering environment. *Polym Degrad Stab* 92:1841–1846. <https://doi.org/10.1016/j.polymdegradstab.2007.07.001>

Compatibilization of Natural Rubber/ Recycled Ethylene Propylene Diene Rubber Blends



Nabil Hayeemasae and Hanafi Ismail

1 Introduction

Ethylene propylene diene rubber (EPDM) is considered a fast-growing rubber compared to other synthetic rubbers (Fukumori et al. 2002; Nabil et al. 2013b). EPDM is mostly used as main matrix for non-tire applications (Ismail and Mathialagan 2012). Although EPDM processes high thermal resistance, it has been discarded after certain period of consumption. Because of its higher thermal resistance, it makes harder to devulcanize it. Therefore, the best solution is to use directly from its form (Phadke et al. 1983; Nabil et al. 2012; Korkut et al. 2013). To conquer this drawback, crumb EPDM waste has been currently used in attention to manufacture a value-added drubber material based on the blend of NR and w-EPDM. This blend has been studied previously (Hayeemasae et al. 2013; Nabil et al. 2013a). But acceptable cure properties and tensile properties are not easy to receive because their cure mismatches between NR and w-EPDM. The dissimilarity in level of diene makes them incompatible. To improve it, proper formulation and processing technique need to be carried out to control the compatibility.

NRL is a unique waterborne polymer gained from para rubber tree (Rathnayake et al. 2012; Rahman et al. 2013). NRL can be further processed into a variety of raw materials and products. NRL is also known to have stickiness and low surface tension which may provide some enhancements to the compatibility of NR and

N. Hayeemasae (✉)

Department of Rubber Technology and Polymer Science, Faculty of Science and Technology,
Prince of Songkla University, Pattani, Thailand
e-mail: nabil.h@psu.ac.th

H. Ismail

School of Materials and Mineral Resources Engineering, Engineering Campus,
Universiti Sains Malaysia, Nibong Tebal, Penang, Malaysia

w-EPDM. Previously, NRL was used to modify the properties of vulcanizates by Awang et al. (2008). Better performance was observed in their materials.

Nowadays, the curing of rubber by introducing radiation has been applied especially in the continuous process. The cross-linking bond of radiated rubber is mainly C-C bond which is like peroxide cross-link. This method can match the curing of different types of rubber and provide high purities to the final product (Rahman et al. 2013; Belkahla et al. 2013). There are many sources of radiation that have been used to cure the rubber. Among them, EB irradiation has been developed; it is claimed to be fast together with well-controlled conditions (Noriman et al. 2010; Shanmugaraj and Bhowmick 2003; Banik and Bhowmick 2000). However, there were two competitive factors that may interfere the cross-linking by this method namely cross-linking and chain scissioning (Munusamy et al. 2009; Zurina et al. 2008; Ismail et al. 2008). It always solves by introducing some polyfunctional monomers, such as trimethylolpropane triacrylate (TMPTA) which assists to decrease the scissioning effect (Vijayabaskar et al. 2008). Improving the tensile properties and dynamic mechanical properties is challenge for NR/w-EPDM blends. This chapter describes the effects NRL and EB irradiation on the properties of NR/wEPDM blends.

2 Materials and Preparation of the Blends

2.1 Materials

Mardec Sdn. Bhd. manufactured the SMR 5L grade NR. NRL with low ammonia and w-EPDM were supplied by Zarm Scientific (M) Sdn. Bhd. Penang, Malaysia. w-EPDM was ground to gain the size around 10–200 μm . The specific gravity of w-EPDM was 1.06 g/cm^3 . The carbon black (CB) content in w-EPDM was 29.33%. Other characteristics can be found in previous work (Hayeemasae et al. 2013). The N330-grade CB was manufactured by Malayan Carbon (M) Ltd., Malaysia. Zinc oxide, stearic acid, N-cyclohexyl-benzothiazyl-sulfenamide (CBS), and sulfur were purchased from Bayer (M) Ltd. Trimethylolpropane triacrylate was purchased from UCB Asia Pacific Ltd., Malaysia.

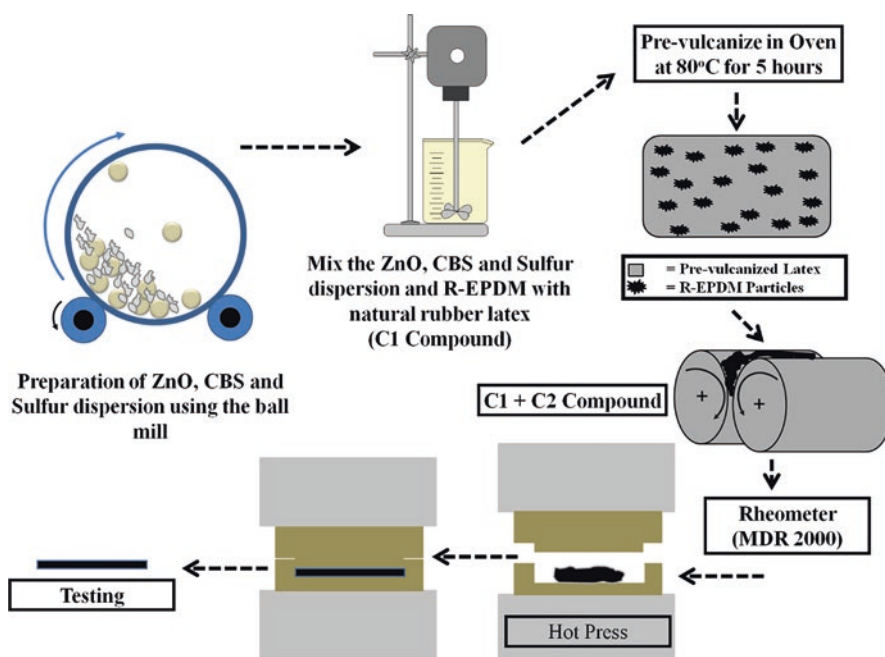
2.2 Preparation of the Blends in the Presence of Natural Rubber Latex

There were two ways of compounding preparation. For control, all the rubbers and additives (see Table 1) were mixed on a laboratory-sized two-roll mill (model XK-160) while different method was proposed for the blends in the presence of NRL. As can be seen from Fig. 1 and Table 2, all the ingredients except for NR,

Table 1 The blending formulation used for blends in the presence of NRL

Conventional mixing		Mixing using NRL				
Materials (phr)	Control	Materials (phr)	L1	L2	L3	L4
SMR L	70.0	SMR L	60.0	50.0	40.0	30.0
R-EPDM	30.0	NRL	10.0	50.0	30.0	40.0
ZnO	5.0	R-EPDM	30.0	30.0	30.0	30.0
Stearic acid	2.0	Stearic acid	2.0	2.0	2.0	2.0
CBS	1.2	N330	30.0	30.0	30.0	30.0
Sulfur	1.8	50% ZnO	5.0	5.0	5.0	5.0
N330	30.0	50% CBS	1.2	1.2	1.2	1.2
		50% Sulfur	1.8	1.8	1.8	1.8

SMR L standard Malaysian rubber L, NRL natural rubber latex, R-EPDM recycled ethylene propylene diene rubber, ZnO zinc oxide, CBS N-cyclohexyl-benzothiazyl-sulfenamide


Fig. 1 Schematic illustration representing the preparation of the blends by natural rubber latex (NRL)

stearic acid, and CB (C2 Compound), were processed in NRL. First, NRL was stirred using the mechanical stirrer at 10 rpm for about 10 min. Next, w-EPDM and 50% zinc oxide (ZnO) were added and stirred. After 5 min of maturation, 50% CBS and 50% sulfur were added to the mixture. Next, the mixing was prevulcanized in oven at 80 °C for 5 h. Finally, the dried sheet of NRL/w-EPDM blends (C1 Compound) was blended with NR, stearic acid, and CB (C2 Compound) on the

Table 2 Preparation of the unmodified (control) and NRL-modified NR/R-EPDM blends

Additives used with respect to		
Control	Mixing using NRL	
Two-Roll Mill at ambient temperature	NRL at ambient temperature (C1)	Two-Roll Mill at ambient temperature (C2)
NR	60% NRL	NR
R-EPDM	R-EPDM	Stearic acid
ZnO	50% ZnO	N330
Stearic acid	50% CBS	
CBS	50% Sulfur	
Sulfur		
N330		

Table 3 The blending formulation used for blends in the presence of electron-beam irradiation

Materials (phr)	Control blend	Irradiated blends in the presence of TMPTA
SMR L	70.0	70.0
R-EPDM	30.0	30.0
ZnO	5.0	5.0
Stearic acid	2.0	2.0
CBS	1.2	1.2
Sulfur	1.8	1.8
N330	30.0	30.0
TMPTA	–	3.0

two-roll mill. The respective compounds were later tested for its curing characteristics by using a Monsanto Moving Die Rheometer (MDR 2000). The compounds were finally compressed using a stainless-steel mold at 150 °C with a pressure of 10 MPa based on the curing times.

2.3 Preparation of the Blends in the Presence of Electron-Beam Irradiation

Our previous work (Hayeemasae et al. 2013) has concluded that the blending ratio at 70/30 (phr/phr) of NR and w-EPDM gave acceptable properties. This ratio was chosen on this work (see Table 3). In the control blend, all the rubbers and additives were mixed on a laboratory-sized two-roll mill (model XK-160) at ambient temperature. On the contrary, the irradiated blends were prepared by adding TMPTA as cross-linking promoter.

The respective compounds from all formulations were tested for their cure properties using a Monsanto Moving Die Rheometer (MDR 2000). Then, they were compressed using a hot press based on their curing times. EB irradiation was carried

at this step where the samples were irradiated using a 3 MeV EB accelerator (NHV EPS-3000) at doses of 0–200 kGy.

3 Effect of Natural Rubber Latex

3.1 Curing Characteristics

A Monsanto Moving Die Rheometer (MDR 2000) was used to determine the curing properties of the blends according to ASTM D2084. Table 4 lists the outputs received from MDR 2000. Adding NRL provided higher $S'M_L$ and it is increased over the addition of NRL. This shows that NRL made the processability slightly harder. As C1 compound was precured before blending with C2 compound, the C1 compound contained partial cross-links as well (see Fig. 2). Higher content of NRL can make sulfur interacts swell with the NRL to perform the cross-linking.

In general, stiffness can be observed for cross-linked rubber. More cross-linking results more stiffness. Thus, less processability was observed over the addition of NRL. Similar finding was observed for $S'M_H$ which indicates the overall stiffness of the compounds. $S'(M_H-M_L)$ increased up to 30 phr (L3) and then decreased as $S'(M_H-M_L)$ relates to the degree of cross-linking (Ismail et al. 1999). This suggested that there was a compatibility between NR and w-EPDM as this value increased significantly but it was not obtained for L4 compound. This is because the C1 compound was mostly cross-linked at this stage and not in a processable form. It may lose its ability to be mixed with C2 compound and leading to a decrease in degree of cross-linking.

Figure 2 illustrates the way that pre-cross-linking was formed in C1 compound. At 10 phr (L1) of NRL, L1 started to form slight cross-linking because L1 already contained unsaturation level from the small portion of NRL. This NRL was prevulcanized and left some remaining amount of sulfur or free sulfur. Somehow, as the NRL content increased, free sulfur may be reduced by the presence of higher level of unsaturation. This observation shows a direct effect to ts_2 , tc_{90} , and CRI of the blends where faster curing process is taken place.

Table 4 Curing characteristics of unmodified (control) and NRL-modified NR/R-EPDM blends

Curing characteristics	Control	L1	L2	L3	L4
$S'M_L$	0.76	0.84	1.13	1.4	3.69
$S'M_H$	16.61	17.01	17.4	18.74	19.43
$S'(M_H-M_L)$	15.85	16.17	16.27	17.34	15.74
ts_2	1.85	1.02	0.83	0.65	0.61
tc_{90}	8.27	8.20	7.62	6.01	4.84
CRI	15.58	13.93	14.73	18.66	23.64

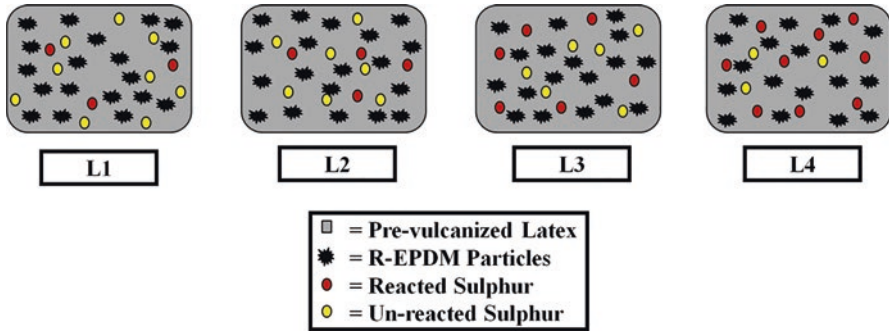


Fig. 2 Characteristics of prevulcanized NRL/R-EPDM blends (C1 compound)

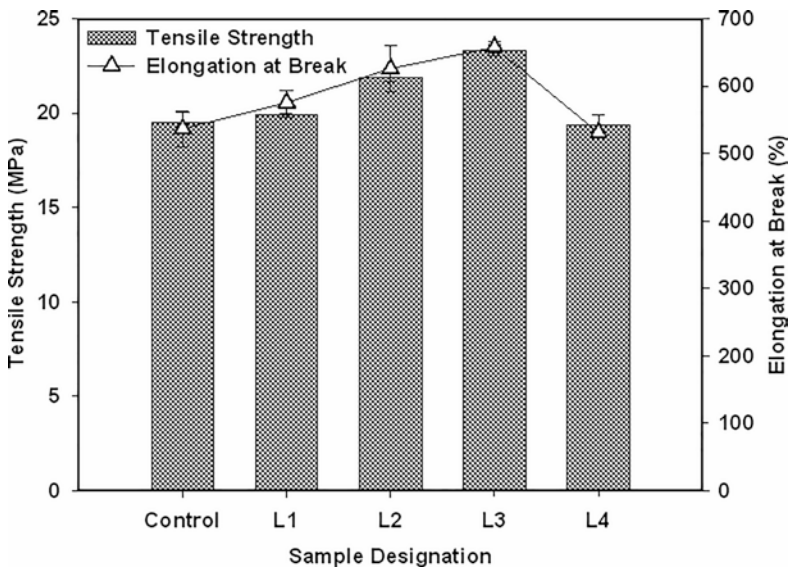


Fig.3 Tensile strength and elongation at break of unmodified and NRL-modified NR/R-EPDM blends

3.2 Tensile Properties

Tensile properties were evaluated according to ASTM D412. Tensile strength and elongation at break of the blends are shown in Fig. 3. NRL has affected to enhance the tensile strength and elongation at break of the blends. The enhancements were 2.05%, 12.37%, and 19.71% higher for L1, L2, and L3 while the improvements for elongation at break were 7.26%, 16.61%, and 22.57%. This assumes that the interaction between the w-EPDM and NR enhances in the presence of NRL. Further explanation on such interactions can be referred to Fig. 4. As C1 compound contained vulcanizing additives, C1 can start a normal sulfur-curing reaction. The

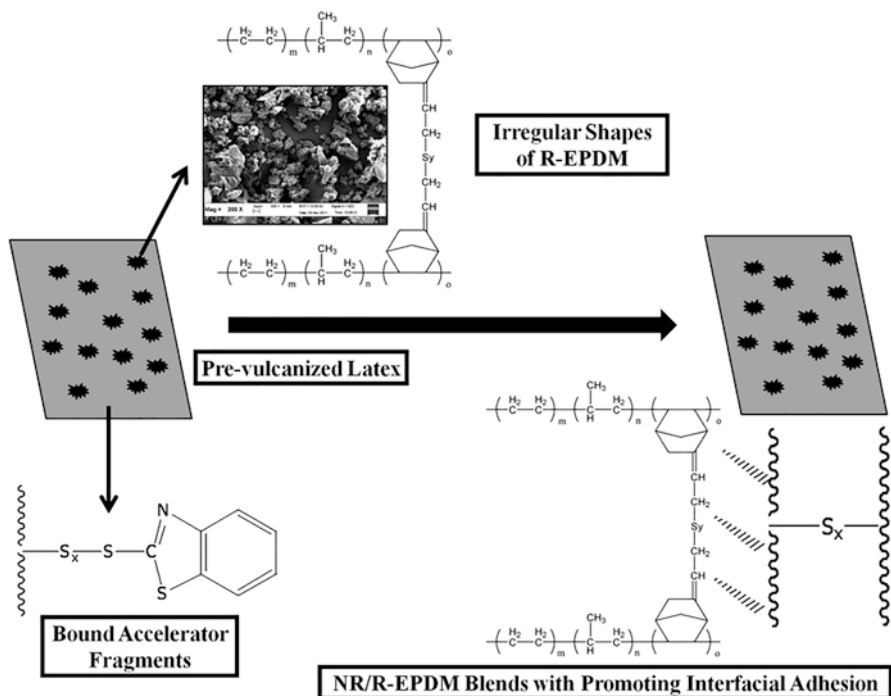


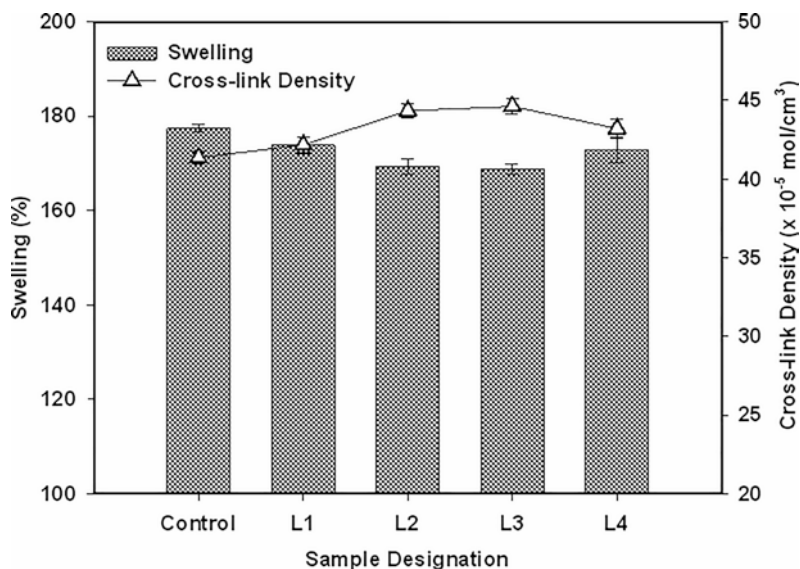
Fig. 4 Possible physical locking between NR and R-EPDM phases

vulcanizing reactions are as usual as other sulfur vulcanization. The reaction started when ZnO creates accelerator complex and later interacts with sulfur to give an active sulfurating agent. After that, the cross-linking reaction takes place (Coran 1965, 2003). At this stage, free sulfur or active sulfurating agents are still free to have further interaction with NR (SMR L). This has made the cross-linking distributed well throughout the rubber chains. Moreover, w-EPDM used in this work was ground and mostly cross-linked. In this case, adding NRL seemed to improve the interfacial adhesion between NRL and w-EPDM. Thus, the migration of CB to NR is reduced while more homogenous CB distribution in the blends is observed. Similar finding was found for elongation at break. Increasing interfacial adhesion with NRL also enhanced the flexibility of the chain (Kumar et al. 2002).

The drastic reduction of elongation at break and tensile strength of L4 compound is simply due to the less ability of mixing between C1 and C2 compound. The heterogenous mixing of these two compounds is responsible for the lower stress transfer to the final blend. Therefore, it fastens the crack initiation and reduced the tensile strength and flexibility to the blend. Table 5 lists the M100, M300, and hardness of the blends. Modulus and hardness indicate the stiffness and also degree of cross-link. This has confirmed the affinity of NRL as compatibilizer in the blends. The occurrence of prevulcanized NRL is responsible for the increment of hardness and modulus.

Table 5 M100, M300, and hardness property of unmodified (control) and NRL-modified NR/R-EPDM blends

Sample codes	M100 (MPa)	M300 (MPa)	Hardness (Shore A)
Control	2.11 ± 0.07	8.31 ± 0.37	65 ± 0.6
L1	2.62 ± 0.06	8.67 ± 0.14	67 ± 0.8
L2	2.68 ± 0.10	8.95 ± 0.25	68 ± 0.9
L3	2.73 ± 0.12	8.96 ± 0.09	69 ± 0.5
L4	2.96 ± 0.15	9.78 ± 0.26	70 ± 0.8

**Fig. 5** Swelling and cross-link density of control and NRL-modified NR/R-EPDM blends

3.3 Swelling Behavior

Swelling uptake was measured according to ASTM D471 based on the gravimetric analysis. The results from swelling uptake were further implemented for calculation of cross-link density by modifying the Flory–Rehner equation (Flory and Rehner Jr. 1943). Figure 5 shows the swelling uptake and cross-link density of the blends. Swelling decreased over the addition of NRL then slightly decreased for L4. This is clear evidence from the previous explanation on the action of NRL as compatibilizer. More homogenous w-EPDM and CB distribution in the blends is responsible for such enhancement. The increment of swelling result and the reduction of cross-link density when using the NRL for 40 phr (L4) is attributed to the heterogeneous mixture of C1 and C2 compounds.

3.4 Scanning Electron Microscopy (SEM)

SEM images were captured to screen the micro-defects of the rubber samples and correlated with previous properties. SEM images of the blends are shown in Fig. 6. The images correlated well with the result from tensile strength. There was rough and torn surface seen in the unmodified blends (Fig. 6a). However, rougher surface and many more tearing lines were clearer in L1, L2, and L3 blends (Fig. 6b–d) particularly for L3 blend, suggesting more resistance for crack growth and thus resulted in highest tensile strength. These findings agreed well with the

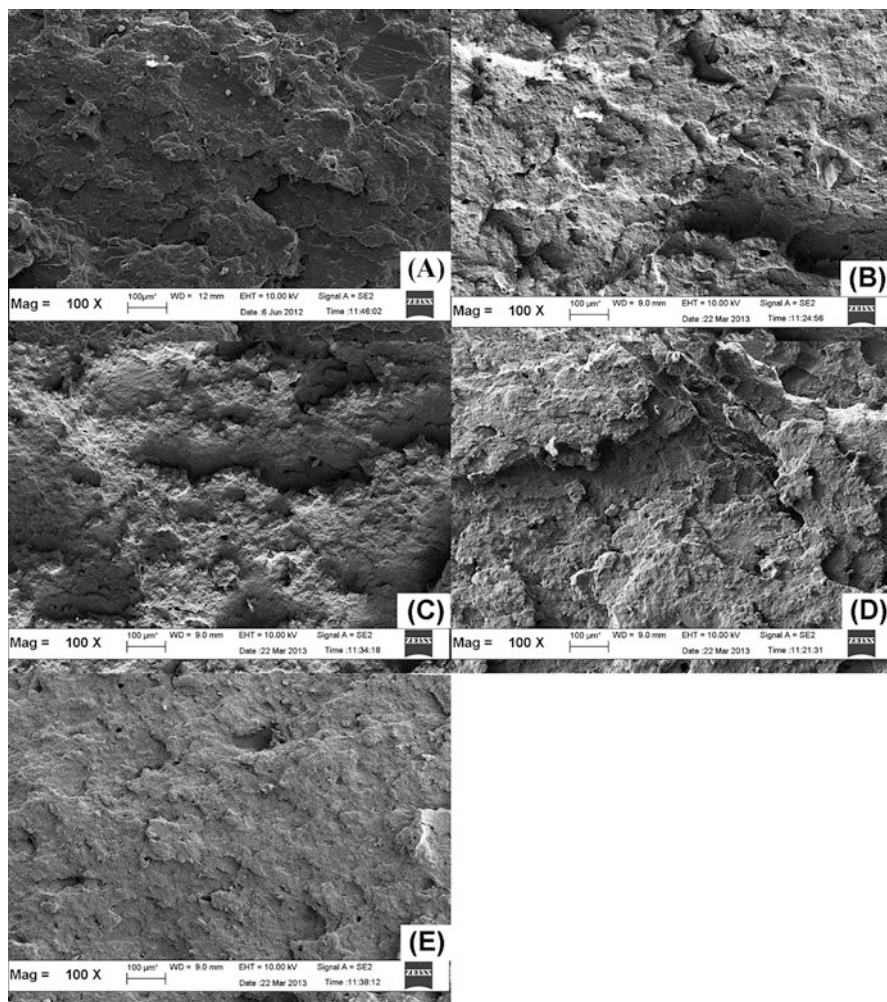


Fig. 6 Tensile fractured surface images obtained from SEM of control (a) and NRL-modified NR/R-EPDM blends: L1 (b), L2 (c), L3 (d), and L4 (e) at 100× magnification

above-mentioned findings related to the enhancement of the tensile strength provided by the NRL modification. Awang et al. (2008) suggested that an enhancement in interfacial adhesion after using NRL to reduce interfacial tensile between w-EPDM and NR. Furthermore, the image was seen to be smoother when the addition of NRL beyond 30 phr (Fig. 6e). This has made less energy used for breaking the sample or decrease the possibility of rubber to deform while subjecting to stretching.

3.5 Thermogravimetric Analysis (TGA)

Thermal stability of the blends was analyzed by thermogravimetric analysis or TGA. TG and DTG curves of the blends are shown in Figs. 7 and 8. The outputs from TG profiles such as the decomposition temperatures at various weight loss and stages and char residue are tabulated in Table 6. First stage of degradation was at about 330 °C which was due to NR degradation while the second stage appeared in the region 450–520 °C which was contributed to the scission of w-EPDM and other components left after the first degradation step. The thermal stability of the blends can be considered from their thermal decomposition temperature. It was found that the decomposition temperature at various weight loss, i.e., 10%, 30%, 50%, and 60% or stages, i.e., $T_{\max I}$ and $T_{\max II}$, increased up to 30 phr of NRL content. An improvement of thermal stability is attributed to the promoting the interfacial adhesion to phases of NR and w-EPDM in the presence of NRL.

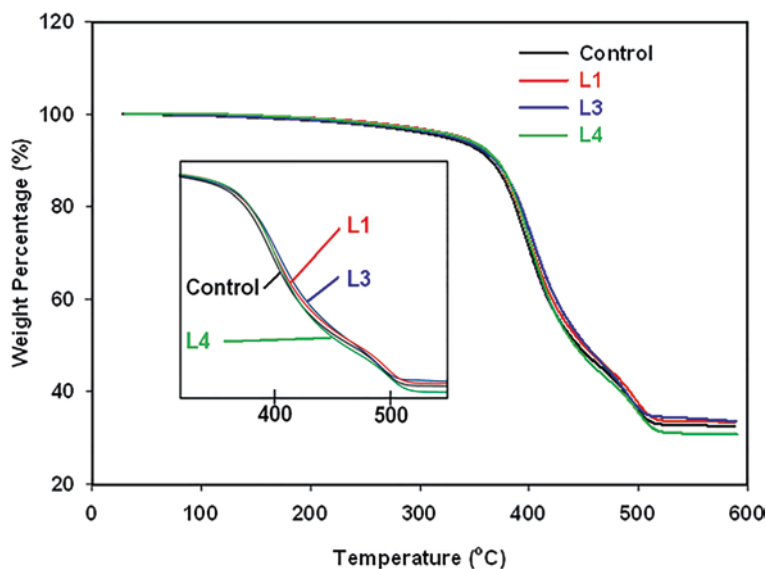


Fig. 7 TG curves of control and NRL-modified NR/R-EPDM blends

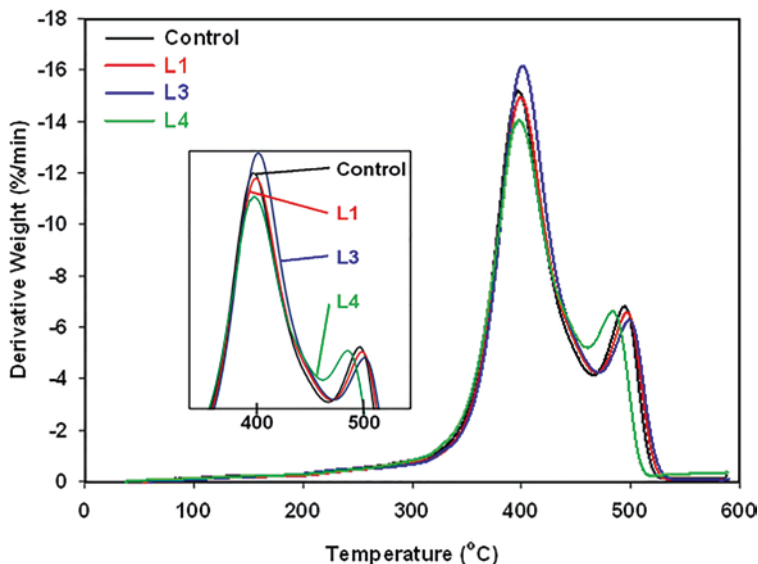


Fig. 8 DTG curves of control and NRL-modified NR/R-EPDM blends

Table 6 The decomposition temperature at various weight losses and stages and char residue (CR) of the control and NRL-modified NR/R-EPDM blends

Sample codes	The decomposition temperature (°C)						Char res. (%)
	T _{-10%}	T _{-30%}	T _{-50%}	T _{-60%}	T _{max I}	T _{max II}	
Control	367.18	403.58	446.97	489.75	399	487	33.6
L1	369.90	404.66	450.19	488.26	399	497	33.6
L3	369.04	407.68	452.35	492.37	401	499	33.4
L4	370.60	404.12	442.17	484.34	398	483	33.9

As a result, higher heat is required to break the bonds or the structure of compatibilized blends. Such temperatures were clearer at the decomposition temperatures above 30% of weight loss. This shows that NRL acted efficiently at higher temperature. Moreover, the char residue of all samples was not changed as there were no additional fillers added in the formulation. The amount of residue is very much dependent to the type and amount of filler (Chakraborty et al. 2011).

3.6 Activation Energy of the Degradation Process

Activation energy value was also calculated to correlate with TG profiles of the blends. It was analyzed by modifying the Coats–Redfern’s method (Coats and Redfern 1964). Coats–Redfern plots of the blends are based on the stages of

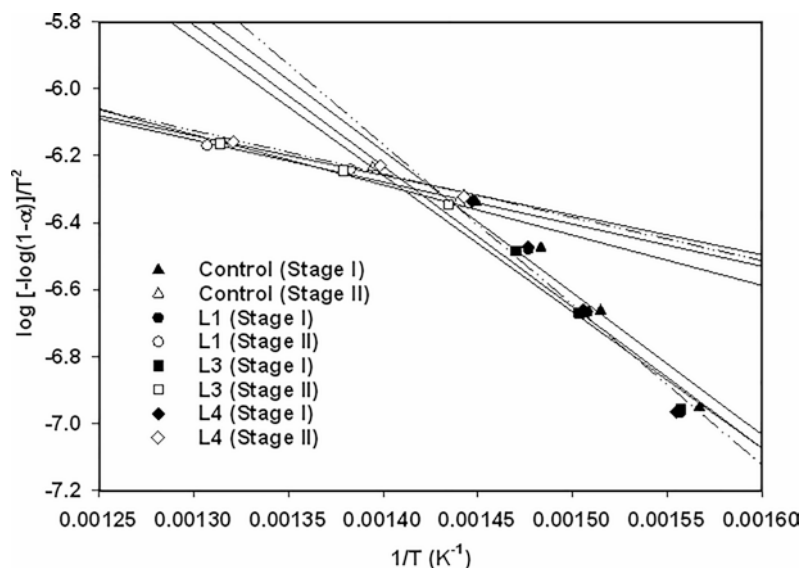


Fig. 9 Coats-Redfern's plots of control and NRL-modified NR/R-EPDM blends

Table 7 Activation energy of control and NRL-modified NR/R-EPDM blends calculated from Coats-Redfern's equation

Sample codes	Activation energy (kJ/mol)	
	E_I	E_{II}
Control	69.24	20.23
L1	70.86	21.75
L3	75.60	25.14
L4	71.56	21.57

degradation received from TG profiles. Figure 9 and Table 7 show the Coats-Redfern plots and their respective outputs. As stated previously that the blends decomposed in two stages, which can be separated as the degradation of NR phase (E_I) and w-EPDM (E_{II}). It was obviously observed that adding NRL has influenced the activation energy of the blends; it kept higher up to the optimum value at 30 phr of NRL content. This confirmed that the thermal stability of the blends is received in the presence of NRL. This is because of the better interfacial adhesion between NR and w-EPDM. The reduction of activation energy for L4 is responsible to an uneven cross-linking distribution as stated in the curing part.

3.7 Dynamic Mechanical Analysis (DMA)

Dynamic mechanical analysis was done under cyclic tensile strain where the data of storage modulus (E'), loss modulus (E''), and damping factor ($\tan \delta$) were recorded and explained. As been clearly observed that introducing NRL has improved the

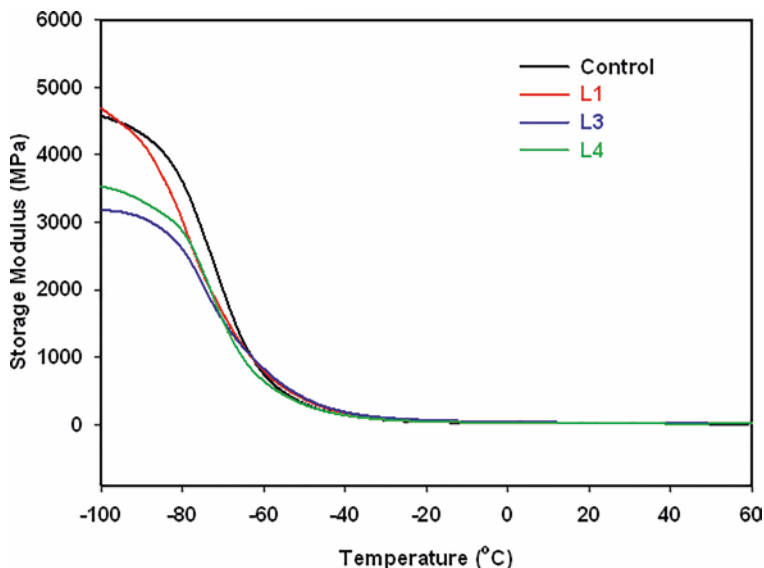


Fig. 10 Storage modulus on temperature of control and NRL-modified NR/R-EPDM blends

performance of the blends, previous results already proposed the respective evidence to support the findings. DMA was also a tool to assess the blending compatibility. Figures 10, 11, and 12 illustrate the E' , E'' , and $\tan \delta$ over the temperatures of the blends. The raw data are also listed in Table 8. E' values increased up to L3 blends and then reduced continuously for L4. This correlated well with prior discussion on the improvement of blending performance in the presence of NRL.

E'' peak indicates hysteresis loss or heat build-up of the blends under cyclic deformation. Higher E'' may not be good for the products that required less heat build-up. As can be seen from E'' values, adding NRL has made the rubber less heat build-up, and this is a good indication that NRL can improve the compatibility of NR and w-EPDM. A similar trend is observed for $\tan \delta_{\max}$, i.e., L3 provides a comparatively lower $\tan \delta_{\max}$, compared with control blend. As the $\tan \delta$ reversely relates to the cross-linking degree, the results again verified that L3 shows the highest cross-linking degree due to the better interfacial adhesion achieved in the blends.

Addition of NRL has also shifted the T_g of the blends, as seen from the temperature at which $\tan \delta_{\max}$ present. Higher restriction of molecular movement in the presence of NRL required higher temperature to loosen it. Thus, the changing rate of free volume over the temperature is increased resulting to the shifting of T_g .

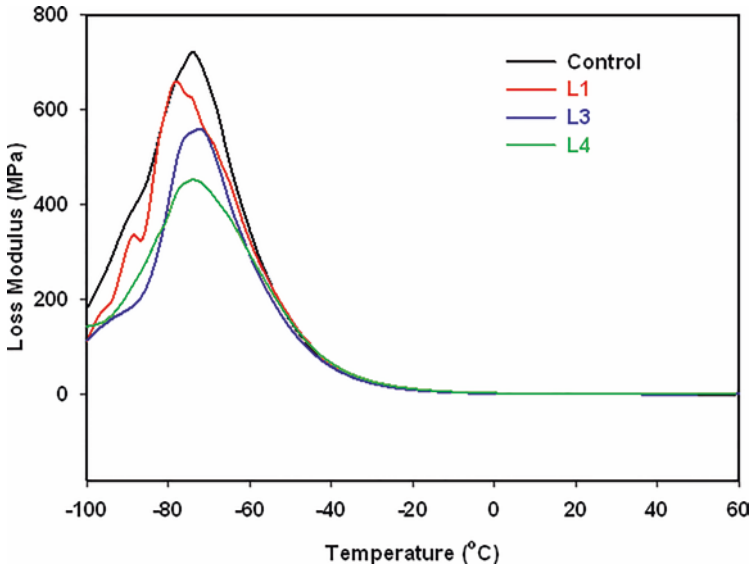


Fig. 11 Loss modulus on temperature of control and NRL-modified NR/R-EPDM blends

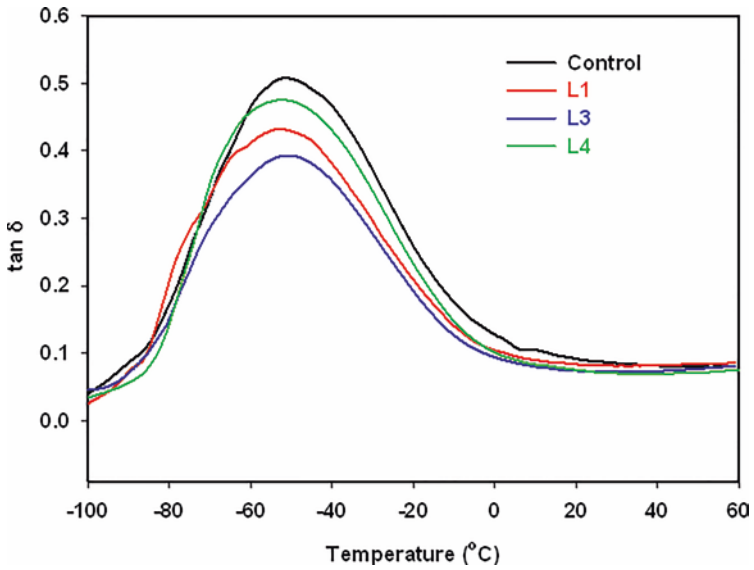


Fig. 12 Damping factor ($\tan \delta$) on temperature of control and NRL-modified NR/R-EPDM blends

Table 8 Storage modulus (E') at 25 °C, maximum loss modulus (E''_{\max}), damping factor ($\tan \delta_{\max}$), and glass transition temperature (T_g) of control and NRL-modified NR/R-EPDM blends

Sample codes	E' (MPa)	E''_{\max} (MPa)	$\tan \delta_{\max}$	T_g (°C) @ $\tan \delta_{\max}$
Control	21.65	721.18	0.5073	-50.67
L1	27.74	657.66	0.4312	-49.68
L3	28.51	559.64	0.3929	-48.24
L4	17.94	452.92	0.4755	-51.12

Table 9 Curing characteristics of NR/R-EPDM blends in the absence and presence of TMPTA

Curing characteristics	Control blend	Irradiated blend + TMPTA
$S'M_L$	0.76	0.70
$S'M_H$	16.61	17.47
$S'(M_H-M_L)$	15.85	16.77
ts_2	1.85	1.83
tc_{90}	8.27	7.7
CRI	15.58	19.08

4 Effect of Electron-Beam Irradiation

4.1 Curing Characteristics

The data obtained from curing characteristics of the blends are listed in Table 9. TMPTA lowered the $S'M_L$ of the blends, indicating that a lower viscosity of the compound was observed. TMPTA is liquid additive; it can act as plasticizer for rubber compound, thus making the compound more processable. $S'M_H$ also increased in the presence of TMPTA. TMPTA is known as co-curing agent which can generate free radical when heated. Thus, it can provide some extra cross-linking and may increase the stiffness of the blends. This has a direct effect to the $S'(M_H-M_L)$ which indicates the extent of cross-linking (Ishiaku et al. 2000). This finding exhibits that the compounds contained more cross-links when adding TMPTA. The ts_2 , tc_{90} , and CRI show that the occurrence of TMPTA fastens the curing process. Previous work also reported the same findings on the role of TMPTA as co-curing agent (Noriman et al. 2010).

4.2 Fourier Transform Infrared Spectroscopy (FT-IR)

Figure 13 shows the FT-IR spectra of the blends with and without EB irradiation. The assignment at various peaks is also tabulated in Table 10. The O-H groups were observed at the peak around 3357.79 cm^{-1} while the peak at 2848.62 and 2912.84 cm^{-1} referred to the CH_2 and CH_3 bands of NR and w-EPDM. C=C and

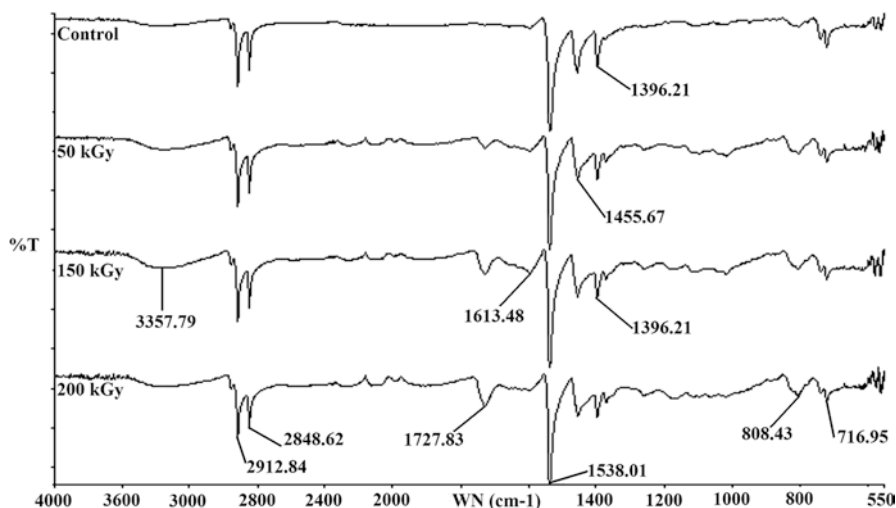


Fig. 13 FT-IR spectrum of NR/R-EPDM blends before and after EB irradiation

Table 10 Fourier transforms infrared positions and assignments of NR/R-EPDM blends before and after EB irradiation

Assignments	Wave number (cm ⁻¹)
C–O stretching	1000–3000
Symmetric C–H stretching vibration of CH ₃	1396.21
CH ₂ scissoring vibration	1455.67
ENB and C=C vibration	1613.48
C=O stretching vibration	1727.83
C–H symmetric stretching bands	2848.62
C–H symmetric stretching bands	2912.84
O–H stretching	3357.79

C=O groups were observed from two small adjoining peaks at 1613.48 and 1727.83 cm⁻¹ where their intensity increases over the dose of EB irradiation (Zhao et al. 2007). A slight broad peak in the region of 1000–1300 cm⁻¹ indicates C-O from the carboxylic acid of TMPTA. The results appeared from FT-IR clearly showed that EB irradiation can induce more cross-links within the NR and w-EPDM.

4.3 Mechanical Properties

Tensile strength and elongation at break of the blends are shown in Fig. 14. It was found that the tensile strength increased up to 50 kGy of EB irradiation dose and then decreased slightly when applying higher dose. The formation of irradiation-induced cross-link may be the main reason contributing to a higher strength. EB

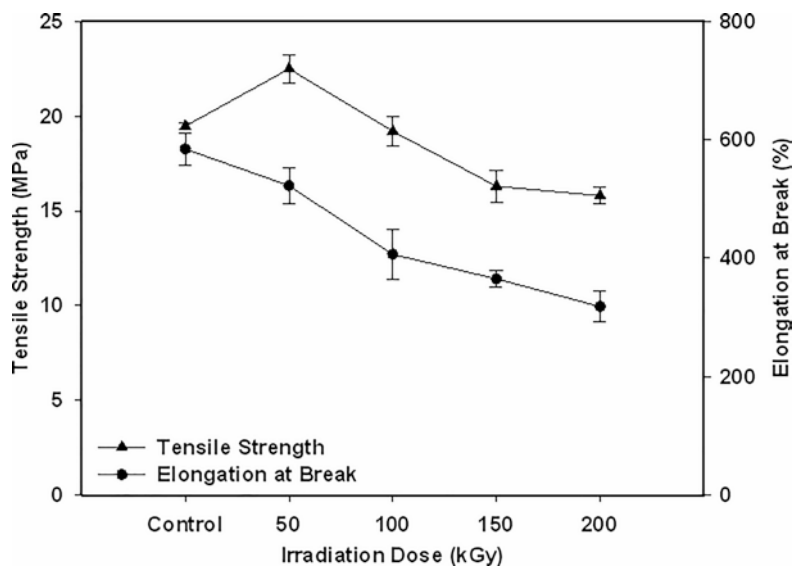


Fig. 14 Tensile strength and elongation at break of NR/R-EPDM blends before and after EB irradiation

Table 11 M100, M300, and hardness property of NR/R-EPDM blends before and after EB irradiation

Sample code	M100 (MPa)	M100 (MPa)	Hardness (Shore A)
Control	2.11 ± 0.04	8.31 ± 0.09	65 ± 0.4
TBBS	2.32 ± 0.10	9.67 ± 0.34	68 ± 0.4
CBS	2.76 ± 0.07	11.67 ± 0.25	69 ± 0.5
TMTD	2.94 ± 0.10	12.35 ± 0.31	70 ± 0.5
MBT	3.21 ± 0.06	13.67 ± 0.09	72 ± 0.5

irradiation together with the TMPTA function well to induce the cross-linking in the blends. However, higher formation of cross-links may interfere the stress transfer; it restrained the chains from structural rearrangement while stretching and thus reducing strength. A good explanation was reported by Rooj et al. (2013); they reveals that when the cross-link density of rubber is high, some energy is partially stored while stretching, more internal heat is present. This can create a failure and reduce the energy to break the sample. Elongation at break also reduced over the EB irradiation. This was simply because of the cross-linking discussed previously. The irradiation induced more cross-linking and caused a restriction molecular chain to move and later reduced the flexibility of the rubber chains. This observation correlated well to the finding observed in the literatures (Ratnam et al. 2001; Senna et al. 2008; Noriman et al. 2010). The formation of irradiation-induced cross-linking is also reflected for the increase in modulus and hardness of the blends (see Table 11). This is because the modulus and hardness relate to the stiffness and rigidity of rubber (Banik and Bhowmick 2000).

4.4 Swelling Uptake and Cross-Link Density

Table 12 tabulates the swelling uptake and cross-link density of the blends. The swelling resistance and cross-link density of the blends increased over the irradiation doses. This is clear applying EB irradiation has induced cross-linking, providing the specimen with less penetration of solvent (Chattopadhyay et al. 2001). Pasbakhsh et al. (2012) previously reported that the swelling uptake gave an evidence of irradiation induced cross-linking.

4.5 Scanning Electron Microscopy (SEM)

Figure 15 illustrates the SEM images of the blends a 100× magnification. The SEM images of the samples agreed well with the results from tensile strength. Typical surface with an appearance of roughness and tearing lines was seen for unmodified blend (see Fig. 15a), indicating a certain energy was required for breaking the sample. Moreover, the surfaces of the specimen changed after applying EB irradiation, more roughness and tearing lines were visible (see Fig. 15b). The specimen altered cracking area, which brought to more resistance to failure and thus leading to an improvement in tensile strength.

The sample tended to be less tearing line and became smoother after 50 kGy of irradiation dose (see Fig. 15c–e). This exhibited that lower force was needed to start and propagate the cracks while stretching. Similar reports were discussed elsewhere (Banik and Bhowmick 2000; Zurina et al. 2008; Munusamy et al. 2009) regarding to the changes in SEM images of rubber sample after being exposed to EB irradiation.

4.6 Thermogravimetric Analysis (TGA)

Figures 16 and 17 shows the TG and DTG curves of the blends before and after EB irradiation. The raw output obtained from TG profiles is listed in Table 13. Two different regions of degradation were observed, one being due to the scission of NR (330–450 °C) and another is due to the degradation of w-EPDM (450–520 °C) (He

Table 12 Swelling and cross-link density of NR/R-EPDM blends before and after EB irradiation

Sample code	Swelling (%)	χ -link density ($\times 10^{-5}$ mol/cm ³)
Control	177.40 \pm 0.77	41.36 \pm 0.42
TBBS	157.38 \pm 0.65	48.77 \pm 0.29
CBS	143.83 \pm 0.45	57.85 \pm 0.18
TMTD	136.80 \pm 0.79	63.45 \pm 0.59
MBT	133.91 \pm 0.83	65.93 \pm 0.42

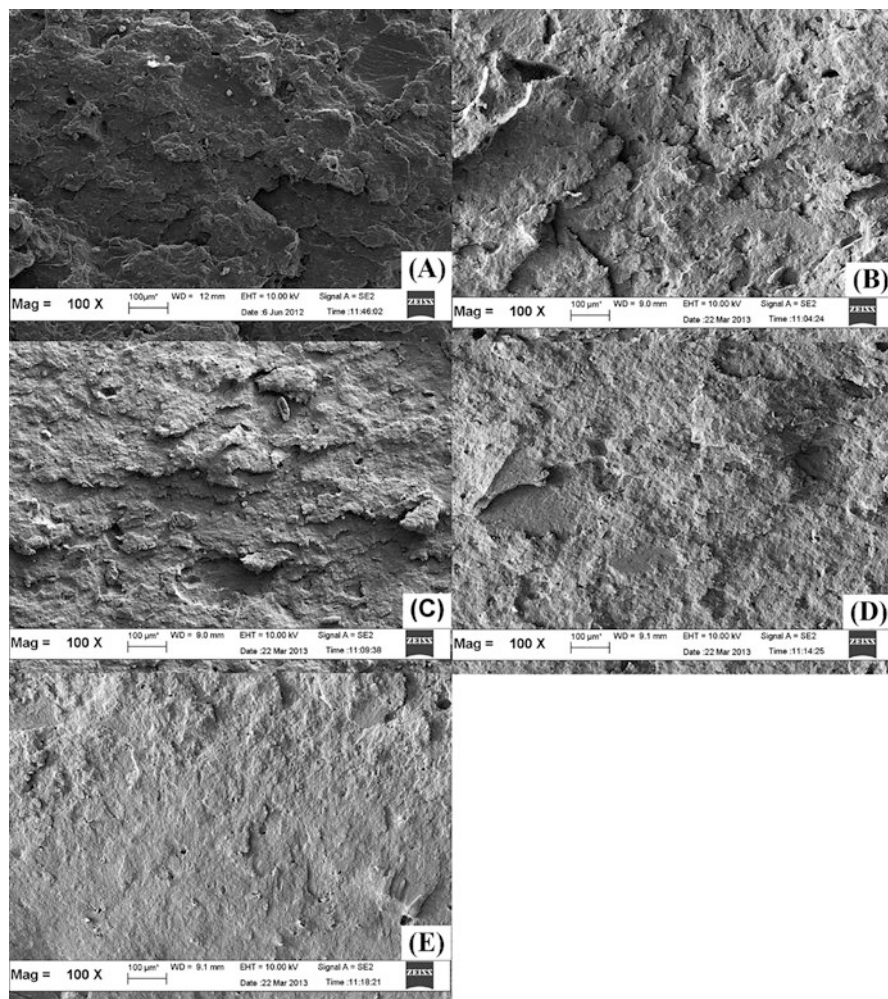


Fig. 15 SEM micrographs of tensile fractured surfaces of control (a) and irradiated NR/R-EPDM blends at 50 kGy (b), 100 kGy (c), 150 kGy (d), and 200 kGy (e) (100× magnification)

et al. 2011). It is noted that EB irradiation has influenced the thermal stability of the blends regardless of their decomposition at various weight loss or maximum weight loss. An improvement in thermal stability is simply because of their cross-linking induction after EB irradiation. This is because a higher temperature is required to decompose the cross-links. Moreover, there was also no change in the char residue of the blends as there was no additional filler added to the rubber formulation.

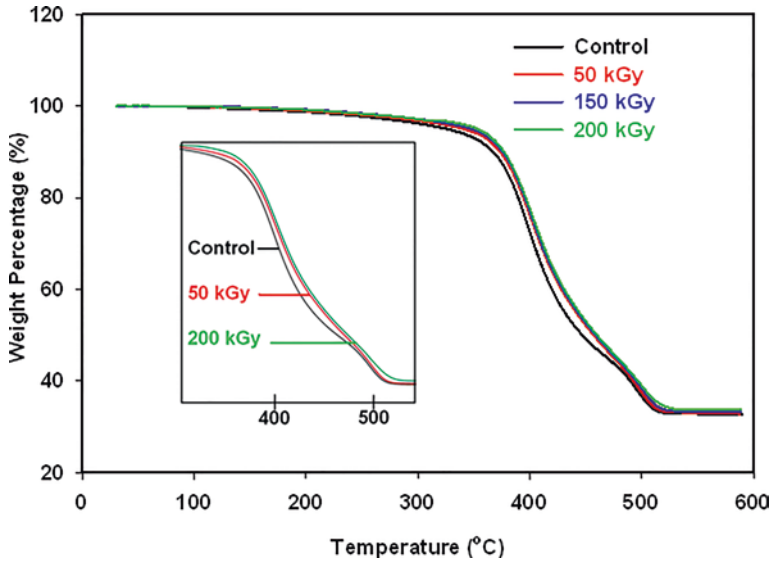


Fig. 16 TG curves of NR/R-EPDM blends before and after EB irradiation

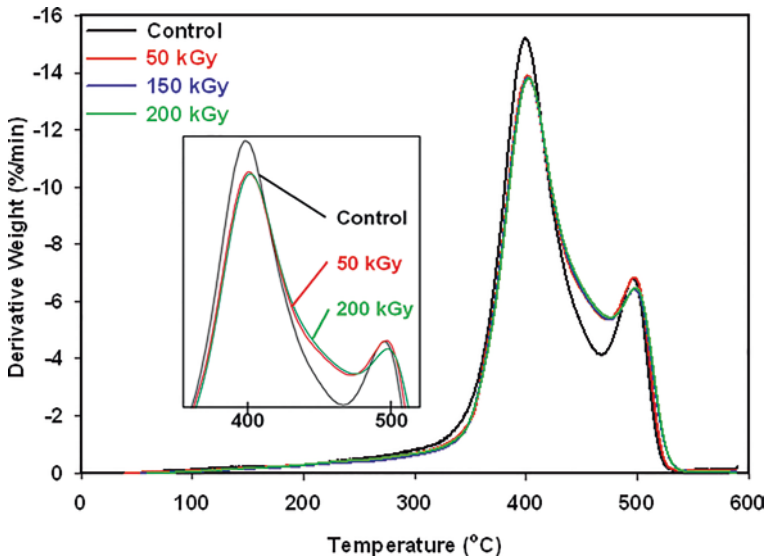


Fig. 17 DTG curves of NR/R-EPDM blends before and after EB irradiation

4.7 Activation Energy of Degradation Process

Coats–Redfern’s plots for the blends with and without EB irradiation are illustrated in Fig. 18. The values of activation energy are also summarized in Table 14. As been

Table 13 The decomposition temperature at various weight losses and stages, activation energy calculated from Coats-Redfern's equation and char residue (CR) of NR/R-EPDM blends before and after EB irradiation

Sample codes	The decomposition temperature (°C)						Char res. (%)
	T _{-10%}	T _{-30%}	T _{-50%}	T _{-60%}	T _{max I}	T _{max II}	
Control	367.18	403.58	446.97	489.75	399	487	33.6
50 kGy	373.43	409.31	456.92	492.50	401	496	33.8
100 kGy	374.76	410.19	457.97	493.93	402	498	33.7
150 kGy	375.85	410.32	458.86	495.05	402	498	33.2
200 kGy	377.05	411.73	460.17	496.73	403	499	33.7

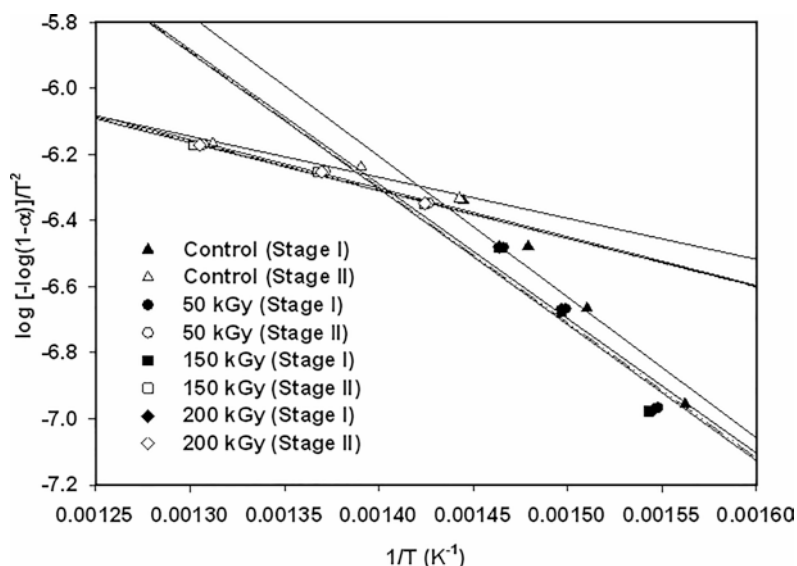


Fig. 18 Coats-Redfern's plot of NR/R-EPDM blends before and after EB irradiation

stated before that the blend between NR and w-EPDM provided the TG profiles with two stages of decomposition, i.e., NR phase (Stage I) and w-EPDM phase (Stage II). When calculating the activation energy, it is very clear that the values increased over the dose of EB irradiation. Previous discussion has reported that thermal stability was improved after EB irradiation. The data reported as activation energy are also the indication confirming their thermal stability irradiated blends. TMPTA is also the key role to enhance the thermal stability of rubber. It was also reported by Kader and Bhowmick (2003) that the special functional groups of TMPTA can help to generate more cross-links in the blends. Thereby, it enabled to reduce the bond breakage at the degradation temperature (He et al. 2011).

Table 14 Activation energy of NR/R-EPDM blends before and after EB irradiation calculated from Coats–Redfern’s equation

Sample codes	Activation energy (kJ/mol)	
	E_I	E_{II}
Control	69.24	20.23
50 kGy	70.91	25.56
100 kGy	71.89	25.91
150 kGy	72.04	26.15
200 kGy	72.06	26.31

4.8 Dynamic Mechanical Analysis (DMA)

Figure 19 illustrates the E' over the temperature of the blends. The raw data are also tabulated in Table 16.15. The values of E' at 25 °C increased over the dose of EB irradiation. Higher cross-linking degree after EB irradiation contributed to E' of the blends. The values of E' agreed well with the modulus and hardness of the blends. The mechanism behind such finding was reported by Akiba and Hashim (1997), the EB irradiation generates free radicals and initiates radical reactions, and this is very similar to peroxide curing system. The vulcanization of rubber by peroxide requires certain temperature to decompose the peroxide but it is not in the case of EB irradiation as it was performed at room temperature. An idealized mechanism regarding the formation of cross-link after EB irradiation was modified from Henning

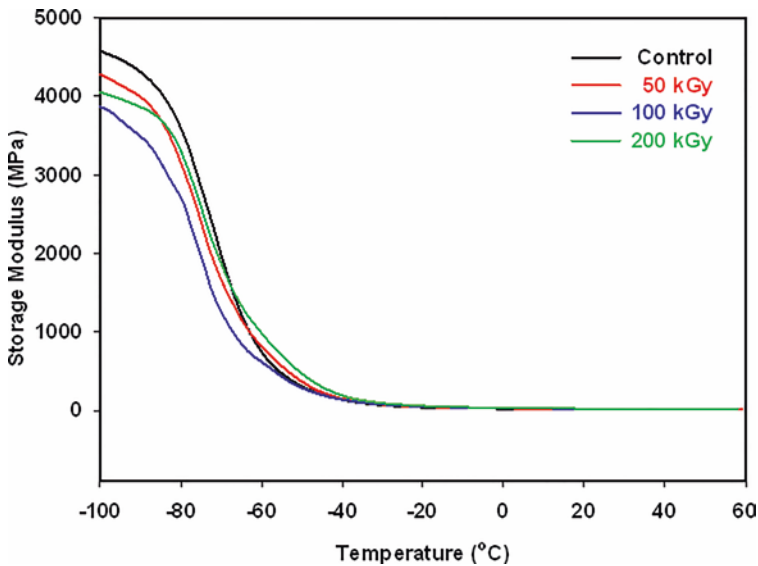


Fig. 19 Storage modulus as a function of temperature of NR/R-EPDM blends before and after EB irradiation

Table 15 Storage modulus (E') at 25 °C, maximum loss modulus (E''_{\max}) and damping factor ($\tan \delta_{\max}$), and the glass transition temperature (T_g) of NR/R-EPDM blends before and after EB irradiation

Sample codes	E' (MPa)	E''_{\max} (MPa)	$\tan \delta_{\max}$	T_g (°C) @ $\tan \delta_{\max}$
Control	21.65	721.18	0.5073	-50.67
50 kGy	21.77	663.10	0.5067	-50.38
100 kGy	22.32	585.91	0.4716	-49.98
200 kGy	23.68	585.31	0.4613	-49.63

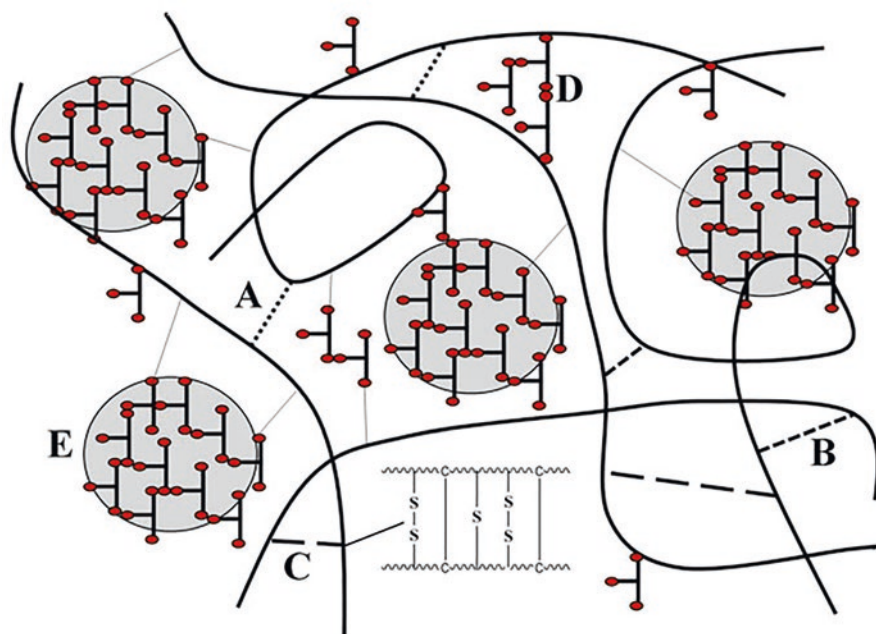


Fig. 20 Idealized network from EB irradiation curing in the presence of cross-linking promoter (TMPTA). Cross-links can be derived from (A) rubber radicals, (B) $-S_x-$ linkages, (C) mixed $-S_x-$ and $-C-C-$ linkages, (D) cross-linking promoter forming cross-links, and (E) thermoset domains of cross-linking promoter grafted to polymer chains. (Adapted from Henning 2007)

(2007) (see Fig. 20). Cross-links can be from rubber radicals (A), $-S_x-$ bonds (B), combined $-S_x-$ and $-C-C-$ bonds (C), cross-linking promoter forming cross-links (D), and thermoset domains of cross-linking promoter grafted to polymer chains (E). A cross-linking promoter or TMPTA provides effective radicals, whether to generate additional cross-links (Keller 1988) or to terminate non-network forming side reactions during irradiation process (Búcsi and Szócs 2000; García-Quesada and Gilbert 2000).

In the presence of EB irradiation, TMPTA enabled to form a high modulus filler-like domain together with the formation of co-cross-links of sulfidic ($-S_x-$) and carbon to carbon ($-C-C-$). This may result in an increase in the level of cross-linking. This finding contributed well to an increase in peak intensity from FT-IR at wavenumber of 1727.83 cm^{-1} ($C=O$ stretching vibrations). It is responsible to be due an interpenetrating network of filler-like cores or homopolymerized cross-link.

Figure 21 shows the E'' over the temperature range variation of the blends. It was observed that the E'' decreased over the dose of EB irradiation. Lower E'' indicates lower energy was stored and changed to heat. Thus, EB irradiation has helped to provide rubber with less heat build-up. This is simple due to the irradiation induced cross-linking as always stated at every point of the discussion. E'' of the blends showed quite a similar observation to the $\tan \delta$, as shown in Fig. 22. The results again verified that EB irradiation gave the rubber with low damping.

The T_g of the blends obtained from $\tan \delta_{\max}$ is also tabulated in Table 16.15. It is clear that the T_g of irradiated samples increased gradually. The T_g is direct indicators of cross-linking or network structures (Banik and Bhowmick 2000). Cross-linking obstructs the molecular deformation under cyclic tension; this kind of phenomenon requires higher heat to loosen the rubber chains. This has brought to an increase in the T_g of the blends.

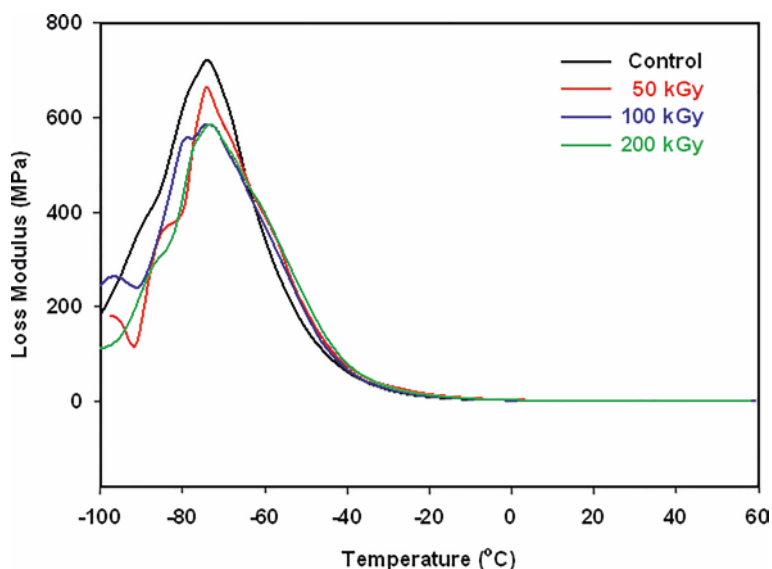


Fig. 21 Loss modulus as a function of temperature of NR/R-EPDM blends before and after EB irradiation

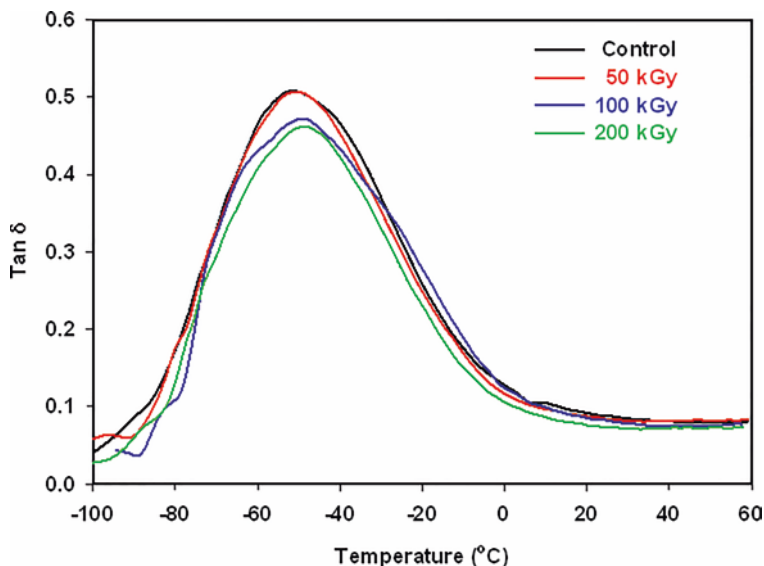


Fig. 22 Damping factor ($\tan \delta$) as a function of temperature of NR/R-EPDM blends before and after EB irradiation

5 Conclusions

5.1 Effect of Natural Rubber Latex

The use of NRL as a compatibilizer in the blends between NR and w-EPDM has improved the interfacial adhesion between these two phases. It had direct effect to the physical and mechanical properties as well as thermal stability and dynamic properties of the blends. The content of NRL at 30 phr gave an obvious effect to the properties of the blends. This content is therefore highly suggested to improve the compatibility of NR and w-EPDM.

5.2 Effect of Electron-Beam Irradiation

TMPTA plays very important role for the rubber exposed to EB irradiation. It helped to provide higher cross-linking to the rubber which later helped to improve the overall performance of the blends. These may include physical and mechanical properties as well as thermal stability and dynamic properties. The dose of EB irradiation of 50 kGy is recommended for this blending system to balance the overall properties of the blends.

References

- Akiba M, Hashim A (1997) Vulcanization and crosslinking in elastomers. *Prog Polym Sci* 22:475–521. [https://doi.org/10.1016/S0079-6700\(96\)00015-9](https://doi.org/10.1016/S0079-6700(96)00015-9)
- Awang M, Ismail H, Hazizan M (2008) Processing and properties of polypropylene-latex modified waste tyre dust blends (PP/WTD_{ML}). *Polym Test* 27:93–99. <https://doi.org/10.1016/j.polymertesting.2007.09.008>
- Banik I, Bhowmick AK (2000) Effect of electron beam irradiation on the properties of crosslinked rubbers. *Radiat Phys Chem* 58:293–298. [https://doi.org/10.1016/S0969-806X\(99\)00371-0](https://doi.org/10.1016/S0969-806X(99)00371-0)
- Belkahlia N, Saidi-Amroun N, Saidi M et al (2013) Influence of gamma radiation on electrical conduction of polyethylene terephthalate (PET) at ambient temperature. *Int J Polym Anal Charact* 18:15–24. <https://doi.org/10.1080/1023666X.2012.723854>
- Búcsi A, Szócs F (2000) Kinetics of radical generation in PVC with dibenzoyl peroxide utilizing high-pressure technique. *Macromol Chem Phys* 201:435–438. [https://doi.org/10.1002/\(SICI\)1521-3935\(20000201\)201:4<435::AID-MACP435>3.0.CO;2-C](https://doi.org/10.1002/(SICI)1521-3935(20000201)201:4<435::AID-MACP435>3.0.CO;2-C)
- Chakraborty S, Roy P, Pathak A et al (2011) Composition analysis of carbon black-filled polychloroprene rubber compound by thermo-oxidative degradation of the compound. *J Elastomers Plast* 43:499–508. <https://doi.org/10.1177/0095244311413442>
- Chattopadhyay S, Chaki T, Bhowmick AK (2001) Structural characterization of electron-beam crosslinked thermoplastic elastomeric films from blends of polyethylene and ethylene-vinyl acetate copolymers. *J Appl Polym Sci* 81:1936–1950. <https://doi.org/10.1002/app.1626>
- Coats A, Redfern J (1964) Kinetic parameters from thermogravimetric data. *Nature* 201:68–69. <https://doi.org/10.1038/201068a0>
- Coran A (1965) Vulcanization. Part VII. Kinetics of sulfur vulcanization of natural rubber in presence of delayed-action accelerators. *Rubb Chem Technol* 38:1–14. <https://doi.org/10.5254/1.3535628>
- Coran A (2003) Chemistry of the vulcanization and protection of elastomers: a review of the achievements. *J Appl Poly Sci* 87:24–30. <https://doi.org/10.1002/app.11659>
- Flory PJ, Rehner J Jr (1943) Statistical mechanics of cross-linked polymer networks II. Swelling. *J Chem Phys* 11:512–520. <https://doi.org/10.1063/1.1723791>
- Fukumori K, Matsushita M, Okamoto H et al (2002) Recycling technology of tire rubber. *JSAE Rev* 23:259–264. [https://doi.org/10.1016/S0389-4304\(02\)00173-X](https://doi.org/10.1016/S0389-4304(02)00173-X)
- García-Quesada J, Gilbert M (2000) Peroxide crosslinking of unplasticized poly (vinyl chloride). *J Appl Polym Sci* 77:2657–2666. [https://doi.org/10.1002/1097-4628\(20000919\)77:12<2657::AID-APP130>3.0.CO;2-G](https://doi.org/10.1002/1097-4628(20000919)77:12<2657::AID-APP130>3.0.CO;2-G)
- Hayemasae N, Ismail H, Azura AR (2013) Blending of natural rubber/recycled ethylene-propylene-diene monomer: cure behaviors and mechanical properties. *Polym Plast Technol Eng* 52:501–509. <https://doi.org/10.1080/03602559.2012.762020>
- He W, Jiang Y, Luyt A et al (2011) Synthesis and degradation kinetics of a novel polyester containing bithiazole rings. *Thermochimica Acta* 525:9–15. <https://doi.org/10.1016/j.tca.2011.07.015>
- Henning SK (2007) The use of coagents in the radical cure of elastomers. In: *The 56th international wire & cable symposium (IWCS conference™)*, Lake Buena Vista, 11–14 Nov 2007, pp 537–593
- Ishiaku U, Chong C, Ismail H (2000) Cure characteristics and vulcanizate properties of a natural rubber compound extended with convoluted rubber powder. *Polym Test* 19:507–521. [https://doi.org/10.1016/S0142-9418\(99\)00021-5](https://doi.org/10.1016/S0142-9418(99)00021-5)
- Ismail H, Mathialagan M (2012) Comparative study on the effect of partial replacement of silica or calcium carbonate by bentonite on the properties of EPDM composites. *Polym Test* 31:199–208. <https://doi.org/10.1016/j.polymertesting.2011.09.002>
- Ismail H, Nasaruddin MN, Rozman HD (1999) The effect of multifunctional additive in white rice husk ash filled natural rubber compounds. *Eur Polym J* 35:1429–1437. [https://doi.org/10.1016/S0014-3057\(98\)00223-7](https://doi.org/10.1016/S0014-3057(98)00223-7)

- Ismail H, Munusamy Y, Jaafar M et al (2008) Preparation and characterization of ethylene vinyl acetate (EVA)/natural rubber (SMR L)/organoclay nanocomposites: effect of blending sequences and organoclay loading. *Polym Plast Technol Eng* 47:752–761. <https://doi.org/10.1080/03602550802188599>
- Kader MA, Bhowmick AK (2003) Thermal ageing, degradation and swelling of acrylate rubber, fluororubber and their blends containing polyfunctional acrylates. *Polym Degrad Stab* 79:283–295. [https://doi.org/10.1016/S0141-3910\(02\)00292-6](https://doi.org/10.1016/S0141-3910(02)00292-6)
- Keller RC (1988) Peroxide curing of ethylene-propylene elastomers. *Rubber Chem Technol* 61:238–254. <https://doi.org/10.5254/1.3536185>
- Korkut T, Umaç ZI, Aygün B et al (2013) Neutron equivalent dose rate measurements of gypsum-waste tire rubber layered structures. *Int J Polym Anal Charact* 18:423–429. <https://doi.org/10.1080/1023666X.2013.814025>
- Kumar A, Dipak G, Basu K (2002) Natural rubber-ethylene propylene diene rubber covulcanization: effect of reinforcing fillers. *J Appl Polym Sci* 84:1001–1010. <https://doi.org/10.1002/app.10361>
- Munusamy Y, Ismail H, Mariatti M et al (2009) Effect of electron beam irradiation on the properties of ethylene-(vinyl acetate) copolymer/natural rubber/organoclay nanocomposites. *J Vinyl Add Technol* 15:39–46. <https://doi.org/10.1002/vnl.20174>
- Nabil H, Ismail H, Rashid AA (2012) Effects of partial replacement of commercial fillers by recycled poly(ethylene terephthalate) powder on the properties of natural rubber composites. *J Vinyl Add Technol* 18:139–146. <https://doi.org/10.1002/vnl.20291>
- Nabil H, Ismail H, Azura AR (2013a) Comparison of thermo-oxidative ageing and thermal analysis of carbon black-filled NR/virgin EPDM and NR/recycled EPDM blends. *Polym Test* 32:631–639. <https://doi.org/10.1016/j.polymertesting.2013.03.019>
- Nabil H, Ismail H, Azura AR (2013b) Effects of virgin ethylene-propylene-diene-monomer and its preheating time on the properties of natural rubber/recycled ethylene-propylene-diene-monomer blends. *Mater Des* 50:27–37. <https://doi.org/10.1016/j.matdes.2013.02.086>
- Noriman N, Ismail H, Ratnam C et al (2010) The effect of electron beam (EB) irradiation in presence of TMPTA on cure characteristics and mechanical properties of styrene butadiene rubber/recycled acrylonitrile-butadiene rubber (SBR/NBRr) blends. *Polym Plast Technol Eng* 49:228–236. <https://doi.org/10.1080/03602550903413805>
- Pasbakhsh P, Ismail H, Mohd Nor A et al (2012) Electron beam irradiation of sulphur vulcanised ethylene propylene diene monomer (EPDM) nanocomposites reinforced by halloysite nanotubes. *Plast Rubber Compos* 41:430–440. <https://doi.org/10.1179/1743289811Y.0000000058>
- Phadke A, Bhattacharya A, Chakraborty S et al (1983) Studies of vulcanization of reclaimed rubber. *Rubber Chem Technol* 56:726–736. <https://doi.org/10.5254/1.3538152>
- Rahman M, Hossain M, Alam M et al (2013) Addition of transition metals to improve physico-mechanical properties of radiation-vulcanized natural rubber latex films. *Int J Polym Anal Charact* 18:479–487. <https://doi.org/10.1080/1023666X.2013.785098>
- Rathnayake I, Ismail H, Azahari B et al (2012) Synthesis and characterization of nano-silver incorporated natural rubber latex foam. *Polym Plast Technol Eng* 51:605–611. <https://doi.org/10.1080/03602559.2012.659310>
- Ratnam CT, Nasir M, Baharin A et al (2001) Evidence of irradiation-induced crosslinking in miscible blends of poly (vinyl chloride)/epoxidized natural rubber in presence of trimethylolpropane triacrylate. *J Appl Polym Sci* 81:1914–1925. <https://doi.org/10.1002/app.1624>
- Roop S, Das A, Morozov IA, Stöckelhuber KW et al (2013) Influence of “expanded clay” on the microstructure and fatigue crack growth behavior of carbon black filled NR composites. *Compos Sci Technol* 76:61–68. <https://doi.org/10.1016/j.compscitech.2012.12.020>
- Senna MM, Hossain FM, El-Naggar AWM (2008) Compatibilization of low-density polyethylene/plasticized starch blends by reactive compounds and electron beam irradiation. *Polym Compos* 29:1137–1144. <https://doi.org/10.1002/pc.20393>
- Shanmugaraj A, Bhowmick AK (2003) Dynamic mechanical properties of styrene-butadiene rubber vulcanizate filled with electron beam modified surface-treated dual-phase filler. *J Appl Polym Sci* 88:2992–3004. <https://doi.org/10.1002/app.12067>

- Vijayabaskar V, Stephan M, Kalaivani S et al (2008) Influence of radiation temperature on the crosslinking of nitrile rubber by electron beam irradiation. *Radiat Phys Chem* 77:511–521. <https://doi.org/10.1016/j.radphyschem.2007.09.011>
- Zhao Q, Li X, Gao J (2007) Aging of ethylene-propylene-diene monomer (EPDM) in artificial weathering environment. *Polym Degrad Stab* 92:1841–1846. <https://doi.org/10.1016/j.polyimdegradstab.2007.07.001>
- Zurina M, Ismail H, Ratnam C (2008) The effect of HVA-2 on properties of irradiated epoxidized natural rubber (ENR-50), ethylene vinyl acetate (EVA), and ENR-50/EVA blend. *Polym Test* 27:480–490. <https://doi.org/10.1016/j.polymertesting.2008.02.001>

Effect of Metal Oxide Content on the Mechanical and Thermal Properties of Natural Rubber/Recycled Chloroprene Rubber Blends



Nabil Hayeemasae, Siti Zuliana Salleh, and Hanafi Ismail

1 Introduction

Blending of rubbers is advantageous method to give a balance set of final properties of rubber products. This method has given much interesting and is better than synthesizing new material when considering the economic scale and technical uncertainties (Sae-oui et al. 2007; Chang et al. 1999; El-Sabbagh 2003). Many types of rubbers have been blended and available in the market. NR is a good example used as blending component in various blends especially in tire application. NR provides many remarkable properties such as its highly mechanical strength and dynamic response. However, the application of NR is still constraint when requiring the heat and oil resistance. This is because an unsaturated molecular chains of NR, making it prone to oxidation and swollen in non-polar solvent.

To conquer all the disadvantages of NR, this rubber is then blended with other rubbers to have compromising performance such as ethylene propylene rubber (EPDM), nitrile rubber (NBR), and chloroprene rubber (CR). The chemical structure of CR is similar where the chlorine (Cl) atoms replaced on methyl groups. The presence of Cl makes CR more polarity as compared to NR. Blending CR and NR

N. Hayeemasae (✉)

Department of Rubber Technology and Polymer Science, Faculty of Science and Technology, Prince of Songkla University, Pattani Campus, Pattani, Thailand
e-mail: nabil.h@psu.ac.th

S. Z. Salleh

Department of Mechanical Engineering, Centre of Advanced Manufacturing and Material Processing (AMMP Centre), Faculty of Engineering, Universiti Malaya, Kuala Lumpur, Malaysia

H. Ismail

School of Materials and Mineral Resources Engineering, Engineering Campus, Universiti Sains Malaysia, Nibong Tebal, Penang, Malaysia

can help NR improved its solvent and thermal resistance. CR also lasts longer at high temperature; this makes CR difficult to degrade after period of usage which later causes abundance of rubber waste (Hayeemasae et al. 2013). Therefore, switching CR waste into processable form is challenging in relation to the continuous growth of CR market. This has brought to a focus to blend CR waste (w-CR) with other virgin rubbers to gain compromising properties obtained from both rubbers.

Blends of NR and w-CR were reported recently (Salleh et al. 2013, 2016), but the main aim was to focus on their curing and mechanical characteristics; they still faced few problems on the curing compatibility between NR and CR as these two rubbers are cured in different systems. Besides, the difference in polarity of NR and CR has also reduced the mechanical performance of the rubber blend. As a result, searching proper design of rubber formulation is very much concerned.

Considering the curing package of sulfur cured system, it is necessary to add metal oxide and fatty acid to act as rubber activator and to increase the cure rate of the compound. Commonly used activators are zinc oxide (ZnO) and stearic acid. There are other types of metal oxide that have been incorporated as activator such as calcium oxide (CaO), magnesium oxide (MgO), lead oxide (Pb₃O₄), and titanium dioxide (TiO₂) but previous report has mentioned that ZnO is suitable for sulfur vulcanization due to chemical reactivity of ZnO. ZnO can effectively form hydrocarbon-soluble zinc stearate during the onset of crosslinking (Heideman et al. 2005). Apart from their role as curing activator, metal oxide can also be used as curing agent in certain rubbers namely CR, CSM, polysulfides, and XNBR (Tinker 1995). In CR, MgO with combination of ZnO is normally added in the compounding formulation, such mixture can give better balance of curing and mechanical characteristics. From the aspect of cure compatibility of NR and CR, the combination of MgO and ZnO is still unexplored especially in the blend of NR and w-CR.

The point of this chapter was to report the mechanical properties and solvent resistance of NR/w-CR blends. Besides, an investigation was also to focus on the action of MgO and ZnO content on the blending performance. This work will give the readers better understanding on the action of MgO and ZnO in the NR/w-CR blends. In this chapter, effects of MgO and ZnO content on the curing properties, mechanical, and dynamic mechanical properties of the blends were reported.

2 Materials and Preparation of the Blends

Standard Malaysian rubber (SMR L) grade of NR was used and manufactured by Mardec Malaysia Sdn. Bhd. W-CR was rejected gloves that collected by Juara One Resources (M) Sdn. Bhd. The compounding ingredients of this rejected glove are shown in Table 1. W-CR was ground prior to be blended with NR. The size of w-CR was below 600 μm (US Standard mesh is 40). W-CR was in irregular shape as shown in Fig. 1. N330 grade of carbon black (CB) was supplied by EXCELKOS Sdn. Bhd., Selangor, Malaysia. Other ingredients such as ZnO, MgO, stearic acid, N-cyclohexyl-2-benzothiazole sulfenamide (CBS), tetramethylthiuram

Table 1 Compounding formulation used for preparing CR glove

Ingredients	Amount (phr)
60% w/w chloroprene rubber	100
25% w/w stabilizer	0.5
43% w/w colorant	0.4
30% w/w accelerator	0.2
11% w/w heat-sensitive agent	0.2
2% w/w thickener	0.2

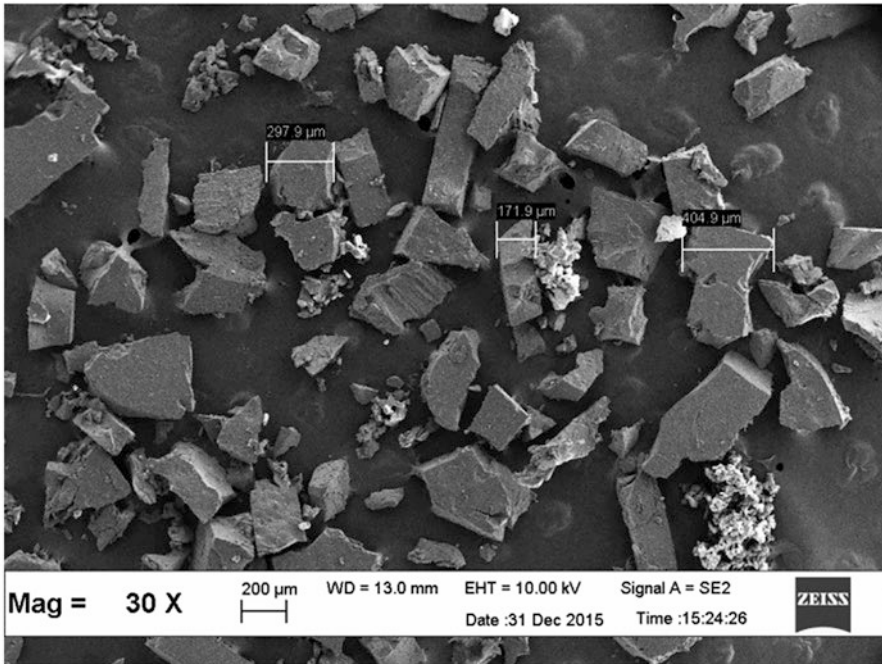


Fig. 1 SEM image for R-CR powder

monosulfide (TMTM), and sulfur were supplied by Bayer (M) Sdn. Bhd., Selangor, Malaysia.

Previous report highlighted that the blend ratio of NR/w-CR at 75/25 (phr/phr) has provided suitable properties (Salleh et al. 2013, 2016). Then, this ratio was selected for this experiment where the amount of other ingredients is listed in Table 2. The content of MgO and ZnO was varied while fixing the ratio of them. The entire amount of compounding ingredients was mixed on a two-roll mill (model XK-160) at room temperature. The respective compounds were then tested for their curing characteristics using a Monsanto Moving Die Rheometer (MDR 2000) and finally compression-molded.

Table 2 Compounding formulation of the blends prepared using various metal oxide contents

Ingredient	Content (phr)				
	M2Z5	M4Z10	M6Z15	M8Z20	M10Z25
Compounding codes					
NR	75	75	75	75	75
R-CR	25	25	25	25	25
CBS	1.0	1.0	1.0	1.0	1.0
TMTM	0.5	0.5	0.5	0.5	0.5
Stearic acid	3.0	3.0	3.0	3.0	3.0
Sulfur	2.5	2.5	2.5	2.5	2.5
CB	30.0	30.0	30.0	30.0	30.0
MgO	2.0	4.0	6.0	8.0	10.0
ZnO	5.0	10.0	15.0	20.0	25.0

Table 3 Curing characteristics of the blends prepared using various metal oxide contents

Compounding code	ts ₂ (min)	tc ₉₀ (min)	M _L (dN.m)	M _H (dN.m)	M _H -M _L (dN.m)
M2Z5	1.02	2.23	1.05	19.57	18.52
M4Z10	0.98	2.19	0.77	20.01	19.24
M6Z15	0.86	2.05	0.83	22.18	21.35
M8Z20	0.85	2.04	0.89	23.71	22.83
M10Z25	0.82	2.00	0.90	23.78	22.88

3 Properties of the Rubber Blends

3.1 Curing Characteristics

Effects of MgO and ZnO content on the curing characteristics of the blends are listed in Table 3. Higher amount of MgO and ZnO has caused to reduce the scorch time (ts₂) and curing time (tc₉₀) of the blends. This shows that MgO and ZnO have given full function as cure activator which can induce the crosslinking during vulcanization (Hernández et al. 2015; da Costa et al. 2003). In general, the vulcanization reaction starts from the reaction between ZnO and stearic acid to give zinc stearate. Then, zinc stearate produces free zinc ions to react further with accelerator. At this stage, a complex of activator and accelerator is formed and get ready to react with sulfur to form an active sulfuring agent (Heideman et al. 2004). Next, such agent reacts further with unsaturated backbones through allylic carbon and provides a crosslinking precursor. This precursor is very active and can bind with other precursors to complete crosslinking process (Heideman et al. 2004). Higher content of MgO and ZnO can give more active accelerator complexes and resulted to shorten the curing process. It is noted that tc₉₀ may not be significant at higher level of MgO and ZnO. This is because the content of stearic and accelerators is constant; the reactions of these two chemicals may be limited when excessing amount of MgO and ZnO was added.

MgO and ZnO are not only act as curing activator, but they also functioned as curing agent for w-CR (Zhang et al. 2010). Considering the curing mechanism in w-CR, it starts with the reaction of ZnO and Cl atoms in w-CR to give an active intermediate, which later react with another rubber to give carbon-carbon (C-C) crosslink through ether linkage (C-O-C) (Roy et al. 2016). Moreover, ZnCl_2 is produced in this reaction as by-product which can be an active catalyst to boost the vulcanization. However, such ZnCl_2 can also generate faster process of dehydrochlorination of w-CR leading to a deterioration of the rubber. Thus, MgO is incorporated to neutralize the hydrochloric acid (HCl) released while vulcanization and scavenges chloride ions that produced during the mixing, thereby limiting the amount ZnCl_2 (Desai et al. 2007). This is a good compromise between ZnO and MgO to optimize the suitable level of crosslinking distribution in the blends.

Minimum torque (M_L) was recorded in this work which indicates the compound's viscosity of the rubber. Highest value of M_L is found for the blend with 2/5 (phr/phr) of MgO/ZnO. This shows that adding MgO/ZnO at this content may interfere the processability to the compound. However, the process became easier when adding higher content of MgO/ZnO. For instance, in the blend with 4/10 (phr/phr) of MgO/ZnO, it provided lowest M_L compared to the other variations. This may be the optimum content of MgO/ZnO to make processing easier in the blend. As the content of MgO/ZnO increased, the value of maximum torque (M_H) continuously increased due to its dilution effect, this is because both MgO and ZnO can act as filler beside being curative in the rubber formulation. Hence, higher level of MgO/ZnO has led to increase the stiffness of the blend and lead to higher restriction of molecular movement.

Another reason may be attributed to a faster formation of reactive sulfur complexes promoted by MgO and ZnO which later increases the degree of crosslinking in the vulcanizates. When considering only NR, its vulcanization happens in the presence of sulfur and is also activated by metal oxide and fatty acid. In this experiment, the presence of MgO and ZnO could form an active complex with accelerator and sulfur while vulcanization. This results to an increase in crosslinking (Sahoo et al. 2007). Moreover, an increase in M_H can also be contributed to the reduction in elastic phase as MgO and ZnO are rigid in nature. Therefore, the stiffness of the compound increases over the addition of MgO and ZnO.

3.2 Mechanical Properties

Tensile properties were carried out using a universal tensile machine (UTM) based on ASTM D412. The outputs received from UTM were tensile modulus at given strain, elongation at break, and tensile strength (see Table 4). The tensile strength increased up to the content of MgO/Zn at 4/10 (phr/phr). After that, the values decreased over the addition of MgO and ZnO. As been stated previously, MgO and ZnO can function as high modulus filler and cure activator, a reason at this point is their significance as reinforcing roles of combined MgO and ZnO at 4/10 (phr/phr).

Table 4 Mechanical properties of the blends prepared using various metal oxide contents

Compounding designation	Tensile strength (MPa)	Elongation at break (%)	M100 (MPa)	M300 (MPa)	Hardness (Shore A)
M2Z5	18.86 ± 0.56	537.23 ± 2.10	2.72 ± 0.03	9.52 ± 0.05	62
M4Z10	18.97 ± 0.42	520.57 ± 1.98	3.19 ± 0.02	10.06 ± 0.04	65
M6Z15	17.37 ± 0.63	473.87 ± 3.25	3.55 ± 0.03	10.61 ± 0.03	66
M8Z20	17.06 ± 0.44	452.23 ± 4.12	3.82 ± 0.05	11.13 ± 0.05	68
M10Z25	15.51 ± 0.34	446.10 ± 3.97	3.98 ± 0.03	11.52 ± 0.07	69

Therefore, the addition of both MgO and ZnO into the blend can lead to give better rubber-filler interactions and enhances the interfacial adhesion between NR and w-CR which later increased the tensile strength. Improved rubber-filler interaction is mainly because of the function of MgO and ZnO as filler; it may disperse well in such content, providing more interfacial contact to the rubber blends.

The decrease of tensile strength at higher content of MgO and ZnO is responsible to the tendency of these metal oxides to agglomerate due to their filler-filler interactions (Nabil et al. 2013a). Uneven distribution of MgO and ZnO may lead to less homogenization within the rubber blends (Sae-Oui et al. 2008). This agreed well with other work, which showed the similar finding when high content of inorganic filler was added to the rubber matrix (Intiya et al. 2017).

As for the elongation at break, MgO and ZnO had brought to a reduction in elasticity of the blends. This is due to a so-called dilution effect where there is less portion of deformable phase (Zhang et al. 2009). The rigid phase of MgO and ZnO occupied the elastic phase in the rubber molecules and hence restrict the movement of rubber chains. More evidence can also be observed from the tensile modulus and hardness. Similar trend of modulus at 100% and 300% elongation (M100 and M300, respectively) and hardness was shown. The presence of MgO and ZnO caused the blends stiffer than ever. Despite acting as an activator, a crosslinker for CR phase, and fillers, their role as filler dominates other functions. Thus, MgO and ZnO acted effectively as filler to increase modulus and hardness of the blends.

3.3 Fatigue Life

Monsanto fatigue-to-failure tester was used as a tool to determine fatigue life of rubber blends with repeated cyclic strain at 100 cpm and 2.01 ± 0.05 extension ratio according to JIS K 6270. The calculated fatigue life values of the rubber blends are listed in Table 5. It was observed that the blend at 4/10 (phr/phr) of MgO/ZnO received an optimum value of fatigue life, and after this content, the values decreased over the content of MgO/ZnO. Adding the MgO and ZnO at this content enabled to enhance rubber-filler interaction and crosslinking formation to the blend, giving a higher resistance toward the cyclic stretching. However, a decrease of fatigue life a

Table 5 Fatigue life of the blends prepared using various metal oxide contents

Compounding code	Fatigue life (kc)
M2Z5	187.1 ± 2.12
M4Z10	190.5 ± 2.56
M6Z15	148.4 ± 3.21
M8Z20	137.7 ± 2.02
M10Z25	100.8 ± 1.91

Table 6 Swelling and crosslink density of the blends prepared using various metal oxide contents

Compounding code	Swelling uptake (%)	Crosslink density ($\times 10^{-5}$ mol/cm ³)
M2Z5	186.73 ± 2.11	4.40 ± 0.54
M4Z10	150.92 ± 3.24	10.84 ± 0.93
M6Z15	146.44 ± 3.85	12.86 ± 0.62
M8Z20	140.58 ± 3.98	14.03 ± 0.19
M10Z25	137.85 ± 2.74	15.36 ± 0.71

high content of MgO and ZnO is related to an increase in filler–filler interaction which make them agglomerated (Nabil et al. 2013a). This has brought to early failure to the rubber sample while cyclic stretching and thus leading to reduce the fatigue life of the blends.

3.4 Swelling Behavior

Swelling uptake was tested for the vulcanizates and the raw data from the swelling test were applied for calculation of crosslink density according to the Flory–Rehner equation (Flory and Rehner 1943). The results of swelling uptake and crosslink density of the blends are listed in Table 6. It is known that the swelling uptake is related to the crosslink density (Sae-oui et al. 2007), and higher crosslink density is from the less swollen sample (Mathialagan and Ismail 2012). Therefore, incorporation of MgO and ZnO has made the samples less swelling due to dilution effect as described earlier. When more rigid phase was added to the rubber formulation, it reduced the elastic phase. Reducing elastic component has then decreased the possibility of solvent to penetrate and to swell the rubber sample.

When calculating the crosslink density, the crosslink density increased over the addition of MgO and ZnO. As metal oxide used in this experiment can also function as cure activator, it can enhance the state of cure and finally increase the crosslinking degree of the rubber blends. The values of crosslink density correlated well with the torque difference (see $M_H - M_L$). This finding supports the assumption of MgO and ZnO as an activator and crosslinking agent in NR/w-CR blends.

3.5 Scanning Electron Microscopy (SEM)

The SEM images of the rubber samples were captured from the tensile-fractured surfaces. The fractured samples were coated with gold palladium to avoid a charge while scanning. Figure 2 shows the SEM images of the rubber blends. Two different images are shown to discuss their surfaces at similar content of MgO/ZnO. Figure 2a, d

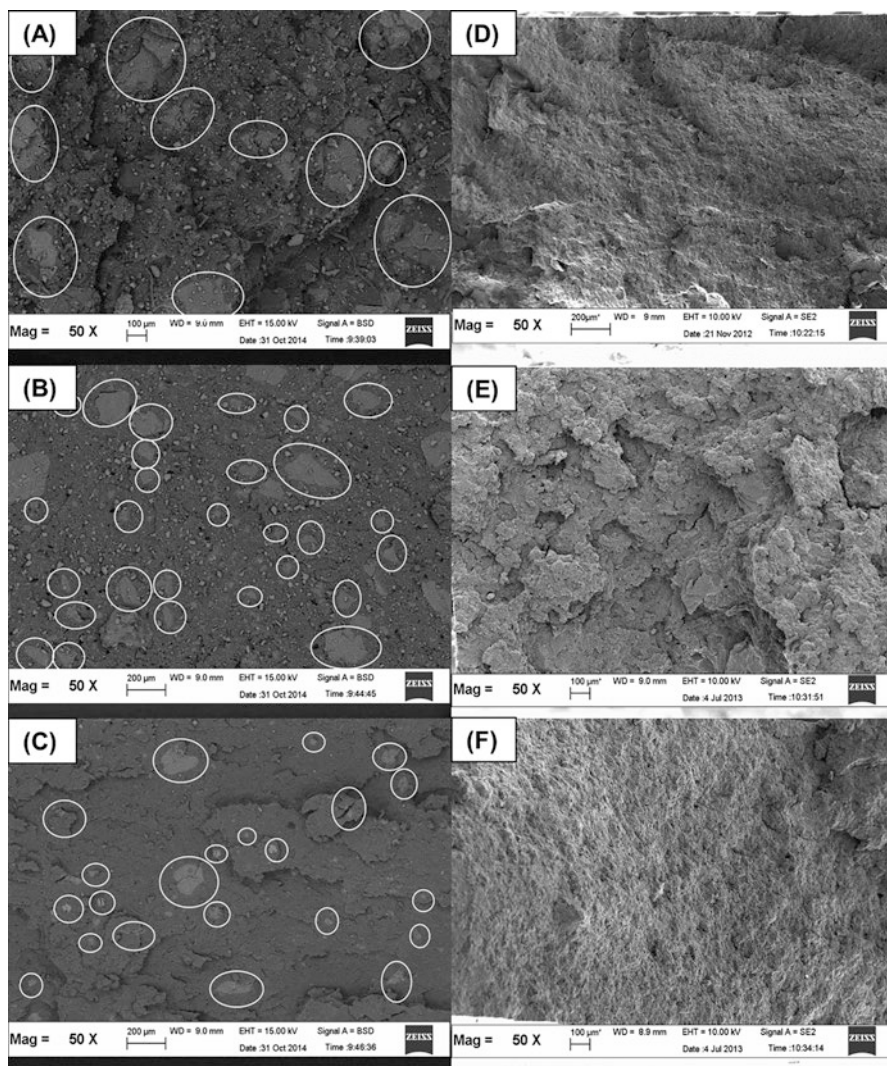


Fig. 2 Backscattered SEM of the tensile-fractured surfaces of the blends prepared using various metal oxide contents. (a) M2Z5, (b) M4Z10, and (c) M10Z25 and secondary electrons SEM of the tensile-fractured surfaces of (d) M2Z5, (e) M4Z10, and (f) M10Z25

show the images of the blend at 2//5 (phr/phr) of MgO/ZnO. Non-homogeneous dispersion of w-CR throughout the NR matrix and smooth surface is seen, indicating that lower force may be required to failure. Figure 2b shows the image of the blends at 4/10 (phr/phr) of MgO/ZnO. Rougher surface and tearing lines are seen, indicating that higher energy was needed to break the sample. This agreed well to the fractured surface seen in Fig. 2e, which showed a broader tortuous path. The SEM images supported that the ability of MgO and ZnO enhances the dispersion and interaction between w-CR and NR phases which resulting to higher values of tensile strength. However, when higher content of MgO and ZnO was added, i.e., 10/25 (phr/phr), both MgO and ZnO tended to agglomerate each other due to the strong filler network. This is seen in Fig. 2c, f, suggesting that low force is required for failure in the specimen. Higher possibility of forming the filler network is contributed for a decrement in tensile strength.

3.6 Thermogravimetric Analysis (TGA)

A Perkin–Elmer Pyris 6 TGA analyzer was used for the thermogravimetric analysis of the rubber blends. The analysis initiated from 30 °C to 600 °C at a heating rate of 20 °C/min in nitrogen gas. The TG and DTG curves were plotted and shown in Figs. 3 and 4. The raw data received from TG profiles such as decomposition temperature at various weight loss, various stages, and their residue are listed in Table 7.

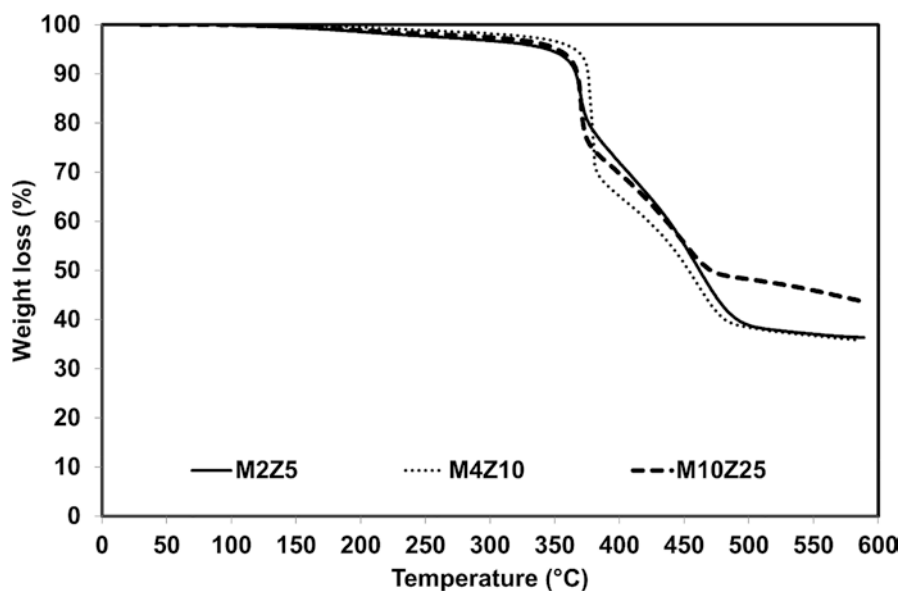


Fig. 3 TG curves of the blends prepared using various metal oxide contents

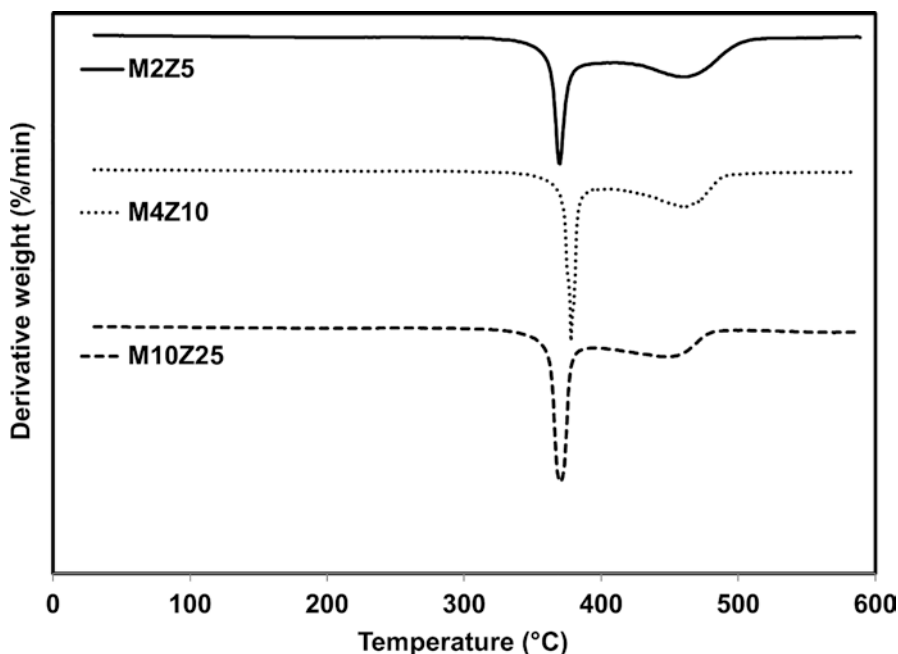


Fig. 4 DTG curves of the blends prepared using various metal oxide contents

Table 7 Thermal decomposition parameter properties of the blends prepared using various metal oxide contents

Thermal properties	M2Z5	M4Z10	M10Z25
$T_{5\%}$ (°C)	344	366	352
$T_{10\%}$ (°C)	366	376	367
$T_{30\%}$ (°C)	399	406	383
$T_{50\%}$ (°C)	462	471	454
$T_{\max I}$ (°C)	370	378	370
$T_{\max II}$ (°C)	459	458	448
Char residue (%)	36.34	35.89	43.69

From the results observed, a very minor mass loss at approximately 150–300 °C was due to the presence of volatile matters such as moisture, stearic acid, and other unreacted substances (Tomer et al. 2007). Beyond such temperatures, there are two regions of thermal degradation observed from TG and DTG curves. First maximum weight loss was responsible to degradation of NR which observed at the temperature range of 350 °C to 400 °C. The second maximum weight loss is relative to the degradation of w-CR and leftover diene after the first stage of degradation. Such steps of degradation were shifted to higher temperature when adding higher content of MgO and ZnO. It affected the decomposition temperature at 5%, 10%, 30%, and 50% weight loss of the blend. The blend at 4 phr of MgO and 10 phr ZnO showed

the most thermally stable at the onset of decomposition. The decomposition temperature of such blend showed very significant particularly at the decomposition temperature of 5% and 10% of weight loss ($T_{5\%}$ and $T_{10\%}$, respectively). The role of MgO and ZnO as cure activator may provide the rubber blends with higher cross-linking which therefore increased the thermal stability of the blends. Another possible reason may be due to the chemical nature of MgO and ZnO. It is known that both MgO and ZnO are considered as inorganic substance, when these two metal oxides dispersed all over the rubber matrices, it can protect the sample from losing their weight while heating due to their high thermal stability. Higher content of MgO and ZnO acts as barrier to reduce the heat transfer which hinders the additive decomposition at lower temperature.

It is interesting to note that the temperature of second maximum weight loss was decreased at highest content of MgO and ZnO (M10Z25). In general, Zn-stearate is defined as a strong Lewis acidity which enables to increase the possibility of dehydrochlorination reaction to w-CR (Liu et al. 2007; Benavides et al. 1995). Therefore, higher content of ZnO is used; there is a high tendency of dehydrochlorination taken place (Kameda et al. 2008). It is well-recognized that dehydrochlorination would result to decrease the thermal stability of CR.

Furthermore, the MgO and ZnO content greatly affected the char residue at all rubber formulations. As the MgO and ZnO are inorganic in nature which possess high thermal stability, the amount of char depends on content of filler, in this case, MgO and ZnO (Chakraborty et al. 2011). Both MgO and ZnO are thermally stable up to 1000 °C. Hence, more residue is left at the end of testing temperature.

3.7 Dynamic Mechanical Analysis (DMA)

Dynamic mechanical analysis (DMA) was studied using a Perkin-Elmer DMA7 to obtain the results of the storage modulus (E') and damping characteristic ($\tan \delta$). The samples were subjected to tension mode with the force amplitude of 0.1 N at a frequency of 10 Hz. The E' of the blends is plotted and shown in Fig. 5 where other data obtained from DMA are also tabulated in Table 8. Three different regions of E' were shown namely a glassy zone below the glass transition temperature (T_g), a transition zone where E' value is reduced over the temperature, and a rubbery region where the samples behave as elastic material. E' values at room temperature are selected and shown in Table 8; it revealed that the E' values of the blends increased over the content of MgO and ZnO. E' is related to the degree of elasticity and cross-link density of the sample (Sae-oui et al. 2007; Nabil et al. 2013b); this is clear that elastic response was significant in the presence of MgO and ZnO which can be attributed to a higher crosslinking degree imparted by MgO and ZnO. An increase of E' in the blends correlated well with the previous findings such as the calculated crosslink density, torque difference, and tensile modulus.

$\tan \delta$ is a crucial characteristic to discuss as it is indirectly related to the elastic response of the vulcanizate. The factors relating to this result are the nature of

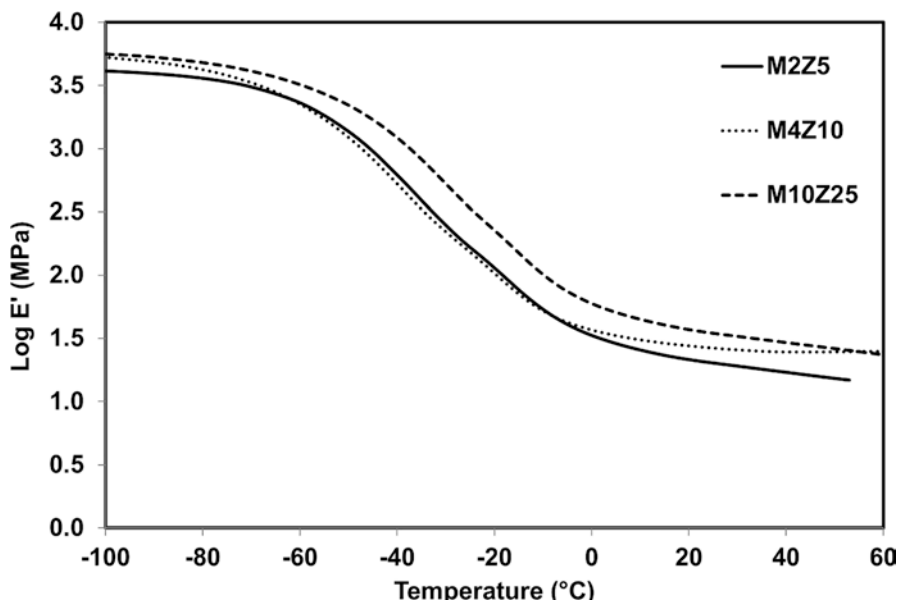


Fig. 5 Storage modulus of the blends prepared using various metal oxide contents

Table 8 Thermal decomposition parameters of the blends containing various types of fillers

Compounding codes	Log E' at 25 °C (MPa)	tan δ_{\max}		T_g @ tan δ_{\max} (°C)	
		tan $\delta_{\max I}$	tan $\delta_{\max II}$	tan $\delta_{\max I}$	tan $\delta_{\max II}$
M2Z5	1.30	0.66	0.48	-40.90	-19.98
M4Z10	1.42	0.60	0.45	-39.10	-16.17
M10Z25	1.55	0.52	0.42	-35.47	-14.05

rubber matrix (NR or w-CR), the nature of interphase (b), the frictional damping between matrix interphases (c), and the energy dissipation in the catastrophic area (d) (Heideman et al. 2004). Variation of tan δ over the temperature is illustrated in Fig. 6, and the respective values are tabulated in Table 8. It is significant that the blends at low content of MgO and ZnO provided higher tan δ_{\max} value. Higher value of tan δ_{\max} indicates higher damping characteristics. Damping indicates the elastic response of the vulcanizate; high damping leads to a low elastic response. Here, it agreed well to the previous discussion on E' value of the vulcanizate. Moreover, the value of tan δ decreased over the content of MgO to ZnO. Increasing MgO and ZnO content has provided the blends with higher crosslinking degree. Such crosslinking network has helped the rubber chain stored the energy and recovered well under cyclic tension, and hence lowering the damping characteristics.

The T_g can also be selected by the temperature at the maximum peak of tan δ . Two peaks are found based on the T_g of NR and w-CR. It is significantly observed that T_g of the blends increases over the content of MgO and ZnO. The T_g of NR phase increased from -40.9 °C (M2Z5) to -36.6 °C (M4Z10) and -35.5 °C

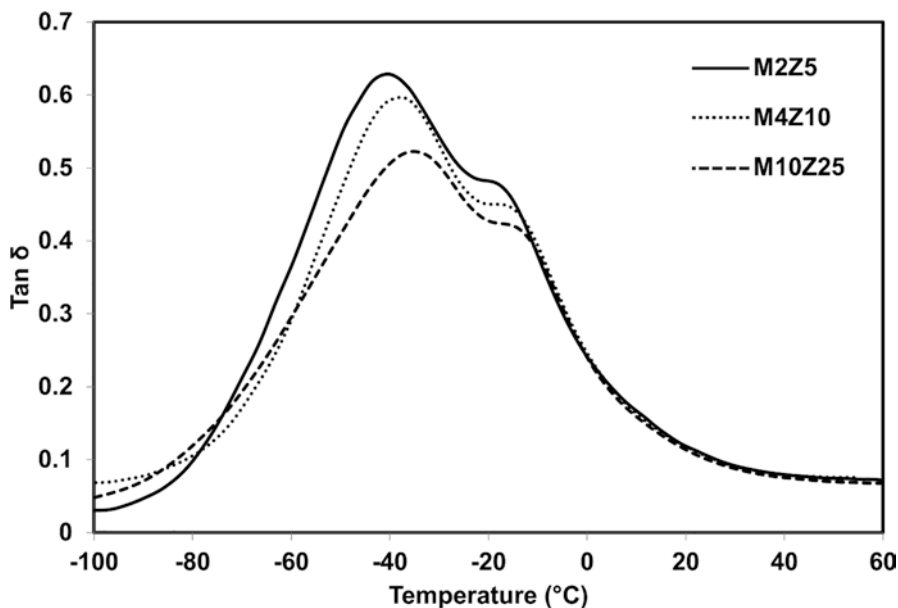


Fig. 6 Tan δ of the blends prepared using various metal oxide contents

(M10Z25) respectively while the T_g of w-CR phase increased from -18.7 °C (M2Z5) to -14.5 °C (M4Z10) and -14.1 °C (M10Z25) consecutively. The shifting of T_g is greatly attributed to the high entanglement and crosslink density assisted by the presence of MgO and ZnO. This has brought to a high molecular restriction. Thus, higher temperature is needed to move the rubber chain while cyclic tension. Any type of additive that can restrict the movement of molecular chain would result to a shift in T_g . A similar observation was found and discussed previously by Ramesan et al. (2001). It was reported that trapped drubber or occluded drubber is contributed to the change in the T_g .

4 Conclusions

MgO and ZnO effectively influenced the cure characteristics of the blends. M_H was observed to be higher for the blends having higher content of MgO and ZnO. The tensile strength and elongation at break of the blends increased up to the amount at 4/10 (phr/phr) of MgO/ZnO. The E' and tan δ correlated well to the calculated crosslink density, torque different, and tensile modulus. The glass transition temperature (T_g) received from damping factor (tan δ) shifted to a higher temperature toward the addition of MgO and ZnO. This was due to the higher molecular restriction when higher content of MgO to ZnO is added. As seen from overall properties, the content of MgO to ZnO at 4/10 (phr/phr) is highly recommended to

compound NR/w-CR blends. It is applicable for the rubber products that required high strength and thermal stability. Apart from that, the use of w-CR can cheapen the manufacturing cost which results to eliminate CR waste.

References

- Benavides R, Edge M, Allen NS et al (1995) The mode of action of metal stearate stabilisers in poly (vinyl chloride). III. Influence of pre-heating on polyene formation and secondary reactions. *Poly Degrad Stab* 48:377–385. [https://doi.org/10.1016/0141-3910\(95\)00086-2](https://doi.org/10.1016/0141-3910(95)00086-2)
- Chakraborty S, Roy P, Pathak A et al (2011) Composition analysis of carbon black-filled polychloroprene rubber compound by thermo-oxidative degradation of the compound. *J Elast Plast* 43:499–508. <https://doi.org/10.1177/0095244311413442>
- Chang YW, Shin YS, Chun H et al (1999) Effects of trans-polyoctylene rubber (TOR) on the properties of NR/EPDM blends. *J Appl Polym Sci* 73:749–756. [https://doi.org/10.1002/\(SICI\)1097-4628\(19990801\)73:5<749::AID-APP15>3.0.CO;2-S](https://doi.org/10.1002/(SICI)1097-4628(19990801)73:5<749::AID-APP15>3.0.CO;2-S)
- da Costa HM, Abrantes TAS, Nunes RCR et al (2003) Design and analysis of experiments in silica filled natural rubber compounds-effect of castor oil. *Polym Test* 22:769–777. [https://doi.org/10.1016/S0142-9418\(03\)00011-4](https://doi.org/10.1016/S0142-9418(03)00011-4)
- Desai H, Hendrikse KG, Woolard CD (2007) Vulcanization of polychloroprene rubber. I A revised cationic mechanism for ZnO crosslinking. *J Appl Polym Sci* 105:865–876. <https://doi.org/10.1002/app.23904>
- El-Sabbagh SH (2003) Compatibility study of natural rubber and ethylene-propylene diene rubber blends. *Polym Test* 22:93–100. [https://doi.org/10.1016/S0142-9418\(02\)00056-9](https://doi.org/10.1016/S0142-9418(02)00056-9)
- Flory PJ, Rehner J Jr (1943) Statistical mechanics of cross-linked polymer networks II. Swelling. *J Chem Phys* 11:512–520. <https://doi.org/10.1063/1.1723791>
- Hayemasae N, Ismail H, Azura AR (2013) Blending of natural rubber/recycled ethylene-propylene-diene monomer: cure behaviors and mechanical properties. *Polym Plast Technol Engineer* 52:501–509. <https://doi.org/10.1080/03602559.2012.762020>
- Heideman G, Datta RN, Noordermeer JWM et al (2004) Activators in accelerated sulfur vulcanization. *Rubb Chem Technol* 77:512–541. <https://doi.org/10.5254/1.3547834>
- Heideman G, Datta RN, Noordermeer JWM et al (2005) Influence of zinc oxide during different stages of sulfur vulcanization. Elucidated by model compound studies. *J Appl Polym Sci* 95:1388–1404. <https://doi.org/10.1002/app.21364>
- Hernández M, Valentín JL, López-Manchado MA et al (2015) Influence of the vulcanization system on the dynamics and structure of natural rubber: comparative study by means of broadband dielectric spectroscopy and solid-state NMR spectroscopy. *Euro Polym J* 68:90–103. <https://doi.org/10.1016/j.eurpolymj.2015.04.021>
- Intiya W, Thepsuwan U, Sirisinha C et al (2017) Possible use of sludge ash as filler in natural rubber. *J Mater Cycles Waste Manag* 19:774–781. <https://doi.org/10.1007/s10163-016-0480-5>
- Kameda T, Watanabe Y, Grause G et al (2008) Dehydrochlorination behavior of polychloroprene during thermal degradation. *Thermochim Acta* 476:28–32. <https://doi.org/10.1016/j.tca.2008.07.004>
- Liu YB, Liu WQ, Hou MH (2007) Metal dicarboxylates as thermal stabilizers for PVC. *Poly Degrad Stab* 92:1565–1571. <https://doi.org/10.1016/j.polymdegradstab.2007.05.003>
- Mathialagan M, Ismail H (2012) Optimization and effect of 3-aminopropyltriethoxysilane content on the properties of bentonite-filled ethylene propylene diene monomer composites. *Polym Compos* 33:1993–2000. <https://doi.org/10.1002/pc.22340>
- Nabil H, Ismail H, Azura AR (2013a) Compounding, mechanical and morphological properties of carbon-black-filled natural rubber/recycled ethylene-propylene-diene-monomer (NR/R--EPDM) blends. *Polym Test* 32:385–393. <https://doi.org/10.1016/j.polymertesting.2012.11.003>

- Nabil H, Ismail H, Azura AR (2013b) Effects of virgin ethylene-propylene-diene-monomer and its preheating time on the properties of natural rubber/recycled ethylene-propylene-diene-monomer blends. *Mater Design* 50:27–37. <https://doi.org/10.1016/j.matdes.2013.02.086>
- Ramesan MT, Mathew G, Kuriakose B et al (2001) Role of dichlorocarbene modified styrene butadiene rubber in compatibilisation of styrene butadiene rubber and chloroprene rubber blends. *Euro Polym J* 37:719–728. [https://doi.org/10.1016/S0014-3057\(00\)00157-9](https://doi.org/10.1016/S0014-3057(00)00157-9)
- Roy K, Alam MN, Mandal SK et al (2016) Development of a suitable nanostructured cure activator system for polychloroprene rubber nanocomposites with enhanced curing, mechanical and thermal properties. *Polym Bull* 73:191–207. <https://doi.org/10.1007/s00289-015-1480-7>
- Sae-oui P, Sirisinha C, Hatthapanit K (2007) Effect of blend ratio on aging, oil and ozone resistance of silica-filled chloroprene rubber/natural rubber (CR/NR) blends. *Express Polym Lett* 1:8–14. <https://doi.org/10.3144/expresspolymlett.2007.3>
- Sae-Oui P, Sirisinha C, Hatthapanit K et al (2008) Influence of magnesium carbonate loading on the compound properties of polychloroprene, natural rubber, and their blends. *J Appl Polym Sci* 110:2763–2769. <https://doi.org/10.1002/app.28786>
- Sahoo S, Maiti M, Ganguly A et al (2007) Effect of zinc oxide nanoparticles as cure activator on the properties of natural rubber and nitrile rubber. *J Appl Polym Sci* 105:2407–2415. <https://doi.org/10.1002/app.26296>
- Salleh SZ, Ismail H, Ahmad Z (2013) Study on the effect of virgin and recycled chloroprene rubber (vCR and rCR) on the properties of natural rubber/chloroprene rubber (NR/CR) blends. *J Polym Eng* 33:803–811. <https://doi.org/10.1515/polyeng-2013-0127>
- Salleh SZ, Ismail H, Ahmad Z (2016) Properties of natural rubber latex-compatible natural rubber/recycled chloroprene rubber blends. *J Elast Plast* 48:640–655. <https://doi.org/10.1177/0095244315613620>
- Tinker AJ (1995) Distribution of crosslinks in vulcanized blends. *Rubb Chem Technol* 68:461–480. <https://doi.org/10.5254/1.3538751>
- Tomer NS, Delor-Jestin F, Singh RP et al (2007) Cross-linking assessment after accelerated ageing of ethylene propylene diene monomer rubber. *Poly Degrad Stab* 92:457–463. <https://doi.org/10.1016/j.polymdegradstab.2006.11.013>
- Zhang P, Huang G, Liu Z (2009) An effect of OMMT on the anti-reversion in NR/CR blend system. *J Appl Polym Sci* 111:673–679. <https://doi.org/10.1002/app.28882>
- Zhang P, Huang G, Wang X et al (2010) The influence of montmorillonite on the anti-reversion in the rubber-clay composites. *J Appl Polym Sci* 118:306–311. <https://doi.org/10.1002/app.32343>

Chloroprene Rubber Waste as Blend Component with Natural Rubber, Epoxidized Natural Rubber, and Styrene Butadiene Rubber



Nabil Hayeemasae, Siti Zuliana Salleh, and Hanafi Ismail

1 Introduction

Earlier efforts on the disposal of rubber waste have been incineration, pyrolysis, and landfills which will end up with environmental issues. Therefore, the development of effective methods to recycle rubber has been keen challenge (Alassali et al. 2018; Hou et al. 2018; Prathiba et al. 2018). Recently, many rubber industries have been forced to include rubber waste in their products to compromise between cost and environmental aspects (Ghavipankeh et al. 2018; Rooj et al. 2011). Simple and cost-effective ways are to use it in their current form and further blend with other types of virgin rubber. Preparing rubber blend is best and potential solutions to make new material from rubber waste. Apart from an environmental issue, blending of rubber is a purpose to promote better balance gained from blending components (Ismail et al. 2002). Reutilizing chloroprene rubber (CR) is an interesting approach, considering the continuous growth of CR market. CR classifies as specialty rubber which was originally developed in 1931 (Bridgwater 1940). The chemical structure

N. Hayeemasae (✉)

Department of Rubber Technology and Polymer Science, Faculty of Science and Technology,
Prince of Songkla University, Pattani, Thailand
e-mail: nabil.h@psu.ac.th

S. Z. Salleh

Centre of Advanced Manufacturing and Material Processing (AMMP Centre),
Department of Mechanical Engineering, Faculty of Engineering, Universiti Malaya,
Kuala Lumpur, Malaysia

H. Ismail

School of Materials and Mineral Resources Engineering, Engineering Campus,
Universiti Sains Malaysia, Nibong Tebal, Penang, Malaysia

of CR is quite similar to natural rubber (NR); the property of CR is also similar except for the heat and oil resistance which are considerably higher than NR (Sae-oui et al. 2007).

NR is one of the first selection for rubber compounder to choose as blending component. This is because NR possesses very special characteristics such as high durability, flexibility, and resilience. Another type of NR-based rubber origin is an epoxidized natural rubber (ENR). ENR was developed to solve few disadvantages of NR. ENR is less durable than NR, but ENR is more resistant to oxidation and oil (Baker et al. 1985). Currently, there have been limited studies on the use of w-CR as blending component with NR and ENR. Previous works have focused on the use of virgin rubbers for preparing these two blends. For examples, Ismail and Leong (2001) prepared NR/CR and ENR/CR blends and found that this blend offered better performance than NR/CR blends. Following study by Sae-oui et al. (2007) verified that durability and thermal stability of NR/CR blend were from its morphological characteristics whereby such properties were enhanced by the addition of CR in the blend. Considering these two blends, CR is more compatible to ENR than NR due to their similar polarity in nature. However, it also requires certain factors such as blending ratio and curing systems to provide effective performance to the blend.

Apart from NR and ENR, styrene butadiene rubber or SBR has always been a replacement of NR when the cost of the rubber is concerned. The use of SBR can lower the price of the production cost and provides good damping and bonding properties. Even SBR possesses lower durability than NR, its heat resistance and cycle-to-crack initiation are higher. Blend of SBR and CR has been prepared by Ramesan et al. (2005). This was to gain compromising properties from these two rubbers such as the strain-induced crystallization, better compression set, and the flame resistance compared to SBR alone.

This chapter provides valuable information about the properties of the blends based on w-CR as blending component. There were three types of virgin rubbers namely NR, ENR50, and SBR. The blends at various ratio, i.e., 95/5, 85/15, 75/25, 65/35, and 50/50 (phr/phr), were prepared. The findings presented in this chapter will be useful and benefits for the rubber manufacturers on manufacturing novel materials with economic and environmental aspects based on w-CR. Therefore, the blends based on these three blends are novel materials and facilitate developing rubber products based on the respective blends.

2 Materials and Preparation of the Blends

w-CR was obtained from rejected CR gloves and was supplied by Juara One Resources (M) Sdn. Bhd. w-CR was ground to processable form until the size was received at below 600 μm (US Standard mesh is 40). SMR L grade NR was manufactured by Mardec Malaysia Sdn. Bhd. SBR 1502 with the 23.5 wt% of styrene content was purchased from Juara One Resources (M) Sdn. Bhd. ENR50

Table 1 Compounding formulation used for preparing CR glove

Ingredients	Amount (phr)
60% w/w Chloroprene rubber	100
25% w/w Stabilizer	0.5
43% w/w Colorant	0.4
30% w/w Accelerator	0.2
11% w/w Heat-sensitive agent	0.2
2% w/w Thickener	0.2

Table 2 Formulations used for compounding NR/CRw, ENR50/CRw, and SBR/CRw blends

Ingredients	Amount (phr)				
	95	85	75	65	50
NR or ENR50 or SBR	95	85	75	65	50
CRw	5	15	25	35	50
ZnO	5.0	5.0	5.0	5.0	5.0
Stearic acid	1.0	1.0	1.0	1.0	1.0
CBS	1.0	1.0	1.0	1.0	1.0
TMTM	0.5	0.5	0.5	0.5	0.5
MgO	2.0	2.0	2.0	2.0	2.0
Sulfur	2.5	2.5	2.5	2.5	2.5
CB (N330)	30.0	30.0	30.0	30.0	30.0

was synthesized by Kumpulan Guthrie Sdn. Bhd. The rubber formulation used for blending the original w-CR is shown in Table 1. Carbon black (CB) type N330, silica (Vulkasil C), and calcium carbonate (CaCO_3) were supplied by EXCELKOS Sdn. Bhd., Bayer (Malaysia) Sdn. Bhd., and Emax Asia Pte Ltd., respectively. Other additives namely zinc oxide, sulfur, N-cyclohexyl-2-benzothiazole sulfenamide (CBS), tetramethylthiuram monosulfide (TMTM), magnesium oxide (MgO), and stearic acid were purchased from Bayer (M) Sdn. Bhd., Selangor, Malaysia. Table 2 shows the ingredients used for preparing the blends. All the ingredients added for each blend were mixed on the two-roll mill (model XK-160). Then, the compounds were tested for their curing times prior for compression molding.

3 Properties of the Rubber Blends

3.1 Curing Characteristics

The information about torques, scorch time (ts_2), and curing time (tc_{90}) of the blends was recorded from a Monsanto Moving Die Rheometer (MDR 2000). It was done at the temperature of 150 °C according to ASTM D5289. All the data are listed in Table 3. As w-CR content increased, the ts_2 and tc_{90} increased. This occurs for all rubber blends and correlates to the chemical structure of each blending component such as NR, ENR50, and SBR. Longer ts_2 and tc_{90} may be contributed to less reactive

Table 3 Curing parameters of NR/CRw, ENR/CRw, and SBR/CRw blends

Blends and their ratio (phr/phr)	ts ₂ (min)	tc ₉₀ (min)	M _L (dN.m)	M _H (dN.m)	M _H -M _L (dN.m)
NR/CRw					
95/5	0.90	1.99	0.75	16.96	16.21
85/15	0.98	2.13	0.95	17.83	16.88
75/25	1.02	2.23	1.05	19.57	18.52
65/35	1.09	2.51	1.27	21.95	20.68
50/50	1.12	3.03	2.25	24.25	22.00
ENR/CRw					
95/5	0.87	2.70	0.19	17.32	17.13
85/15	0.89	2.73	1.40	18.69	17.29
75/25	0.93	2.79	1.03	21.15	20.12
65/35	1.00	2.88	1.93	23.89	21.96
50/50	1.13	3.38	4.02	26.29	22.27
SBR/CRw					
95/5	2.42	4.66	1.79	19.43	17.64
85/15	2.33	4.97	1.93	19.67	17.74
75/25	2.37	5.37	2.33	23.87	21.54
65/35	2.49	6.56	2.54	25.30	22.76
50/50	2.61	6.78	3.82	27.40	23.58

site due to an increase in w-CR content. The difference in unsaturation resulted to promote cure incompatibility, especially in sulfur-cured systems. Another reason may be because of the w-CR itself (Ismail and Leong 2001). Chlorine (Cl) atom in CR possesses high electronegativity; it can de-activate reactivity of allylic carbon to generate the free radical. This has later retarded the sulfur vulcanization process (Chokanandsombat and Sirisinha 2013). At similar blending ratio, it was found that both ts₂ and tc₉₀ of SBR/w-CR blends were longer than NR/w-CR and ENR50/w-CR which exhibited the same. SBR has less diene content styrene than NR and ENR50. Thus, it needs longer time to complete vulcanization. Moreover, the ts₂ was not much different especially at low content of w-CR; there may be less effect at the beginning of cross-link.

Minimum torque (M_L) increased over the content of w-CR regardless of whether NR, ENR50, or SBR was used as blending component. M_L indicates the viscosity of the rubber compound (Hayeemasae et al. 2013); lower M_L exhibits better processing of the rubber compound. Here, w-CR provided poor processability to the blends. At similar blend ratio (especially at high w-CR content), the blends exhibited higher M_L. As the w-CR is originally hard due to its crumb form, it may interfere the processability of the blends. The maximum torque (M_H) also increased over the addition of w-CR but not much different when comparing among different types of blends. Higher M_H may be came from w-CR which possesses harder phase from its crumb form as the cross-linking precursors in w-CR. This phenomenon also occurred for the torque difference (M_H-M_L). M_H-M_L correlated well with the M_H; it may be related to the cross-linking degree of vulcanizate (Rattanasom et al. 2007).

3.2 Mechanical Properties

The mechanical properties of all blends were evaluated through tensile strength, elongation at break, tensile modulus, and hardness. The tensile tests were carried out using universal tensile machine whereas the hardness was tested by Shore A type durometer. Tensile properties and hardness values are tabulated in Table 4. w-CR has reduced the tensile strength and elongation at break of all blends regardless of blending types. w-CR was cross-linked prior to be used; such cross-link can create different interfacial tension with its blending component. Thus, non-homogeneous phase structure was formed and later reduced the stress transfer to the blends. Comparing each blending type, NR/w-CR blends exhibited highest tensile strength and elongation at break which is simply due to the original characteristics of NR. NR has very good mechanical performance, owing to its ability to crystallize while stretching (Baker et al. 1985; George et al. 2000). Also, the sulfur vulcanization system provided an advantage to the NR-based blends because NR contains more allylic sites than ENR50 and SBR. NR has highest possibility to have created the cross-linking formation than other rubbers which resulted to enhance the tensile strength and elongation at break.

It is noted that the tensile strength of the blends is controlled by certain characteristics of blending components. NR has high strength due to its strain-induced crystallization (SIC). This behavior is diminished after epoxidation (ENR50). This can be seen from the reduction of tensile strength. Moreover, SBR/w-CR blends

Table 4 Tensile properties and hardness of NR/CRw, ENR50/CRw, and SBR/CRw blends

Blends and their ratio (phr/phr)	Tensile strength (MPa)	Elongation at break (%)	M100 (MPa)	Hardness (Shore A)
NR/CRw				
95/5	24.96 ± 0.59	670.00 ± 5.11	2.03 ± 0.02	59
85/15	22.47 ± 0.61	600.77 ± 4.87	2.37 ± 0.03	61
75/25	18.86 ± 0.56	537.23 ± 2.10	2.72 ± 0.03	62
65/35	15.49 ± 0.43	445.43 ± 2.26	3.15 ± 0.04	68
50/50	12.80 ± 0.22	324.43 ± 2.55	3.92 ± 0.03	75
ENR/CRw				
95/5	16.16 ± 0.57	393.90 ± 3.07	3.34 ± 0.02	71
85/15	14.61 ± 0.63	375.57 ± 4.85	3.15 ± 0.03	71
75/25	12.35 ± 0.44	284.43 ± 6.40	4.06 ± 0.06	74
65/35	12.05 ± 0.31	237.20 ± 5.41	5.05 ± 0.05	78
50/50	11.22 ± 0.47	224.43 ± 3.06	6.44 ± 0.03	81
SBR/CRw				
95/5	10.27 ± 0.55	300.85 ± 6.09	2.60 ± 0.04	64
85/15	9.10 ± 0.27	278.87 ± 4.51	2.55 ± 0.02	65
75/25	8.59 ± 0.33	226.63 ± 3.03	2.98 ± 0.03	68
65/35	8.24 ± 0.41	204.47 ± 4.09	3.67 ± 0.05	70
50/50	9.23 ± 0.48	200.53 ± 3.44	4.33 ± 0.04	77

exhibited lowest tensile strength. SBR has very low mechanical properties; it always requires the addition of reinforcing filler to enhance the strength. This is because styrene unit destroys the regularity of rubber chains, which is needed for SIC (Ramesan et al. 2001). Similar findings were also observed for elongation at break. The flexibility of NR is originally higher than of ENR50 and SBR.

The modulus at 100% elongation (M100) and hardness of NR/w-CR, ENR50/w-CR, and SBR/w-CR blends are shown in Table 4. w-CR has increased M100 and hardness of all blends. This clearly confirmed that the rigidity in nature of w-CR has made the vulcanizates more stiffness. Increasing the content of rubber waste, the modulus was then increased (Poh et al. 2001). ENR50/w-CR was seen to provide the blends with highest M100 and hardness. ENR can be self-cross-linked during epoxidation by forming ether bonds (Baker et al. 1985). This cross-linking enables to promote high modulus rubber. Another reason may be because of its higher glass transition temperature (T_g) of ENR50. It makes this rubber harder at ambient temperature unlike other rubbers. Similar report was also mentioned by Nagode and Roland (1991), who emphasized that the T_g contributes to the final stiffness of the rubber vulcanizate. As for the SBR/w-CR blends, the presence of styrene in the SBR restrains the mobility of rubber chain and makes the final rubber harder (Chakraborty et al. 2011; Poh et al. 2001).

3.3 Fatigue Life

Monsanto fatigue-to-failure tester was used as a tool to determine fatigue life of rubber blends with repeated cyclic strain at 100 cpm and 2.01 ± 0.05 extension ratio according to JIS K 6270. The calculated cycles of fatigue life of all blends are shown in Table 5. Increasing w-CR content has reduced the fatigue life of all blends, which is due to deterioration of vulcanizate in the presence of w-CR. Noriman and Ismail (2011) reported that an addition of rubber waste especially in crumb form may create defect while stretching the sample. Such defect cannot transfer the stress from one phase to another; this has ended up with the broken sample at unexpected cycle of fatigue test. This shows that w-CR reduced the elasticity of the blends and made them unable to sustain any longer under cyclic deformations. Comparing among the blends, SBR/w-CR blends showed less fatigue cycle than NR/w-CR or ENR50/w-CR blends. As stated before, the unique property of NR over synthetic rubber (SR) is the ability to crystallize while elongation. Such crystals can inhibit the propagation of crack during cyclic deformations, thus reducing the crack growth to the rubber sample (Poh et al. 2001). This is again due to its SIC which helps to enhance the fatigue life. In fact, the major consideration for the products having high fatigue life is toward the ability of rubber to perform SIC (George et al. 2000).

In addition to SIC, the fatigue cycle of the SBR/w-CR blends showed lowest value, which is simply because SBR does not perform SIC. SBR is an amorphous

Table 5 Fatigue life of NR/CRw, ENR50/CRw, and SBR/CRw blends

Blends and their ratio (phr/phr)	Fatigue life (kc)
NR/CRw	
95/5	402.1 ± 2.95
85/15	297.3 ± 2.09
75/25	187.1 ± 2.12
65/35	166.2 ± 3.17
50/50	28.3 ± 4.05
ENR/CRw	
95/5	68.2 ± 5.02
85/15	45.5 ± 5.31
75/25	31.2 ± 4.44
65/35	29.0 ± 3.51
50/50	15.5 ± 3.33
SBR/CRw	
95/5	54.6 ± 4.12
85/15	42.3 ± 4.56
75/25	27.9 ± 6.74
65/35	24.3 ± 5.04
50/50	14.0 ± 6.12

rubber due to the presence of styrene along the main chain; it causes poor fatigue life especially when considering the crack propagation during cyclic tension. Legorju-jago and Bathias (2002) confirmed that the fatigue cycle of NR and SR strongly depends on their chemical constituents.

3.4 Swelling Uptake and Cross-Link Density

Swelling uptake was tested for the vulcanizates and the raw data from the swelling test were applied for calculation of cross-link density according to the Flory–Rehner equation (Flory and Rehner 1943). The results of swelling uptake and cross-link density of all blends are listed in Table 6. The swelling resistance was investigated by equilibrium toluene uptake at room temperature. Swelling uptake correlates with the overall cross-link density of rubber vulcanizate (Flory and Rehner 1943). Less swelling uptake indicates more cross-linking because cross-links can inhibit the penetration of solvent to the rubber molecules. The swelling uptake of all blends reduced over the addition of w-CR. This was simply due to the nature of w-CR, as CR possesses good oil and solvent resistances (Ismail and Leong 2001). Adding w-CR has then reduced the swelling uptake. Moreover, w-CR was cross-linked due

Table 6 Swelling percentage and cross-link density of NR/CRw, ENR50/CRw, and SBR/CRw blends

Blends and their ratio (phr/phr)	Swelling uptake (%)	Cross-link density ($\times 10^{-5}$ mol/cm ³)
NR/CRw		
95/5	243.60 \pm 3.15	3.98 \pm 0.35
85/15	225.82 \pm 2.54	4.25 \pm 0.25
75/25	182.62 \pm 2.78	4.48 \pm 0.46
65/35	167.64 \pm 2.55	4.55 \pm 0.39
50/50	161.83 \pm 4.65	5.63 \pm 0.25
ENR/CRw		
95/5	162.77 \pm 2.52	6.78 \pm 0.17
85/15	160.82 \pm 2.33	6.89 \pm 0.56
75/25	147.48 \pm 2.29	7.63 \pm 0.48
65/35	139.51 \pm 3.21	7.56 \pm 0.51
50/50	127.10 \pm 1.67	9.41 \pm 0.24
SBR/CRw		
95/5	180.66 \pm 2.49	5.34 \pm 0.37
85/15	172.52 \pm 3.12	5.58 \pm 0.55
75/25	158.12 \pm 1.52	6.11 \pm 0.61
65/35	150.88 \pm 2.44	6.14 \pm 0.49
50/50	130.12 \pm 2.07	8.35 \pm 0.31

to its recycled form; this may be another reason to reduce the possibility of solvent to penetrate the molecules of rubber blends.

Types of blending component have also influenced the overall swelling uptake of the blends. The blends containing NR as blending component showed highest swelling uptake followed by SBR and ENR, respectively. NR is non-polar rubber, so it is very prone to non-polar solvent when immersing. Although SBR is also classified considered a non-polar rubber like NR, but the presence of styrene on SBR backbones has made SBR more insoluble with non-polar solvent like toluene. The sulfur content in the formulation of SBR/w-CR might be another condition that made this blend more swelling resistance. As SBR has less unsaturated level than NR, it normally requires less amount of sulfur for vulcanization. However, all formulations used in this work were similar except for the types of blending component. Therefore, the possibility of cross-linking in SBR based blend is higher which then made the vulcanizate more swelling resistance. In addition to this, the highest swelling resistance observed for ENR50/w-CR blends is simply because of the presence of epoxide group. The epoxide group increases the polarity of the ENR and affected the final swelling uptake. Another consideration was due to the self-cross-linked formation of ENR through the ether linkage. This may also contribute additional cross-links to the ENR50/w-CR blends.

3.5 Scanning Electron Microscopy (SEM)

The SEM images of all blends were taken from the fractured specimen after tensile test. Figure 1 shows the SEM images at 50× magnification for all blends. Figure 1a, c, e show the SEM images of NR/w-CR, SBR/w-CR and ENR50/w-CR blends with low content of w-CR (25 phr). The rough surfaces still can be seen from their

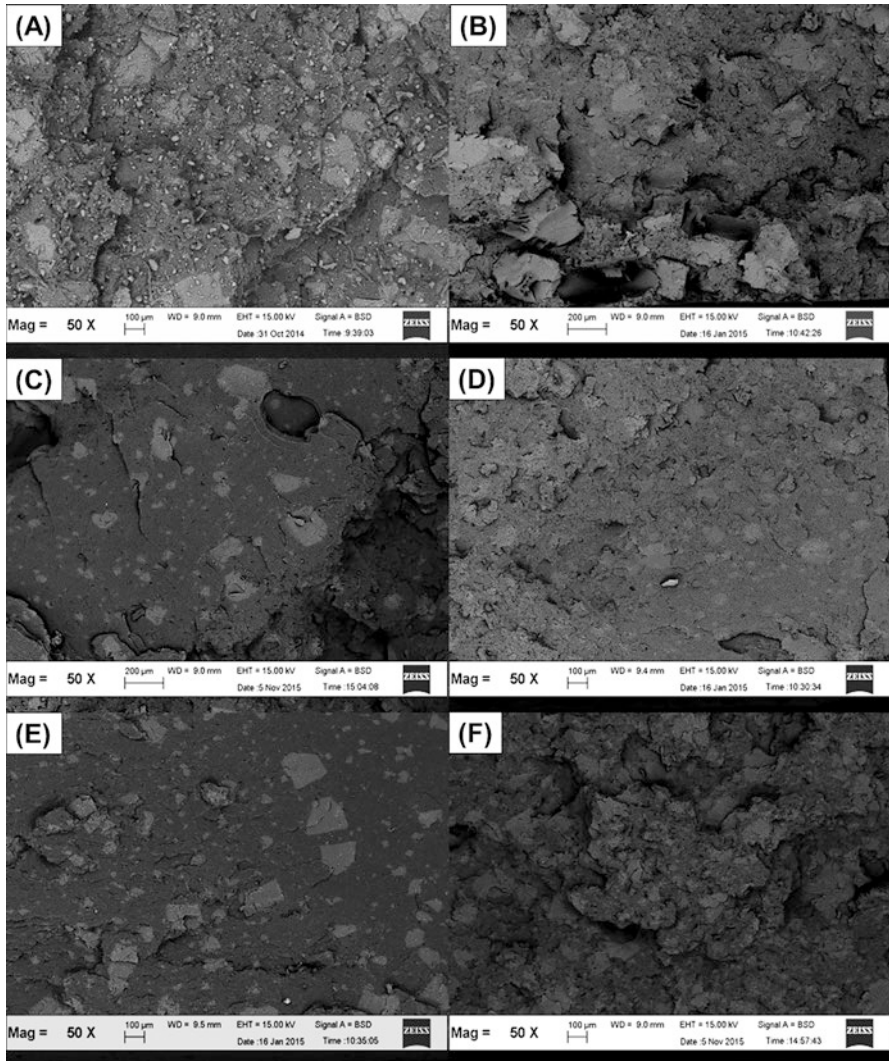


Fig. 1 SEM images of the blends at various blending ratios, i.e., NR/CRw blends at 75/25 (a) and 50/50 (b), ENR50/CRw blends at 75/25 (c) and 50/50 (d), and SBR/CRw blends at 75/25 (e) and 50/50 (f)

surfaces; this indicates the crack was difficult to create under tensile test. At higher content of w-CR (see Fig. 1b, d, f), less roughness and smoother surfaces are seen in the images. This agreed well with the values of tensile strength tested. Apart from that, detachment of w-CR was visible when more w-CR was added, this is simply to the poor compatibility among the blending components; this resulted to reduce the tensile strength.

3.6 Thermogravimetric Analysis (TGA)

A Perkin–Elmer Pyris 6 TGA analyzer was used for the thermogravimetric analysis of the rubber blends. The analysis initiated from 30 to 600 °C at a heating rate of 20 °C/min in nitrogen gas. The TG and DTG curves of all blends were plotted and shown in Figs. 2, 3 and 4. The raw data received from TG profiles such as decomposition temperature at various weight loss, various stages, and their residue are listed in Table 7. Two regions are observed in the degradation of these blends. From the results observed, a very minor mass loss at approximately 150–300 °C was due to the presence of volatile matters such as moisture, stearic acid, and other unreacted substances (Tomer et al. 2007). Beyond such temperatures, there are two regions of thermal degradation observed from TG and DTG curves. First maximum weight loss was responsible to degradation of NR and ENR and the styrene and butadiene components of SBR, respectively, which observed at the temperature range of 350–400 °C. The second maximum weight loss is relative to the degradation of w-CR and leftover diene after the first stage of degradation. The thermal stability of all blends can be evaluated from the temperature at certain weight loss. Here, the weight loss at 5% and 5% were selected. It is found that the temperature decreased

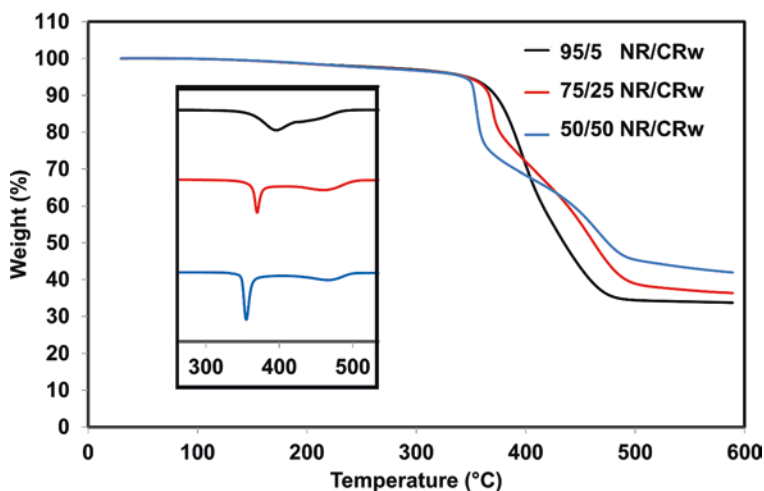


Fig. 2 TG and DTG curves of NR/CRw blends

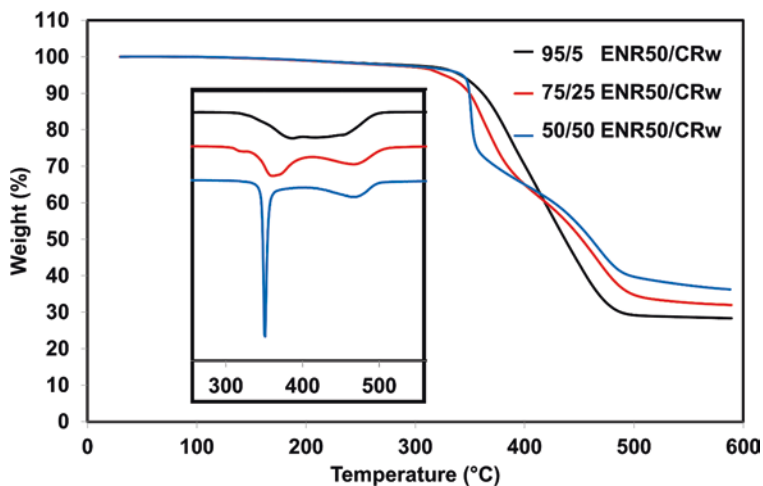


Fig. 3 TG and DTG curves of ENR50/CRw blends

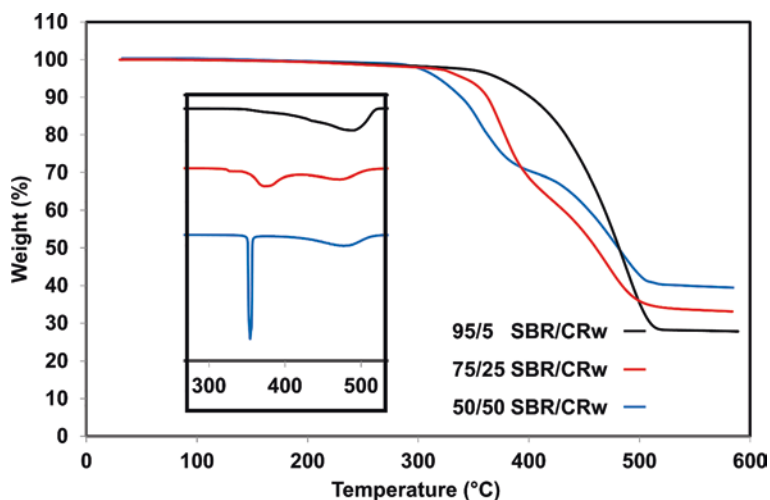


Fig. 4 TG and DTG curves of SBR/CRw blends

over the content of w-CR for all types of blends, particularly for the initial stage of degradation (see $T_{10\%}$ – $T_{30\%}$). However, the degradation rates were fastened after 50% loss (see $T_{50\%}$). In general, the temperature at initial stage of degradation correlates to the first maximum peak of decomposition (T_{max1}) while the second maximum peak of degradation contributes to the second stage of degradation. Here, it can be summarized that w-CR provides great effect to the thermal stability of all blends, particularly at the lower temperatures. This correlates well to the temperature at which volatile matter evaporized and the elimination of HCl from w-CR; this contributes to faster loss of weight at this stage (Aracil et al. 2007).

Table 7 Thermal decomposition parameters of NR/CRw, ENR50/CRw, and SBR/CRw blends

Blends and their ratio (phr/phr)	T _{5%} (°C)	T _{10%} (°C)	T _{30%} (°C)	T _{50%} (°C)	T _{max1} (°C)	T _{max2} (°C)	Char residue (%)
NR/CRw							
95/5	346	372	401	435	391	426	33.69
75/25	344	366	406	462	370	459	36.34
50/50	342	353	390	475	354	465	41.96
ENR 50/CRw							
95/5	341	361	400	437	387	417	28.35
75/25	326	349	384	452	360	467	32.01
50/50	343	349	373	461	351	463	36.22
SBR/CRw							
95/5	374	402	453	481	–	472	27.83
75/25	342	362	396	461	376	476	33.11
50/50	353	353	388	477	354	488	37.79

According to Kameda et al. (2008), chlorine-based rubber material tends to perform dehydrochlorination; this reaction is initiated at 150 °C and continues to about 350 °C. As can be seen from the decomposition temperature of the blends, dehydrochlorination happened at the initial stage of degradation. However, once the dehydrochlorination is complete, the HCl is then released and neutralized, and there is only the scission of some cross-linked CR and conjugated polyene left after the initial stage of degradation. It still can enhance the thermal stability at the later stage of decomposition.

This resulted to increase the decomposition temperatures of the blends. It is interesting to highlight that using only 5 phr of w-CR note for SBR/w-CR blend did not show the second peak of decomposition temperature. This is because SBR implies stable decomposition. The decomposition of SBR involved many chemical substances such as 4-phenyl cyclohexene, 4-vinylcyclohexene, styrene, ethylbenzene, methylbenzene, and α -methyl styrene. They are all classified as low molecular weight substances (Ghosh et al. 2018). This has made the SBR/w-CR blends showed highest thermal stability over other types of blending component. The structure of blending component greatly affects the thermal stability of the blends (Tangudom et al. 2014). Furthermore, the char residue of all blends changed considerably over the content of w-CR. As w-CR was in crumb form and contained certain content of inorganic additives as evidently shown in Table 1. This may be the reason behind the variation in char residue at the final decomposition temperature.

3.7 Dynamic Mechanical Analysis (DMA)

Dynamic mechanical analysis (DMA) was studied using a Perkin–Elmer DMA7 to obtain the results of the storage modulus (E') and damping characteristic ($\tan \delta$). The samples were subjected to tension mode with the force amplitude of 0.1 N at a

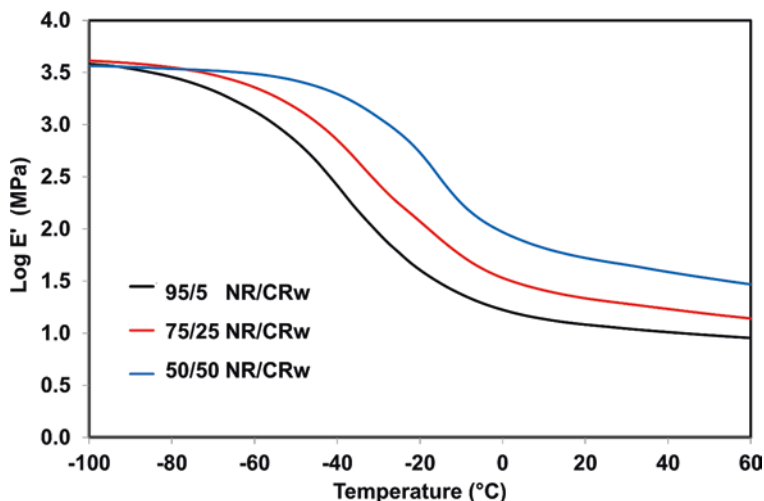


Fig. 5 Storage modulus of NR/CRw blends

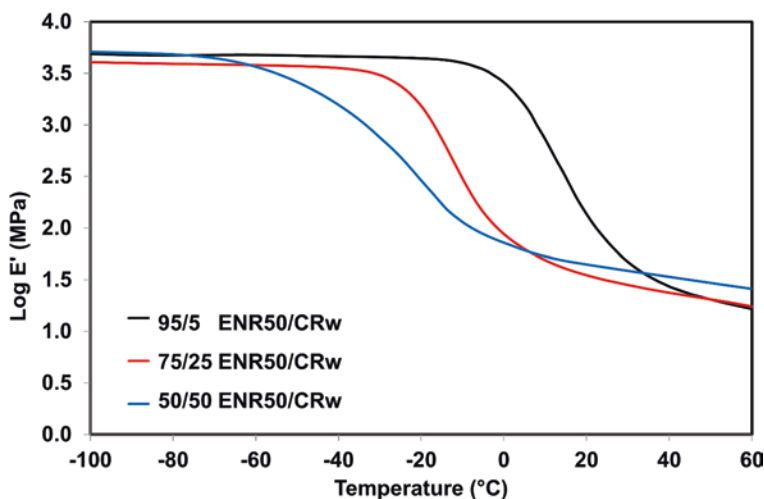


Fig. 6 Storage modulus of ENR50/CRw blends

frequency of 10 Hz. Figures 5, 6, 7, 8, 9 and 10 show results recorded from DMA of all blends. The raw data are also tabulated in Table 8. As for the E' (see Figs. 5, 6 and 7), three different regions of E' were shown namely a glassy zone below the glass transition temperature (T_g), a transition zone where E' value is reduced over the temperature, and a rubbery region where the samples behave as elastic material. The result clearly showed that E' of the blends increased over the content of w-CR, except for the ENR50/w-CR blends. E' is related to the elastic and cross-linking

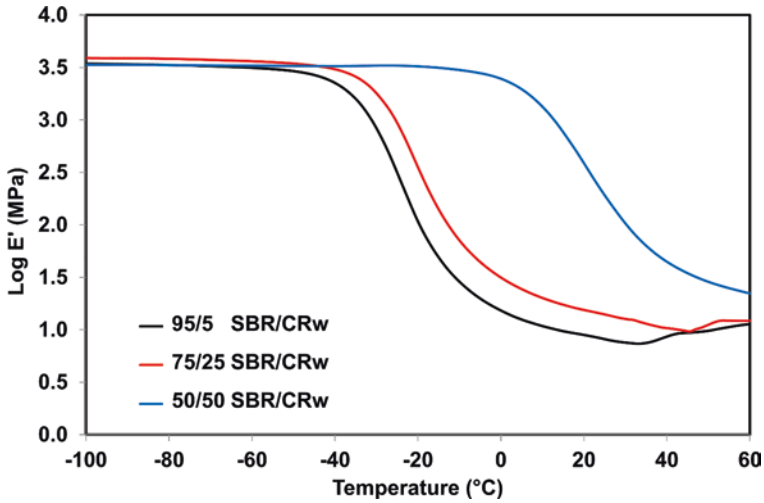


Fig. 7 Storage modulus of SBR/CRw blends

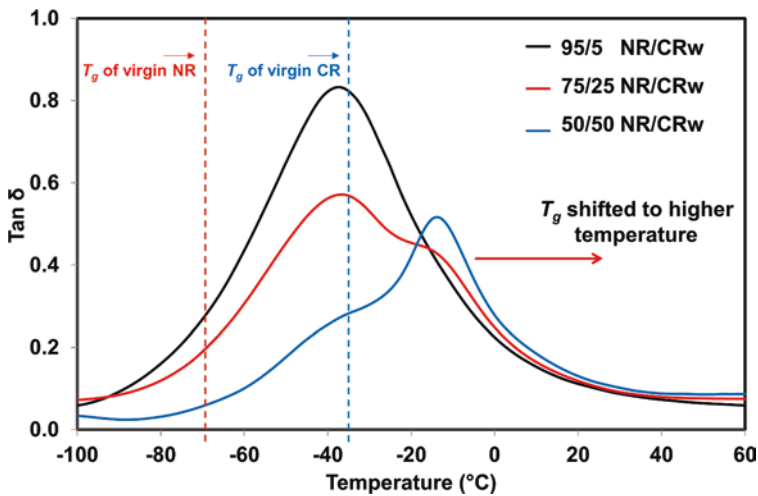


Fig. 8 Damping factor ($\tan \delta$) of NR/CRw blends

degree (Nabil et al. 2013); this is clear that elastic response was significant in the presence of w-CR which can be attributed to a higher cross-linking degree imparted by w-CR.

The different observation found for ENR50/w-CR blends related to the side reaction from taken place between ENR50 and w-CR phases. The CB may catalyze HCl during dehydrochlorination process of w-CR; this may cause the separation of rubber phases (Bandyopadhyay et al. 1995). Moreover, the formation of ether bonds during the synthesis of ENR may attribute such observation. As for NR/w-CR and

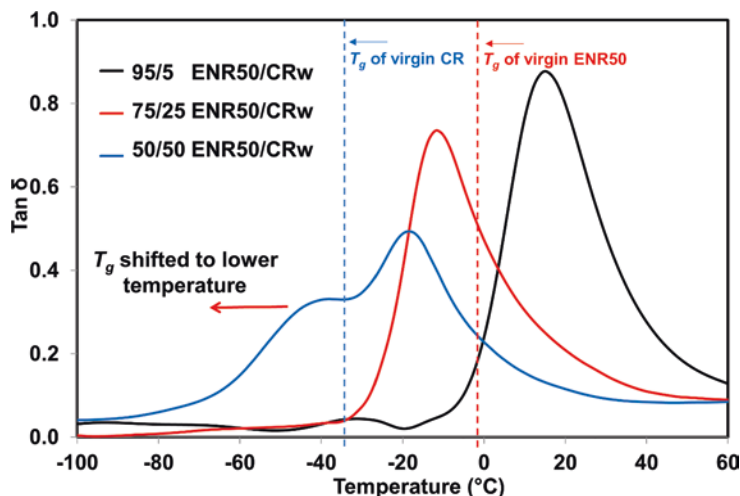


Fig. 9 Damping factor ($\tan \delta$) of ENR50/CRw blends

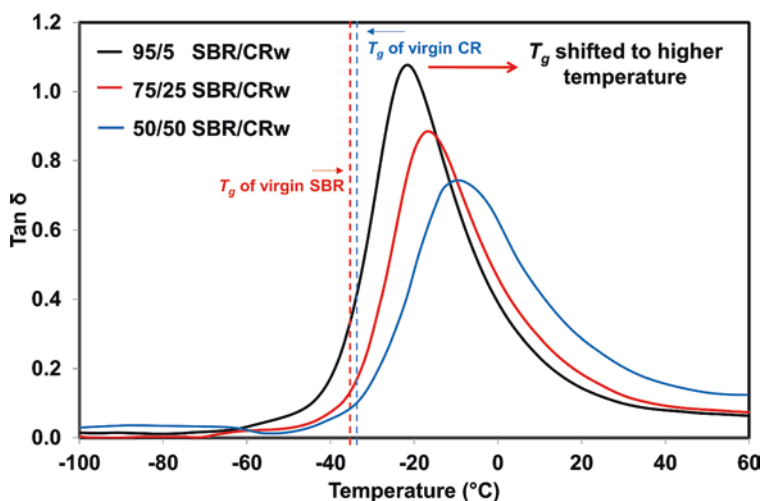


Fig. 10 Damping factor ($\tan \delta$) of SBR/CRw blends

SBR/w-CR blends, E' remained the same; although the styrene group may provide harder vulcanizate, it may have great effect only at higher content of SBR (50/50 phr/phr of SBR/w-CR blend) High E' at higher content of SBR may be due to the designed formulation as discussed previously. SBR has less unsaturated level than NR, but the content of sulfur remained constant to all over the blends, so the sulfur content is more than enough to complete the vulcanization. Thus, SBR consisted of more cross-linking than NR in the blends. This agreed well with the cross-link density reported previously.

Table 8 Dynamic mechanical properties of NR/CRw, ENR50/CRw, and SBR/CRw blends

Blends and their ratio (phr/phr)	Log E' at 25 °C (MPa)	tan δ_{\max}		T_g @ tan δ_{\max} (°C)	
		tan $\delta_{\max1}$	tan $\delta_{\max2}$	tan $\delta_{\max1}$	tan $\delta_{\max2}$
NR/CRw					
95/5	1.06	0.83	–	–36.30	–
75/25	1.30	0.66	0.48	–36.59	–19.98
50/50	1.69	0.28	0.51	–34.89	–14.73
ENR50/CRw					
95/5	1.85	0.06	0.87	–31.05	14.39
75/25	1.50	0.03	0.73	–38.19	–12.13
50/50	1.62	0.32	0.49	–42.88	–19.12
SBR/CRw					
95/5	0.92	1.07	–	–22.88	–
75/25	1.15	0.87	–	–14.91	–
50/50	2.31	0.75	–	–9.42	–

Tan δ is a crucial characteristic to discuss as it is indirectly related to the elastic response of the vulcanizate. The factors relating to this result are the nature of rubber matrix (NR, SBR, ENR50 or w-CR), the nature of interphase (b), the frictional damping between matrix interphases (c), and the energy dissipation in the catastrophic area (d) (Jacob et al. 2006). Besides, tan δ also relates to the impact resistance of the material (Atiqah et al. 2018). Variation of tan δ over the temperature is illustrated in Figs. 8, 9 and 10 and the respective values are tabulated in Table 8.

Considering the available figures, the blue straight line represents the T_g for virgin CR, which is roughly at -33 °C, while the red straight line indicates the T_g for virgin NR, ENR50, and SBR, which are at -70 °C, -1 °C, and -34.5 °C, consecutively (Baker et al. 1985; Arrighi et al. 2003). The T_g of NR and SBR is lower than CR. This was the reason behind the the shifting of T_g over the content of w-CR in the blend. Besides, the T_g of SBR and CR is almost equal which are -34.5 °C and -33 °C, respectively. This is simply the possible reason of having only one peak of tan δ . As for the ENR50/w-CR blends, the T_g of ENR50 is way higher than CR; this has made the T_g of vulcanizate lower when adding more w-CR. Moreover, the tan δ peak is reduced in the presence of w-CR, irrespective of the types of blending component. The w-CR restricted the mobility of rubber chains because of the rigidity of w-CR, resulting to lower elasticity, higher restriction of molecular movement, and thus lowering the damping characteristics. This agreed well with the cross-link density reported previously.

It is interesting to highlight that the types of rubber namely NR, SBR, and ENR50 greatly influence the damping behavior of all blends. It is known that damping behavior is opposite to elasticity of vulcanizate. Low tan δ also indicates low tire rolling resistance, while a high tan δ shows good wet grip. NR/w-CR and ENR50/w-CR blends have low tan δ , which is special characteristic of NR, while the SBR/w-CR blends showed quite higher tan δ values. This is simply because of the nature

SBR itself. SBR is known to have very high rolling resistance due to the presence of styrene group, a high $\tan \delta$ seen correlates well with the property of SBR.

4 Conclusions

In this chapter, the utilization of w-CR as blending component in NR, SBR and ENR50 was carried out. The overall performance of the blends was evaluated from many characteristics such as mechanical properties, thermal stability, and dynamic mechanical properties. Before undergoing the respective testing, the curing characteristics were observed; it was found that w-CR has prolonged the ts_2 and tc_{90} due to unsaturation level which led to cure mismatch between the blends. M_L , M_H , and $M_H - M_L$ of all blends increased over the content of w-CR. This is because w-CR has cross-links before blending with virgin rubbers. This also increased the swelling resistance, cross-link density, and storage modulus. Tensile strength reduced over the content of w-CR; the change in tensile strength can be correlated with the SEM images. The rougher surfaces with more tearing lines indicate the requirement of higher energy for breaking the sample. w-CR greatly affected the thermal stability of all blends by elevating the decomposition temperature. In summary, each blend regardless of whether NR/w-CR, ENR50/w-CR, or SBR/w-CR possess their own characteristics. The blend based on NR as blending component is suitable for the products where flexibility and strength are required. However, the blend based on SBR is more appropriate when requiring high thermal resistance and damping characteristic. Finally, the blend based on ENR50 as blending component is suggested when the rubber compounders request for a synergistic property among physical and thermal stability of the rubber vulcanizate. As for the ENR50/CRw blends, it provided a compromise in the physical and thermal properties. On top of that, the use of w-CR is considered the key role for preparing rubber products based on rubber waste and can be ended up with cost-effective and environmentally friendly issues.

References

- Alassali A, Fiore S, Kuchta K (2018) Assessment of plastic waste materials degradation through near infrared spectroscopy. *Waste Manag* 82:71–81. <https://doi.org/10.1016/j.wasman.2018.10.010>
- Aracil I, Font R, Conesa JA et al (2007) TG-MS analysis of the thermo-oxidative decomposition of polychloroprene. *J Anal Appl Pyrolysis* 79:327–336. <https://doi.org/10.1016/j.jaap.2006.12.027>
- Arrighi V, McEwen IJ, Qian H et al (2003) The glass transition and interfacial layer in styrene-butadiene rubber containing silica nanofiller. *Polymers* 44:6259–6266. [https://doi.org/10.1016/S0032-3861\(03\)00667-0](https://doi.org/10.1016/S0032-3861(03)00667-0)
- Atiqah A, Jawaid M, Sapuan SM et al (2018) Thermal properties of sugar palm/glass fiber reinforced thermoplastic polyurethane hybrid composites. *Compos Struct* 202:954–958. <https://doi.org/10.1016/j.compstruct.2018.05.009>

- Baker CSL, Gelling IR, Newell R (1985) Epoxidized natural rubber. *Rubber Chem Technol* 58:67–85. <https://doi.org/10.5254/1.3536059>
- Bandyopadhyay S, De PP, Tripathy DK et al (1995) Dynamic mechanical spectroscopic studies on the miscibility of polychloroprene-epoxidized natural rubber blend in presence of carbon black filler. *Polymer* 36:1979–1984. [https://doi.org/10.1016/0032-3861\(95\)91441-9](https://doi.org/10.1016/0032-3861(95)91441-9)
- Bridgwater ER (1940) Neoprene, the chloroprene rubber. *Ind Eng Chem* 32:1155–1156. <https://doi.org/10.1021/ie50369a004>
- Chakraborty SK, Sabharwal S, Das PK et al (2011) Electron beam (EB) radiation curing—a unique technique to introduce mixed crosslinks in cured rubber matrix to improve quality and productivity. *J Appl Polym Sci* 122:3227–3236. <https://doi.org/10.1002/app.34340>
- Chokanandsombat Y, Sirisinha C (2013) MgO and ZnO as reinforcing fillers in cured polychloroprene rubber. *J Appl Polym Sci* 128:2533–2540. <https://doi.org/10.1002/app.38579>
- Flory PJ, Rehner J Jr (1943) Statistical mechanics of cross-linked polymer networks II. Swelling *J Chem Phys* 11:512–520. <https://doi.org/10.1063/1.1723791>
- George SC, Ninan KN, Groeninickx G et al (2000) Styrene-butadiene rubber/natural rubber blends: morphology, transport behavior, and dynamic mechanical and mechanical properties. *J Appl Polym Sci* 78:1280–1303. [https://doi.org/10.1002/1097-4628\(20001107\)78:6<1280::AID-APP150>3.0.CO;2-S](https://doi.org/10.1002/1097-4628(20001107)78:6<1280::AID-APP150>3.0.CO;2-S)
- Ghaviyanjeh F, Ziaei Rad Z, Pazouki M (2018) Devulcanization of ground tires by different strains of bacteria: optimization of culture condition by taguchi method. *J Polym Environ* 26:3168–3175. <https://doi.org/10.1007/s10924-017-1169-0>
- Ghosh J, Ghorai S, Bhunia S et al (2018) The role of devulcanizing agent for mechanochemical devulcanization of styrene butadiene rubber vulcanizate. *Polym Eng Sci* 58:74–85. <https://doi.org/10.1002/pen.24533>
- Hayemasae N, Ismail H, Azura AR (2013) Blending of natural rubber/recycled ethylene-propylene-diene monomer: cure behaviors and mechanical properties. *Polym-Plast Technol Eng* 52:501–509. <https://doi.org/10.1080/03602559.2012.762020>
- Hou P, Xu Y, Taiebat M et al (2018) Life cycle assessment of end-of-life treatments for plastic film waste. *J Clean Prod* 201:1052–1060. <https://doi.org/10.1016/j.jclepro.2018.07.278>
- Ismail H, Leong HC (2001) Curing characteristics and mechanical properties of natural rubber/chloroprene rubber and epoxidized natural rubber/chloroprene rubber blends. *Polym Test* 20:509–516. [https://doi.org/10.1016/S0142-9418\(00\)00067-2](https://doi.org/10.1016/S0142-9418(00)00067-2)
- Ismail H, Nordin R, Noor AM (2002) The comparison properties of recycle rubber powder, carbon black, and calcium carbonate filled natural rubber compounds. *Polym-Plast Technol Eng* 41:847–862. <https://doi.org/10.1081/PPT-120014392>
- Jacob M, Francis B, Thomas S et al (2006) Dynamical mechanical analysis of sisal/oil palm hybrid fiber-reinforced natural rubber composites. *Polym Compos* 27:671–680. <https://doi.org/10.1002/pc.20250>
- Kameda T, Watanabe Y, Grause G et al (2008) Dehydrochlorination behavior of polychloroprene during thermal degradation. *Thermochim Acta* 476:28–32. <https://doi.org/10.1016/j.tca.2008.07.004>
- Legorju-Jago K, Bathias C (2002) Fatigue initiation and propagation in natural and synthetic rubbers. *Int J Fatigue* 24:85–92. [https://doi.org/10.1016/S0142-1123\(01\)00062-7](https://doi.org/10.1016/S0142-1123(01)00062-7)
- Nabil H, Ismail H, Azura AR (2013) Effects of virgin ethylene-propylene-diene-monomer and its preheating time on the properties of natural rubber/recycled ethylene-propylene-diene-monomer blends. *Mater Design* 50:27–37. <https://doi.org/10.1016/j.matdes.2013.02.086>
- Nagode JB, Roland CM (1991) Miscible mixtures of polychloroprene and epoxidized polyisoprene. *Polymers* 32:505–509. [https://doi.org/10.1016/0032-3861\(91\)90457-T](https://doi.org/10.1016/0032-3861(91)90457-T)
- Noriman N, Ismail H (2011) The effects of electron beam irradiation on the thermal properties, fatigue life and natural weathering of styrene butadiene rubber/recycled acrylonitrile-butadiene rubber blends. *Mater Design* 32:3336–3346. <https://doi.org/10.1016/j.matdes.2011.02.020>
- Poh BT, Ismail H, Quah EH et al (2001) Cure and mechanical properties of filled SMR L/ENR 25 and SMR L/SBR blends. *J Appl Polym Sci* 81:47–52. <https://doi.org/10.1002/app.1411>

- Prathiba R, Shruthi M, Miranda LR (2018) Pyrolysis of polystyrene waste in the presence of activated carbon in conventional and microwave heating using modified thermocouple. *Waste Manag* 76:528–536. <https://doi.org/10.1016/j.wasman.2018.03.029>
- Ramesan MT, Mathew G, Kuriakose B et al (2001) Role of dichlorocarbene modified styrene butadiene rubber in compatibilisation of styrene butadiene rubber and chloroprene rubber blends. *Eur Polym J* 37:719–728. [https://doi.org/10.1016/S0014-3057\(00\)00157-9](https://doi.org/10.1016/S0014-3057(00)00157-9)
- Ramesan MT, Alex R, Khanh NV (2005) Studies on the cure and mechanical properties of blends of natural rubber with dichlorocarbene modified styrene-butadiene rubber and chloroprene rubber. *React Funct Polym* 62:41–50. <https://doi.org/10.1016/j.reactfunctpolym.2004.08.002>
- Rattanasom N, Saowapark T, Deeprasertkul C (2007) Reinforcement of natural rubber with silica/carbon black hybrid filler. *Polym Test* 26:369–377. <https://doi.org/10.1016/j.polymertesting.2006.12.003>
- Rooj S, Basak GC, Maji PK et al (2011) New route for devulcanization of natural rubber and the properties of devulcanized rubber. *J Polym Environ* 19:382–390. <https://doi.org/10.1007/s10924-011-0293-5>
- Sae-oui P, Sirisinha C, Hatthapanit K (2007) Effect of blend ratio on aging, oil and ozone resistance of silica-filled chloroprene rubber/natural rubber (CR/NR) blends. *Express Polym Lett* 1:8–14. <https://doi.org/10.3144/expresspolymlett.2007.3>
- Tangudom P, Thongsang S, Sombatsompop N (2014) Cure and mechanical properties and abrasive wear behavior of natural rubber, styrene-butadiene rubber and their blends reinforced with silica hybrid fillers. *Mater Design* 53:856–864. <https://doi.org/10.1016/j.matdes.2013.07.024>
- Tomer NS, Delor-Jestin F, Singh RP et al (2007) Cross-linking assessment after accelerated ageing of ethylene propylene diene monomer rubber. *Polym Degrad Stab* 92:457–463. <https://doi.org/10.1016/j.polyimdegradstab.2006.11.013>

Recycled Cellulose and Cellulose-Based Materials by Gamma Rays and Its Use as Reinforcement in Composites



Irna Zukeyt Garduño-Jaimes, Gonzalo Martínez-Barrera,
Enrique Viguera-Santiago, and Julián Cruz-Olivares

1 Introduction

Some studies are related to composites produced with cellulose and polyester resin. For example, (I) unsaturated polyester resin was reinforced with cellulose nanofibers (CNF) (up to 45 vol%), which were obtained from wood. When adding 45 vol% CNF, the strength and the elasticity modulus increase up to three times, while ductility and fracture toughness twice. Moreover, the glass transition temperature (T_g) increases with cellulose concentration increases (Ansari et al. 2015). (II) Improvements on the tensile modulus, impact resistance, viscoelasticity, and thermal resistance were obtained for composites produced with unsaturated polyester resin and up to 6 wt% cellulose nanocrystals modified by silane (Kargarzadeh et al. 2015). Cellulose is the most abundant natural polymer around the world, with $(C_6H_{10}O_5)_n$ chemical formula. Cellulose contains D-glucopyranose units linked by β -1,4-glycosidic bonds, containing up to 25,000 repeating units; which constitute a straight-chain molecular structure, enabling the production of soft and flexible fibers. Cellulose I is referred to nature cellulose, while cellulose II is produced by mercerization (alkali treatment) or regeneration (solubilization and subsequent recrystallization). Cellulose III_I and III_{II} can be formed from cellulose I and II, respectively, by reversible reaction with liquid ammonia. Finally, cellulose IV_I and

I. Z. Garduño-Jaimes

Posgrado en Materiales, Facultad de Química, Universidad Autónoma del Estado de México, Toluca, Mexico

G. Martínez-Barrera (✉) · E. Viguera-Santiago

Laboratorio de Investigación y Desarrollo de Materiales Avanzados (LIDMA), Facultad de Química, Universidad Autónoma del Estado de México, Toluca-Atlaquemulco, Mexico

J. Cruz-Olivares

Facultad de Química, Universidad Autónoma del Estado de México, Toluca, Estado de México, Mexico

IV_{II} can be produced by heating cellulose III_I and III_{II}, respectively. The main components of natural fibers are cellulose, hemicellulose, and lignin. Each one content can vary according to the species, climate, and age (Bledzki and Gassan 1999; Park et al. 2010).

2 Cellulose Irradiated by Gamma Rays

Because cellulose is a biodegradable material, its recycling processes have been improved; one of them is carried out by electromagnetic radiation, coming from radioactive sources such as cobalt 60. Gamma radiation causes or enhances polymer breakdown, particularly by scissions of polymer chains, that produce low-molecular-weight materials, which can be used as raw materials or additives. Also, gamma rays have been used to improve the mechanical properties and performance of waste materials, by cross-linking processes. Furthermore, they can be used to upgrade natural polymers and to produce products having added value. Polymers submitted to ionizing radiation, even at low doses, often undergo structural changes accompanied by chain cleavage, cross-linking, and grafting reactions. In some polymers, cleavage and cross-linking reactions happen at the same time. Cross-linking produced by gamma rays has great advantages since it does not require any additional chemical agents and it is easily controlled by radiation dose. Cross-linking process is widely used for hydrogel manufacturing. Modifications on the strength and color of polymers can be getting by controlled conditions. Chain length disruption initiates the primary break called aging, and various external factors, such as temperature and chemicals, also increase the degradation rate. In addition, gamma radiation has shown being a simple and environmentally friendly technology (Burillo et al. 2002; Ndiaye and Tidjani 2014; Wan Ishak et al. 2018).

2.1 Degree of Polymerization (DP) and Molecular Weight

Polymerization can be carried out continuously or discontinuously by using different processes such as suspension, mass, emulsion, gas phase, and solution. Degree of polymerization (DP) is the number of repeating units in the formed polymer chain. In materials containing cellulose, this depends on its age, physical, and chemical properties. For example, higher molecular weight means higher degree of polymerization, as shown in Table 1.

Composites containing nanocellulose have shown great scientific advances, for example, (I) those made with sugar palm starch reinforced with nanofibrillated sugar palm cellulose, which were produced by a high-pressure homogenization process. They show good compatibility between the components. Moreover, at 1 wt% sugar palm starch, the tensile strength increased from 4.80 to 10.68 MPa and Young's modulus from 53.97 to 121.26 MPa (Ilyas et al. 2019a, b, c); the

Table 1 Degree of polymerization and molecular weight of materials containing cellulose (Hallac and Ragauskas 2011)

Material	Molecular weight (units $\times 10^3$)	Degree of polymerization (DP $\times 10^3$)
Cotton (closed fruit)	2478.6	15.3
Poplar cellulose	1668.6	10.3
Cotton (open fruit)	1344.6	8.3
Fir cellulose	1296.0	8.0
Pine cellulose	1279.8	7.9
Spruce-bleached kraft pulp	203.31	1.2
Pine-bleached kraft pulp	144.18	0.89
Bleached bisulfite pulp of eucalyptus	105.30	0.65
Rayon regenerated cellulose	49.41	0.30

nanofibrillated cellulose was obtained from sugar palm fibers, by using chemical and mechanical processes. This has 82% crystallinity, 92% yield, 5.5 ± 1.0 nm average diameter, and several micrometer length, as well as thermal stability with respect to raw fibers (Ilyas et al. 2019a, b, c). In other study, nanocrystalline cellulose was extracted from sugar palm fibers by delignification and mercerization treatments, at 60 wt% sulfuric acid. The results show nanocrystals with 9 ± 1.96 nm diameter and 130 ± 30 nm length (Ilyas et al. 2018a, b); (II) many studies are focused on the reuse and recycling of biobased packaging products. The plastics aging is influenced by different factors, such as exposure to sunlight, oxygen, air, water, heat, cold, and microorganisms (Ilyas et al. 2021); (III) agroindustrial wastes such as starch and sugar palm fibers were used for producing nanocomposites by using the solution casting method, adding 0.1–1.0 wt% nanocellulose. The highest mechanical and thermal stability was obtained with 1.0 wt% nanocellulose. Moreover, burial tests in the soil showed biodegradability resistance (Ilyas et al. 2020); (IV) bionanocomposite films were produced with sugar palm starch and sorbitol/glycerol. The nanocrystalline cellulose was obtained from sugar palm fiber, which was treated with NaClO_2 , bleached with NaOH and hydrolyzed with acid. The nanocrystalline cellulose showed 8.5 ± 1.82 nm diameter and 130 ± 30.23 nm length. The films showed higher crystallinity, tensile strength, Young's modulus, thermal, and water resistance (Ilyas et al. 2018a, b); (V) nanofibrillated sugar palm cellulose was extracted by using delignification and mercerization processes. Such nanofibers were mechanically extracted by high-pressure homogenization. The resulting sizes are cycle dependent, particularly when increased from 5 to 15 cycles produce decrease in diameter from 21.37 nm to 5.5 nm, but increase crystallinity from 38% to 81.19% (Ilyas et al. 2019a, b, c).

The effects of ionizing radiation on cellulose as well as in other polysaccharides result in physicochemical property modifications that include decomposition, chemical structure, mechanical resistance, solubility in fluids, and reactivity. For example, in a study *Miscanthus* biomass containing cellulose, hemicellulose, and lignin was irradiated by gamma rays at 1200 kGy dose. The results show that after

irradiating, the DP values decreased from 366,225 to 11,354, which means 96% less. Moreover, the weight average molecular mass (Mw) and the number average molecular mass (Mn) decreased with increasing absorbed doses. Non-irradiated biomass had Mw = 542,342 Da and Mn = 45,544 Da, which decreasing up to 72% (namely 150,821) and 33% (30,237 Da), respectively, after irradiation at 1200 kGy dose. For non-irradiated biomass, the Mw/Mn ratio was 11.9, while those irradiated at 1200 kGy decrease up to 4.98. Moreover, gamma rays can partially destroy the intra- or intermolecular hydrogen bonds into biomass. Thus, cellulose and hemicellulose content decrease with increasing absorbed doses. However, the lignin content before and after irradiation was almost stable (Su et al. 2020).

2.2 Degree of Crystallinity

Polymers have crystalline and amorphous regions. In the case of polymer fibers, they are uniaxially oriented filaments with cylindrical symmetry, sometimes the chain axis direction coincides with the cylindrical symmetry axis. In the case of cellulose, linear molecules are linked laterally by hydrogen bonds to form linear bundles and crystalline structures. As known, the degree of crystallinity allows to establish the relationship between structure and properties, which can be calculated by X-ray diffraction, calorimetry, mass density measurements, among others. The degree of crystallinity for materials containing cellulose varies, for example, 90% for ramie fibers, 80–85% for cotton, and 60–85% for wood (Ioelovich and Veveris 1987; Park et al. 2010).

The amorphous regions are reactive during pulping processes; thus, amorphous cellulose is more reactive than fully crystalline and therefore more easily degradable. In some materials, the crystalline regions are interrupted every 60 nm with amorphous regions. The crystalline regions may contain occasional kinks or folds on the polymer chain. As known, cellulose is difficult to hydrolyze due to its crystalline structure. However, high degree of crystallinity allows to cellulose be more resistant to chemical attack during the pulping process. Moreover, with high crystalline/amorphous regions ratio, the rigidity of cellulose fibers increases, but flexibility decreases (Akerholm, et al. 2004). Materials containing cellulose with high degree of crystallinity show increase or decrease on their properties, as shown in Table 2.

Table 2 Properties of materials containing cellulose with high crystallinity (Ioelovich and Veveris 1987)

Properties that increase	Properties that decrease
Tensile strength	Deformation
Scratch resistance	Water absorption
Stiffness	Swelling
Dimensional stability	Colorants absorption
Density	Flexural
Young modulus	Chemical reactivity

Regarding the effects of gamma rays on cellulose; at a dose of 25 kGy the degree of crystallinity decreases by 1%, while at 31.6 kGy it decreases by 12%. However, this unchanged up to 300 kGy. For higher doses (> 300 kGy), the crystallinity decreases gradually. In other study, the crystallinity remains unchanged up to 1000 kGy, then decrease for higher doses. Finally, at 6.5 MGy crystallinity totally disappears (Glegg and Kertesz 1957).

Regenerated cellulose films prepared by NaOH/urea solvent system were irradiated (5–50 kGy). Cellulose fibers are surrounded by hemicellulose and lignin structures. During irradiation, gamma rays produce degradation in the hemicelluloses, releasing individual crystallites, due to the glycosidic bond cleavage, located between cellulose, and hemicellulose. At low doses, the crystallinity percentage increases up to 12%, due to the hemicellulose degradation, which is more amorphous than cellulose. Moreover, amorphous area is more reactive to gamma rays compared to crystalline one. Thus, improved arrangement of cellulose chains is due to cross-linking induced by gamma radiation. However, at higher doses than 10 kGy, crystallinity decreases up to 20%, which is attributed to chains cleavage, which occurs preferentially in the amorphous regions (Tanvir et al. 2016).

After irradiation, glucose units into cellulose are destroyed by cleavages, which produce weight loss. Moreover, bond fracture is randomly affected by high-energy radiation along each molecular chain; then, as a result of random fracture, the crystallite sizes decrease as degradation proceeds. The bonds in the amorphous and crystalline domains are expected to be equally sensitive to radiation (Horio et al. 1963).

2.3 Chemical Structure and Morphology

Cellulose irradiated at high doses in oxygen produces carbonyl and carboxyl groups due to oxidative degradation. The 1732 cm^{-1} peak corresponding to C=O stretching vibration of the carbonyl group appears at 200 kGy dose. Moreover, its intensity increases gradually with the dose, up to 1200 kGy. In the case of its morphology, cellulose microfibrils have crystalline and amorphous zones, where chemicals can penetrate. Gamma radiation causes breakup of cellulose to shorter chains (which are water soluble), as well as additional microcracks, in which water molecules can easily penetrate. Scanning electron microscopy images of non-irradiated cellulose show smooth and homogeneous surfaces with some dispersed particles. However, at 50 kGy dose, more dispersed particles and some cracks are observed. For higher doses, more space between cellulose surfaces appears, along with small voids. Such modifications are due to the scission and cross-linking of molecular chains.

2.4 *Thermal Properties and Mechanical Properties*

The chemical decomposition of irradiated cellulose (0.2–2.2 MGy doses) is a process related with the temperature. Such decomposition stimulates a monotonous increase on the production of valuable organic products through chain mechanisms. The results shown that irradiation reduces the yield of carbon and water. The hydrolysis of water-soluble fractions results in the formation of xylose, arabinose, glucuronic and formic acids, malondialdehyde, among others. Moreover, water-soluble products, cellobiose, glucose, glyoxal, and 2-ketogluconic are detected. The cellulose decomposition efficiency depends on the irradiation and heating rates. For specific irradiation dose, if the temperature increases, then the degree of polymerization decreases. At 100 °C, low decomposition was obtained, but for higher temperatures resulting notable decomposition. Furthermore, the fragmentation efficiency at 190 °C was six times higher than that obtained at room temperature (Kholodkova and Ponomarev 2011; Ponomarev and Ershov 2014).

The degree of crystallinity is one of the most important structural parameters in cellulose, since its values have great influence on the physical and mechanical properties. Regenerated cellulose films were prepared with NaOH and urea, and exposed to gamma rays (5–50 kGy dose). The results show free radical production on the cellulose chains, due to the hydrogen and hydroxyl abstraction. At irradiation doses less than 10 kGy, the cellulose chains crosslink, thus improvements on the mechanical properties are obtained, resulting in a stronger but more brittle material. At higher doses, chain cleavage degradation predominates over cross-linking. Glycosidic bond cleavage occurs by random depolymerization which produces molecular weight decrease and lower mechanical properties values.

The mechanical characteristics for non-irradiated and irradiated cellulose films show that the tensile strength for non-irradiated ones was 62.37 MPa, which increase 9% at 10 kGy dose, but for higher doses decrease up to 51%. In case of Young modulus, 56.44 MPa was obtained for non-irradiated films, but such value increases 42% at 10 kGy dose. Furthermore, the elongation at break decreases gradually, from 1.41% to 0.59%, which means 58% less, which was due to the polymer chains cross-linking, that reduces their mobility (Tanvir et al. 2016).

3 **Effects of Gamma Radiation in Materials Containing Cellulose**

Gamma radiation has proven to be an effective process for recycling of materials containing cellulose, due to its easy handling at room temperature and great penetration. It is considered a fast, clean, and environmental-friendly process. Moreover, such ionizing radiation can be used in composite materials as an alternative to coupling or compatibilizing agents, for improvement of the filler/matrix interfaces.

Moreover, recycled materials by gamma rays can be reused for producing novel materials with specific characteristics.

3.1 Cotton

As is known, after scouring and bleaching, cotton contains 99% cellulose. In one study, waste cotton fabrics containing 95–99% cellulose were irradiated with gamma rays (doses of 10–100 kGy, at a rate of 10 kGy/h, at room temperature) to produce microcrystalline cellulose (MCC). Waste dry cotton was used, and wet cotton was immersed in 35% H₂O₂ solution. The results show that the degradation of the dry cellulose was due to the formation of macroradicals, while that of the aqueous solution was due to the indirect effects of the products of water radiolysis after irradiation. Free radicals such as hydroxyl formed by water radiolysis are effective for enhancing cellulose degradation. The oxidizing species presence, such as hydrogen peroxide, can enhance the hydroxyl radical formation as well as the degradation process, in order to reduce the degree of polymerization of cellulose (Swantomo et al. 2017).

The degree of polymerization (DP) of cellulose decreases with increasing irradiation dose. DP was higher in the medium wet phase (hydrogen peroxide) than that in dry phase after irradiation. Moreover, the water solubility of the cotton cellulose irradiated at the middle wet and dry phase decreases with radiation dose increase. In the case of crystallinity, waste cotton fabrics showed 62.63%, which was increasing for MCC irradiated at 50 kGy, namely 70.8%; but lower than those values for commercial MCC. The crystallite sizes were 5.92 nm for waste cotton fabrics, which decreased for MCC irradiated at 50 kGy at 4.65 nm, and even more for commercial MCC, namely 4.0 nm (Swantomo, et al. 2017).

In view of the ecological and economic restrictions imposed on the textile industry, innovative surface modification on the textile surfaces (as cotton fibers) has been made by high-energy irradiation methods, such as gamma rays, which improve wettability, dyeability, printability, color fastness, hydrophilicity, and effective antimicrobial activity. Gamma rays improve the accessibility of the functional group without affecting other bulk properties. Moreover, such modified textile fibers have been mixed with other materials to produce novel materials, such as upholstery panels for the automotive industry, for helping the vehicle acoustic properties (Shahid-ul-Islam and Mohammad 2015). The combined process including alkaline chemical treatment and gamma radiation was applied to cotton, the results showed a decrease in the degree of polymerization, as well as an increase in the content of carbonyl, nitrogen (19.16%) and oxygen. In addition, an increase of 3 °C in the decomposition temperature is observed, with respect to that of untreated cotton (358 °C), but a high increase in the exothermic peak, located at 450 °C, for treated cotton, with respect to untreated cotton, located at 382 °C. Such thermal changes are used for textile fabrics improvements.

Cotton cellulose was irradiated with gamma rays at 10 kGy/h dose ratio. Radiolysis was carried out at 77 K for cellulose, followed by heating to 190–200 K, for the appearance of the secondary thermal reactions. The radiolysis results show production of H-C=O formyl radical, while for heating cellulose formation of ROO peroxide radicals. For the primary radicals, thermal transformations consisted of polycarbohydrate complex dehydration as well as bond dissociation (CH, C-OH, and CC), elimination (H₂O, H₂, CO, and CO₂), radical formation (allyl and polyene) (Kuzina and Mikhailov 2006).

After irradiation by electron beam at room temperature, cotton cellulose showed decomposition on its carbonyl groups rather than carboxyl groups. The carbonyl group yield was 6.5 ± 0.5 at 100 eV, but lower for the carboxyl groups, namely 0.9–1.8. Radiation at room temperature and low-dose rates leads chemical transformations. Moreover, irradiated cellulose decomposes efficiently at temperatures below the pyrolysis initiation threshold. At 50 kGy, H groups were produced. Higher doses become the cellulose in condensate liquid (Ponomarev and Ershov 2014).

3.2 Paper

Paper-based products contain 90–99% cellulose, which provides strength, flexibility, and water sensitivity. It has intramolecular (within molecule) and intermolecular (with adjacent molecules) very strong hydrogen bonds. In a study, paper with kraft cellulose was irradiated with gamma rays. As known, drainability is the measurable index for refining degree of the pulps. The freeness term is used to appoint the pulp quality. Moreover, recycled fibers have lower drainage rates comparing to virgin fibers, namely they have poor quality due to the paper forming and drying process. The Schopper-Riegler freeness index (°SR) and the strength increase with the radiation dose increase (Dienes et al. 2005).

3.3 Cellophane

Cellophane is produced by cellulose from wood, cotton, hemp, or other source, which is called dissolving pulp that contains 92–98% cellulose. Cellophane is widely used as a packaging material for food and pharmaceutical products. Certain coatings are applied to improve its barrier properties, although these may present difficulties for its biodegradability. For solving such problems, some investigations have been carried out, for example, (I) cellophane membranes were irradiated at 30–60 kGy. As known, cellophane is used for dialysis membranes since its high hydrophilicity; however, it is not soluble in water, but allows the diffusion of ions and low-molecular-weight solutes, which is related to crystallinity and the intermolecular hydrogen bonding between hydroxyl groups. The cellophane membranes were modified at low irradiation dose, but for longer exposure was hardly affected.

Gamma rays produce changes on the salt permeability, electrical resistance, and OH moieties. The wide absorption band located at $3200\text{--}3400\text{ cm}^{-1}$ becomes narrower with irradiation dose increases, due to the weakening of the intermolecular hydrogen bonds (Vázquez et al. 2004); (II) three types of cellophane films (uncoated cellophane, coated cellophane nitrocellulose, and cellophane coated with PVDC) were irradiated by gamma rays in air. The results show remarkable biodegradation in the uncoated cellophane. The formed peroxy free radicals can cause reactions on the polymer chains, continue for long periods, and cause structural changes. The mineralization percentage of irradiated uncoated cellophane after 3 months storage was 103%, higher than that for non-irradiated, namely 71%. The aging of the irradiated samples increased their biodegradation with storage time, due to irradiation-induced free radicals and chain cleavage (Benyathiar et al. 2015).

3.4 *Sisal*

The sisal fibers contain cellulose (65.8%), hemicellulose (12%), lignin (9.9%), pectin (0.8%), wax (0.3%), and water-soluble compounds. Composites with sisal fibers have been studied, for example, (I) composites made with woven sisal fibers and castor oil polyurethane, without compatibility agents were irradiated at 25 kGy dose. The results show a flexural strength of 42 ± 3 MPa for the non-irradiated composites, and an increase of 31% for the irradiated ones; while the modulus of elasticity of 1.64 ± 0.12 GPa for the non-irradiated composites, increases by 22% for the irradiated ones. High impact values were obtained for composites due to the well sisal fiber dispersion. Moreover, probably the ends of the fibers act as crack blockers, preventing the cracks propagation and consequently the impact resistance increase (Vasco, et al. 2021); (II) polypropylene with 20% sisal fibers was irradiated up to 70 kGy (at 4.8 kGy/h ratio), in air at room temperature. After irradiating, at 10 kGy the tensile strength increases 24% and the elongation at break 25%, while impact resistance decreases 24%. Such results can be related with the fractured surfaces after mechanical testing, where the sisal fiber dispersion is not optimal. Furthermore, hydrophilicity for irradiated polypropylene increases since the OH functional groups increase and slight cross-linking is produced on it (Albano et al. 2002).

3.5 *Bamboo*

Bamboo contains 60% cellulose with high content of lignin. Gamma rays are used for eliminate moisture and biological agents (mold fungi) in native bamboo, which affect long-term durability and dimensional stability. Cell walls of bamboo were irradiated up to 1000 kGy dose. At doses less than 100 kGy, the crystallinity and the cellulose content increase, but at higher doses (300 kGy), it was degraded showing

decrease on the crystalline regions, with more concentration of carbonyl and methoxyl groups. Small fragments easily soluble in water are produced. In the case of the hemicellulose, it was degraded at doses lower than 100 kGy, via scission of molecular chains; its degradation continues up to 1000 kGy doses. Moreover, non-phenolic lignin changed to phenolic with the irradiation dose increase (Sun, et al. 2014).

Low gamma radiation doses (<5 kGy) have been applied to extend the shelf life of bamboo shoots after harvest. Unfortunately, a lot of bamboo shoots are lost due to microbial spoilage during storage and transportation. *Dendrocalamus asp* shoots were irradiated (0.5–5.0 kGy), immersed in 2% NaCl solution, and stored at 5 ± 2 °C. At 2.5 kGy and 5.0 kGy, no microbial load was detected up to 240 days at 5 ± 2 °C storage; thus, the cells were destroyed at these conditions. The moisture content of non-irradiated bamboo shoots ranged between 90.77% and 94.73%, while for those irradiated ones, it increased from 94.24% to 96.31% (Singh, et al. 2021).

3.6 Wood

Gamma rays can produce free radicals and covalent bonds breaking, so molecular weight decreases. The polymer chains can be attached to the initial split point or reorganized by covalent cross-linking with neighboring chains. During irradiation, peroxy and hydroperoxy radicals are produced in the amorphous regions. When more molecules are breaking into the crystallites, the chain cleavage process increases the stress concentration in the crystals. Moreover, better adhesion between fibers and the matrix is getting when moisture is removed from the composite by gamma radiation.

Wood is the primary source of cellulose fibers. The wood cell walls contain cellulose (45–60%), hemicellulose (20–40%), lignin (25%), and pectin (5%). For wood cellulose, the degree of polymerization (DP) decreases when increasing radiation dose. For non-irradiated, the DP value was 1200, which decreases drastically up to 88% at 200 kGy (Ioelovich and Plotnikov 1999). As known, when the irradiation dose increases, some processes occur, including depolymerization, crystalline structure distortion (or dislocation), changes on the inter-plane distances as well as macro-radical formation. In wood irradiated at 500 kGy, high solubility is obtained due to the depolymerization and degradation of the hemicellulose. Their side-chain constituents (galactans) are affected earlier, more than those located at the primary backbone, namely xylan or mannan. Furthermore, softening temperature (T_s) was located at 235 °C for non-irradiated cellulose, which decreases linearly up to 300 kGy, due to the scission of chemical bonds such as glycosidic (Ioelovich and Plotnikov 1999).

Bleached wood cellulose was irradiated; the results show chains scission and local dislocations in crystalline domains. The distance between (020) crystalline planes increased linearly with the radiation dose increases. At doses above 1000 kGy,

the crystallinity percentage and the crystallite size decrease (Ioelovich and Plotnikov 1999).

Wood species (*Pinus patula*, *Pinus cunninghamia*, *Cedrela fissilis*, and *Ocotea porosa*) were irradiated up to 100 kGy. The results did not show significant changes, which allowed irradiate the wood several times, even if microorganism re-infestation occurs. Therefore, gamma rays are efficient as disinfection and decontamination treatment, since it does not damage the wood structure or generate by-products. Thus, wood sterilization by gamma rays is an easy, fast, and effective process. Thermal curves for irradiated wood species showed two stages, the first corresponding to the depolymerization and the second to the cellulose combustion. The thermal behavior shows 9% mass loss up to 130 °C, while at 250 °C, thermal oxidation of the cellulose components (crystalline and amorphous) was obtained. At 330 °C, mass loss was 64%; low-molecular-weight fragments were obtained as consequence of rupture of both glucosidal groups and anhydroglucose units. Finally, at 330–440 °C, the lignin oxidation occurred, with 20% mass loss. Moreover, lignin content decreases gradually from 29.5% to 27.5%, according to irradiation dose increases (Severiano et al. 2011).

Composites produced with wood flour, polypropylene, and 3% maleic anhydride graft polypropylene as compatibilizer were irradiated (5–30 kGy doses). At 10 kGy dose, the highest mechanical values were obtained. The highest flexural modulus (9.6 GPa) was 23% higher than that for non-irradiated; such improvement was due to the predominant cross-linking, which strengthens the wood flour/polypropylene interactions. The flexural strength was 48.6 MPa for non-irradiated composites, which increase 4% for irradiated ones. In the same way, the tensile modulus for irradiated composites increased 10% (from 2.29 to 2.53 GPa) and the tensile strength 3% (from 28.6 to 29.5 MPa). For doses higher than 10 kGy, the chain cleavage had a greater effect than cross-linking and the mechanical properties decrease (Rimdisit et al. 2010).

Wood/polypropylene composites were irradiated up to 100 kGy. The results show minor changes on the tensile strength values but improvement on the bending strength is up to 50 kGy dose, as shown in Table 3.

Table 3 Tensile and bending strength of wood/polypropylene composites (Ndiaye and Tidjani 2014)

Dose (kGy)	Tensile strength (MPa)	Bending strength (MPa)
0	12.00	12.35
10	12.25	13.75
25	12.50	14.15
50	11.75	14.50
100	11.25	12.40

3.7 *Microcrystalline Cellulose (MCC)*

Cellulose microcrystals are fine crystalline powder, odorless, white, and biodegradable materials. Microcrystals are obtained from pulp of fibrous plants with mineral acids, by depolymerized of alpha cellulose (type I β). Microcrystalline cellulose degradation by gamma rays is one of the most promising methods, due to easy handling at room temperature, with great penetration, fast, and clean.

Microcrystalline cellulose (MCC) was irradiated by gamma rays at 400–1200 kGy doses. The results show that the degree of polymerization (DP) decreases gradually with absorbed gamma dose increases. The DP decreases from 183,045 to 47,495 at 400 kGy dose, which meant 74% less. Moreover, non-irradiated MCC shows a smooth surface, but this was changing according to the gamma dose increase. At doses higher than 400 kGy, holes on the surface were produced. The waste cotton fabrics have great potential as raw materials for producing low-cost microcrystalline cellulose (MCC). The DP of waste cotton decreased with increasing radiation, which is due to direct chain scission at the β -glycosidic bonds, an increase in reactive radicals due to hydrogen bond cleavage or an oxidation process.

3.8 *Cellulose Nanocrystals (CNC)*

Cellulose nanocrystals (CNC) can be obtained by mechanical, chemical, enzymatic, or biological processes and have high potential uses as reinforcing materials in nanocomposites. For example, addition of irradiated biodegradable CNCs is being used in packaging applications. Cellulose nanocrystals were irradiated by gamma rays. After irradiation, the molecular weight increases. At higher doses, the degree of polymerization (DP) decreases 30%, while the aldehyde group content increases to 379 mmol CHO/kg due to the cleavage of glycosidic bonds. Moreover, irradiated CNCs provide easy interaction with aqueous biopolymer matrices (i.e., alginate), due to their wettability and removal properties. They increase stability in food since preventing lipid oxidation. For non-irradiated CNC, the concentration of carboxylic acid groups (COOH) was 43 mmol COOH/kg, but increased to 631 mmol COOH/kg at 80 kGy dose. These physicochemical changes allowed improvement on the antioxidant properties (Criado et al. 2017).

Cellulose nanocrystals (CNC), extracted from kraft pulp, are crystalline nanomaterials produced by hydrolysis. Dispersed suspensions of cellulose nanocrystals were irradiated up to 80 kGy. The results show changes on its molecular structure as well as in adsorbed water on the CNC surfaces. Changes in the ketones were observed at 1750 cm^{-1} and 1650 cm^{-1} in the FT-IR spectrum. After irradiation, aldehyde and carboxylic acid were formed; the last improved the hydrophilic behavior, which was corroborated by decrease of contact angle. Moreover, for non-irradiated CNC, the degree of polymerization (DP) was 135, which was decreasing to 95 at 80 kGy.

In other study, cellulose was extracted from rice husk by alkaline and bleaching treatments, after cellulose nanocrystals (CNC) were produced by acid hydrolysis. Finally, gamma radiation was used to prepare hydrogels (α -cellulose reinforced gelatin) and cellulose nanocrystals (CNC) in absence of cross-linking agents. Addition of CNC produced higher swelling capacity and improved dynamic mechanical properties, and the absorption/release drug performance, Moreover, the CNC sizes affected the performance of the cross-linked hydrogels. Such gelatin/CNC hydrogels are suitable for drug delivery applications (Wan Ishak et al. 2018).

3.9 Cellulose and Polylactic Acid

Composites with polylactic acid (PLA), microcrystalline cellulose fibers (MCC), cellulose nanowhiskers (CNW), and maleic anhydride (AM) were produced by a melt spinning process and irradiated with gamma rays at 5–30 kGy doses (1.92 kGy/h ratio, at room temperature). Due to the fiber fineness variation, the tensile strength is expressed as toughness (cN/tex), related to force per fineness unit. Fineness relates the fiber mass and its length (tex, g/km). After irradiation, chain cleavage and decrease on the molecular weight were obtained for the PLA matrix, probably due to structural changes that occurred in the amorphous/crystalline fractions. Moreover, the tenacity, Young modulus, and elongation at break decrease gradually on the composites, becoming a brittle material. Table 4, shows the data for toughness, Young's modulus and elongation at break of the composites, while Table 5 shows the decrease in mechanical characteristics.

Table 4 Mechanical properties of PLA/cellulose composites as a function of absorbed dose (Aouat, et al. 2019)

Material	Dose (kGy)	Tenacity (CN/tex)	Young modulus (GPa)	Elongation at break (%)
PLA	0	7.74 ± 0.2	3.27 ± 0.5	77.77 ± 1.5
	30	5.74 ± 0.2	2.64 ± 0.2	45.52 ± 1.5
92% PLA/7% MA/1% MCC	0	8.04 ± 0.1	3.38 ± 0.2	91.60 ± 0.8
	30	6.52 ± 0.1	2.91 ± 0.1	65.22 ± 1.9
92% PLA/7%/1% CNW	0	6.88 ± 0.4	2.94 ± 0.5	36.46 ± 1.1
	30	6.78 ± 0.7	2.92 ± 0.1	36.81 ± 0.9

Table 5 Decrease percentages of PLA/cellulose composites (Aouat et al. 2019)

Fibers	Tenacity (%)	Young modulus (%)	Elongation at break (%)
PLA	25	19	41
PLA/MCC	18	13	28
PLA/CNW	3	1	3

With respect to the thermal behavior, after irradiation the temperature decreases for the glass transition (T_g), cold crystallization (T_{cc}), and melting (T_m). For PLA, at 30 kGy dose the temperatures for T_g , T_{cc} , and T_m decrease 7, 14, and 4 °C, respectively, while for irradiated composites 5, 11, and 3 °C, respectively. Thus, composites are thermally more stable. Moreover, The PLA crystallinity increases, due to the chain cleavage and the crystallite formation with a smaller size (Aouat, et al. 2019).

4 Conclusions

Investigations concerning to cellulose-based composites have shown their effectiveness on diverse applications. Furthermore, recycling based on the structural modifications in cellulose has allowed that it has been used as reinforcement in composites. Such modifications can be got by gamma rays, which have advantages over other processes such as chemical attacks or thermal treatments. Thus, benefits offered by gamma rays as recycling tool include to be chemical-free, environmental-friendly, clean, and easy handling.

Acknowledgments The authors thank Council of Science and Technology of the State of Mexico (COMECYT), for the scholarship granted to one of the authors (I.Z. Garduño-Jaimes).

References

- Akerholm M, Hinterstoisser B, Salmen L (2004) Characterization of the crystalline structure of cellulose using static and dynamic FT-IR spectroscopy. *Carbohydr Res* 339(3):569–578. <https://doi.org/10.1016/j.carres.2003.11.012>
- Albano C, Reyes J, Ichazo M, González J, Brito M, Moronta D (2002) Analysis of the mechanical, thermal and morphological behaviour of polypropylene compounds with sisal fibre and wood flour, irradiated with gamma rays. *Polym Degrad Stab* 76:191–203. [https://doi.org/10.1016/S0141-3910\(02\)00014-9](https://doi.org/10.1016/S0141-3910(02)00014-9)
- Ansari F, Skrifvars M, Berglund L (2015) Nanostructured biocomposites based on unsaturated polyester resin and a cellulose nanofiber network. *Compos Sci Technol* 117:298–306. <https://doi.org/10.1016/j.compscitech.2015.07.004>
- Aouat T, Kaci M, Lopez-Cuesta J, Devaux E, Mahlous M (2019) The effect of gamma-irradiation on morphology and properties of melt-spun poly (lactic acid)/cellulose fibers. *Polym Degrad Stab* 160:14–23. <https://doi.org/10.1016/j.polymdegradstab.2018.11.014>
- Benyathiar P, Selke S, Auras R (2015) Effect of irradiation on the biodegradation of cellophane films. *J Polym Environ* 23:449–458. <https://doi.org/10.1007/s10924-015-0740-9>
- Bledzki AK, Gassan J (1999) Composites reinforced with cellulose based fibres. *Prog Polym Sci* 24:221–274. [https://doi.org/10.1016/S0079-6700\(98\)00018-5](https://doi.org/10.1016/S0079-6700(98)00018-5)
- Burillo G, Clough R, Czvikovszky T, Güven O, Moel A, Liu W, Singh A, Yang J, Zaharescu T (2002) Polymer recycling: potential application of radiation technology. *Radiat Phys Chem* 64:41–51. [https://doi.org/10.1016/S0969-806X\(01\)00443-1](https://doi.org/10.1016/S0969-806X(01)00443-1)

- Criado P, Fraschini C, Jamshidian M, Salmieri S, Safrany A, Lacroix M (2017) Gamma-irradiation of cellulose nanocrystals (CNCs): investigation of physicochemical and antioxidant properties. *Cellulose* 24:2111–2124. <https://doi.org/10.1007/s10570-017-1241-x>
- Dienes D, Kemény S, Egyházi A, Réczey K (2005) Improving the capability of the Schopper–Riegler freeness measurement. *Measurement* 38:194–203. <https://doi.org/10.1016/j.measurement.2005.07.011>
- Glegg RE, Kertesz ZI (1957) Effect of gamma-radiation on cellulose. *Polym Chem* 26(114):289–297. <https://doi.org/10.1002/pol.1957.1202611403>
- Hallac BB, Ragauskas AJ (2011) Analyzing cellulose degree of polymerization and its relevancy to cellulosic ethanol. *Biofuels Bioprod Biorefin* 5(2):215–225. <https://doi.org/10.1002/bbb.269>
- Horio M, Imamura R, Mizukami H (1963) Effect of gamma irradiation upon cellulose. *Bull Inst Chem Res Kyoto Univ* 41(1):17–38. <http://hdl.handle.net/2433/75947>
- Ilyas R, Sapuan S, Ishak M (2018a) Isolation and characterization of nanocrystalline cellulose from sugar palm fibres (*Arenga Pinnata*). *Carbohydr Polym* 181:1038–1051. <https://doi.org/10.1016/j.carbpol.2017.11.045>
- Ilyas R, Sapuan S, Ishak M, Zainudin E (2018b) Development and characterization of sugar palm nanocrystalline cellulose reinforced sugar palm starch bionanocomposites. *Carbohydr Polym* 202:186–202. <https://doi.org/10.1016/j.carbpol.2018.09.002>
- Ilyas R, Sapuan S, Ishak M, Zainudin E (2019a) Sugar palm nanofibrillated cellulose (*Arenga pinnata* (Wurmb.) Merr): effect of cycles on their yield, physic-chemical, morphological and thermal behavior. *Int J Biol Macromol* 123:379–388. <https://doi.org/10.1016/j.jbiomac.2018.11.124>
- Ilyas R, Sapuan S, Ibrahim R et al (2019b) Sugar palm (*Arenga pinnata* (Wurmb.) Merr) cellulosic fibre hierarchy: a comprehensive approach from macro to nano scale. *J Mater Res Technol* 8:2753–2766. <https://doi.org/10.1016/j.jmrt.2019.04.011>
- Ilyas R, Sapuan S, Ibrahim R et al (2019c) Effect of sugar palm nanofibrillated cellulose concentrations on morphological, mechanical and physical properties of biodegradable films based on agro-waste sugar palm (*Arenga pinnata* (Wurmb.) Merr) starch. *J Mater Res Technol* 8:4819–4830. <https://doi.org/10.1016/j.jmrt.2019.08.028>
- Ilyas R, Sapuan S, Ibrahim R et al (2020) Thermal, biodegradability and water barrier properties of bio-nanocomposites based on plasticised sugar palm starch and Nanofibrillated celluloses from sugar palm fibres. *J Biobased Mater Bioenergy* 14:234–248. <https://doi.org/10.1166/jbmb.2020.1951>
- Ilyas R, Sapuan S, Sabaruddin F et al (2021) Reuse and recycle of biobased packaging products. In: *Bio-based packaging: material, environmental and economic aspects*. Wiley, pp 413–426. <https://doi.org/10.1002/9781119381228.ch23>
- Ioelovich M, Plotnikov O (1999) Influence of high-energy irradiation on structure and properties of cellulose. *Sci Israel Technol Advant J* 1:11–15
- Ioelovich MY, Veveřis GP (1987) Determination of cellulose crystallinity by X-ray diffraction method. *J Wood Chem* 5:72–80
- Kargarzadeh H, Sheltami RM, Ahmad I, Abdullah I, Dufresne A (2015) Cellulose nanocrystal reinforced liquid natural rubber toughened unsaturated polyester: effects of filler content and surface treatment on its morphological, thermal, mechanical, and viscoelastic properties. *Polymer* 71:51–59. <https://doi.org/10.1016/j.polymer.2015.06.045>
- Kholodkova E, Ponomarev A (2011) Phase distribution of the products of radiation and post-radiation distillation of cellulose. *High Energy Chem* 45:386–389. <https://doi.org/10.1134/s0018143911040072>
- Kuzina S, Mikhailov A (2006) The oxidation and thermal transformations of macro radicals in gamma irradiated cellulose. *Russ J Phys Chem* 80:1666–1670. <https://doi.org/10.1134/s0036024406100207>
- Ndiaye D, Tidjani A (2014) Physical changes associated with gamma doses on wood/polypropylene composites. *IOP Conf Ser Mater Sci Eng* 62:012025. <https://doi.org/10.1088/1757-899x/62/1/012025>

- Park S, Braker JO, Himmel ME, Parilla PA, Johnson D (2010) Cellulose crystallinity index: measurement techniques and their impact on interpreting cellulase performance. *Biotechnol Biofuels* 3:10–16. <https://doi.org/10.1186/1754-6834-3-10>
- Ponomarev A, Ershov B (2014) Radiation-induced high-temperature conversion of cellulose. *Molecules* 19:16877–16908. <https://doi.org/10.3390/molecules191016877>
- Rimdisut S, Wongsongyot S, Jittarom S, Suwanmala P, Tiptipakorn S (2010) Effects of gamma irradiation with and without compatibilizer on the mechanical properties of polypropylene/wood flour composites. *J Polym Res* 18:801–809. <https://doi.org/10.1007/s10965-010-9477-2>
- Severiano L, Lahr F, Bardi M, Machado L (2011) Evaluation of the effects of gamma radiation on thermal properties of wood species used in Brazilian artistic and cultural heritage. *J Therm Anal Calorim* 106:783–786. <https://doi.org/10.1007/s10973-011-1840-y>
- Shahid-ul-Islam, Mohammad F (2015) High-energy radiation induced sustainable coloration and functional finishing of textile materials. *Ind Eng Chem Res* 54:3727–3745. <https://doi.org/10.1021/acs.iecr.5b00524>
- Singh D, Chatterjee R, Chauhan A, Aggarwal M, Varma A, Kharkwal A (2021) Effect of gamma irradiation technique on the microbial and nutritional quality of edible bamboo shoot (*den-drocalamus asper*) for shelf-life enhancement. *J Exp Biol Agric Sci* 9(4):517–527. [https://doi.org/10.18006/2021.9\(4\).517.527](https://doi.org/10.18006/2021.9(4).517.527)
- Su Z, Li W, Liu L (2020) Radiation-induced structural changes of *Miscanthus* biomass. *Appl Sci* 10:1130. <https://doi.org/10.3390/app10031130>
- Sun F, Jiang Z, Sun Q, Lu F (2014) Changes in chemical composition and microstructure of bamboo after gamma ray irradiation. *Bioresources* 9(4):5794–5800. <https://doi.org/10.15376/biores.9.4.5794-5800>
- Swantomo D, Giyatmi G, Adiguno SH, Wongsawaeng D (2017) Preparation of microcrystalline cellulose from waste cotton fabrics using gamma irradiation. *Eng J* 21(2):173–182. <https://doi.org/10.4186/ej.2017.21.2.173>
- Tanvir A, Al-Maadeed M, Hassan M (2016) Secondary chain motion and mechanical properties of γ -irradiated-regenerated cellulose films. *Starch – Stärke* 69:1500329. <https://doi.org/10.1002/star.201500329>
- Vázquez M, Galán P, Casado J, Ariza M, Benavente J (2004) Effect of radiation and thermal treatment on structural and transport parameters for cellulose regenerated membranes. *Appl Surf Sci* 238:415–422. <https://doi.org/10.1016/j.apsusc.2004.05.161>
- Vasco M, Claro Neto S, Nascimento E, Azevedo E (2021) Gamma radiation effect on sisal/polyurethane composites without coupling agents. *Polymers* 27(2):165–170. <https://doi.org/10.1590/0104-1428.05916>
- Wan Ishak W, Ahmad I, Ramli S, Mohd AM (2018) Gamma irradiation-assisted synthesis of cellulose nanocrystal-reinforced gelatin hydrogels. *Nano* 8:749. <https://doi.org/10.3390/nano8100749>

Tensile, Thermal Properties, and Biodegradability Test of Paddy Straw Powder-Filled Polyhydroxybutyrate-3-Valerate (PHBV) Biocomposites: Acrylation Pretreatment



Noorulnajwa Diyana Yaacob, Hanafi Ismail, and Sam Sung Ting

1 Introduction

Over the past few years, there has been increasing interest in using natural fibres as a reinforcing agent in composite materials (Ilyas et al. 2021; Salwa et al. 2021; Chandrasekar et al. 2021; Li et al. 2015; Rubio et al. 2015; Sarifuddin et al. 2015; Pang and Ismail 2014; Anuar et al. 2012; Bertini et al. 2012). A combination of industry-applicable properties such as low cost, low density, non-toxicity, high specific properties, no abrasion during processing, and recyclability has contributed to an increase of interest from the manufacturing industry. However, several problems arise when incorporating such fibres into the matrices. The most notable problem is fibre-matrix incompatibility where a polar polymer (i.e. matrix) is concerned. This process generates a weak interface, hence causing low thermal and tensile properties (Chun et al. 2012).

Paddy straw powder (PSP)-filled polyhydroxybutyrate-3-valerate (PHBV) is a member of the polyhydroxyalkanoate (PHA) family. PHAs are biodegradable polyesters that are synthesised and accumulated intra-cellularly as a carbon or energy storage material during unbalanced growth by a large variety of bacteria. Currently, more than 80 hydroxyalkanoates have been detected as constituents of PHAs, and more than 300 different microorganisms are known to synthesise and accumulate PHAs intra-cellularly. Poly(β -hydroxybutyrate-co- β -hydroxyvalerate) (PHBV) is

N. D. Yaacob (✉) · S. S. Ting
Faculty of Chemical Engineering & Technology, Universiti Malaysia Perlis, Perlis, Malaysia
e-mail: noorulnajwa@unimap.edu.my

H. Ismail
School of Materials and Mineral Resources Engineering, Engineering Campus, Universiti Sains Malaysia,
Nibong Tebal, Penang, Malaysia

an optically active thermoplastic aliphatic polyester with high stereoregularity (Tao et al. 2009).

Paddy straw is one of the lignocellulosic fillers. Paddy (*Oryza sativa*) is an agricultural co-product which is found abundantly in Malaysia. By comparison with mineral, the lignocellulosic filler is shown to be able to demonstrate some outstanding properties (Gordobil et al. 2015; Berthet et al. 2015; Faludi et al. 2013; Bertini et al. 2012; Chun et al. 2012; Danjaji et al. 2001). However, there are strong polarised hydroxyl groups which are placed upon lignocellulosic fillers. Hence, it is hard to produce a tough interfacial bonding via a non-polar polymer matrix because hydrogen bonds hinder the filler surfaces from becoming wet. Because of the inadequacy of interfacial adhesion, low mechanical properties in polymer composites are portrayed by lignocellulosic fillers (Rahnama et al. 2013). Through altering the surface of filler, the interfacial adhesion between matrix and filler can be enhanced. Presently, a lot of approaches are applied in order to develop the interfacial adhesion between polymer matrices and lignocellulose filler, including silane treatment (Kargarzadeh et al. 2015; Ramamoorthy et al. 2014; Chun et al. 2012), esterification (Siyamak et al. 2012), using compatibilizers (Wu and Hakkarainen 2015), alkaline treatment (Obasi et al. 2014; Ramamoorthy et al. 2014; Rahnama et al. 2013; Njoku et al. 2012), and treatment with other chemical compounds.

Recently, scientific research and commercial industry have been focusing on the development and application of biodegradable plastic materials. The American Society for Testing and Materials Biodegradable (ASTM) defines plastics as degradable plastics where the degradation happens from the enzymatic action of naturally occurring microorganisms such as bacteria, fungi, and algae. Based on scientific reports, PHB can be degraded by numerous microorganisms in the various ecosystem (Kim et al. 2000). *Alternaria* sp., *Penicillium simplicissimum*, *P. funiculosum*, *P. notatum*, and *Eupenicillium* sp. are among the microbial species which are known to be able to degrade PHB (Rapa et al. 2011, 2014; Volova et al. 2010; Shah et al. 2007).

Hence, this study was conducted to examine the impacts of acrylic acid (AA) and filler loading of PSP upon thermal and tensile properties as well as morphology of PHBV/PSP biocomposites. Other than that, the biodegradability of these biocomposites was studied by using two different strains of *Aspergillus* species.

2 Experimental Work

2.1 Materials

PHBV was provided by Hasrat Bestari Sdn. Bhd. in Penang. The paddy straw was gained from the paddy field in Perlis. The paddy straw was cut, grounded into powder, and dried at a temperature of 80 °C for 24 h. The Malvern Particle Size Analyser Instrument (Italy) was used to measure the average particle size of PSP, and a measurement of 63µm was obtained. The ethanol and acrylic acid (grade 01730) were

Table 1 Formulation of treated and untreated of PHBV/PSP biocomposites

Materials	PHBV/PSP (untreated)	PHBV/PSP (AA treated)
PHBV (% wt.)	100	100
PSP (% wt.)	0, 5, 10, 15, 20	0, 5, 10, 15, 20
Acrylic acid (%) ^a	–	3

AA acrylic acid, PSP paddy straw powder, PHBV polyhydroxybutyrate-3-valerate

^a 3% based on the weight of PSP

provided by Fluka in Penang. Table 1 portrays the formulation of treated and untreated PHBV/PSP biocomposites.

2.2 Filler Treatment

AA was dissolved into 3% (v/v) ethanol. PSP was then added slowly into the solution and remained stirred for 1 h for a complete esterification. Lastly, PSP was filtered and dried in an oven at a temperature of 80 °C for 24 h.

2.3 The Blending of PHBV/PSP

PHBV was dried in a vacuum oven for 24 h at 60 °C while PSP was dried for 3 h at 105 °C prior to blending. Both PHBV and PSP were compounded in an internal mixer (Haake Rheomix Polydrive R 600/610) via co-rotating blades and a mixing head with a volumetric capacity of 69 cm³. Compounding temperature and rotor speed were set to 170 °C and 50 rpm. PHBV was put into the mixing chamber and was allowed to melt for 3 min, followed by sequential feeding of PSP which was done for 5 min. The materials were mixed for 7 min, making the total mixing time of 15 min. Compounded materials were gathered at the end of the mixing and were kept in a sealed plastic bag for subsequent compression moulding experiment.

2.4 Compression Moulding

Materials which were collected from the internal mixer underwent compression moulding in order to get test specimens. The compounded materials were put into a suitable steel mould which was covered by aluminium plates at both sides. The materials were pressed at 170 °C into tensile specimens of 3 mm thickness, respectively, via Kao Tieh Go Tech compression moulding machine. The moulding cycle involved 3 min of preheating without pressure, 3 min of compression under 14 MPa pressure, and 5 min of cooling under 6.21 MPa pressure. The cooling

process was conducted in an adjacent cool press which were equipped with tap water cooling.

2.5 Tensile Testing

Instron Machine model 5569 was applied to conduct the tensile testing based on ASTM D638. The tensile testing was carried out at 25 ± 3 °C while applying the crosshead speed of 50 mm/min. The tensile properties for five similar samples with different compositions were assessed and the average values were recorded.

2.6 Morphological Analysis

A variable pressure field emission scanning electron microscope (VPFESEM) model Zeiss SUPRA 35VP was applied to conduct SEM of fracture surfaces of tensile pieces. The microscope was operated at 10 kV. The test specimens were attached to an aluminium mount using double sticky tape and were sputtered with gold (10-nm thicknesses) in order to remove electron charging impacts.

2.7 Thermal Analysis

Thermogravimetric analysis Diamond, Perkin-Elmer (Malaysia) was applied to conduct thermal analysis. With the heating rate of 20 °C/min under nitrogen atmosphere, samples of 6 ± 2 mg were scanned from 30 to 600 °C.

2.8 Differential Scanning Calorimetry (DSC) Analysis

The thermal properties of biocomposites can be analysed using differential scanning calorimetry (DSC). This can be done through measuring heat changes which happen within bio-molecules under the controlled temperature. A hermetically sealed aluminium pan was used to encapsulate 10 mg of sample formulation. A Perkin-Elmer DSC 7 instrument was used to examine the sample. In order to eliminate the thermal history of the sample, it was initially heated up from room temperature to 300 °C at a heating rate of 10 °C/min for 5 min. After that, it was cooled down to room temperature with a heating rate of 20 °C/min. Lastly, it was reheated again to a temperature of 220 °C at a heating rate of 20 °C/min. The analysis was carried out under a nitrogen atmosphere.

The values of crystallisation temperature (T_c) and melting temperature (T_m) were shown by the maximum peak in the graph. The calculation of heat of fusion (ΔH) was performed via merging areas under the endothermic curve. The calculation of the percentage of crystallinity of biocomposites and PHBV was performed via Eq. (1).

$$\% \text{crystallinity} = \frac{\Delta H}{\Delta H_m} \times 100 \quad (1)$$

where ΔH represents the heat of fusion of sample and ΔH_m represents the heat of fusion of 100% semicrystalline PHBV.

2.9 Biodegradability Test

Biodegradability test was conducted using solid-state fermentation method (Cosgrove et al. 2010). Briefly, 100 g of PSP was put into 500-ml Erlenmeyer flasks and was sterilised via autoclaving at a temperature of 121 °C for 15 min. 50 ml of filter-sterilised mineral salt medium was added to every flask in order to produce moisture. Two types of strains which are *Aspergillus fumigatus* strain SGE57 and *Aspergillus niveus* isolate A17 were grown in PDA media for 7 days (30 °C). The mycelium was roughly chopped with a sterile scalpel blade and was added to the Erlenmeyer flasks. The cultures were grown for a week at a temperature of 30 °C with occasional shaking and triplicate biocomposites were added after sterilising surface with 70% (v/v) ethanol. Total weight loss was determined at the end of the fermentation.

3 Results and Discussion

3.1 Tensile Properties

Figure 1 shows the impacts of different PSP contents upon tensile properties of both treated and untreated PHBV/PSP biocomposites. The data demonstrated a decrease in the tensile strength of the untreated PHBV/PSP biocomposites when the PSP content creased. This phenomenon might occur because of the low interfacial adhesion between fibres and matrix as well as poor dispersion and low wettability between hydrophobic PHBV matrix and hydrophilic PSP. Nevertheless, the surface treatment of PSP via AA lead to an increase of tensile strength. Joseph et al. stated that the tensile strength of natural fibre which was altered chemically was enhanced (Joseph et al. 1996). Previous research conducted by Li et al. (2007) portrayed that the tensile strength of acrylic acid-treated flax fibre–HDPE composites was

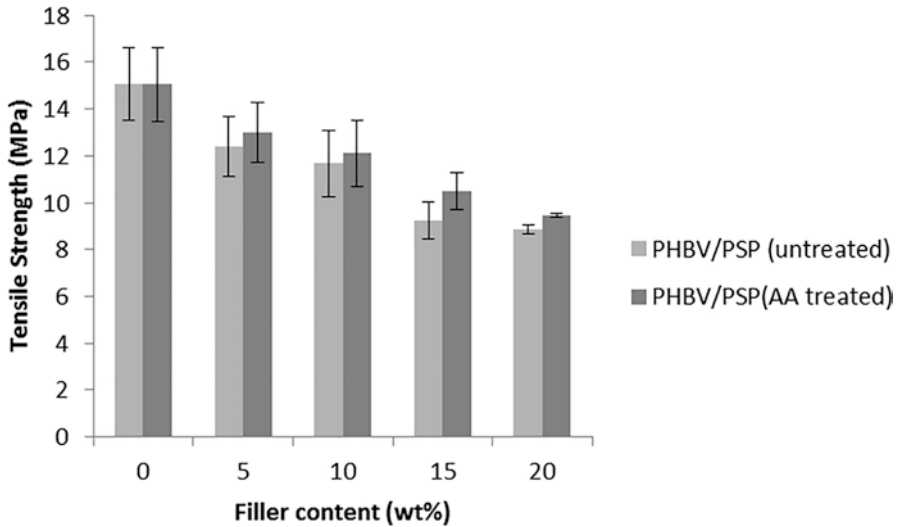


Fig. 1 Tensile strength of PHBV/PSP biocomposites with and without acrylic acid treatment

enhanced. The study conducted by Vilay et al. also demonstrated an increase in tensile strength of the acrylic acid-treated bagasse fibre-reinforced unsaturated polyester (Vilay et al. 2008).

This behaviour was formed due to good dispersion and tough interfacial adhesion that existed between PHBV and PSP. AA responded via the process of esterification with the hydroxyl group of PSP in order to produce a hydrogen bond. The tensile strength of PHBV/PSP biocomposites increased because of the enhanced interfacial adhesion that existed between PHBV matrix and the treated PSP. While conducting acrylic acid treatment, hydrophobic ester groups were introduced, and most of the lignin and hemicelluloses were eliminated. Therefore, stress transfer capacity at the interface is improved while fibre surface area with polymeric matrix which has better adhesion is increased (Dhanalakshimi et al. 2015a, b; Bessadok et al. 2007). According to prior study, the tensile strength of biocomposites decreased. This phenomenon happened because of the existence of voids, which were formed by fibres and pulled out at low fibre content while high fibre content led to agglomeration (Dong et al. 2014). Based on the SEM micrographs shown in Fig. 5, agglomeration, voids and uneven surfaces were produced in biocomposites when comparing to surface of pure PHBV which was smoother. Hence, biocomposites exhibited lower tensile strength than pure PHBV.

Figure 2 portrays the impacts of different PSP content upon the elongation at break (Eb) of treated PHBV/PSP biocomposites and untreated acrylic acid. Based on the graph, the overall Eb of treated and untreated biocomposites decreased when the PSP content increased. This phenomenon might occur because of the hardening impact of PSP and reduced deformability of a firm interface between PHBV matrix and PSP. However, the treated PHBV/PSP biocomposites with AA demonstrated

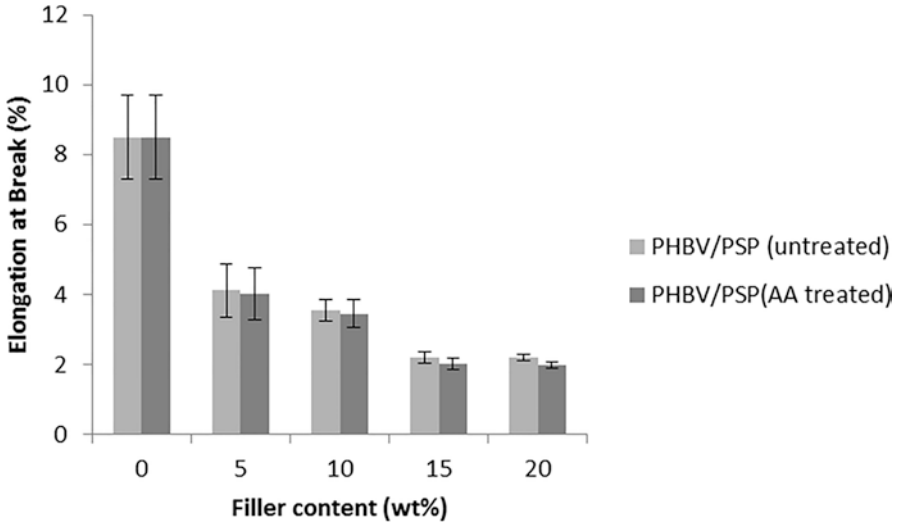


Fig. 2 Elongation at break (Eb) of PHBV/PSP biocomposite with and without acrylic acid treatment

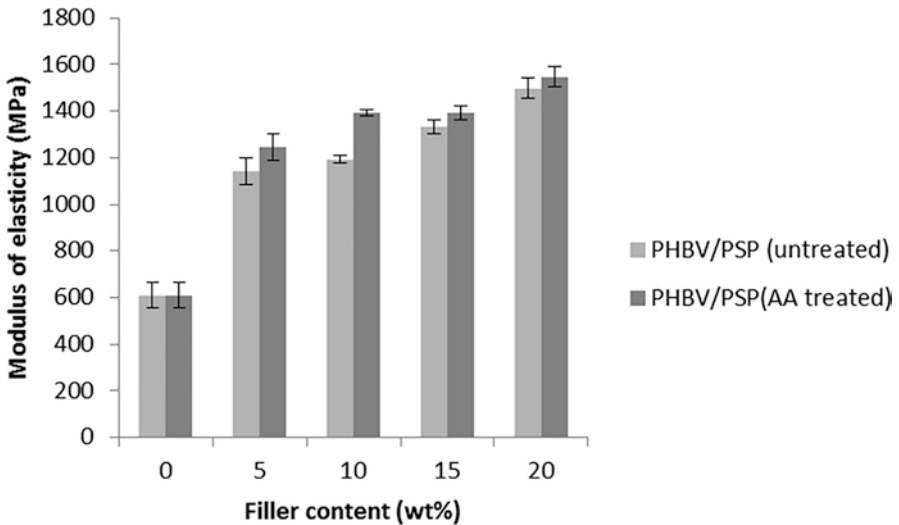


Fig. 3 Modulus of elasticity of untreated PHBV/PSP and treated PHBV/PSP biocomposites

slightly lower elongation at break than untreated biocomposites. The PSP surfaces with AA treatment reduced the ductility of biocomposites and improved the firmness of biocomposites. Other than that, the interfacial adhesion between matrix and filler would be increased by the treated surface of PSP. This would produce good

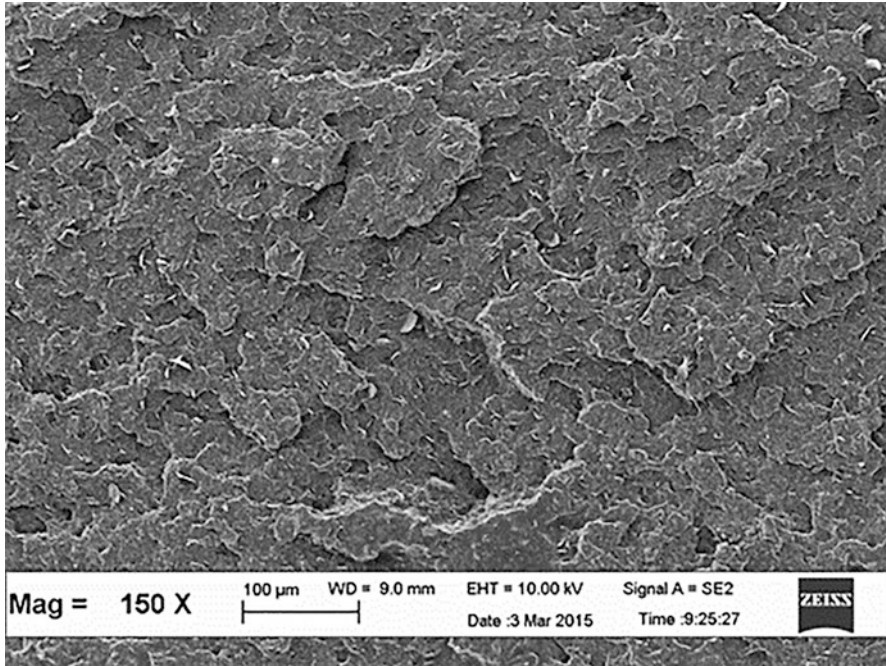


Fig. 4 SEM micrographs of pure PHBV

stress propagation and enhance tensile strength; however, the biocomposites would be more fragile than the polymer matrix (Salmah et al. 2012).

Figure 3 shows the modulus of elasticity for AA-treated and untreated biocomposites. The modulus of elasticity of PHBV/PSP biocomposites was greater compared to the pure PHBV. This phenomenon might happen because of high toughness strength of PSP fibres. In addition, the modulus of elasticity of treated PHBV/PSP biocomposites was greater compared to the untreated PHBV/ PSP biocomposites. The results demonstrated an increase in the toughness of the PHBV/PSP biocomposites through chemical treatment.

3.2 Morphological Study

The fracture surface of pure PHBV is shown in Fig. 4. Based on the micrograph, the surface of pure PHBV was smooth without any voids. Figure 5a, c shows micrographs of the tensile fracture surface of untreated PHBV/ PSP biocomposites with 10 and 20 wt. % of PSP content. Those two micrographs demonstrated a low adhesion and dispersion at the surface of PSP in PHBV matrix. The filler was removed from the unwetted PSP and matrix in PHBV matrix. Agglomeration happened when the PSP content was high (Fig. 5c).

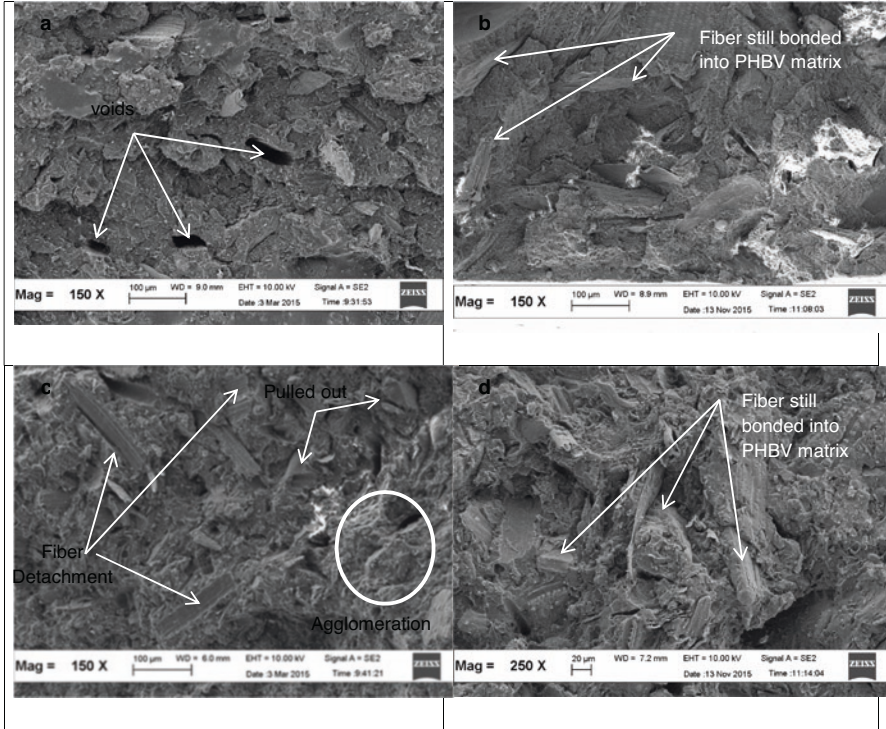


Fig. 5 SEM micrographs of (a) PHBV/10PSP (untreated), (b) PHBV/10PSP (AA treated), (c) PHBV/20PSP (untreated), (d) PHBV/20PSP (AA treated)

The polar feature of PSP does not have the ability to generate good connection between filler-matrix and non-polar PHBV matrix. The SEM micrographs of AA-treated PHBV/PSP biocomposites in Fig. 5b, d showed that the adhesion and wettability of PSP in the matrix were good. The filler agglomeration was decreased via AA treatment while the interfacial connection between filler and matrix was enhanced. It is interesting to note that there is little evidence of fibre which is pulled out in the AA-treated fibre-based composites, which indirectly indicating better adhesion that exists at the interphase.

3.3 Thermal Analysis

The TGA thermogram of weight loss curves for PHBV/PSP biocomposites along with temperature is shown in Fig. 6. Pure PHBV recorded a temperature of 295 °C at the highest degradation peak than its composites. This might be because of the hydrophilic characteristic of PSP, which would enable the water to be evaporated at a faster rate (Dong et al. 2014). According to Yussuf et al. (2010), there are three phases of degradation of biocomposites. The first phase takes place at a temperature

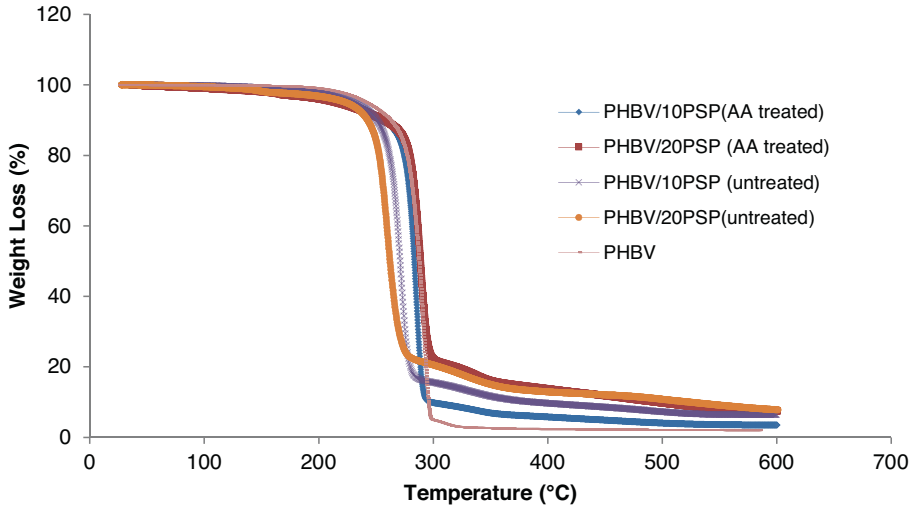


Fig. 6 TGA of pure PHBV, untreated and treated PHBV/PSP biocomposites

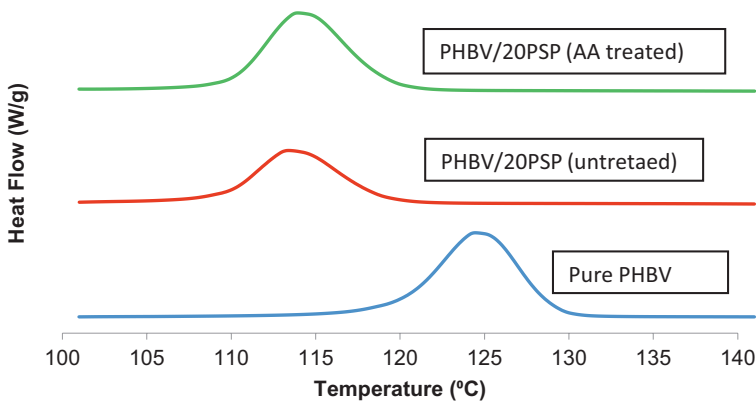


Fig. 7 DSC cooling of PHBV/PSP biocomposites

between 0 and 150 °C because the moisture which is absorbed into fibres evaporates. The second stage occurs at a temperature between 230 and 370 °C, and this is because of thermal degradation of cellulose, lignin, and hemicellulose in natural fibre. The third phase happens after 370 °C and this is because non-cellulosic materials are degraded in fibres (Yussuf et al. 2010). Based on Fig. 7, the degradation temperature of biocomposites decreased when the PSP content increased.

Table 2 summarises degradation temperatures of pure PHBV, PHBV/10PSP; PHBV/20PSP, PHBV/10PSP (AA treated), and PHBV/20PSP (AA treated) biocomposites. The initial degradation at 5 wt% and 30 wt% of sample weight loss was

Table 2 TGA data for pure PHBV, untreated, and AA-treated PHBV/PSP biocomposites

Samples	T _{5%} (°C)	T _{30%} (°C)	Char residue (wt.%)
PHBV	235.52	284.69	1.57
PHBV/10PSP (untreated)	232.65	280.64	4.38
PHBV/20PSP (untreated)	230.03	275.74	6.40
PHBV/10PSP (AA treated)	225.62	272.68	5.45
PHBV/20PSP (AA treated)	222.61	269.62	7.05

Table 3 DSC data for Pure PHBV, untreated, and AA-treated PHBV/PSP biocomposites

Samples	T _m (°C)	T _c (°C)	ΔH (J/g)	Crystallinity (%)
Pure PHBV	165.50	124.47	65.52	44.87
PHBV/20PSP (untreated)	164.68	113.39	38.32	26.24
PHBV/20PSP (AA treated)	165.26	93.77	44.07	30.18

shown by T values correspondingly. At 5% and 30% of weight loss, pure PHBV recorded the highest temperature. PHBV reduced the degradation temperature through adding fibres. When natural fibres were added, the replacement of some parts of polymer by less thermally stable fibres reduced the thermal stability of composites (Yussuf et al. 2010).

By comparison with the untreated PHBV/20PSP biocomposites, the degrading temperature of PHBV/20PSP (AA treated) biocomposites reduced. By adding treated PSP fibres, the thermal stability of the composites was improved because of the presence of enhanced interfacial adhesion between PSP fibre filler and PHBV matrix via the acrylation treatment (Praveenkumara et al. 2021). The study conducted by Dhanalakshmi et al. showed that the thermal stability of areca fibre composite increases when the acrylic acid is introduced to the fibre (Dhanalakshmi et al. 2017). Ester groups, which are introduced into the fibres via acrylation treatments, enhance the thermal stability of fibres that are treated chemically.

PSP fibre-filled biocomposites possess more char residue than pure PHBV due to the presence of natural fibres. By comparison with the untreated biocomposites, the treated biocomposites tended to have more char residue. This is due to the increase in thermal stability of treated fibres loaded biocomposites and there was a stronger interaction between the PHBV matrix and PSP fibres (Sundar et al. 2010). The thermal stability of biocomposites can be improved with the good interaction between filler and polymer matrix in the biocomposites.

3.4 Differential Scanning Calorimetry (DSC) Properties

Figure 7 shows the cooling thermogram of pure PHBV and PHBV/PSP biocomposites. By comparison with pure PHBV, it could be observed that the peak of biocomposites moved slightly to left, indicating a lower T_c for all biocomposites compared

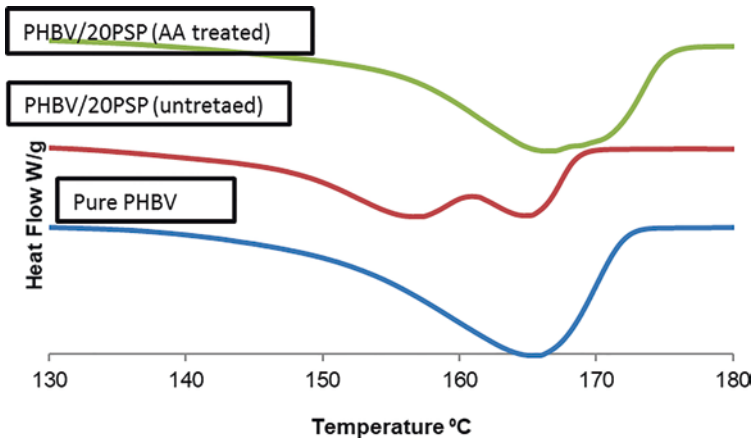


Fig. 8 DSC melting of PHBV/PSP biocomposites

to the pure PHBV. This might take place because of low miscibility between fillers and the matrix, thus portraying low dispersion and incorporation of fibres within the biocomposites (Margem et al. 2015). Based on Table 3, the T_c value of PHBV/PSP biocomposites (untreated and treated) was lower than pure PHBV. This phenomenon occurs as the crystallisation process of PHBV is accelerated effectively by fibres, hence enabling the growth rate of crystal to be advanced (Praveenkumara et al. 2021).

From Fig. 8, there were no substantial alterations in the T_m of biocomposites. Chemical modification of PSP slightly improved the T_m ; nevertheless, the T_m of biocomposites were lower than pure PHBV ($T_m = 165.5$ °C). Table 3 depicts the alterations in T_m and T_c as well as crystallinity of pure PHBV and its composites. Pure PHBV had a crystallinity value which was greater compared to untreated biocomposites. By putting untreated fibres into PHBV, its melting enthalpy became lower compared to pure PHBV, thus resulting in its amorphosity of materials to increase and eventually causing its crystallinity value to decrease (Faruk et al. 2012). The crystallinity of pure PHBV and PHBV/20PSP (untreated) was 44.87% and 26.24%, respectively. With the disarrangement of polymeric molecules in the biocomposites via fibres, the enthalpy value and crystallinity percentage were thus appeared to be low (Faruk et al. 2012).

The crystallinity of the PHBV/20PSP (AA treated) biocomposites was slightly higher than untreated biocomposites, which were 30.18% and 26.24%, respectively. This increment might be because of the capability of acrylic acid to lengthen the prevalence of crystallisation process. High crystallinity value reflects the mechanical properties of polymer biocomposites. Higher crystallinity will give the higher tensile strength of the polymer biocomposites (Praveenkumara et al. 2021). Based on Fig. 1, pure PHBV had tensile strength which was greater compared to others.

Table 4 Weight loss of the PHBV/PSP biocomposites after 7-day fermentation

Types of strains	Weight loss (%)
<i>Aspergillus fumigatus</i> strain SGE57	2.42
<i>Aspergillus niveus</i> isolate A17	3.65

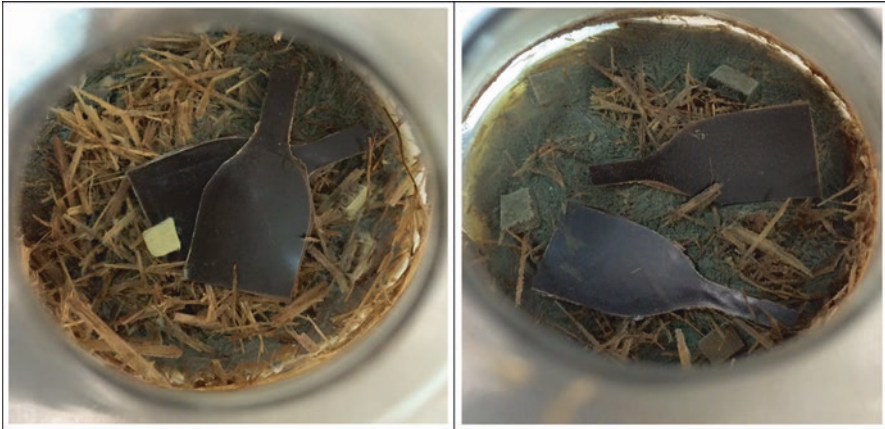


Fig. 9 Photographs of the (a) *Aspergillus fumigatus* strain SGE57 (b) *Aspergillus niveus* isolate A17 growth on the PHBV/PSP biocomposites

3.5 Biodegradability Test

Biodegradability test was carried out to investigate the efficiency of PHBV/PSP biocomposites on the biodegradation via two potential strains, namely *Aspergillus fumigatus* strain SGE57 and *Aspergillus niveus* isolate A17. Table 4 shows the weight loss (%) for each strain after 7 days of fermentation.

Based on Table 4, both strains showed a positive effect on their ability to degrade the biocomposites. However, *Aspergillus niveus* isolate A17 showed a higher rate of biodegradation, where the total weight loss of the biocomposites was higher compared to another strain. Theoretically, the PHBV/PSP served as the only carbon which were present throughout the process of fermenting these microorganisms. The biocomposites experienced an initial breakdown due to numerous enzymes which were produced by the microorganisms. Depolymerisation process includes extracellular and intracellular enzymes. Depolymerisation is defined as the breakdown of complex polymers into simple monomers in order to allow the molecules to pass through the cell wall and further utilise as carbon and energy sources (Dey et al. 2012). Figure 9 shows the photographs of the growth of the strain on the PHBV/PSP biocomposites.

4 Conclusions

- The incorporation of PSP in the PHBV matrix decreased tensile strength and Eb but increased the modulus of elasticity of PHBV/PSP biocomposites.
- Treatment of PSP via acrylic acid improved tensile strength and slightly enhanced the Eb.
- Morphology of the treated PHBV/PSP biocomposites showed better wettability and adhesion of PSP in the matrix.
- Thermal stability and crystallinity of treated PHBV/PSP biocomposites were greater compared to the untreated PHBV/PSP biocomposites.
- Two strains from *Aspergillus* species gave positive effect on biodegradation of the PHBV/PSP biocomposites.

Acknowledgement The authors acknowledge and greatly appreciate the financial support from the Fundamental Research Grant, MOSTI (grant no: 9003-00385).

References

- Anuar H, Zuraida A, Kovacs JG et al (2012) Improvement of mechanical properties of injection-molded polylactic acid-kenaf fiber biocomposite. *J Thermoplast Compos Mater* 25(2):153–164. <https://doi.org/10.1177/0892705711408984>
- Berthet MA, Angellier-Coussy H, Machado D et al (2015) Exploring the potentialities of using lignocellulosic fibres derived from three food by-products as constituents of biocomposites for food packaging. *Ind Crop Prod* 69:110–122. <https://doi.org/10.1016/j.indcrop.2015.01.028>
- Bertini F, Canetti M, Cacciamani A et al (2012) Effect of ligno-derivatives on thermal properties and degradation behavior of poly(3-hydroxybutyrate)-based biocomposites. *Polym Degrad* 97(10):1979–1987. <https://doi.org/10.1016/j.polymdegradstab.2012.03.009>
- Bessadok A, Marais S, Gouanve F, Colasse L, Zimmerlin I, Me'tayer S, Roudesli M (2007) Effect of chemical treatments of Alfa (*Stipa tenacissima*) fibres on water-sorption properties. *Compos Sci Technol* 67:685–697. <https://doi.org/10.1016/j.compscitech.2006.04.013>
- Chandrasekar M, Kumar TSM, Senthilkumar K, Radoor S, Ilyas RA, Sapuan SM et al (2021) Performance of natural fiber reinforced recycled thermoplastic polymer composites under aging conditions. In: Ilyas RA, Sapuan SM, Bayraktar E (eds) *Recycling of plastics, metals, and their composites*, 1st edn. CRC Press, Boca Raton. <https://doi.org/10.1201/9781003148760-7>
- Chun KS, Husseinsyah S, Osman H (2012) Mechanical and thermal properties of coconut shell powder filled polylactic acid biocomposites: effects of the filler content and silane coupling agent. *J Polym Res* 19(5):9859. <https://doi.org/10.1007/s10965-012-9859-8>
- Cosgrove L, McGeechan PL, Handley PS et al (2010) Effect of biostimulation and bioaugmentation on degradation of polyurethane buried in soil. *Appl Environ Microbiol* 76(3):810–819. <https://doi.org/10.1128/AEM.00534-09>
- Danjaji ID, Nawang R, Ishiaku US et al (2001) Sago starch-filled linear low-density polyethylene (LLDPE) films: their mechanical properties and water absorption. *J Appl* 79(1):29–37. [https://doi.org/10.1002/1097-4628\(20010103\)79:1%3C29::AID-APP40%3E3.0.CO;2-R](https://doi.org/10.1002/1097-4628(20010103)79:1%3C29::AID-APP40%3E3.0.CO;2-R)
- Dey U, Mondal N, Das K et al (2012) An approach to polymer degradation through microbes. *IOSR J Pharm* 2(3):385–388. <https://doi.org/10.9790/3013-0230385388>

- Dhanalakshmi S, Ramadevi P, Basavaraju B (2015a) Influence of chemical treatments on flexural strength of areca fiber reinforced epoxy composites. *Chem Sci Trans* 4:409–418. <https://doi.org/10.7598/cst2015.1033>
- Dhanalakshmi S, Ramadevi P, Basavaraju B et al (2015b) *Orient J Chem* 31(2):763–769. <https://doi.org/10.13005/ojc/310218>
- Dhanalakshmi S, Ramadevi P, Basavaraju B (2017) A study of the effect of chemical treatments on areca fiber reinforced polypropylene composite properties. *Sci Eng Compos Mater* 24(4):501–520. <https://doi.org/10.1515/secm-2015-0292>
- Dong Y, Ghataura A, Takagi H et al (2014) Polylactic acid (PLA) biocomposites reinforced with coir fibres: evaluation of mechanical performance and multifunctional properties. *Compos Part A Appl Sci Manuf* 63:76–84. <https://doi.org/10.1016/j.compositesa.2014.04.003>
- Faludi G, Dora G, Renner K et al (2013) Biocomposite from polylactic acid and lignocellulosic fibers: structure-property correlations. *Carbohydr Polym* 92(2):1767–1775. <https://doi.org/10.1016/j.carbpol.2012.11.006>
- Faruk O, Bledzki AK, Fink HP et al (2012) Biocomposites reinforced with natural fibers: 2000–2010. *Prog Polym Sci* 37(11):1552–1596. <https://doi.org/10.1016/j.progpolymsci.2012.04.003>
- Gordobil O, Delucis R, Egiúés I et al (2015) Kraft lignin as filler in PLA to improve ductility and thermal properties. *Ind Crop Prod* 72:46–53. <https://doi.org/10.1016/j.indcrop.2015.01.055>
- Ilyas RA, Sapuan SM, Sabaruddin FA et al (2021) Reuse and recycle of biobased packaging products. In: *Bio-based packaging: material, environmental and economic aspects*. Wiley, West Sussex, pp 413–426. <https://doi.org/10.1002/9781119381228ch23>
- Joseph K, Pavithran C, Thomas S (1996) Effect of chemical treatment on the tensile properties of short sisal fibre-reinforced polyethylene composites. *J Reinf Plast Compos* 12:139. [https://doi.org/10.1016/0032-3861\(96\)00144-9](https://doi.org/10.1016/0032-3861(96)00144-9)
- Kargarzadeh H, Sheltami R, Ahmad I et al (2015) Cellulose nanocrystal reinforced liquid natural rubber toughened unsaturated polyester: effects of filler content and surface treatment on its morphological, thermal, mechanical, and viscoelastic properties. *Br Polym J* 71:51–59. <https://doi.org/10.1016/j.polymer.2015.06.045>
- Kim MN, Lee AR, Yoon JS et al (2000) Biodegradation of poly(3-hydroxybutyrate), Sky-Green® and Mater-Bi® by fungi isolated from soils. *Eur Polym J* 36(8):1677–1685. [https://doi.org/10.1016/S0014-3057\(99\)00219-0](https://doi.org/10.1016/S0014-3057(99)00219-0)
- Li X, Tabil LG, Panigrahi S (2007) Chemical treatments of natural fiber for use in natural fiber-reinforced composites: a review. *J Polym Environ* 15:25–33. <https://doi.org/10.1007/s10924-006-0042-3>
- Li L, Huang W, Wang B et al (2015) Properties and structure of polylactide/poly (3-hydroxybutyrate-co-3-hydroxyvalerate) (PLA/PHBV) blend fibers. *Polymers* 68:183–194. <https://doi.org/10.1016/j.polymer.2015.05.024>
- Margem JI, Gomes VA, Margem FM et al (2015) Flexural behavior of epoxy matrix composites reinforced with malva fiber 2. *Exp Proc* 18(Suppl 2):114–120. <https://doi.org/10.1590/1516-1439.359514>
- Njoku RE, Ofili I, Agbiogwu DO et al (2012) Effect of alkali treatment and fiber content variation on the tensile properties of coir fiber reinforced cashew nut shell liquid (Cnsl) composite. *Niger J Technol* 31(2):107–110
- Obasi HC, Iheaturu NC, Onuoha FN et al (2014) Influence of alkali treatment and fibre content on the properties of oil palm press fibre reinforced epoxy biocomposites. *Am J Eng Res* 3(02):117–123
- Pang A, Ismail H (2014) Effects of kenaf loading and 3-aminopropyltriethoxysilane coupling agent on the properties of polypropylene/waste tire dust/kenaf composites. *J Thermoplas Compos Mater* 27(12):1607–1619. <https://doi.org/10.1177/0892705712475002>
- Praveenkumara J, Madhu P, Sanjay MR, Suchart S (2021) A review on extraction, chemical treatment, characterization of natural fibers and its composites for potential applications. *Polym Compos* 42(12):6239–6264. <https://doi.org/10.1002/pc.26312>

- Rahnama N, Mamat S, Ling FH et al (2013) Effect of alkali pretreatment of Rice straw on cellulase and xylanase production by local *Trichoderma harzianum* SNRS3 under solid state fermentation. *Bioresources* 8(2):2881–2896. <https://doi.org/10.15376/biores.8.2.2881-2896>
- Ramamoorthy SK, Skrifvars M, Rissanen M (2014) Effect of alkali and silane surface treatments on regenerated cellulose fibre type (Lyocell) intended for composites. *Cellulose* 22(1):637–654. <https://doi.org/10.1007/s10570-014-0526-6>
- Râpă M, Popa ME, Grosu E et al (2011) Evaluation of the biodegrading action of the *Penicillium* Sp. on some composites based on PHB. *Rom Biotechnol Lett* 16(1):9–18
- Rapa M, Popa ME, Cornea PC et al (2014) Degradation study by *Trichoderma* spp. of poly(3-hydroxybutyrate) and wood fibers composites. *Rom Biotechnol Lett* 19(3):9390–9399
- Rubio-lópez A, Olmedo A, Díaz-álvarez A et al (2015) Manufacture of compression moulded PLA based biocomposites: a parametric study. *Compos Struct* 131:995–1000. <https://doi.org/10.1016/j.compstruct.2015.06.066>
- Salmah H, Koay S, Hakimah O (2012) Surface modification of coconut shell powder filled polylactic acid biocomposites. *J Thermoplast Compos Mater* 26(6):809–819. <https://doi.org/10.1177/0892705711429981>
- Salwa HN, Sapuan SM, Mastura MT, Zuhri MYM, Ilyas RA (2021) Life cycle assessment (LCA) of recycled polymer composites. In: Ilyas RA, Sapuan SM, Bayraktar E (eds) *Recycling of plastics, metals, and their composites*, 1st edn. CRC Press/Taylor & Francis Group, Boca Raton, p 15. <https://doi.org/10.1201/9781003148760-27>
- Sarifuddin N, Ismail H, Ahmad Z (2015) Studies of properties and characteristics of low-density polyethylene/thermoplastic sago starch-reinforced kenaf core fiber composites. *J Thermoplast Compos Mater* 28(4):445–460. <https://doi.org/10.1177/0892705713486125>
- Shah AA, Hasan F, Hameed A et al (2007) Isolation and characterisation of poly(3-hydroxybutyrate-co-3-hydroxyvalerate) degrading actinomycetes and purification of PHBV depolymerase from newly isolated *Streptovorticillum kashmirensis* AF1. *Ann Microbiol* 57(4):583–588. <https://doi.org/10.1016/2Fj.ibiod.2007.01.004>
- Siyamak S, Ibrahim NA, Abdolmohammadi S et al (2012) Enhancement of mechanical and thermal properties of oil palm empty fruit bunch fiber poly(butylene adipate-co-terephthalate) biocomposites by matrix esterification using succinic anhydride. *Molecules* 17(2):1969–1991. <https://doi.org/10.3390/molecules17021969>
- Sundar S, Sain M, Oksman K (2010) Thermal characterisation and electrical properties of Fe-modified cellulose long fibers and micro crystalline cellulose. *J Therm Anal Calorim* 104(3):841–847. <https://doi.org/10.1007/s10973-011-1338-7>
- Tao J, Song C, Cao M et al (2009) Thermal properties and degradability of poly(propylene carbonate)/poly(β -hydroxybutyrate-co- β -hydroxyvalerate) (PPC/PHBV) blends. *Polym Degrad* 94(4):575–583. <https://doi.org/10.1016/j.polymdegradstab.2009.01.017>
- Vilay V, Mariatti M, Mat Taib R et al (2008) Effect of fiber surface treatment and fiber loading on the properties of bagasse fiber-reinforced unsaturated polyester composites. *Compos Sci Technol* 68:631–638. <https://doi.org/10.1016/j.compscitech.2007.10.005>
- Volova TG, Boyandin AN, Vasiliev AD et al (2010) Biodegradation of polyhydroxyalkanoates (PHAs) in tropical coastal waters and identification of PHA-degrading bacteria. *Polym Degrad* 95(12):2350–2359. <https://doi.org/10.1016/j.polymdegradstab.2010.08.023>
- Wu D, Hakkaraianen M (2015) Recycling PLA to multifunctional oligomeric compatibilisers for PLA/starch composites. *Eur Polym* 64:126–137. <https://doi.org/10.1016/2Fj.eurpolymj.2015.01.004>
- Yussuf AA, Massoumi I, Hassan A (2010) Comparison of polylactic acid/kenaf and polylactic acid/rise husk composites: the influence of the natural fibers on the mechanical, thermal and biodegradability properties. *J Polym Environ* 18(3):422–429. <https://doi.org/10.1007/s10924-010-0185-0>

Comparison Between Natural Rubber, Liquid Natural Rubber, and Recycled Natural Rubber as Secondary Matrix in Epoxy/Natural Rubber/Graphene Nano-platelet System



K. W. Kam, P. L. Teh, and C. K. Yeoh

1 Introduction

This study focuses on the effect of natural rubber (NR), liquid natural rubber (LNR), and recycled natural rubber (rNR) as secondary matrices on the properties of filled epoxy systems. NR is classified as a renewable and sustainable biopolymer, which is usually tapped and extracted from tropical rubber trees, known as *Hevea Brasiliensis* (Krishna Kumar et al. 2021; Radabutra et al. 2021). NR is extensively used in an enormous range of applications due to its high elongation, high elasticity, and resilience (Chawalitsakunchai et al. 2021). The main application of natural rubber latex is in glove application, like household or medical gloves. The NR gloves waste has created landfill problems. Thus, it is necessary to overcome the landfill problems by recycling the NR gloves. Therefore, NR was used to improve the toughness properties of epoxy resins, since it is a renewable resource and is easily available in Malaysia (Rotrekl et al. 2013).

Epoxy resins are one of the most important classes of amorphous highly cross-linked thermosetting polymers and exhibit prominent properties such as high stiffness, creep resistance, chemical resistance, corrosion resistance, thermal resistance, good dimensional stability, and low shrinkage (Puglia et al. 2013). Epoxy resins are extensively used in aerospace applications, automotive, electronic components, electrical laminates, adhesives, coating, and energy devices (Mathew et al. 2010). The most widely used epoxy resins are epichlorohydrin and bisphenol-A-derived

K. W. Kam

Faculty of Chemical Engineering & Technology, Arau, Perlis, Malaysia

P. L. Teh (✉) · C. K. Yeoh

Faculty of Chemical Engineering & Technology, Arau, Perlis, Malaysia

Centre of Excellence Frontier Materials Research (CFMR), Universiti Malaysia Perlis, Arau, Perlis, Malaysia

e-mail: plteh@unimap.edu.my

resin (Cantoni et al. 2021). Once epoxy resins are cured with the corresponding hardener, a highly cross-linked three-dimensional network structure is formed. The high cross-link density is essential for thermosetting resin to attain excellent mechanical properties. However, the chief drawbacks of epoxy are their low toughness and impact resistance (Wang et al. 2013a, b). In order to address this issue, one of the successful approaches to modify the epoxy resin involved incorporation of natural rubber (NR) as the secondary matrix into the epoxy matrix, thereby forming an immiscible two-matrix morphology (two-phase structure). Two-matrix system can be obtained by reaction-induced phase separation (RIPS) of an initially epoxy/NR co-continuous structure. According to the Flory-Huggins mean field theory, epoxy/NR systems no longer remain homogenous as the average molecular weight of epoxy resin is increased up to an extent. During the curing reaction, the molecular weight of the epoxy matrix increases to a critical extent and the system starts phase separating through spinodal decomposition. The curing rate of the epoxy matrix is significantly higher, resulting in the precipitation of spherical NR phases (Hong and Chan 2004; Tan et al. 2013).

Epoxy resins and NR are polymeric materials, which are usually classified as insulating materials. The incorporation of promising conductive nano-fillers like copper (Pargi et al. 2015) and even recycled metal (Ilyas et al. 2021a, b) causes the material to gradually transition from an insulator to a conductor. In this regard, the discovery of graphene is an important addition. Graphene consists of two-dimensional nano-fillers with a single atom thick structure of sp² bonded carbon atoms, which is densely packed in a hexagonal honeycomb crystal lattice structure (Verma et al. 2014). Graphene nano-platelets (GNP) have outstanding properties such as high aspect ratio, high strength, modulus, and surface conductivity, which make them ideal fillers for polymer nanocomposites used in advanced materials applications (Yue et al. 2014). It is important to note that graphene is much cheaper than single-walled carbon nanotubes (CNTs) because it can easily be derived from graphite precursors in large quantities (Du and Cheng 2012). The wrinkled topology and nano-scale surface roughness of graphene have increased mechanical interlocking with polymer chains, thus strengthening the interaction and increasing the maximum load transfer between graphene and polymer matrix.

The present work attempts to investigate the effect of different forms of vulcanized NR on the physical, mechanical, thermal, and electrical performances of filled epoxy systems. For effective rubber toughening epoxy, the optimum particle sizes of rubber phases are within the range of 0.1–5 μm . Large rubber phases (>5 μm) are too large to interact with the stress field at the crack tip, while small rubber phases (<0.1 μm) are too small to cavitate effectively and do not take part in the toughening epoxy matrix (Kam et al. 2018). Tan et al. have indicated liquid epoxidized natural rubber is a good potential toughening agent for epoxy resins (Tan et al. 2013). Tan et al. described the use of natural rubber as toughening agent in low-density polyethylene systems (Tan et al. 2013). Ozturk et al. indicated mechanical and thermal properties of epoxy resins can be enhanced with hydroxyl terminated polybutadiene (HTPB) liquid rubber (Ozturk et al. 2001). The incorporation of GNP nano-fillers

has transformed the two-matrix system from an insulator to a semiconductor. The percolation threshold of GNP nano-fillers, that is 0.8 vol.%, was applied in the filled systems based on previous studies (Kam et al. 2018). The electrical performance of the filled epoxy system can be further enhanced by rubber phases (elastomer spacers). The elastomer spacers pushed the GNP nano-fillers closer to each other, leading to the formation of more effective conductive pathways for electron conduction. Similar findings reported by Phua et al. (2017) identified that electrical conductivity of filled systems improved with 10 vol.% of thermoplastic spacer. With the incorporation of 10 vol.% PMMA-spacer, the filled system shows promising improvement in electrical conductivity, with an order of magnitude increase at 15 vol.% CB loading (Phua et al. 2017). The fractured surface and two-matrix morphology were examined by scanning electron microscope (SEM) to observe the deformation and toughening mechanism. Different forms of vulcanized NR acted as elastomer spacers that aided in the improvement on electrical conductivity of filled systems were compared.

2 Experimental

2.1 Materials

Epoxy resin (DGEBA) with epoxide equivalent weight 182–192 and epoxy hardener with amine value 260–284 (mg KOH/gm) were purchased from Euro Chemo-Pharma Sdn. Bhd. (Malaysia). Natural rubber (cis 1,4-polyisoprene) was purchased from Malaysian Rubber Board (Malaysia). Liquid natural rubber (LNR) was purchased from Zarm Scientific & Supplies Sdn. Bhd. (Malaysia). Recycled natural rubber (rNR) derived from recycled gloves was purchased from SWJ Global Enterprise Sdn. Bhd. (Malaysia). GNP was purchased from SkySpring Nanomaterials (USA), with thickness of 11–15 nm. Toluene (C_6H_5OH) was purchased from Fisher Scientific Company L.L.C. (USA). Hydrogen peroxide (H_2O_2) was purchased from HmbG Chemical (Germany). Acetic acid (CH_3COOH) was purchased from HmbG chemical (Germany). Vulcanizing agents such as zinc oxide (ZnO), stearic acid ($CH_3(CH_2)_{16}COOH$), n-cyclohexyl-2-benzothiazolesulfenamide (CBS), and sulfur were purchased from Malaysian Rubber Board (Malaysia).

2.2 Sample Preparation

2.2.1 Photo-Depolymerization of NR and LNR

Photo-depolymerization was carried out under sunlight as reported by Radhakrishnan. For both NR and LNR, photo-depolymerization of rubber in a fixed volume of toluene was done using 30 wt.% of hydrogen peroxide and 0.35 mol of acetic acid (Kam

et al. 2018). The mixture was stirred for 1 h. The milky NR solution was then left under sunlight for 2 weeks. The milky NR solution turned pale yellow after 2 weeks. The depolymerized NR was coagulated using methanol to remove the residues. Finally, the coagulants were dried in oven at 90 °C for 2 days. Before photo-depolymerization, the molecular weight of NR was determined, M_n (number average molecular weight) = 68,699 g/mol, M_w (weight average molecular weight) = 183,510 g/mol, and PDI (polydispersity index) = 2.671. After depolymerization, the molecular weight of depolymerized NR was reduced to M_n = 1688 g/mol, M_w = 38,527 g/mol, and PDI = 22.824 while the molecular weight of depolymerized LNR was reduced to M_n = 675 g/mol, M_w = 6427 g/mol, and PDI = 9.521.

2.2.2 Compounding of Two-Matrix Filled Epoxy/NR/GNP and Epoxy/LNR/GNP Systems

For filled epoxy/NR/GNP system, the compositions of epoxy/NR were prepared (95/5, 90/10, 85/15, 80/20, 75/25, and 70/30 vol.%). During the initial stage, depolymerized NR (DNR) was dissolved in epoxy resin via magnetic stirring at 60 °C. After NR was completely dissolved, vulcanizing agents such as zinc oxide (5 phr), stearic acid (2 phr), and CBS (1.2 phr) based on 100 phr of NR were added into the epoxy/NR mixture and stirred for 10 min. 0.8 vol.% of GNP nano-fillers were added into the mixture and stirred for another 20 min. Afterward, the mixture was placed in an ultrasonic water bath for 30 min (53 kHz and 60 °C). Sonication is an effective way to suppress the re-aggregation of GNP nano-fillers. The sulfur (1.5 phr) was added into the mixture and stirred for 5 min. At last, the mixture was stirred together with epoxy hardener and cured in an oven, at 90 °C for 2 h. The compounding of two-matrix filled epoxy/LNR/GNP system was done similarly as two-matrix filled epoxy/NR/GNP systems, except LNR was used instead of NR.

2.2.3 Compounding of Two-Matrix Filled Epoxy/rNR/GNP System

For filled epoxy/rNR/GNP system, the composition of epoxy/NR was prepared (95/5, 90/10, 85/15, 80/20, 75/25, and 70/30 vol.%). The rNR was milled and sieved to obtain a maximum particle size of 250 μm . During the initial stage, rNR was added into the epoxy resins and mixed for 2 h. 0.8 vol.% of GNP nano-fillers were added into the mixture and stirred for 20 min. The mixture was placed in an ultrasonic water bath for 30 min (53 kHz and 60 °C). The mixture was stirred together with epoxy hardener and cured in an oven, at 90 °C for 2 h.

2.3 Characterizations

Density measurements were performed using a pycnometer, model Micromeritics AccuPyc II 1340, under the flow of helium gas at room temperature. The theoretical density of the filled systems was calculated based on previous finding (Fuad et al. 1993). Flexural properties were measured under a three-point bending approach according to ASTM D790, using an Instron machine (Model 5569), with a span length of 50 mm and a cross-head speed of 2.38 mm/min. The applied load was 50 kN (Kutz 2002). The size of rectangular samples used was $60 \times 12.7 \times 3$ mm. Fracture toughness (K_{IC}) was performed using Universal Instron testing machine (Model 5569), with a cross-head speed at 1 mm/min, according to the standard of ISO 13586 under Mode I (tensile opening). The rectangular samples were notched at one-third of the sample width and dimension of samples used were $60 \times 12.7 \times 3$ mm. The morphological study was performed using SEM, JEOL JSM-6460 LA with an accelerating voltage of 5 kV. The flexural fractured surfaces of cross-sectional samples were coated with palladium, which prevent accumulation of electrostatic charges. Thermogravimetric analysis (TGA) of the samples (5 mg) was performed based on ASTM E1131 under inert nitrogen atmosphere, with a heating rate of $10 \text{ }^\circ\text{C}\cdot\text{min}^{-1}$ from 25 to 800 $^\circ\text{C}$. X-ray diffraction analysis was performed using Shimadzu X-ray diffractometer XRD-6000 with Cu-K α radiation, at an accelerating voltage of 40 kv. The measured 2θ was recorded from 10° to 70° with a scan rate of 5°min^{-1} . The d-spacing of GNP nano-fillers was calculated using Bragg's law. Electrical bulk conductivity was conducted according to ASTM D257-14, using a Fluke 8845A/8846A 6.5-digit precision multimeter, with a voltage supply of 5 V. To ensure a good surface contact in between electrodes and samples, silver conductive paint was applied on the top and bottom surfaces of the samples. The diameter and thickness of circular-shaped samples were 10 mm and 0.2 mm, respectively.

3 Results and Discussion

3.1 Density

Figure 1 illustrates the effect of different forms of vulcanized NR content on the density of filled systems. By using pycnometer density analyzer, the density of the pure epoxy and GNP nano-fillers was obtained as 1.169 and 2.8 g/cm³, respectively. Comparing at the same rubber content (5 vol.%), the density of filled system with rNR was higher as compared to those with NR and LNR. The density of neat rNR is reported as 1.103 g/cm³, which is relatively higher than NR (0.949 g/cm³) and LNR (0.785 g/cm³). Since the ratio of epoxy to rubber for three filled systems was

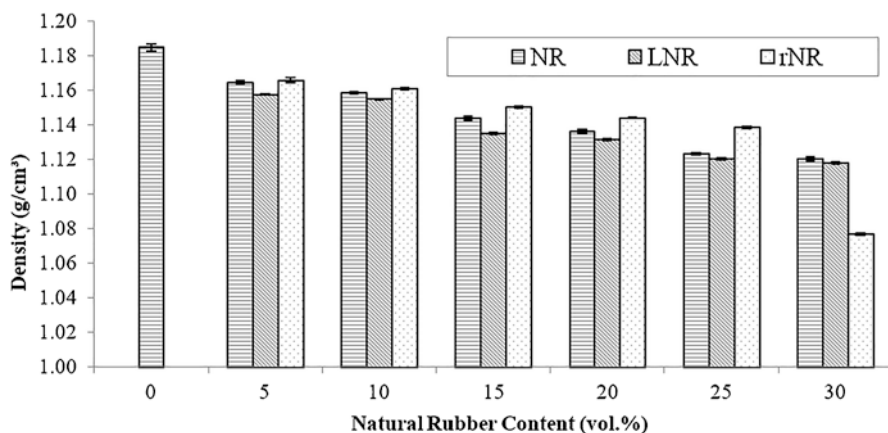


Fig. 1 Effect of different forms of vulcanized NR on the density of filled systems, at different NR contents

the same, hence, the incorporation of high-density neat rNR has increased the density values of the filled epoxy system. At 30 vol.% of rubber content, the filled epoxy system added with rNR showed the lowest density value as compared to NR and LNR. This is because the rNR particles agglomerated, forming large cluster particles, where it trapped voids inside the epoxy medium. Hence, the presence of voids has obstructed the cross-linking reaction of epoxide groups (epoxy matrix) and amine-based groups (hardener).

For all three systems (NR, LNR, and rNR), the density decreased steadily with increasing rubber content from 5 up to 30 vol.%. At high NR content, more NR phases hindered and obstructed the cross-linking reaction in between the epoxy and hardener, thereby impairing the cross-linking reaction at that particular site (Tan et al. 2013). This is attributed to rubber molecular chains (bearing epoxide group) forming cross-links with the hardener, thereby disrupting the cross-link network of epoxy matrix. In addition, the density of neat NR, LNR, and rNR was relatively lower as compared to the pure epoxy resin. The increase of NR content from 5 up to 30 vol.% has led to a decrease in the ratio of epoxy to NR, therefore contributing to a reduction in density.

Table 1 summarizes the theoretical (T.D) and experimental density (E.D) of three filled systems with different forms of vulcanized NR (NR, LNR, and rNR). The theoretical density of filled systems was calculated based on the measured density values of epoxy, NR, LNR, rNR, GNP nano-fillers, and vulcanizing agents that was determined using the pycnometer. Filled epoxy systems at 0 vol.% of NR content showed higher density as compared to filled epoxy systems with NR content from 5 up to 30 vol.%. This is because the rubber phases functioned as a flexibilizer that occupy the spaces in between the reactive sites, thereby impairing the cross-linking reaction at that particular site (Thamos et al. 2008). As a result, it reduces the cross-link density of the filled systems corresponding to the decrease in density. This became more significant when the rubber content increased up to 30 vol.%.

Table 1 Comparison between theoretical and experimental density of filled system with different forms of vulcanized rubber

NR content (vol.%)	Vulcanized filled epoxy/NR/GNP system		Vulcanized filled epoxy/LNR/GNP system		Vulcanized filled epoxy/rNR/GNP system	
	T.D (g/cm ³)	E.D (g/cm ³)	T.D (g/cm ³)	E.D (g/cm ³)	T.D (g/cm ³)	E.D (g/cm ³)
0	1.180	1.185	1.180	1.185	1.180	1.185
5	1.175	1.165	1.160	1.158	1.187	1.166
10	1.163	1.159	1.135	1.155	1.189	1.161
15	1.152	1.144	1.112	1.135	1.190	1.151
20	1.142	1.137	1.089	1.132	1.191	1.144
25	1.132	1.124	1.068	1.121	1.193	1.139
30	1.121	1.121	1.047	1.118	1.194	1.077

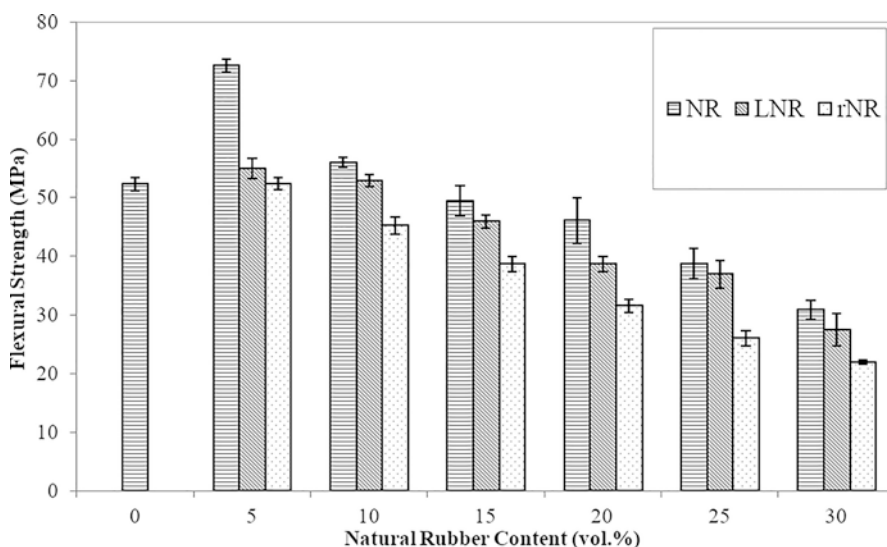


Fig. 2 Effect of different forms of vulcanized NR on the flexural strength of filled systems, at different NR contents

3.2 Flexural Properties

Figure 2 depicts the effect of different forms of vulcanized NR on the flexural strength of filled systems. The formation of rubber phases is related to phase separation starting from the initial epoxy/rubber co-continuous structure induced by the addition of epoxy hardener. The effectiveness of NR phases acting as energy dissipating centers in the epoxy matrix can be influenced by the particle sizes. Similar finding has been reported by Thomas et al. (2008); they identified those mechanical properties of epoxy/liquid rubber as greatly influenced by the particle sizes of NR particles (Thomas et al. 2008).

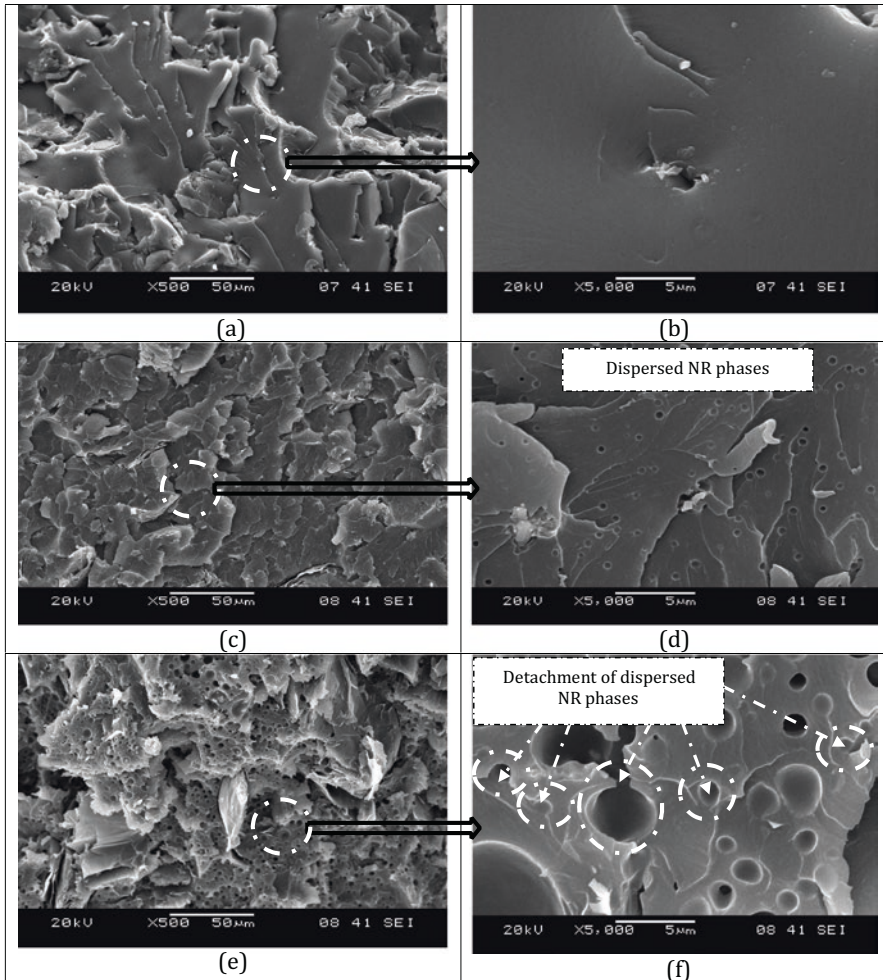


Fig. 3 SEM micrographs of the flexural fractured surfaces of filled systems with (a, b) 5 vol.%, (c, d) 20 vol.%, and (e, f) 30 vol.% of vulcanized NR content

Comparing samples at the same level of rubber content, flexural strength of filled epoxy systems with NR was relatively higher as compared to filled epoxy systems with LNR and rNR. In order to correlate the flexural properties with the morphological analysis, the flexural fractured surfaces were analyzed using SEM. Based on Figs. 3 and 4, the flexural fractured surfaces of filled systems have demonstrated two distinct phases, which included a continuous epoxy matrix and the spherical rubber phases. The effect of different forms of vulcanized rubber content on the average particle sizes of rubber phases is summarized in Table 2. The particle sizes of rubber phases were measured using software ImageJ, and the average results were obtained.

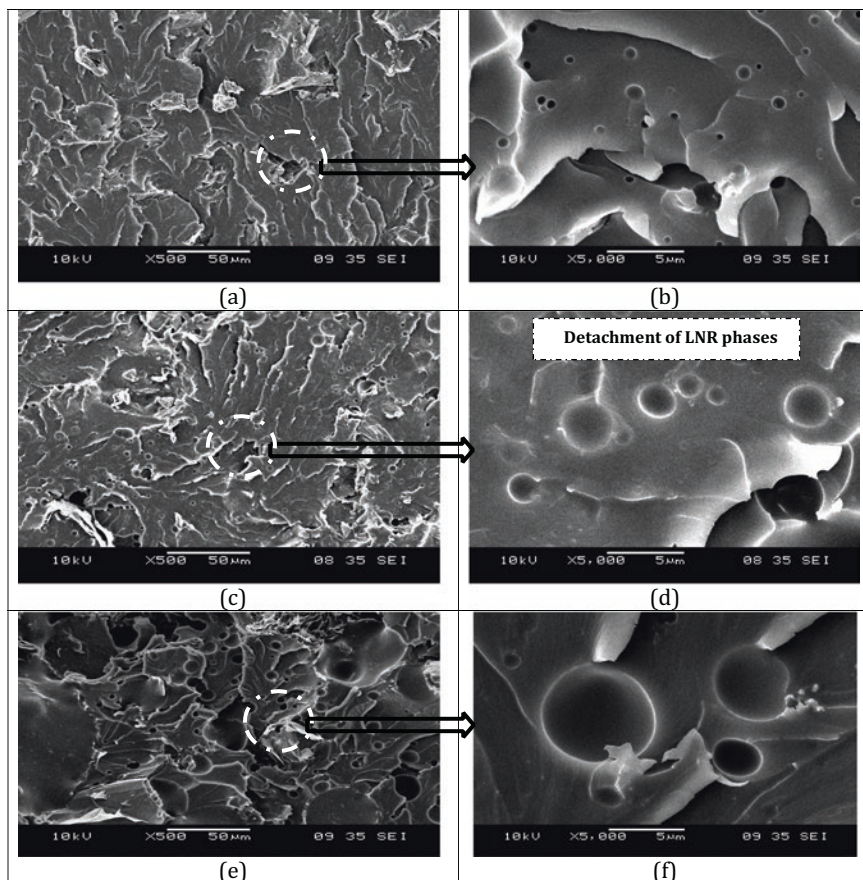


Fig. 4 SEM micrographs of the flexural fractured surfaces of filled systems with (a, b) 5 vol.%, (c, d) 20 vol.%, and (e, f) 30 vol.% of vulcanized LNR content

Table 2 Effect of different forms of vulcanized rubber contents on the range and average particle sizes of rubber phases in filled system

	NR content (vol.%)	5	20	30
Average particle sizes (μm)	NR	0.287	0.369	1.659
	LNR	0.641	2.020	3.571
	rNR	≥ 250	≥ 250	≥ 250
Range of particle sizes (μm)	NR	0.120–0.410	0.168–0.597	0.876–4.457
	LNR	0.226–1.118	0.568–4.033	0.732–7.757
	rNR	≥ 250	≥ 250	≥ 250

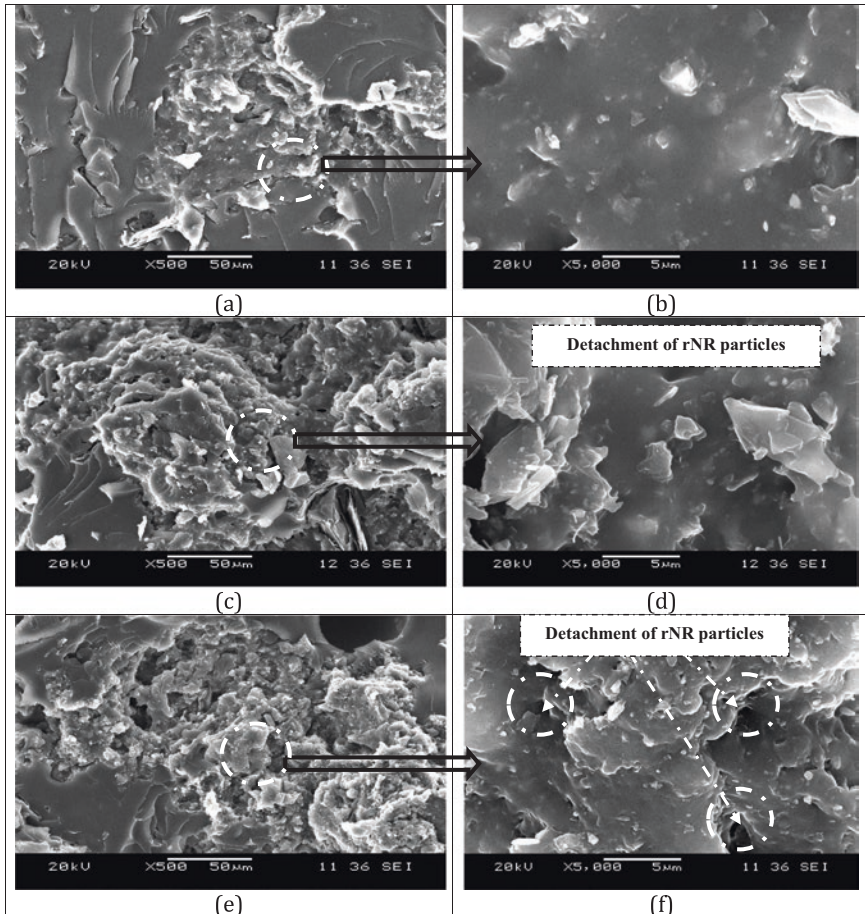


Fig. 5 SEM micrographs of the flexural fractured surfaces of filled systems with (a, b) 5 vol.%, (c, d) 20 vol.%, and (e, f) 30 vol.% of vulcanized rNR content

When comparing the flexural fractured surfaces of NR (Fig. 3), LNR (Fig. 4), and rNR (Fig. 5), the particle sizes of NR phases within the epoxy matrix were smaller and dispersed more uniformly as compared to LNR and rNR phases, as summarized in Table 2. This may be due to the fact that LNR has lower molecular weight than NR; the LNR molecules easily migrated and agglomerated into larger phases during the phase-separation process. This is agreed by researchers who have noted that particle sizes of liquid carboxyl terminated butadiene acrylonitrile copolymer (CTBN) phases were larger due to low molecular weight. In addition, poor dispersion of rNR in the epoxy matrix was attributed to the presence of cross-link precursors in the rubber molecular structure (Ahmad et al. 2016). The smaller particle sizes of NR phases have contributed to large surface area to interact with the

surrounding epoxy matrix (Zhang et al. 2013). Hence, the NR phases absorbed and transferred the stress that was applied on it more effectively (Phinyocheep et al. 2007). In addition, the propagation of cracks in filled epoxy/NR/GNP system (Fig. 3b) was found to be finer than LNR (Fig. 4b) and rNR (Fig. 5a). This proves that the NR phase has higher potential to act as effective energy dissipating centers in the epoxy matrix.

At low rubber content (5 vol.%), the particle sizes of NR, LNR, and the rNR phases were smaller and function as energy dissipating centers in epoxy matrix. Based on Figs. 3b and 4b, the small NR and LNR phases were able to prevent the growth of the cracks, while Fig. 5b shows that small rNR particles were partially compatible with the epoxy matrix. However, the flexural strength of filled systems decreased gradually with increasing NR, LNR, and rNR contents from 5 up to 30 vol.%, respectively. Figure 3b, d, f shows the particle sizes of NR phases in epoxy matrix increased with increasing NR contents. In Fig. 4b, d, f, the particle sizes of LNR phases also increased with increasing LNR content. The presence of large particle sizes of rubber phases is attributed to the agglomeration and coalescence of the rubber phases during the phase-separation process. Based on Fig. 5b, d, f, the compatibility between epoxy and rNR was reduced with increasing rNR content. Figure 5d, e shows there was detachment of rNR particles from the epoxy matrix, which indicated weak interfacial adhesion in between epoxy matrix and large rNR particles.

Figure 6 illustrates the effect of different forms of vulcanized NR on the flexural modulus of filled systems. It is interesting to find that the addition of small volume

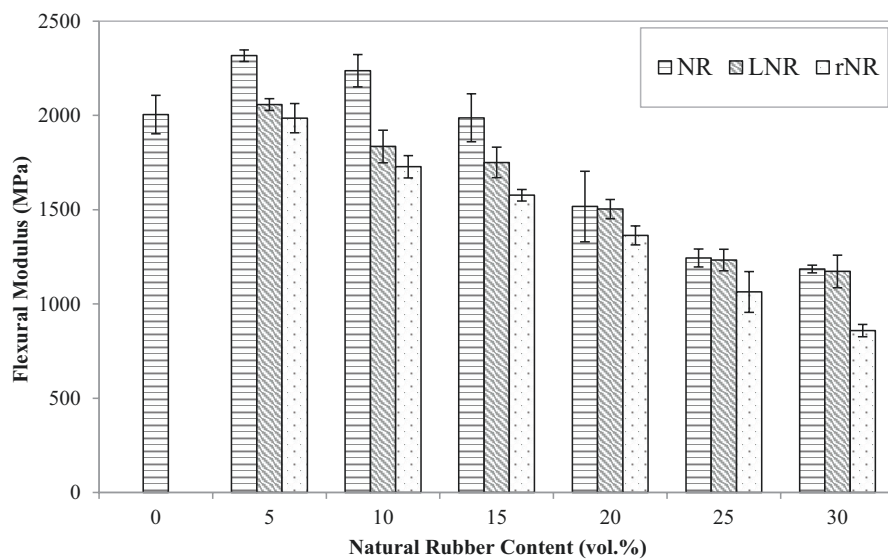


Fig. 6 Effect of different forms of vulcanized NR on the flexural modulus of filled systems, at different NR content

fraction of rubber has improved the flexural modulus of the filled systems. The increase in flexural modulus of filled epoxy system with 5 vol.% of NR and LNR content was 15.61% and 2.62% as compared to filled epoxy system with 0 vol.% of rubber content, respectively. The highest flexural modulus was achieved at 5 vol.% of NR content (2317.508 MPa). When the stress is applied to the specimens, the small NR phases within the epoxy matrix bear the entire stress that is applied. It is important noted that small NR phases have large surface area of contact with the surface of GNP nano-fillers. In addition, the inherent stiffness of GNP nano-fillers restricted the chain mobility of epoxy molecules and NR phases, hence increasing the flexural modulus of filled systems.

At the same rubber content, the flexural modulus has been enhanced by the addition of NR phases, as compared with LNR and rNR. This is because the particle sizes of NR phases were relatively smaller and more uniform as compared to the LNR and rNR phases. Low molecular weight of LNR molecular chains is easily migrated and coalesce to form large rubber phases, while the poor dispersion of rNR in the epoxy matrix was due to the presence of cross-link precursor in the rubber phases. Similar finding reported by other researchers indicated the poor dispersion of recycled acrylonitrile-butadiene rubber (NBRr) in the NR and ENR-50 matrix due to the presence of cross-link precursor (Ahmad et al. 2016). Thus, the small NR phases acted as effective energy dissipating centers within the epoxy matrix, which promoted effective load transfer from the epoxy matrix to NR phases.

The flexural modulus of filled epoxy systems decreased gradually with increasing NR, LNR, and rNR content from 5 up to 30 vol.%, respectively. Epoxy matrices are relatively hard and brittle compared to rubber which is classified as ductile materials. Therefore, the increase of rubber content in epoxy matrix has promoted a reduction in the flexural modulus. At high rubber content (30 vol.%), there are more large rubber phases which disrupts the cross-link density of the epoxy network. Since the depolymerized NR and LNR molecules contain epoxide groups, the rubber molecules could form cross-links with the amine-based hardener, thereby disrupting the continuous cross-link network of epoxy. As discussed earlier, the formation of large rNR particles is attributed to the poor dispersion of rNR in epoxy matrix. This is proven by Figs. 3f, 4f and 5f which indicated that there were large rubber phases within the epoxy matrix. The large NR, LNR, and rNR phases acted as crack initiators, where the cracks were more likely propagated along the weak interfacial bonding in between large rubber phases and epoxy matrix. Thus, the detachment of rubber phases from the epoxy matrix resulted in a decrease in mechanical properties (Mohamad et al. 2013).

3.3 Fracture Toughness

Figure 7 illustrates the effect of different forms of vulcanized NR on the fracture toughness (K_{IC}) of filled systems. The K_{IC} value of filled systems was significantly enhanced at 5 vol.% of NR content, in average 38.5% as compared to filled epoxy

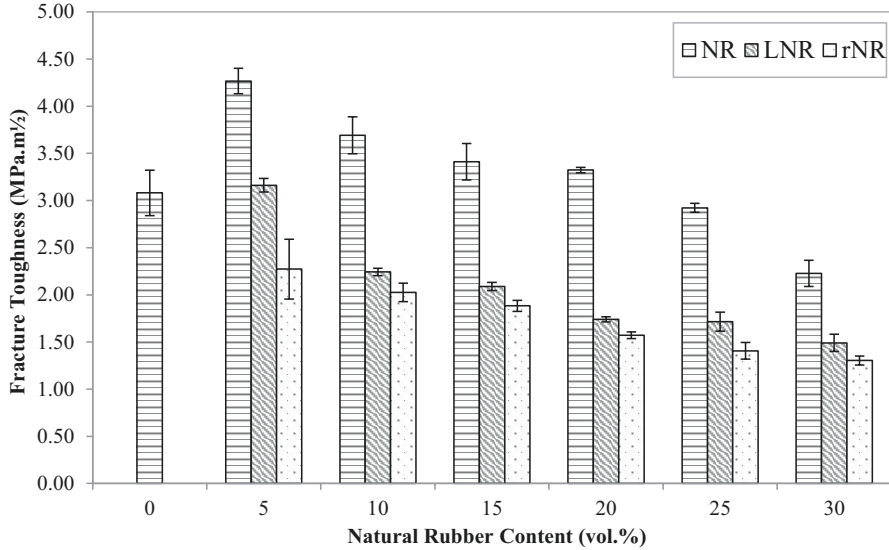


Fig. 7 Effect of different forms of vulcanized NR on the fracture toughness of filled systems, at different NR content

systems with 0 vol.% of rubber content. The K_{IC} value of filled system was slightly improved by adding with 5 vol.% of LNR content with an increase of 2.63% as compared to a filled system with 0 vol.% rubber content. The optimum K_{IC} value was achieved at 5 vol.% NR content (4.267 MPa.m^{1/2}). It is interesting to find that toughness properties of pure epoxy can be improved by adding small volume fraction of NR content (5 vol.%). At low rubber content (5 vol.%), the small vulcanized NR and LNR phases acted as effective energy dissipating centers in the epoxy matrix. When stress is applied, the vulcanized NR and LNR phases absorb and dissipate the stress to the surrounding matrix with significant ductile deformation occur in the epoxy matrix (Kumar and Kothandaraman 2008). The small NR and LNR phases were able to prevent the growth of the cracks and induced significant plastic deformation in epoxy matrix. However, the K_{IC} value of the filled systems did not improve with rNR. This is attributed to the formation of weak interfacial bonding in between epoxy matrix and large rNR particles, although at low rNR content.

Based on Fig. 7, the filled epoxy systems with NR showed higher K_{IC} values as compared to LNR and rNR. At 5 vol% rubber content, the K_{IC} value of filled epoxy systems with NR (4.267 MPa.m^{1/2}) was significantly 25.87% and 46.73% higher than LNR (3.162 MPa.m^{1/2}) and rNR (2.273 MPa.m^{1/2}), respectively. At 20 vol% rubber content, the K_{IC} value of filled system with NR (3.324 MPa.m^{1/2}) was 47.65% and 52.71% higher than LNR (1.740 MPa.m^{1/2}) and rNR (1.572 MPa.m^{1/2}), respectively. This indicated that the addition of NR has greatly enhanced the toughness properties of the filled epoxy system more than those with LNR and

rNR. The increase in toughness was due to the elastic energy stored in the NR phases during stretching (Mathew et al. 2012).

At 5 vol.% rubber content, the K_{IC} value of filled system added with NR was higher than those with LNR and rNR. Based on Fig. 3b, the particle sizes of NR phases were significantly smaller and more uniform as compared to LNR (Fig. 4b) and rNR (Fig. 5b). The mean particle sizes are as summarized in Table 2. The small vulcanized NR phases formed good interfacial bonding with the surrounding epoxy matrix, allowing effective load transfer from the epoxy matrix to the NR phases (Seng et al. 2011). The propagation of cracks in the filled system added with NR (Fig. 3a) was found to be finer as compared to LNR (Fig. 4a) and rNR (Fig. 5a). This has proven that NR acted as effective energy dissipating centers, which absorbed and dissipated the stress to the surrounding matrix with obvious shear yielding. The high molecular weight of NR molecules causes a higher difficulty in molecular migration; thus, smaller NR phases have formed. As discussed earlier, the particle sizes of LNR phases were significantly larger than those of NR. This is because LNR molecules have lower molecular weight than NR; the LNR molecules easily migrate and agglomerate to form large LNR phases during the phase-separation process (Zhou and Xu 2014). The filled epoxy system with rNR exhibited the lowest K_{IC} value, which attributed to the poor dispersion of rNR in epoxy matrix. This may due to the presence of cross-link precursor in the rNR molecular structure (Ahmad et al. 2016). Similar trends were observed and reported at rubber content from 5 vol.% up to 30 vol.%.

For each form of vulcanized rubber (NR, LNR, and rNR), the K_{IC} values of filled epoxy systems decreased with increasing rubber content from 5 vol.% up to 30 vol.%. The toughness properties of epoxy resin reduced with increasing rubber content. This phenomenon was mainly due to plasticization of the matrix by incorporation with rubber. At high rubber content (30 vol.%), the small rubber phases coalesce and agglomerate to form large rubber phases. This was proven by the SEM micrographs in Figs. 3f, 4f and 5f, at 30 vol.% of rubber content for all systems. The large rubber phases have formed weak interfacial bonding with the surrounding matrix. Therefore, the cracks were more likely to propagate along the weak interfacial bonding, which resulted in rubber phases being detached from the surfaces of epoxy matrix as revealed in Figs. 3f, 4f and 5f. This failure occurred at lower toughness value. Similar findings were reported by Chikhi et al., who observed the formation of weak interface between large rubber phases and epoxy matrix under excessive liquid rubber composition (Jansen et al. 1999).

3.4 Thermal Properties

Figure 8 illustrates thermogravimetric (TG) curves for thermal degradation behavior of vulcanized filled epoxy/NR/GNP, epoxy/LNR/GNP, and epoxy/rNR/GNP systems at 5 vol.% of rubber content. Regardless of the different forms of NR (NR, LNR, and rNR), all filled epoxy systems exhibited two stages of decomposition,

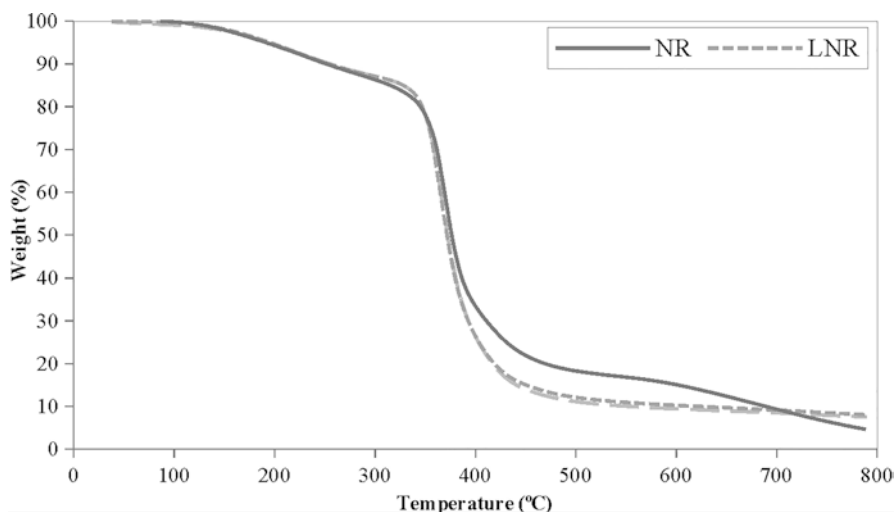


Fig. 8 TGA curves of vulcanized filled epoxy/NR/GNP, epoxy/LNR/GNP, and epoxy/rNR/GNP systems, comparing at 5 vol.% of rubber content

Table 3 Effect of different forms of vulcanized rubber on T_5 , T_{50} , T_{d1} , and T_{max} of filled system, comparing at 5 vol.% of rubber content

	T_5 (°C)	T_{50} (°C)	T_{d1} (°C)	T_{max} (°C)
Pure epoxy	193.43	378.17	222.52	368.61
Vulcanized filled epoxy/NR/GNP system	191.57	376.34	227.03	374.16
Vulcanized filled epoxy/LNR/GNP system	195.33	371.33	224.67	366.00
Vulcanized filled epoxy/rNR/GNP system	192.67	368.67	211.33	363.33

similar to pure epoxy as reported previously (Kam et al. 2021). This indicated that thermal degradation mechanism of epoxy matrix was not significantly altered by incorporation with different forms of vulcanized NR and GNP nano-fillers.

Initial decomposition temperature indicated temperature at which 5% weight losses was designated as T_5 . The effect of different forms of vulcanized NR on T_5 , T_{50} , T_{d1} , and T_{max} of filled epoxy systems is summarized in Table 3. Filled epoxy/LNR/GNP system has higher T_5 values (195.33 °C) among the others, indicating that LNR additions delayed the initial degradation of the epoxy matrix. However, filled epoxy/NR/GNP system has higher T_{50} values as compared to those with LNR and rNR. This is attributed to the higher heat energy required to force the NR molecular chains to flow, which has proven by gel permeation chromatography (GPC) result. The high molecular weights of NR molecular chains have absorbed more heat energy in order to flow.

Based on Table 3, the initial degradation of pure epoxy occurred at about 193.43 °C and continued up to 368.61 °C. For pure epoxy and filled systems, the weight loss (T_{d1}) at temperature around 200 °C is attributed to the partial decomposition of epoxy pre-polymer. The first stage was due to the decomposition

of unreacted epoxy resin apart from the cured epoxy resin. The main weight losses took place at temperature in the range from 350 to 500 °C, corresponding to thermal degradation of the cured epoxy network (Jin and Park 2012).

Based on Table 3, filled epoxy/NR/GNP systems showed higher T_{\max} value as compared to pure epoxy resins. High thermal stability of filled system is attributed to more heat energy being required to overcome good interfacial bonding in between epoxy matrix and vulcanized NR phases. In filled epoxy system, the vulcanized NR phases and GNP nano-fillers acted as effective toughening agent and reinforcement, respectively. The presence of NR phases and GNP nano-fillers has enhanced the mechanical performance of epoxy matrix with improved thermal stability.

At the same rubber content (5 vol.%), the filled epoxy/NR/GNP systems showed higher T_{\max} value, followed by LNR and rNR. This is attributed to the good interfacial bonding between epoxy matrix and small vulcanized NR phases formed in the filled epoxy system. The NR molecular chains facing difficulty in migration due to its molecular weight are higher as compared to LNR; therefore, smaller NR phases were formed in filled system. Thus, more heat energy is needed to overcome the good interfacial bonding in between the epoxy matrix and small vulcanized NR phases. The filled epoxy/rNR/GNP system exhibited lowest T_{\max} value among others. The presence of cross-link precursors in the rNR caused poor dispersion of rNR particles within the epoxy matrix. Thus, less heat energy is needed to overcome the weak interfacial bonding between epoxy matrix and large rNR particles. This was observed in the flexural strength, modulus, and K_{IC} values as discussed in the previous sections.

3.5 X-Ray Diffraction (XRD)

By monitoring the diffraction angles, shape, and intensity of the characteristic peak of GNP nano-fillers in the filled systems, the d-spacing in between the GNP nano-fillers can be determined. Figure 9 illustrates the XRD patterns of filled systems incorporated with different forms of vulcanized NR, at 5 and 20 vol.% of rubber content. All the XRD patterns of filled systems with different forms of vulcanized NR (NR, LNR, and rNR) showed an initial broad diffraction peak of epoxy matrix at 2θ range between 10° and 20°. The single amorphous and broad peak indicated the highly amorphous nature of epoxy matrix (Wang et al. 2013a, b; Arshad et al. 2014). In addition, XRD patterns of filled systems (NR, LNR, and rNR) have showed three basal reflection peaks at 2θ of about 31.9°, 34.5°, and 36.4° corresponding to (1 0 0), (0 0 2), and (1 0 1) lattice planes of the hexagonal wurtzite structure of zinc oxide (ZnO), respectively (Valentini et al. 2016; Jurablu et al. 2015). The intensity of these three peaks is correlated to structurally changing of ZnO, which is involved in vulcanization process of rubber phases (Allahbakhsh et al. 2013).

Based on the previous finding, XRD pattern of pristine GNP nano-fillers have showed an intense and high-intensity basal reflection peak at $2\theta = 26.125^\circ$, attributed

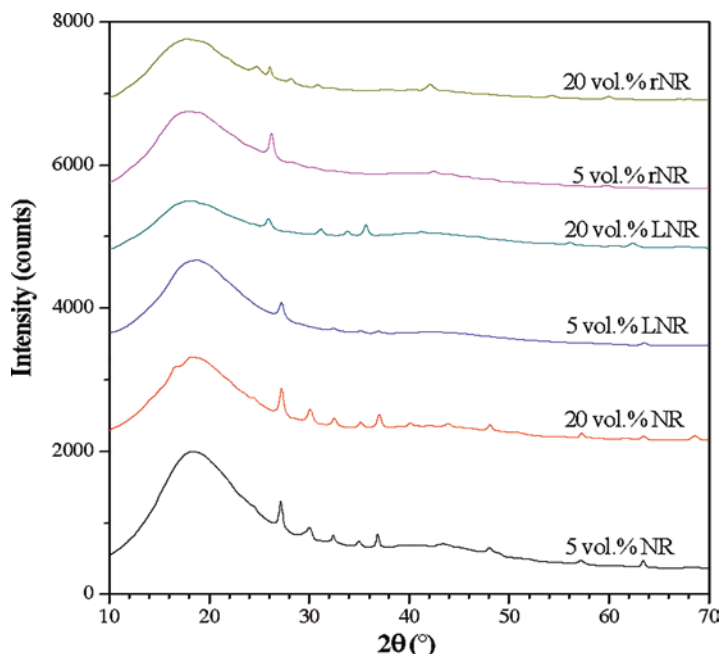


Fig. 9 XRD patterns of filled systems incorporated with different forms of vulcanized rubber, at 5 and 20 vol.% of rubber content

to the (0 0 2) lattice plane, corresponding to d-spacing value of 0.3408 nm (Kam et al. 2018). At 0.8 vol.% of GNP loading (with 0 vol.% of rubber content), the characteristic peak (0 0 2) of pristine GNP nano-fillers has shifted from $2\theta = 26.125^\circ$ to 26.784° . The decrease in d-spacing values from 0.3408 to 0.3326 nm indicated that GNP nano-fillers tend to be closer to each other in high viscosity epoxy medium.

Table 4 shows the diffraction angles (2θ) and d-spacing (nm) of filled epoxy systems with different forms of vulcanized NR (NR, LNR, and rNR). At the same rubber content, the filled epoxy/NR/GNP system showed the highest 2θ values, as compared to those with LNR and rNR. Based on Table 2, the particle sizes of vulcanized NR phases were relatively smaller than that of LNR and rNR phases. As a result, there were more particles of vulcanized NR phases per unit volume. The vulcanized NR phases acted as elastomer spacers and provided better “GNP packing efficiency”, which pushed and forced the GNP nano-fillers to come closer with each other. Therefore, the d-spacing values in between the GNP nano-fillers in filled epoxy/NR/GNP system showed the lowest value. This is supported by filled epoxy/NR/GNP systems which exhibited the highest electrical bulk conductivity values as discussed in Sect. 3.6. With the aid of elastomer spacers, the GNP nano-fillers easily realigned together to form more effective conductive pathways for electron flow, thus improving the electrical conductivity of the filled epoxy systems. For filled epoxy/rNR/GNP systems, the d-spacing in between GNP nano-fillers was largest. The individual rNR particle was easily re-agglomerated to form large rNR particles,

Table 4 Effect of different forms of vulcanized rubber on the XRD values of filled system, comparing at 0, 5, 20, and 30 vol.% of rubber contents

	Rubber content (vol.%)	2 θ ($^{\circ}$)	d-spacing (nm)
Pristine GNP	–	26.125	0.3408
Vulcanized filled epoxy/NR/GNP system	0	26.784	0.3326
	5	27.225	0.3273
	20	27.302	0.3264
	30	28.782	0.3099
Vulcanized filled epoxy/LNR/GNP system	5	27.197	0.3276
	20	27.210	0.3275
	30	28.426	0.3137
Vulcanized filled epoxy/rNR/GNP system	5	26.411	0.3372
	20	26.432	0.3369
	30	27.676	0.3221

which led to poor distribution of rNR particles in the epoxy matrix. This was shown clearly by the SEM micrographs in Fig. 6b, d, f. The presence of large rNR particles in epoxy matrix has promoted less rNR particles per unit volume; thus, the realignment of GNP nano-fillers would be more difficult as compared to NR and LNR. Therefore, the electrical bulk conductivity of filled epoxy/rNR/GNP system showed the lowest values due to the large d-spacing in between the GNP nano-fillers.

For each filled epoxy systems with different forms of vulcanized rubber (NR, LNR, and rNR), the characteristic peak (0 0 2) of GNP nano-filler has shifted toward higher 2 θ values, indicating d-spacing in between the GNP nano-fillers has reduced with increasing of rubber content from 5 up to 30 vol.%. The number of vulcanized rubber phases (NR, LNR, and rNR) per unit volume increased with increasing rubber content from 5 up to 30 vol.%. The vulcanized rubber phases (NR, LNR, and rNR) acted as elastomer spacers, which pushed and forced the GNP nano-fillers to come closer to each other, thus increasing the packing efficiency. This phenomenon has led to increment in the number of effective conductive pathways in the filled epoxy systems (Khanam et al. 2015). As the numbers of effective conductive pathways are increased, electrons moving from one layer to another layer occurred at faster rate. Hence, the electrical bulk conductivity increased with increasing of rubber content from 5 up to 30 vol.% as discussed in Sect. 3.6.

3.6 Electrical Bulk Conductivity

Figure 10 illustrates the effect of different forms of vulcanized NR on the bulk conductivity of filled epoxy systems, comparing rubber contents from 0 up to 30 vol.%. The two-phase morphology and selective localization of conductive nano-fillers could affect the electrical performances of the filled systems (Pan et al. 2016). Selective localization of conductive nano-fillers in one phase of two-matrix system

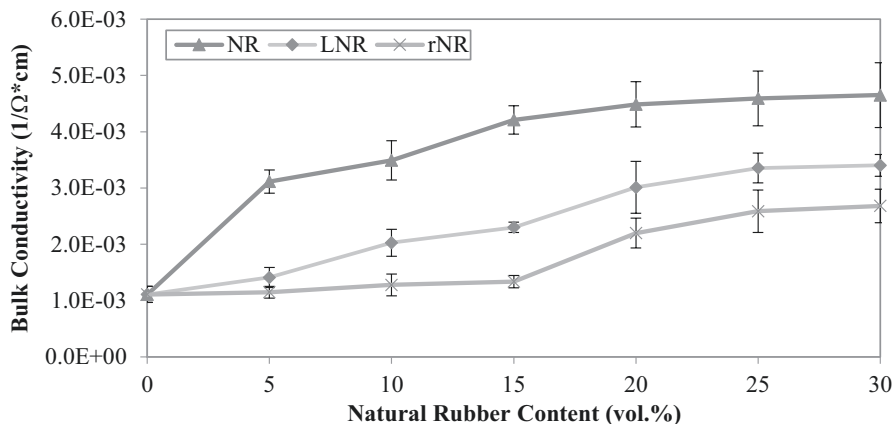


Fig. 10 Effect of different forms of vulcanized NR on the bulk conductivity of filled systems, at different rubber content

has reduced the percolation thresholds by forming conductive pathways in the selected phases, and this concept is known as double percolation. Based on the previous findings, the GNP nano-fillers were selectively localized in epoxy matrix rather than in NR phases (Kam et al. 2017, 2021).

Similar findings were reported by researchers, which identified that carbon black (CB) particles were selectively located in polystyrene (PS) rather than polypropylene and CB need to build up percolated pathways in PS phases to achieve insulator-to-conductor transition (Chen et al. 2017). In addition, Mao et al. (2012) have used the concept of double percolation to obtain conductive composites with a lower electrical percolation threshold. They identified that electrical conductivity of composites can be optimal as polystyrene (PS) and poly (methyl methacrylate) (PMMA) formed a co-continuous structure and octadecylamine-functionalized graphene (GE-ODA) were selectively localized in the PS phase (Mao et al. 2012).

Comparing the same rubber content, the filled epoxy/NR/GNP systems showed the highest bulk conductivity value, followed by filled epoxy/LNR/GNP and epoxy/rNR/GNP systems. However, all of the filled systems have bulk conductivity values which remained at the same order of magnitude (10^{-3} 1/Ω.cm). The morphology of the two-matrix systems has provided a great impact on its electrical performances (Huang et al. 2014). Based on Table 2, the particle sizes of vulcanized NR phases were relatively smaller and more uniform as compared to LNR and rNR phases. Since the particle sizes of vulcanized NR phases were relatively smaller, they provided a better “GNP packing density” with more NR phases per unit volume. In this case, the vulcanized NR, LNR, and rNR phases acted as elastomer spacers in the filled systems. With the aid of vulcanized NR phases, they realigned and forced the GNP nano-fillers to contact each other more easily as compared to LNR and rNR phases; hence, the d-spacing value in between GNP nano-fillers become smaller. This was proven by the XRD results which indicated d-spacing in between

GNP nano-fillers was the shortest in the filled epoxy/NR/GNP system, as shown in Table 4. The reduction in d-spacing value allowed more tunneling activity and electrons hopping in between GNP nano-fillers, resulted in an increase in bulk conductivity. The highest bulk conductivity value of filled epoxy/NR/GNP system is attributed to the formation of more effective conductive pathways for the ease of tunneling activity and electrons hopping. Hence, the electrons can move through the seamlessly interconnected three-dimensional networks constructed by the GNP nano-fillers in epoxy matrix.

However, the particle sizes of vulcanized LNR phases were relatively smaller as compared to the aggregated rNR particles. Thus, the vulcanized LNR phases have pushed and forced the GNP nano-fillers close contact each other more easily as compared to large rNR particles, where there were more LNR phases per unit volume. There are more electrical conductive pathways in filled epoxy/LNR/GNP system, compared to filled epoxy/rNR/GNP system. Therefore, the bulk conductivity values of filled epoxy/LNR/GNP system were higher than filled epoxy/rNR/GNP system, but slightly lower as compared to filled epoxy/NR/GNP system. However, further increasing of rubber (NR, LNR, and rNR) contents does not cause a significant increase in bulk conductivity values of filled systems, but has leveled off. At 30 vol.% of rubber content, bulk conductivity was stabilized at a magnitude of 10^{-3} $1/\Omega\cdot\text{cm}$, which indicated there exists an optimum formation of conductive networks for the electrons to travel.

4 Conclusion

The filled epoxy/NR/GNP system showed the highest flexural strength, modulus, and toughness properties, at 5 vol.% of rubber content. The SEM micrographs have revealed that particle sizes of NR phases were smaller and more uniform than those of LNR and rNR while the filled epoxy/rNR/GNP system showed the lowest flexural strength, modulus, and toughness, attributed to poor dispersion of rNR particles in the epoxy matrix. Vulcanized filled epoxy/NR/GNP system has the highest thermal stability, followed by LNR and rNR due to the good interfacial bonding in between epoxy matrix and small NR phases. In terms of electrical conductivity, highest bulk conductivity values were reported to the filled epoxy/NR/GNP system. The vulcanized NR phases (smaller and more uniform) were acted as elastomer spacers, which provided better “GNP packing density” with more NR phases per unit volume. The XRD results also indicated d-spacing values in between GNP nano-fillers in filled epoxy/NR/GNP system were the nearest for electrons hopping. Thus, the electrons can move easily through the seamlessly interconnected networks of GNP nano-fillers.

Acknowledgments The authors wish to express their gratitude for the support of the Ministry of Higher Education (MOHE). The financial support of Fundamental Research Grant Scheme (FRGS) under grant number FRGS/1/2018/TK05/UNIMAP/02/13 is gratefully acknowledged.

References

- Ahmad HS, Ismail H, Rashid AA (2016) Tensile properties and morphology of epoxidized natural rubber/recycled acrylonitrile-butadiene rubber (ENR 50/NBRr) blends. *Procedia Chem* 19:359–365. <https://doi.org/10.1016/j.proche.2016.03.024>
- Allahbakhsh A, Mazinani S, Kalae MR et al (2013) Cure kinetics and chemorheology of EPDM/graphene oxide nanocomposites. *Thermochim Acta* 563:22–32. <https://doi.org/10.1016/j.tca.2013.04.010>
- Arshad MA, Maaroufi A, Benavente R et al (2014) Kinetics of the thermal decomposition mechanisms of conducting and non-conducting epoxy/Al composites. *J Mater Environ Sci* 5:1342–1354
- Cantoni B, Cappello Riguzzi A, Turolla A et al (2021) Bisphenol A leaching from epoxy resins in the drinking water distribution networks as human health risk determinant. *Sci Total Environ* 783:146908. <https://doi.org/10.1016/j.scitotenv.2021.146908>
- Chawalitsakunchai W, Dittanet P, Loykulnant S et al (2021) Properties of natural rubber reinforced with nano cellulose from pineapple leaf agricultural waste. *Mater Today* 28:102594. <https://doi.org/10.1016/j.mtcomm.2021.102594>
- Chen J, Cui X, Sui K et al (2017) Balance the electrical properties and mechanical properties of carbon black filled immiscible polymer blends with a double percolation structure. *Compos Sci Technol* 140:99–105. <https://doi.org/10.1016/j.compscitech.2016.12.029>
- Du J, Cheng HM (2012) The fabrication, properties and uses of graphene/polymer composites. *Macromol Chem Phys* 213:1060–1077. <https://doi.org/10.1002/macp.201200029>
- Fuad MA, Yaakob I, Ishak ZM et al (1993) Density measurement of rice husk ash filler particles in polypropylene composites. *Polym Test* 12:107–112. [https://doi.org/10.1016/0142-9418\(93\)90033-L](https://doi.org/10.1016/0142-9418(93)90033-L)
- Hong SG, Chan CK (2004) The curing behaviors of the epoxy/dicyanamide system modified with epoxidized natural rubber. *Thermochim Acta* 417(1):99–106. <https://doi.org/10.1016/J.TCA.2003.12.015>
- Huang J, Mao C, Zhu Y (2014) Control of carbon nanotubes at the interface of a co-continuous immiscible polymer blend to fabricate conductive composites with ultralow percolation thresholds. *Carbon* 73:267–274. <https://doi.org/10.1016/j.carbon.2014.02.063>
- Ilyas RA, Sapuan SM, Jailani AK et al (2021a) Introduction to recycling of polymers and metal composites. In: Ilyas RA, Sapuan SM, Bayraktar E (eds) *Recycling of plastics, metals, and their composites*, 1st edn. CRC Press/Taylor & Francis Group, Boca Raton
- Ilyas RA, Sapuan SM, Bayraktar E et al (2021b) *Recycling of plastics, metals, and their composites*, 1st edn. CRC Press, Boca Raton. <https://doi.org/10.1201/9781003148760>
- Jansen BJP, Tamminga KY, Meijer HEH et al (1999) Preparation of thermoset rubbery epoxy particles as novel toughening modifiers for glassy epoxy resins. *Polymer* 40:5601–5607. [https://doi.org/10.1016/S0032-3861\(98\)00774-5](https://doi.org/10.1016/S0032-3861(98)00774-5)
- Jin FL, Park SJ (2012) Thermal properties of epoxy resin/filler hybrid composites. *Polym Degrad Stab* 97:2148–2153. <https://doi.org/10.1016/j.polymdegradstab.2012.08.015>
- Jurablu S, Farahmandjou M, Firoozabadi TP et al (2015) Sol-gel synthesis of zinc oxide (ZnO) nanoparticles: study of structural and optical properties. *J Sci Islam Repub Iran* 26:281–285
- Kam KW, Teh PL, Husseniayah S et al (2017) The effect of graphene and natural rubber content on mechanical and electrical conductivity properties of epoxy/natural rubber/graphene conductive materials. *Mater Sci Forum* 888:209–215. <https://doi.org/10.4028/www.scientific.net/MSF.888.209>
- Kam KW, Teh PL, Osman H et al (2018) Comparison study: effect of un-vulcanized and vulcanized NR content on the properties of two-matrix filled epoxy/natural rubber/graphene nanoplatelets system. *J Polym Res* 25:15. <https://doi.org/10.1007/s10965-017-1418-x>
- Kam KW, Teh PL, Yeoh CK (2021) Comparison study: the effect of unmodified and modified graphene nano-platelets (GNP) on the mechanical, thermal, and electrical performance of

- different types of GNP-filled materials. *Polym Adv Technol* 32(9):3588–3608. <https://doi.org/10.1002/pat.5368>
- Khanam PN, Ponnamma D, Al-Madeed MA et al (2015) Graphene-based polymer nanocomposites in electronic: electrical properties of graphene polymer nanocomposites. Springer
- Krishna Kumar KS, Varuni SJ, Promsung R et al (2021) Synergistic effects of soap nut extract and glutaraldehyde on the properties of natural rubber: a waste to wealth approach. *Ind Crop Prod* 172:114063. <https://doi.org/10.1016/j.indcrop.2021.114063>
- Kumar KD, Kothandaraman B (2008) Modification of (DGEBA) epoxy resin with maleated depolymerised natural rubber. *Express Polym Lett* 2:302–311. <https://doi.org/10.3144/expresspolymlett.2008.36>
- Kutz M (2002) Handbook of materials selection. Wiley. <https://doi.org/10.1002/9780470172551>
- Mao C, Zhu Y, Jiang W (2012) Design of electrical conductive composites: tuning the morphology to improve the electrical properties of graphene filled immiscible polymer blends. *ACS Appl Mater Interfaces* 4:5281–5286. <https://doi.org/10.1021/am301230q>
- Mathew VS, Sinturel C, George SC et al (2010) Epoxy resin/liquid natural rubber system: secondary phase separation and its impact on mechanical properties. *J Mater Sci* 45:1769–1781. <https://doi.org/10.1007/s10853-009-4154-8>
- Mathew VS, Jyotishkumar P, George S et al (2012) High performance HTLNR/epoxy blend-phase morphology and thermo-mechanical properties. *J Appl Polym Sci* 125:804–811. <https://doi.org/10.1002/app.35446>
- Mohamad N, Sharafina ZN, Ab Maulod HE et al (2013) Morphological and mechanical properties of polypropylene/epoxidized natural rubber thermoplastic vulcanizates treated with maleic anhydride-grafted polypropylene. *Int J Automot Mech Eng* 8:1305–1315. <https://doi.org/10.15282/ijame.8.2013.19.0107>
- Ozturk A, Kaynak C, Tincer T (2001) Effects of liquid rubber modification on the behavior of epoxy resin. *Eur Polym J* 37:2353–2363. [https://doi.org/10.1016/S0014-3057\(01\)00158-6](https://doi.org/10.1016/S0014-3057(01)00158-6)
- Pan Y, Liu X, Hao X et al (2016) Enhancing the electrical conductivity of carbon black-filled immiscible polymer blends by tuning the morphology. *Eur Polym J* 78:106–115. <https://doi.org/10.1016/j.eurpolymj.2016.03.019>
- Pargi MNF, Teh PL, Hussiensyah S et al (2015) Recycled-copper-filled epoxy composites: the effect of mixed particle size. *Int J Mech Mater Eng* 10:3. <https://doi.org/10.1186/s40712-015-0030-2>
- Phinyocheep P, Saelao J, Buzare JY (2007) Mechanical properties, morphology and molecular characteristics of poly(ethylene terephthalate) toughened by natural rubber. *Polymer* 48:5702–5712. <https://doi.org/10.1016/j.polymer.2007.07.016>
- Phua JL, Teh PL, Ghani SA et al (2017) Influence of thermoplastic spacer on the mechanical, electrical, and thermal properties of carbon black filled epoxy adhesives. *Polym Adv Technol* 28:345–352. <https://doi.org/10.1002/pat.3894>
- Puglia D, Maria HJ, Kenny JM et al (2013) Clay nanostructure and its localization in epoxy/liquid rubber blend. *RSC Adv* 3:24634–24643. <https://doi.org/10.1039/C3RA44844D>
- Radabutra S, Khemthong P, Saengsuwan S (2021) Effect of silane coupling agent pretreatment on the properties of rice straw particleboard bonded with prevulcanized natural rubber latex. *J Rubber Res* 24:157–163. <https://doi.org/10.1007/s42464-021-00081-z>
- Rotrekl J, Sikora A, Kaprálková L et al (2013) Effect of an organoclay on the reaction-induced phase-separation in a dynamically asymmetric epoxy/PCL system. *Express Polym Lett* 7(2013):1012–1019. <https://doi.org/10.3144/expresspolymlett.2013.99>
- Seng LY, Ahmad S, Rasid R et al (2011) Effect of liquid natural rubber (LNR) on the mechanical properties of LNR toughened epoxy composite. *Sains Malaysiana* 40:679–683
- Tan SK, Ahmad S, Chia CH et al (2013) A comparison study of liquid natural rubber (LNR) and liquid epoxidized natural rubber (LENR) as the toughening agent for epoxy. *Am J Mater Sci* 3(3):55–61. <https://doi.org/10.5923/j.materials.20130303.02>
- Thomas R, Yumei D, Yuelong H et al (2008) Miscibility, morphology, thermal and mechanical properties of a DGEBA based epoxy resin toughened with a liquid rubber. *Polymer* 49:278–294. <https://doi.org/10.1016/j.polymer.2007.11.030>

- Valentini L, Bon SBB, Lopez-Manchado MA et al (2016) Synergistic effect of graphene nanoplatelets and carbon black in multifunctional EPDM nanocomposites. *Compos Sci Technol* 128:123–130. <https://doi.org/10.1016/j.compscitech.2016.03.024>
- Verma D, Gope PC, Shandilya A et al (2014) Mechanical-thermal-electrical and morphological properties of graphene reinforced polymer composites: a review. *Trans Indian Inst Metals* 67:803–816. <https://doi.org/10.1007/s12666-014-0408-5>
- Wang D, Zhang X, Zha JW et al (2013a) Dielectric properties of reduced graphene oxide/polypropylene composites with ultralow percolation threshold. *Polymer*:1916–1922. <https://doi.org/10.1016/j.polymer.2013.02.012>
- Wang X, Jin J, Song M (2013b) An investigation of the mechanism of graphene toughening epoxy. *Carbon* 65:324–333. <https://doi.org/10.1016/j.carbon.2013.08.032>
- Yue L, Pircheraghi G, Monemian SA et al (2014) Epoxy composites with carbon nanotubes and graphene nanoplatelets – dispersion and synergy effects. *Carbon* 78:268–278. <https://doi.org/10.1016/j.carbon.2014.07.003>
- Zhang C, Wang W, Huang Y et al (2013) Thermal, mechanical and rheological properties of polylactide toughened by epoxidized natural rubber. *Mater Des* 45:198–205. <https://doi.org/10.1016/j.matdes.2012.09.024>
- Zhou H, Xu S (2014) A new method to prepare rubber toughened epoxy with high modulus and high impact strength. *Mater Lett* 121:238–240. <https://doi.org/10.1016/j.matlet.2014.01.160>

Recycling of Commonly Used Waste Plastics to Fabricate Membranes for Filtration Applications



Abichal Ghosh, Anirban Roy, and A. K. Ghosh

1 Introduction

The accumulation of plastic solid waste (PSW) is one of the largest concerns worldwide as the environmental consequences of such wastes are clearly visible through the increasing levels of global plastic pollution both on the land and in the oceans. Over the years, several waste management methods have been developed for PSW disposal such as incineration-gasification, burying the waste, reuse/recycling, etc. (Awasthi et al. 2017; Ilyas et al. 2021a, b; Salwa et al. 2021). Incineration of the PSW followed by the collection of heat energy is useful for the treatment of mixed waste as presorting of mixed plastics is not required here. However, the recovery or reuse of any of the starting materials in this process is not possible and the burning process also leads to the release of harmful gases to the atmosphere. Burying the waste can cause surface and groundwater pollution which hinders the growth of agricultural products. Hence, the importance of recycling plastics is quite obvious due to the environmental and economic consequences. Thermosetting polymers and composites such as epoxy polymers are generally incinerated or landfilled as they cannot be reformed (Pastine 2012). However, the end-of-life treatment options for

A. Ghosh
Department of Computer Science and Information Systems, Birla Institute BITS Pilani,
Goa, India

A. Roy
Department of Chemical Engineering, BITS Pilani, Goa, India

A. K. Ghosh (✉)
Desalination and Membrane Technology Division, Bhabha Atomic Research Centre,
Mumbai, India
e-mail: akghosh@barc.gov.in

plastic solid wastes are quite limited. These limitations can be perceived in many ways, such as in the form of presorting of plastics before recycling which is costly both in terms of money and time along with which it also requires an excess amount of energy; often leading to unwanted residual polymers; and it is not being able to be applied to many polymeric materials. Subsequently, newer research methods are able to overcome these limitations with lower energy requirements, avoiding sorting through compatibilization of mixed plastic wastes (Hamad et al. 2013), and expanding recycling technologies to traditionally nonrecyclable polymers (Garcia and Robertson 2017).

One of the newest widely used technologies for the large-scale treatment of PSW is that of mechanical recycling. In this technology, several steps are present such as the removal of organic residue through washing followed by shredding, melting, and remolding of the polymer through which the original product is remade (Schyns and Shave 2021). The mechanical recycling technologies however, have limitations which arise due to each type of plastic responding differently to the recycling process depending on their chemical, thermal, and mechanical properties. Another limitation in the mechanical recycling technology is that temperature-sensitive plastics like thermosetting plastics cannot be processed. Currently, chemical recycling technologies such as pyrolysis (thermolysis) are able to overcome the limitations of mechanical recycling (Ragaert et al. 2017). The technology of pyrolysis includes selectively producing gases, fuels, or waxes through the use of catalysts. However, this method is not commonly used as a recycling practice due to its high energy costs. Some of the recent important research directions for plastic recycling practices are that of: (i) Chemical recycling using advanced catalysts to improve the performance, (ii) Compatibilizer design to minimize the need for sorting, and (iii) expanding recycling beyond thermoplastics (Garcia and Robertson 2017). Fabrication of recycled plastic product with same/equivalent properties to the original material is the main challenge for the recycle and reuse of waste material.

To convert polymer plastic wastes into functional polymer with a new application always gives added value. Among other recycling methods, waste plastics are nowadays being converted into products used for energy generation, mechanical recycling, filtration membrane manufacturing, etc. Fabrication of filtration membranes requires plastics with specific properties like film-forming ability, lower cost, and easy processability. Table 1 gives the list of common polymeric wastes and the recycle methods used. Polyethylene terephthalate (PET), polyvinyl chloride (PVC), polystyrene (PS), polycarbonate (PC), etc. are some of the common membrane filter materials that are discarded as PSW, but could be used to fabricate useful membranes with improved eco-efficiency characteristics and technical performance toward filtration applications like water purification and gas separation. This chapter covers the current methods and challenges for the fabrication of filtration membranes using widely used reusable plastics namely, PET, PVC, PS, and PC.

Table 1 Types of PSW and their present recycling methods including fabrication of filtration membranes

Name of the polymer	Abbreviation	Uses	Recycling methods
Polyethylene terephthalate	PET	Water bottles, clothings, combs, bean bags, rope, carpet, packaging foods, and beverages	Recycled polyethylene terephthalate is known as RPET, and it is the most widely recycled plastic in the world. Recycled by remelting and by chemically breaking to its component materials to make new PET resin; <i>filtration membranes for water purification and gas separation.</i>
Polyvinyl chloride	PVC	Pipes, electrical cable insulation, shoes, flooring, imitation leather, plumbing	Used PVC recycled through mechanical recycling (grinds plastic into a powder base for new products); <i>filtration membranes for water purification</i>
Polystyrene or styrofoam	PS	Drinking glasses, soup bowls, salad boxes, sunglass, packing foam egg cartons	Expanded polystyrene (or EPS) can be immediately reused. Three common methods of recycling known as granulation, compacting, and densifying. <i>Filtration membranes for gas separation and water purification after chemical modification</i>
Polycarbonate	PC	Safety glasses, plastic CDs and DVDs, baby feeding bottles	PC sheets are 100 percent recyclable. Usual process for recycling polycarbonate is to sort, shred, wash, and then turn into a granulate ready for manufacturers to use again. Also PC waste was recycled into useful products such as phenol and bisphenol A by chemical recycling. <i>Filtration membranes for water purification.</i>
Polypropylene	PP	Plastic parts for machinery and equipment, plastic containers, reusable water bottles, medical components, toys.	Polypropylene is widely recyclable and either processed as a recycle for reuse or remelted directly into new products.
High-density and low-density polyethylene	HDPE & LDPE	HDPE: Chemical containers, milk jugs, recycling bins, flower pots LDPE: Dispensing bottles, wash bottles, tubing, plastic parts for computer components	HDPE is widely recyclable and recycled HDPE often used to make piping, plastic lumber, recycling bins, and rope. <i>Filtration membranes for water purification.</i> LDPE is the material used to make things like ice-cream lids, garbage bags, sandwich bags, etc. and is usually a soft and flexible material that can be recycled into the same thing.

(continued)

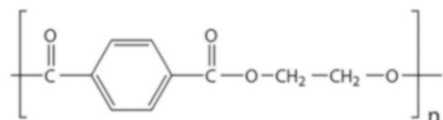
Table 1 (continued)

Name of the polymer	Abbreviation	Uses	Recycling methods
Other polymers (acrylic, polyacrylonitrile)	PAN, acrylonitrile butadiene styrene (ABS), etc.	PAN: Fibers in hot gas filtration systems, synthetic wool. ABS: Electronic housings, auto parts, consumer products, pipe fittings, protective head gear	PAN may not be possible to recycle through traditional recycling methods and recycled through blending with other polymers to develop different products. ABS plastic is biocompatible and recyclable material. Recycled ABS generally blended with virgin material to produce products with lower cost while preserving the high quality.

2 Polyethylene Terephthalate (PET)

Polyethylene terephthalate is one of the highest used plastics produced worldwide for single-used drink packaging bottles in the food industries. PET polymers are resistant to a wide variety of solvents with good stability in free chlorine & acid environments and have very good mechanical, processability, and barrier properties (Stevenson 1989).

The chemical structure of the PET polymer is given below:



After use, making of fabric for cloth is the commonly used recycle method for PET. Making of filtration membrane from PET is a better-value product in comparison to making cloth fabrics and hence it is economically more feasible and also has the advantages of reduction in membrane production costs using green technology which minimizes environmental pollution.

PET is commonly used to make nonwoven support for preparation of all types of filtration membranes. With respect to preparation of membranes for water purification, PET membranes manufactured without additives are found rigid with poor mechanical properties. Mulyati et al. (2018) reported performance-enhanced PET-based membrane preparation via thermal-induced phase separation method using the wasted plastic bottle for humic acid separation by adding cellulose acetate and silica. Cellulose acetate acts as a sub-polymer to increase mechanical strength and silica as a membrane pore-forming agent. Nanofiber-based microfiltration membranes were developed by Zander et al. (2016) from recycled PET plastic bottles and used as prefilter for wastewater treatment system. Washed and dried PET shreds were dissolved in hexafluoroisopropanol (HFIP) (5–10 wt.%) and nanofiber membranes were prepared via solution electrospinning with fiber diameters as low as

100 nm and finally the fibers were functionalized with biguanide and quaternary ammonium compound to make the membrane biofouling resistant.

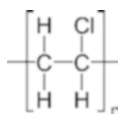
For use of filtration membranes in high-temperature solvents and other harsh environments, Pulido et al. (2019) reported the development of membranes with pore size range of 35–100 nm using recycled water bottles made of PET by nonsolvent-induced phase separation in methanol or ethanol solvent. From Fig. 1, it can be seen that the PET membranes can be used for permeation of various organic solvents along with the water and these membranes were found stable in dimethylformamide (DMF) at temperatures up to 100 °C and highly acidic (pH:1) & alkaline (pH:13) conditions.

Strain et al. (2015) reported the development of PET-based tough fibrous membranes using recycled PET bottles for smoke filtration by solution electrospinning. It was found that when air filtration study was carried out using cigarette smoke as a model substance through these fiber membranes, it absorbs 32–43 times of its weight of the smoke. Figure 2 shows scheme of smoke filtration, photographs of mat before and after smoke filtration, and the IR-spectra of a clean and smoke-exposed fiber membrane with average fiber diameters of 0.4, 1.0, and 4.3 mm to confirm the absorption of carcinogenic hydrocarbons from the tobacco smoke.

3 Polyvinyl Chloride (PVC)

Polyvinyl chloride is a thermoplastic polymer synthesized mostly by suspension polymerization of vinyl chloride monomer. After polyethylene and polypropylene, PVC polymer is the world's third-most produced synthetic polymer and has applications across a broad range of industrial, technical, and household uses for making electrical cable insulation, flooring, imitation leather, plumbing, etc.

The chemical structure of the PVC polymer is given below:



Efficient use and control of PVC throughout its life cycle is one of the challenges for sustainability. Being a chlorinated hydrocarbon, pure PVC has molecular instability towards light and heat. It releases highly corrosive gas/vapor of hydrochloric acid on burning and also ash from PVC incineration contains toxic elements like cadmium and lead. PVC has great advantage of being a highly versatile polymer gets dissolved in a various organic solvent like tetrahydrofuran (THF), N-methyl pyrrolidone (NMP), N, N-dimethylacetamide (DMAc), N, N-dimethylformamide (DMF), etc. and hence wide range of formulation possibilities can be explored to reuse and recycle into new products with improved eco-friendly and safety characteristics without loss of technical performance. One of the very attractive applications can be the development of suitable filtration membranes for water purification.

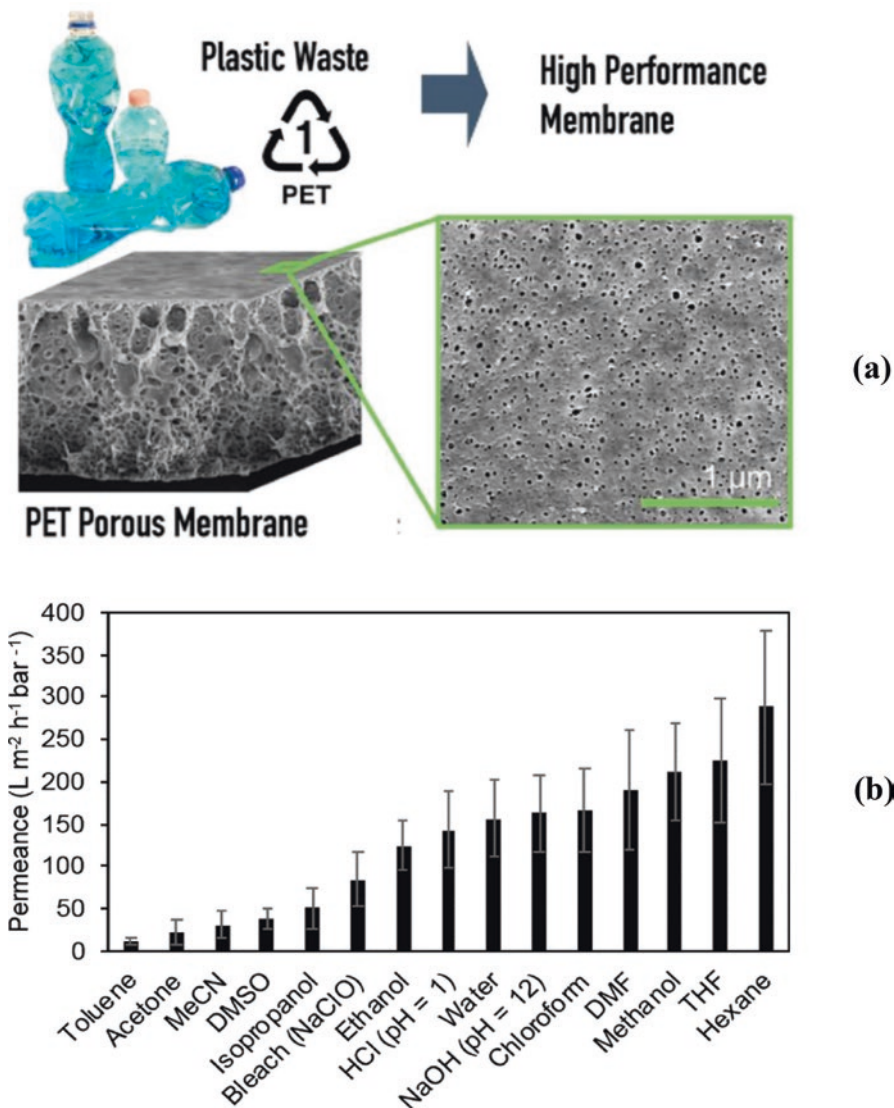


Fig. 1 (a) Recycled PET bottles and SEM images of membranes prepared. (b) Permeance of different solvents using a PET membrane (prepared by casting of 10 wt.% PET solutions in TFA with 4 wt.% PEG 1 kg mol^{-1} , with 0 s evaporation time, immersed in ethanol. (Adopted from Pulido et al. 2019)

PVC is an outstanding membrane material due to robust mechanical strength, suitable chemical resistance, low cost, and other excellent properties such as high resistance to acids, bases, and solvents. Hence on the way of recycling, the used PVC waste can be dissolved first in a suitable organic solvent like N-methyl pyrrolidone (NMP) followed by separation of undissolved additives/binder by filtration

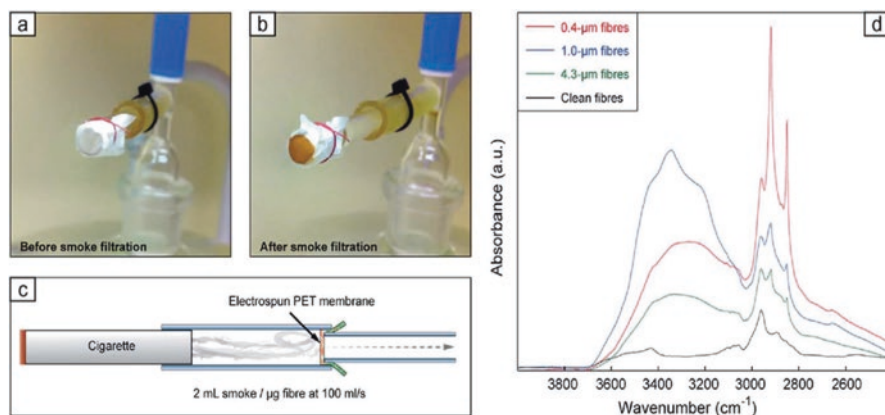


Fig. 2 Photographs of fiber mats (a) before and (b) after smoke filtration (1.0 mm diameter), conducted according to the scheme shown in (c). IR-spectroscopy (d) of a clean fiber mat compared to that of smoke-exposed fiber mats with average fiber diameters of 0.4, 1.0, and 4.3 mm. (Adopted from Strain et al. 2015)

with filter paper. Then the PVC solution is allowed to precipitate in water as NMP leached out and recover pure PVC for membrane making.

There are number of published literatures discussed on use of commercially available neat PVC polymer for useful membrane fabrication and their probable applications in water treatment (Ghazanfari et al. 2017; Dizajikan et al. 2018; Bhran et al. 2018). The only literature found where Aji et al. (2020) reported the utilization of waste PVC into fabrication of a useful ultrafiltration membranes. PVC derived from PSW was blended with cellulose acetate in N, N-dimethyl formamide solvent and membranes were prepared via nonsolvent-induced phase inversion techniques. From Fig. 3, it can be seen that the pure PVC membranes have very few pores and the number of pores increase with increase in cellulose acetate concentration in the PVC/CA blend membrane. Ultrafiltration membranes having pure water flux (PWF) of 85 L/m² h with more than 90% bovine serum albumin (BSA) rejection were developed.

4 Polystyrene (PS)

Polystyrenes is a thermoplastic polymer synthesized mostly by free radical vinyl polymerization of styrene monomers. Polystyrenes are commonly used in our home, office, local grocery as reusable plastic items like drinking glasses, drinking bottles, soup bowls, salad boxes, sunglass, foam egg cartons, etc. Styrofoam is basically expanded polystyrene (EPS) consists of ~98% air and ~ 2% of polystyrene. The chemical structure of the PS polymer or also known as Styrofoam is given below:

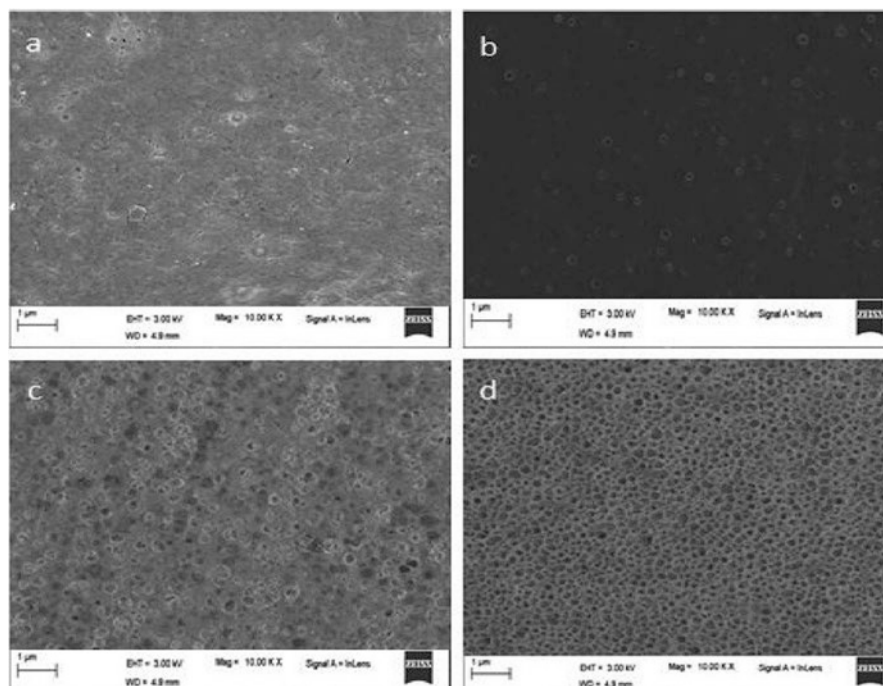
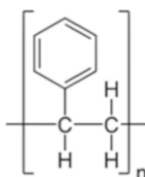


Fig. 3 FESEM images of PVC/CA membranes. PVC-20 wt.% with different amount of CA (a) 0 wt.% of CA, (b) 1 wt.% of CA, (c) 3 wt.% of CA, and (d) 5 wt.% of CA. (Adopted from Aji et al. 2020)



Ramos-Olmos et al. (2008) used recycled polystyrene foam for fabrication of asymmetric ultrafiltration membranes for water purification. Polystyrene foam (20 wt.%) without prior processing was dissolved in N-methyl-2-pyrrolidone (NMP) solvent with polyethylene glycol (PEG) of different molecular weights (10–20 wt.%) and dioctyl phthalate (DOP) (2 wt.%) as additives and prepared the membranes by phase inversion technique. Membranes prepared using casting solution with PEG-600 (20 wt.%) give the highest pure water permeability of $120 \text{ L}\cdot\text{m}^{-2}\cdot\text{h}^{-1}$ with molecular weight cutoff of $\sim 750 \text{ KDa}$. Adamczak et al. (2020) reported the utilization of waste polystyrene polymers as base material for preparation of ultrafiltration membrane and tested using feed prepared by mixing river surface water with micro-pollutants (1 g/L in methanol). It was demonstrated that ultrafiltration membranes prepared using recycled polystyrene in N, N-dimethyl formamide solvent with

single-walled carbon nanotube as additives give product water with final concentration of 1 mg/L micropollutants and the performances of these membranes are on par with commercial membranes. Garcia et al. (2017) reported the utilization of virgin commercial high-impact polystyrene (HIPS) and postconsumer recycled high-impact polystyrene (HIPS-R) independently as base polymer for the preparation of membranes suitable for low-pressure membrane processes like microfiltration and ultrafiltration. The polymers were dissolved in N, N-Dimethylacetamide (DMAC) solvent for preparation of casting solution and membranes were prepared via phase inversion method. The membranes prepared using HIPS-R show similar thermal properties and asymmetric membrane structures with slightly higher porosity than the control membranes prepared with HIPS. Membranes from HIPS-R minimize irreversible fouling and show high humic acid rejection (~ 95–96%).

Zhuang et al. (2016) used polystyrene waste comprise of three types of styrenes [Oriented polystyrene (OPS), expandable polystyrene (EPS), and high-impact polystyrene (HIPS)] for preparation of gas separation membrane by a solution casting method. The gas permeabilities were measured for all the membranes using H₂, CO₂, O₂, N₂, and CH₄ at 1 atm and room temperature at 27 °C. The results for O₂/N₂ and CO₂/N₂ separation indicate that the membranes fabricated from waste polymer maintain same gas-permeation properties compared to the membrane fabricated from the raw polystyrene. Out of all types of polystyrene waste, HIPS membranes showed high CO₂ permeability and also highest CO₂/N₂ selectivity.

Waste polystyrene was directly used to fabricate ultrafiltration/microfiltration types of membranes previously where only colloidal and suspended matters can be removed. We have attempted to develop nanofiltration-type membranes from waste polystyrene-based drinking glasses after suitable chemical modification of polystyrene for removal of multivalent ions from water and treatment of industrial dye effluents. All the steps to make the polymer casting solution for filtration membrane preparation starting from white coffee cups are shown in Fig. 4.

White coffee cups were cut into small pieces and the known amount was put into a conical flask and known volume of dense sulfuric acid, 95% was added under agitation. After 4–5 h of reaction, the white pieces become brownish after sulfonation and washed the sulfonated polymers with DI water till it is free from residual acids and finally dried for making polymer casting solution. The degree of sulfonation of the modified brownish polystyrenes was evaluated after dissolved it in a toluene/methanol (9:1) followed by titration with 0.1 N of sodium hydroxide in methanol with phenolphthalein as indicator. The polymer casting solution was prepared by adding 18.0 gm of dried sulfonated polystyrene (SPS) into 44.0 gm of 1,4-Dioxane and 38.0 gm of N,N-Dimethylacetamide (DMAC) solvent mixture and the solution was kept agitated for several hours for complete dissolution. Nanofiltration membranes were prepared by phase inversion technique. The casting solution was spread over a nonwoven fabric support using doctor knife edge under a steady casting shear. After coating of polymer solution over fabric, it was kept in air for 50–60 s for evaporation of solvents followed by immersion in a gelling bath containing DI water at room temperature. After complete leaching of the solvents from the membrane matrices, the resulting membranes were taken out of the gelling water bath

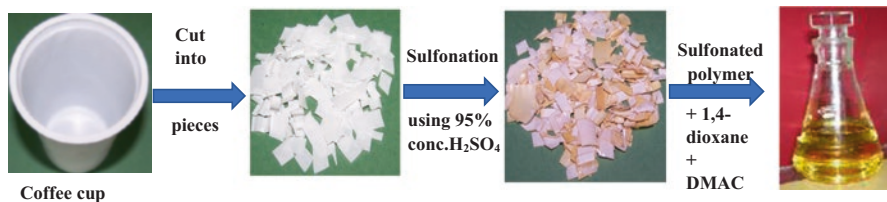


Fig. 4 Steps of preparation of polymer casting solution from waste polystyrene for making nano-filtration membranes

Table 2 Separation performances of sulfonated polystyrene (SPS) membranes for different solutes

Parameters	NaCl	Na ₂ SO ₄	Rhodamine-B
Pure water permeability (L.m ⁻² .h ⁻¹)	25.6	26.4	24.3
% solute rejection	54.0	88.7	91.0

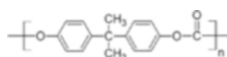
Pressure: 1 MPa; temperature: 25 °C; feed concentration: 1000 ppm

and rinsed in fresh water for several times. The membranes were characterized in terms of product permeability or flux and solute rejection using 1000 ppm Na₂SO₄ feed at 1.0 MPa pressure. The performance evaluation of the membranes from SPS has been carried out for separation behavior for Rhodamine dye solution. The performance of the SPS membrane for different solutes, namely, NaCl, Na₂SO₄, and Rhodamine-B is given in Table 2.

It can be seen that the polystyrene from polymer waste after chemical modification through sulfonation can give very good NF membranes suitable for removal of dyes and multivalent salts from feed solution.

5 Polycarbonate (PC)

Polycarbonate is a polyester family of thermoplastic polymers commonly synthesized by polycondensation reaction of bis-phenol A with phosgene monomer. Polycarbonates are commonly used in making electrical and telecommunications hardware, construction materials, data storage devices, aircraft & security components, etc. The chemical structure of the PC polymer is given below:



Saijun and Chinpa (2020) used waste compact discs of ~95% polycarbonate (PC) to successfully prepare the asymmetric ultrafiltration membranes using nonsolvent-induced phase inversion technique. To recover PC polymer from waste CDs, first the coating layers were removed by mechanical abrasion and then after drying, the cut pieces of CDs were dissolved in chloroform to make homogeneous solution followed by precipitation in methanol. The recovered polycarbonate (PC-R) was

dissolved in N-methyl pyrrolidone (NMP) solvent to prepare casting solution with PC-R concentration of 18, 20, 22, and 24 wt.%. For preparation of membranes via phase inversion method, the casted membranes were gelled in deionized water at 70 °C for 1 h followed by washing in deionized water to remove residual solvent. As shown in the SEM images in Fig. 5, it is found that regardless of the concentration of the casting solution, all the membranes have tight skin layer in the top and a finger-like structure or macrovoid sublayer beneath the skin layer.

More numbers of macrovoids were found in the sublayer of the PC-R membranes prepared with lower polymer concentrations casting solution of 18 and 20 wt.% but sponge-like sublayer was generated in the membranes prepared from higher polymer concentration casting solutions of 22 and 24 wt.%. Ultrafiltration membranes having pure water flux (PWF) of 80 L/m² h with ~70% bovine serum albumin (BSA) rejection were developed.

Previously reported work by Saijun et al. (2020) was on fabrication of asymmetric ultrafiltration membranes only which cannot be used for removal of ions and dyes from effluents. Hence, similar to waste polystyrene, we have attempted to develop nanofiltration-type membranes from waste polycarbonate-based CDs/DVDs. All the steps to prepare the polymer casting solution for nanofiltration membrane preparation starting from CD/DVD are shown in Fig. 6.

Similar to sulfonated polystyrene in previous section, the polymer concentration in mixed solvent system has been optimized and it is found that the casting solution prepared by adding 18.0 gm of dried sulfonated polycarbonate (SPC) into 56.0 gm of 1,4-Dioxane and 26.0 gm of N, N-Dimethylacetamide (DMAC) solvent mixture gives better nanofiltration membranes.

6 Other Polymers and Future Perspective

Altalhi et al. (2013) reported the method developed to convert commercially available grocery plastic bags into useful carbon nanotube membranes with desired molecular transport properties. Inside Nanoporous anodic alumina membranes (NAAMs), carbon nanotubes were synthesized using chemical vapor deposition (CVD) system consisting of a two-stage furnace equipped with a cylindrical quartz tube with dimension of 43 mm diameter with 1000 mm length. The performance testing of CNTs–NAAMs was performed toward selectivity of both charged (positive and negative) and neutral dyes.

Zulfi et al. (2019) successfully recycled Acrylonitrile butadiene styrene (ABS) waste into nanofiber membranes for air filtration. Polymer solutions were prepared using DMAc, DMF, and THF solvents at concentrations of 10, 20, and 30 wt.% and the nanofiber membranes were prepared by electrospinning. From the air filtration performance test, it was found that membranes fabricated using DMAc and DMF solvents had the best criteria as air filter.

Zukimin et al. (2017) reported on the successful preparation of membrane from plastic waste of high-density polyethylene (HDPE) for treatment of contaminated

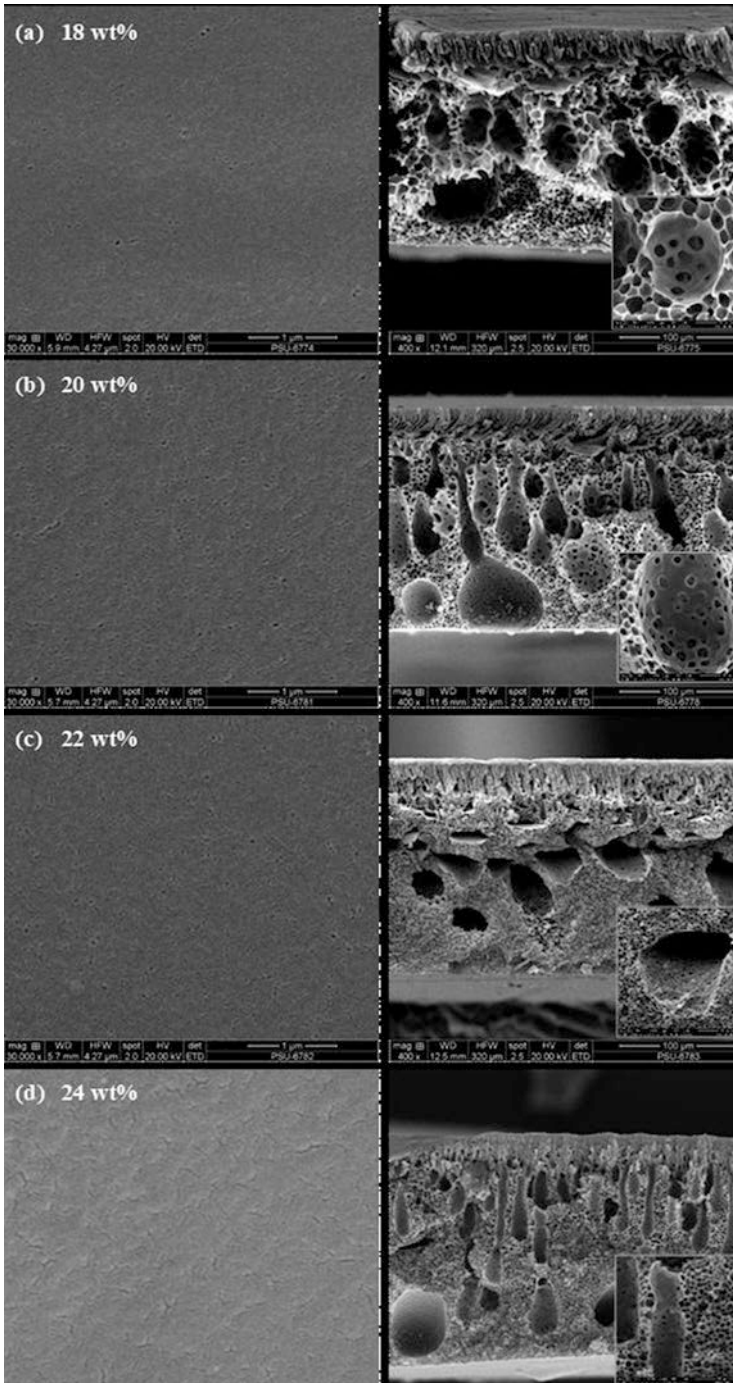


Fig. 5 Surface and cross-sectional SEM micrographs of membranes from PC-R casting solutions at concentrations of (a) 18 wt.%, (b) 20 wt.%, (c) 22 wt.%, and (d) 24 wt.%. (Adopted from Saijun et al. 2020)

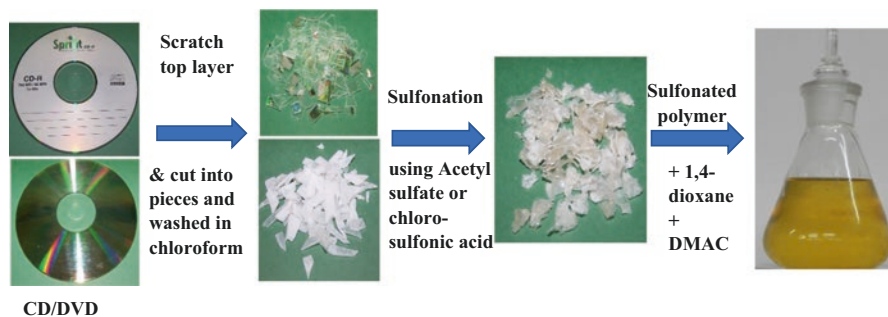


Fig. 6 Steps of preparation of polymer casting solution from waste polycarbonate (CD/DVD) for making nanofiltration membranes

river water. HDPE from plastic waste was grinded first into various particle size powders (in the range of 93.5–270.7 μm using plastic granulator and automatic continuous hammer mill herb grinder machine) followed by preparation of filtration membrane by sintering method and finally the effect of particle size and temperature on the final filtration performances of the membranes was studied. The HDPE powder was mixed with different solvents like olive oil, cooking oil, water, and ethylene glycol and then sintering was carried out in the temperature in the range of 120 $^{\circ}\text{C}$ –180 $^{\circ}\text{C}$ (the temperature set at 100 $^{\circ}\text{C}$ and increases 10 $^{\circ}\text{C}$ for every 5 min). Microfiltration membranes prepared were tested using river water turbidity of ~ 49.5 NTU as feed at 0.85 bar pressure. The HDPE membranes prepared with no solvents showed highest percentage of product permeate rejection compared to the membranes prepared with four other solvents. Increase in heating temperature directly increases the percentage rejection in permeate till it exceeds the temperature of 180 $^{\circ}\text{C}$. Membrane prepared with HDPE powder having average particle size of ~ 270.7 μm has better separation in terms of higher percentage rejection compared to the membranes prepared using powder with average particle size of ~ 93.5 μm .

One of the future prospects of reuse of selected plastic wastes for manufacturing useful filtration membranes is to suitably modify the waste polymer so as to make it better candidate for development of filtration membranes with desired performance characteristics rather than to use the virgin polymer recovered from waste. For example, crushed transparent drinking glasses, DVDs as waste polymers made up of polycarbonate and polystyrene can give moderate ultrafiltration/microfiltration membranes for water filtration but sulfonated polycarbonate and polystyrene can be used to make nanofiltration-type membranes useful for removal of multivalent ions, treatment of industrial dye effluents, etc. The chemical modification can be that of carboxylation, amination, nitration or even by polymer blending with a compatible polymer or through nanocomposite with addition of a suitable nanoparticle.

Regarding scope of use of waste plastic in commercial manufacturing of filtration membranes, an additional step of crushing, washing, and drying of waste polymer needs to be added prior to making polymer casting solution. A typical scheme of membrane making starting from waste plastic is given in Fig. 7. New practices

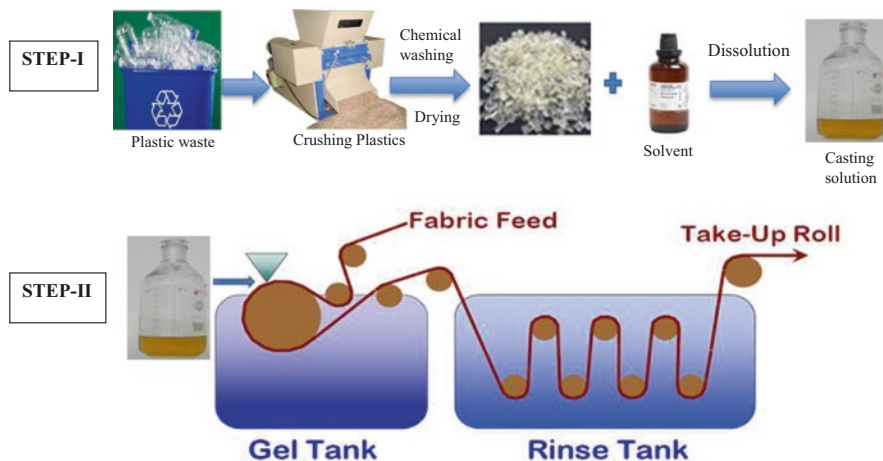


Fig. 7 A scheme of filtration membrane making from waste plastic

for making membranes from recyclable polymer waste should be adopted by membrane manufacturing companies for establishment of sustainable uses of some of the waste plastics.

7 Conclusions

This chapter highlights the key developments on fabrication of useful membrane filters from different reusable waste plastics. Membrane making using the polymers from zero carbon footprint sources, such as plastic waste can make the technology more sustainable, attractive and also the cost of filtration membranes would be cheaper. The use of waste polymers like polyethylene terephthalate, polyvinyl chloride, polystyrene, polycarbonate, etc. for fabrication of useful filtration membrane can contribute to the sustainability of various separation applications like water purification, effluent treatment, gas separation, etc.

Polyethylene terephthalate polymer wastes were used successfully for fabrications of ultrafiltration membranes for humic acid separation, microfiltration membranes for prefiltration of wastewater treatment, organic solvent-resistant membranes for permeation of various organic solvents, and fiber membranes for air filtration. Polyvinyl chloride polymer wastes were used for fabrications of 90% bovine serum albumin (BSA) rejecting ultrafiltration membranes. Polystyrene polymer wastes were used for fabrications of microfiltration and ultrafiltration membranes for removal of humic acid and micropollutants, nanofiltration membranes for treatment of dye effluents and gas separation membranes with high CO_2/N_2 selectivity. Polycarbonate polymer wastes were used for fabrications of ultrafiltration and nanofiltration membranes. Similarly, high-density polyethylene (HDPE)-based microfiltration membranes were fabricated for treatment of contaminated river water.

References

- Adamczak M, Kamińska G, Bohdziewicz J (2020) Application of waste polymers as basic material for ultrafiltration membranes preparation. *Water* 12(1):179. <https://doi.org/10.3390/w12010179>
- Aji MM, Narendren S, Purkait M, Katiyar V (2020) Utilization of waste polyvinyl chloride (PVC) for ultrafiltration membrane fabrication and its characterization. *J Environ Chem Eng* 8:103650. <https://doi.org/10.1016/j.jece.2019.103650>
- Altalhi T, Kumeria T, Santos A, Losic D (2013) Synthesis of well-organised carbon nanotube membranes from non-degradable plastic bags with tuneable molecular transport: towards nanotechnological recycling. *Carbon* 63:423–433. <https://doi.org/10.1016/j.carbon.2013.07.003>
- Awasthi AK, Shivashankar M, Majumder M (2017) Plastic solid waste utilization technologies: a review. *IOP Conf. Series: Mater Sci Eng* 263:022024. <https://iopscience.iop.org/article/10.1088/1757-899X/263/2/022024>
- Bhran A, Shoaib A, Elsideq D, El-gendi A, Abdallah H (2018) Preparation of PVC/PVP composite polymer membranes via phase inversion process for water treatment purposes. *Chinese J Chem Eng* 26:715–722. <https://doi.org/10.1016/j.cjche.2017.09.003>
- Dizajikan B, Asadollahi M, Musavi MA, Bastani D (2018) Preparation of poly(vinyl chloride) (PVC) ultrafiltration membranes from PVC/additive/solvent and application of UF membranes as substrate for fabrication of reverse osmosis membranes. *J Appl Polym Sci* 135:46267. <https://doi.org/10.1002/app.46267>
- Garcia JM, Robertson ML (2017) The future of plastics recycling. *Science* 358(6365):870–872. <https://www.science.org/doi/10.1126/science.aq0324>
- Garcia J, Wang-Xu X, Iborra-Clar MI (2017) Application of post-consumer recycled high-impact polystyrene in the preparation of phase-inversion membranes for low-pressure membrane processes. *Sep Purif Technol* 175:340–351. <https://doi.org/10.1016/j.seppur.2016.11.061>
- Ghazanfari D, Bastani D, Mousavi SA (2017) Preparation and characterization of poly (vinyl chloride) (PVC) based membrane for wastewater treatment. *J Water Process Eng* 16:98–107. <https://doi.org/10.1016/j.jwpe.2016.12.001>
- Hamad K, Kaseem M, Deri F (2013) Recycling of waste from polymer materials: an overview of the recent works. *Polym Deg Stabil* 98(12):2801–2812. <https://doi.org/10.1016/j.polymdegradstab.2013.09.025>
- Ilyas RA, Sapuan SM, Jailani AK, Yusof AHM, Norizan MN, Norrahim MNF, Atikah MSN, Atiqah A, Bayraktar E (2021a) Introduction to recycling of polymers and metal composites. In: Ilyas RA, Sapuan SM, Bayraktar E (eds) *Recycl. Plast. Met. Their Compos*, 1st edn. CRC Press/Taylor & Francis Group; Chapter 1, Boca Raton. <https://doi.org/10.1201/9781003148760>
- Ilyas RA, Sapuan SM, Sabaruddin FA, Atikah MSN, Ibrahim R, Asyraf MRM, Huzaifah MRM, Saiful Azry SOA, Ainun ZMA (2021b) Reuse and recycle of biobased packaging products. In: Sapuan SM, Ilyas RA (eds) *Bio-based packaging: material, environmental and economic aspects*, 1st edn. Wiley; Chapter 23, pp 414–426. <https://doi.org/10.1002/9781119381228.ch23>
- Mulyati S, Armando MA, Mawardi H, Fahrina A, Malahayati N, Syawaliah (2018) Fabrication of hydrophilic and strong PET-based membrane from wasted plastic bottle. *Rasayan J. Chem* 11(4):1609–1617. <https://doi.org/10.31788/RJC.2018.1144047>
- Pastine S (2012) Can epoxy composites be made 100% recyclable? *Reinf Plast* 56(5):26–28. [https://doi.org/10.1016/S0034-3617\(12\)70109-1](https://doi.org/10.1016/S0034-3617(12)70109-1)
- Pulido BA, Habboub OS, Aristizabal SL, Szekely G, Nunes SP (2019) Recycled poly(ethylene terephthalate) for high-temperature solvent resistant membranes. *ACS Appl Polym Mater* 1:2379–2387. <https://doi.org/10.1021/acsapm.9b00493>
- Ragaert K, Delva L, Geem KV (2017) Mechanical and chemical recycling of solid plastic waste. *Waste Manag* 69:24–58. <https://doi.org/10.1016/j.wasman.2017.07.044>
- Ramos-Olmos R, Rogel-Hernandez E, Flores-López L, Lin SW, Espinoza-Gómez H (2008) Synthesis and characterization of asymmetric ultrafiltration membrane made with recycled polystyrene foam and different additives. *J Chil Chem Soc* 53(4):1705–1708. <https://doi.org/10.4067/S0717-97072008000400015>

- Saijun D, Chinpa W (2020) Feasibility study of membrane preparation using polycarbonate from waste compact discs by phase separation, *Songklanakarin J. Sci. Technol* 42(5):967–974. <https://doi.org/10.14456/sjst-psu.2020.125>
- Salwa HN, Sapuan SM, Mastura MT, Zuhri MYM, Ilyas RA (2021) Life cycle assessment (LCA) of recycled polymer composites. In: Ilyas RA, Sapuan SM, Bayraktar E (eds) *Recycl. Plast. Met. Their Compos*, 1st edn. CRC Press/Taylor & Francis Group; Chapter 27, Boca Raton. <https://doi.org/10.1201/9781003148760>
- Schyns ZOG, Shaver MP (2021) Mechanical recycling of packaging plastics: a review. *Macromol Rapid Commun* 42:2000415. <https://doi.org/10.1002/marc.202000415>
- Stevenson JF (1989) 10 – extrusion of rubber and plastics, *comprehensive polymer science and supplements*. Oxford, Pergamon, pp 303–354
- Strain IN, Wu Q, Pourrahimi AM, Hedenqvist MS, Olsson RT, Andersson RL (2015) Electrospinning of recycled PET to generate tough mesomorphic fibre membranes for smoke filtration. *J Mater Chem A* 3:1632–1640. <https://doi.org/10.1039/C4TA06191H>
- Zander NE, Gillan M, Sweetser D (2016) Recycled PET nanofibers for water filtration applications. *Materials* 9(4):247–257. <https://doi.org/10.3390/ma9040247>
- Zhuang G, Tseng H, Wey M (2016) Feasibility of using waste polystyrene as a membrane material for gas separation. *Chem Eng Res & Design* 111:204–217. <https://doi.org/10.1016/j.cherd.2016.03.033>
- Zukimin NW, Jullok N, Razi ANM, Fadzilah MHH (2017) Membrane from plastic waste for the treatment of contaminated river water. *J Teknol Sci Eng* 79(1-2):83–88. <https://doi.org/10.11113/jt.v79.10441>
- Zulfi A, Hapidin D, Munir M, Iskandar F, Khairurrijal K (2019) The synthesis of nanofiber membranes from acrylonitrile butadiene styrene (ABS) waste using electrospinning for use as air filtration media. *RSC Adv* 9:30741–30749. <https://doi.org/10.1039/C9RA04877D>

Recycled Polymer Bio-based Composites: A Review of Compatibility and Performance Issues



Khalid Alzebdeh, Nasr Al Hinai, Mahmoud Al Safy, and Mahmoud Nassar

1 Background

Natural fiber-reinforced polymer composites (NFRPCs) have remarkable properties such as low specific gravity, cost-competitiveness, high flexibility, high impact resistance, reliability and ease of processing, etc. (Kerni et al. 2020; Nurazzi et al. 2021a). Because of their eco-friendliness, nontoxicity, and good biocompatibility, such composites are gradually replacing conventional composites. However, there are several drawbacks to employing natural fillers, which prevent their wider spread in different applications. Efficient handling of these drawbacks will improve their properties and increase their workability (Chang et al. 2020; Alsubari et al. 2021). These fillers are generated from plant sources and are classified as fibers or particulates. Natural fillers, such as wheat, pulp, lignin, hemicellulose, pectin, or cellulose derivatives, are widely recognized for their applicability as polyolefin and other varieties of polymer reinforcements (Bari et al. 2021; Nassar et al. 2021b). Because of these benefits, the use of natural fibers in polymeric composites has captured the attention of numerous materials engineers and researchers. Nonetheless, these gained benefits have to be balanced against expected drawbacks as summarized in Table 1. Contemporary breakthroughs in this field of study, as well as recent environmental concerns, have accelerated the growing interest among businesses in using NFRPCs in the design of a range of goods (Girijappa et al. 2019).

Ecocomposites provide a new category of composite materials obtained by mixing recycled plastics and biomass waste to develop better biomaterials. Creating

K. Alzebdeh (✉) · N. Al Hinai · M. Al Safy
Department of Mechanical and Industrial Engineering, Sultan Qaboos University,
Al-Khod, Sultanate of Oman
e-mail: alzebdeh@squ.edu.om

M. Nassar
College of Applied Professions, Palestine Polytechnic University, Hebron, State of Palestine

Table 1 Benefits and drawbacks of NFRPCs

Benefits	Drawbacks
Excellent acoustic and electrical insulation capabilities	Low fire resistance
Water absorption can be chemically cut down	Moisture absorption causes fibers to swell
Biodegradability of fibers through the activity of fungus and/or bacteria	Variability in quality due to uncontrollable conditions like weathering
Combustibility: energy can be created when dumped or disposed	Maximum processing temperature is limited
Reasonable mechanical characteristics, particularly flexural strength	Low impact strength
Low abrasive characteristics of natural fibers and better composite processability	Dimensional instability and material hygroscopicity
Renewable resources and sustainability	Low durability

innovative eco-composites using agro-residue fillers and recycled polymers while gaining a fundamental grasp of overall quality will optimize accumulated benefits and broaden applications (Nassar et al. 2021b; Shanmugam et al. 2021). One circular economy approach is to reuse products and resources while also regenerating natural systems. This approach raises the employment rate linked to waste collection and increases plastic pollution management. Involvements at the local and the national levels have sought to enhance the status of waste disposal through methods such as regulated pricing and government agreements. As a response, the need to establish additional selection procedures aims at initiating qualifying requirements for recovered plastics in a variety of sectors (Barford and Ahmad 2021; Shanmugam et al. 2021).

This chapter describes current breakthroughs in the production of new eco-composite materials derived from recycled polymers and natural fillers developed by researchers. It provides the profound related to the compatibility of polymers and natural fillers when using filler treatments and polymer chemical modification, namely crosslinking agents. Furthermore, the chapter presents the mechanical, physical, thermal, and morphological characteristics of recently developed eco-composites. Finally, it concludes with future perspectives and insights on this research subject.

2 Recycled Polymers and Natural Fillers

Plastic pollution is seen as a major environmental concern. This has necessitated concerted efforts to decrease Municipal Solid Waste (MSW) and identify potential reuse opportunities. The utilization of recycled plastic solid waste to generate new eco-friendly composites with natural fillers has emerged as a feasible solution (Gu et al. 2017; Anjum et al. 2020; Nizamuddin et al. 2021). Polyolefins are the most commonly used reprocessed plastic for attempting to make eco-composites because

of their distinctive and acceptable achievement, outstanding impact and abrasion resistance, high strength-to-weight ratio, low cost, good durability, low melting point, recyclability, and high resistance to microorganisms' assimilation (Chandrasekar et al. 2021). These qualities classify them as viable materials for a wide range of products and design standards (Aldousiri and Shalwan 2013; Chamas et al. 2020). To generate ecocomposites, recyclable thermoplastic polymers such as low-density polyethylene (rLDPE), high-density polyethylene (rHDPE), polypropylene (rPP), and polyethylene terephthalate (rPET) were mixed with reinforcing filler including such flax, cotton, sisal, coir, hemp, and palm. Polyolefin thermoplastics account for a considerable portion of the plastic waste that is often recycled or disposed of in landfills (Ragaert et al. 2017; Joseph et al. 2021). Figure 1 presents the planning of design solutions within the life cycle context of bio-based and synthetic biomaterials designed to motivate implementation of the circular economy paradigm for long-term recovery (Lee et al. 2021).

Plastics such as polyethylene (PE) are commonly used in the packaging industry. Every year, it creates around 60 million tons of waste. rLDPE is an important element of the PE class in the synthesis of polymers due to its wide range of applications (Siracusa and Blanco 2020). This polymeric material offers outstanding characteristics such as opacity, high flexibility, strong resistance to acids and bases, alcohols, and esters, impact resistance, electrical insulation, high toughness, dimensional stability, and adaptability even at low temperatures. In addition, it is a low-cost substance that is simple to prepare (George et al. 2020; AL-Oqila 2021). Similarly, high-density polyethylene (HDPE) is a widely utilized polymer with a wide range of uses, including bottles, containers, and everyday items (Chianelli-Junior et al. 2013; Evode et al. 2021). HDPE is also a low-cost synthetic polymer

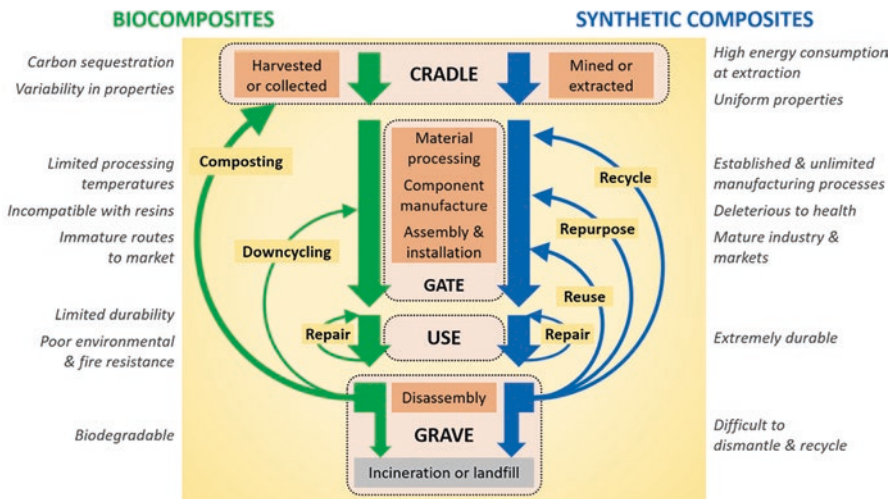


Fig. 1 Design solutions within the life cycle structure of bio-based and synthetic composites. (Lee et al. 2021)

with good features such as low density, hard surface, resistance to abrasion, and electrical insulation. Furthermore, HDPE is environmentally benign throughout its manufacturing and functional life, and as such, it is easily recyclable and may be reused several times (Jesus et al. 2022). When they are not qualified to fulfill the manufacturer/consumer criteria, HDPE has the benefit of being relatively easily recyclable. As a result, rHDPE is readily accessible, simple to process, and the most often utilized matrix material for ecocomposites. The characteristics of rHDPE derived from postconsumer materials are not significantly different from those of virgin HDPE. Hence, they might be employed for a wide range of applications (Adhikary et al. 2008; Su et al. 2021).

Polypropylene (PP) is an olefin with a linear structure that may be melted and remolded several times. Similar to PE, PP is a hydrophobic material that is utilized in a broad range of applications. It has a high softening point and steady mechanical characteristics at room temperature (Kim et al. 2019). Its low density, strong impact resistance, and dimensional stability, make it appropriate for a wide range of structural applications. For long, PP is commonly employed with a diverse range of reinforcing fibers and particles (Jannah et al. 2009; Amieva et al. 2014). A main gain of this material is its low-cost alongside its ability to be treated repeatedly without deterioration of qualities. Due to this, polyolefin thermoplastics contribute a significant amount of plastic waste that is frequently recycled or discarded (Kim et al. 2019; Kar et al. 2020; Nassar et al. 2021b).

Polyethylene Terephthalate (PET) is a manmade semi-crystalline thermoplastic polymer that is comparable to polyester material in terms of weight, versatility, and durability. It is among the most common forms of plastic found in MSW (Wang et al. 2019; Benavides et al. 2020). PET is utilized in a variety of purposes, but it is most widely and well-known in the production of soft drink plastic-bottles (Čuk et al. 2015). Due to the steady-state growth in the bottle industry, PET demand has been estimated to have the quickest rate of expansion in the market of plastics. Although PET causes no direct harm to the environment, it may be classified as a toxic substance due to its vast size and great resistance to atmospheric and biological agents (Farahani et al. 2012; Wang et al. 2019).

The use of available resources, such as date palm agro-waste, for the production of biocomposites can minimize the shortage of raw materials in the Wood Plastic Composites (WPC) sector. Date palm tree fronds, rachis, and pedicels have traditionally been used to make mats, baskets, and ropes in various regions around the world (Benaniba et al. 2020; Supian et al. 2021). However, the vast majority of the material is dumped as waste, which is either disposed of in a landfill or burnt. Several research works have been conducted to investigate the appropriateness of using date palm leaves, mesh, and rachis in biocomposites for different applications (Abdel-Shafy and Mansour 2018; Alzebeleh et al. 2019). The geometric features of numerous natural fibers, such as diameter and length, are summarized in Table 2.

Natural fibers come in a wide range of (a) fiber's diameter (5–76 μm), (b) fiber bundles width (10–1000 μm), and (c) lengths (1.2–300 mm). This divergence causes significant variances in the characteristics of polymer composites made from these fibers. Furthermore, the inherent discrepancies in natural fiber characteristics provide significant challenges in developing production methods for reinforcing

Table 2 Geometrical characteristics of natural fibers (Balla et al. 2019)

Fiber	Shape	Diameter/width (μm)	Bundle width, (μm)	Length, (mm)
Sisal	Round/polygon	4–47	9–460	0.5–8
Jute	Polygon/rectangular	5–30	25–200	1–5
Hemp	Polygonal/ribbon-shape	5–40	25–500	8–55
Wood	Rectangular/round	5–50	–	1.2–3.6
Flax	Polygon	5–76	40–620	4–140
Abaca	Polygon/round	6–46	10–1000	2–12
Coir	Round /oval	10–30	50–460	150–300
Kenaf	Round/polygon	12–50	30–247	1.5–11

Table 3 Density and strength properties of natural and synthetic fibers (Balla et al. 2019)

Fiber	Density (g/cm^3)	Elongation (%)	Tensile strength (MPa)	Young's modulus (MPa)
<i>Natural fibers</i>				
Abaca	1.5	1–12	12–980	12–72
Bamboo	0.6–1.1	3.8–5.8	140–230	11–17
Banana	1.35	1–10	430–914	7.7–42
Coir	1.2	30	160–250	3.3–6
Cotton	1.5–1.6	2–10	220–840	4.5–12.6
Flax	1.5	1.2–4	343–1834	8–100
Hemp	1.48	1.5–51.4	95–1735	2.8–90
Jute	1.3–1.5	1.5–1.8	187–800	3–64
Kapok	1.3	1.2–4	45–93	1.7–4
Kenaf	1.45	1.5	215–930	35–53
Pineapple	0.8–1.6	0.8–14.5	170–627	2–128
Ramie	1.5	1.2–4.6	290–1060	5–128
Sisal	1.5	1.9–14	80–855	9–38
<i>Synthetic fibers</i>				
E-glass	2.5	2.5	2000–3500	70
Carbon	1.4–1.7	1.4–1.8	4000	230–240
Aramid	1.4	3.2–3.7	3000–3150	63–67

materials. As a result, precise feedstock material assessment and control are critical in achieving targeted performance. In addition, natural fibers do possess a lower tensile strength than synthetic materials; however, they offer a larger range of mechanical attributes. This qualifies them to be considered as alternatives to replace synthetic fibers in a variety of applications (Balla et al. 2019; Lee et al. 2021). On the other hand, while the variety in the qualities of synthetic fibers is limited, the properties of natural fibers clearly vary, both within the same kind of fiber and across different types of fibers. Such a wide variety of mechanical properties of natural fibers may generate severe concerns regarding the mechanical performance of produced composites being dependent on the fiber source (Balla et al. 2019). For completeness, Table 3 shows the mechanical characteristics of popular natural fibers and synthetic fibers.

3 Polymer-Filler Compatibility

Enhancing the compatibility between natural filler and surrounding polymer assists in handling number of challenges including poor fiber/matrix adhesion, wettability, low fire resistance, insufficient mechanical properties, low heat resistance, and constrained production temperature of the biocomposite (Aisyah et al. 2021; Andrew and Dhakal 2022). Researchers have applied a variety of physical and chemical approaches to boost the compatibility of fillers and/or polymers. For example, the fiber/matrix interlocking, as well as moisture and heat resistance, are increased using fiber and polymer subjected to physical and chemical modification processes, which ultimately improve the quality of biocomposites produced (Kannan and Thangaraju 2021; Zwawi 2021). The following subsections provide thorough discussions of recent filler and polymer modification processes.

3.1 Filler Modification

Natural fillers are well known to have poor hydrophilicity and wettability. This makes it more challenging to diversify their industrial applications. Therefore, it is necessary to strengthen and improve the polymer composites. One possible approach to achieve this is by performing filler treatment therapy (Kerni et al. 2020; Obasi et al. 2021). Different chemical procedures were employed to treat natural materials. Treatments procedures using acetylation, alkalization, benzoylation, silane, and malleated coupling are of the most prevalent treatment methods that qualified natural fibers as reinforcing agents for both virgin and recycled polymers (Sanjay et al. 2019; Syduzzaman et al. 2020). Chemical treatments that improve filler/matrix consistency and adherence likely improve the mechanical characteristics of designed biocomposites (Hassaini et al. 2017; Kuan et al. 2021). Based on empirical data, the alkaline treatment with NaOH is recognized as the most traditional modification treatment method of natural fibers (Karthi et al. 2019). In general, one of the major goals of the treatment is to modify the surface of the fiber by removing contaminants and roughening it, hence, improving adhesion between both the fiber and the surrounding matrix. Furthermore, chemical treatment methods weaken the hydrogen bond in the fibril structure, triggering fiber/polymer crosslinking (Rahman et al. 2018). They also effectively eliminate hemicellulose, lignin, wax, and oils that cover the outer layer of the fiber's cell wall, depolymerize cellulose, and expose short length crystallites. When the hydroxyl group in hemicellulose is replaced with an alkoxide or acetyl group, the fiber's behavior shifts from hydrophilic to hydrophobic (Rahman et al. 2018). It is viable to perform chemical reactions either at room temperature or at increased temperatures by utilizing an external source of heat such as traditional oven. Yet, the use of an accelerated heat source (electrical microwave) is proven to be successful and efficient (Mohammed et al. 2018; Nassar et al. 2020).

The use of natural filler-reinforced composites made from date palm waste and recycled plastics resulted in considerable environmental advantages (Nassar et al. 2020). Natural strands formed from date palm agro-residue stand out owing to its high material properties and affordable cost when compared to certain other varieties such as kenaf, hemp, coir, and sisal fibers (Rajeshkumar 2020). Because these biodegradable fibers are considered waste and abundant, using date palm fronds as fillers in plastics is a potential alternative. Recently, Nassar et al. (2020) developed a novel chemical treatment procedure for extracting rich cellulose fiber from date palm agro-residues. An experimental characterization of the treated fibers' thermal, physical, and mechanical properties revealed a considerable improvement over their untreated counterparts, confirming the new process's efficacy. Figure 2 illustrates the stress-strain diagrams for treated and untreated date fibers. The plot can be used to calculate the elastic modulus, tensile strength, and elongation at break. The figure clearly shows that fiber processed using the accelerated heating (AH) option yields the highest strength but with lower ductility in contrast to conventional heating option. The largest ductility is accomplished after using conventional heat (CH) source to derive fibers; however, achieved strength was approximately 33% less than that of the AH-derived fiber. A typical material behavior noted in this work is the balance between strength and ductility. Clearly, the AH-based fiber is less ductile than the CH-based fiber due to the altered microstructure, which contributes to higher strength and lower ductility.

For natural fibers, surface modification methods were adopted to adjust the surface topography and expose the OH groups at the fiber surface. Moreover,

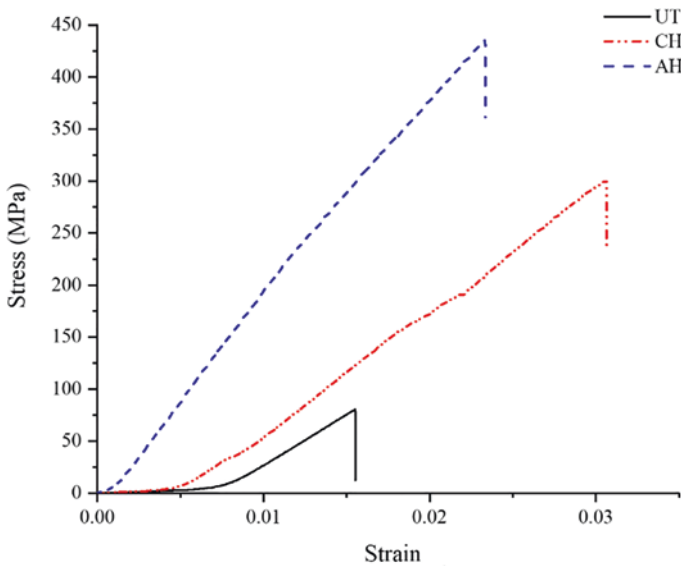


Fig. 2 Stress-strain curves of untreated and treated date palm fibers

functionalization of the natural filler by substituting the OH groups with different reactive modifiers boosts the filler reactivity with polymer and reduces the filler hydrophilicity, particularly when superhydrophobic agents are utilized (Gu et al. 2019). If intended chemical reaction takes place among ingredients of biocomposite, intermolecular bonding and crosslinking between the fiber and polymer will be introduced. Therefore, effective properties of the developed biocomposites will be improved depending on the filler surface roughness and type of chemical crosslinking. Robust filler-polymer bonding supports load-bearing capacity and develops better mechanical and water repellent properties (Charlet et al. 2015; Gu et al. 2019).

Applying functional groups for effective surface modification of date palm powder (DPP) and improved chemical synthesis can be performed using Azide and Alkyne chemical-based methods (Nassar et al. 2021c). The two methods demonstrated a considerable capacity to modify lignocellulosic material efficiently, with improved surface roughness prompting mechanical interlocking. It also reduces the filler hydrophilic nature, which is especially important when water repellent agents are used (Gars et al. 2020). The morphology of original and modified DPP is analyzed by SEM as shown in Fig. 3. If the expected chemical reaction occurs among the bioconstituents, then composite's intermolecular binding and crosslinking between the fiber and polymer will occur. As a result, depending on the filler surface quality and type of chemical crosslinking, the effective characteristics of the generated biocomposites will be improved. Strong

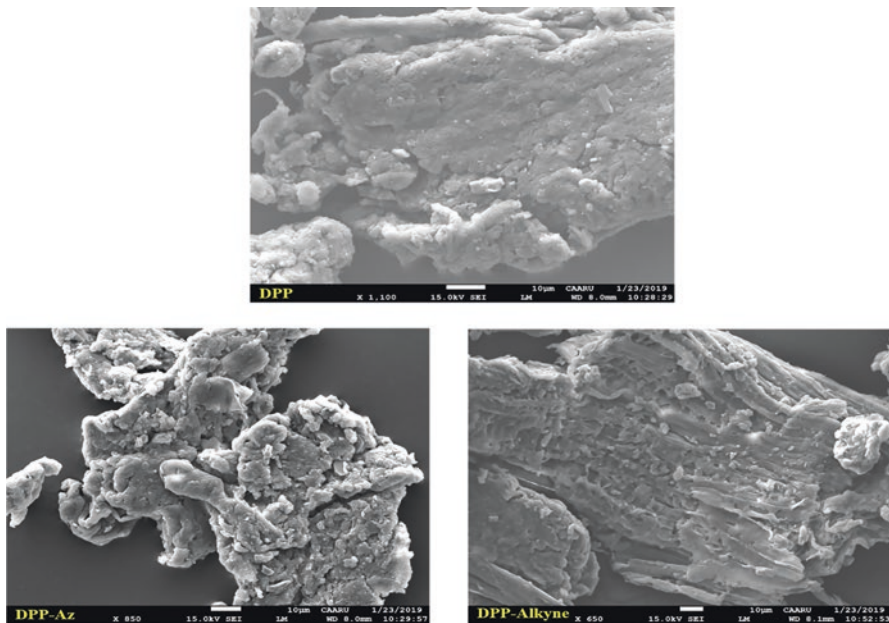


Fig. 3 SEM images of (a) DPP, (b) DPP-Azide, and (c) DPP-Alkyne. (Nassar et al. 2021c)

filler-polymer bonding promotes load transmission while also improving mechanical and water-resistant characteristics (Charlet et al. 2015; Gu et al. 2019).

3.2 Polymer Functionalization

Similar to the filler modification, polymer functionalization aims to improve filler/polymer bonding by modifying molecules by using chemical or physical methods. The presence of hydroxyl groups on the biomass surface, particularly on the cellulose backbone, indicates that the biomass is polar. It is conceivable to employ hydroxyl groups to create more chemically reactive groups on the natural fiber's surface (Zhang et al. 2018; Nassar and Sider 2021). Polymer functionality is achieved by a variety of approaches that include coupling agents and compatibilizers. This builds sustainable ecomposites with appropriate gradient compatibility as shown in Fig. 4 for a newly developed biocomposite (Hubbe and Grigsby 2020; Nassar et al. 2021b). Further, performing chemical modification and irradiation for fiber and polymer, respectively, results in ecomposites with more compatibility than chemical treatment alone. Irradiated ecomposites containing treated natural fillers exhibited superior mechanical characteristics, decreased moisture content, and greater thermal stability (Abdel-Hakim et al. 2021; Lazim and Samat 2019).

Most thermoplastic polymers possess nonpolar functionality and have low surface-free energy, resulting in poor adhesion qualities (Pearson et al. 2022). Therefore, coupling agents are used to boost adhesion between fillers and hosting polymers as illustrated in Fig. 4. Indeed, the functionalization of a polymer surface by an isocyanate group is a new and rarely utilized approach. As exemplified in Fig. 5a, the hydroxyl group is very reactive and can establish urethane linkages between bio-fillers and polymer matrix (Chauhan et al. 2016; Karmarkar et al. 2007). In Fig. 5b, which is adopted from a work by Yeo et al. (2015), the aim is to modify both

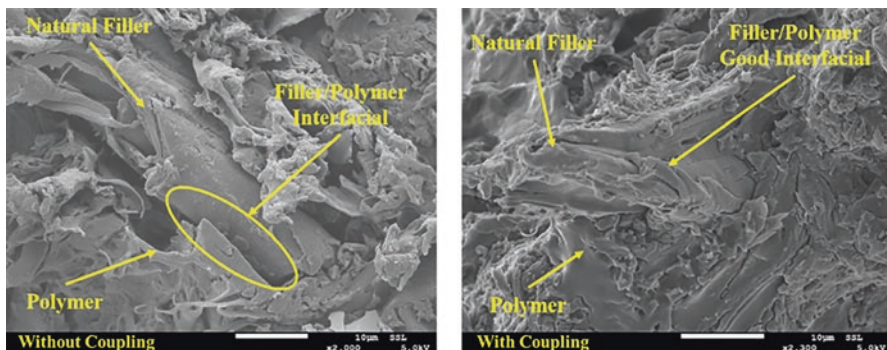


Fig. 4 SEM images of DPP reinforced polypropylene without and with coupling agent. (Nassar et al. 2021b)

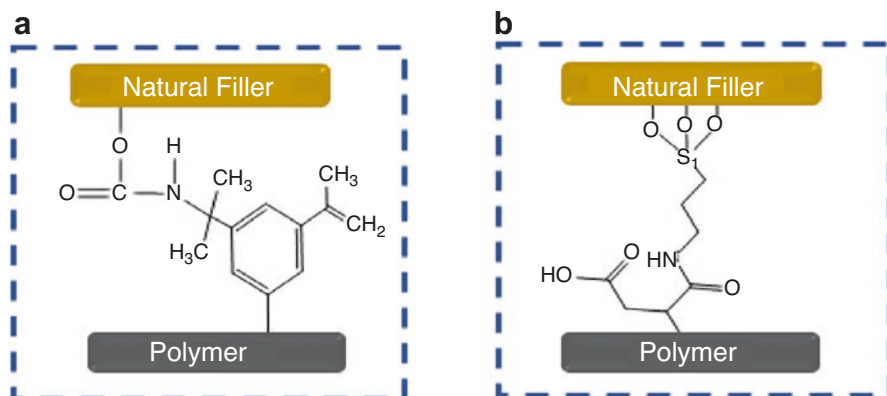


Fig. 5 Natural filler-polymer chemical crosslinking: (a) filler and functionalized polymer, (b) functionalized filler and functionalized polymer. (Nassar et al. 2021b)

biomass and polymer by amine bonding and maleic anhydride (MAH), respectively. This process, known as amidation process, generates polypropylene-graft-MAH connected to lignin. It enhances the interfacial connection between the particulate filler and the mating matrix, as well as particles distribution within the matrix, thus, developing a considerable increase in strength properties.

In relation to the above, an attempt to employ the coupling agent (PP-g-MA) and dried coffee ground (CG) to form biocomposites caused chemical interfacial crosslinking among ingredients, resulting in an enhancement in the mechanical characteristics of the manufactured material (Chitra et al. 2014; Anbupalani et al. 2020). Similarly, Jute/rPP composites produced using (m-TMI)-grafted-polypropylene as the coupling agent demonstrated a considerable growth in mechanical tensile, flexural, impact, and tensile modulus at 50 wt.%. This increase in mechanical characteristics revealed that rPP reinforced with jute fibers efficiently transmitted load from matrix to fibers (Aggarwal et al. 2013; Nassar and Sider 2021). According to recent research, LDPE-filled composites containing corn stalk powder (CSP) that used Maleic Anhydride Polyethylene (MAPE) as coupling agents established stronger interfacial bonding between polymer and filler. Tensile strength and breaking elongation were also enhanced. Young's modulus, on the other hand, appeared to decrease as a result of this alteration (Eze and Madufor 2020; Ismail et al. 2020). Biological treatment using microbial films is a straightforward and clean technology that allows for the grafting of any polymeric substrate without affecting the bulk polymer characteristics (Pearson and Urban 2014; Gafri et al. 2019). When compared to untreated CM/LDPE, the treatment of the composite containing 2 wt.% Citrus Maxima (CM)-filled LDPE with silane revealed a substantial improvement in tensile strength, percent elongation, and impact strength as filler content increases. Furthermore, the CM filler influenced the elasticity and deformation characteristics of LDPE (Joglekar et al. 2021).

4 Recycled Polymer Bio-based Composites Performance

In recent times, eco-composites generated from waste have become competitive materials for an increasing range of industrial sectors. The main leading factors for this is the customizable features and low cost. As a consequence, their overall quality and performance are rigorously evaluated, studied, and improved in order to widen their usage in a variety of applications (Olatunji 2015; Vidakis et al. 2021). Despite this, due to the low levels of strength of such materials in relation to design specifications, the application of eco-composites is confined to non-load-bearing applications. Accordingly, further in-depth research and development activities are essential to raise their performance to the level of structural requirements. The following subsections cover recent achievements in this field as well as the realized performance of eco-composites in terms of mechanical, morphological, physical, and thermal properties to emphasize the relevance of such an attempt.

4.1 Mechanical Properties

The mechanical characteristics of recycled plastic bio-based composites are strongly connected to the natural filler's interfacial bonding, compatibility, and engagement with the encapsulated matrix (Hasan et al. 2021; Wu et al. 2021). The inclusion of suitable compatibilizers, nano-fillers, and coupling agents at optimal concentrations helps to increase their mechanical performance. As discussed in Sect. 3, it has been established that surface treatment of fillers can have a comparable effect (Singh et al. 2019; Omran et al. 2021). Furthermore, mechanical recycling factors such as extruder speed and torque, mold temperature, and the number of recycling cycles, among others, have a significant impact on the mechanical characteristics made of eco-composites (Chan et al. 2018; Ilyas et al. 2021b). In practice, the kind and qualities of the eco-ingredients of the composite define the level of total mechanical properties. Research that investigated using Olive fibers in rLDPE, for example, revealed the ideal reinforcing conditions for increasing the composites' overall flexural capabilities (AL-Oqla 2021; Valvez et al. 2021). Mechanical interlocking within the components of eco-composite generates a strong interfacial connection between the olive fiber and the matrix due to sufficient surface roughness of the olive particle (Sider and Nassar 2021). Thus far, the greatest flexural strength of the biocomposite with different fiber contents was estimated to be 34.6 MPa at 40% fiber content and tensile strength of 32 MPa. This enhanced the flexural modulus of rLDPE by more than 200%. Moreover, the effect of rLDPE seemed to have a far larger impact on the tensile strength WPCs than the wood filler. As a result, the type of polymer used in WPC goods should be carefully selected (Acheampong et al. 2021).

Of the main challenges that limit the applicability of biocomposites is the gradual reduction in their tensile strength compared to that when using pure polymer.

For example, the tensile strength of composites formed completely of rLDPE matrix is nearly 13 MPa; however, the inclusion of 40% cocoa waste may lower this value to 3.5 MPa. This is a huge drop in the tensile strength. Many literatures explored different means to resolve this issue. It is reported that the properties of ecocomposites can be upgraded by using compatibilizers such as alkaline pretreatments to remove extractives that may impair compatibility, and by controlling the optimum wt.% content and form of the fiber, filament, staple, chopped, or powder (de Araújo Veloso et al. 2021; Ilyas et al. 2021a). Gebremedhin and Rotich (2020) developed an ecocomposite material made of rLDPE filled with treated pineapple leaf fiber. This developed material had improved properties in tensile, flexural, impact, and water absorption at the optimal fiber weight of 30% and length of 30 mm. Further, when polyethylene-graft maleic anhydride (PE-g-MA) was employed as a coupling agent for *Pennisetum Purpureum*/rLDPE at 30 wt.% fiber content, the modulus of elasticity and tensile strength reached 251 MPa and 11.3 MPa, respectively. These results are equivalent to those of various natural woods, allowing them to be used in non-load-bearing applications such as furniture and doors (Grillo and Saron 2020).

Furthermore, rLDPE reinforced with irradiation crosslinked fibers demonstrated improved mechanical performance and crystalline characteristics while retaining the key benefits of self-reinforced biocomposites that are simpler to recycle than pure LDPE material (Mészáros et al. 2020). In the case of recycled blends such as rLDPE/rHDPE, rTP/rHDPE, and others, it has been revealed that the processing time has a greater impact on mechanical strength than the composition of the blend itself (Aranda-García et al. 2020). The bio-based composite PP/rLLDP with 2 wt.% compatibilizer exceeded the uncompatibilized composite in terms of strength. In comparison to the uncompatibilized composite blend, the tensile and flexural strengths improved by 24.4% and 14.1%, respectively (Chowdhury et al. 2021). Furthermore, maleic anhydride-grafted PP/PE (13 wt.%) was employed, which outperformed maleic anhydride-grafted PP/rLLDPE in terms of mechanical and thermomechanical characteristics. It was shown that the addition of 2 wt.% compatibilizer improved the mechanical characteristics of PP/rLLDPE mix (Chowdhury et al. 2021).

In spite of the presence of surface “pin-holes,” the mechanical performance of the composite LLDPE filled with 2.5 wt.% and 5 wt.% wheat bran did not decline appreciably. Tensile strength and resilience were practically comparable from 16.5 to 17 MPa. However, hardness was reduced from 52.5 to 50.5 MPa due to the structure’s porosity. Reduced filler loadings had no effect on rheological characteristics. Composites comprising 10% and 20% fibers of total weight, on the other hand, displayed rotational molding-suitable behavior (Hejna et al. 2020). Another study found that the composite 30%wood/rHDPE had higher strength (15.87 MPa) and lower water absorption qualities than other variants of the same composite. Particle sizes, plastic types, and blending ratio all exhibited a significant effect on the dimensional stability and mechanical behavior of the composites at the 0.05 significance level. Appropriate WPCs for nonstructural purposes were made from *Cordia millenii* waste and rPE (Omoniyi 2020). Because of the hydrophilic filler, the strength of the polyethylene (PE) composites dropped as the amount of

Table 4 Tensile strength of biocomposites

Polymer	Fiber	Fiber content wt. %	Tensile strength MPa	References
LDPE	Olive fiber	40%	32	Al-Oqla (2021)
	Coca	40%	3.5	de Araújo Veloso et al. (2021)
	PALF-treated	30%	1.5	Gebremedhin and Rotich (2020)
	P. purpureum	30%	11.3	de Camargo and Saron (2020)
rLLDPE	Wheat bran	2.5%	16.5	Hejna et al. (2020)
	Wheat bran	5%	17	Hejna et al. (2020)
rHDPE	Wood	30%	15.87	Omoniyi (2020)
rPP	Jute fiber	50%	60.6	Aggarwal et al. (2013)
Epoxy	Kenaf-treated	6%	45	Ismail et al. (2021)
	Kenaf-untreated	6%	68	Ismail et al. (2021)

filler increased. However, with 10% and 20% infill, the creep behavior was improved (Kohl et al. 2020).

Over virgin PP, the tensile strength of rPP composite filled with 50 wt.% jute fiber improved by 87%, while the flexural strength increased by roughly 95%. The tensile strength of composites was roughly double that of virgin PP (60.6 vs. 32 MPa), but as filler content rises, the failure strain and impact strength of the composites decrease while the notched impact strength increases (Aggarwal et al. 2013). In certain instances, therapy produces undesirable outcomes in terms of material strengthening. A research done by Ismail et al. (2021) showed that the tensile strength of untreated kenaf fiber/epoxy composite was greater (68 MPa) than the strength of treated kenaf fiber/epoxy composite (45 MPa.). In this example, the 6 wt.% alkali treatment lowered tensile strength by 34% and Young's modulus by 12%. Table 4 summarizes the tensile strength of numerous polymers with varying fiber contents.

4.2 Morphological Properties

The overall performance of eco-composites is contributed not only to the base-recycled polymer, chemical additives, and production techniques as established above, but also to the natural fiber fundamental features such as kind and shape. The irregular structure of natural fibers typically reduces the strength of eco-composite due to low interfacial strength, poor compatibility, and moisture between polar plant fibers and nonpolar polymers. Furthermore, the filler material should be fine-tuned to get the intended result. A high natural fiber content incorporated in polymer may result in dominating fiber aggregation, leading to poor fiber dispersion and excess

voids or cavities in eco-composites (Xie et al. 2010; Nassar et al. 2021a). Coupling agents help to reduce voids, cracks, and fiber agglomeration. Additionally, they enhance the filler encapsulating in the matrix. As a result, the total strength and performance of the created eco-composites are determined by the uniformity of fiber/particle dispersion in the matrix. Optical microscopy and scanning electron microscopy (SEM) are commonly employed to assess the dispersion of fillers and other microstructural characteristics (Nassar et al. 2021b). The morphological examination of the char layer in a produced composite from HDPE filled with 5% talc fibers revealed that the addition of this fiber aids flame-penetration prevention and enhances the composite's overall fire resistance. This is in contrast to other types of biocomposites. For instance, the surface of typical wood-filled HDPE-featured broad fissures, which allows for rapid fire penetration and decreased fire resistance. Furthermore, as compared to composites with unaltered HDPE shells, there is a small increase in the flame resistance properties of the composite at low-fiber loading (25 wt.%). However, at this 25 wt.% fiber loading, the composite's rate and total heat emission were dramatically decreased (Huang et al. 2020).

SEM and AFM images in Fig. 6 indicate that chemical treatment alters the fiber shape. Fiber treatment is an effective approach for modifying the topography of the surface and an important strategy for improving the quality of the fiber. In certain conditions, the properties of the fiber are degraded by fibrillation and damage in the treatment. In order to minimize such harm, it is therefore necessary to carefully control the treatment conditions. The cellulosic ingredients obtained from natural agro-residues as a bio-filler can be used effectively for the modification of different processes in recycled polymers. For instance, surface treatment, delignification, and hydrolysis provided further insights to these processes (Nassar et al. 2021b).

4.3 Physical Properties

Among critical physical properties of biocomposites is the water absorption as it impacts the mechanical performance and durability of the materials. To generate economically feasible natural fiber bio-based composites, synthetic resins are quite often reinforced with hydrophilic fibers, resulting in incompatibility issues such as void formation and delamination at fiber–matrix interfaces (Al-Maharma and Al-Huniti 2019). Consequently, the water intake of the biocomposite will increase with outlined mechanism as shown in Fig. 7. Then, it is necessary to employ chemical and/or physical treatment procedures in order to mitigate the impact of these issues. The treatment technique should be carefully chosen and applied while taking into account numerous parameters with respect to fiber and matrix characteristics (Al-Maharma and Al-Huniti 2019).

The water absorption performance of jute/PP composites without crosslinking agents was 2–3 times higher than that of the composites with additives (Aggarwal et al. 2013). The water absorption of DPE/HDPE and TP/HDPE blends is affected by processing time, which has been investigated by immersing them in water for

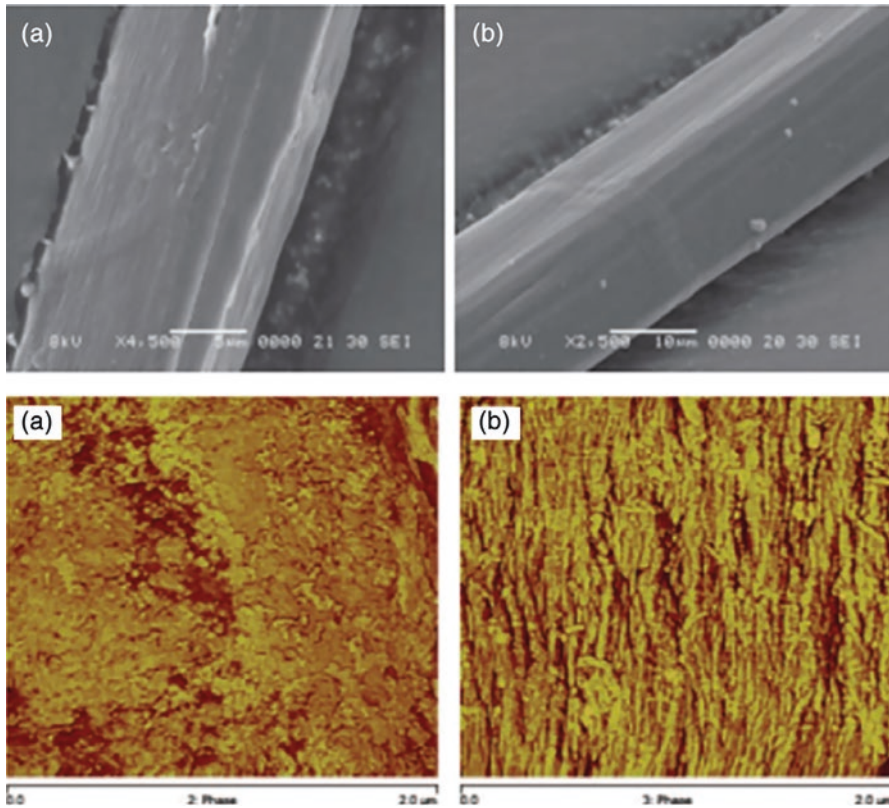


Fig. 6 SEM and AFM micrographs of (a) raw flax fiber and (b) 10% NaOH-treated flax fiber. (Nassar et al. 2021b)

17 days and absorbing 60 wt.% of their dry weight (Aranda-García et al. 2020). With combining of lignocellulosic biomass to the matrix, the density of a cocoa almond husk/rLDPE composite decreased from 0.81 to 0.61 g/cm³, while moisture increased from 0.03% to 0.60% and water absorption increased from 0.17% to 2.68%, indicating good potential for use in civil construction. Incorporating additives into cocoa waste-based composites, on the other hand, improves their water repellency and hence qualifies them for outdoor applications (de Araújo Veloso et al. 2021). Furthermore, the water uptake capability of the composites PALF-treated/rLDPE increases at higher fiber weight and length in the application of wall tiles (Gebremedhin and Rotich 2020). It has been found that DPP/rPP composites are much more resistant to water absorption than virgin polypropylene-based composites. This improvement might be attributable to the reprocessed plastic polymer's better surface modification (Alzabdeh et al. 2019).

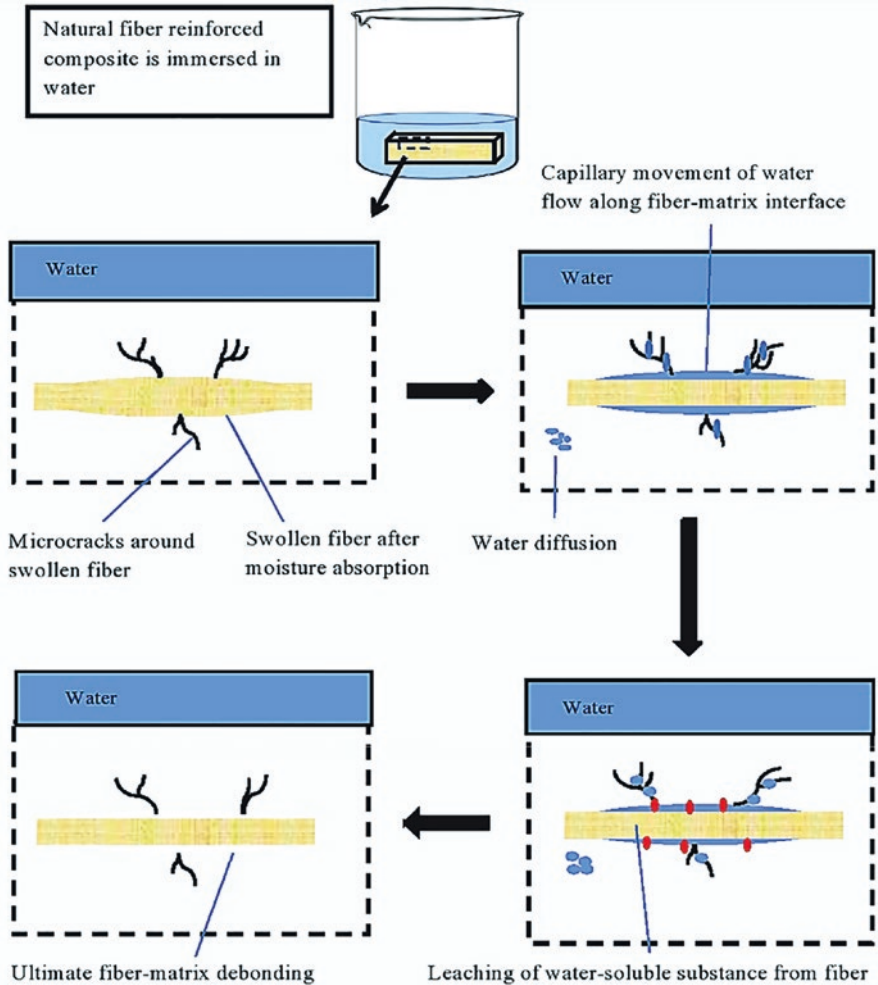


Fig. 7 Mechanics of water swelling in NFRPCs. (Rahman and Nur 2021)

4.4 Thermal Properties

The basic thermal properties of biocomposites of interest are coefficient of thermal expansion, decomposition and transition temperatures, crystallinity index. These properties are often assessed using Differential Scanning Calorimetry (DSC) and Thermogravimetric Analysis (TGA). Thermal degradation of composites made from natural fiber/rLDPE composites typically occurs at temperatures over 200 °C, allowing thermomechanical processing of the constituents by extrusion and injection molding (Grillo and Saron 2020). For example, the chemically treated kenaf fiber-filled composite materials offer superior heat stability over the untreated counterpart. In addition, an epoxy filled with untreated kenaf fiber showed temperature

sensitivity and loss threshold of 82% in the temperature range 25–150 °C. The treated kenaf/epoxy composite performs the best at ambient temperature, while the tensile strength starts to decline at temperatures over 50 °C. In another case where rice husk fillers are added to rPE matrix, a weight loss or breakdown of the composite seems to begin around 250 °C, but decomposition (weight loss) of PE without the rice husk filler appears to begin around 325 °C. Because roofing tiles are the most typical application for rPE with rice husk filler composites, it is critical to comprehend how the material responds to high temperatures that tiles may be subjected to. As a result, creep resistance is crucial in such application, and studies suggest that adding rice husk improves it. The increased storage moduli at 50 °C provided further confirmation of improved high-temperature performance of rice husk filler-based composites at 10% and 20% filler loading (Kohl et al. 2020). Overall, research into the thermal behavior of natural fiber-reinforced polymer composites is currently being conducted, and hence this area of study has a promising future (Kerni et al. 2020; Nurazzi et al. 2021b).

5 Applications

The use of eco-composites generated from natural sources and recycled polymers is motivated by the low-production cost, functional capabilities, and ingredient availability. They have recently acquired popularity in a range of applications such as transportation (automotive, locomotive, and aerospace), military items, building (ceiling panels, partition boards), packaging, consumer products, and so on (Suhaily et al. 2012; Atuanya and Aigbodion 2014; Paul et al. 2021). Furthermore, light-weight biocomposites are finding uses in the automobile industry for making components mostly made of recycled plastics (rPP, rPE, rPVC, etc.) and natural fibers (wood, sisal, hemp, banana, flax, and rice husk), with certain additives to boost strength and density. To provide a better understanding of how cost-effective biocomposite may be, glass fibers are priced between 0.30 and 2.00 \$/kg, whereas natural fibers are priced between 0.22 and 1.10 \$/kg (Zajac et al. 2014; Rodríguez et al. 2018).

Adaptive manufacturing and 3D printing of eco-composites to create new products with geometric flexibility are developing. Recent advancements in the production of complex structures may pave the way for natural fiber-based composites to overcome considerable constraints in structural components. Adaptive printing has great potential in biomedical applications such as functional replicas for surgical rehabilitation, dentistry, individualized implants, medication delivery devices, and organ fabrication (Ngo et al. 2018; Oladele et al. 2020; Aliyeva et al. 2021). Therefore, eco-composites have a tremendous potential to fulfill the growing need for high-strength modern materials, such as those required by the automotive and aerospace industries. Researchers and scientists all around the globe are working hard to produce more industrially applicable eco-composites.

6 Future Perspectives

More research and development will be necessary in the future to effectively produce eco-composites that are economically and operationally compatible with commercial design. One of the difficulties in this respect is to improve mechanical characteristics by creating more tailored morphologies with homogenous filler distribution and strong bonding with the surrounding polymer. Appropriate and efficient functionalization and ingredient modification procedures will result in improved attributes of newly produced eco-composites.

Until now, only a limited quantity of plastic rubbish has been collected and recycled mechanically. The relatively high costs of collecting, cleaning, sorting, and treating waste are a major hindrance to this method. Effective strategies to enhance the qualities of recycled plastics must be introduced to boost people's motivation to recycle plastic garbage, eliminate its disposal, and lessen its negative influence on the environment. Designers, manufacturers, and end users should collaborate to develop novel recycling processing technologies in the future. The fact that the natural fiber composite market in many industries is largely driven by increased demand for lightweight and environmentally friendly goods is a contributing factor in improving recycled plastic adaptation. Similarly, demand for recyclable items is increasing in the worldwide biocomposite industry. This expands the worldwide market for such commodities and may lead to increased global demand. As a result, eco-composite supply chain management must be carefully assessed in order to collect adequate resources to meet market demand in a sustainable manner.

In recent years, a variety of nano-scale additives for reinforcing polymeric materials have also been used. Still, a modest number of mixtures of ecological composites including nanoparticles and postconsumer recycled polymers have been manufactured. The incorporation of clay nano-fillers into biopolymers may increase the overall impact of the created eco-composites. More research into acquiring new and diverse types of production processes and procedures for eco-composites would help to boost the economic value of industrial items. Furthermore, qualifying and testing of nano-eco-composites are still in its early stages. The goal is to develop completely biodegradable bioplastics at a reasonable cost. Furthermore, in order to lower overall vehicle weight and increase performance, the contemporary aerospace and automotive sectors are striving to move from high-density materials to composites. To summarize, more research is crucial to clarify the behavior of natural fiber sandwich composites in engineering applications. Treatment will be required in the future to strengthen the durability of the adopted production procedures, which include biological and nanoparticles.

7 Concluding Remarks

Recycled-based polymer biocomposites have developed as a significant class of natural filler-reinforced polymer composites with high-good properties and performance. Several recycled polymers were tested for compatibility and performance when supplemented with natural fillers. Furthermore, bio-fillers' cellulosic substances derived from modified natural agro-residues using various procedures have been employed in processing of recycled polymer-based biocomposites. Chemical alteration of the polymer or natural fillers improves the compatibility of composite materials. Water is absorbed by biocomposites through fine voids and gaps at the interface between both the polymer and the filler, as well as microfractures in the polymeric matrix. Thus, the filler/polymer interfacial bonding has a significant impact on water absorption and related mechanical characteristics. Mechanical (chemical or physical) interlocking can be achieved by carefully modifying the surface of the filler. The results demonstrated enhanced heat stability of the eco-composites created by including a natural filler into the recycled matrix.

Overall, this chapter has shed light on latest advances in the development of eco-based composites derived from natural and waste resources. Its goal was to assist researchers in the planning, selection, and development of various types of eco-composite materials. The utilization of recycled polymers to create usable goods is primarily advocated. To achieve a high rate of adoption of such goods, new manufacturing processes capable of producing high-quality environmental composites for usage in a variety of applications are required.

Acknowledgments The authors would like to appreciate The Research Council (TRC) in Oman for their financial assistance in this research endeavor as well as for giving substantial funding through a research project (RC/RG-ENG/MIED/18/01).

References

- Abdel-Hakim A, El-Gamal AA, El-Zayat MM, Sadek AM (2021) Effect of novel sucrose-based polyfunctional monomer on physico-mechanical and electrical properties of irradiated EPDM. *Radiat Phys Chem* 189:109729. <https://doi.org/10.1016/j.radphyschem.2021.109729>
- Abdel-Shafy HI, Mansour MSM (2018) Solid waste issue: sources, composition, disposal, recycling, and valorization. *Egypt J Pet* 27:1275–1290. <https://doi.org/10.1016/j.ejpe.2018.07.003>
- Acheampong JB, de Angelis M, Krause A, Meincken M (2021) The effect of raw material selection on physical and mechanical properties of wood plastic composites made from recycled LDPE and wood from invasive trees in South Africa. *Wood Mater Sci Eng* 16:118–123. <https://doi.org/10.1080/17480272.2019.1635207>
- Adhikary KB, Pang S, Staiger MP (2008) Dimensional stability and mechanical behaviour of wood-plastic composites based on recycled and virgin high-density polyethylene (HDPE). *Compos Part B Eng* 39:807–815. <https://doi.org/10.1016/j.compositesb.2007.10.005>

- Aggarwal PK, Raghu N, Karmarkar A, Chuahan S (2013) Jute-polypropylene composites using m-TMI-grafted-polypropylene as a coupling agent. *Mater Des* 43:112–117
- Aisyah HA, Paridah MT, Sapuan SM et al (2021) A comprehensive review on advanced sustainable woven natural fibre polymer composites. *Polymers (Basel)* 13:1–45. <https://doi.org/10.3390/polym13030471>
- Aldousiri B, Shalwan CWC (2013) A review on tribological behaviour of natural reinforced composites. *Adv Mater Sci Eng* 2013:1–9. <https://doi.org/10.1155/2013/645923>
- Aliyeva N, Sas HS, Saner Okan B (2021) Recent developments on the overmolding process for the fabrication of thermoset and thermoplastic composites by the integration of nano/micron-scale reinforcements. *Compos Part A Appl Sci Manuf* 149:106525. <https://doi.org/10.1016/j.compositesa.2021.106525>
- Al-Maharma AY, Al-Huniti N (2019) Critical review of the parameters affecting the effectiveness of moisture absorption treatments used for natural composites. *J Compos Sci* 3. <https://doi.org/10.3390/jcs3010027>
- Al-Oqla FM (2021) Flexural characteristics and impact rupture stress investigations of sustainable green olive leaves bio-composite materials. *J Polym Environ* 29:892–899. <https://doi.org/10.1007/s10924-020-01889-3>
- Alsubari S, Zuhri MYM, Sapuan SM et al (2021) Potential of natural fiber reinforced polymer composites in sandwich structures: a review on its mechanical properties. *Polymers (Basel)* 13:1–20. <https://doi.org/10.3390/polym13030423>
- Alzebeleh KI, Nassar MMA, Arunachalam R (2019) Effect of fabrication parameters on strength of natural fiber polypropylene composites: statistical assessment. *Meas J Int Meas Confed* 146:195–207. <https://doi.org/10.1016/j.measurement.2019.06.012>
- Amieva EJCJ-C, Velasco-Santos C, Martínez-Hernández AL et al (2014) Composites from chicken feathers quill and recycled polypropylene. *J Compos Mater* 49:275–283. <https://doi.org/10.1177/0021998313518359>
- Anbupalani MS, Venkatachalam CD, Rathanasamy R (2020) Influence of coupling agent on altering the reinforcing efficiency of natural fibre-incorporated polymers – a review. *J Reinf Plast Compos* 39:520–544. <https://doi.org/10.1177/0731684420918937>
- Andrew JJ, Dhakal HN (2022) Sustainable biobased composites for advanced applications: recent trends and future opportunities – a critical review. *Compos Part C Open Access* 7:100220. <https://doi.org/10.1016/j.jcomc.2021.100220>
- Anjum M, Miandad R, Waqas M et al (2020) Solid waste management in Saudi Arabia: a review. *J Appl Agric Biotechnol* 1(1):13–26
- Aranda-García FJ, González-Pérez MM, Robledo-Ortíz JR et al (2020) Influence of processing time on physical and mechanical properties of composite boards made of recycled multilayer containers and HDPE. *J Mater Cycle Waste Manag* 22:2020–2028. <https://doi.org/10.1007/s10163-020-01092-5>
- Atuanya CU, Aigbodion VS (2014) Effect of wear parameter on wear behavior of recycled polyethylene/snail shell waste particulate bio-composites. *J Fail Anal Prev* 14:509–518. <https://doi.org/10.1007/s11668-014-9841-3>
- Balla VK, Kate KH, Satyavolu J et al (2019) Additive manufacturing of natural fiber-reinforced polymer composites: processing and prospects. *Compos Part B Eng* 174:106956. <https://doi.org/10.1016/j.compositesb.2019.106956>
- Barford A, Ahmad SR (2021) A call for a socially restorative circular economy: waste pickers in the recycled plastics supply chain. *Circ Econ Sustain* 1:761–782. <https://doi.org/10.1007/s43615-021-00056-7>
- Bari E, Sistani A, Morrell JJ et al (2021) Current strategies for the production of sustainable biopolymer composites. *Polymers (Basel)* 13:1–15. <https://doi.org/10.3390/polym13172878>
- Benaniba S, Driss Z, Djendel M et al (2020) Thermo-mechanical characterization of a bio-composite mortar reinforced with date palm. *Fiber J Eng Fiber Fabr* 15. <https://doi.org/10.1177/1558925020948234>
- Benavides PT, Lee U, Zarè-Mehrjerdi O (2020) Life cycle greenhouse gas emissions and energy use of polylactic acid, bio-derived polyethylene, and fossil-derived polyethylene. *J Clean Prod* 277:1–26. <https://doi.org/10.1016/j.jclepro.2020.124010>

- Chamas A, Moon H, Zheng J et al (2020) Degradation rates of plastics in the environment. *ACS Sustain Chem Eng* 8:3494–3511. <https://doi.org/10.1021/acssuschemeng.9b06635>
- Chan CM, Vandi LJ, Pratt S et al (2018) Composites of wood and biodegradable thermoplastics: a review. *Polym Rev* 58:444–494. <https://doi.org/10.1080/15583724.2017.1380039>
- Chandrasekar M, Kumar TSM, Senthilkumar K et al (2021) Performance of natural fiber-reinforced recycled thermoplastic polymer composites under aging conditions. In: *Recycling of plastics, metals, and their composites*. CRC Press, p 13
- Chang BP, Mohanty AK, Misra M (2020) Studies on durability of sustainable biobased composites: a review. *RSC Adv* 10:17955–17999. <https://doi.org/10.1039/c9ra09554c>
- Charlet K, Saulnier F, Dubois M, Béakou A (2015) Improvement of wood polymer composite mechanical properties by direct fluorination. *Mater Des* 74:61–66
- Chauhan S, Aggarwal P, Karmarkar A (2016) The effectiveness of m-TMI-grafted-PP as a coupling agent for wood polymer composites. *J Compos Mater* 50:3515–3524
- Chianelli-Junior R, Reis JML, Cardoso JL, Castro PF (2013) Mechanical characterization of sisal fiber-reinforced recycled HDPE composites. *Mater Res* 16:1393–1397. <https://doi.org/10.1590/S1516-14392013005000128>
- Chitra NJ, Vasanthakumari R, Amanulla S (2014) Preliminary studies of the effect of coupling agent on the properties of spent coffee grounds polypropylene bio-composites. *Int J Eng Res Technol* 7:9–16
- Chowdhury IH, Abdelwahab MA, Misra M, Mohanty AK (2021) Sustainable biocomposites from recycled bale wrap plastic and agave fiber: processing and property evaluation. *ACS Omega* 6:2856–2864. <https://doi.org/10.1021/acsomega.0c05186>
- Čuk N, Fabjan E, Grželj P, Kunaver M (2015) Water-blown polyurethane/polyisocyanurate foams made from recycled polyethylene terephthalate and liquefied wood-based polyester polyol. *J Appl Polym Sci* 132:1–7. <https://doi.org/10.1002/app.41522>
- de Araújo Veloso MCR, Scatolino MV, Gonçalves MMBP et al (2021) Sustainable valorization of recycled low-density polyethylene and cocoa biomass for composite production. *Environ Sci Pollut Res* 28:32810–32822. <https://doi.org/10.1007/s11356-021-13061-y>
- de Camargo RV, Saron C (2020) Mechanical–chemical recycling of low-density polyethylene waste with polypropylene. *J Polym Environ* 28:794–802
- De Jesus RA, Alves T, Fernando L et al (2022) Conversion of plastic waste into supports for nanostructured heterogeneous catalysts: application in environmental remediation. *Surfaces* 5:35–66
- Evode N, Qamar SA, Bilal M et al (2021) Plastic waste and its management strategies for environmental sustainability. *Case Stud Chem Environ Eng* 4:100142. <https://doi.org/10.1016/j.csee.2021.100142>
- Eze WU, Madufor IC (2020) Effect of maleic anhydride graft-polyethylene (MAPE) on mechanical properties of cow dung and poultry dung filled low-density polyethylene (LDPE) composites. *Int J Adv Res Innov Idea Educ* 4(1):18–27
- Farahani GN, Ahmad I, Mosadeghzad Z (2012) Effect of fiber content, fiber length and alkali treatment on properties of kenaf fiber/UPR composites based on recycled PET wastes. *Polym-Plast Technol Eng* 51:634–639. <https://doi.org/10.1080/03602559.2012.659314>
- Gafri HFS, Mohamed Zuki F, Aroua MK, Hashim NA (2019) Mechanism of bacterial adhesion on ultrafiltration membrane modified by natural antimicrobial polymers (chitosan) and combination with activated carbon (PAC). *Rev Chem Eng* 35:421–443. <https://doi.org/10.1515/revce-2017-0006>
- Gars M, Le Delvart A, Roger P et al (2020) Amidation of TEMPO-oxidized cellulose nanocrystals using aromatic aminated molecules neat CNC TEMPO-mediated oxidation distilled water TEMPO, NaBr, NaClO TEMPO-CNC amidation with 1-methyl-3-phenylpropylamine distilled water 1-M-3-PP, EDC, NHS CNC-1-M. *Colloid Polym Sci* 298:603–617
- Gebremedhin N, Rotich GK (2020) Manufacturing of bathroom wall tile composites from recycled low-density polyethylene reinforced with pineapple leaf fiber. *Int J Polym Sci* 2020:1. <https://doi.org/10.1155/2020/2732571>

- George A, Sanjay MR, Srisuk R et al (2020) A comprehensive review on chemical properties and applications of biopolymers and their composites. *Int J Biol Macromol* 154:329–338. <https://doi.org/10.1016/j.ijbiomac.2020.03.120>
- Girijappa YGT, Mavinkere Rangappa S, Parameswaranpillai J, Siengchin S (2019) Natural fibers as sustainable and renewable resource for development of eco-friendly composites: a comprehensive review. *Front Mater* 6:1–14. <https://doi.org/10.3389/fmats.2019.00226>
- Grillo CC, Saron C (2020) Wood-plastic from *Pennisetum Purpureum* fibers and recycled low-density polyethylene. *J Nat Fiber* 00:1–14. <https://doi.org/10.1080/15440478.2020.1764436>
- Gu F, Guo J, Zhang W et al (2017) From waste plastics to industrial raw materials: a life cycle assessment of mechanical plastic recycling practice based on a real-world case study. *Sci Total Environ* 601–602:1192–1207. <https://doi.org/10.1016/j.scitotenv.2017.05.278>
- Gu L, Jiang B, Song J et al (2019) Effect of lignin on performance of lignocellulose nanofibrils for durable superhydrophobic surface. *Cellulose* 26:933–944
- Hasan KMF, Horváth PG, Bak M, Alpár T (2021) A state-of-the-art review on coir fiber-reinforced biocomposites. *RSC Adv* 11:10548–10571. <https://doi.org/10.1039/d1ra00231g>
- Hassaini L, Kaci M, Touati N et al (2017) Valorization of olive husk flour as a filler for biocomposites based on poly(3-hydroxybutyrate-Co-3-hydroxyvalerate): effects of silane treatment. *Over Rim*:191–199. <https://doi.org/10.2307/j.ctt46nrzt.12>
- Hejna A, Barczewski M, Andrzejewski J et al (2020) Rotational molding of linear low-density polyethylene composites filled with wheat bran. *Polymers (Basel)* 12. <https://doi.org/10.3390/POLYM12051004>
- Huang R, Zhang X, Chen Z et al (2020) Thermal stability and flame resistance of the coextruded wood-plastic composites containing talc-filled plastic shells. *Int J Polym Sci* 2020. <https://doi.org/10.1155/2020/1435249>
- Hubbe MA, Grigsby W (2020) From nanocellulose to wood particles: a review of particle size vs. the properties of plastic composites reinforced with cellulose-based entities. *Bioresources* 15:2030–2081. <https://doi.org/10.15376/biores.15.1.2030-2081>
- Ilyas RA, Sapuan SM, Bayraktar E (2021a) Recycling of plastics, metals, and their composites. CRC Press
- Ilyas RA, Sapuan SM, Sabaruddin FA et al (2021b) Reuse and recycle of biobased packaging products. In: *Bio-based packaging: material, environmental and economic aspects*, pp 413–426. <https://doi.org/10.1002/9781119381228.ch23>
- Ismail AB, Bakar HBA, Shafei SB (2020) Comparison of LDPE/corn stalk with eco degradant and LDPE/corn stalk with MAPE: influence of coupling agent and compatibiliser on mechanical properties. *Mater Today Proc* 31:360–365. <https://doi.org/10.1016/j.matpr.2020.06.234>
- Ismail NF, Mohd Radzuan NA, Sulong AB et al (2021) The effect of alkali treatment on physical, mechanical and thermal properties of kenaf fiber and polymer epoxy composites. *Polymers (Basel)* 13. <https://doi.org/10.3390/polym13122005>
- Jannah M, Mariatti M, Abu Bakar A, Abdul Khalil HPS (2009) Effect of chemical surface modifications on the properties of woven banana-reinforced unsaturated polyester composites. *J Reinf Plast Compos* 28:1519–1532. <https://doi.org/10.1177/0731684408090366>
- Joglekar JJ, Munde YS, Jadhav AL et al (2021) Mechanical and morphological properties of citrus maxima waste powder filled low-density polyethylene composites. *Mater Today Proc*:3–8. <https://doi.org/10.1016/j.matpr.2021.03.684>
- Joseph B, James J, Kalarikkal N, Thomas S (2021) Recycling of medical plastics. *Adv Ind Eng Polym Res* 4:199–208. <https://doi.org/10.1016/j.aiepr.2021.06.003>
- Kannan G, Thangaraju R (2021) Recent progress on natural lignocellulosic fiber-reinforced polymer composites: a review. *J Nat Fiber* 00:1–32. <https://doi.org/10.1080/15440478.2021.1944425>
- Kar GP, Saed MO, Terentjev EM (2020) Scalable upcycling of thermoplastic polyolefins into vitrimers through transesterification. *J Mater Chem A* 8:24137–24147. <https://doi.org/10.1039/d0ta07339c>
- Karmarkar A, Chauhan SS, Modak JM, Chanda M (2007) Mechanical properties of wood-fiber reinforced polypropylene composites: effect of a novel compatibilizer with isocyanate functional group. *Compos Part A* 38:227–233. <https://doi.org/10.1016/j.compositesa.2006.05.005>

- Karthi N, Kumaresan K, Sathish S et al (2019) An overview: natural fiber-reinforced hybrid composites, chemical treatments and application areas. *Mater Today Proc* 27:2828–2834. <https://doi.org/10.1016/j.matpr.2020.01.011>
- Kerni L, Singh S, Patnaik A, Kumar N (2020) A review on natural fiber-reinforced composites. *Mater Today Proc* 28:1616–1621. <https://doi.org/10.1016/j.matpr.2020.04.851>
- Kim DY, Cha JH, Seo KH (2019) Effects of chain extender on properties and foaming behavior of polypropylene foam. *RSC Adv* 9:25496–25507. <https://doi.org/10.1039/c9ra04824c>
- Kohl JG, Kohl AG, Licea-Claverie A et al (2020) Mechanical and thermal characterization of As-received recycled polyethylene filled with rice husk and their relationship to the end use of these composites. *Polym Technol Mater* 59:1463–1472. <https://doi.org/10.1080/25740881.2020.1744013>
- Kuan HTN, Tan MY, Shen Y, Yahya MY (2021) Mechanical properties of particulate organic natural filler-reinforced polymer composite: a review. *Compos Adv Mater* 30:263498332110075. <https://doi.org/10.1177/26349833211007502>
- Lazim NH, Samat N (2019) The influence of irradiated recycled polypropylene compatibilizer on the impact fracture behavior of recycled polypropylene/microcrystalline cellulose composites. *Polym Compos* 40:E24–E34. <https://doi.org/10.1002/pc.24430>
- Lee CH, Padzil FNBM, Lee SH et al (2021) Potential for natural fiber reinforcement in PLA polymer filaments for fused deposition modeling (FDM) additive manufacturing: a review. *Polymers (Basel)* 13. <https://doi.org/10.3390/polym13091407>
- Mészáros L, Kara Y, Fekete T, Molnár K (2020) Development of self-reinforced low-density polyethylene using γ -irradiation cross-linked polyethylene fibres. *Radiat Phys Chem* 170:108655. <https://doi.org/10.1016/j.radphyschem.2019.108655>
- Mohammed AA, Bachtiar D, Rejab MRM, Siregar JP (2018) Effect of microwave treatment on tensile properties of sugar palm fibre reinforced thermoplastic polyurethane composites. *Def Technol* 14:287–290. <https://doi.org/10.1016/j.dt.2018.05.008>
- Nassar MMA, Sider I (2021) Evaluation of novel compatibility strategies for improving the performance of recycled low-density polyethylene-based biocomposites. *Polymers (Basel)* 13. <https://doi.org/10.3390/polym13203486>
- Nassar MMA, Alzebedeh K, Munam A et al (2020) Preparation of high-performance fiber from natural fiber (date palm). *World Intellectual Prop Organ (WIPO)*, WO2020139088A1, pp 1–22
- Nassar MMA, Alzebedeh K, Munam A et al (2021a) Polymer powder and pellets comparative performances as bio-based composites. *Iran Polym J* 30:269–283. <https://doi.org/10.1007/s13726-020-00888-4>
- Nassar MMA, Alzebedeh KI, Pervez T et al (2021b) Progress and challenges in sustainability, compatibility, and production of eco-composites: a state-of-art review. *J Appl Polym Sci* 138:1–31. <https://doi.org/10.1002/app.51284>
- Nassar MMA, Munam A, Alzebedeh KI et al (2021c) Efficient methods of surface functionalization of lignocellulosic waste toward surface clickability enhancement. *Compos Interface* 29:79. <https://doi.org/10.1080/09276440.2021.1897924>
- Ngo TD, Kashani A, Imbalzano G et al (2018) Additive manufacturing (3D printing): a review of materials, methods, applications and challenges. *Compos Part B Eng* 143:172–196. <https://doi.org/10.1016/j.compositesb.2018.02.012>
- Nizamuddin S, Boom YJ, Giustozzi F (2021) Sustainable polymers from recycled waste plastics and their virgin counterparts as bitumen modifiers: a comprehensive review. *Polymers (Basel)* 13. <https://doi.org/10.3390/polym13193242>
- Nurazzi NM, Asyraf MRM, Khalina A et al (2021a) A review on natural fiber reinforced polymer composite for bullet proof and ballistic applications. *Polymers (Basel)* 13:1–42. <https://doi.org/10.3390/polym13040646>
- Nurazzi NM, Asyraf MRM, Rayung M et al (2021b) Thermogravimetric analysis properties of cellulosic natural fiber polymer composites: a review on influence of chemical treatments. *Polymers (Basel)* 13. <https://doi.org/10.3390/polym13162710>

- Obasi HC, Mark UC, Mark U (2021) Improving the mechanical properties of polypropylene composites with coconut shell particles. *Compos Adv Mater* 30:263498332110074. <https://doi.org/10.1177/26349833211007497>
- Oladele IO, Omosho TF, Adediran AA (2020) Polymer-based composites: an indispensable material for present and future applications. *Int J Polym Sci* 2020:1. <https://doi.org/10.1155/2020/8834518>
- Olatunji O (2015) Natural polymers: industry techniques and applications. *Nat Polym Ind Tech Appl*:1–370. <https://doi.org/10.1007/978-3-319-26414-1>
- Omoniyi TE (2020) Influence of particle size and fibre content on the dimensional stability and mechanical behaviour of composites produced from Cordiamillenii and recycled polyethylene. *Int J Adv Eng Res Sci* 7:155–165. <https://doi.org/10.22161/ijaers.76.19>
- Omran AAB, Mohammed AABA, Sapuan SM et al (2021) Micro-and nanocellulose in polymer composite materials: a review. *Polymers (Basel)* 13:1–30. <https://doi.org/10.3390/polym13020231>
- Paul S, Sen B, Das S et al (2021) Incarnation of bioplastics: recuperation of plastic pollution. *Int J Environ Anal Chem* 00:1–24. <https://doi.org/10.1080/03067319.2021.1983552>
- Pearson HA, Urban MW (2014) Simple click reactions on polymer surfaces leading to antimicrobial behavior. *J Mater Chem B* 2:2084–2087. <https://doi.org/10.1039/c3tb21865a>
- Pearson A, Liao W, Kazemi Y et al (2022) Fiber-matrix adhesion between high-density polyethylene and carbon fiber. *Polym Test* 105:107423. <https://doi.org/10.1016/j.polymertesting.2021.107423>
- Ragaert K, Delva L, Van Geem K (2017) Mechanical and chemical recycling of solid plastic waste. *Waste Manag* 69:24–58
- Rahman R, Nur RM (2021) Water absorption properties of natural fibres reinforced PLA bio-composite. In: *Biocomposite materials*, pp 251–271. https://doi.org/10.1007/978-981-33-4091-6_9
- Rahman NSA, Yhaya MF, Azahari B, Ismail WR (2018) Utilisation of natural cellulose fibres in wastewater treatment. *Cellulose* 25:4887–4903. <https://doi.org/10.1007/s10570-018-1935-8>
- Rajeshkumar G (2020) A new study on tribological performance of phoenix Sp. fiber-reinforced epoxy composites. *J Nat Fiber* 00:1–12. <https://doi.org/10.1080/15440478.2020.1724235>
- Rodríguez LJ, Orrego CE, Ribeiro I, Peças P (2018) Life-cycle assessment and life-cycle cost study of banana (*Musa sapientum*) fiber biocomposite materials. *Procedia CIRP* 69:585–590. <https://doi.org/10.1016/j.procir.2017.11.145>
- Sanjay MR, Siengchin S, Parameswaranpillai J et al (2019) A comprehensive review of techniques for natural fibers as reinforcement in composites: preparation, processing and characterization. *Carbohydr Polym* 207:108–121. <https://doi.org/10.1016/j.carbpol.2018.11.083>
- Shanmugam V, Mensah RA, Försth M et al (2021) Circular economy in biocomposite development: state-of-the-art, challenges and emerging trends. *Compos Part C Open Access* 5:100138. <https://doi.org/10.1016/j.jcomc.2021.100138>
- Sider I, Nassar MMA (2021) Chemical treatment of bio-derived industrial waste filled recycled low-density polyethylene: a comparative evaluation. *Polymer* 13:1–13
- Singh AK, Bedi R, Kaith BS (2019) Mechanical properties of composite materials based on waste plastic – a review. *Mater Today Proc* 26:1293–1301. <https://doi.org/10.1016/j.matpr.2020.02.258>
- Siracusa V, Blanco I (2020) Bio-polyethylene (Bio-PE), Bio-polypropylene (Bio-PP) and Bio-poly(ethylene terephthalate) (Bio-PET): recent developments in bio-based polymers analogous to petroleum-derived ones for packaging and engineering applications. *Polymers (Basel)* 12. <https://doi.org/10.3390/APP10155029>
- Su QZ, Vera P, Salafranca J, Nerin C (2021) Decontamination efficiencies of post-consumer high-density polyethylene milk bottles and prioritization of high concern volatile migrants. *Resour Conserv Recycl* 171:105640. <https://doi.org/10.1016/j.resconrec.2021.105640>
- Suhaily SS, Jawaid M, Abdul Khalil HPS, Ibrahim F (2012) A review of oil palm biocomposites for furniture design and applications: potential and challenges. *Bioresources* 7:4400–4423. <https://doi.org/10.15376/biores.7.3.4400-4423>

- Supian ABM, Jawaid M, Rashid B et al (2021) Mechanical and physical performance of date palm/bamboo fibre reinforced epoxy hybrid composites. *J Mater Res Technol* 15:1330–1341. <https://doi.org/10.1016/j.jmrt.2021.08.115>
- Syduzzaman M, Al Faruque MA, Bilisik K, Naebe M (2020) Plant-based natural fibre-reinforced composites: a review on fabrication, properties and applications. *CoatingsTech* 10:1–34. <https://doi.org/10.3390/coatings10100973>
- Valvez S, Maceiras A, Santos P, Reis PNB (2021) Olive stones as filler for polymer-based composites: a review. *Materials* 14(4):845
- Vidakis N, Petousis M, Tzounis L et al (2021) Sustainable additive manufacturing: mechanical response of polypropylene over multiple recycling processes. *Sustainability* 13:1–16. <https://doi.org/10.3390/su13010159>
- Wang W, Themelis NJ, Sun K et al (2019) Current influence of China's ban on plastic waste imports. *Waste Dispos Sustain Energy* 1:67–78. <https://doi.org/10.1007/s42768-019-00005-z>
- Wu CS, Wu DY, Wang SS (2021) Preparation, characterization, and functionality of bio-based polyhydroxyalkanoate and renewable natural fiber with waste oyster shell composites. *Polym Bull* 78:4817–4834. <https://doi.org/10.1007/s00289-020-03341-x>
- Xie Y, Hill CAS, Xiao Z et al (2010) Silane coupling agents used for natural fiber/polymer composites: a review. *Compos Part A Appl Sci Manuf* 41:806–819. <https://doi.org/10.1016/j.compositesa.2010.03.005>
- Yeo JS, Seong DW, Hwang SH (2015) Chemical surface modification of lignin particle and its application as filler in the polypropylene composites. *J Ind Eng Chem* 31:80–85. <https://doi.org/10.1016/j.jiec.2015.06.010>
- Zajac J, Hutyrková Z, Orlovský I (2014) Investigation of surface roughness after turning of one kind of the bio-material with thermoplastic matrix and natural fibers. *Adv Mater Res* 941–944:275–279. <https://doi.org/10.4028/www.scientific.net/AMR.941-944.275>
- Zhang X, Li BW, Dong L et al (2018) Superior energy storage performances of polymer nanocomposites via modification of filler/polymer interfaces. *Adv Mater Interfaces* 5:1–28. <https://doi.org/10.1002/admi.201800096>
- Zwawi M (2021) A review on natural fiber bio-composites, surface modifications and applications. *Molecules* 26. <https://doi.org/10.3390/molecules26020404>

Production and Recycling of Biocomposites: Present Trends and Future Perspectives



Venitalitya A. S. Augustia and Achmad Chafidz

1 Present Trends in Biocomposites Production and Its Applications

Composites are considered one of the most important manifestations of the integrated mechanism in structures, technology, and materials creation, and one of their main components is a polymer. There is a quick increase in the development of material creation such as composites as human technologies develop rapidly but there is a need to place attention on the environment due to the fact that these technologies also have certain negative effects (Ilyas et al. 2021a, b, c). For example, humans frequently use polymers which are mostly known as plastics in their daily life in the twentieth century because they are cheap, durable, and convenient. However, the uncontrolled use of this material which is mostly nondegradable, has led to the accumulation of plastic waste globally, thereby causing significant damages to the environment (Ilyas et al. 2021a, b, c).

Environmental scientists predicted that the quantity of global plastic waste in landfills is estimated to reach 12,000 million tons in 2050 (AccessScience 2017). A previous study also showed that the degradation process of different types of plastic usually produces some harmful volatile compounds such as ketones, esters, lactones, carboxylic acid, aldehydes, alcohol, and ethers (Shanmugam et al. 2021). This means there is a need to innovate and find more eco-friendly materials which are safe for humans and easy to degrade. Biocomposites are recyclable, lightweight,

V. A. S. Augustia

Department of Chemical Engineering, Universitas Islam Indonesia, Yogyakarta, Indonesia

A. Chafidz (✉)

Department of Chemical Engineering, Universitas Islam Indonesia, Yogyakarta, Indonesia

Department of Chemical Engineering, National Taiwan University, Taipei, Taiwan

e-mail: achmad.chafidz@uii.ac.id

and cost-effective materials that have been discovered to have a high potential to serve as the substitute for nondegradable materials such as plastics (Kumar et al. 2020; Righetti et al. 2019; Das et al. 2018a, b).

Biocomposites are composed of bio-based polymer and filler made from renewable natural sources and degradable materials (Sundarakannan et al. 2020; Das et al. 2018a, b, 2019). These natural fillers also known as bio-filler can be classified into two groups of raw materials which include the first- and second-generation (Sheldon and Norton 2020). Wood is an example of first-generation materials while the lignocellulosic wastes produced from wood, forest, and agricultural residues are second-generation materials. This shows that second-generation materials are more widely used in the production of biocomposites due to their eco-friendly properties and availability at a very low cost. Moreover, plastics and some other renewable natural sources can also be used in producing biocomposites (Sheldon and Norton 2020) with the renewable natural sources usually applied to minimize the use of nonrenewable sources and to repair the existing waste streams (Mohanty et al. 2018).

Bio-fillers are also normally used to strengthen the structure of biocomposites through the addition of a coupling agent and to enhance the biodegradability of the composites (Shanmugam et al. 2021). The types of natural fibers and fillers commonly used in the production process are presented in Fig. 1 while the matrix polymers including the petrochemical-based and bio-resourced materials which are both advanced technologies are indicated in Fig. 2. It is also important to note that biocomposites are also known as hybrid composites (Mohanty et al. 2018).

There are several methods used in producing biocomposites with each having different materials and applications. For example, the melt mixing processes, through the extrusion and injection mold, are usually used to manufacture short-fiber, particulate-type, and filler-reinforced thermoplastic biocomposites (Mohanty et al. 2018) while the thermoforming and compressing molding-type are used in reinforcing fabric thermoplastic-type. Moreover, thermoset resins are manufactured through the resin infusion process while thermoset biocomposites are mainly produced through hand-layup, vacuum-assisted resin, transfer molding, and sheet

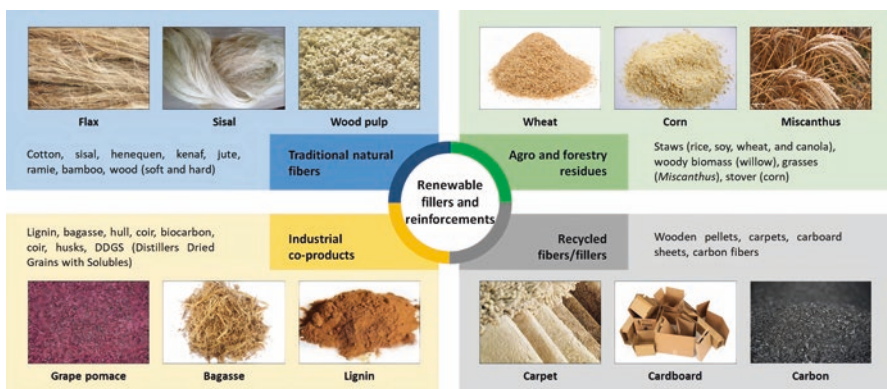


Fig. 1 Several types of natural fibers and fillers. (Adopted from Mohanty et al. 2018)

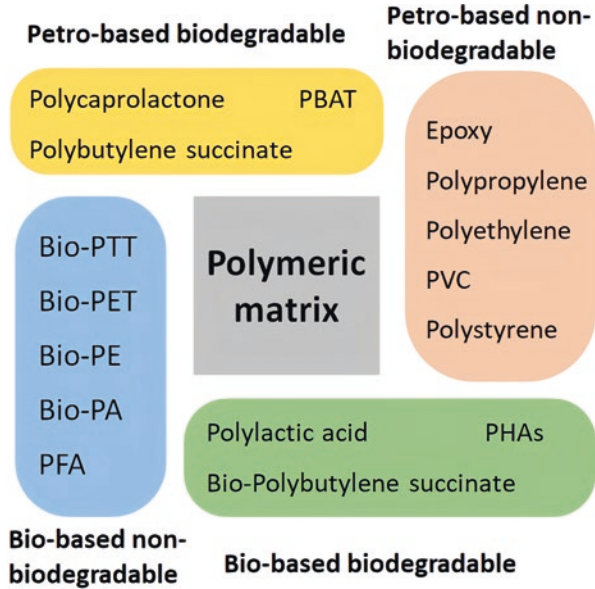


Fig. 2 Several types of matrix polymers used for biocomposites. (Adopted from Mohanty et al. 2018)

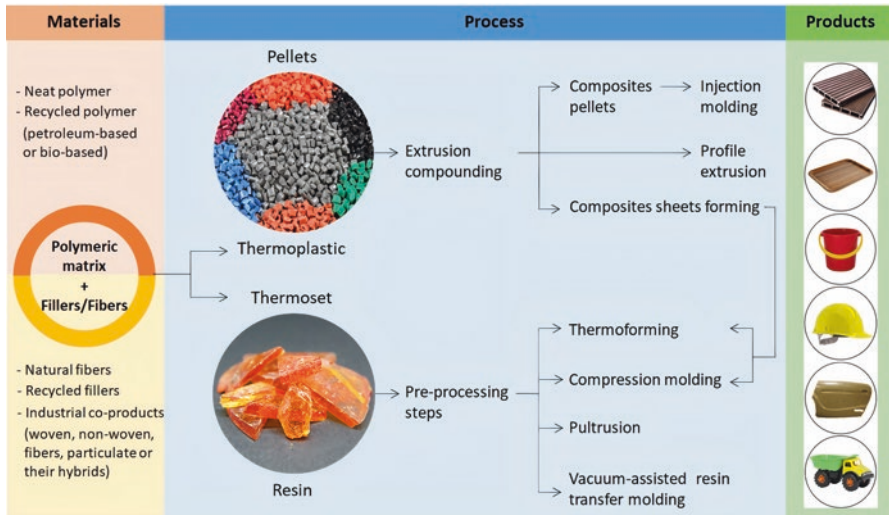


Fig. 3 The examples of biocomposites manufacturing processes. (Adopted from Mohanty et al. 2018)

molding processes (Mohanty et al. 2018). The examples of the materials, processes, and types of products in biocomposite production are presented in Fig. 3.

Table 1 Different applications of biocomposites

Type of resin	Type of filler	Application	References
Polypropylene	Coir fiber	Load-floor production for the 2012 model ford Focus battery-electric vehicles	Malnati (2018)
Thermoplastic elastomer	Ground coconut shells	Structural guards for ford F-250 super duty pickups in 2013	
Thermoplastic polyolefin	Ground coconut shells, shredded battery cases, unique synthetic mineral-based fiber (magnesium silica)	Rear decklid applique brackets and side-door cladding for 2015 MY ford mustang sports cars	
Natural resins	Lignin	Construction, electronics, headphones, and furniture	Kun and Pukánszky (2017)
No information	Wood fibers with an oil-based binder	Door panels for Mercedes Benz S-class	Akampunguza et al. (2017)
Polyols	Natural fibers	Interior auto components (door panel and seats) by Johnson Controls interiors	Sajjan et al. (2020)
Poly(3-hydroxybutyrate-co-3-hydroxyvalerate)	Coffee Silverskin	Plastic materials at food contact	Gigante et al. (2021)
Thermoplastic polymer	Lignocellulosic components (e.g., pulp fibers, nanocellulose, and lignin)	Construction, household items, interior design, and automotive industries	Zarna et al. (2021)
Enzymatically synthesized Levan from <i>Erwinia amylovora</i>	Montmorillonite clay, bovine serum albumin	Drug delivery system and short peptide	Xu et al. (2020)
Natural mucilage biopolymer	Nanophase yttrium-substituted hydroxyapatite particles from eggshell	Biomedical fields	Sridevi et al. (2021)
Polyaniline-modified almond	Walnut shells	Adsorbents for removing Orange G dye in industrial wastewater	Imgharn et al. (2021)
Chitosan-gelatin (biopolymers)	Allantoin	Biocomposite film for wound dressing	Sakthiguru and Sithique (2020)
Poly(methyl methacrylate)	Hybrid materials (e.g., ZrO ₂ /Kraft lignin and ZrO ₂ -SiO ₂ /Kraft lignin)	Building facades, noise barriers, and other construction applications	Jędrzejczak et al. (2021)
Poly(ϵ -caprolactone)	Lignocellulosic hemp	Lightweight applications	Dhokal et al. (2018)

(continued)

Table 1 (continued)

Type of resin	Type of filler	Application	References
Poly(lactic acid)	Nanofillers (e.g., metallic nanofillers, cellulose nanocrystals, and carbon-based nanoparticles)	Biomedical and pharmaceutical applications, packaging, and sensors	Liu et al. (2020)
Bio-epoxy and acrylate-epoxidized soybean oil resin (thermoset bioresin)	Denim waste	Automotive interior parts, furniture, interior construction and sport, and leisure equipment	Temmink et al. (2018)

Different types of biocomposites such as natural fiber composites are applied in construction, automotive part, electronic, and sporting goods industries as indicated in Table 1 (Mohanty et al. 2018). They are widely applied in automotive industries due to their great properties such as moisture repellence, structural stability, good finishing, and flame-retardant (Mohanty et al. 2018), and their ability to provide long-term price stability for auto manufacturers. The use of eco-friendly materials such as the wastes and by-products of agroforestry industries also makes the products cheaper than traditional materials (Malnati 2018). Moreover, it is also possible to recycle the polymer matrix (i.e., thermoplastic) and use it in the production of biocomposites. This is considered advantageous due to the increase in environmental and ecological awareness around the world which has made recycling and reuse of thermoplastics to be very important. Several countries were observed to have implemented policies to ban single-use of plastics in some applications such as cups, straws, water bottles, bags, and others and also to promote the usage of recycled or reusable plastics (Chandrasekar et al. 2021; Ilyas et al. 2021a, b, c).

2 Life-Cycle Analysis of Biocomposites

Conventional polymer composites have certain environmental issues due to their nondegradable and harmful residues. Therefore, innovations of composite fabrication were discovered over the last decade in the form of biocomposites (Zini and Scandola 2011) which have been previously explained to consist of bio-based or natural fiber as the filler and polymer matrix (Beigbeder et al. 2019). The application of natural and renewable components in these materials makes it possible to manage their end-of-life stage (Beigbeder et al. 2019) using several methods, including recycling, incineration, composting, or landfilling as well as some mechanical methods such as extrusion after washing, shredding, and sorting (Le Duigou et al. 2008; Soccalingame et al. 2015; Srebrenkoska et al. 2008; Beigbeder et al. 2019).

A life-cycle assessment was developed to evaluate the environmental effects of a system or product (Pennington et al. 2004). This is also known as life-cycle analysis

(LCA) and designed as the methodology to analyze the environmental performances of commercial materials/products, processes, or services in all stages. For example, the environmental performances of a product being manufactured are normally analyzed starting from the raw material into final disposal with the focus on the extraction of raw material, processing, manufacturing, transportation or distribution, use or re-use, maintenance, and recycling or final disposal (Song et al. 2009). The standard associated with this assessment has been outlined by the International Organization for Standardization (ISO) 14,040:2006—Environmental Management (Salwa et al. 2021).

Corbière-Nicollier et al. (2001) studied the use of LCA on biofibers to determine the environmental impact of substituting glass fibers with reed fibers in plastic products and the use of natural fibers was observed to be generally more eco-friendly compared to glass fibers. It is important to note that the cutoff approach is the model mostly applied in the recycling process of LCA. This means the recycling steps of the biocomposites produced using recycled materials need to be considered (Frischknecht 2010). LCA was also applied by Beigbeder et al. (2019) to polypropylene/wood flour and polylactic acid/flax fibers which are two kinds of biocomposites commonly used in France while the environmental impacts of the end-of-life options such as landfill, incineration, mechanical recycling, and industrial composting were also studied. Some system boundaries were selected as indicated in Fig. 4 and the results showed that the lowest environmental impacts were found with the recycling end-of-life option.

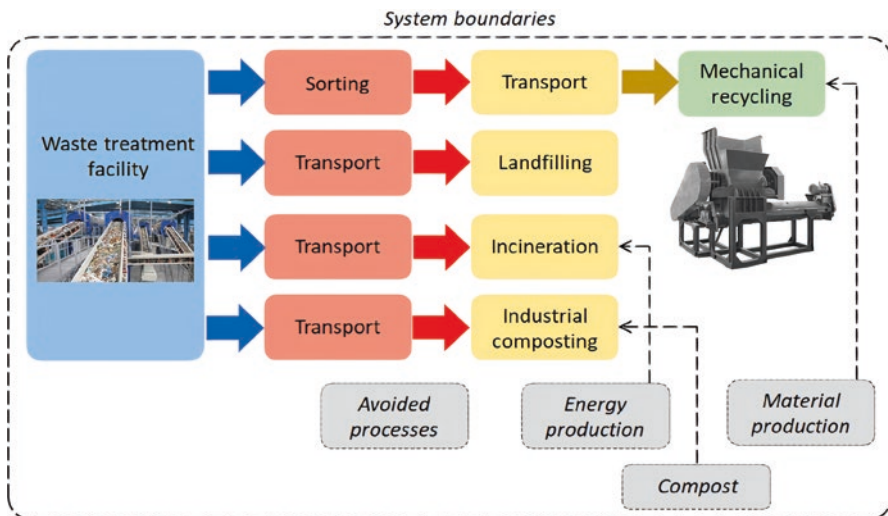


Fig. 4 System boundaries of LCA applied to polypropylene and PLA/flax fiber composites. (Adopted from Beigbeder et al. 2019)

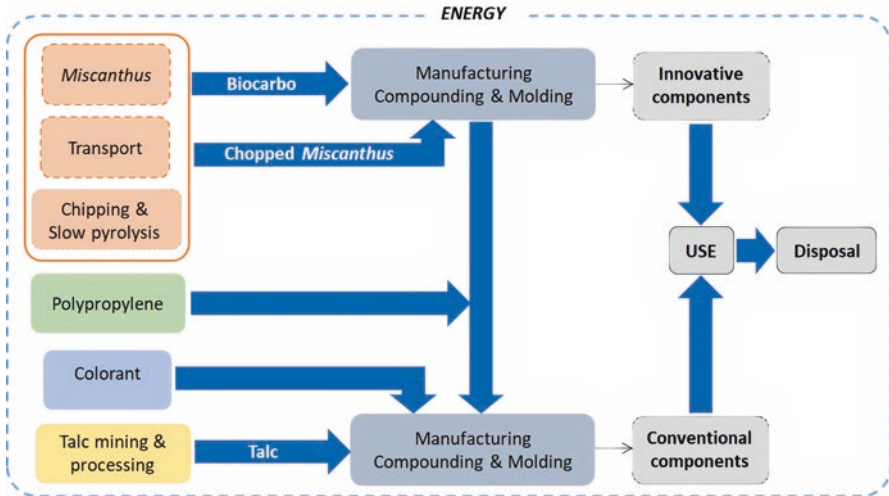


Fig. 5 System boundaries used in the application of LCA on the biocarbon from Miscanthus, polypropylene-reinforced biocarbon biocomposites, and biocomposites for automotive component. (Adopted from Roy et al. 2020)

Roy et al. (2020) also applied LCA to determine the environmental impacts and advantages of using biocomposites in producing automotive components considering the fact that the transportation industry is one of the sectors that mostly use this material. The boundaries used in the study are presented in Fig. 5 and it was discovered that the colorant used in automotive components normally produces the highest environmental impacts while the biocarbon contained in biocomposites has the lowest. This means biocomposites also have greater environmental impacts compared to conventional composites (Roy et al. 2020).

3 Recycling Technologies of Biocomposites

There are three types of biocomposite recycling methods which are mechanical, chemical, and thermal methods (Shanmugam et al. 2020). The first is the mechanical recycling method which involves conducting remelting and remolding processes simultaneously (Shanmugam et al. 2021), and the steps include cutting of the biocomposites to form granules, pellets, or flakes followed by extruding and the addition of virgin plastics into the new recycled product to improve the quality (Grigore 2017; Shanmugam et al. 2021). It is important to note that some properties such as molecular weight of recycled plastics and aspect ratio of reinforcements usually reduce after the mechanical process (Grigore 2017). This means it is better to use

these composites only one time even though the recycling process is more eco-friendly (Shanmugam et al. 2021).

The second is the chemical recycling method which involves the use of a solvent to dissolve the matrix of the polymer followed by the separation of the recycled material and the matrix polymer (Rybicka et al. 2016; Yang et al. 2012). These chemical processes are normally used to convert plastics to monomers or to ensure partial depolymerization to oligomer (Shanmugam et al. 2021) while some other reactions are for polymer decomposition such as the degradation through microwave, thermal or catalytic cracking, hydrogenation, glycolysis, and methanolysis, depolymerization using chemical processes, gasification, pyrolysis, photodegradation, and degradation using ultrasound, reforming, and hydrolysis (Grigore 2017). The last is the thermal recycling method which involves an important process of incineration or combustion in recycling biocomposites. It is considered promising due to the energy usually generated from the polymer but observed to be disadvantageous because it produces toxic and harmful airborne compounds (Grigore 2017).

Mechanical recycling is the best method among the three due to the fact that it has more advantages such as low cost, ease to process, and eco-friendly (Chaitanya et al. 2019; Badia et al. 2012). Figure 6 shows the two types of recycling methods typically for thermoplastic and thermosetting-based composites as reported by Yang et al. (2012) while the structure of the recycling process is presented in Fig. 7.

Types	Recycling methods	Technology features	Status of technology
Thermoset-matrix composites	Mechanical recycling	<ul style="list-style-type: none"> ➢ Comminution - grinding – milling ➢ Products: fibres and fillers ➢ Degradation of fibre properties 	<ul style="list-style-type: none"> ➢ Commercialization (e.g. ERCOM (Germany), Phoenix Fibreglass (Canada))
	Thermal recycling	<ul style="list-style-type: none"> ➢ Combustion/incineration with energy recovery ➢ Fluidised-bed thermal process for fibre recovery ➢ Pyrolysis for fibre and matrix recovery 	<ul style="list-style-type: none"> ➢ Promising Technology
	Chemical recycling	<ul style="list-style-type: none"> ➢ Chemical dissolution of matrix ➢ Solvolysis (supercritical organic solvent)/hydrolysis (supercritical water) ➢ Product of high quality fibres, potential recovery of resin ➢ Inflexibility of solvent and potential pollution 	<ul style="list-style-type: none"> ➢ Laboratory scale, promising technology
Thermoplastic-matrix composites	Thermal processing	<ul style="list-style-type: none"> ➢ Combustion or incineration for energy recovery (option for old scrap) 	<ul style="list-style-type: none"> ➢ Commercialization (e.g. ERCOM (Germany), Phoenix Fibreglass (Canada))
	Chemical recycling	<ul style="list-style-type: none"> ➢ Dissolution of matrix ➢ Fluidised-bed thermal process for fibre recovery ➢ Fibre breakage – property degradation 	<ul style="list-style-type: none"> ➢ Promising Technology
	Remelting and remoulding	<ul style="list-style-type: none"> ➢ No separation of matrix from the fibre ➢ Regrinding – compression or injection moulding/extrusion – compression moulding ➢ Product as pellets or flakes for moulding ➢ Fibre breakage – property degradation 	<ul style="list-style-type: none"> ➢ Laboratory scale, promising technology

Fig. 6 Two recycling methods for composites. (Adopted from Yang et al. 2012)

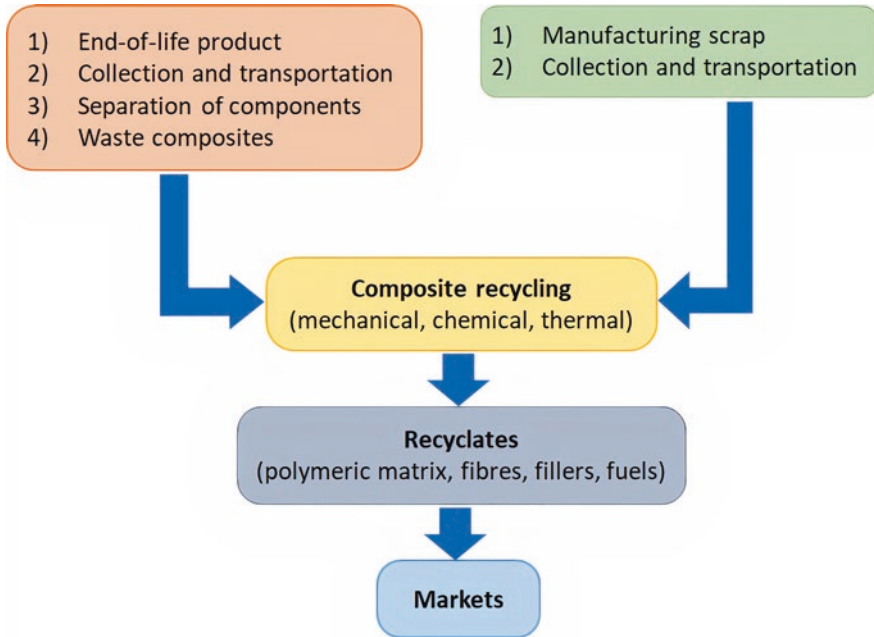


Fig. 7 The recycling processes for composites. (Adopted from Yang et al. 2012)

4 Properties of Recycled Biocomposites

There are two types of polymers, namely thermosets and thermoplastics. Thermoplastics are usually used in daily life such as the large range of plastic products due to their affordable price, lightweight, low density, user-friendly design, high strength, and durability (Grigore 2017). The three types of thermoplastics are crystalline, amorphous, and semi-crystalline (Nicholson 2017). It is important to note that plastics have some drawbacks despite their numerous benefits and these include the difficulty in degrading, thereby leading to their accumulation in landfills and the subsequent effect on the natural ecosystems (Grigore 2017). Therefore, this makes the recycling processes an interesting idea to solve this problem.

Previous studies have been conducted on recycling processes, specifically with the focus on biocomposite components, and recycled biocomposites were reported to have many advantages in the automotive industries (Mohanty et al. 2018) but require good properties to ensure their continuous application. The mechanical properties of some biocomposites are presented in Table 2 while the practical advantages and benefits of the biocarbon in their application are described in Fig. 8.

Table 2 Several biocomposites and their properties

Types of fillers	Types of resins	Tensile strength (MPa)	Tensile modulus (GPa)	Impact strength (kJ/m ²)	References
Carbon fibers, jute fibers	Polylactic acid	57–185	5.1–19.5	–	Matsuzaki et al. (2016)
Flax fibers	Polybutylene succinate/polylactic acid	39–55	3.6–7.4	9.1–17.8	Bourmaud et al. (2015)
Glass fibers	Epoxy/acrylate	532	37	237	Hosseini et al. (2016)
Sisal fibers	Bio polyurethane	57–119	1.2–2.2	–	Bakare et al. (2010)
Wood, poultry litter biochar	Polypropylene	27	4.3	8.1	Das et al. (2016)
Flax fibers	Polypropylene	40	6.5	0.751	Oksman (2000)

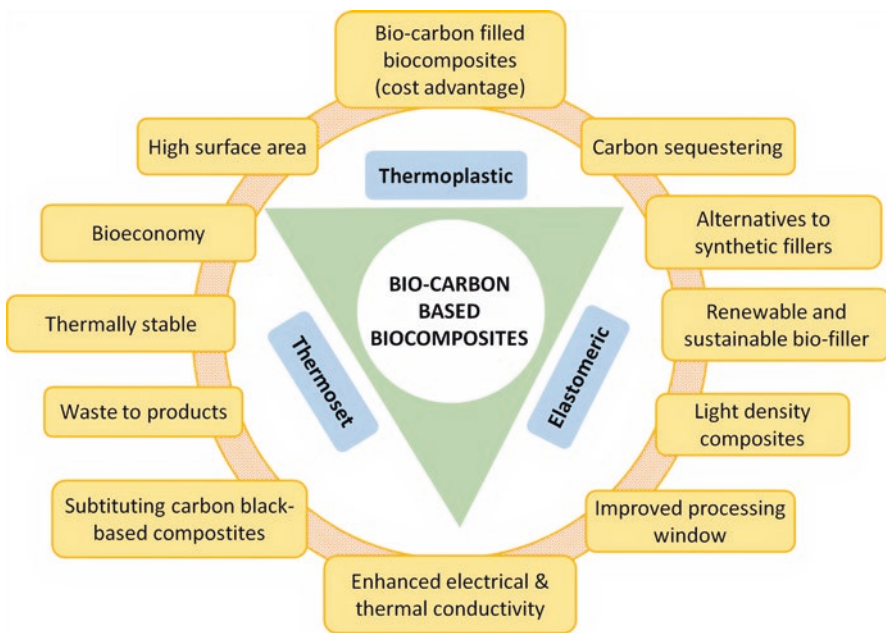


Fig. 8 Practical advantages and benefits of biocarbon in biocomposite applications. (Adopted from Chang et al. 2021)

5 Future Perspectives of Recycled Biocomposites

Previous explanations showed that biocomposites have several advantages which led to their wide application in automotive and construction industries (Gurunathan et al. 2015) due to the need to replace conventional composites with renewable and degradable materials. However, biocomposites need to be developed to make sure they have good functional and structural stability for storage and usage condition and also to degrade effectively after disposal (Satyanarayana et al. 2009). This means there is a need for more technologies to produce eco-friendly biocomposites using different efficient processes (Gurunathan et al. 2015).

Faruk et al. (2012) explained that the main obstacle to the commercialization of biocomposites in developing countries is the absence of study and development despite the abundance of natural resources for fibers in these areas. This means there is a need for more studies and development on the technology associated with biocomposite production as well as waste management (Gurunathan et al. 2015). This is necessary because the products need to be sustainable, biodegradable, recyclable, affordable, and have good mechanical properties to ensure wider applications.

The inclusion of natural materials as the main raw material in addition to synthetic ones such as plastics can also be a challenge to the wide-scale production of biocomposites due to the availability and sustainability of natural feedstock or biomass. This shows the need to plan the biomass supply chains with a focus on the strategies to be applied in harvesting, collecting, transporting, and also storing the biomass (Mohanty et al. 2018). This is necessary because the availability and quality of raw materials usually affect the quality of biocomposites produced. Some other factors to be considered include the energy consumed during the manufacturing process, durability of the product, health impacts after using the product, the economic value, and the wastes (Álvarez-Chávez et al. 2012; Ilyas et al. 2021a, b, c).

6 Conclusions

High usage of conventional composites is creating new problems for the environment due to their nonbiodegradability and this led to the introduction of biocomposites because they use natural or biomaterials as their filler. These biocomposites can be applied in several industries such as healthcare, food packaging, and automotive, but the availability and sustainability of green materials have been discovered to be the challenge to the mass production of these materials. Moreover, there is the need to consider the quality and economic feasibility due to the importance of these factors to the consumers and also to maintain the end-of-life recycling and disposal of the products to prevent new harmful impacts on the environment and achieve their purpose of being alternative eco-friendly materials.

References

- AccessScience, AccessScience Editors O P (2017) Plastic waste pollution. McGraw-Hill Education. <https://doi.org/10.1036/1097-8542.BR0802171>
- Akampunguza O, Wambua PM, Ahmed A, Li W, Qin X-H (2017) Review of the applications of biocomposites in the automotive industry. *Polym Compos* 38(11):2553–2569. <https://doi.org/10.1002/pc.23847>
- Álvarez-Chávez CR, Edwards S, Moure-Eraso R, Geiser K (2012) Sustainability of bio-based plastics: General comparative analysis and recommendations for improvement. *J Clean Prod* 23(1):47–56. <https://doi.org/10.1016/j.jclepro.2011.10.003>
- Badia JD, Strömberg E, Karlsson S, Ribes-Greus A (2012) Material valorisation of amorphous polylactide. Influence of thermo-mechanical degradation on the morphology, segmental dynamics, thermal and mechanical performance. *Polym Degrad Stab* 97(4):670–678. <https://doi.org/10.1016/j.polymdegradstab.2011.12.019>
- Bakare IO, Okieimen FE, Pavithran C, Abdul Khalil HPS, Brahmakumar M (2010) Mechanical and thermal properties of sisal fiber-reinforced rubber seed oil-based polyurethane composites. *Mater Des* 31(9):4274–4280. <https://doi.org/10.1016/j.mates.2010.04.013>
- Beigbeder J, Soccalingame L, Perrin D, Bénézet JC, Bergeret A (2019) How to manage biocomposites wastes end of life? A life cycle assessment approach (LCA) focused on polypropylene (PP)/wood flour and polylactic acid (PLA)/flax fibres biocomposites. *Waste Manag* 83:184–193. <https://doi.org/10.1016/j.wasman.2018.11.012>
- Bourmaud A, Corre YM, Baley C (2015) Fully biodegradable composites: use of poly-(butylene-succinate) as a matrix and to plasticize l-poly-(Lactide)-flax blends. *Ind Crop Prod* 64(1):251–257. <https://doi.org/10.1016/j.indcrop.2014.09.033>
- Chaitanya S, Singh I, Song JI (2019) Recyclability analysis of PLA/sisal fiber biocomposites. *Compos Part B* 173(April):106895. <https://doi.org/10.1016/j.compositesb.2019.05.106>
- Chandrasekar M, Kumar TSM, Senthilkumar K, Radoor S, Ilyas RA, Sapuan SM et al (2021) Performance of natural fiber reinforced recycled thermoplastic polymer composites under aging conditions. In: Ilyas RA, Sapuan SM, Bayraktar E (eds) *Recycl. Plast. Met. Their compos*, 1st edn. CRC Press/Taylor & Francis Group, Boca Raton, p 13
- Chang BP, Rodriguez-Urbe A, Mohanty AK, Misra M (2021) A comprehensive review of renewable and sustainable bioinsourced carbon through pyrolysis in biocomposites uses: current development and future opportunity. *Renew Sustain Energy Rev* 152(September):111666. <https://doi.org/10.1016/j.rser.2021.111666>
- Corbière-Nicollier T, Gfeller Laban B, Lundquist L, Leterrier Y, Månson JAE, Joliet O (2001) Life cycle assessment of biofibres replacing glass fibres as reinforcement in plastics. *Resour Conserv Recycl* 33(4):267–287. [https://doi.org/10.1016/S0921-3449\(01\)00089-1](https://doi.org/10.1016/S0921-3449(01)00089-1)
- Das O, Sarmah AK, Bhattacharyya D (2016) Biocomposites from waste-derived biochars: mechanical, thermal, chemical, and morphological properties, vol 49. *Waste Management*, New York, pp 560–570. <https://doi.org/10.1016/j.wasman.2015.12.007>
- Das O, Kim NK, Hedenqvist MS, Lin RJT, Sarmah AK, Bhattacharyya D (2018a) An attempt to find a suitable biomass for biochar-based polypropylene biocomposites. *Environ Manag* 62(2):403–413. <https://doi.org/10.1007/s00267-018-1033-6>
- Das O, Loho TA, Capezza AJ, Lemrhari I, Hedenqvist MS (2018b) A novel way of adhering PET onto protein (wheat gluten) plastics to impart water resistance. *Coatings* 8(11). <https://doi.org/10.3390/COATINGS8110388>
- Das O, Hedenqvist MS, Johansson E, Olsson RT, Loho TA, Capezza AJ et al (2019) An all-gluten biocomposite: comparisons with carbon black and pine char composites. *Compos A: Appl Sci Manuf* 120:42–48. <https://doi.org/10.1016/j.compositesa.2019.02.015>
- Dhakal HN, Ismail SO, Zhang Z, Barber A, Welsh E, Maignet J-E et al (2018) Development of sustainable biodegradable lignocellulosic hemp fiber/polycaprolactone biocomposites for light weight applications. *Compos A: Appl Sci Manuf* 113:350–358. <https://doi.org/10.1016/j.compositesa.2018.08.005>

- Faruk O, Bledzki AK, Fink HP, Sain M (2012) Biocomposites reinforced with natural fibers: 2000–2010. *Prog Polym Sci* 37(11):1552–1596. <https://doi.org/10.1016/j.progpolymsci.2012.04.003>
- Frischknecht R (2010) LCI modelling approaches applied on recycling of materials in view of environmental sustainability, risk perception and eco-efficiency. *Int J Life Cycle Assess* 15(7):666–671. <https://doi.org/10.1007/s11367-010-0201-6>
- Gigante V, Seggiani M, Cinelli P, Signori F, Vania A, Navarini L et al (2021) Utilization of coffee Silverskin in the production of poly(3-Hydroxybutyrate-co-3-Hydroxyvalerate) biopolymer-based thermoplastic biocomposites for food contact applications. *Compos A: Appl Sci Manuf* 140:106172. <https://doi.org/10.1016/j.compositesa.2020.106172>
- Grigore ME (2017) Methods of recycling, properties and applications of recycled thermoplastic polymers. *Recycling* 2(4):1–11. <https://doi.org/10.3390/recycling2040024>
- Gurunathan T, Mohanty S, Nayak SK (2015) A review of the recent developments in biocomposites based on natural Fibres and their application perspectives. *Compos A: Appl Sci Manuf* 77:1–25. <https://doi.org/10.1016/j.compositesa.2015.06.007>
- Hosseini N, Webster DC, Ulven C (2016) Advanced biocomposite from highly functional Methacrylated Epoxidized Sucrose Soyate (MAESS) resin derived from vegetable oil and fiberglass fabric for composite applications. *Eur Polym J* 79:63–71. <https://doi.org/10.1016/j.eurpolymj.2016.04.012>
- Ilyas RA, Sapuan SM, Bayraktar E (2021a) Recycling of plastics, metals, and their composites, 1st edn. CRC Press, Boca Raton. <https://doi.org/10.1201/9781003148760>
- Ilyas RA, Sapuan SM, Jailani AK, Yusof AHM, Norizan MN, Norrahim MNF et al (2021b) Introduction to recycling of polymers and metal composites. In: Ilyas RA, Sapuan SM, Bayraktar E (eds) *Recycl. Plast. Met. Their Compos*, 1st edn. CRC Press/Taylor & Francis Group, Boca Raton, p 35
- Ilyas RA, Sapuan SM, Sabaruddin FA, Atikah MSN, Ibrahim R, Asyraf MRM, Ainun ZMA (2021c) Reuse and recycle of biobased packaging products. *Bio-based Packaging*, pp 413–426. <https://doi.org/10.1002/9781119381228.ch23>
- Imgharn A, Ighnih H, Hsini A, Naciri Y, Laabd M, Kabli H et al (2021) Synthesis and characterization of polyaniline-based biocomposites and their application for effective removal of orange G dye using adsorption in dynamic regime. *Chem Phys Lett* 778:138811. <https://doi.org/10.1016/j.cplett.2021.138811>
- Jędrzejczak P, Puzska A, Kubiak A, Podkościelna B, Klapiszewski Ł (2021) New lignin-based hybrid materials as functional additives for polymer biocomposites: from design to application. *Int J Biol Macromol* 190:624–635. <https://doi.org/10.1016/j.ijbiomac.2021.09.025>
- Kumar A, Jyske T, Möttönen V (2020) Properties of injection molded biocomposites reinforced with wood particles of short-rotation Aspen and willow. *Polymers* 12(2). <https://doi.org/10.3390/polym12020257>
- Kun D, Pukánszky B (2017) Polymer/lignin blends: interactions, properties, applications. *Eur Polym J* 93 (December 2016): 618–641. doi:<https://doi.org/10.1016/j.eurpolymj.2017.04.035>
- Le Duigou A, Pillin I, Bourmaud A, Davies P, Baley C (2008) Effect of recycling on mechanical behaviour of biocompostable flax/poly(l-Lactide) composites. *Compos A: Appl Sci Manuf* 39(9):1471–1478. <https://doi.org/10.1016/j.compositesa.2008.05.008>
- Liu S, Qin S, He M, Zhou D, Qin Q, Wang H (2020) Current applications of poly(lactic acid) composites in tissue engineering and drug delivery. *Compos Part B* 199:108238. <https://doi.org/10.1016/j.compositesb.2020.108238>
- Malnati P (2018) Recycled waste products get new life as lightweight. *Cost-Effective Auto Parts Plastic Eng* 74(6):18–25. <https://doi.org/10.1002/j.1941-9635.2018.tb01899.x>
- Matsuzaki R, Ueda M, Namiki M, Jeong T-K, Asahara H, Horiguchi K et al (2016) Three-dimensional printing of continuous-fiber composites by in-nozzle impregnation. *Sci Rep* 6(1):23058. <https://doi.org/10.1038/srep23058>

- Mohanty AK, Vivekanandhan S, Pin JM, Misra M (2018) Composites from renewable and sustainable resources: challenges and innovations. *Science* 362(6414):536–542. <https://doi.org/10.1126/science.aat9072>
- Nicholson JW (2017) The chemistry of polymers. The Royal Society of Chemistry
- Oksman K (2000) Mechanical properties of natural fibre mat reinforced thermoplastic. *Appl Compos Mater* 7(5):403–414. <https://doi.org/10.1023/A:1026546426764>
- Pennington DW, Potting J, Finnveden G, Lindeijer E, Jolliet O, Rydberg T et al (2004) Life cycle assessment part 2: current impact assessment practice. *Environ Int* 30(5):721–739. <https://doi.org/10.1016/j.envint.2003.12.009>
- Righetti MC, Cinelli P, Mallegni N, Massa CA, Aliotta L, Lazzeri A (2019) Thermal, mechanical, viscoelastic and morphological properties of poly(lactic acid) based biocomposites with potato pulp powder treated with waxes. *Materials* 12(6). <https://doi.org/10.3390/ma12060990>
- Roy P, Defersha F, Rodriguez-Urbe A, Misra M, Mohanty AK (2020) Evaluation of the life cycle of an automotive component produced from biocomposite. *J Clean Prod* 273:123051. <https://doi.org/10.1016/j.jclepro.2020.123051>
- Rybicka J, Tiwari A, Leeke GA (2016) Technology readiness level assessment of composites recycling technologies. *J Clean Prod* 112:1001–1012. <https://doi.org/10.1016/j.jclepro.2015.08.104>
- Sajjan SM, Bongale VKA, Yogesha DB (2020) Natural fiber reinforced polymer composites for automobile applications: recent trends. *Int Res J Eng Technol* 07(11):1101–1113. <https://doi.org/10.3844/ajessp.2013.494.504>
- Sakthiguru N, Sithique MA (2020) Fabrication of bioinspired chitosan/gelatin/Allantoin biocomposite film for wound dressing application. *Int J Biol Macromol* 152:873–883. <https://doi.org/10.1016/j.ijbiomac.2020.02.289>
- Salwa HN, Sapuan SM, Mastura MT, Zuhri MYM, Ilyas RA (2021) Life cycle assessment (LCA) of recycled polymer composites. In: Ilyas RA, Sapuan SM, Bayraktar E (eds) *Recycl. Plast. Met. Their Compos*, 1st edn. CRC Press/Taylor & Francis Group, Boca Raton, p 15
- Satyanarayana KG, Arizaga GGC, Wypych F (2009) Biodegradable composites based on lignocellulosic fibers—an overview. *Prog Polym Sci* 34(9):982–1021. <https://doi.org/10.1016/j.progpolymsci.2008.12.002>
- Shanmugam V, Das O, Neisiany RE, Babu K, Singh S, Hedenqvist MS, Berto F, Ramakrishna S (2020) Polymer recycling in additive manufacturing: an opportunity for the circular economy. *Mater Circular Econ* 2(1). <https://doi.org/10.1007/s42824-020-00012-0>
- Shanmugam V, Mensah RA, Försth M, Sas G, Restás Á, Addy C et al (2021) Circular economy in biocomposite development: state-of-the-art, challenges and emerging trends. *Composites Part C: Open Access* 5(March):100138. <https://doi.org/10.1016/j.jcomc.2021.100138>
- Sheldon RA, Norton M (2020) Green chemistry and the plastic pollution challenge: towards a circular economy. *Green Chem* 22(19):6310–6322. <https://doi.org/10.1039/D0GC02630A>
- Soccalingame L, Perrin D, Bénézet J-C, Mani S, Coiffier F, Richaud E et al (2015) Reprocessing of artificial UV-weathered wood flour reinforced polypropylene composites. *Polym Degrad Stab* 120:313–327. <https://doi.org/10.1016/j.polymdegradstab.2015.07.013>
- Song YS, Youn JR, Gutowski TG (2009) Life cycle energy analysis of fiber-reinforced composites. *Compos A: Appl Sci Manuf* 40(8):1257–1265. <https://doi.org/10.1016/j.compositesa.2009.05.020>
- Srebrnkoska V, Gaceva GB, Avella M, Errico ME, Gentile G (2008) Recycling of polypropylene-based eco-composites. *Polym Int* 57(11):1252–1257. <https://doi.org/10.1002/pi.2470>
- Sridevi S, Sutha S, Kavitha L, Gopi D (2021) Valorization of biowaste-derived nanophase yttrium-substituted hydroxyapatite/citrate cellulose/opuntia mucilage biocomposite: a template assisted synthesis for potential biomedical applications. *Mater Chem Phys* 273(April):125144. <https://doi.org/10.1016/j.matchemphys.2021.125144>
- Sundarakannan R, Arumugaprabu V, Manikandan V, Vigneshwaran S (2020) Mechanical property analysis of biochar derived from cashew nut Shell waste reinforced polymer matrix. *Mater Res Express* 6(12):125349. <https://doi.org/10.1088/2053-1591/ab6197>

- Temmink R, Baghaei B, Skrifvars M (2018) Development of biocomposites from denim waste and thermoset bio-resins for structural applications. *Compos A: Appl Sci Manuf* 106:59–69. <https://doi.org/10.1016/j.compositesa.2017.12.011>
- Xu W, Peng J, Ni D, Zhang W, Wu H, Mu W (2020) Preparation, characterization and application of Levan/montmorillonite biocomposite and Levan/BSA nanoparticle. *Carbohydr Polym* 234:115921. <https://doi.org/10.1016/j.carbpol.2020.115921>
- Yang Y, Boom R, Irion B, van Heerden DJ, Kuiper P, de Wit H (2012) Recycling of composite materials. *Chem Eng Process Process Intensif* 51:53–68. <https://doi.org/10.1016/j.cep.2011.09.007>
- Zarna C, Opedal MT, Echtermeyer AT, Chinga-Carrasco G (2021) Reinforcement ability of lignocellulosic components in biocomposites and their 3D printed applications – a review. *Composites Part C: Open Access* 6:100171. <https://doi.org/10.1016/j.jcomc.2021.100171>
- Zini E, Scandola M (2011) Green composites: an overview. *Polym Compos* 32(12):1905–1915. <https://doi.org/10.1002/pc.21224>

Recycled Polyethylene Blends and Composites: Current Trend, Technology, and Challenges



Yamuna Munusamy, Zunaida Zakaria, Hanafi Ismail,
and Nor Azura Abdul Rahim

1 Polyethylene Blends and Composite Consumption

Polyethylene (PE) could be classified into four types based on its structure, molecular weight, and crystallinity; low-density polyethylene (LDPE), linear low-density polyethylene (LLDPE), high-density polyethylene (HDPE), and ultrahigh molecular weight polyethylene (UHMWPE). PE is the most widely used polymer worldwide, and in 2019, the annual production and consumption of PE is higher than 100 million tons. This figure accounts for 40% of the total consumption of thermoplastic polymers (Gaurh and Pramanik 2018). PE is used in wide range of applications as shown in Fig. 1. PE is often blended with various thermoplastics, elastomers, and fillers to produce blends and composites. Examples of PE blends and composites are listed in Table 1.

Y. Munusamy (✉)

Faculty of Engineering and Green Technology, Universiti Tunku Abdul Rahman,
Jalan Universiti, Kampar, Perak, Malaysia
e-mail: yamunam@utar.edu.my

Z. Zakaria · N. A. A. Rahim

Fakulti Teknologi Kejuruteraan Kimia, Universiti Malaysia Perlis, Arau, Perlis, Malaysia

H. Ismail

School of Materials and Mineral Resources Engineering, Engineering Campus,
Universiti Sains Malaysia, Nibong Tebal, Penang, Malaysia



Fig. 1 Products from PE

2 Polyethylene Blends and Composite Waste

PE blends and composite waste could be classified into two types which are the postindustrial scraps which are generated during the manufacturing process and postconsumer waste which is generated by end users. According to statistics, PE contributes to 69% of all plastic waste especially in the form of packaging materials (Gaurh and Pramanik 2018). It is harder to recycle postconsumer PE products. The postconsumer PE products are often collected as mixed waste which leads to incineration for energy recovery or recycled through open-loop recycling which results in low-quality end products. Postconsumer material also consists contamination which causes color changes or imparts odor to recycled products. The postconsumer PE waste is normally cleaned using absorber, biological treatment technology, and specialized washing techniques.

3 PE Waste Treatment Options

PE waste treatment options could be divided into options shown in Fig. 2. For each recycling pathway, the circular economy performance indicator is calculated based on minimal required effort in the recycling process. In that perspective, close-loop recycling is the best option while incineration is the least. Another indicator that often been used is recyclability benefit rate indicators which are expressed by the potential environmental saving by the choice of recycling method compared with virgin material production or disposal of material to landfill. Study shows that

Table 1 Example of PE composites and blends

Polymer blends or composites	Properties	Reference
Blends		
PE Rigidex™ or Innovex™ blended with liquid crystal polyester	Good melt processability, reduction of specific energy during compounding, and reduction of viscosity.	Akkapeddi (2014)
PE copolymer blended with ethylene propylene diene monomer (EPDM), PP, and talc	Excellent moldability and surface finish. Improved hardness and good impact resistance.	Utracki (2003)
PP blended with LLDPE and ethylene-butene plastomer	The blend is used for melt-spun or melt-blown fibers and fabrics. The blends showed good processability, resistance to tearing, and tensile strength.	Utracki et al. (2014)
LLDPE blended with starch and ionic compound	The blend is used to produce weldable and sealable multilayer films. Starch improved biodegradation of the blend.	Utracki (2014)
HDPE blended with acrylonitrile-butadiene copolymer	The blend is used for injection-molded plastic bottles, automobile gasoline tanks, and other containers having limited or restricted permeability to gases, vapors, or organic liquids. These materials also showed good chemical resistance, strength, and processability.	Utracki (2014)
LLDPE blended with PMMA	The blends were found to produce blown films with improved tear in the machine direction, modulus, and impact strength.	Utracki et al. (2014)
Composites		
PE filled with aluminum hydroxide (ATH) or magnesium hydroxide (MH) up to 60 wt.%	Improvement of flame retardancy	Hippi et al. (2003)
UHMWPE reinforced with carbon fiber	CF improves the strength, wear, and abrasion resistance of the composite for tribotechnical materials.	Gogoleva et al. (2019)
Injection-molded HDPE biocomposites with rice straw	Addition of rice straw has increased the tensile and flexural modulus.	Rahman et al. (2009)
LDPE filled with ultrafine iron (Fe)	Produce multifunctional materials that respond to external mechanical pressure and magnetic field, as well as have radio-absorbing properties.	Kabirov et al. (2021)
LLDPE filled with calcium carbonate and talc	LLDPE used to produce cast films is filled with high amount of calcium carbonate and talc to reduce the cost of the product.	Barczewski et al. (2016)

close-loop recycling has 60% environmental benefits compared to virgin material production while open-loop recycling shows 26–39% environmental benefits (Larrain et al. 2020). However, in terms of economic performance in plastic blend or mixed plastic system, open-loop recycling has better economic performance than close-loop system (Salwa et al. 2022).

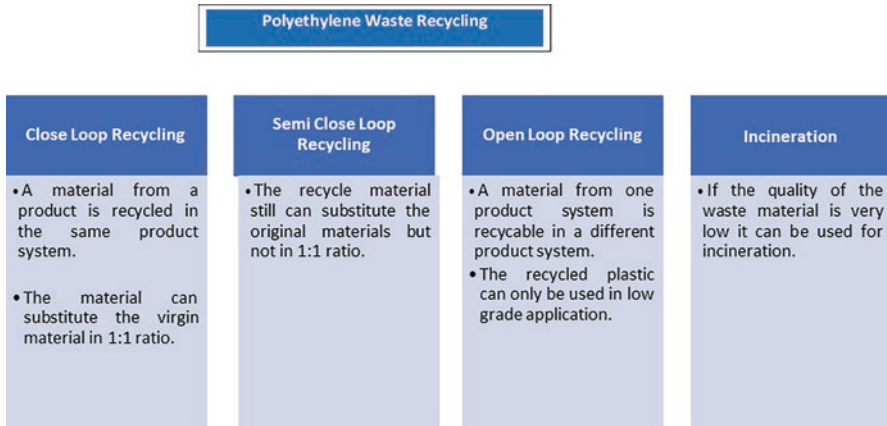


Fig. 2 Options for recycling of PE

3.1 Close-Loop Recycling of PE Composites

PE composites are made of two or more materials with distinct phase such as matrix and fillers. The phases are mixed together and thus it is not worthwhile to separate them and recycle. The most economical route will be to reprocess the composite through melt mixing and used it for new product development (Grigore 2017).

Many studies reported reduction of molecular weights and chain entanglement in neat PE due to recycling which then leads to reduction in elastic properties (Ilyas et al. 2022). Macroradicals are formed during repeated reprocessing. In recycling of neat HDPE, chain branching is reported as the main structural change during first 30 recycling process through extrusion. After 30 cycles, chain scission takes place and after 60 cycles cross-linking occurs. While in recycling of neat LDPE, 100 reprocessing cycles cause thermal degradation and gelation caused by chain scission, reticulation, and branching. In HDPE, chain scission is the dominant structural change while in LDPE, branching and reticulation are the main structural changes (Benoit et al. 2017). The dominant degradation pathway of PE could be determined by studying the shear rheology of the material during reprocessing. Large changes in the zero-shear viscosity (η_0) regions indicate structural changes due to chain entanglement; however, significant change to the onset of shear thinning or time relaxation (λ) and the width of the transition zone between zero-shear rate region and power law region (a) will indicate degradation due to main chain session (Berzin et al. 2001).

In recycling of natural fiber PE composites, properties such as fiber dimensions, polymer matrix number average molecular mass, crystallinity, and viscosity are largely affected (Chandrasekar et al. 2022). Appropriate choice of parameters during recycling such as screw rotational speed, throughput rate, and temperature profile in the barrel is crucial to minimize thermal degradation and color deterioration of natural fiber composites. Recycling of compatibilized composite system also

causes less deterioration of properties. Some study also reported that even though the recycled composite undergone chain scission, fiber breakup, and universal degradation, the mechanical properties are still at the considerable level and the composite could be used in industrial application (Berzin et al. 2001). All the reported work only consider recycling cycle less than 10. However due to these issues, most of the effort to recycle natural fiber PE composites involves dissolution of PE matrix and recovery of fibers (Maris et al. 2018).

The largest change in molecular weight of PE composites during recycling happens in the first cycle and does not show any particular trend in subsequent cycles. This is in contrary with recycling of neat PE where continuous reduction in molecular weight will be observed. A study conducted by Kabamba et al. (2011) shows that the η_0 of the recycled LDPE fiber composites is higher compared to recycled neat PE. The a , λ , and n for the PE composite are generally lower than the value for neat PE because addition of fiber reduces elasticity and fluidity of the polymer matrix. It is noteworthy that these values increase with reprocessing cycles. Moreover, the differences between η_0 of neat PE and composite PE decrease as the number of reprocessing increases. The observe change in rheological properties is caused by the decreasing fiber length due to reprocessing. The elongational strains in the extruder are mostly transferred to the PE matrix while the shear strains are subjected to the fibers to cause breakage. Some works have reported that the usage of coupling agent or compatibilizer could reduce fiber breakage during reprocessing by improving the transfer of shear strain to PE matrix (Gosselin et al. 2006). However, all the other mechanical properties will be higher for recycled neat PE compared to PE composites at all reprocessing cycle.

In recent years, attention is also given to recycling of PE nanocomposites due to the increment in the production of these materials for industrial and consumer usage. Studies found that in nanocomposites, the dispersion of the nanofillers improves due to repeat extrusion and the degradation of the polymer matrix is also influenced by degradation of modifiers on the nanofillers (Stan et al. 2017). Modifiers are often used to improve the dispersion of the nanofillers in polymer matrix and increase the interaction between the filler and matrix. The findings on PE nanocomposite recycling show that the properties of PE nanocomposite recycled products are depended on the degradation of each component and recycling parameters as shown in Table 2. The influence of several factors on recycling of PE composite and nanocomposites is shown in Fig. 3.

3.2 Close-Loop Recycling of Polymer Blends

Blends of HDPE, LDPE with PP are used vastly and cause major waste stream. In this type of blends, the polymers are hard to be separated from each other during recycling due to their similar densities. In a close-loop recycling of these blends, the properties of the recycled products are mainly depended on the compatibility between the phases. Factors such as reduction of molecular weight, detachment,

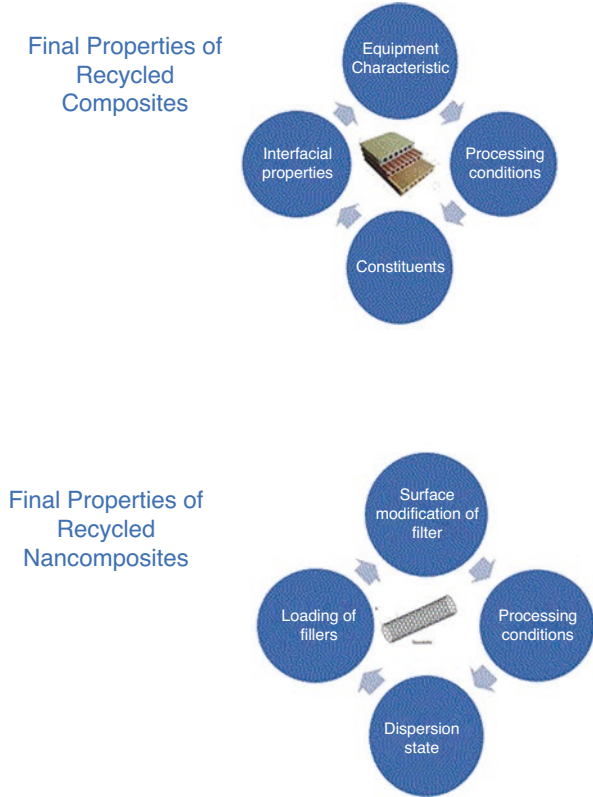
Table 2 Recycling of PE nanocomposites

Nanocomposite system	Effect of recycling	Reference
LDPE/organically modified nanoclay nanocomposites. Four extrusion cycle at different temperature (low 160 °C and high 210 °C).	At low-processing temperature, the viscosity increases after reprocessing because the dispersion of nanoclay was improved. At high-processing temperature, the viscosity decreases after reprocessing due to disruption of intercalated structure of nanoclay. Degradation of organo-modified nanoclay through Hoffmann reaction.	Stan et al. (2017)
HDPE/carbon nanotubes (CNT) nanocomposite. Ten extrusion cycle	The mechanical properties of the neat HDPE and HDPE composites does not change much after ten cycles of extrusion. In fact, nanocomposite does not exhibit any reduction in molecular weight while in neat HDPE, a large reduction in molecular weight could be observed after ten extrusion cycle. It is noteworthy that the CNT were not surface modified. The loading of CNT was less than 3 wt.%	La Mantia et al. (2013)
HDPE/multiwall carbon nanotubes (MWCNT)	Below 3 wt.%, loading MWCNT reprocessing does not affect the properties of the composites. However, when the loading of MWCNT increases to be more than 3 wt.%, reprocessing caused large degradation due to percolation of MWCNT.	Svensson et al. (2020)

and changes of crystallinity can cause phase separation during recycling. Some of the approaches to reduce the effect of phase separation include usage of compatibilizer, chain extender, and radiation during melt extrusion of recycled products. For example, usage of gamma radiation on recycled LDPE/HDPE blends showed improvement in mechanical properties due to increment in compatibility between the two phases by cross-linking (Stan et al. 2021). Usage of modifiers and compatibilizers such as very low-density PE (VLDPE), ethylene vinyl acetate (EVA), and poly(1-butene) in HDPE-PP blends could improve the recycle ability of the blends (Miguez Suarez et al. 2000).

PE is also often used to produce multilayer films with polyethylene terephthalate (PET) and these layers are immiscible to each other. To increase the compatibility between these layers during film production, an intermediary polymer adhesive is added to tie the two layers together. The polymer adhesive has functional groups such as maleic anhydrides which can chemically react with the layers and form covalent bond or they could also form secondary bonding like hydrogen bonding. The compatibility between the layers could also be improved by using physical method such as ion sputtering, corona irradiation or plasma irradiation. The recycling of these multilayer films is very difficult due to the presence of adhesion between the layers. PE and PET could not be separated and thus need to be melt processed together during recycling to produce a product. However, melt processing PE and PET multilayer films results in product with poor mechanical properties due to immiscibility of the blend components which then causes phase separations. Thus, a compatibilizer with functional groups that can interact with the components

Fig. 3 Factors influencing recycling of PE composites and nanocomposites



of the blends or resembling PE or PET needs to be added when recycling the film. The properties of polymers blended with PE are also depended on the amount of PE loading. At loading less than 10 wt.%, PE was found not to influence the properties of the recycled blends (Tall et al. 1998).

Blending of PE with natural polymers such as starch is also quite common nowadays in order to produce a more environmentally friendly polymer (Saikrishnan et al. 2020). Thermoplastic starch was found to be stable and does not degrade up to ten extrusion cycles. LDPE blended with thermoplastic starch shows not much reduction in properties up to ten extrusion cycles. Imaging equipment shows reduction in the average size of thermoplastic starch-rich phase upon reprocessing. This increases the interaction between starch and LDPE phase. Addition of 50 wt.% starch led to 25% reduction in elastic modulus and tensile strength (Abioye and Obuekwe 2020). Oxidation of PE which then form groups with oxygen functional group also improves the interaction between PE and natural polymers.

Open-loop recycling becomes a choice when the PE composite and blends could not be melt processed again and used to substitute the virgin PE. Often in open-loop recycling, the composite or blends are mixed in some proportion together with virgin plastic or other forms of materials. The waste composite and blends will be

Table 3 Additives used in open-loop recycling of PE multilayer films

Film components	Additives	Reference
PA/PE	PP-based elastomer—Viscosity modifier elastomer Talc filler	Eriksen et al. (2019)
PET/HDPE	Ethylene-glycidyl-methacrylate (EGMA) Ethylene-butylene-styrene-grafted with maleic anhydride (SEBS-g-MA)	Pawlak et al. (2002)
PET/PE	EGMA and copolymer of ethylene- α -olefin grafted with maleic anhydride (PE-g-MA)	Uehara et al. (2015)

either melt reprocessed and blended with other thermoplastics or grinded to powder and mixed with thermosets, rubber or even materials such as cement. For instance, LDPE composites could be dissolved in a solvent, quenched, and powdered. The PE powder then could be mixed into cement matrix. Addition of PE powder into cement was found to increase fracture toughness of the cement product.

Open-loop recycling is also popular in multilayer PE composite films used for packaging purposes. The layers are physically attached, thus each polymer components are hard to be separated from each other. Therefore, they are processed together as mixture most of the time. The polymers used to produce these layers are not miscible to each other due to difference in polarity or chemical structure such as PE/PA or PE/PET multilayer films. Melting these films for recycling will produce immiscible blend. The immiscibility between different polymers will have negative effect on mechanical properties and processability which makes recycling challenging. Thus, in open-loop recycling of multilayer films, additives such as compatibilizer are often used. Compatibilizer improves the interaction between the immiscible component. The mechanical properties of recycled blends are improved by improving the interphase adhesion between the immiscible component of the blends. In addition, additives such as viscosity modifier, plasticizer, stabilizer, and mineral fillers are also often added. The common additives used in recycling of multilayer PE films are shown in Table 3.

Delamination method is also used to segregate the different layers of films and recycling the polymer multilayer films separately. The adhesive between the layers is dissolved using specific solvent. Research is also conducted to improve delamination of multilayer PE film by using protein-based adhesive as substitute for common adhesive. The protein layer can be removed by washing the film with enzymatic detergents (Uehara et al. 2015).

4 Challenges and Future Perspective in PE Composites and Blends Recycling

The main challenges faced by recycling of composites are lack of adequate market, high cost of recycling, and low quality of recycled products. Extensive R&D has to be carried out to develop better recyclable composites. The separation of plastic waste

stream also needs to be improved. A synergistic effort is required from design aspect, manufacturing method, and end-of-life management for the composites to be recycled. The current available recycling technologies have difficulties to meet requirements from products quality, environment regulations, and operation economics.

Innovations are necessary areas listed below to increase the recyclability of composites:

- (i) Development of new and easily recyclable composite materials
- (ii) Development of more intensified separation and purification technique
- (iii) Environmental legislation to recycle composites

In terms of collection and transport of PE composites and blends, an efficient system is required for collection of both postindustrial and postconsumer scrap. The product has to be cut and shredded to smaller size for easy handling. Insufficient collect rate and small volume of collection will reduce the interest of industry to use recycled PE composite and blends. Market requirement for high quality and price competitive of recycled product compared to virgin material is another important factor, especially when the price of virgin material fluctuates (Sabau 2018).

5 Conclusions

In general, PE composite and blends could be classified into two category; postindustrial and postconsumer scrap. This type of waste could be recycled through four approaches; close-loop recycling, semi close-loop recycling, open-loop recycling, and incineration. Close-loop recycling shows minimal required effort for recycling while incineration shows maximum effort based on circular economy indicators. Close-loop recycling also shows more environmental benefits compared to open-loop recycling of PE. In close-loop recycling of PE composites, the properties of recycle products are dependent on equipment design, processing parameters, filler properties, and loading. While in close-loop recycling of PE blends, the properties of recycle products are mainly dependent on compatibility between phases. Open-loop recycling becomes a choice when PE composites and blends cannot be melt processed again to substitute virgin PE in a product. However, development of new and easily recyclable composite materials and better separation technology of waste streams could drive closer-loop recycling of composite and blends.

References

- Abioye AA, Obuekwe CC (2020) Investigation of the biodegradation of low-density polyethylene-starch bi-polymer blends. *Results Eng* 5:100090. <https://doi.org/10.1016/j.rineng.2019.100090>
- Akkapeddi MK (2014) Commercial polymer blends. In: Utracki L, Wilkie C (eds) *Polymer blends handbook*. Springer, Dordrecht. https://doi.org/10.1007/978-94-007-6064-6_22
- Barczewski M, Lewandowski K, Schmidt M, Szostak M (2016) Melt fracture and rheology of linear low-density polyethylene – calcium carbonate composites. *Polymer Eng Sci* 57:998–1004. <https://doi.org/10.1002/pen.24477>

- Benoit N, González-Núñez R, Rodrigue D (2017) High-density polyethylene degradation followed by closed-loop recycling. *Prog Rubber Plast Recycl Technol* 33:17–38. <https://doi.org/10.1177/147776061703300102>
- Berzin F, Vergnes B, Delamare L (2001) Rheological behavior of controlled-rheology polypropylenes obtained by peroxide-promoted degradation during extrusion: comparison between homopolymer and copolymer. *J Appl Polym Sci* 80:1243–1252. <https://doi.org/10.1002/app.1210>
- Chandrasekar M, Kumar TSM, Senthilkumar K et al (2022) Performance of natural fiber reinforced recycled thermoplastic polymer composites under aging conditions. In: *Recycling of plastics, metals, and their composites*. CRC Press
- Eriksen MK, Christiansen JD, Daugaard AE, Astrup TF (2019) Closing the loop for PET, PE and PP waste from households: influence of material properties and product design for plastic recycling. *Waste Manag* 96:75–85. <https://doi.org/10.1016/j.wasman.2019.07.005>
- Gaurh P, Pramanik H (2018) A novel approach of solid waste management via aromatization using multiphase catalytic pyrolysis of waste polyethylene. *Waste Manag* 71:86–96. <https://doi.org/10.1016/j.wasman.2017.10.053>
- Gogoleva OV, Petrova PN, Kolesova ES (2019) Development of polymer composite materials based on ultrahigh-molecular weight polyethylene and carbon fillers. *Mater Sci Forum* 945:362–368. <https://doi.org/10.4028/www.scientific.net/msf.945.362>
- Gosselin R, Rodrigue D, Riedl B (2006) Injection molding of postconsumer wood–plastic composites I: morphology. *J Thermoplast Compos Mater* 19:639–657. <https://doi.org/10.1177/08927057060067484>
- Grigore M (2017) Methods of recycling, properties and applications of recycled thermoplastic polymers. *Recycling* 2:24. <https://doi.org/10.3390/recycling2040024>
- Hippi U, Mattila J, Korhonen M, Seppälä J (2003) Compatibilization of polyethylene/aluminum hydroxide (PE/Ath) and polyethylene/magnesium hydroxide (PE/MH) composites with functionalized polyethylenes. *Polymer* 44:1193–1201. [https://doi.org/10.1016/s0032-3861\(02\)00856-x](https://doi.org/10.1016/s0032-3861(02)00856-x)
- Ilyas RA, Sapuan SM, Jailani AK et al (2022) Introduction to recycling of polymers and metal composites. *Recycling of plastics, metals, and their composites*. CRC Press, Boca Raton
- Kabirov Y, Sidorenko E, Prutsakova N et al (2021) Elasto-elastic composite materials with a polymer matrix based on ultrafine iron and polyethylene. *Letter Mater* 11:17–21. <https://doi.org/10.22226/2410-3535-2021-1-17-21>
- La Mantia FP, Mistretta MC, Morreale M (2013) Recycling and thermomechanical degradation of LDPE/modified clay nanocomposites. *Macromol Mater Eng* 299:96–103. <https://doi.org/10.1002/mame.201200449>
- Larrain M, Van Passel S, Thomassen G et al (2020) Economic performance of pyrolysis of mixed plastic waste: open-loop versus closed-loop recycling. *J Clean Prod* 270:122442. <https://doi.org/10.1016/j.jclepro.2020.122442>
- Maris J, Bourdon S, Brossard J-M et al (2018) Mechanical recycling: compatibilization of mixed thermoplastic wastes. *Polym Degrad Stab* 147:245–266. <https://doi.org/10.1016/j.polyimdegradstab.2017.11.001>
- Miguez Suarez JC, Biasotto Mano E, Abrahão Pereira R (2000) Thermal behavior of gamma-irradiated recycled polyethylene blends. *Polym Degrad Stab* 69:217–222. [https://doi.org/10.1016/s0141-3910\(00\)00065-3](https://doi.org/10.1016/s0141-3910(00)00065-3)
- Pawlak A, Morawiec J, Pazzagli F et al (2002) Recycling of postconsumer poly(ethylene terephthalate) and high-density polyethylene by compatibilized blending. *J Appl Polym Sci* 86:1473–1485. <https://doi.org/10.1002/app.11307>
- Rahman WA, Isa NM, Rahmat AR et al (2009) Rice husk/high-density polyethylene bio-composite: effect of rice husk filler size and composition on injection molding processability with respect to impact property. *Adv Mat Res* 83-86:367–374. <https://doi.org/10.4028/www.scientific.net/amr.83-86.367>
- Sabău E (2018) Recycling of polymeric composite materials. *Product Lifecycle Management - Terminology and Applications*. <https://doi.org/10.5772/intechopen.81281>

- Saikrishnan S, Jubinville D, Tzoganakis C, Mekonnen TH (2020) Thermo-mechanical degradation of polypropylene (PP) and low-density polyethylene (LDPE) blends exposed to simulated recycling. *Polym Degrad Stab* 182:109390. <https://doi.org/10.1016/j.polymdegradstab.2020.109390>
- Salwa HN, Sapuan SM, Mastura MT et al (2022) Life cycle assessment (LCA) of recycled polymer composites. Recycling of plastics, metals, and their composites. CRC Press, Boca Raton
- Stan F, Sandu LI, Fetecau C, Rosculeț R (2017) Effect of reprocessing on the rheological, electrical, and mechanical properties of polypropylene/carbon nanotube composites. *J Micro Nano-Manuf.* <https://doi.org/10.1115/1.4035955>
- Stan F, Sandu I-L, Turcanu A-M et al (2021) The influence of carbon nanotubes and reprocessing on the morphology and properties of high-density polyethylene/carbon nanotube composites, vol 2. Manufacturing Processes; Manufacturing Systems; Nano/Micro/Meso Manufacturing; Quality and Reliability. <https://doi.org/10.1115/msec2021-63499>
- Svensson S, Åkesson D, Bohlén M (2020) Reprocessing of high-density polyethylene reinforced with carbon nanotubes. *J Polym Environ* 28:1967–1973. <https://doi.org/10.1007/s10924-020-01739-2>
- Tall S, Albertsson A-C, Karlsson S (1998) Recycling of mixed plastic fractions: mechanical properties of multicomponent extruded polyolefin blends using response surface methodology. *J Appl Polym Sci* 70:2381–2390
- Twite-Kabamba E, Fehri ZF, Rodrigue D (2011) Properties of recycled LDPE/birch fibre composites. *Prog Rubber Plast Recycl Technol* 27:1–20. <https://doi.org/10.1177/147776061102700101>
- Uehara GA, França MP, Canevarolo SV Jr (2015) Recycling assessment of multilayer flexible packaging films using design of experiments. *Polímeros* 25:371–381. <https://doi.org/10.1590/0104-1428.1965>
- Utracki LA (2003) Introduction to polymer blends. In: Utracki LA (ed) *Polymer Blends Handbook*. Springer, Dordrecht. https://doi.org/10.1007/0-306-48244-4_1
- Utracki LA (2014) Polyethylenes and their blends. In: Utracki L, Wilkie C (eds) *Polymer blends handbook*. Springer, Dordrecht. https://doi.org/10.1007/978-94-007-6064-6_21
- Utracki LA, Mukhopadhyay P, Gupta RK (2014) Polymer blends: introduction. In: Utracki L, Wilkie C (eds) *Polymer blends handbook*. Springer, Dordrecht. https://doi.org/10.1007/978-94-007-6064-6_3

Recycled Polyethylene Terephthalate Blends and Composites: Impact of PET Waste, Engineering Design, and Their Applications



Zunaida Zakaria, Hakimah Osman, Nor Azura Abdul Rahim, Yamuna Munusamy, and Hanafi Ismail

1 Introduction

In 2020 alone, around 22.66 million metric tons of polyethylene terephthalate (PET) resin have been produced worldwide and the growth rate is expected to increase by 4% annually until 2025. PET is a general-purpose thermoplastic made of polyester (Zhang et al. 2020). Semi-aromatic PET is made by combining two monomers of modified ethylene glycol and purified terephthalic acid through synthesis. PET has a glass transition temperature of 67–81 °C and a melting point of 260 °C, and exists as an amorphous (transparent) or semicrystalline (opaque and white) thermoplastic

Z. Zakaria (✉)

Faculty of Chemical Engineering Technology, Universiti Malaysia Perlis, Arau, Perlis, Malaysia

Polymer Advanced Group, Geopolymer & Green Technology, Centre of Excellence (CEGeoGTech), Universiti Malaysia Perlis (UniMAP), Arau, Perlis, Malaysia

H. Osman

Faculty of Chemical Engineering Technology, Universiti Malaysia Perlis, Arau, Perlis, Malaysia

Centre of Excellence for Biomass Utilization, Universiti Malaysia Perlis (UniMAP), Arau, Perlis, Malaysia

N. A. A. Rahim

Faculty of Chemical Engineering Technology, Universiti Malaysia Perlis, Arau, Perlis, Malaysia

Y. Munusamy

Faculty of Engineering and Green Technology, Universiti Tunku Abdul Rahman, Jalan Universiti, Kampar, Perak, Malaysia

H. Ismail

School of Materials and Mineral Resources Engineering, Engineering Campus, Universiti Sains Malaysia, Nibong Tebal, Penang, Malaysia

material. Semicrystalline PET has excellent mechanical properties in terms of strength, ductility, stiffness, and hardness. Meanwhile, PET with an amorphous structure has better ductility than that of semicrystalline PET but has to compromise with less stiffness and hardness (Ragaert et al. 2017). PET exhibits good dimensional stability, thermostability, and resistance to impact, and it has excellent moisture and fair oxygen barrier characteristics. Therefore, PET has become the material of choice in industrial applications especially for the packaging of fruit juice and soft drink bottles (de Moura Giraldo et al. 2005).

Today, PET is the most recyclable plastic in the world and it can be easily identified from the number 1 indicator in the triangular code printed on the bottle or container. Recognizing the critical threats posed by PET waste, various organizations and entities have collaborated to promote the importance of PET waste recycling. Through numerous attempts, a minimum reduction of 24% carbon emissions can be eradicated and this makes the utilization of rPET a more sustainable option (Khoonkari et al. 2015; Raheem et al. 2019). Predominantly, PET can be recycled multiple times before ending up in a landfill. Plastic waste from other products may be utilized as a low-cost and long-term feedstock in other new production processes (Salwa et al. 2021). Material recycling is essential due to the increasing use of composites in many sectors as well as stricter legislation and concerns about the disposal or incineration of composites in landfills (Ilyas et al. 2021). Apart from recycling, rPET has been successfully blended with various thermoplastics, namely polypropylene (PP) (Subhashini et al. 2021), polyethylene (PE) (Lei et al. 2009), and polyamide 11 (Khan et al. 2021). The improved blending properties have been confirmed by mechanical testing based on tensile and flexural strengths. In addition, studies on the utilization of solid fillers from fly ash (Sharma and Mahanwar 2010; Zaichenko and Nefedov 2018), mineral-based fillers (Negoro et al. 2016; Pivsa-Art et al. 2021), glass fiber (Monti et al. 2021), carbon-based fillers (Baek et al. 2018), and nanoparticles (Chowreddy et al. 2019) in rPET have also gained significant interest among researchers. To provide clear insight, this chapter focuses on the progress of rPET blends and rPET-based composites as well as their impact on engineering design and performance.

2 Source of PET Waste

With the increasing use of PET plastics, the waste will accumulate in the environment and will generate unknown long-term impacts. PET was initially assumed to be harmless and inert, but later researchers have claimed that it could take more than 400 years to completely decompose (Hamad et al. 2013). Based on the Springer Report 2019, China is the world's largest PET resin manufacturer encompassing more than 15% of the global market. Moreover, China is also the largest consumer of PET products in the world. Previously, PET accounted for about 50% of China's waste plastic imports (Sardon and Dove 2018). Between 2000 to 2018, the cumulative amount of waste PET bottles was around 78 million tons in China which

was equivalent to about 7 tons of waste PET bottles generated per minute. Remarkably, China is also a net importer of waste PET bottles, and the number of waste PET bottles imported are 290 times that of export. To address this issue, the Chinese government has taken action to restrict the import of waste plastics in 2018 (Wang et al. 2020).

PET plastic bottles are a popular choice for packaging soft drinks due to their numerous benefits to manufacturers and consumers. About 70% of soft drinks (carbonated drinks, fruit juices, and bottled water) are largely packaged in PET plastic bottles (Singh et al. 2021a). By 2016, annual sales of bottled water in the United States (US) officially surpassed soft drinks. As a result, plastic bottles and bottle caps are the third and fourth most collected plastic waste in the US. Most of the beverages we consume regularly are in single-use bottles and cans for water, sodas, iced tea, cold-brewed coffee, fruit juices, energy drinks, and others (Wang et al. 2020). Furthermore, PET is frequently used as packaging for a variety of products including beverages, bakery goods, frozen foods, salad dressings, cosmetics, and household cleaners. These materials accumulate a large portion of the PET waste in landfills as well as in the ocean.

Moreover, Norway has a recycling rate of PET bottles over 97% as of 2018, making it a world leader in recycling (Mallakpour & Behranvand 2016). In the same year, the recycling rate of PET bottles in the US was only 29% (Yamada and Thumsorn 2013). The high recycling rate in Norway can be attributed to the country's efficient deposit return system. When customers purchase a plastic bottle, they pay a modest surcharge in addition to the product price, which will be refunded when the bottle is returned to reverse vending machines. Other countries have adopted this approach as it has been proven effective. In the United Kingdom (UK), 86% of the population favored the supermarket deposit return scheme for plastic and glass bottles as well as beverage cans (Raheem et al. 2019).

3 Impact of PET Waste to Humans

Initially, PET was considered harmless and inert, but over the years, perceptions have changed owing to the massive amount of PET being disposed into the environment. Sardon and Dove (2018) predicted that by 2050, the size of plastic waste will continue to grow, and the recycling process will be insufficient causing the mass of plastic waste to exceed the number of fish. Similarly, PET waste has accumulated at landfills progressively and the amount continues to increase yearly, comprising PET-based product and packaging materials (Feng et al. 2013).

Before being converted to the final product, various additives are added into the PET resin during processing for different reasons. The most significant reason is to retain the properties of the resin for a sufficient period. Typically, an inorganic compound, such as antimony trioxide, is used as a catalyst for PET production and rubber vulcanization, and this additive can leach when exposed to extreme and rigorous conditions. For PET plastics, the waste is buried, compressed in layers, and

exposed to rain and hot weather constantly at landfills (Ioakeimidis et al. 2016; Yesil 2013). Although the degradation process can decelerate in the long run, it can greatly expose landfills to toxic additives due to the leaching issue from PET waste.

In addition, PET waste is considered a major burden to the aquatic environments where there is prolonged biophysical breakdown of plastics, negative impacts on ocean habitats, and limited plastic removal options. For synthetic polymer, PET plastic, the degradation process begins as soon as it is disposed into the oceans due to the synergistic effects of environmental variables and inherent material instability. Ioakeimidis et al. (2016) performed FTIR characterization on PET collected from the submarine environment and indicated that the degradation behavior of PET was attributed to environmental conditions. Based on the findings, it was proven that PET remained robust after 15 years of floating in the ocean. Subsequently, a significant decrease in native functional groups has been documented and some have disappeared (Chowreddy and Nord-Varhaug 2019). The PET will then slowly degrade and turn into large amounts of floating marine waste microplastics. Microplastics are small pieces of plastic that are less than 4.76 mm in length, and now they have sparked a huge controversy that seriously endangers marine ecosystems (Gan et al. 2021). According to Cox et al. (2021), Americans consume more than 50,000 microscopic bits of plastic from the food chain each year. Through the food chain, toxins attached to plastics can also move and accumulate in animal fats and tissues through the bioaccumulation process.

In addition, man-made CO₂ emissions pose a serious hazard to both humans and ecosystems. PET bottle releases more than 100 times toxins into the air and water. Moreover, the production process of PET can be classified as a process that is hazardous to workers. Over the years, serious accidents including explosions, chemical fires, chemical spills, and clouds of toxic vapor were unprecedented. On the other hand, PET bottles have contributed significantly to CO₂ emissions in recent years. If preventative actions are not taken, CO₂ emissions from plastic bottles are expected to quadruple by 2021 compared to 2006 (Zhang et al. 2020). Activated carbon derived from industrial waste, especially plastic waste, is considered a promising CO₂ adsorbent that can address PET waste recycling and CO₂ mitigation simultaneously. Wang et al. (2020) studied the PET waste-derived activated carbon for CO₂ capture and revealed that the life cycle process stipulated a large primary energy demand of 5481 MJ kg⁻¹ activated carbon. This suggested that a large portion of the total energy was used for CO₂ desorption. The study also revealed the environmental trade-offs associated with this technique, with primary energy use, water resource depletion, and freshwater ecotoxicity being the most significant.

4 Recycling Methods

The general terminology for plastic recycling is described through recycling steps including collection, separation, manufacturing, and marketing (Grigore 2018). This terminology is based on various recycling and recovery processes (Table 1).

Table 1 Different terminologies of plastic recycling and recovery

ASTM D5033 definitions	ISO 15270 definitions	Other equivalent terms
Primary recycling	Mechanical recycling	Closed-loop recycling
Secondary recycling	Mechanical recycling	Downgrading
Tertiary recycling	Chemical recycling	Feed stock recycling
Quaternary recycling	Energy recovery	Valorization

Primary (mechanical reprocessing into goods with equivalent attributes), secondary (mechanical reprocessing into products with lesser properties), tertiary (recovery of chemical constituents), and quaternary (recovery of chemical constituents) are the four types (recovery of energy) (Hopewell et al. 2009).

4.1 Mechanical Recycling

Primary recycling (closed-loop recycling) and secondary recycling are two types of mechanical recycling (downgrading). Primary recycling is the most practical as it successfully separates contaminants from the source and stabilizes them against degradation during reprocessing and subsequent use. It is used to produce an identical product that was recovered in the beginning. This innovative product can be constructed entirely from recycled plastics or a mixture of recycled and virgin polymers. The method of dilution ensures that the product can be recycled at the same rate as the material recovered. All PET bottles, for example, are constructed from similar PET grades appropriate for the manufacture and reprocessing of bottles to polyester fibers (Ragaert et al. 2017). Meanwhile, secondary recycling (downgrading) is used for products that are different from those recovered. For example, textile fibers are made from PET bottles and printer components are made from polycarbonate water bottles (Hopewell et al. 2009).

A physical approach is used to describe the mechanical process, which includes waste collecting, sorting, washing, material grinding, and melting to manufacture new products through extrusion (Fig. 1). Automatic and manual sorting is used to sort items by shape, density, size, color, or chemical composition. Furthermore, Fourier transform near-infrared (FT-NIR) is used to separate the mixed plastic waste, which is then segregated into clear, blue, and green PET using an optical color recognition sorter. Finally, all of these sorted streams pass through a sorting cabin, where trained operators inspect them for false positives and negatives (Ragaert et al. 2017; Grigore 2018). In addition, product washing is required to remove food residues, pulp fibers, and adhesives. To remove residues, several approaches are used, such as wet (water) or dry (friction) surface cleaning (Hopewell et al. 2009). The final step in mechanical recycling is the size reduction from goods to flakes via grinding. Optional treatments for converting flakes into granulates include compounding and pelletizing (Al-Salem et al. 2009; Ragaert et al. 2017).



Fig. 1 Basic steps in mechanical recycling

Table 2 Chemical processes involved in the decomposition of polymers into monomers

Types	Definitions
Chemolysis	New approaches are being developed using garbage as a precursor in the production of pure value-added goods for a variety of industrial and commercial purposes.
Pyrolysis	Multilayer packaging, fiber-reinforced composites, polyurethane building, demolition waste, and other plastic waste feeds that are difficult to depolymerize and are not currently (mechanically) recycled but burnt and/or disposed of at landfills.
Fluid catalytic cracking (FCC)	The skewed carbon distribution of the reactor effluent results from the thermal degradation of solid plastic waste.
Hydrogenation	The method is similar to fluid catalytic cracking (FCC), but hydrogen is added to the mixture.
Gasification combined with methanol production	Waste is converted to methanol using Enerkem's cutting-edge technology. Methanol is then converted to chemicals such as acetic acid, thickening agents, and dimethyl ether, e.g., for fibers and adhesives (clean propellant gases).
Katalytische Drucklose Verölung (KDV)	The catalytic pressureless depolymerization process converts biomass and plastic waste into liquid fuels at pressures close to atmospheric pressure.
Toxicity of pyrolysis and gasification products	The toxicity of gaseous compounds produced under different thermal decomposition settings is a major problem.

4.2 Chemical Recycling

Chemical recycling is the process of chemically converting a polymer to monomers or partially depolymerizing a polymer to oligomers (chemical structure change) (Singh et al. 2017). The resulting monomers can be utilized to create further polymerization to replicate the original or similar polymer product. Starting with monomers, oligomers, or a combination of various hydrocarbon compounds, this process can convert plastic materials into smaller molecules appropriate for use as feedstocks. Table 2 lists the chemical processes that convert polymers to monomers (Ragaert et al. 2017).

4.3 Energy Recovery

Energy recovery from plastics is a good solution and an effective way to reduce the volume of organic materials through incineration. This method generates considerable energy from polymers, but it is ecologically unacceptable due to the health risk from airborne toxic substances including heavy metals, chlorine-containing polymers, toxic carbon, and oxygen-based free radicals (Grigore 2018).

5 Engineering Design of Recycled PET

While Covid-19 is an immediate challenge, new recycling technologies and alternative feedstocks will become increasingly important in the subsequent five years. The engineering design of recycled PET (rPeT) into new blends and composites is considered an eco-strategy to overcome a large amount of PET waste. rPET is often used as a matrix material in blends and composites and also as a filler in composites. Blending rPET with new virgin materials or with other recycled materials can reduce total production costs. In addition, the utilization of rPET as a filler can enhance the properties of the composites. This section reviews the engineering designs of various types of rPETs (i.e., commercial rPET resin and rPET flakes from PET waste) used in blends and composites and their final properties.

5.1 Recycled PET Blends

Recycled PET blends can be combined with virgin PET or with other/more materials to produce new materials with unique physical and mechanical properties. Due to the incompatible properties of rPET with other materials, several studies have been conducted to seek an effective compatibilizer for rPET blends. Compatibilization is crucial to ensure an increase in microstructural uniformity, and also enhance the interfacial adhesion between phases. Among the examples of compatibilizers currently used in rPET blends are polypropylene-graft-maleic anhydride (PP-g-MA), polyethylene-graft-maleic anhydride (PE-g-MA), styrene-ethylene-butylene-styrene (SEBS-g-MA), and ethylene-glycidyl methacrylate copolymer (E-GMA) (Lei et al. 2009; Ahmadlouydarab et al. 2020; Adekunle et al. 2020; Subhashini et al. 2021). Furthermore, several researchers have proposed chemical approaches, such as chain extender, to enhance the properties of rPET blends apart from compatibilizers. In this section, the properties and potential applications of several rPET blends combined with compatibilizer or/and chain extender are summarized in Table 3.

Table 3 Recent studies on processing methods, potential applications, and properties of rPET blends

Blend and processing method	Potential application	Properties
rPET/rHDPE—Extrusion	Container for packaging material	This blend has poor compatibility in the presence of HDPE exceeding 5%, where the two phases were clearly differentiated from SEM micrographs (Navarro et al. 2008).
rPET/rHDPE with compatibilizer (PE-g-MA, SEBS-g-MA, and E-GMA)—Reactive extrusion and postextrusion strand stretching	Packaging material	The compatibility of rPET and rHDPE was improved. 5% E-GMA blended with rHDPE/rPET (75/25 w/w) indicated the best performance among compatibilizer with significantly improved toughness and impact strength, and increased tensile fracture elongation by 83% (Lei et al. 2009).
PP/rPET-compatibilizer PP-g-MA—Twin-screw extrusion	Industrial applications	The yield stress and elastic modulus of the blends increased with increasing rPET concentrations in the blends from 0% to 30%. Sample with compatibilizer demonstrated higher yield strength, modulus of elasticity, and impact energy compared to blends without compatibilizer (Ahmadlouydarab et al. 2020).
PP/rPET PP-g-MA—Extrusion	Low-speed wheel material	The tensile strength, Young's modulus, and flexural strength were improved with increasing rPET content from 10% to 30%. The elongation at break reduced when more r-PET was included in the blends (Subhashini et al. 2021).
RPET/PETV—Melt blending—Haake rheometer Melt spinning	Filament yarn for textile	The melting temperature of the blend fibers decreased with increasing rPET content. The crystallization rate decreased with the addition of rPET into the PETV. The mechanical properties of 30/70 wt.% rPET/PETV blended fibers were comparable to those of virgin PET fibers (Lee et al. 2013).
rPET/PET—Single-screw extrusion	Food contact packaging	The degree of crystallinity of the blends slightly improved at rPET composition of 10–30%. The Young's modulus for the rPET composition of 30/70 showed the highest tensile strength (Masmoudi et al. 2020).
rPET/PET with 5-amino isophthalic acid (C ₈ H ₇ NO ₄) as additive—Reactive extrusion	Matrices for composites	Reactive extrusion has improved the flowability and elastic modulus of the blends (Asensio et al. 2020a).
rPET/PBT—Single-screw extruder	Not mentioned	Tensile strength, impact strength, and degree of crystallinity of PET/PBT (40w/60w) blends containing 60 wt.% rPET improved (Baxi et al. 2010).

(continued)

Table 3 (continued)

Blend and processing method	Potential application	Properties
rPET/PBT with multifunctional epoxide as chain extender—Reactive extrusion	Not mentioned	The addition of only 0.2 wt.% Joncryl to the rPET/PBT (75/25) blends dramatically improved its thermal stability, dynamic rheological properties, and processability (Guclu et al. 2021).
rPET/PBT—Twin-screw extruder	Home appliances, electrical, and automotive applications	The addition of a chain extender increased the melt viscosity of the blend. In the amorphous region, the blends were totally miscible, but after rapid cooling, the crystalline phases became immiscible. The chain extender did not significantly influence the mechanical properties (Nofar and Oğuz 2019).
rPP/rPET with compatibilizer SEBS-g-MA—Internal mixer (Brabender)	Fibers applications	50/50 rPP/rPET blend with 20 phr compatibilizer showed better tensile strength, impact resistance, and resilience modulus compared to those without compatibilizer (Araujo and Morales 2018).
rPP/rPET uncompatibilized—Injection molding	Substituted to rPP for similar applications	The elastic modulus improved at 20% and 30% of opaque rPET (rPET-O). An increase in rPET-O from 10% to 30% has improved the fatigue life, diminished overall deformation, prevented local heating, and changed fatigue failure to quasi-static failure (Tramis et al. 2021).
rPET/PC—With styrene acrylic copolymer as chain extender—Single-screw extruder		The tensile modulus improved with the addition of 30% PC in the blend. The tensile strength and modulus further increased by adding chain extender from 0.5% to 2% (Srithep et al. 2017).
rPET/EVA with pyromellitic dianhydride (PMDA) as chain extender—Extrusion & reactive extrusion	Microfibrillar composite	The rate and degree of crystallinity of rPET decreased with the addition of PMDA and EVA. rPET/EVA showed co-continuous morphology, while the addition of 0.5 wt.% PMDA showed microfibrillar matrix-disperse state (Moghanlou and Pourabbas 2020).
rPET/PA11 uncompatibilized—Twin-screw extruder	Automobile, packaging, and various industries	Tensile and flexural strength improved significantly with the addition of PA11 into the rPET (Khan et al. 2021).
rPET/PE/PP/PS with EGMA as compatibilizer—Extrusion	Not mentioned	The Izod impact strength improved with increasing EGMA content in the rPET/PE/PP/PS blend. The miscibility of the blends also improved with increasing EGMA content and was evidenced by SEM images (Imamura et al. 2014).
rPET/rHDPE/rPP (ethylene-glycidyl methacrylate copolymer (EGMA)—Injection molding	Automobile bumper	Blending 164 g rPET, 18 g rHDPE, and 18 g rPP with 10% EGMA produced the best mechanical properties of a car bumper (Adekunle et al. 2020).

5.2 Recycled PET Composites

Recently, rPET has also been used as a matrix material in the production of various polymer composites, which is economically effective. It also has the potential to reduce the consumption of virgin materials and address the environmental contamination issue that results from postconsumer PET waste. In rPET composites, several fillers have been widely used such as organoclay, glass fiber, wood, titanium dioxide, carbon fiber, rubber particles, kenaf, and others (Singh et al. 2021a, b). The type of fillers, compounding process, and performance of rPET blends and composites are summarized in Table 4.

6 Applications of Recycled PET Blends and Composites

The evolution of rPET in new plastic packaging was introduced in 2002 by Triantafyllou et al. (2002). PET Recycling Company NPC or known as PETCO is one of the companies established in 2004 to handle the rPET (Petco n.d.). PETCO has commercialized new food grade and nonfood grade packaging from rPET. Then, Artenius (LSB) has commercialized a new packaging material in early 2012 which was a combination of virgin PET with recycled PET (Gallant 2012). Moreover, Artenius UNIQUE F10 currently uses a chemical recycling process to produce rPET-Artenius FLOW (virgin resin with 10% clean recycled PET). Furthermore, Coca-Cola Great Britain has recently stated that Sprite bottles would be changed from green to clear plastic to allow bottle-to-bottle recycling, with the quantity of rPET in all bottles increased to 50% (Maile 2019). It has good mechanical properties and was intended for stretch blow molding processes to make packaging for highly carbonated soft drinks and all direct food contact applications.

In addition, Greiner Packaging has also shifted to sustainable materials by combining PET with 30% rPET in new packaging for ketchup and sauce bottles (Edbauer 2019). Extensive research on this area is escalating over the years due to the increased production and consumption of PET plastics as new plastic packaging. Meanwhile, Covestro introduced Arnite® AM2001 GF (G)-recycled PET, high-performance, glass-fiber-filled rPET for 3D printing filament in 2021 (Product News 2021). It allows fast and cost-effective of additive manufacturing for large-scale items. It has potential for structure, small recreational boats, tooling, and infrastructures such as footbridges and cycling, or pedestrian tunnels as well as architectural applications. Konica Minolta was another pioneering business that has successfully produced a new rPC/rPET for the exterior parts of a multifunction printer (MFP). The strength, flame resistance, and molding of rPET were successfully enhanced with polycarbonate (PC) to produce composite materials (Business solution, n.d.). The rPET/PC combination is also commonly utilized in automobile applications for bumpers, wheel covers, body panels, and electrical components.

Table 4 Recent studies on processing methods, potential applications, and properties of rPET composites

Composites	Compounding process	Properties
rPET/organoclay nanocomposites	Twin-screw extruder	The glass transition temperature (T_g) and melting temperature (T_m) of the composite decreased slightly in the presence of 1 wt.% clay. However, concentrations higher than 1 wt.% did not cause further reduction in T_g and T_m . Yield strength and modulus improved with increasing MMT up to 5 wt.% (Bizarria et al. 2007).
rPET/ clay nanocomposites	Twin-screw extruder via masterbatch dilution	The composite with 1 wt.% clay exhibited Newtonian behavior, while more than 1 wt.% up to 6 wt.% showed the shear thinning effect. In contrast, the viscosity of the composite decreased with increasing clay content. The T_g decreased with increasing clay content. The tensile strength increased gradually with the clay content. The impact strength did not change when 4 wt.% clay was added but decreased by 28% at 6 wt.% clay (Chowreddy et al. 2019).
rPET/glass fiber	Twin-screw extruder	The impact strength and tensile strength improved with the addition of 30% glass fiber (de Moura Giraldi et al. 2005).
rPET /recycled LDPE-HDPE	Single-screw extruder & injection molding	Different rPE/rPET ratios were used. The time taken to extrude the composite increased with increasing rPET. The viscosity also increased, but the compressive strength decreased with decreasing rPET ratio (Laria et al. 2020).
rPET/micronized rubber	Extrusion	The T_g and degree crystallinity increased with the addition of rubber. The toughness improved by adding rubber powder (Zander and Boelter 2021).
rPET/glass fiber/ wood laminated composites	Compression molding	The alternating arrangement of rPET and wood layers influenced the final properties of the sandwich composite. The rPET layers decreased water absorption by the composites. The addition of an rPET layer decreased the flexural strength and modulus (Bakir et al. 2021).
rPET/glass fiber	Pultrusion	Different types of rPET were used. Composites with chemically modified rPET showed higher flexural strength and modulus compared to unmodified rPET and colored rPET. Composites with chemically modified rPET showed the highest tensile strength (441 MPa) (Asensio et al. 2020b).
rPET/glass fiber composites with impact modifier	Twin-screw extruder	The addition of an impact modifier slightly improved the impact properties. Composite with E-MA/24-GMA impact modifier showed the highest impact. From SEM images, the impact modifier tended to form the largest rubber particles (Monti et al. 2021).

(continued)

Table 4 (continued)

Composites	Compounding process	Properties
rPET/TiO ₂	Semi-industrial extrusion calendaring process	Two composites made of two types of rPET (i.e., transparent bottle grade (rPET-T) and mix transparent colored with opaques (rPET-O)) containing 1.45 wt.% TiO ₂ were produced. The glass transition of rPET-T was higher than that of rPET-O. rPET-O showed stable and uniform color. Both samples demonstrated almost similar Young's modulus and yield strength. Physically aged rPET-T showed higher tensile strength than the physically aged rPET-O sample (Loeza et al. 2021).
rPET/nano-TiO ₂	Twin-screw extruder and melt spinning	The tenacity and elongation at break of bicomponent fibers increased with the increase of nano-TiO ₂ up to 3 wt.%. The 90/10 bicomponent multifilament fiber with 3 wt.% TiO ₂ achieved the highest antibacterial activity (Pivsa-Art et al. 2021).
rPET/sawdust	Dry blending & hot flat pressing	The modulus of elasticity decreased with increasing sawdust content (40–70%). The modulus of rupture also decreased gradually (Rahman et al. 2013).
rPET/carbon fibers	Hot pressing	Tensile strength improved by increasing the processing temperature up to 270 °C. The interlaminar shear stress (ILSS) also showed a similar trend (Baek et al. 2018).
rPET/fly ash	Injection molding	The compressive strength of the composite increased by adding modified fly ash (Zaichenko and Nefedov 2018).
rPET/talc	Twin-screw extruder	The rPET was more crystallized using air cooling than the water cooling system during extrusion. Tensile strength and modulus improved with the addition of 5 wt.% talc. The tensile modulus of the composite prepared by water cooling was higher than that of the air cooling system (Negoro et al. 2016).
rPET/ newspaper fiber	Twin-screw extruder	The tensile and flexural strength improved by adding newspaper fiber (NPF) up to 5 wt.%, then gradually decreasing at 10 wt.% and 15 wt.% NPF. The impact strength decreased with increasing NPF content up to 15 wt.%. The degree of crystallinity of the composites increased with increasing NPF content (Ardekani et al. 2014).
rPET/rPP/kenaf	Twin-screw extruder	Composites reinforced with kenaf bast fiber have higher mechanical properties than kenaf core fiber composites. For both bast- and core-filled composites, the maximum tensile strength was 5 phr and the highest impact strength was 20 phr (Marzuki et al. 2021).
rPET/PAN composite nanofibers	Electrospinning	The compressive and flexural strength of the mortar improved by adding rPET/PAN fibers. Water penetration decreased with increasing rPET/PAN composite nanofibers (Chinchillas-Chinchillas et al. 2020).

(continued)

Table 4 (continued)

Composites	Compounding process	Properties
rPET/PBAT/wood	Twin-screw extruder	The tensile strength improved by increasing wood content up to 30 wt.%. The impact strength decreased in proportion to the decrease in rPET content. The flexural strength increased when wood content increased up to 15 wt.% (Chaiwutthinan et al. 2019).
rPET/ poly (ϵ -caprolactone) (PCL)/sawdust	Cryogenic solid-state milling & hot flat pressing	The optimal tensile strength for 25% sawdust was 35.8 MPa, with a high modulus of elasticity of 1100 MPa (Allaf et al. 2020).

The rPET content employed is between 50% and 80%, while the PC content ranges from 25% to 30%, and this is cheaper than materials made of acrylonitrile butadiene styrene (ABS) (Thakur 2015). Glass-filled rPET composites have also been used in automotive applications for headlamp bracket, window hardware, roof rack, and others, and Ford uses them for grille opening reinforcing panels of cars and trucks (Koester 1997).

7 Challenges in PET Recycling

Washing is required prior to mechanical and chemical recycling to remove impurities from the surface of plastic waste. Contaminants are critical factors affecting the suitability of postconsumed PET flakes for recycling in terms of the amount and nature of contaminants present in the flakes, resulting in deterioration of physical and chemical properties during reprocessing and problems of recycling postconsumed PET (Giannotta et al. 1994). PET (contaminated flakes) produces 43.9% carbon dioxide/acetaldehyde and 3.66% 4-(vinylloxycarbonyl) benzoic acid as its main components. The most prevalent by-products of faster pyrolytic breakdown due to the catalytic effects of remaining pollutants (i.e., D-limonene, chlorobenzene, benzophenone) are products with low molecular weight (CO_2 , acetaldehyde) (Dimitrov et al. 2013). Several contaminants can contaminate rPET (Table 5).

Contamination issues can be solved by improving the recycling process. The super-clean PET recycling technique based on pellets, according to Damayanti and Wu (2021), is an alternative to overcome the difficulties. This approach is extremely similar to current mechanical procedures and uses the same apparatus, but it uses solid-state polycondensation (SSP) technology to accomplish it. The first stage involves the removal of all pollutants that have adhered to the PET surface. The PET is thoroughly cleaned in the second stage using SSP technology. With parameters such as residence time, temperature, vacuum, and inert gas stream, the SSP can be operated in a batch or continuous mode. Depending on the reaction temperature and the desired viscosity of the PET material, the residence time for the solid-state

Table 5 Types of contaminants that can affect properties of recycled PET

Type of contaminants	Effect	Problem solving
Water	Before the molten PET reacts rapidly, the hydrolytic chain cleavage and moisture content are devolatilized. The viscosity of the polymer can be lowered by a small amount of moisture (La Mantia 1996). PET hydrolysis is aided by its starting pace. It results in water loss in the sample, whereas the slower pace is due to thermooxidative chain depolymerization by thermal energy (Seo and Cloyd 1991).	PET should be rigorously dried before melt-reprocessing. The drying temperature for recovering PET flakes is 160–180 °C (La Mantia 1996).
Coloring	Before melt-reprocessing, the PET should be thoroughly dried. To recover PET flakes, the drying temperature ranges from 160 to 1800 °C (La Mantia 1996).	A few additives (Bacha et al. 2012) can be used.
Acetaldehyde	(i) Food packaging and containers use copper phthalocyanine blue.	
Heavy metal	(ii) UV stabilizers, such as benzotriazole, are used to protect food from the sun.	

reactions is between 6 and 20 h. For this scenario, the temperature range is 180–220 °C. The virgin rPET is homogenous, and postconsumer PET contamination is evenly dispersed, according to the findings.

The main difference is the presence of oxygen in the atmosphere. This leads to the formation of oxygenated groups on the polymer chain and affects the final properties of the material. In addition, the subsequent challenge is the processing of complex mixtures as the polymers in the mixed plastic waste differ in melting points and processing temperatures. When reprocessing these mixtures, recyclers often need to reprocess them at the highest melting component processing temperature. This often leads to overheating and degradation of some of the lower melting components, which in turn reduces the final properties (Ragaert et al. 2017).

Mechanical recycling has several obstacles, including (1) thermal-mechanical degradation, (2) degradation over time, and (3) complex mixed processing. The polymer is heated and mechanically sheared during melt processing, causing thermal-mechanical deterioration. Chain scission and chain branching are the most typical processes observed in commercial polymers (Beyler and Hirschler 2002). The photooxidation process, due to the mixture of heat, oxygen, light, radiation, moisture, and mechanical stress, causes the degradation of plastic items over their lifetime. Thermomechanical degradation and structural changes in polymers are extremely comparable. When comparing mechanical and chemical recycling, the industry promotes chemical recycling more aggressively, despite the fact that it consumes a lot of energy and does not mitigate CO₂. Chemical recycling, in reality, has its own set of obstacles and disadvantages. The production of fuel from plastic waste through chemical recycling is inconvenient as more CO₂ is released into the atmosphere when this fuel is consumed.

As a result, it is preferable to convert waste into energy (quaternary recycling) in a waste incineration plant rather than using fuel as an intermediary step. If the plastic waste contains too many distinct materials or is too filthy, the quality of the product will be affected, and the entire process will become economically unsustainable. Chemical recycling currently receives more funding than mechanical recycling. A chemical recycling factory, for example, will be developed in Rotterdam, Netherlands. It will convert 360,000 tons of plastic waste to methanol annually. Meanwhile, Air Liquide of France, AkzoNobel Specialty Chemicals of the Netherlands, Enerkem of Canada, and the Port of Rotterdam each spent a total of EUR nine million at the start. The factory is projected to cost around EUR 200 million in total (ChemViews Magazine 2020).

8 Conclusion

PET waste has dominated the world ranging from large pieces of water bottles to tiny-sized microplastics that are harmful to the environment, humans, and wildlife. The recycling method has evolved since the first existed to address the PET waste issues globally and continue to seek ways to utilize rPET. The evolution involving engineering design through reactive blending and chemical approach (i.e., chain extenders and compatibilizer) for rPET blends, as well as the addition of various fillers and fibers for rPET composites has created different high-end products for many industries and offered an economically feasible rPET business.

References

- Adekunle AS, Adeleke AA, Sam Obu CV et al (2020) Recycling of plastics with compatibilizer as raw materials for the production of automobile bumper. *Cogent Eng* 7:1801247. <https://doi.org/10.1080/23311916.2020.1801247>
- Ahmadlouydarab M, Chamkouri M, Chamkouri H (2020) Compatibilization of immiscible polymer blends (R-PET/PP) by adding PP-g-MA as compatibilizer: analysis of phase morphology and mechanical properties. *Polym Bull* 77(11):5753–5766. <https://doi.org/10.1007/s00289-019-03054-w>
- Allaf RM, Albarahmeh E, Futian M et al (2020) Preparation of sawdust-filled recycled-PET composites via solid-state compounding. *PRO* 8(1):100. <https://doi.org/10.3390/pr8010100>
- Al-Salem SM, Lettieri P, Baeyens J (2009) Recycling and recovery routes of plastic solid waste (PSW): a review. *Waste Manag* 29(10):2625–2643. <https://doi.org/10.1016/j.wasman.2009.06.004>
- Araujo LMG, Morales AR (2018) Compatibilization of recycled polypropylene and recycled poly (ethylene terephthalate) blends with SEBS-g-MA. *Polimeros* 28:84–91. <https://doi.org/10.1590/0104-1428.03016>
- Ardekani SM, Dehghani A, Al-Maadeed MA et al (2014) Mechanical and thermal properties of recycled poly (ethylene terephthalate) reinforced newspaper fiber composites. *Fiber Polym* 15(7):1531–1538. <https://doi.org/10.1007/s12221-014-1531-y>

- Asensio M, Nuñez K, Guerrero J et al (2020a) Rheological modification of recycled poly (ethylene terephthalate): blending and reactive extrusion. *Polym Degrad Stab* 179:109258. <https://doi.org/10.1016/j.polymdegradstab.2020.109258>
- Asensio M, Esfandiari P, Nuñez K et al (2020b) Processing of pre-impregnated thermoplastic tow-preg reinforced by continuous glass fibre and recycled PET by pultrusion. *Compos Part B-Eng* 200:108365. <https://doi.org/10.1016/j.compositesb.2020.108365>
- Bach C, Dauchy X, Chagnon MC et al (2012) Chemical migration in drinking water stored in polyethylene terephthalate (PET) bottles: a source of controversy. *Water Res* 46:571–583. <https://doi.org/10.1016/j.watres.2011.11.062>
- Baek YM, Shin PS, Kim JH et al (2018) Investigation of interfacial and mechanical properties of various thermally-recycled carbon fibers/recycled PET composites. *Fiber Polym* 19(8):1767–1775. <https://doi.org/10.1007/s12221-018-8305-x>
- Bakır AA, Atik R, Özeriç S (2021) Effect of fused deposition modeling process parameters on the mechanical properties of recycled polyethylene terephthalate parts. *J Appl Polym Sci* 138(3):49709. <https://doi.org/10.1002/app.49709>
- Baxi RN, Pathak SU, Peshwe DR (2010) Mechanical, thermal, and structural characterization of poly (ethylene terephthalate) and poly (butylene terephthalate) blend systems by the addition of postconsumer poly (ethylene terephthalate). *J Appl Polym Sci* 115:928–934. <https://doi.org/10.1002/app.30647>
- Beyler CL, Hirschler MM (2002) Thermal decomposition of polymer. *SFPE Hand. Fire Protect Eng* 2:110–131. [http://refhub.elsevier.com/S0956-053X\(17\)30535-4/h0115](http://refhub.elsevier.com/S0956-053X(17)30535-4/h0115)
- Bizarria MT, Giraldo AL, de Carvalho CM et al (2007) Morphology and thermomechanical properties of recycled PET–organoclay nanocomposites. *J Appl Polym Sci* 104(3):1839–1844. <https://doi.org/10.1002/app.25836>
- Business Solution (n.d.) Recycled PC/PET for exterior materials. Konica Minolta. <https://www.konicaminolta.com/about/research/business/pcpet.html>
- Chaiwuthinon P, Pimpong A, Larpkasemsuk A et al (2019) Wood plastic composites based on recycled poly (ethylene terephthalate) and poly (butylene adipate-co-terephthalate). *Journal of Metals, Materials and Minerals* 29:29
- ChemViews (2020) Chemical versus mechanical recycling of plastic waste. *Nacricten aus der Chemie/GDCh* 68:22. <https://doi.org/10.1002/nadc.20204095088>
- Chinchillas-Chinchillas MJ, Gaxiola A, Alvarado-Beltrán CG et al (2020) A new application of recycled-PET/PAN composite nanofibers to cement-based materials. *J Clean Prod* 252:119827. <https://doi.org/10.1016/j.jclepro.2019.119827>
- Chowreddy RR, Nord-Varhaug K, Rapp F (2019) Recycled poly (ethylene terephthalate)/clay nanocomposites: rheology, thermal and mechanical properties. *J Polym Environ* 27:37. <https://doi.org/10.1007/s10924-018-1320-6>
- Cox HJ, Li J, Saini P (2021) Bioinspired and eco-friendly high-efficacy cinnamaldehyde antibacterial surfaces. *J Mater Chem B* 9(12):2918–2930. <https://doi.org/10.1039/d0tb02379e>
- Damayanti WS-H (2021) Strategic possibility routes of recycled PET. *Polymers* 13:1475. <https://doi.org/10.3390/polym13091475>
- de Moura Giraldo AL, de Jesus RC, Mei LI (2005) The influence of extrusion variables on the interfacial adhesion and mechanical properties of recycled PET composites. *J Mater Process Tech* 15(162):90–95. <https://doi.org/10.1016/j.jmatprotec.2005.02.046>
- Dimitrov N, Krehula LK, Siročić AP et al (2013) Analysis of recycled PET bottles products by pyrolysis-gas chromatography. *Polym Degrad Stab* 98:972–979. <https://doi.org/10.1016/j.polymdegradstab.2013.02.013>
- Edbauer T (2019) Greiner packaging creates packaging solution containing r-PET. Greiner Packaging. https://www.greiner-gpi.com/en/Media/Greiner-Packaging-creates-packaging-solution-containing-r-PET_s_166790
- Feng N, Wang X, Wu D (2013) Surface modification of recycled carbon fiber and its reinforcement effect on nylon 6 composites: mechanical properties, morphology and crystallization behaviors. *Curr Appl Phys* 13(9):2038–2050. <https://doi.org/10.1016/j.cap.2013.09.009>

- Gallant A (2012) PET resin unit of Spain-based LSB, Artenius, announces development of new PET packaging material that combines virgin PET resin with post-consumer recycled PET as feedstock in production process. Industry Intelligence Inc. <https://www.industryintel.com/public2:news/read/3225179544/PET%20resin%20unit%20of%20Spain-based%20LSB%2C%20Arten%2E%80%A6/ur/55601>
- Gan L, Xiao Z, Pan H, Xu W et al (2021) Efficiently production of micron-sized polyethylene terephthalate (PET) powder from waste polyester fibre by physicochemical method. *Adv Powder Technol* 32(2):630–636. <https://doi.org/10.1016/j.apt.2021.01.010>
- Giannotta G, Po R, Cardi N et al (1994) Processing effects on poly(ethylene terephthalate) from bottle scraps. *Polym Eng Sci* 34:1219–1223. <https://doi.org/10.1002/pen.760341508>
- Grigore ME (2018) Methods of recycling, properties and applications of recycled polymers. *Recycling* 2:24. <https://doi.org/10.3390/recycling2040024>
- Guclu M, Göksu YA, Özdemir B et al (2021) Thermal stabilization of recycled PET through chain extension and blending with PBT. *J Polym Environ* 30:719. <https://doi.org/10.1007/s10924-021-02238-8>
- Hamad K, Kaseem M, Deri F (2013) Recycling of waste from polymer materials: an overview of the recent works. *Polym Degrad Stab* 98(12):2801–2812. <https://doi.org/10.1016/j.polymdegradstab.2013.09.025>
- Hopewell J, Dvorak R, Kosior E et al (2009) Plastics recycling: challenges and opportunities. *Phil Trans R Soc B* 364:2115–2126. <https://doi.org/10.1098/rstb.2008.0311>
- Ilyas R, Sapuan SM, Bayraktar E (2021) Recycling of plastics, metals, and their composites, 1st edn. CRC Press, Boca Raton. <https://doi.org/10.1201/9781003148760>
- Imamura N, Sakamoto H, Higuchi Y et al (2014) Effectiveness of compatibilizer on mechanical properties of recycled PET blends with PE, PP, and PS. *Mater Sci Appl* 05:548. <https://doi.org/10.4236/msa.2014.58057>
- Ioakeimidis C, Fotopoulou KN, Karapanagioti HK et al (2016) The degradation potential of PET bottles in the marine environment: an ATR-FTIR based approach. *Sci Rep* 6(1):1–8. <https://doi.org/10.1038/srep23501>
- Khan ZI, Mohamad ZB, Rahmat ARB et al (2021) A novel recycled polyethylene terephthalate/polyamide 11 (rPET/PA11) thermoplastic blend. *Prog Rubber Plast Re* 37(3):233–244. <https://doi.org/10.1177/14777606211001074>
- Khoonkari M, Haghghi AH, Sefidbakht Y et al (2015) Chemical recycling of PET wastes with different catalysts. *Int J Polym Sci* 29:2015. <https://doi.org/10.1155/2015/124524>
- Koester E (1997) Friendly old PET VS cheap new PET. *Mater World* 5(9):525–528
- La Mantia FP (1996) Recycling of PVC and mixed plastic waste. ChemTec Publishing, Toronto
- Laria JG, Gaggino R, Kreiker J et al (2020) Mechanical and processing properties of recycled PET and LDPE-HDPE composite materials for building components. *J Thermoplast Compos* 36:0892705720939141. <https://doi.org/10.1177/0892705720939141>
- Lee JH, Lim KS, Hahn WG et al (2013) Properties of recycled and virgin poly (ethylene terephthalate) blend fibers. *J Appl Polym Sci* 128(2):1250–1256. <https://doi.org/10.1002/app.38502>
- Lei Y, Wu Q, Zhang Q (2009) Morphology and properties of microfibrillar composites based on recycled poly (ethylene terephthalate) and high-density polyethylene. *Compos Part A-Appl S* 40(6–7):904–912. <https://doi.org/10.1016/j.compositesa.2009.04.017>
- Loaeza D, Cailloux J, Santana Pérez O et al (2021) Impact of titanium dioxide in the mechanical recycling of post-consumer polyethylene terephthalate bottle waste: tensile and fracture behavior. *Polymers* 13(2):310. <https://doi.org/10.3390/polym13020310>
- Maile K (2019) Sustainability alert: sprite replaces iconic green bottle with clear plastic. *Recycling Today*. <https://www.recyclingtoday.com/article/sprite-pepsico-mcdonalds-trash-wheel-project-sustainability/>
- Mallakpour S, Behranvand V (2016) Manufacture and characterization of nanocomposite materials obtained from incorporation of d-glucose functionalized MWCNTs into the recycled poly (ethylene terephthalate). *Des Monomers Polym* 19(4):283–289. <https://doi.org/10.1080/015685551.2015.1136533>

- Marzuki NH, Wahit MU, Arsad A et al (2021) The effect of kenaf loading on the mechanical properties of kenaf-reinforced recycled poly (ethylene terephthalate)/recycled poly (propylene)(rPET/rPP) composite. *Mater Today Proc* 39:959–964. <https://doi.org/10.1016/j.matpr.2020.04.333>
- Masmoudi F, Alix S, Buet S et al (2020) Design and characterization of a new food packaging material by recycling blends virgin and recovered polyethylene terephthalate. *Polym Eng Sci* 60(2):250–256. <https://doi.org/10.1002/pen.25278>
- Moghanlou S, Khamseh M, Aghjeh MR et al (2020) Influence of chain extension and blending on crystallinity and morphological behavior of recycled-PET/ethylene vinyl acetate blends. *J Polym Environ* 1-8:1526. <https://doi.org/10.1007/s10924-020-01699-7>
- Monti M, Scrivani MT, Kociolek I (2021) Enhanced impact strength of recycled PET/glass fiber composites. *Polymers* 13(9):1471. <https://doi.org/10.3390/polym13091471>
- Navarro R, Ferrandiz S, Lopez J et al (2008) The influence of polyethylene in the mechanical recycling of polyethylene terephthalate. *J Mater Process Tech* 195(1–3):110–116. <https://doi.org/10.1016/j.jmatprotec.2007.04.126>
- Negoro T, Thodsaratpreeyakul W, Takada Y et al (2016) Role of crystallinity on moisture absorption and mechanical performance of recycled PET compounds. *Energy Procedia* 89:323–327. <https://doi.org/10.1016/j.egypro.2016.05.042>
- Nofar M, Oğuz H (2019) Development of PBT/recycled-PET blends and the influence of using chain extender. *J Polym Environ* 27:1404–1417. <https://doi.org/10.1007/s10924-019-01435-w>
- Petco (n.d.) Commercial-scale recycling projects. Petco. <https://petco.co.za/petco-industry-projects/>
- Pivsa-Art S, Sunyikhan K, Pivsa-Art W (2021) Bicomponent multifilament yarns of recycled poly (ethylene terephthalate) and nano-titanium dioxide for antibacterial carpet. *J Ind Text* 27:1034S. <https://doi.org/10.1177/15280837211011774>
- Product News (2021) Covestro introduces glass fiber-filled rPET for 3D pellet printing. Omnexus. <https://omnexus.specialchem.com/news/product-news/covestro-rpet-3d-pellet-printing-000224678>
- Ragaert K, Delva L, Van Geem K (2017) Mechanical and chemical recycling of solid plastic waste. *Waste Manag* 69:24–58. <https://doi.org/10.1016/j.wasman.2017.07.044>
- Raheem AB, Noor ZZ, Hassan A, Abd Hamid MK et al (2019) Current developments in chemical recycling of post-consumer polyethylene terephthalate wastes for new materials production: a review. *J Clean Prod* 225:1052–1064. <https://doi.org/10.1016/j.jclepro.2019.04.019>
- Rahman KS, Islam MN, Rahman MM et al (2013) Flat-pressed wood plastic composites from sawdust and recycled polyethylene terephthalate (PET): physical and mechanical properties. *Springer Plus* 2(1):1–7. <https://doi.org/10.1186/2193-1801-2-629>
- Salwa HN, Sapuan SM, Mastura MT et al (2021) Life cycle assessment (LCA) of recycled polymer composites. In: Ilyas RA, Sapuan SM, Bayraktar E (eds) *Recycl. Plast. Met. Their Compos*, 1st edn. CRC Press/Taylor & Francis Group, Boca Raton, p 15
- Sardon H, Dove AP (2018) Plastics recycling with a difference. *Science* 360(6387):380–381. <https://doi.org/10.1126/science.aat4997>
- Seo KS, Cloyd JD (1991) Kinetics of hydrolysis and thermal degradation of polyester melts. *J Appl Polym Sci* 42:845–850. <https://doi.org/10.1002/app.1991.070420330>
- Sharma AK, Mahanwar PA (2010) Effect of particle size of fly ash on recycled poly (ethylene terephthalate)/fly ash composites. *Int J Plast Technol* 14(1):53–64. <https://doi.org/10.1007/s12588-010-0006-2>
- Singh N, Hui D, Singh R et al (2017) Recycling of plastic solid waste: a state of art review and future applications. *Compos Part B Eng* 115:409–422. <https://doi.org/10.1016/j.compositesb.2016.09.013>
- Singh A, Rorrer NA, Nicholson SR et al (2021a) Techno-economic, life-cycle, and socioeconomic impact analysis of enzymatic recycling of poly (ethylene terephthalate). *Joule* 5(9):2479–2503. <https://doi.org/10.1016/j.joule.2021.06.015>
- Singh AK, Bedi R, Kaith BS (2021b) Composite materials based on recycled polyethylene terephthalate and their properties—a comprehensive review. *Compos Part B Eng* 219:108928. <https://doi.org/10.1016/j.compositesb.2021.108928>

- Srithep Y, Pholharn D, Dassakorn A et al (2017) Effect of chain extenders on mechanical and thermal properties of recycled poly (ethylene terephthalate) and polycarbonate blends. *IOP Conf Ser-Mat Sci* 213(1):012008
- Subhashini S, Rajapaksha SM, Ranatunga S et al (2021) Development of PP/recycled-PET blended low speed wheels to reduce the virgin plastic usage in the industry. *Polym Technol* 1(1):7–24. <https://doi.org/10.31357/ait.v1i1.4893>
- Thakur VK (2015) *Recycled polymers: properties and applications*, volume 2. Smithers Rapra
- Tramis O, Garnier C, Yus C et al (2021) Enhancement of the fatigue life of recycled PP by incorporation of recycled opaque PET collected from household milk bottle wastes. *Waste Manag* 125:49–57. <https://doi.org/10.1016/j.wasman.2021.02.006>
- Triantafyllou VI, Karamani AG, Akrida-Demertzi K et al (2002) Studies on the usability of recycled PET for food packaging applications. *Eur Food Res Technol* 215(3):243–248. <https://doi.org/10.1007/s00217-002-0559-1>
- Wang Y, Gu Y, Wu Y et al (2020) Performance simulation and policy optimization of waste polyethylene terephthalate bottle recycling system in China. *Resour Conserv Recycl* 162:105014. <https://doi.org/10.1016/j.resconrec.2020.105014>
- Yamada K, Thumsorn S (2013) Effectiveness of talc filler on thermal resistance of recycled PET blends. *Advances in Materials Physics and Chemistry* 1;3(8):327:327. <https://doi.org/10.4236/ampc.2013.38045>
- Yesil S (2013) Effect of carbon nanotube reinforcement on the properties of the recycled poly (ethylene terephthalate)/poly (ethylene naphthalate)(r-PET/PEN) blends containing functional elastomers. *Mater Des* 52:693–705. <https://doi.org/10.1016/j.matdes.2013.05.101>
- Zaichenko N, Nefedov V (2018) Composite material based on the polyethylene terephthalate polymer and modified fly ash filler. In: *MATEC web of conferences 2018*, vol 245. EDP Sciences, p 3007. <https://doi.org/10.1051/mateconf/201824503007>
- Zander NE, Boelter ZR (2021) Rubber toughened recycled polyethylene terephthalate for material extrusion additive manufacturing. *Polym Int* 70(6):742–748. <https://doi.org/10.1002/pi.6079>
- Zhang R, Ma X, Shen X et al (2020) PET bottles recycling in China: an LCA coupled with LCC case study of blanket production made of waste PET bottles. *J Environ Manag* 260:110062. <https://doi.org/10.1016/j.jenvman.2019.110062>

Index

A

Accelerators, 184, 194, 209–225, 231, 233, 257–259, 273
Acrylic acid (AA), 308, 309, 311–319
Agro residue, 364, 369, 376, 381
Alginate, 67, 68, 71–75, 77–80, 95, 302

B

Bibliometric analysis, 98
Biocomposites, 9, 10, 37–44, 56, 308, 310–319, 366, 368, 370–376, 378–381, 389–399
Biodegradability, 38, 87, 123, 134, 293, 298, 308, 311, 318–319, 364, 390
Blend, 5, 20, 39, 53, 97, 113, 152, 180, 209, 229, 262, 279, 353, 374, 405, 418
Blends recycling, 412–413

C

Cellulose, 4, 8, 19, 20, 43, 45, 57, 67, 147, 159, 291–304, 315, 350, 353, 363, 368, 369, 371, 393
Chloroprene rubber, 255–267, 271–287
Commingled recycling, 116, 122, 123
Compatibility, 38, 39, 56, 114, 120–122, 160, 165, 169, 184, 214, 223, 227, 231, 239, 251, 256, 280, 292, 299, 333, 363–381, 409, 410, 413, 424
Composite, 3, 27, 35, 49, 82, 97, 116, 134, 204, 291, 307, 341, 347, 363, 389, 405, 418

E

Electron beam irradiation, 230–231, 241–251
End of life tires, 97, 98, 103, 106, 107
Environment, 1, 2, 4, 5, 7, 9, 12, 17–19, 23, 28, 51–53, 97, 104, 106, 111, 112, 124, 133, 134, 139, 142, 150, 152, 189, 199, 201, 350, 351, 366, 380, 389, 399, 413, 418–420, 431
Epoxidized natural rubber (ENR), 272, 274–278, 280, 282, 284, 324
Epoxies, 61, 114, 323–342, 347, 375, 378, 379, 398
Excess sludge, 67, 68, 81, 82, 84–91, 93, 95

F

Filtration applications, 348
Flexural, 40–43, 45, 60, 61, 122, 299, 301, 327, 329–334, 342, 373–375, 418
Forward osmosis (FO), 72, 73, 95
Functionalization, 38, 39, 370–372, 380

G

Gamma radiation, 292, 295–304, 410
Green fillers, 133–173
Ground tire rubber, 97–107

H

Heavy metal ion adsorbent, 68, 78–88
Hybrid, 9, 60–61, 390

I

Impact, 6–11, 18, 19, 39–45, 52, 55, 56, 58, 89, 101, 106, 112, 121, 122, 133, 136, 139, 142, 143, 148, 169, 286, 299, 308, 310, 311, 324, 341, 365, 372–376, 394, 395, 399, 417–431

L

Life-cycle analysis (LCA), 393–395
Liquid natural rubber (LNR), 323–342

M

Mechanical properties, 5, 6, 28, 37–42, 49–62, 98, 101, 102, 104, 107, 115, 120, 121, 123, 124, 138, 141, 143–150, 171, 180, 183, 194, 210, 223, 225, 228, 242–244, 256, 259–260, 275–276, 286, 287, 292, 296, 301, 303, 308, 324, 329, 334, 348, 350, 367–369, 373–375, 397, 399, 409, 410, 412, 418, 424–426, 428
Mechanical recycling, 4, 9, 11–13, 28, 36, 37, 53, 113–115, 120, 124, 136, 155, 348, 349, 373, 394–396, 421–422, 430, 431
Membrane fabrication, 353
Membrane recoveries, 68, 84
Metal oxides, 256, 258–267
Microfiltration, 71, 78–80, 95, 121, 350, 355, 359, 360

N

Nanocellulose, 292, 293, 392
Nanocomposite, 23, 59, 60, 143, 148, 150, 293, 302, 324, 359, 409–411
Natural fiber, 35–45, 56, 57, 123, 139–142, 165, 292, 363, 366–369, 371, 379, 380, 390, 393, 408, 409
Natural fillers, 141, 150, 155, 159, 164, 165, 363–368, 370, 371, 373, 381, 390
Natural rubber (NR), 98, 102, 103, 107, 179–205, 209–225, 227–251, 255–268, 271–287, 323–342
Natural rubber latex, 228–239, 251, 323

P

Paddy straw powder (PSP), 145, 307–309, 311–319

PE composites, 407–409, 411–413
Performance, 5, 10, 18, 21, 23–25, 28, 49, 51, 52, 54, 58, 59, 62, 68, 79, 82, 114, 121, 123–125, 139, 152, 157–159, 173, 180, 199, 209, 210, 228, 239, 251, 255, 256, 272, 275, 287, 292, 303, 324, 325, 338, 340, 341, 348, 351, 355–357, 359, 363–381, 394, 406, 407, 418, 424, 426
PET waste, 11, 39, 41, 417–431
PE waste treatment, 406–412
Physical and mechanical properties, 139, 251, 296, 423
Plastic recycling, 2, 4, 8, 12, 35, 112, 113, 122, 348, 420, 421
Polyethylene terephthalate (PET), 2, 11, 12, 20, 35, 37–41, 44, 51–53, 55, 57–59, 61, 112, 113, 115, 116, 121, 122, 124, 156, 348–351, 360, 365, 366, 410–412, 417–431
Polyhydroxybutyrate-3-valerate (PHBV), 307–319
Polymer blend, 5–7, 9, 40, 44, 104, 111–125, 161, 409–412
Polymer composites, 5, 7, 39, 54, 60, 61, 134, 139, 149, 158, 159, 308, 363, 366, 368, 379, 381, 393, 426
Polymeric matrices, 39, 381
Polymeric substance (PS), 52, 67, 68, 86–89, 93, 95, 112, 115, 116, 120, 122, 425
Polymers, 2, 18, 35, 50, 69, 97, 112, 133, 188, 217, 249, 291, 307, 323, 347, 363, 389, 405, 420
Polypropylene (PP), 2, 6, 8, 12, 19, 20, 35, 38, 40–45, 51, 53, 55–59, 103, 105, 111–116, 120–124, 133–173, 299, 301, 341, 349, 351, 365, 366, 371, 374–376, 392, 394, 398, 407, 409, 418, 424, 425
Processing, 6, 37, 51, 113, 135, 227, 259, 354, 363, 394, 410, 419
Processing methods, 138, 155–158, 172, 424–425, 427–429
Production, 1, 3, 5, 10–12, 17–19, 21, 26, 28, 35–38, 42, 53, 56, 60, 67, 68, 97, 100, 101, 111–113, 116, 120, 123, 124, 138, 142, 155, 162–168, 172, 272, 296, 298, 350, 364, 366, 368, 375, 379, 380, 389–393, 399, 405–407, 409, 410, 418–420, 422, 423, 426, 430

R

Recycled Chloroprene Rubber, 255–268
Recycled ethylene propylene diene rubber (R-EPDM), 179–205, 209–225, 229–251
Recycled natural rubber (rNR), 323–342
Recycled PET, 423, 426, 430
Recycled Polyethylene Blends, 405–413
Recycled polymer, 5, 10, 35, 44, 53, 139, 171, 363–381
Recycled thermoplastics, 38, 61, 62, 139
Recycling, 2, 18, 35, 52, 67, 97, 112, 133, 179, 209, 292, 323, 347, 373, 393, 406, 418
Recycling bioplastics, 8–12, 116, 125
Recycling composites, 123
Recycling strategies, 19, 28, 116, 120, 161, 380
Recycling technologies, 100, 172, 209, 348, 395–397, 413, 423
Resource recovery, 67

S

Solid waste, 4, 13, 28, 37, 111–113, 348, 364
Styrene butadiene rubber (SBR), 184, 272–282, 284–287
Surfactant-enhanced ultrasonic extraction, 68, 89
Sustainable polymer, 134, 139, 158

T

Tensile, 6–9, 40–45, 51, 54–61, 120–122, 138, 143–145, 148–150, 180, 184–189,

195, 202, 205, 213–215, 217, 222, 227, 228, 232, 243, 259, 263, 275, 278, 287, 291, 293, 296, 301, 307–319, 369, 372–375, 379, 411

Thermal properties, 40, 42, 60, 102, 121, 152, 180, 264, 287, 296, 310, 324, 336–338, 355, 373, 378–379
Thermal stability, 10, 11, 38, 40, 42, 122, 123, 152, 157, 180, 188, 199, 203, 205, 210, 218, 219, 222, 225, 236, 238, 245, 247, 251, 265, 268, 272, 280–282, 287, 293, 316, 317, 319, 338, 342, 371, 425

U

Ultrafiltration, 21–23, 68–71, 78, 79, 85, 95, 121, 353–357, 359, 360

V

Value-added materials, 35, 62, 134, 172, 227

W

Waste, 2, 18, 35, 51, 84, 101, 112, 133, 179, 209, 256, 271, 292, 323, 347, 363, 389, 406, 418
Waste management, 2, 3, 7, 28, 35, 37, 98, 100, 102–104, 106, 107, 112, 113, 134, 171, 172, 347, 399
Waste plastics, 3, 7, 134, 140, 348, 359, 360, 418, 419